The Illustrative Book of Cartilage Repair

Deepak Rajkumar Goyal
Editor

Springer

The Illustrative Book of Cartilage Repair

Deepak Rajkumar Goyal
Editor

The Illustrative Book of Cartilage Repair

Springer

Editor
Deepak Rajkumar Goyal
Saumya Arthroscopy and Sports Knee Clinic
Ahmedabad
India

Visiting Professor of Orthopaedics
Graduate School of Biomedical and Health Sciences
Hiroshima University
Hiroshima
Japan

ISBN 978-3-030-47153-8 ISBN 978-3-030-47154-5 (eBook)
https://doi.org/10.1007/978-3-030-47154-5

This Springer imprint is published by the registered company Springer Nature Switzerland AG
The registered company address is: Gewerbestrasse 11, 6330 Cham, Switzerland

Foreword

Injury and degeneration of articular cartilage continue to present a therapeutic conundrum that challenges the best minds in translational biology and orthopedic surgery. In this one volume, Deepak Goyal and colleagues offer the clinical specialist all the information needed to understand the nature of cartilage lesions, historical and contemporary approaches to their treatment, and a peek into what the future might hold. Dr. Goyal has assembled an outstanding group of experts in the field to provide the reader with the most authoritative information available on each relevant topic. The hallmark of this book is the exhaustive collection of illustrations that augment the text and thoroughly clarify each teaching point. Arthroscopic and gross photographs, photomicrographs, computed tomograms, magnetic resonance images, and original artwork all do their part to bring the text to life. *The Illustrative Book of Cartilage Repair* provides every reader, from novice to expert, with the knowledge needed to navigate this dynamic medical field.

Bruce Reider MD
Editor-in-Chief
American Journal of Sports Medicine
Orthopaedic Journal of Sports Medicine
Professor of Orthopaedic Surgery, Emeritus
University of Chicago
Chicago, IL, USA

Foreword

Hunter's observation in 1743 that cartilage "once destroyed, is not repaired," had a great impact on the attempts of cartilage repair for almost 250 years.

When young individuals suffer from articular cartilage defects of the knee caused by trauma or osteochondritis dissecans, it is difficult to expect a spontaneous healing of the defects because articular cartilage has poor spontaneous healing capacity, due to its lack of blood vessels and nerve supply. They will often result in osteoarthritis in the long run. Total knee replacement is a last possible procedure left for severe OA of the knee.

In order to prevent such early progression to secondary osteoarthritis, various techniques such as mosaicplasty and bone marrow stimulating technique have been developed to repair articular defects.

In 1994, a milestone paper published by M. Brittberg and L. Peterson came up with a new treatment procedure for cartilage repair. In their procedure, a small amount of cartilage slices was harvested from non-weight-bearing areas of the femur, which were expanded in a monolayer culture system, and then implanted in suspension into a prepared recipient site in the region of the chondral defect, which was covered with a periosteal flap. It was astonishing that the repaired area was demonstrated to be hyaline-like cartilage.

However, I personally thought that their implantation method had several probable weak points such as leakage and inhomogeneous distribution of implanted chondrocytes. In 1996, we addressed these concerns for the first time by implanting autologous chondrocytes, cultured in three-dimensional atelocollagen gel, into the cartilage defect site, and reported the early results in 2001 and 2002. This procedure has been listed as an item covered by the National Health Insurance in Japan since 2013, and so far, more than 1000 cases have been performed there.

Since then, in order to overcome the statement made by Hunter about 250 years ago about cartilage—"once destroyed, is not repaired"—many treatment methods and medical products using different types of autogenic or allogenic stem cells have been developed, and such efforts are still being made so as to achieve more optimal clinical outcomes in cartilage repair.

This book has comprehensibly outlined the chronological development of surgical procedures for the cartilage repair. The editor of this book, Deepak Rajkumar Goyal has had several appointments at domestic and international associations such as ICS (Indian Cartilage Society), where he had served as

President for four years, ACRS (Asian Cartilage Repair Society), and ESSKA (European Society of Sports Traumatology, Knee Surgery and Arthroscopy) in the past; currently, he has been serving as President of Asian Cartilage Repair Society (ACRS). Up until today, throughout his academic life, Dr. Deepak has been passionately pursuing clinical practices and his research in the field of cartilage repair. My first encounter with Dr. Deepak Rajkumar Goyal goes back to an international conference held in September 2005 when I was invited to deliver a lecture presentation in Budapest in Hungary. At that time, Dr. Deepak was being trained under Prof. Dr. Berkes István. Since then, more than 15 years have passed, and his zest for cartilage repair has not shown any sign of cooling down.

I am certain that *The Illustrative Book of Cartilage Repair* will contribute significantly to the continued evolution of cartilage repair procedures in orthopedics. For that, I am truly grateful to Dr. Deepak Rajkumar Goyal for having successfully compiled this book, while securing many world-famous talented authors for their excellent contributions. Congratulations to the editor and the authors on this splendid accomplishment.

Mitsuo Ochi, MD, PhD.
President, Hiroshima University
Hiroshima, Japan

President, JOSKAS
(Japanese Orthopaedics Society of Knee,
Arthroscopy and Sports Medicine), 2009-2018
First President, APKAS (Asia-Pacific Knee,
Arthroscopy and Sports Medicine Society)
First President, ACRS (Asian Cartilage Repair Society)

Preface

From "no treatment" to 3-D bioprinting technologies in cartilage repair, the science of cartilage repair has grown out of its infancy and is fast maturing up. The illustrative book of cartilage repair is aimed to provide a visual and first-hand impression of the different concepts behind cartilage repair to the young aspiring as well as the established cartilage surgeons. Young surgeons, who are inadvertently confused with this rapidly evolving science, can understand the basics of cartilage repair along with a broad outlook of the various commonly performed cartilage repair surgeries through a pictorial display of the techniques. It is not uncommon for the established cartilage surgeons to follow some of the cartilage repair procedures while remaining away from the remaining spectrum of cartilage repair surgeries options. The established cartilage surgeons can also have a quick deeper insight into the cartilage repair techniques that they do not commonly perform due to either a lack of availability or a lack of training or due to a disbelief towards a procedure. Pioneers and masters in their respective fields have contributed to the book so as to provide a major insight into the latest technology and the operative techniques. Some of the authors are the basic researchers of their respective techniques and have shared their rich experience in the form of a detailed case presentation as well as step-by-step pictorial guide to the respective technique. I wish this book will find its place in the major libraries as well as on the coffee table of the surgeon's room across the globe.

"Let us preserve the joints"

Ahmedabad, Gujarat, India

Deepak Rajkumar Goyal
President, Asian Cartilage
Repair Society (ACRS)
Founder and Past President,
Indian Cartilage Society (ICS)
Fellow Member and Past Committee
Chair, International Cartilage
Repair Society (ICRS)

Acknowledgement

The patient does not care about your science; what he wants to know is, can you cure him?—Martin H. Fischer

Let the young know they will never find a more interesting, more instructive book than the patient himself.—Giorgio Baglivi

We, as medical professionals continue to learn, understand, and implement the advances in medical science for the welfare of our patients. But we should not forget that at the end, what patient wants is a cure. We learn from the patients and patients expect a cure. Both the philosophies go parallel and will continue to remain so.

While writing the acknowledgement, the first thing that comes to my mind is my patients. The medical education and the professional training made me an educated doctor but my patients made me a human doctor. Their pains and disabilities had lots of human feelings that are not written in the medical books. I learnt a lot treating them and implemented a lot that I learnt from them. I am deeply thankful to my patients who have trusted me for the last three decades and have allowed me to treat them. I have applied lots of information in this book that I gathered while treating them.

It takes tremendous time while writing, editing, and reviewing a book. My wife, Anjali, not only allowed me to utilize our personal time for the preparation of this book, but also served as a great helping hand. My kids, Aarju and Saumya, helped me in managing the technical part of the images while in fact, I was utilizing their quality time. I am thankful to my wife, children, and my parents who had been a backbone of my professional and academic activities all these years.

The contributors of the book have also worked very hard to provide sequential images for their respective chapters. While the surgeons do have many images of a surgical technique, we discovered that it is very difficult to have a complete series of one patient, from clinico-radiological preoperative diagnosis to the sequential surgical steps and then the long-term follow-up confirmation of the results. However, I am so glad that each corresponding author of the book worked very hard to collect the required information and transformed their respective cases into a chapter. The reviewers were also very exemplary. They understood the concept behind the book very well and then contributed immensely in giving their suggestions. I immensely thank all the contributors and reviewers for this detailed and easy-to-understand collection of the illustrated cartilage repair techniques.

Lastly, I thank the editorial support team of Springer who put a deep trust in me and supported me from the conceptualization to the publication of this book.

Deepak Rajkumar Goyal MB, MS, DNB
Consultant Arthroscopy & Sports Knee Surgeon

Saumya Arthroscopy and Sports Knee Clinic,
Ahmedabad, India

Visiting Professor of Orthopaedics
Graduate School of Biomedical
and Health Sciences, Hiroshima
University, Hiroshima,
Japan

Contents

Contributors

Nobuo Adachi Department of Orthopaedic Surgery, Biomedical & Health Sciences, Hiroshima University, Hiroshima, Japan

Sante Alessandro Altamura Clinic IRCCS Istituto Ortopedico Rizzoli, Bologna, Italy

Luca Andriolo Clinic IRCCS Istituto Ortopedico Rizzoli, Bologna, Italy

Michael Banffy Kerlan Jobe Institute, Los Angeles, CA, USA

Angelo Boffa Clinic IRCCS Istituto Ortopedico Rizzoli, Bologna, Italy

Mats Brittberg Cartilage Research Unit, University of Gothenburg, Region Halland Orthopaedics, Kungsbacka Hospital, Kungsbacka, Sweden

Ezequiel Santa Coloma Orthopaedic Arthroscopic Surgery International (O.A.S.I.) Bioresearch Foundation, Gobbi N.P.O., Milan, Italy

Ignacio Dallo Orthopaedic Arthroscopic Surgery International (O.A.S.I.) Bioresearch Foundation, Gobbi N.P.O., Milan, Italy

Alessandro Di Martino Clinic IRCCS Istituto Ortopedico Rizzoli, Bologna, Italy

Giuseppe Filardo Applied and Translational Research center (ATRc), IRCCS Istituto Ortopedico Rizzoli, Bologna, Italy

Alberto Gobbi Orthopaedic Arthroscopic Surgery International (O.A.S.I.) Bioresearch Foundation, Gobbi N.P.O., Milan, Italy

Deepak Rajkumar Goyal Saumya Arthroscopy and Sports Knee Clinic, Ahmedabad, Gujarat, India

Visiting Professor of Orthopaedics, Graduate School of Biomedical and Health Sciences, Hiroshima University, Hiroshima, Japan

Daniel A. Grande Donald and Barbara Zucker School of Medicine at Hofstra/Northwell, Hempstead, NY, USA

Orthopaedic Research Laboratory at Feinstein Institute for Medical Research, Northwell Health, Manhasset, NY, USA

Department of Orthopaedic Surgery, Northwell Health, Great Neck, NY, USA

Laszlo Hangody Hungarian Academy of Sciences, Budapest, Hungary

Department of Traumatology, Semmelweis University, Budapest, Hungary

Department of Orthopaedics, Uzsoki Hospital, Budapest, Hungary

Katarzyna Herman Orthopaedic Arthroscopic Surgery International (O.A.S.I.) Bioresearch Foundation, Gobbi N.P.O., Milan, Italy

Eleonora Irlandini Orthopaedic Arthroscopic Surgery International (O.A.S.I.) Bioresearch Foundation, Gobbi N.P.O., Milan, Italy

Tunku Kamarul Tissue Engineering Group, Department of Orthopedics Surgery, NOCERAL, Faculty of Medicine, University of Malaya, Kuala Lumpur, Malaysia

Elizaveta Kon Department of Biomedical Sciences, Humanitas, University, Milan, Italy

Humanitas Clinical and Research Center, Milan, Italy

Henning Madry Center of Experimental Orthopaedics, Saarland University, Homburg, Germany

Department of Orthopaedic Surgery, Saarland University Medical Center, Homburg, Germany

Pradeep Mandapalli Arthroscopy Service, Kokilaben Dhirubhai Ambani Hospital, Mumbai, India

Bert Mandelbaum Kerlan Jobe Institute, Los Angeles, CA, USA

Byoung-Hyun Min Department of Orthopedic Surgery, Ajou University School of Medicine, Suwon, Korea

Department of Molecular Science and Technology, Ajou University, Suwon, Korea

Cell Therapy Center, Ajou University Hospital, Suwon, Korea

Malliga Raman Murali Tissue Engineering Group, Department of Orthopedics Surgery, NOCERAL, Faculty of Medicine, University of Malaya, Kuala Lumpur, Malaysia

Taylor L. Mustapich Orthopaedic Research Laboratory at Feinstein Institute for Medical Research, Northwell Health, Manhasset, NY, USA

Tomoyuki Nakasa Department of Orthopaedic Surgery, Biomedical & Health Sciences, Hiroshima University, Hiroshima, Japan

Alessandra Nannini Department of Biomedical Sciences, Humanitas, University, Milan, Italy

Humanitas Clinical and Research Center, Milan, Italy

Tamás Oláh Center of Experimental Orthopaedics, Saarland University, Homburg, Germany

Dinshaw N. Pardiwala Arthroscopy Service, Kokilaben Dhirubhai Ambani Hospital, Mumbai, India

Drushi Patel Gujarat Imaging Centre, Samved Hospital, Ahmedabad, Gujarat, India

Shantanu Sudhakar Patil SRM Medical College and Hospitals, SRM University, Kattankulathur, Tamil Nadu, India

Alberto Poggi Clinic IRCCS Istituto Ortopedico Rizzoli, Bologna, Italy

Nicholas Ramos Kerlan Jobe Institute, Los Angeles, CA, USA

Anjaneyulu Purnachandra Tejaswi Ravipati Division of Orthoapedics, Dalhousie University, Halifax, NS, Canada

Timothy F. Reed Donald and Barbara Zucker School of Medicine at Hofstra/Northwell, Hempstead, NY, USA

Orthopaedic Research Laboratory at Feinstein Institute for Medical Research, Northwell Health, Manhasset, NY, USA

Iacopo Romandini Clinic IRCCS Istituto Ortopedico Rizzoli, Bologna, Italy

Ankur Shah Sadbhav Imaging Centre, Ahmedabad, Gujarat, India

Anshu Shekhar The Orthopaedic Speciality Clinic, Pune, India

Martyn Snow The Royal Orthopaedic Hospital, Birmingham, UK

Department of Chemical Engineering, University of Birmingham, Birmingham, UK

Kushalappa Subbiah Arthroscopy Service, Kokilaben Dhirubhai Ambani Hospital, Mumbai, India

Pooja N. Swami Orthopaedic Research Laboratory at Feinstein Institute for Medical Research, Northwell Health, Manhasset, NY, USA

Sachin Ramchandra Tapasvi The Orthopaedic Speciality Clinic, Pune, India

Ivan Wong Division of Orthopaedic Surgery, Dalhousie University, Halifax, NS, Canada

Stefano Zaffagnini Clinic IRCCS Istituto Ortopedico Rizzoli, Bologna, Italy

1 The Science of Illustrated Cartilage Repair and Its Rationale

Deepak Rajkumar Goyal

A historic statement by Hunter [1], "Ulcerated cartilage is a troublesome thing, once destroyed…. is not repaired" had a great impact on the attempts of cartilage repair for almost 250 years. The observation came when he was studying inflammation, suppuration, or lymph collection around a wound and found none appearing around the cartilage and the corneal lesions. Though true in a research context, the statement was not true in the context of a surgical intervention. Hunter brother's findings were questioned by many authors [2–4] but still, no attempts were made to repair the cartilage until the latter half of the last century [5].

Cartilage repair is presently a fast-changing science with a very fast evolution process. The last two decades have seen a plethora of surgical techniques and products that can keep even a veteran cartilage surgeon guessing. Many products have come and have vanished. There are huge controversies and concurrences for each and every cartilage repair technique; be it a marrow stimulation technique, an osteochondral cylinder transfer technique, a cell-based technique or a scaffold-based technique. But then, every change in the technique is making us more equipped to better understand the science behind the cartilage repair. Young surgeons are very keen to learn and understand this emerging field of cartilage repair. However, as the cartilage science is yet to reach a consensus plateau, they are unable to have a clear and a long-lasting message about the cartilage repair. Diversities of the opinions also make it nearly impossible for young surgeons to have a first-hand experience of all the existing technologies.

The basic science of cartilage repair, diagnosis and classifications of cartilage lesions, understanding concepts behind each cartilage repair technique and its step-by-step execution, postoperative rehabilitation and long term results etc are the important fundamentals that must be understood properly before any cartilage repair is attempted. Illustrated portray of various concepts with a step-by-step description is a unique way to understand the major concepts of cartilage repair. Oláh et al. [6, 7] have produced many gross and histological sections in the laboratory and have described the anatomy and histology of the healthy and the degenerative cartilage in a step wise manner. Their chapters also include a basic information about the special stains and the immunohistochemical stains. The subchondral (SC) bone plays many important roles, like cartilage nourishment, support to the overlying cartilage and a supplier of cells and growth factors [8]. SC bone also behaves differently in response to injury, necrosis, arthritis, and to a surgical procedure. The role of SC bone and its response to

D. R. Goyal (✉)
Saumya Arthroscopy and Sports Knee Clinic, Ahmedabad, India

Visiting Professor of Orthopaedics, Graduate School of Biomedical and Health Sciences, Hiroshima University, Hiroshima, Japan
e-mail: deepak@knee.in

D. R. Goyal (ed.), *The Illustrative Book of Cartilage Repair*,
https://doi.org/10.1007/978-3-030-47154-5_1

various pathologies and surgical procedures are discussed by Nakasa and Adachi [9]. Many traumatic and degenerative chondral lesions have abnormal biomechanical forces working behind them, aptly discussed by Goyal [10]. While arthroscopic classification is the gold standard as described by Goyal [11], a magnetic resonance imaging (MRI) classification and assessment is the first insight into the cartilage lesion that has been discussed by Patel et al. [12]. Cells and scaffolds form the basis of any cartilage repair; and hence a basic knowledge about their sources, properties, and their construct is a must. While Min [13] has beautifully discussed the roles of the various cells that have a potential to repair the cartilage, Poggi et al. [14] have created beautiful pictures to describe various scaffolds. Microfracture technique is one of the simplest cartilage repair technique that was once considered as the first line of treatment by many. An insight into the detailed operative technique, along with a discussion about the guarded expectations, has been discussed by Herman et al. [15]. Two elaborative chapters have been dedicated to the osteochondral cylinder transfer techniques using two different surgical techniques: mosaicplasty by Hangody [16] and the osteoarticular autogenous transfer system by Tapasvi et al. [17]. The autologous chondrocytes implantation (ACI) technique was first published by Brittberg et al. [18] in 1994. The technique was revolutionary but had many challenges, leading to its evolution to many generations. While the first-generation technique used the periosteum to cover the chondrogenic chamber, the second-generation ACI replaced the periosteum with a collagen membrane. Both first and second-generations are now gradually being replaced by the third-generation ACI techniques; still a basic insight into these two techniques is a must which has been covered by none another but the pioneer of the technique, Brittberg [19] himself. In the third-generation ACI, instead of making a chondrogenic chamber at the defect site, a scaffold loaded with the cultured chondrocytes is prepared. While membrane-based third-generation ACI is two dimensional ACI as described by Ramos et al. [20], the three-dimensional third-generation scaffold-based ACI is also available as discussed by Goyal [21]. The biggest challenge with the ACI procedures is two stage surgeries that put lots of economic, social, psychological and physical load on the patient, and the healthcare industry. To overcome these issues, there are simultaneous efforts to evolve into the single stage cartilage repair procedures. To develop a single stage procedure, the major concentration is on supplying an optimum scaffold while relying on in vivo cells. BST-Cargel™, bone marrow aspirate concentrate (BMAC), and artificial single to multilayer scaffolds are the various single stage cartilage repair techniques that have shown good midterm results in various publications. Wong and Ravipati [22] have described the basic concept behind the BST-Cargel technique, where chitin-based scaffold uses cells coming from a microfracture technique [15]. Multiphasic scaffolds like MaioRegen™ as described by Kon and Nannini [23] give specific signals to the cells coming from the bone marrow to differentiate into either chondrocytes or osteocytes depending on the properties of the scaffold material. Gobbi et al. [24] have discussed the application of bone marrow aspirate concentrate as a source of cells while using the hyaluronan membrane as a scaffold.

Chondral lesions may not be purely chondral but can also be combined osteochondral lesions. While chondral lesions with a small bony defect may be treated with an isolated cartilage repairing technique, large or extra-large osteochondral lesions require a combination of bone grafting in conjunction with the cartilage repair surgery as described by Goyal [25] in the overlay ACI technique. Alternatively, such lesions can be treated with an osteochondral allograft as discussed by Snow [26]. Cartilage science must grow out of the current scenario and find solutions using the latest technology. A 3D bioprinting is a promising technology that can ensure a near-perfect scaffold-cell construct and ensure a hyaline repair. Reed et al. [27] have discussed the potential of 3D bioprinting technology in cartilage repair while also discussing its advantages and the limitations. Apart from the clinical analysis, MRI provides a first insight into the ongoing cartilage repair process after a cartilage repair surgery. Pardiwala et al. [28] have pro-

vided a significant insight into the MRI analysis after an untreated lesion as well as after various cartilage repair procedures are carried out.

This book is aimed to display the different aspects of cartilage repair, from the basic science to the clinical application, for a quick visual understanding along with a pictorial display of all the major cartilage repair techniques. While the aspiring cartilage surgeons can have a quick perception of the cartilage repair science, existing cartilage surgeons can refresh their observations about the various cartilage repair technologies.

References

1. Hunter W. Of the structure and diseases of articulating cartilages. Philos Trans. 1742;42:514–21.
2. Brodie BC. Pathological and surgical observations on the diseases of the joints. 3rd ed. Washington: D. Green; 1834. Chap. 4. p. 35.
3. Leidy J. On the intimate structure and history of the articular cartilages. Am J Med Sci. 1849;34:277–294 (a) 287; a 291.
4. Buckwalter JA. Were the Hunter brothers wrong? Can surgical treatment repair articular cartilage? The Iowa Orthopaedic Journal. 1997;17:1–13.
5. Pridie K. A method of resurfacing osteoathritic knee joints. J Bone Joint Surg Br. 1959;41-B:618–9.
6. Oláh T, Kamarul T, Madry H, Murali MR. The illustrative anatomy and the histology of the healthy hyaline cartilage. In: Goyal D, editor. The illustrative book of cartilage repair. Berlin: Springer; 2021; In Press.
7. Oláh T, Goyal D, Madry H. The illustrative anatomy and the histology of the degenerative hyaline cartilage. In: Goyal D, editor. The illustrative book of cartilage repair. Berlin: Springer; 2021; In Press.
8. Goyal D, Goyal A, Adachi N. Subchondral bone: healthy soil for the healthy cartilage. In: Bioorthopaedics. Berlin: Springer; 2017. p. 479–86.
9. Nakasa T, Adachi N. The illustrative role of the subchondral bone and the overlying cartilage. In: Goyal D, editor. The illustrative book of cartilage repair. Berlin: Springer; 2021; In Press.
10. Goyal D. The illustrative biomechanics of a chondral injury. In: Goyal D, editor. The illustrative book of cartilage repair. Berlin: Springer; 2021, In Press.
11. Goyal D. The classifications of the chondral lesions. In: Goyal D, editor. The illustrative book of cartilage repair. Berlin: Springer; 2021, In Press.
12. Patel D, Shah A, Goyal D. The illustrative description of the imaging of the damaged cartilage. In: Goyal D, editor. The illustrative book of cartilage repair. Berlin: Springer; 2021, In Press.
13. Min B-H. The illustrative role of cells in cartilage repair. In: Goyal D, editor. The illustrative book of cartilage repair. Berlin: Springer; 2021; In Press.
14. Poggi A, Andriolo L, Boffa A, Altamura SA, Romandini I, Di Martino A, Zaffagnini S, Filardo G. The illustrative chondral and osteochondral scaffolds in cartilage repair. In: Goyal D, editor. The illustrative book of cartilage repair. Berlin: Springer; 2021; In Press.
15. Herman K, Irlandini E, Dallo I, Coloma ES, Gobbi A. The illustrative marrow stimulation techniques for cartilage repair: the microfracture technique. In: Goyal D, editor. The illustrative book of cartilage repair. Berlin: Springer; 2021; In Press.
16. Hangody L. The illustrative osteochondral cylinder transfer techniques for cartilage repair: the mosaicplasty technique. In: Goyal D, editor. The illustrative book of cartilage repair. Berlin: Springer; 2021; In Press.
17. Tapasvi SR, Shekhar A, Patil SS. The illustrative osteochondral cylinder transfer techniques for cartilage repair: the OATS technique. In: Goyal D, editor. The illustrative book of cartilage repair. Berlin: Springer; 2021, In Press.
18. Brittberg M, Lindahl A, Nilsson A, Ohlsson C, Isaksson O, Peterson L. Treatment of deep cartilage defects in the knee with autologous chondrocyte transplantation. N Engl J Med. 1994;331(14):889–95.
19. Brittberg M. The illustrative 1st and 2nd generation autologous chondrocyte implantation (ACI) for the cartilage repair. In: Goyal D, editor. The illustrative book of cartilage repair. Berlin: Springer; 2021, In Press.
20. Ramos N, Mandelbaum B, Banffy M. The illustrative membrane based autologous chondrocyte implantation for the cartilage repair. In: Goyal D, editor. The illustrative book of cartilage repair. Berlin: Springer; 2021, In Press.
21. Goyal D. The illustrative third generation autologous chondrocyte implantation for the cartilage repair-the gel based ACI technique. In: Goyal D, editor. The illustrative book of cartilage repair. Berlin: Springer; 2021; In Press.
22. Wong I, Ravipati APT. The illustrative single stage cartilage repair technique with chitosan-based bioscaffold (BST-cargel). In: Goyal D, editor. The illustrative book of cartilage repair. Berlin: Springer; 2021; In Press.
23. Kon E, Nannini A. The illustrative multilayer scaffolds for the single stage cartilage repair in the osteochondral lesions. In: Goyal D, editor. The illustrative book of cartilage repair. Berlin: Springer; 2021; In Press.
24. Gobbi A, Dallo I, Herman K, Irlandini E. The illustrative bone marrow aspirate concentrate and hyaluronan-based scaffold technique for single stage cartilage

repair. In: Goyal D, editor. The illustrative book of cartilage repair. Berlin: Springer; 2020.
25. Goyal D. The illustrative overlay autologous chondrocytes implantation (overlay ACI) technique for repair of the extra-large osteochondral defects. In: Goyal D, editor. The illustrative book of cartilage repair. Berlin: Springer; 2021; In Press.
26. Snow M. The illustrative osteochondral allograft based cartilage repair. In: Goyal D, editor. The illustrative book of cartilage repair. Berlin: Springer; 2021, In Press.
27. Reed TF, Swami PN, Mustapich TL, Grande DA. The illustrative 3-D bioprinting in cartilage repair. In: Goyal D, editor. The illustrative book of cartilage repair. Berlin: Springer; 2021; In Press.
28. Pardiwala DN, Subbiah K, Mandapalli P. The illustrative magnetic resonance image (MRI) assessment of cartilage repair. In: Goyal D, editor. The illustrative book of cartilage repair. Berlin: Springer; 2021; In Press.

2 The Illustrative Anatomy and the Histology of the Healthy Hyaline Cartilage

Tamás Oláh, Tunku Kamarul, Henning Madry, and Malliga Raman Murali

2.1 Introduction

Hyaline articular cartilage is a 2–4 mm thick, avascular and aneural tissue, consisting of chondrocytes (only 1–2% of the total cartilage volume) embedded in an extracellular matrix [1, 2]. Its principal function is to provide a smooth, lubricated surface for articulation and to facilitate the transmission of loads with a low frictional coefficient [1]. The extracellular matrix contains mainly water (>70%) and two major organic components: type II collagen and the proteoglycan aggrecan, which provide tensile strength and compressive resilience to the tissue [2–4]. Histologically, the articular cartilage can be divided into the superficial, transitional, and deep (radial) zones based on the general orientation of the collagen fibrils, the morphology and arrangement of the chondrocytes, and the staining properties of the matrix [4–6]. Between the deep zone and the calcified cartilage layer, a radiologically denser, 5 μm thin discrete band of mineralized cartilage, called tidemark, can be found. Located below the tidemark, the calcified cartilage is a 20–250 μm thick transitional zone, which reduces the "stress riser" between the much stiffer bone and cartilage. Its physiological function is to form an interface between the cartilage and the bone for the transmitting forces, attaching cartilage to bone, and limiting diffusion from the bone to the deeper layers of cartilage [4, 7]. Under the calcified cartilage lies the subchondral bone which provides mechanical and metabolic support to the articular cartilage, absorbs shock, and maintains the joint shape [4, 5]. The subchondral bone consists of two parts with different macroscopic structures: the subchondral bone plate and the subarticular spongiosa [4]. The subchondral bone plate is a dense bony lamella, similar to the cortical bone of other bony structures, separating the calcified cartilage from the marrow cavity. The subarticular spongiosa is a more porous and metabolically active network of trabecular bone containing innervation and blood vessels [4]. This chapter describes the normal gross anatomy and histological characteristics of the hyaline articular cartilage that give the tissue its extraordinary load-bearing characteristics.

T. Oláh
Center of Experimental Orthopaedics, Saarland University, Homburg, Germany
e-mail: tamas.olah@uni-saarland.de

T. Kamarul · M. R. Murali
Tissue Engineering Group, Department of Orthopedics Surgery, NOCERAL, Faculty of Medicine, University of Malaya, Kuala Lumpur, Malaysia
e-mail: tkzrea@um.edu.my; drmurali@um.edu.my

H. Madry (✉)
Center of Experimental Orthopaedics, Saarland University, Homburg, Germany

Department of Orthopaedic Surgery, Saarland University Medical Center, Homburg, Germany
e-mail: henning.madry@uks.eu

D. R. Goyal (ed.), *The Illustrative Book of Cartilage Repair*,
https://doi.org/10.1007/978-3-030-47154-5_2

2.2 The Illustrations

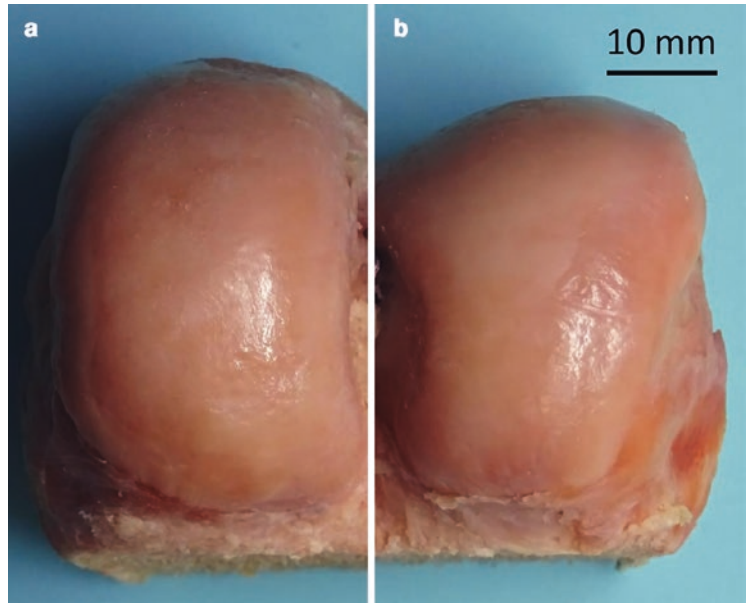

Figure 2.2.1: The Healthy Hyaline Cartilage: The Gross Anatomy of the Femoral Condyles. The gross anatomy of the healthy hyaline cartilage of the femoral condyles from a cadaveric specimen. Macroscopic image of a left (**a**) medial and (**b**) lateral normal human femoral condyle sample of a 96-year-old woman. The medial femoral condyle is larger and more oval than the lateral femoral condyle. The condyles and their radiuses are larger in males than in females, depending on the body height [8]. Healthy hyaline cartilage forms a smooth, shiny, and glassy surface on the diarthrodial joints, such as the femoral condyles and the tibial plateaus of the knee. (Picture Courtesy—Henning Madry)

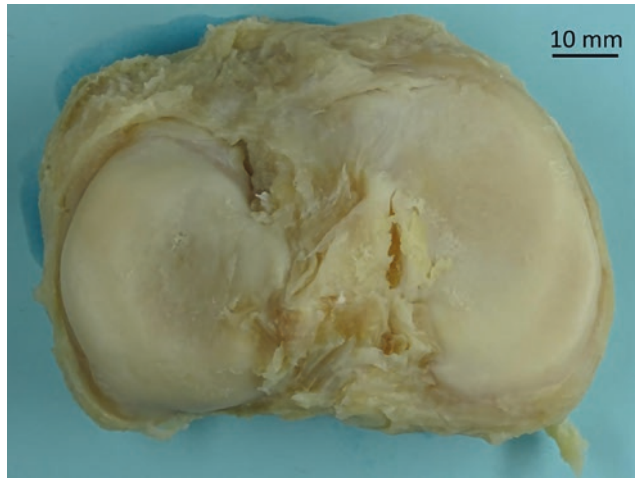

Figure 2.2.2: The Healthy Hyaline Cartilage: The Gross Anatomy of the Tibial Plateau. The gross anatomy of the healthy hyaline cartilage of the tibial plateau from a cadaveric specimen of a 52-year-old man. The proximal tibia is composed of the medial and lateral tibial condyles. The superior surface of these condyles (the tibial plateau) consists of the superior articular surfaces (facets) and the fossae. The central portion of the superior articular surface is the intercondylar eminence (the spine of the tibia). The spine is characterized by two prominences, the medial and lateral tubercles [9]. The macroscopic image of a left normal human tibial plateau shows largely smooth, intact articular cartilage surface and the remnants of the meniscal roots and ligaments which were removed in order to obtain better view of the cartilage. Since the articular cartilage and the underlying subchondral bone forms a very tight functional unit, called the osteochondral unit, studying them simultaneously is desirable [4]. (Picture Courtesy—Henning Madry)

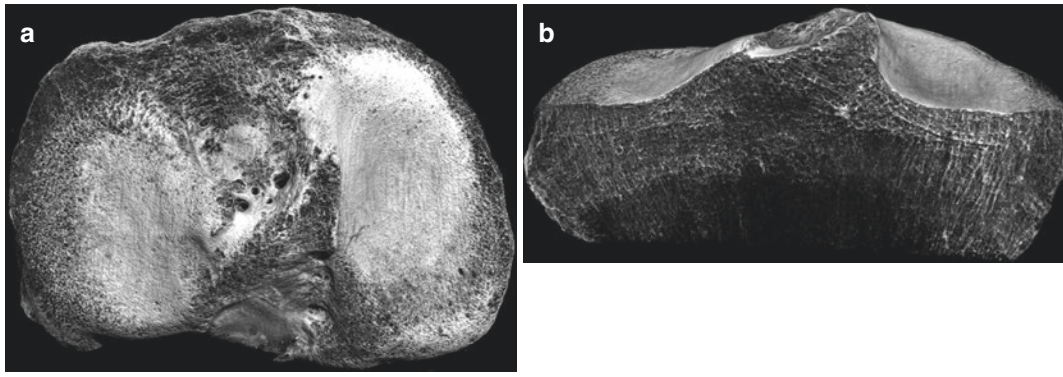

Figure 2.2.3: The Healthy Subchondral Bone: The Gross Anatomy. The gross anatomy of the healthy subchondral bone of the left tibial plateau from a cadaveric specimen of a 52-year-old man shown in Figure 2.2.2. (**a**) A superior view of the 3D reconstructed micro-CT (computed tomography) image showing the subchondral bone plate of the articulating surface. Micro-CT allows to study the morphology of the bone, normally hidden by soft tissues at high resolution. Note the absence of osteophytes on the margins of this healthy specimen, which are generally present in diseases like osteoarthritis. (**b**) The sample was cut in the coronal plane to illustrate the microstructure of the subchondral bone. Below the thin subchondral bone plate, the intricate trabecular architecture of the subarticular spongiosa following the Wolff's law is visible. The datasets of the micro-CT images allow to retrieve the detailed 3D characteristics (including bone volume fraction, bone surface/volume ratio, bone surface density, trabecular number, trabecular separation, connectivity density, structure model index, degree of anisotropy) of the bone microarchitecture using specific analyzing software. (Picture Courtesy—Henning Madry)

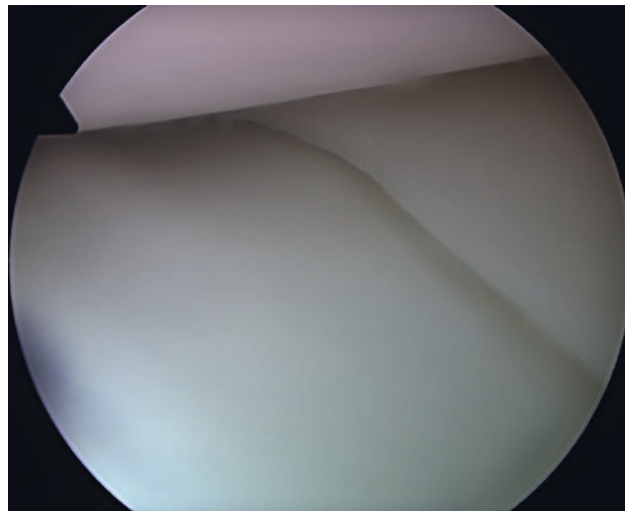

Figure 2.2.4: The Healthy Hyaline Cartilage: The Arthroscopic View. The gross anatomy of the healthy hyaline cartilage of the tibial plateau and femoral condyles from an arthroscopy surgery of a 17-year-old male. The smooth shiny articular cartilage surface of medial femoral condyle (top) and medial tibial plateau (bottom) is seen from the anterolateral portal, without evidence of cartilage defects or osteoarthritis changes. A normal medial meniscus is seen on the right corner. (Picture Courtesy—Henning Madry)

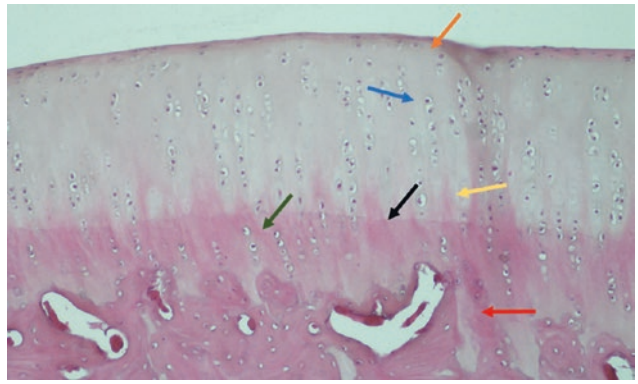

Figure 2.2.5: The Histology of the Healthy Hyaline Cartilage: The Routine Stains. All four zones of cartilage; the superficial zone (orange arrow), the middle zone (blue arrow), the deep zone (yellow arrow), and the calcified zone (green arrow) is seen along with the tidemark (black arrow) and the subchondral bone (red arrow) in the hematoxylin-eosin stained sample of the healthy hyaline cartilage. Superficial zone has the highest proportion of collagen, mainly collagen type II arranged in parallel direction to the surface of the tissue. The main function of high collagen content in superficial zone is to resist the shear stress applied on the cartilage tissue. Middle zone will have randomly oriented collagen fibers and proteoglycans to keep the tissue hydrated, and deep zone will have collagen fibers aligned perpendicular to the surface. Chondrocytes are the cellular components in the cartilage that are responsible for synthesizing and maintaining the extracellular matrix of the cartilage and are located in the matric cavities known as the lacunae. (Picture Courtesy—Tunku Kamarul)

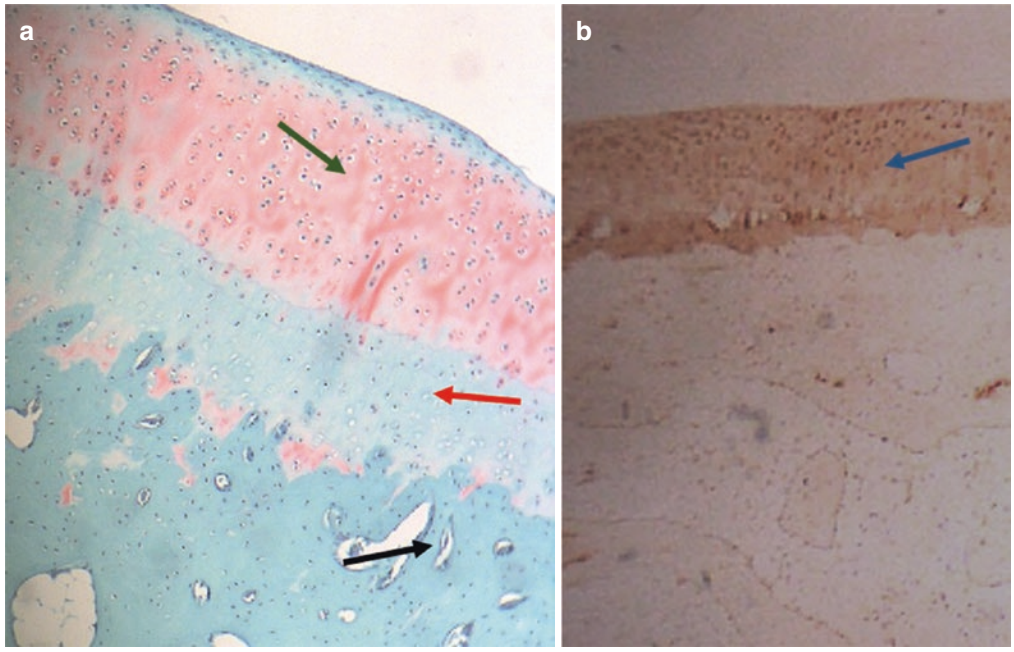

Figure 2.2.6: The Histology of the Healthy Hyaline Cartilage: The Special Stains. The special stains for histological examination of the healthy hyaline cartilage. (**a**) The healthy cartilage and the healthy subchondral bone are stained using a special staining technique, the safranin O technique, where cartilage is stained orange to red (green arrow) and all other areas such as bone is stained blue (red arrow). Safranin O is a basic stain which binds with the proteoglycans in the cartilage with a strong affinity, forming an orange to red complex, and the nuclei are stained black. Note that by controlling the quantity of stain to the adequate levels, the subchondral bone and the cortical bone regions can be clearly differentiated (black arrow). (**b**) The IHC stains for histological examination of the healthy hyaline cartilage can include a number of staining types, for example, picrosirius red (to detect cartilage). Immunostaining using antibodies against collagen type II (the predominant collagen of the cartilage tissue) has been used in this image. Higher intensity of brown color denotes a higher presence of collagen type II (blue arrow). (Picture Courtesy—Tunku Kamarul)

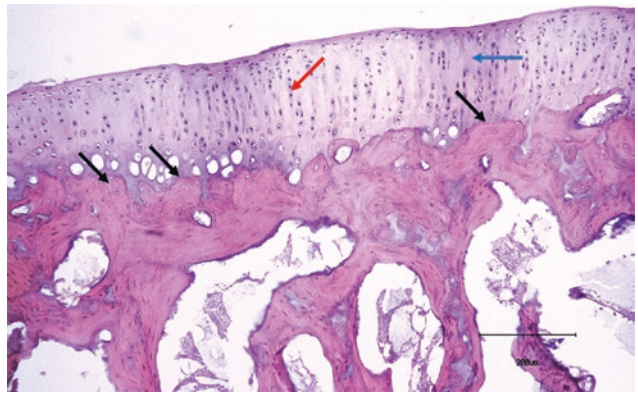

Figure 2.2.7: The Histology of the Healthy Subchondral Bone: The Routine Stains. Healthy cartilage and the healthy subchondral bone sample is stained using hematoxylin and eosin staining method (H&E staining). The cell nuclei were stained in blue-purple (red arrow) and the cartilage matrix was stained in purple-pinkish (blue arrow) color. Areas of high proteoglycan in general appear bluish as seen in this picture. Black arrows marks tidemark in the subchondral bone plate connecting the cartilage to the bone, and the green arrow shows the fenestrae connecting to the bone marrow. (Picture courtesy—Tunku Kamarul)

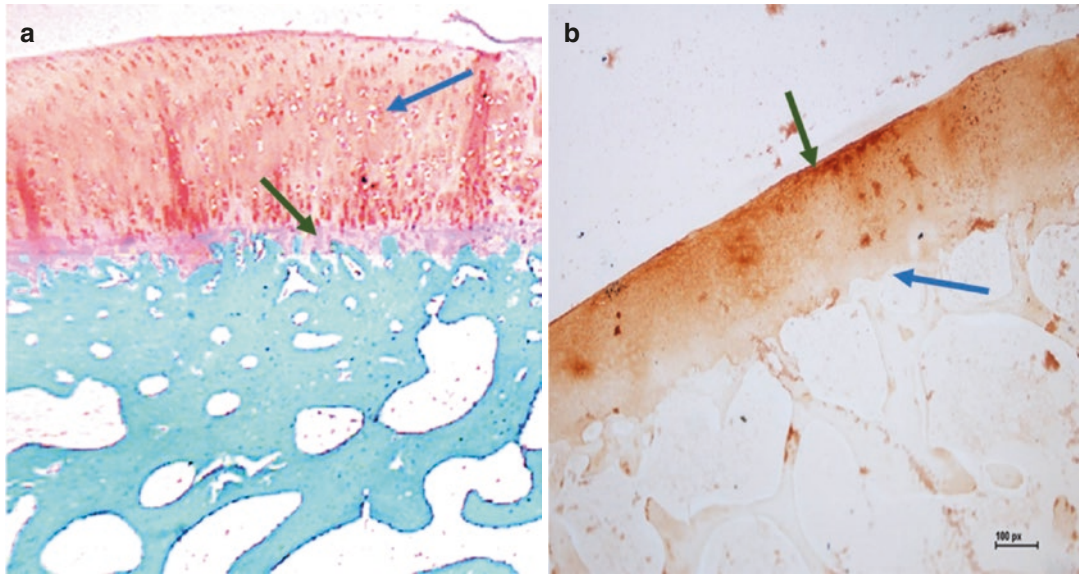

Figure 2.2.8: The Histology of the Healthy Subchondral Bone: The Special Stains. Safranin O is a cationic dye that stains the proteoglycan as well as the glycosaminoglycan. The staining also provides a proportional dye intensity to the proteoglycan content, thereby providing some form of indication of the proteoglycan quantity. (**a**) A high intensity of orange-red staining is observed in the cartilage tissue due to the presence of higher amount of proteoglycans (indicated by blue arrow) as compared to a lower intensity of staining in the cartilage-bone interphase due to a poor glycoprotein content (indicated by the green arrow). The subchondral bone region shows only a light green counterstain indicating the absence of proteoglycans. (**b**) The IHC stains are also used for the histological examination of the healthy subchondral bone. An image of the cartilage to the subchondral bone can be observed in a smooth nice transition of color intensity, as noted in the areas which are of high collagen type II from the surface region (green arrow) to the area where the collagen type II is diminished at the subchondral region (blue arrow). (Picture courtesy—Tunku Kamarul)

2.3 Take-Home Message

The osteochondral unit is a mechanically, physiologically, and biochemically interdependent, tight functional association of the articular cartilage, calcified cartilage, and the underlying subchondral bone [4]. Together they are responsible for transferring loads during weight-bearing and a smooth joint motion [4]. Hyaline articular cartilage is an important element of osteochondral unit ensuring smooth joint movements and a proper load transmission. Due to its avascular and aneural nature, it has limited intrinsic repair capability which makes it vulnerable to traumatic and aging-related injuries and degeneration.

Musculoskeletal disorders and diseases are a leading cause of disability. Over half of the adults aged 50 years and older, in the western world, have a chronic musculoskeletal condition [10]. In the USA, the economic burden is considerable; the cost of musculoskeletal conditions is approaching $1 trillion annually, which represents over 7.4% of the gross domestic product. The societal cost for the treatment for OA alone has surpassed that of both cardiovascular disease and cancer [10]. Understanding the anatomy, physiology, and the complex biomechanical and biochemical interactions of the articular cartilage and the underlying subchondral bone and their degeneration pattern in joint diseases, such as in osteoarthritis, is a major research question in order to be able to develop successful cartilage restoration strategies. Though still in its infancy, the biological treatments for this burdensome disorder have been a focus of intense investigations. In spite of the recent advances, a significant divergence of opinion on the future of early detection and biological treatments for orthopedic injuries remains. Even though new biomarkers for the early detection of OA are promising, there is a considerable need to improve the scientific knowledge, expand the technical capacities, and advance the clinical practice through the acceleration of translational research and an identification of the areas of high-yield research topics in this field [10].

References

1. Sophia Fox AJ, Bedi A, Rodeo SA. The basic science of articular cartilage: structure, composition, and function. Sports Health. 2009;1:461–8.
2. Goldring SR, Goldring MB. Changes in the osteochondral unit during osteoarthritis: structure, function and cartilage-bone crosstalk. Nat Rev Rheumatol. 2016;12:632–44.
3. Imhof H, Breitenseher M, Kainberger F, Rand T, Trattnig S. Importance of subchondral bone to articular cartilage in health and disease. Top Magn Reson Imaging. 1999;10:180–92.
4. Oláh T, Madry H. The Osteochondral unit: the importance of the underlying subchondral bone. In: Farr J, Gomoll AH, editors. Cartilage restoration: practical clinical applications. Cham: Springer International Publishing; 2018. p. 13–22.
5. Imhof H, Sulzbacher I, Grampp S, Czerny C, Youssefzadeh S, Kainberger F. Subchondral bone and cartilage disease: a rediscovered functional unit. Investig Radiol. 2000;35:581–8.
6. Madry H, van Dijk CN, Mueller-Gerbl M. The basic science of the subchondral bone. Knee Surg Sports Traumatol Arthrosc. 2010;18:419–33.
7. Oegema TR Jr, Carpenter RJ, Hofmeister F, Thompson RC Jr. The interaction of the zone of calcified cartilage and subchondral bone in osteoarthritis. Microsc Res Tech. 1997;37:324–32.
8. Biscevic M, Hebibovic M, Smrke D. Variations of femoral condyle shape. Coll Antropol. 2005;29:409–14.
9. McLeod WD, Moschi A, Andrews JR, Hugston JC. Tibial plateau topography. Am J Sports Med. 1977;5:13–8.
10. Madry H, Kon E, Condellao V, Peretti GM, Steinwachs M, Seil R, Berruto M, Engebretsen L, Filardo G, Angele P. Early osteoarthritis of the knee. Knee Surg Sports Traumatol Arthrosc. 2016;24:1753–62.

3 The Illustrative Anatomy and the Histology of the Degenerative Hyaline Cartilage

Tamás Oláh, Deepak Rajkumar Goyal, and Henning Madry

3.1 Introduction

Osteoarthritis is a degenerative disease of the entire joint, including the articular cartilage, the subchondral bone, muscles, ligaments, synovium, capsules, and the menisci [1, 2]. It is the most prevalent debilitating joint disorder in the elderly, and its occurrence is continuously increasing with the increasing age and obesity of the global population [3]. Osteoarthritic degeneration is also commonly initiated by previous injuries of the articular cartilage [4].

T. Oláh
Center of Experimental Orthopaedics, Saarland University, Homburg, Germany
e-mail: tamas.olah@uni-saarland.de

D. R. Goyal
Saumya Arthroscopy and Sports Knee Clinic, Ahmedabad, India

Visiting Professor of Orthopaedics, Graduate School of Biomedical and Health Sciences, Hiroshima University, Hiroshima, Japan
e-mail: deepak@knee.in

H. Madry (✉)
Center of Experimental Orthopaedics, Saarland University, Homburg, Germany

Department of Orthopaedic Surgery, Saarland University Medical Center, Homburg, Germany
e-mail: henning.madry@uks.eu

Signs of osteoarthritic joint degeneration, affecting the articular cartilage and the subchondral bone, are well described on open surgeries, arthroscopy, and histological sections and on the macroscopic and the micro-computed tomographic (microCT) images. In earlier, milder stages of the disease, the cartilage surface becomes slightly irregular, and the developing fissures and fibrillations do not reach the deeper tissue layers. The loss of proteoglycans, reflected in the safranin-O staining intensity on the histological sections, is of a low degree, and the cell clones are not frequent [5, 6]. In the subchondral bone, a prominent degradation of the trabecular structure is observed, including decreased trabecular volume, number, connectivity density, and degree of anisotropy, and an increased trabecular separation [7].

With the progression of the disease, clefts, and fibrillations reach the deeper layers of the articular cartilage and finally peak in the complete erosion down to the subchondral bone. The chondrocytes in the remaining cartilage form doublets, triplets, or cell nests, or they are absent from the matrix, and the tidemark is duplicated or triplicated. The loss of proteoglycans is significant [5, 6]. In this stage of the disease, the subchondral bone is thought to undergo a compensatory trabecular thickening and local stiffening, possibly contributing to the osteoarthritic cartilage degradation [8, 9].

D. R. Goyal (ed.), *The Illustrative Book of Cartilage Repair*,
https://doi.org/10.1007/978-3-030-47154-5_3

3.2 The Illustrations

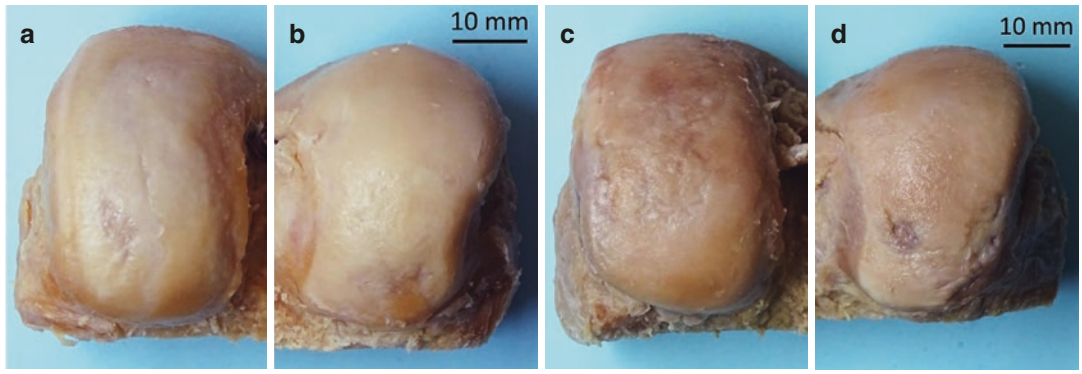

Figure 3.2.1: The Gross Anatomy of the Degenerated Hyaline Femoral Cartilage: Various Stages. The gross anatomy of the degenerated hyaline cartilage of the femoral condyles from a cadaveric specimen, different stages. Macroscopic image of the degenerated hyaline cartilage of the (**a**) medial and the (**b**) lateral femoral condyle from the left knee of a 92-year-old woman with mild osteoarthritis. A diffuse thinning of the cartilage is visible throughout the condyles, while a localized erosion of the articular cartilage is visible only in a small area on the surface of the medial condyle. A macroscopic image of the degenerated hyaline cartilage of the (**c**) medial and (**d**) lateral femoral condyle from the left knee of a 75-year-old woman showing advanced osteoarthritis. The surface of the articular cartilage is severely roughened in both the condyles. On the lateral condyle, the erosion reaches the subchondral bone. (Picture Courtesy—Henning Madry)

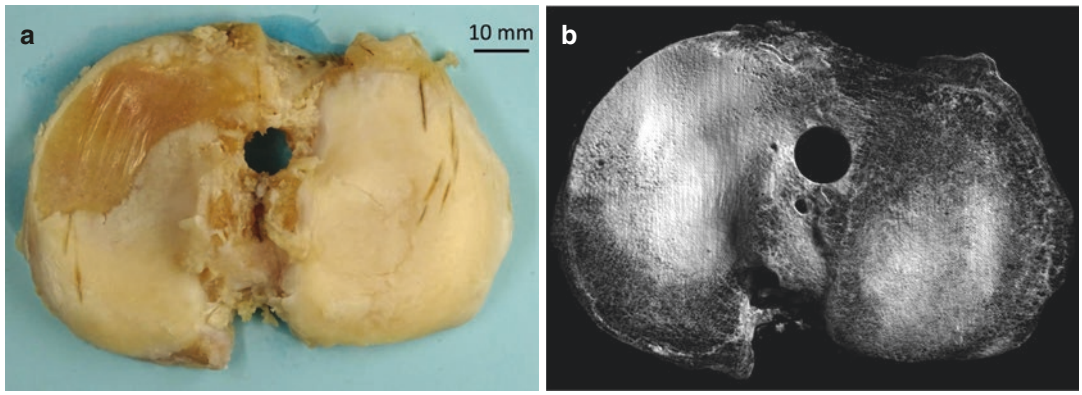

Figure 3.2.2: The Gross Anatomy of the Degenerated Hyaline Tibial Cartilage: Various Stages. The gross anatomy of the degenerated hyaline cartilage of the tibial plateau retrieved post total knee arthroplasty showing late osteoarthritis in (**a**) cadaveric gross picture and (**b**) 3D reconstructed microCT (micro-computed tomography) image. Note the complete erosion of the articular cartilage on the anterior and the intermediate peripheral regions of the medial tibial plateau, originally protected by the meniscus. The subchondral bone is only slightly affected. The gross anatomy of the degenerated hyaline cartilage of the tibial plateau showing advanced osteoarthritis in (**c**) cadaveric gross picture and (**d**) 3D reconstructed microCT image. On the internal and external margins of the medial and the lateral tibial plateaus, a pronounced osteophyte formation is visible. Osteophyte development is a physiological response of the bone thought to stabilize the osteoarthritic joint [10]. An erosion of the subchondral bone plate is prominent, and the subarticular spongiosa containing bone marrow is exposed. (Picture Courtesy—Henning Madry)

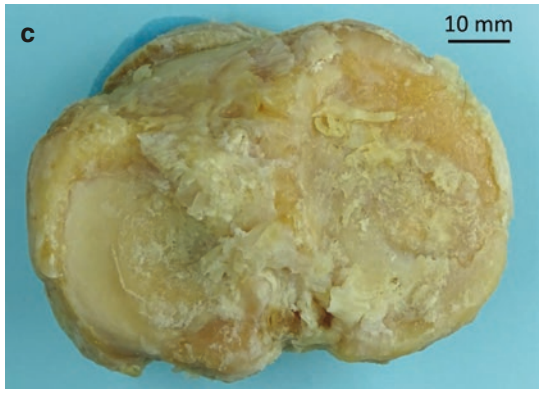

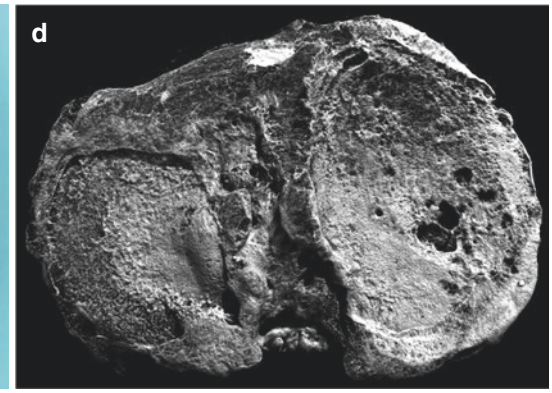

Figure 3.2.2: (continued)

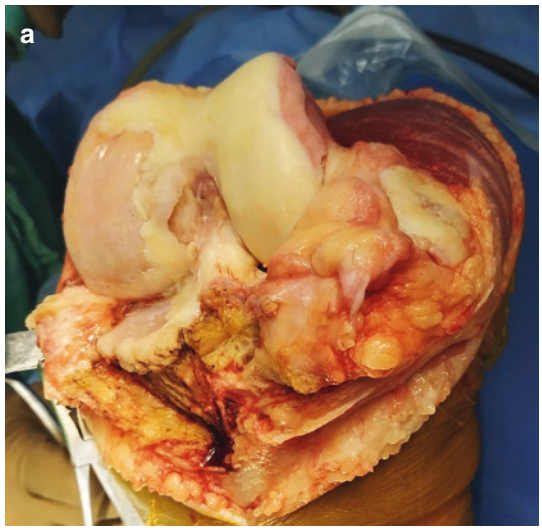

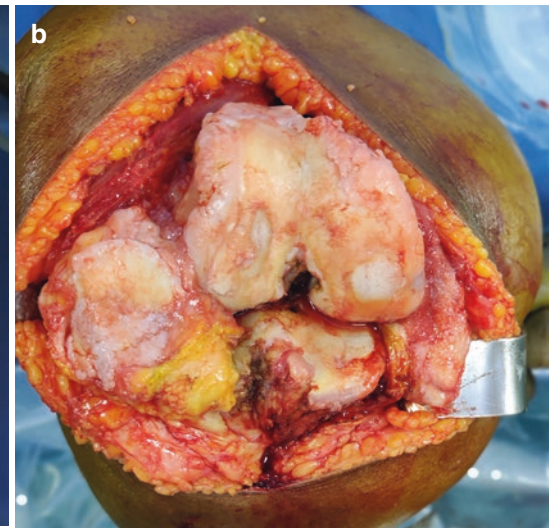

Figure 3.2.3: The Gross Anatomy of the Degenerated Hyaline Femoral Cartilage During Open Surgery: Various Stages. The degenerative process starts from one compartment of the knee joint and gradually spreads to all the compartment of the knee joint. The extent of the degenerative cartilage can easily be assessed during total knee arthroplasty surgery, which also allows the inspection of the gross anatomy of the knee joint as well as its articular surface. (**a**) A 63-year-old female underwent total knee arthroplasty for left-side medial compartment osteoarthritis and patellofemoral arthritis. Her knee was examined for gross anatomic features while standing on the foot end of her left side. The medial femoral condyle shows a completed eburnated cartilage with exposed subchondral bone in its entire extent. Osteophyte formation on the medial tibial plateau is also seen. While there are significant arthritic changes in the medial compartment, the trochlea, and the lateral femoral condyle show normal hyaline cartilage in the form of a glistening white smooth surface. (**b**) A peroperative image of a 68-year-old male undergoing a right-side total knee arthroplasty, with the knee flexed while viewing from the foot end. The articular surfaces of the medial and the lateral femoral condyles are nearly totally eroded with exposed subchondral (SC) bone at multiple places. There is nearly total loss of cartilage in the surrounding areas. The exposed SC bone on the medial femoral condyle is shiny indicative of a chronic erosion of the affected area leading to a partial loss of the SC bone plate. Also note the osteophytes all around the articular surface of the femur. The patella is also showing similar changes, while similar changes are seen on the medial half of the medial tibial plateau. All these changes indicate a severe osteoarthritis of the knee joint. (Picture Courtesy—Manish Shah, Shah Hospital, Ahmedabad, India)

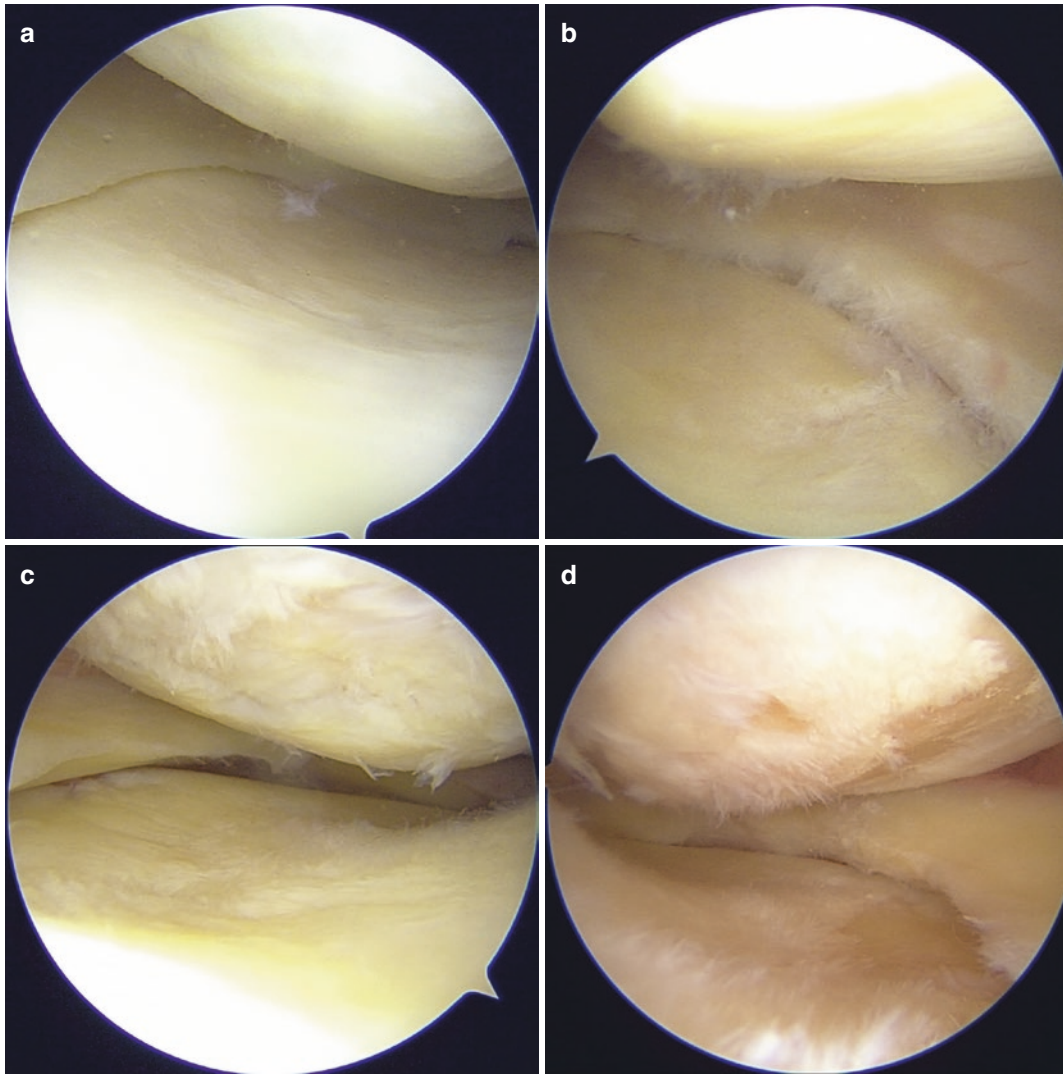

Figure 3.2.4: The Gross Anatomy of the Degenerated Hyaline Femoral Cartilage on Arthroscopy: Various Stages. The degenerative process of the articular cartilage is apparent very nicely on an arthroscopy. The normal glistening, congruous, white, and the smooth surface of the cartilage gradually gets damaged as the degenerative process progresses. (**a**) A male aged 50 years suffered a left lateral meniscus tear (not shown in the figure) and was operated arthroscopically. Arthroscopic examination of his medial compartment revealed early roughening of the articular surface with loss of the normal glistening appearance. Also apparent is a few early fibrillations, all suggesting the beginning of an early osteoarthritis. (**b**) A 53-year-old male patient had a right-side complete anterior cruciate ligament (ACL) tear 5 weeks back and was operated for an ACL reconstruction. Arthroscopic examination of the medial compartment showed degenerative changes in the body of the medial meniscus along with more pronounced roughening of the medial femoral and the medial tibial cartilage. The chondral surface was lusterless, all changes indicative of a mild osteoarthritis of the medial compartment. (**c**) A 47-year-old female, who was suffering from osteoarthritis of the left knee, was taken to operation theatre for a knee preservation surgery. The medial compartment showed erosion and cartilage loss at the medial femoral condyle up to 50% thickness of the cartilage, along with multiple fissures and fibrillations. The medial tibial articular surface also shows roughened chondral surface. These changes are suggestive of a moderate osteoarthritis. (**d**) A 56-year-old male patient suffering from medial compartment osteoarthritis and tibia vara was taken for knee preservation surgery (arthroscopy and high tibial osteotomy). On examination of the medial compartment, there was a total cartilage loss covering the medial half of the medial femoral condyle and the posteromedial corner of the medial tibial plateau. The remaining cartilage also shows signs of degeneration in the form of extensive fibrillations and fissures. These changes are indicative of a severe osteoarthritis of the knee. (Picture Courtesy—Deepak Rajkumar Goyal)

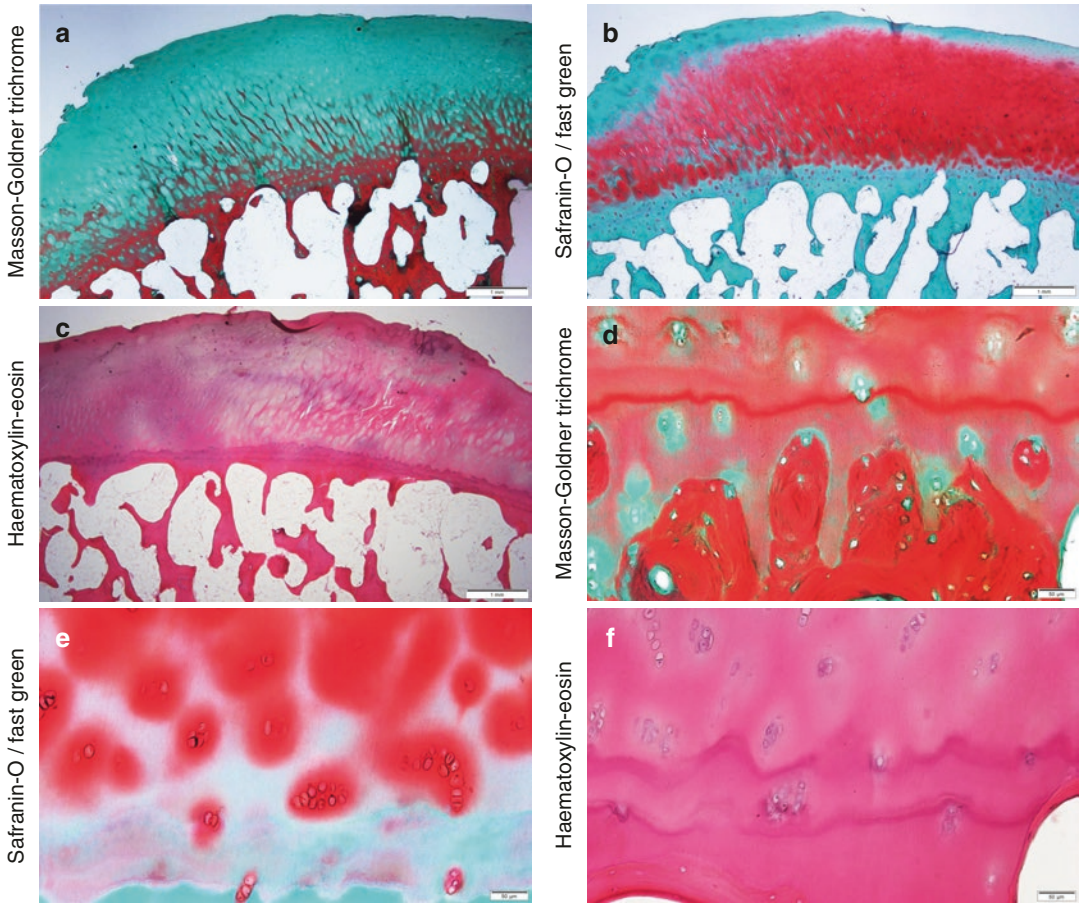

Figure 3.2.5: The Histology of the Degenerated Hyaline Cartilage: Early Osteoarthritis. (**a**) Masson-Goldner trichrome, (**b**) safranin-O/fast green, and (**c**) haematoxylin-eosin stained histological sections of a sample from a femoral condyle with early osteoarthritic changes. The articular cartilage surface is irregular, but deep clefts and fissures are not yet present. The duplication (or even triplication) of the tidemark and a slight loss of safranin-O staining are important hallmarks of early cartilage degeneration. Original magnification: 2×; scale bar: 1 mm. High-magnification images of (**d**) Masson-Goldner trichrome, (**e**) safranin-O/fast green, and (**f**) haematoxylin-eosin stained histological sections of an early osteoarthritic femoral condyle sample, showing the deep zone of the articular cartilage, the tidemark, the calcified cartilage, and the subchondral bone. Note the duplication of the tidemark and the cloning of the chondrocytes, characteristic of osteoarthritis. Original magnification: 20×; scale bar: 50 µm. (Picture Courtesy—Henning Madry)

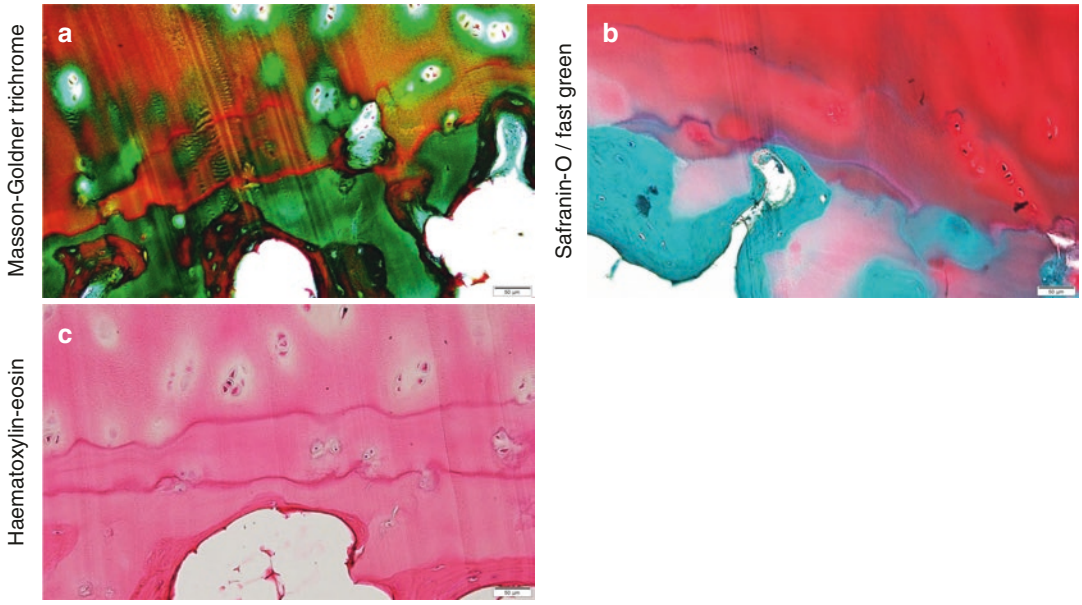

Figure 3.2.6: The Histology of the Degenerated Hyaline Cartilage: Mid-stage Osteoarthritis. (**a**) Masson-Goldner trichrome, (**b**) safranin-O/fast green, and (**c**) haematoxylin-eosin stained histological sections of a mid-stage osteoarthritic tibial plateau sample showing the deep zone of the articular cartilage, the tidemark, the calcified cartilage, and the subchondral bone. Original magnification: 20×; scale bar: 50 µm. Note the duplication of the tidemark, the decreased cellularity, and the occurrence of multiple cell nests, all characteristic of osteoarthritic cartilage degeneration. (Picture Courtesy—Henning Madry)

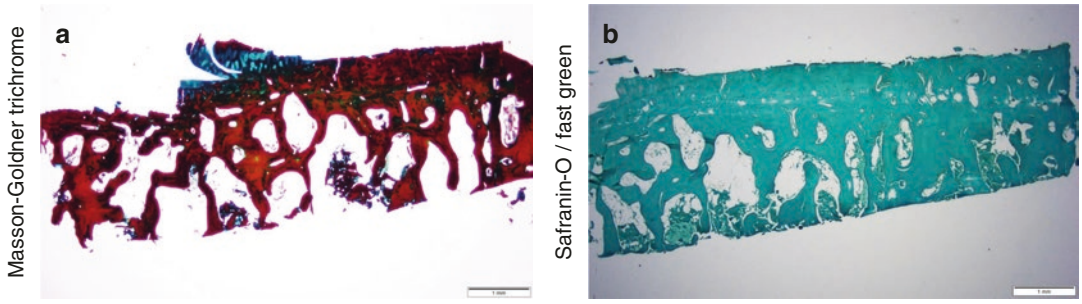

Figure 3.2.7: The Histology of the Degenerated Hyaline Cartilage: Late Osteoarthritis. (**a**) Masson-Goldner trichrome, (**b**) safranin-O/fast green, and (**c**) haematoxylin-eosin stained histological sections of a late osteoarthritic tibial plateau sample showing the remnants of the deep zone of the articular cartilage, the tidemark, the calcified cartilage, and the subchondral bone. Original magnification: 2×; scale bar: 1 mm. Note the severe erosion of the cartilage to the subchondral bone. High-magnification images of (**d**) Masson-Goldner trichrome, (**e**) safranin-O/fast green, and (**f**) haematoxylin-eosin stained histological sections of the same late osteoarthritic tibial plateau sample showing the remnants of the deep zone of the articular cartilage, the tidemark, the calcified cartilage, and the subchondral bone. Original magnification: 20×; scale bar: 50 µm. The articular cartilage is severely eroded, and its remnants can only be found in small areas of the section. The subchondral bone is exposed. Safranin-O staining of the interterritorial matrix is absent, indicating a severe loss of proteoglycans in the remaining cartilage. This degree of cartilage degeneration is characteristic of end-stage osteoarthritis. (Picture Courtesy—Henning Madry)

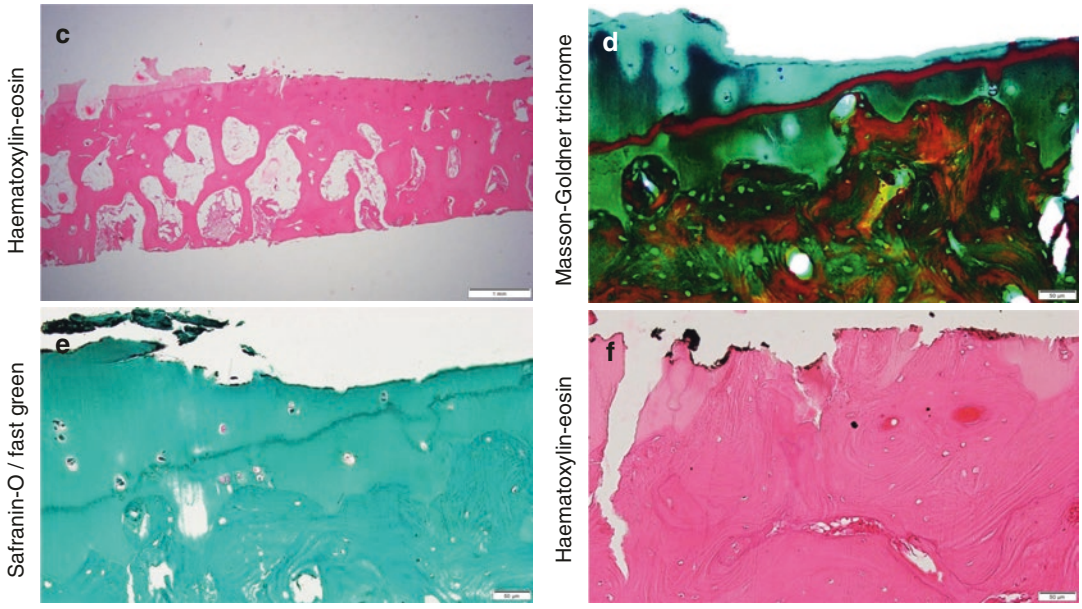

Figure 3.2.7: (continued)

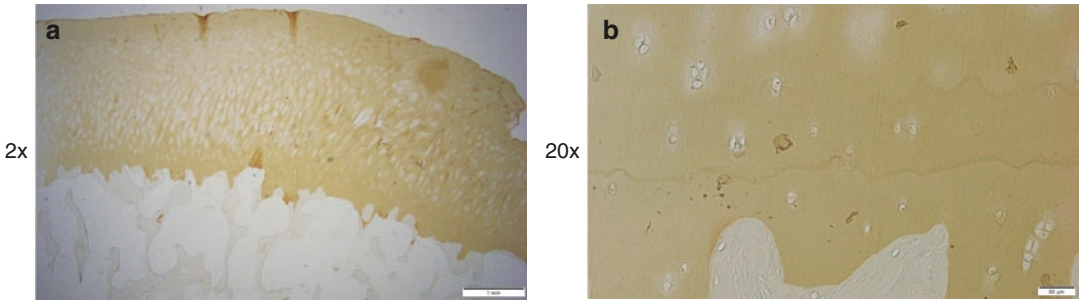

Figure 3.2.8: The Histology of the Degenerated Hyaline Cartilage: Immunohistochemical Staining. The IHC stains for histological examination of the degenerated hyaline cartilage (early osteoarthritis). Type II collagen is the most abundant form of collagen in the healthy hyaline cartilage, representing more than 90% of the total collagen amount. In hypertrophic and degenerated hyaline cartilage, the type II collagen content decreases, and the type X collagen content increases. Immunohistochemical staining of type II collagen in an early osteoarthritic femoral condyle sample shows relatively high staining intensity, indicating a normal or only slightly decreased expression level of the protein. Original magnification: (**a**) 2×, scale bars: 1 mm, (**b**) 20×; scale bars: 50 µm. Note the duplication of the tidemark, characteristic for osteoarthritis, and the absence of staining in the subchondral bone. (Picture Courtesy—Henning Madry)

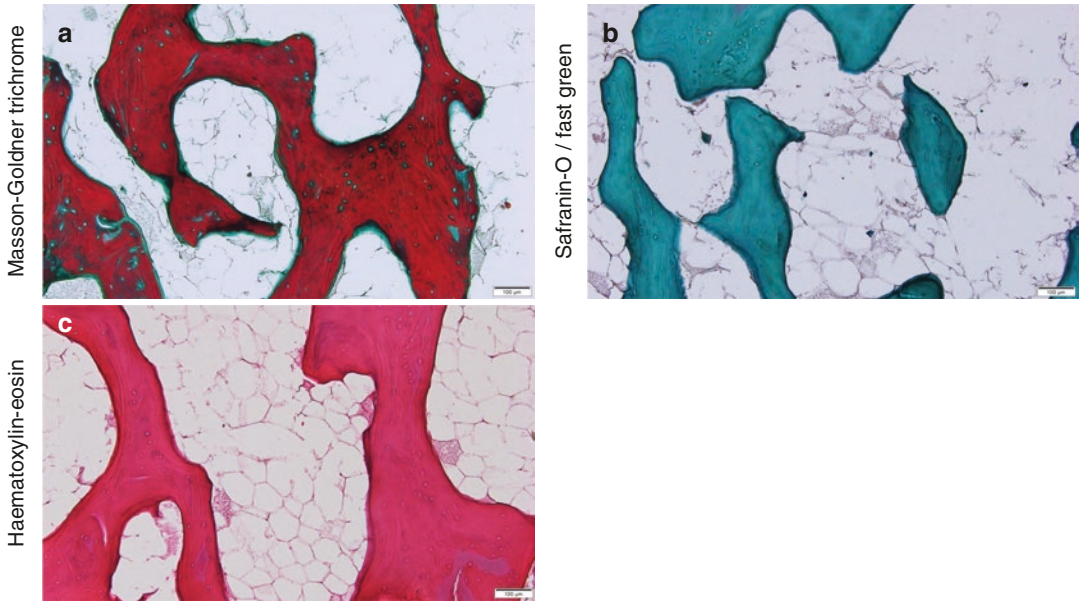

Figure 3.2.9: The Histology of the Degenerated Subchondral Bone. The routine and special stains for the histological examination of the degenerated subchondral bone (early osteoarthritis). (**a**) Masson-Goldner trichrome, (**b**) safranin-O/fast green, and (**c**) haematoxylin-eosin stained histological sections of an early human osteoarthritic femoral condyle sample showing the subarticular spongiosa. Original magnification: 10×; scale bar: 100 µm. Most of the current information on early osteoarthritis originates from large animal models, showing thinner trabeculae and decreased trabecular complexity (decreased trabecular number, connectivity density, bone surface density, degree of anisotropy, and fractal dimension, together with the increased trabecular separation) and relative bone volume (BV/TV) of the subarticular spongiosa. These changes are reversed in late osteoarthritis, reflecting a dynamic remodelling of the subchondral bone during the course of the disease [7]. (Picture Courtesy—Henning Madry)

3.3 Take-Home Message

Osteoarthritis, a painful, slowly progressive disease with an irreversible structural change, affects all the components of the osteochondral unit [11] and manifests in a certain structural pattern of the articular cartilage degeneration, including surface irregularities and erosion, cell cloning, tidemark duplication, and loss of proteoglycans [6], together with a dynamic remodelling of the subchondral bone [8].

As first-line treatment non-pharmacological methods such as education and self-management, exercise, weight loss, and walking aids are widely recommended [12]. When symptoms are not relieved, in early stages of osteoarthritis and for the patients that are too young to undergo a total joint arthroplasty, joint preserving surgical therapy is indicated. It aims at preserving joint function and may include debridement, removal of osteophytes, unstable articular cartilage flaps or loose bodies, the treatment of mechanically problematic meniscal lesions, marrow-stimulating techniques to induce fibrocartilaginous repair, and a correction of axial malalignment among other procedures [13]. As a surgical treatment of the end-stage osteoarthritis, a total joint arthroplasty is frequently applied. However, the possible complications may necessitate further operations and increase healthcare costs [14].

Osteoarthritis is increasingly affecting the global population, and in the coming decades it will become one of the most frequent diseases. The disease needs early and proactive management, and hence the research for efficient causative therapies and a validated early-stage diagnostic criteria is of high clinical importance [3].

References

1. Goldring SR, Goldring MB. Changes in the osteochondral unit during osteoarthritis: structure, function and cartilage-bone crosstalk. Nat Rev Rheumatol. 2016;12:632–44.
2. Madry H, Luyten FP, Facchini A. Biological aspects of early osteoarthritis. Knee Surg Sports Traumatol Arthrosc. 2012;20:407–22.
3. Hunter DJ, Bierma-Zeinstra S. Osteoarthritis. Lancet. 2019;393:1745–59.
4. Heijink A, Gomoll AH, Madry H, Drobnič M, Filardo G, Espregueira-Mendes J, et al. Biomechanical considerations in the pathogenesis of osteoarthritis of the knee. Knee Surg Sports Traumatol Arthrosc. 2012;20:423–35.
5. Little CB, Smith MM, Cake MA, Read RA, Murphy MJ, Barry FP. The OARSI histopathology initiative—recommendations for histological assessments of osteoarthritis in sheep and goats. Osteoarthr Cartil. 2010;18(Suppl 3):S80–92.
6. Mankin HJ, Dorfman H, Lippiello L, Zarins A. Biochemical and metabolic abnormalities in articular cartilage from osteo-arthritic human hips. II. Correlation of morphology with biochemical and metabolic data. J Bone Joint Surg Am. 1971;53:523–37.
7. Olah T, Reinhard J, Gao L, Haberkamp S, Goebel LKH, Cucchiarini M, et al. Topographic modeling of early human osteoarthritis in sheep. Sci Transl Med. 2019;11(508):eaax6775.
8. Chen Y, Hu Y, Yu YE, Zhang X, Watts T, Zhou B, et al. Subchondral trabecular rod loss and plate thickening in the development of osteoarthritis. J Bone Miner Res. 2018;33:316–27.
9. Orth P, Cucchiarini M, Wagenpfeil S, Menger MD, Madry H. PTH [1-34]-induced alterations of the subchondral bone provoke early osteoarthritis. Osteoarthr Cartil. 2014;22:813–21.
10. Menkes CJ, Lane NE. Are osteophytes good or bad? Osteoarthr Cartil. 2004;12(Suppl A):S53–4.
11. Cucchiarini M, de Girolamo L, Filardo G, Oliveira JM, Orth P, Pape D, et al. Basic science of osteoarthritis. J Exp Orthop. 2016;3:22.
12. Martel-Pelletier J, Barr AJ, Cicuttini FM, Conaghan PG, Cooper C, Goldring MB, et al. Osteoarthritis. Nat Rev Dis Primers. 2016;2:16072.
13. Madry H, van Dijk CN, Mueller-Gerbl M. The basic science of the subchondral bone. Knee Surg Sports Traumatol Arthrosc. 2010;18:419–33.
14. Weinstein AM, ome BN, Reichmann WM, Collins JE, Burbine SA, Thornhill TS, et al. Estimating the burden of total knee replacement in the United States. J Bone Joint Surg Am. 2013;95:385–92.

4 The Illustrative Role of the Subchondral Bone and the Overlying Cartilage

Tomoyuki Nakasa and Nobuo Adachi

4.1 Introduction

Articular cartilage has the ability to absorb the loading stress and create a low friction and high resistance to the wear and tear, which provides a smooth joint movement and weight-bearing capability to the joint. A loss of function of the articular cartilage due to trauma or osteoarthritis (OA) induces a functional disability of the joint. The subchondral bone plays a crucial role in the cartilage metabolism, load-bearing, and nourishment and is a warehouse of the cartilage cells and the growth factors. A damaged subchondral bone no longer maintains cartilage homeostasis, which leads to a loss of proteoglycan, glycoprotein, load-bearing capacity, and the vascularity [1]. In the treatment of articular cartilage, it is important to know the importance of the subchondral bone including the relationship of the articular cartilage and the subchondral bone.

There are various surgical treatments for the chondral/osteochondral defects, and an appropriate procedure is chosen according to the defect size, the condition of the subchondral bone, and the surface of the articular cartilage. Bone marrow stimulation techniques such as drilling or microfracture have been widely used. It is reported that the microfracture technique induces a subchondral bone remodeling by endochondral ossification and hence may induce complications such as intralesional osteophytes and subchondral bone cysts depending on the condition of the subchondral bone [2, 3]. The outcome of the autologous chondrocyte implantation (ACI) is also affected by the subchondral bone condition [4]. A proper subchondral bone reconstruction promotes a good cartilage repair since the subchondral bone properties like load-bearing, nourishment, and a warehouse of cells and growth factors are restored.

T. Nakasa (✉) · N. Adachi
Department of Orthopaedic Surgery, Graduate School of Biomedical and Health Sciences, Hiroshima University, Hiroshima, Japan
e-mail: tnakasa0@gmail.com; nadachi@hiroshima-u.ac.jp

D. R. Goyal (ed.), *The Illustrative Book of Cartilage Repair*,
https://doi.org/10.1007/978-3-030-47154-5_4

4.2 The Illustrations

4.2.A The Role of the Subchondral Bone for the Healthy Cartilage and the Healthy Osteochondral Unit

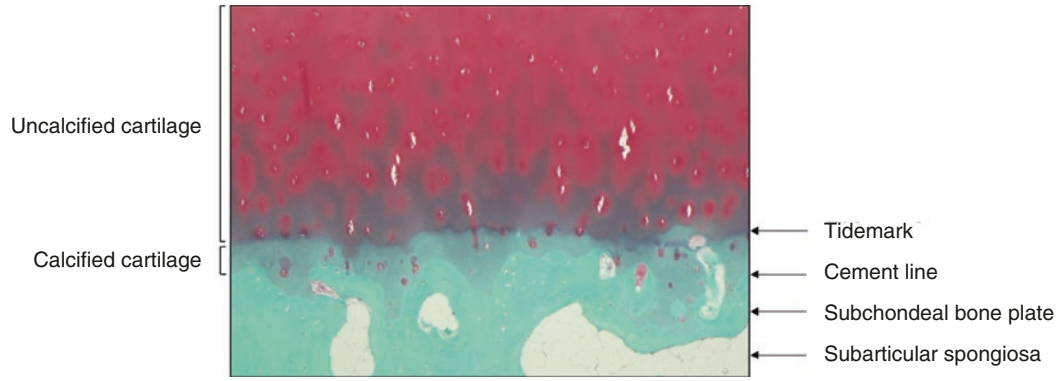

Figure 4.2.A.1: The Normal Subchondral Bone. The structure of normal osteochondral junction. Subchondral bone plays important role on the articular cartilage homeostasis, shock absorbing and nourishment for articular cartilage. The tidemark is the transition zone between the calcified and uncalcified cartilage. Tidemark has the tri-laminated structure which can reduce the shear forces. On the other hand, cement line has no crossing collagen fibrils, and this makes the weakest point in the osteochondral unit. The constant remodeling in the calcified cartilage occurs to help natural healing at the base of the cartilage from the injuries. In the uncalcified cartilage, chondrocytes synthesized the proteoglycans and collagen fibrils by the loading to help the natural healing

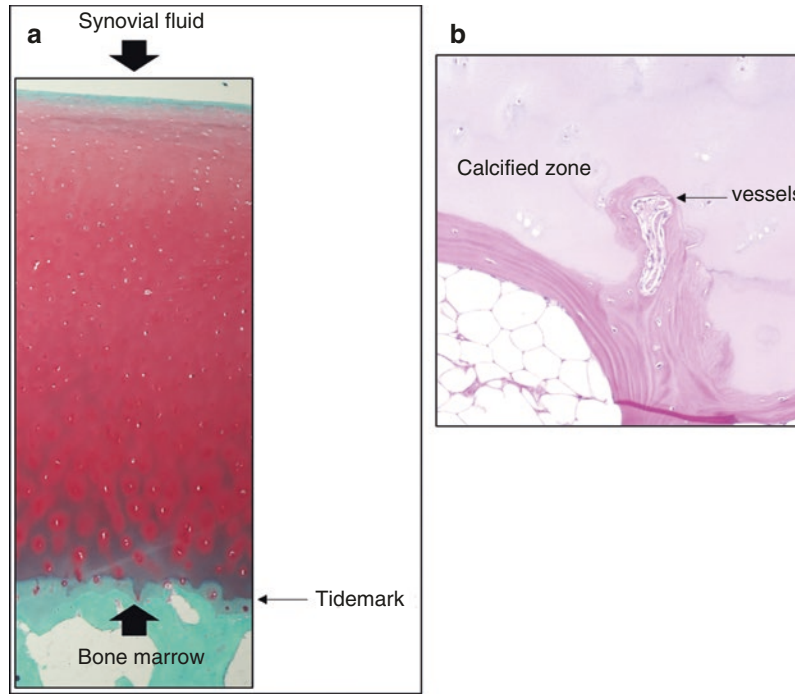

Figure 4.2.A.2: The Role of Subchondral Bone in Cartilage Nourishment. (**a**) Nutrition of the articular cartilage. Nutrients enter articular cartilage from its surface via the synovial fluid or from the underlying subchondral bone. (**b**) Blood vessels can be seen in the subchondral bone plate, penetrating into the calcified zone. Nutrients can reach chondrocytes in the calcified zone [5]. The uncalcified cartilage also gets nutrients from the subchondral bone

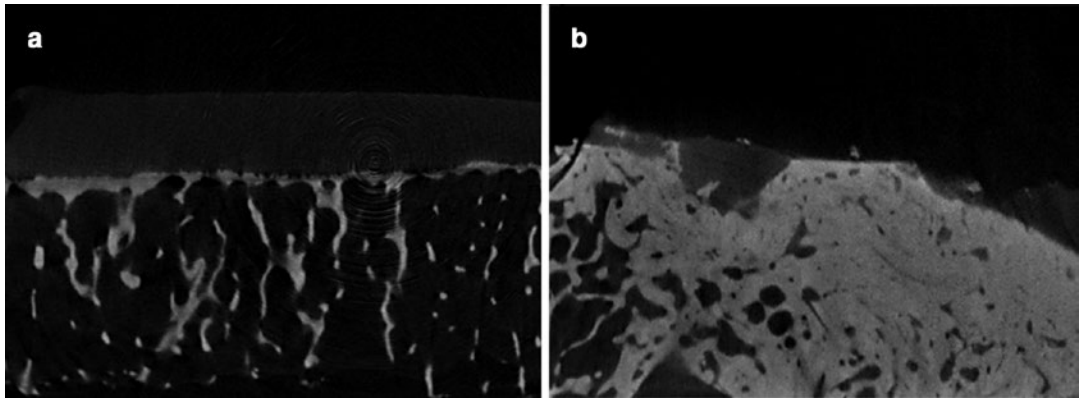

Figure 4.2.A.3: The Role of Subchondral Bone in Load Bearing. (**a**) CT image of the subchondral bone underlying normal articular cartilage. (**b**) CT image of the subchondral bone in OA. Subchondral trabecular bone has an important role in shock absorption. However, subchondral bone with dense and sclerotic changes can no longer absorb the loads and subsequently induces OA progression [6]

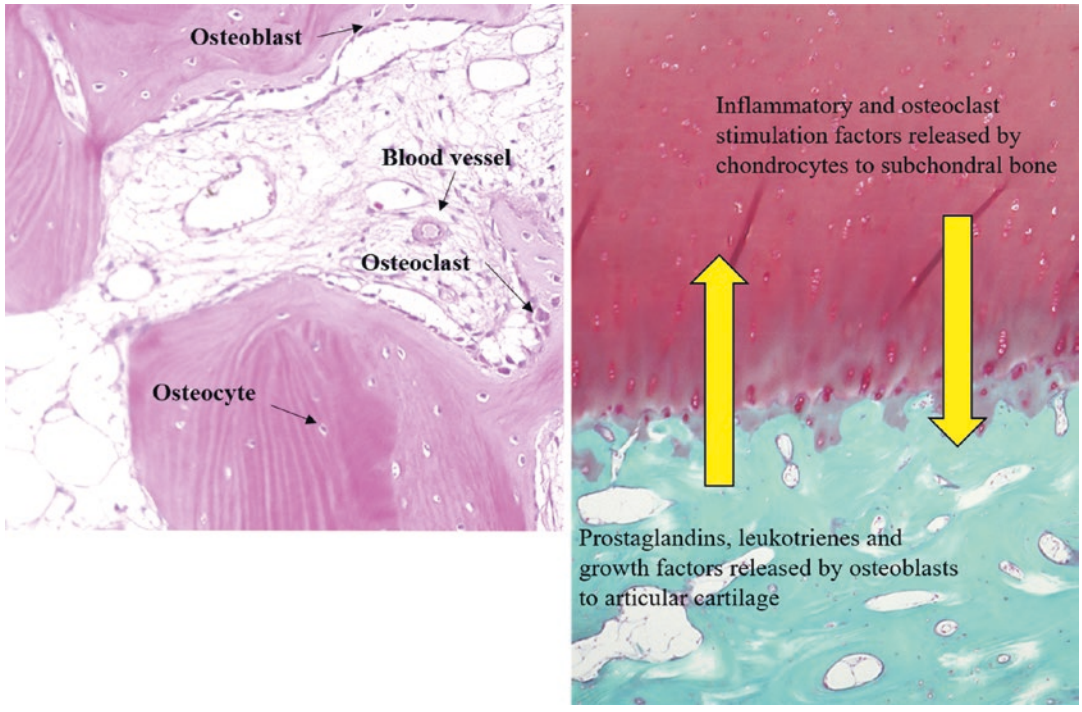

Figure 4.2.A.4: The Role of Subchondral Bone as a Source of Cells and Growth Factors. In the subchondral bone, bone remodeling occurs by osteoblasts and osteoclasts. An imbalance of bone formation and resorption in the subchondral bone results in OA progression. Prostaglandins, leukotrienes, and growth factors released by osteoblasts during subchondral bone remodeling reach to articular cartilage [7]. In OA progression, inflammatory and osteoclast stimulation factors released by articular cartilage induce subchondral bone change including bone sclerosis [8]

4.2.B The Importance of Subchondral Bone in Pathology of Osteochondral/ Chondral Lesions

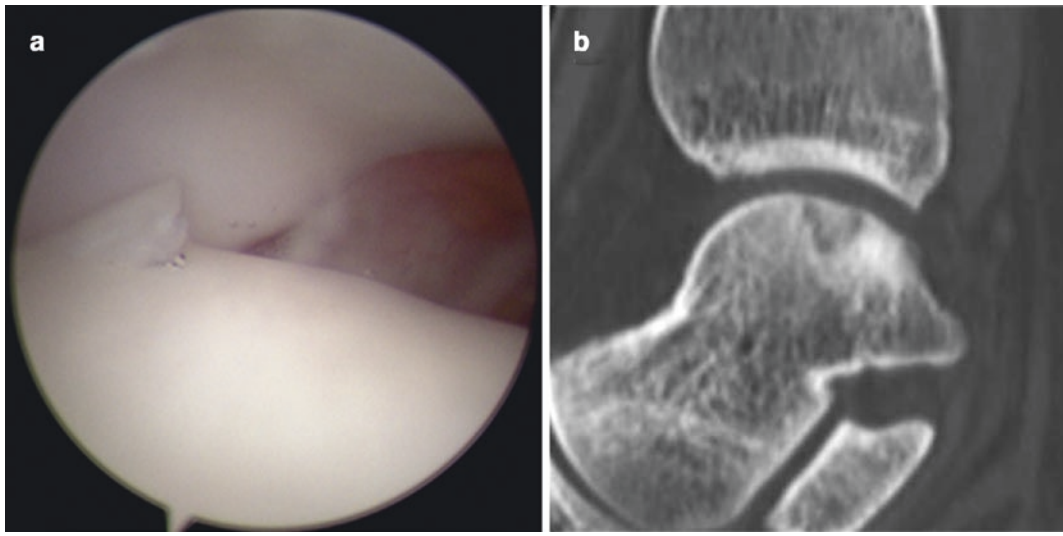

Figure 4.2.B.1: The Subchondral Bone and the Overlying Cartilage After an Injury. A 16-year-old woman with the left ankle pain due to ankle sprain. (**a**) A chondral injury at talus from anterolateral portal view. (**b**) Sagittal image of CT. A pure cartilage injury leads to change in the subchondral bone. Subchondral bone plate is also damaged during cartilage injury, and joint fluid flows into the subchondral bone through the damaged subchondral bone plate. High pressurized fluid activates osteoclasts, subsequently causing bone resorption in the subchondral bone [9]

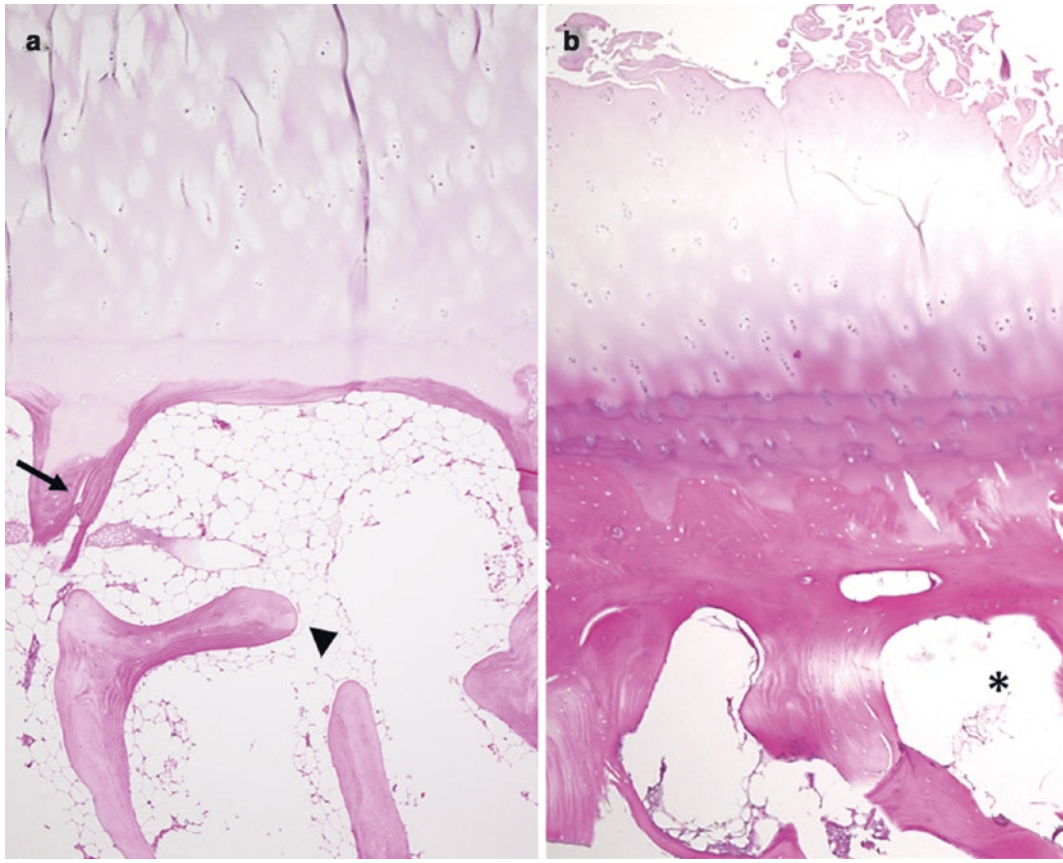

Figure 4.2.B.2: The Subchondral Bone and the Overlying Cartilage in Osteoarthritis. Subchondral bone change of early- and late-stage osteoarthritis (OA). (**a**) In early-stage OA, subchondral bone plate thickness is decreased and osteoporotic changes are progressed. Subchondral microdamage (arrow) and subchondral trabeculae deterioration (arrow head) are seen on the lateral tibial plateau of 74-year-old woman. The mechanism of the thinning of subchondral bone plate is not fully elucidated, but it is suggested that increasing the bone remodeling and vascularity by microdamage of the subchondral bone are the reasons. (**b**) In late-stage OA, subchondral bone plate thickness is increased and subchondral cyst is observed (*) in the medial tibial plateau of 78-year-old woman. Overlying calcified cartilage is thickened with duplication of tidemark [10]

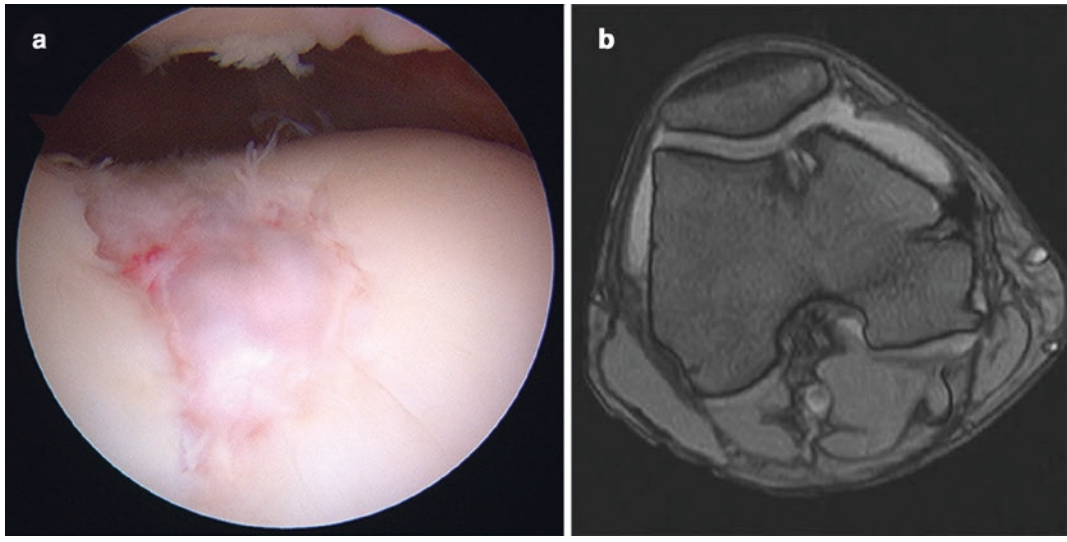

Figure 4.2.B.3: The Subchondral Bone and the Overlying Cartilage in Osteochondral Injury. A 42-year-old female volleyball player who suffered from left side persistent knee pain, occurring mainly during the knee flexion. (**a**) Arthroscopic finding of articular cartilage defect at patella groove from anterolateral portal. (**b**) Proton density weighted MRI image shows the subchondral bone cyst under the articular cartilage defect. Damage of the subchondral bone plate under the articular cartilage defect induces the high-pressurized joint fluid flow into the subchondral bone and subsequently causes the osteolytic change via osteoclast activation

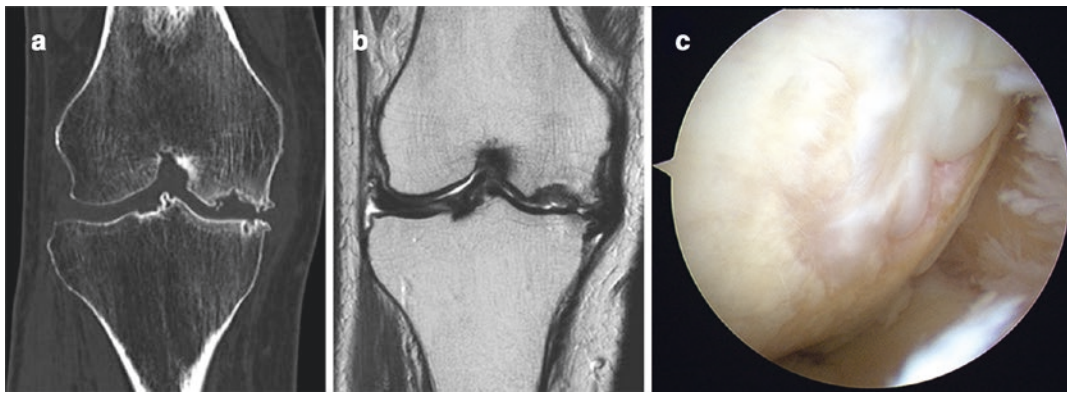

Figure 4.2.B.4: The Subchondral Bone and the Overlying Cartilage in Osteonecrosis. A 81-year-old woman who suffered from severe right knee pain and was diagnosed as osteonecrosis. (**a**) CT image shows osteonecrosis of the medial femoral condyle. The subchondral bone defect at medial femoral condyle was seen. (**b**) T2-weighted MRI reveals the disruption of the articular cartilage layer and degenerative tear of medial meniscus. (**c**) In the arthroscopic findings from anterolateral view, articular cartilage at medial femoral condyle is severely damaged. Disrupted subchondral bone no longer maintains the articular cartilage homeostasis and causes the progression of articular cartilage injury

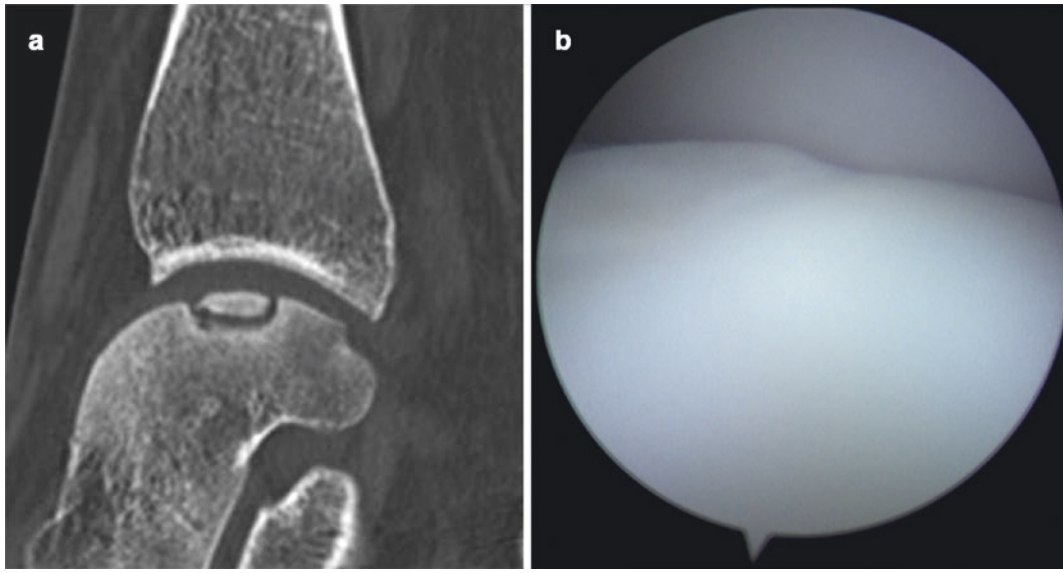

Figure 4.2.B.5: The Subchondral Bone and the Overlying Cartilage in Osteochondral Lesion of Talus. Osteochondral lesion of the left talar dome in a 15-year-old teen. (**a**) CT shows the normal contour of the subchondral bone plate in the osteochondral fragment, but it is separated from its bed. (**b**) Arthroscopic finding from anterolateral portal shows that the surface of articular cartilage is smooth on the osteochondral fragment. Microdamage of subchondral bone induces the high pressurized flow into subchondral bone, which activates osteoclasts. It results in the separation of osteochondral fragment. So far, preserved subchondral bone plate has maintained the articular cartilage homeostasis in the osteochondral fragment

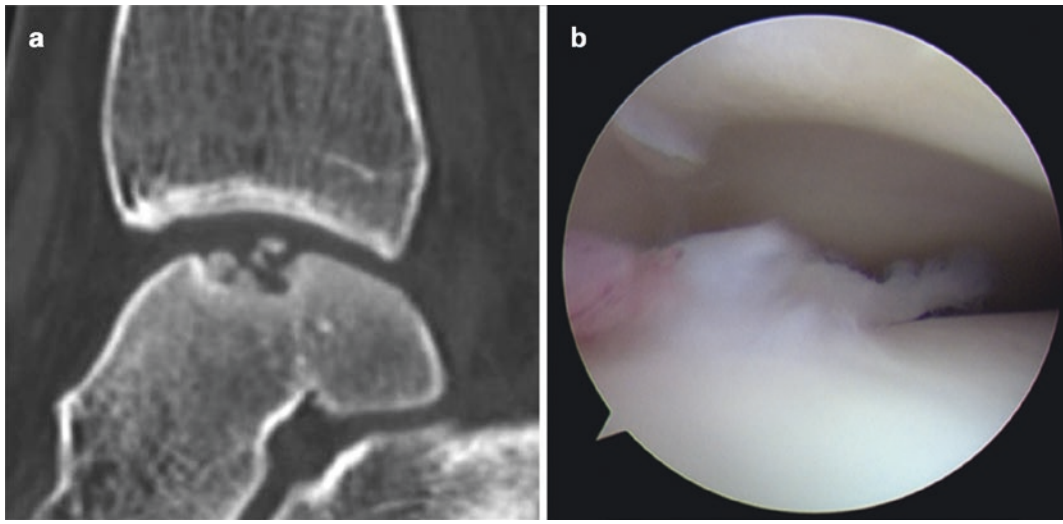

Figure 4.2.B.6: The Subchondral Bone and the Overlying Cartilage in Osteochondral Lesion of Talus. Osteochondral lesion of the left talar dome in a 16-year-old woman. (**a**) CT shows the disruption of subchondral bone plate in the osteochondral fragment. (**b**) Arthroscopic findings from anterolateral portal shows that the articular cartilage on the osteochondral fragment is damaged due to the subchondral bone plate disruption. Subchondral bone in the separated osteochondral fragment is gradually resorbed, and disruption of the subchondral bone plate is not able to maintain articular cartilage function

4.2.C The Importance of Subchondral Bone in Healing of Osteochondral/ Chondral Lesions

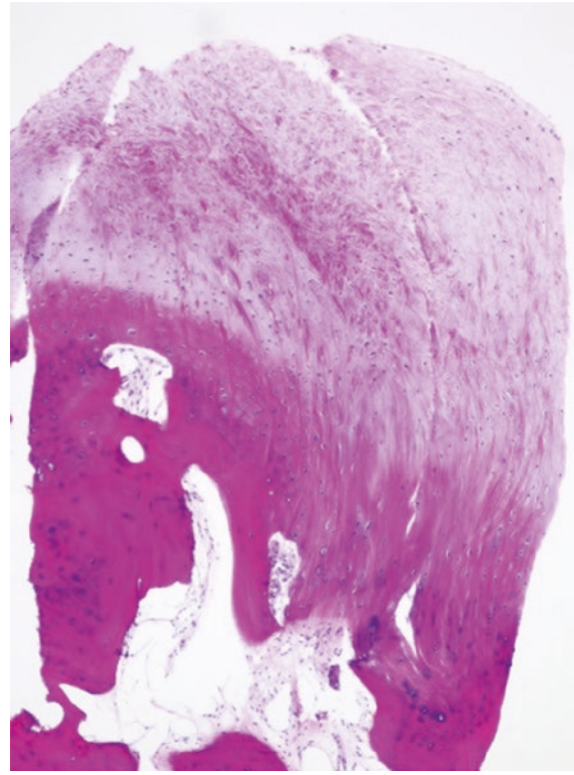

Figure 4.2.C.1: The Subchondral Bone and the Overlying Cartilage Healing in Autologous Chondrocyte Implantation. Biopsy specimen of autologous chondrocyte implantation (ACI) from lateral femoral condyle of a 25-year-old woman at 1 year postoperatively (hematoxylin-eosin staining). For the cartilage defect at the size of 400 mm^2 in lateral femoral condyle, ACI was performed. However, her symptoms have not improved after surgery. The thickened subchondral bone and irregularity of subchondral bone plate are observed. IKDC score of this patient is 58.6 points, which means the condition of subchondral bone after ACI may have been an important factor to obtain good clinical results

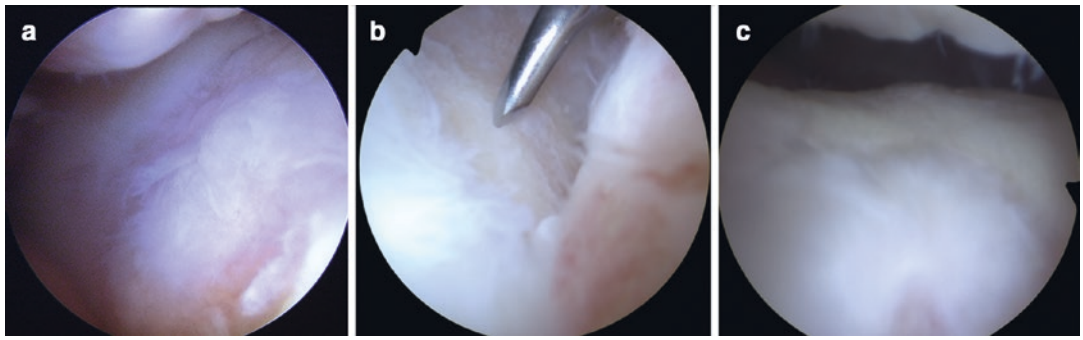

Figure 4.2.C.2: The Subchondral Bone and the Overlying Cartilage in a Successful Microfracture Technique. A 42-year-old woman with symptoms of right knee pain, occurring mainly during the knee flexion. (**a**) Articular cartilage injury at patella groove is seen from anteromedial portal. (**b**) Microfracture after the curettage of the remained degenerated cartilage is seen from anterolateral portal. (**c**) At 1 year after microfracture, cartilage defect is covered with fibrocartilaginous tissue as seen from anterolateral portal

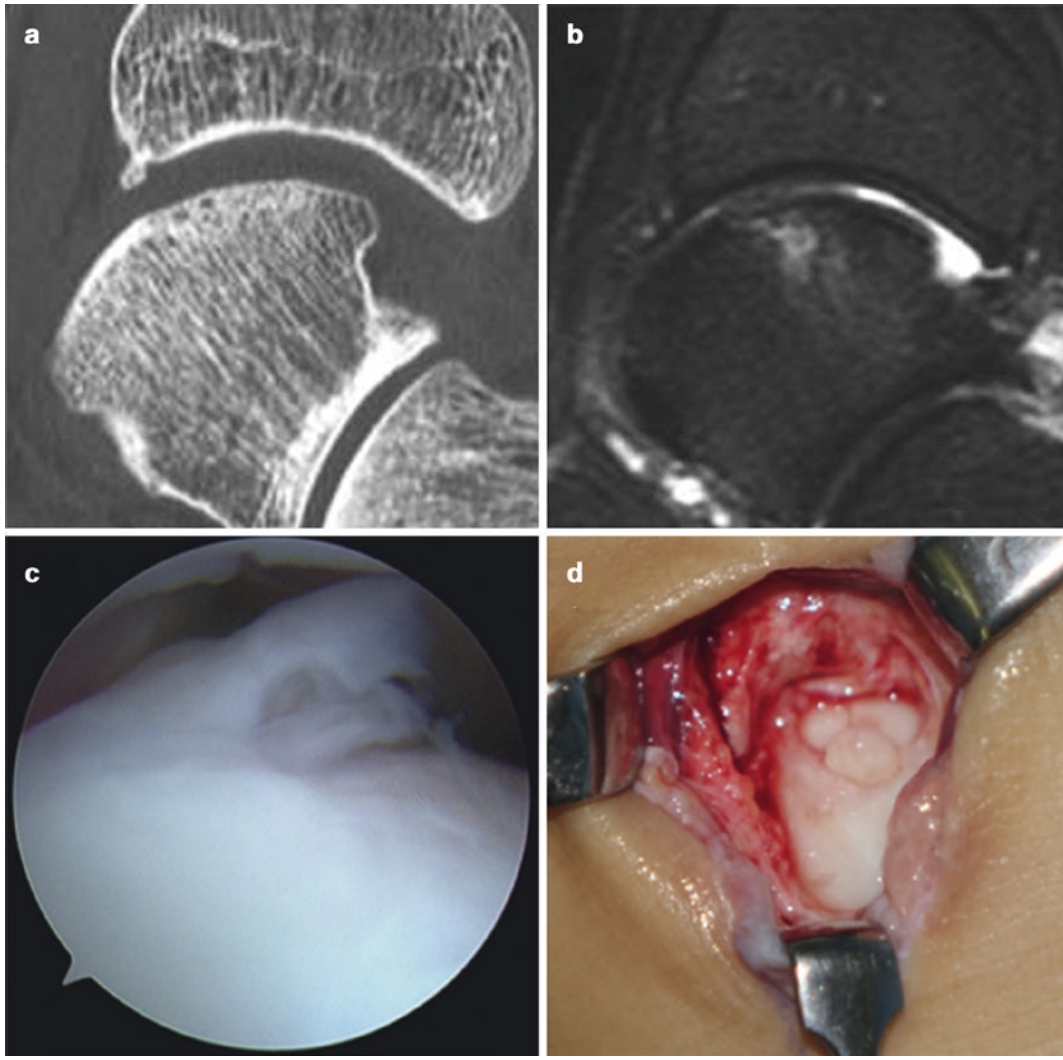

Figure 4.2.C.3: The Subchondral Bone and the Overlying Cartilage Healing in a Failed Microfracture Technique. Failure case of the microfracture for the articular cartilage defect. A 23-year-old man with right ankle pain had been treated by the microfracture technique for the cartilage defect of the talus. However, his ankle pain did not improve. (**a**) CT on sagittal image shows small subchondral bone cysts at microfracture site and (**b**) T2-weighted MRI reveals the subchondral bone edema just under the articular cartilage defect. (**c**) In the arthroscopic finding from anteromedial portal, fibrous tissue covers the articular cartilage defect. (**d**) Autologous osteochondral transplantation was performed to improve the condition of subchondral bone and to replace the articular cartilage. Microfracture gives the subchondral damage; therefore, if the condition of subchondral bone does not improve after microfracture, it will be a failure case

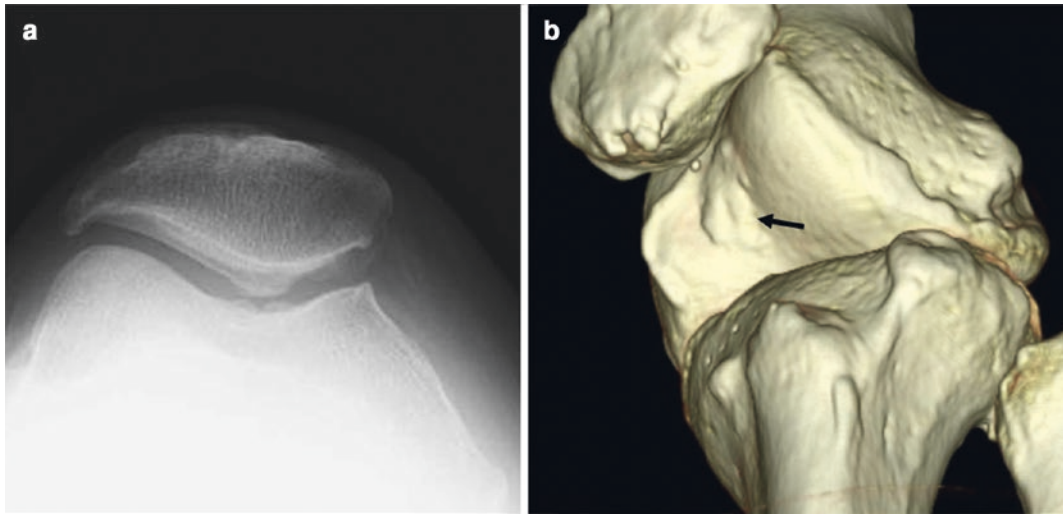

Figure 4.2.C.4: The Side Effects of Microfracture Technique on the Subchondral Bone and the Overlying Cartilage. Intralesional osteophytes after microfracture. A 42-year-old woman who had been treated by arthroscopic microfracture for the cartilage defect of right patella groove. However, she started to suffer from severe knee pain and fluid collection of her knee joint due to intralesional osteophytes after the microfracture technique 10 years later. Plain radiograph at skyline view (**a**) and 3D CT (**b**) shows osteophyte formation (black arrow) at patellofemoral joint after microfracture. Microfracture stimulates the activity of the bone metabolism in the subchondral bone and results the formation of the osteophytes in the articular cartilage defect

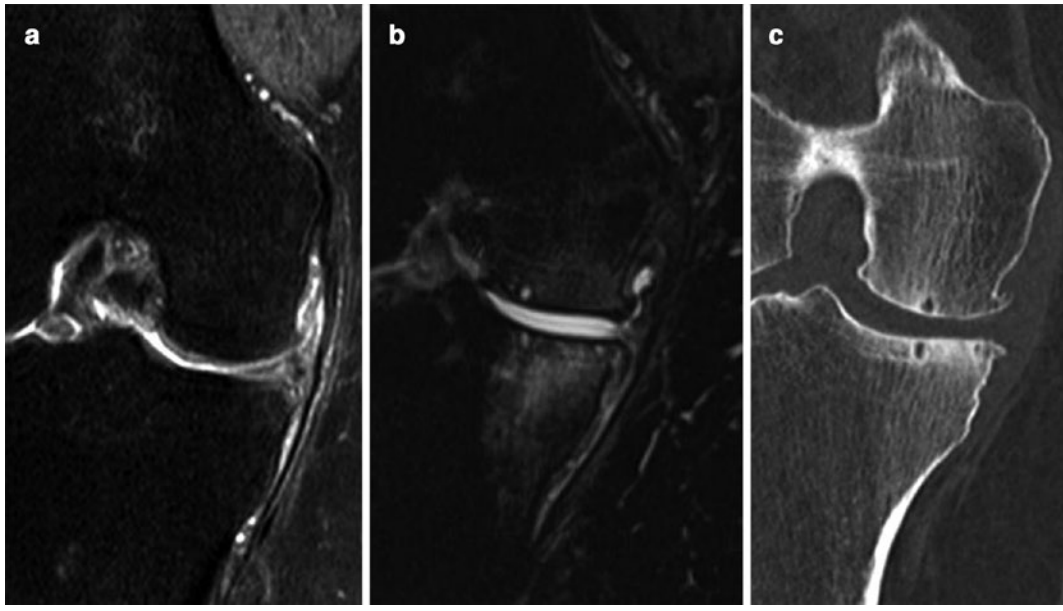

Figure 4.2.C.5: The Side Effects of Microfracture Technique on the Subchondral Bone and the Overlying Cartilage. Subchondral bone cyst after the microfracture technique. A 62-year-old woman with severe right side knee pain. She was diagnosed as early-stage OA with degenerative tear of the medial meniscus. She was treated by arthroscopic partial menisectomy and microfracture. (**a**) T2-weighted MRI image of the osteoarthritis with the cartilage thinning at medial compartment. (**b**) T2-weighted MRI images at 6 months after microfracture. (**c**) Coronal CT images at 6 months after microfracture. Subchondral bone cysts at medial femoral and tibia plateau. Depending on the subchondral bone condition such as osteoporosis, subchondral bone cysts can occur due to the joint fluid flowing through the canals of the microfracture technique. The joint fluid induces the osteoclast activation, which results in the subchondral bone cysts

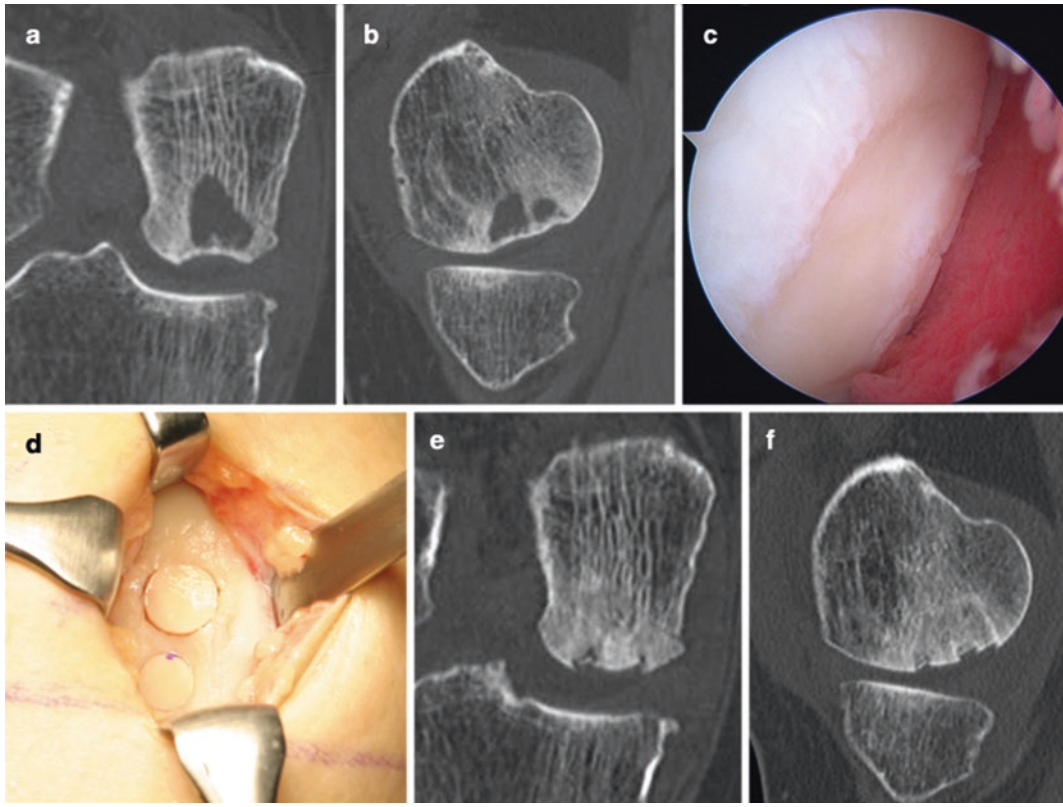

Figure 4.2.C.6: The Subchondral Bone and the Overlying Cartilage in a Successful Osteochondral Cylinder Transfer Technique. A 70-year-old woman who suffered from right side severe knee pain due to spontaneous osteonecrosis of the medial femoral condyle. Coronal (**a**) and sagittal (**b**) CT image shows large subchondral bone defect at the medial femoral condyle. (**c**) Arthroscopic finding from anterolateral portal shows depressed articular surface and cartilage degeneration. (**d**) Osteochondral cylinder transfer was performed to reconstruct subchondral bone and articular surface. At 1 year after osteochondral cylinder transfer technique, bone union is achieved and joint surface is reconstructed on coronal (**e**) and sagittal (**f**) CT images

4.3 Take-Home Message

The subchondral bone plays an important role in cartilage metabolism, load-bearing, nourishment, and as a warehouse of various cells and growth factors [11]. Articular cartilage injury induces the subchondral bone changes, whereas subchondral bone changes such as bone resorption and sclerosis induce articular cartilage degeneration. Even though articular cartilage and subchondral bone have specific properties, both interact with each other, and injury to either has influence on other. Thus, both must be treated as one unit – the osteochondral unit. Good clinical outcome of the articular cartilage repair cannot be obtained without restoring the function of the subchondral bone. Subchondral bone has the persistent bone metabolism, which can affect the pathophysiology of chondral/osteochondral injuries and clinical outcomes.

In early osteoarthritis, microdamage of the subchondral bone induces the structural change in form of osteoporosis with thinning of the subchondral bone plate, which causes the progression of cartilage degeneration. In late-stage osteoarthritis, sclerotic change by excessive bone formation of subchondral bone occurs, and it no longer plays a role as subchondral bone such as cartilage metabolism, load bearing, and nourishment to cartilage.

In cartilage repair procedure such as microfracture and ACI, the response of the subchondral

bone to the cartilage repair procedure affects the results. For example, after microfracture technique, imbalance of bone metabolism causes the complications such as the intralesional osteophytes or subchondral bone cysts. Similarly, cultured chondrocytes after ACI will not survive within the cartilage defect if the subchondral bone condition is poor. A proper knowledge of subchondral bone metabolism and its role in articular cartilage is important for a successful result after a cartilage repair procedure. It is important to know the role of the subchondral bone on the articular cartilage and how to manage these structures to obtain good clinical results.

References

1. Radin EL, Rose RM. Role of subchondral bone in the initiation and progression of cartilage damage. Clin Orthop Relat Res. 1986;213:34–40.
2. Hayashi S, Nakasa T, Ishikawa M, Nakamae A, Miyaki S, Adachi N. Histological evaluation of early-phase changes in the osteochondral unit after microfracture in a full-thickness cartilage defect rat model. Am J Sports Med. 2018;46(12):3032–9.
3. Mithoefer K, Williams RJ 3rd, Warren RF, Potter HG, Spock CR, Jones EC, Wickiewics TL, Marx RG. The microfracture technique for the treatment of articular cartilage lesions in the knee. A prospective cohort study. J Bone Joint Surg Am. 2005;87:1911–20.
4. Pestka JM, Bode G, Salzmann G, Südkamp NP, Niemeyer P. Clinical outcome of autologous chondrocyte implantation for failed microfracture treatment of full-thickness cartilage of the knee joint. Am J Sports Med. 2012;40(2):325–31.
5. Madry H, van Dijk CN, Mueller-Gerbl M. The basic science of the subchondral bone. Knee Surg Sports Traumatol Arthrosc. 2010;18:419–33.
6. Castaneda S, Roman-Blas JA, Largo R, Herrero-Beaumont G. Subchondral bone as a key target for osteoarthritis treatment. Biochem Pharmacol. 2012;83:315–23.
7. Lajeunesse D, Reboul P. Subchondral bone in osteoarthritis: a biologic link with articular cartilage leading to abnormal remodelling. Curr Opin Rheumatol. 2003;15:628–33.
8. Bellido M, Lugo L, Roman-Blas JA, Castaneda S, Caeiro JR, Dapia S, Calvo E, Largo R, Herrero-Beaumont G. Subchondral bone microfractural damage by increased remodelling aggravates experimental osteoarthritis preceded by osteoporosis. Arthritis Res Ther. 2010;12:R152.
9. Van Dijk CN, Reilingh ML, Zengerink M, van Bergen CJ. Osteochondral defects in the ankle: why painful? Knee Surg Sports Traumatol Arthrosc. 2010;18(5):570–80.
10. Li G, Yin J, Gao J, Cheng TS, Pavlos NJ, Zhang C, Zheng MH. Subchondral bone in osteoarthritis: insight into risk factors and microstructural changes. Arthritis Res Ther. 2013;15:223.
11. Goyal D, Goyal A, Adachi N. Subchondral bone: healthy soil for the healthy cartilage. In: Bioorthopaedics. Berlin: Springer; 2017. p. 479–86.

The Illustrative Biomechanics of a Chondral Injury

5

Deepak Rajkumar Goyal

5.1 Introduction

A chondral lesion can occur due to various reasons like trauma, degeneration, pathologies like osteochondritis dissecans (OCD) or a vascular insult. While most of the traumatic lesions are due to the impact of an acute abnormal biomechanical force on the chondral or the osteochondral surface, chronic degenerative lesions occur due to a gradual alteration of the biomechanics over the years. It is the type, force, direction and the repetitions of the load that determine whether the abnormal biomechanics will cause chondral injury or not. While it is not true that there will be abnormal biomechanics behind every cartilage lesion, every abnormal biomechanics will indeed put abnormal loads on the articular surface. Pathologies like OCD and vascular causes may not have abnormal biomechanics all the time.

The common forces working on the knee joint are the vertical loads, the angular loads, the shear forces and the rotatory forces. For example, an acute lateral patellar dislocation imparts a shearing force on the lateral femoral condyle leading to either an osteochondral impaction or an osteochondral fracture of the lateral femoral condyle, depending on the amount of the abnormal biomechanical shear force [1, 2]. An anterior cruciate ligament (ACL) deficient knee results in abnormal rotatory loads on the medial tibiofemoral compartment. These repetitive abnormal rotatory loads in a "chronically ACL deficient knee" result in an increased incidence of a cartilage lesion in the knee, and this incidence of a cartilage lesion increases sharply with time in an untreated ACL tear. Chen et al. [3] reported the incidence of cartilage lesions in the knee as 27.2% when ACL tear was treated in less than a month of injury, while the incidence increased to 62.7% when ACL tear was treated between 1 and 12 months of an injury. In an untreated ACL tear, the cartilage lesions are more prominent in the medial compartment with the reported incidence of 10–22% at the medial femoral condyle and 1–2% at the medial tibial plateau in various literatures [4–6]. Angular deformities like tibia vara or genu vara transmit chronic repetitive loads on the medial compartment, leading to a medial compartment degenerative lesion [7].

A surgeon needs to understand the abnormal biomechanical loads behind the cartilage lesions, since treating the cartilage lesions without correcting the abnormal biomechanics could fail a cartilage repair surgery. The purpose of this chapter is to discuss some of the abnormal biomechanics that imparts abnormal loads on the articular surfaces of the knee, resulting in a chondral damage. The chapter should open up a thought process in a cartilage surgeon's mind to understand the importance of the abnormal biomechanics vis-à-vis a chondral lesion.

D. R. Goyal (✉)
Saumya Arthroscopy and Sports Knee Clinic, Ahmedabad, India

Visiting Professor of Orthopaedics, Graduate School of Biomedical and Health Sciences, Hiroshima University, Hiroshima, Japan
e-mail: deepak@knee.in

D. R. Goyal (ed.), *The Illustrative Book of Cartilage Repair*,
https://doi.org/10.1007/978-3-030-47154-5_5

5.2 The Illustrations

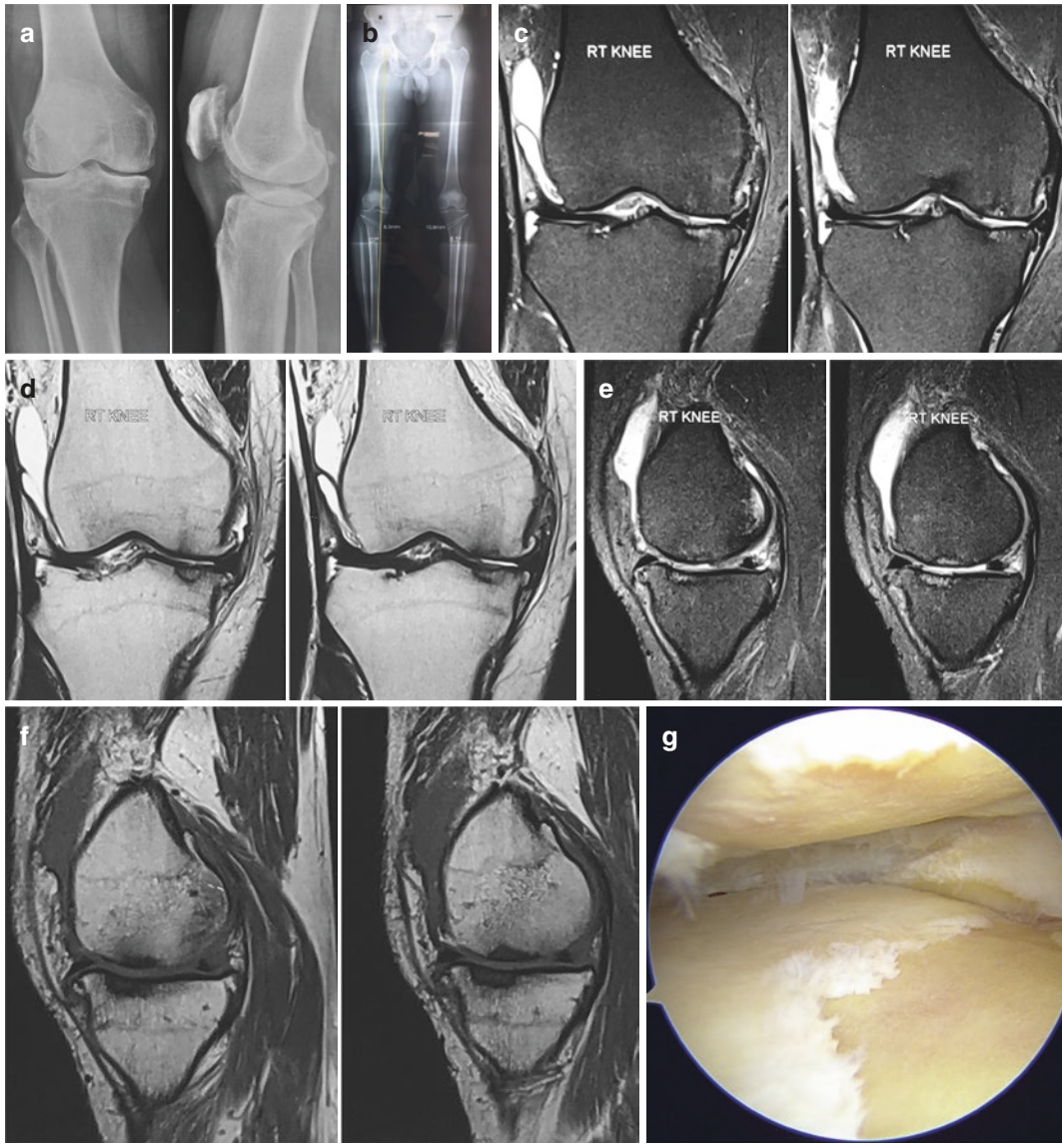

Figure 5.2.1: The Biomechanics of a Chondral Damage: The Chronic Varus Load on the Medial Compartment of the Knee. A 45-year-old male had a persistent knee pain for 3 years in the right knee and was associated with occasional swelling and catching sensations. (**a**) The standing X-ray of the right knee was suggestive of moderate medial joint space reduction along with a few osteophytes on the medial joint line. (**b**) The long limb alignment X-ray confirmed varus deformity on both the sides. (**c**–**f**) An magnetic resonance imaging (MRI) was done that revealed a near total cartilage loss on the medial side of the medial tibial articular surface and medial femoral condyle, with the presence of subchondral (SC) cysts in the medial tibial plateau and the medial femoral condyle. A degenerative tear in the post part of the medial meniscus is also seen. (**g**) His right knee arthroscopy confirmed the MRI findings, showing a total loss of cartilage from the medial side of the medial tibial plateau and the medial femoral condyle. A gradually increasing varus deformity of the knee puts chronic repetitive loads on the medial surface of the medial compartment of the knee. The abnormal loads subsequently lead to a degenerative tear of the medial meniscus and chondral loss of the medial compartment, which is usually more pronounced on the medial side of the medial compartment [7]

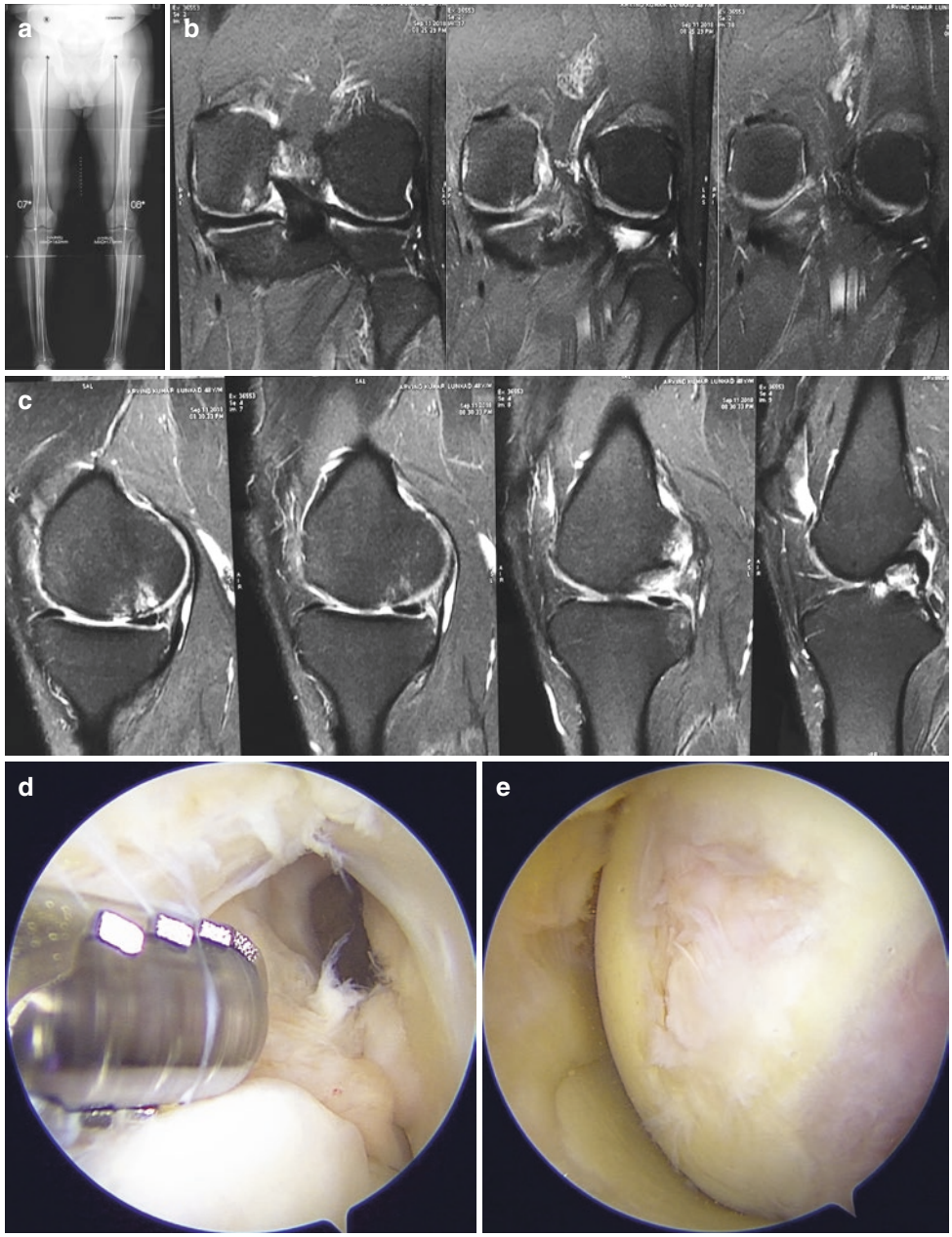

Figure 5.2.2: The Biomechanics of a Chondral Damage: The Chronic Rotatory Forces in an Anterior Cruciate Ligament Deficient Knee. A 48-year-old male presented with left knee pain for 2 years, with a history of fall while playing cricket 6 years back. On clinical examination, all the tests of anterior instability like Lachman's sign, anterior drawer test and pivot shift test were positive. He also had pain on McMurry's examination and had a mild medial joint line tenderness. (**a**) His long limb alignment X-ray showed early tibia vara, comparable on both the sides. (**b**) The T2 fat-suppressed coronal and (**c**) the PD fat-suppressed sagittal magnetic resonance imaging (MRI) showed a thinning of the cartilage on the medial femoral and tibial articular surfaces, in addition to a distinct chondral defect on the lateral half of the medial femoral condyle with subchondral bone marrow oedema. MRI also confirmed a complete anterior cruciate ligament tear. (**d**) On arthroscopy of the left knee, while visualising through the anterolateral portal, a complete ACL tear was evident with its substance loss, confirming a chronic tear. (**e**) The medial femoral condyle showed an around 14 mm × 18 mm chondral lesion on the lateral half of the medial femoral condyle. Chronic ACL tear leads to anterior instability of the knee joint causing excessive rotatory biomechanical forces on the medial joint surface. The commonest structures that can get damaged by these abnormal rotatory forces are the medial meniscus and the medial tibiofemoral chondral surfaces [4–6]

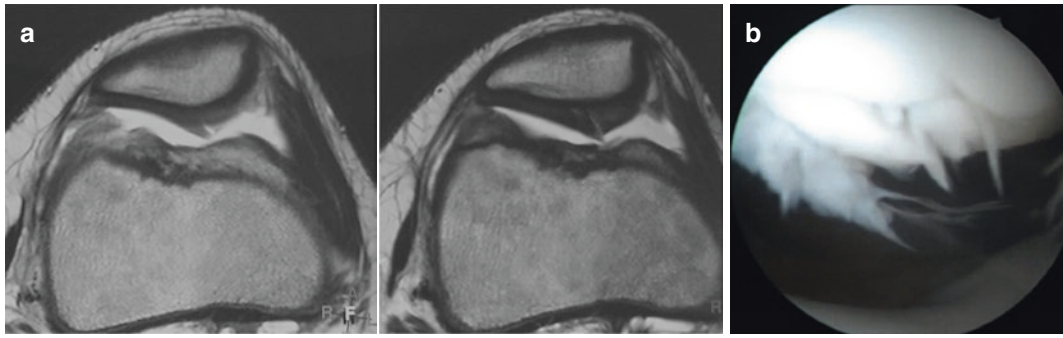

Figure 5.2.3: The Biomechanics of a Chondral Damage: An Acute Impaction on Patella. A 16-year-old male teen jumped from 4 ft height while playing. His right side patella hit directly on the floor, causing a significant impact force of the patella on the trochlea. The clinical examination didn't show any evident intraarticular injury, and his knee X-ray examination was normal. As he had persistent pain and mild swelling, an MRI (magnetic resonance imaging) examination was carried out. (**a**) The T2-weighted axial images on MRI showed a focal fissure at the apex of the patella with a resultant chondral flap formation. The surrounding cartilage also showed small fissures, while the remaining cartilage and bones were normal. As his pain persisted for more than 6 weeks in spite of a conservative trial, he was asked to undergo an arthroscopy surgery. (**b**) Arthroscopy confirmed a chondral burst fracture due to the direct impact of the patellar cartilage on the trochlear surface, leading to multiple chondral flaps and fissuring of the surrounding cartilage. The direct impact on the patella can cause either patella fracture or a chondral damage of the patellar articular surface. Here, the patellar bone could absorb the impact forces while the patellar cartilage couldn't, leading to a chondral damage

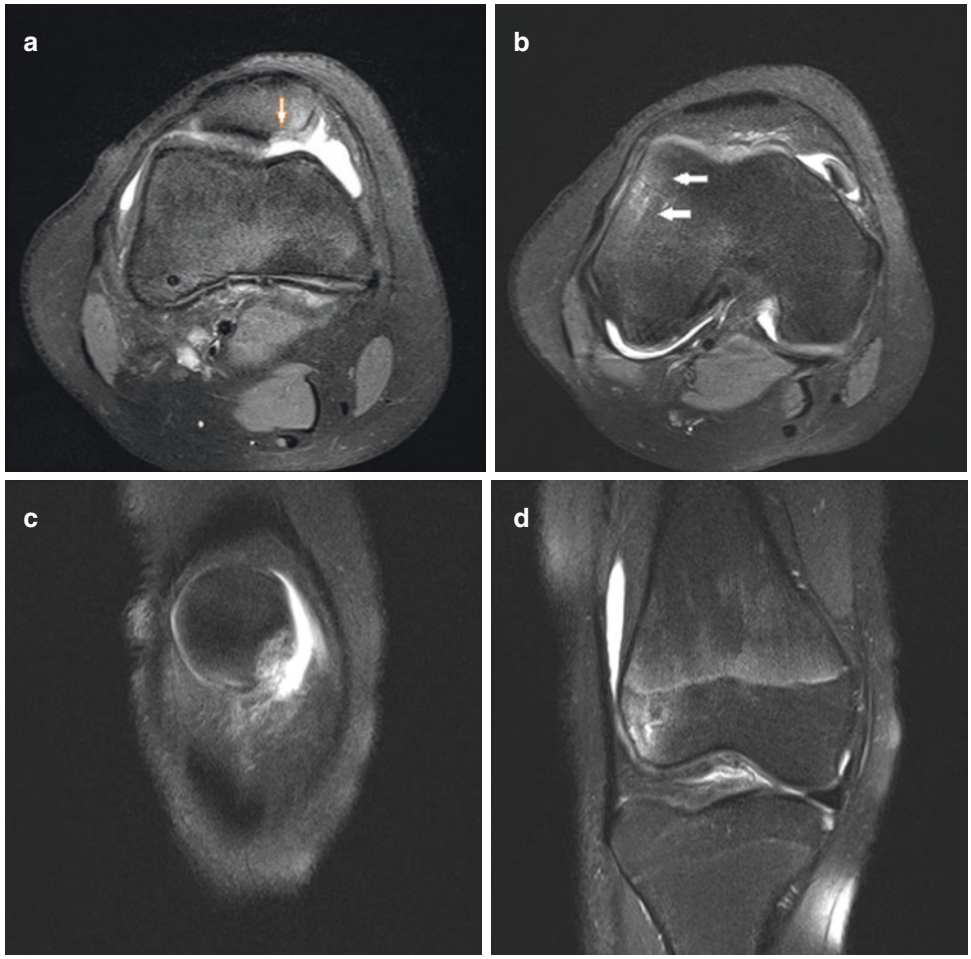

Figure 5.2.4: The Biomechanics of a Chondral Damage: The Acute Shear Rotatory Force of the Lateral Patella Dislocation. A 15-year-old female slipped on the wet bathroom floor, with rotational and valgus movements at the right knee. She developed intense pain and swelling and was diagnosed with acute lateral dislocation of the patella. The patellar dislocation was reduced in the emergency department. In the following weeks, the pain and the swelling subsided, but she continued to experience persistent apprehension in the right knee. (**a**) The proton density (PD) fat-suppressed Magnetic resonance imaging (MRI) axial cuts revealed an osteochondral defect in the patella extending from the apex of the patella till its medial border. (**b**) Another PD image on MRI showed a loose osteochondral fragment lying in the medial gutter. Also note the bone marrow oedema in the lateral femoral condyle. (**c**) The coronal fat-suppressed T2 images confirmed an osteochondral defect at the inferomedial facet of the patella. (**d**) Another fat-suppressed T2 weighted coronal image showed an extensive lateral femoral condylar subchondral bone marrow oedema without a loss of continuity of the articular surface. (**e**) On arthroscopy of the right knee joint, while viewing from the anterolateral portal, a big osteochondral defect was seen on the inferomedial patellar articular surface. The patella was found to be subluxated in the lateral gutter. (**f**) On flexion of the knee, the patella was found tracking back towards the centre of the trochlea with the apex of the patella hitting the lateral femoral condyle. The increased vascularity of the lateral femoral condylar surface is indicative of a recent insult. (**g**) On further flexion, the patella was seen tracking over the centre of the trochlea with an evident osteochondral fracture from the inferomedial facet of the patella. Acute lateral patella dislocation causes a shear force on the lateral femoral condyle while dislocating and can lead to an osteochondral chip fracture of the lateral femoral condyle. The patella, while re-locating, causes an opposite shear load on the medial patellar facet, and this time, it can cause an osteochondral fracture of the medial patellar facet. In this case, the dislocating force was enough to cause an impaction on the subchondral bone of the lateral femoral condyle but not enough to cause a chip fracture. However, during re-location, the forces must be significant enough to cause an osteochondral chip fracture of the medial patellar facet

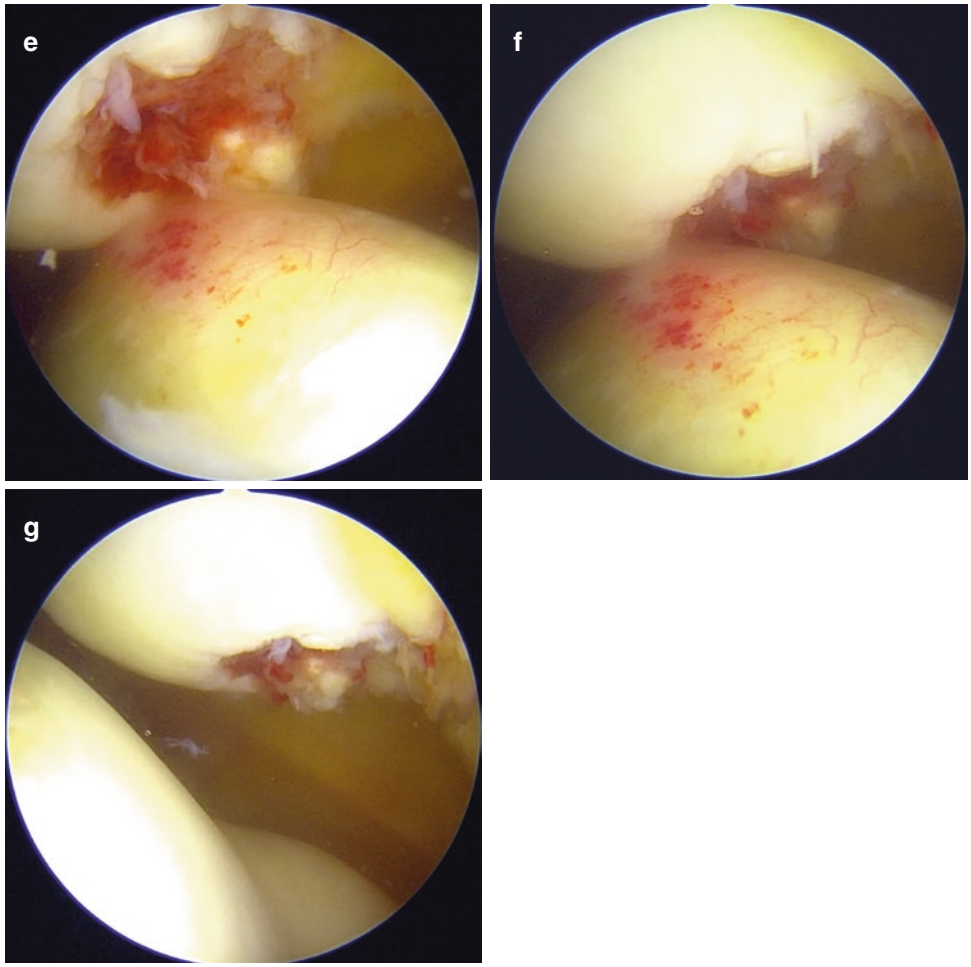

Figure 5.2.4: (continued)

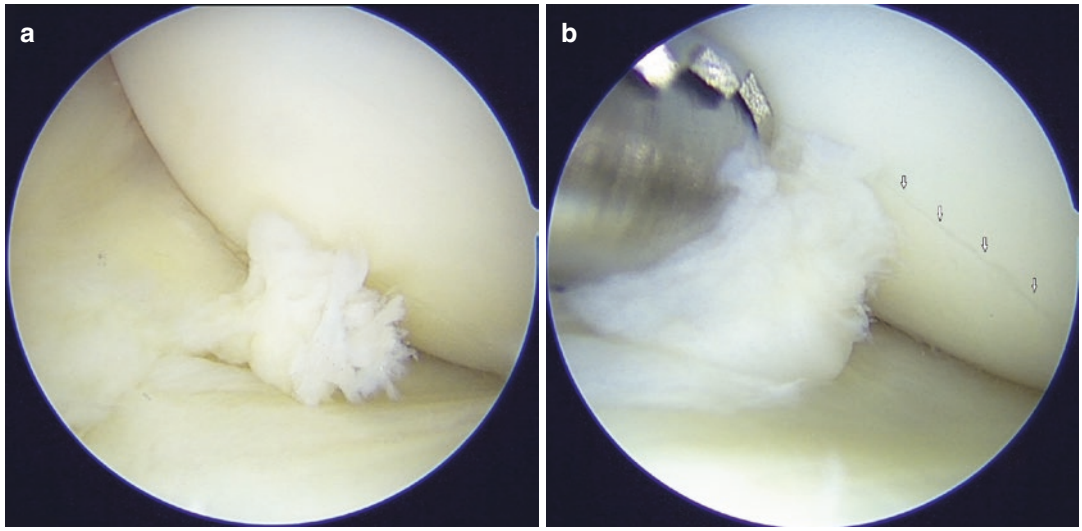

Figure 5.2.5: The Biomechanics of a Chondral Damage: The Impingement Force of Pathological Intraarticular Structures. Intraarticular pathologies cause impingement on the chondral surface during the range of movements [8]. A 23-year-old female had a blunt injury to the front of the left knee, 6 months ago. She had a persistent pain on extension with episodes of knee joint swelling on exertion. Her radiological examinations were normal. A diagnostic arthroscopy revealed hypertrophied synovial tissues on the anteromedial aspect of the knee joint causing (**a**) an impingement of the medial femoral condyle chondral surface. (**b**) On closer look, a vertical crack (see white arrows) on the medial femoral condylar chondral surface is evident, which could be the source of pain

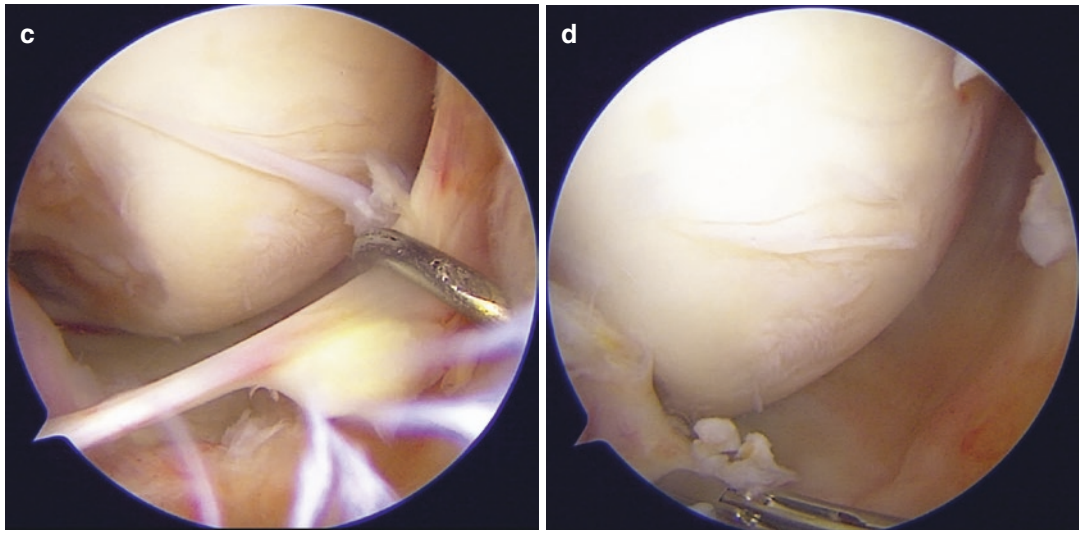

Figure 5.2.5: A 37-year-old female suffered a fall while playing volleyball and injured her right knee 6 months ago. Her family physician advised immobilisation in a long leg brace for 6 weeks. Due to prolonged immobilisation, she developed a stiff knee and was then advised to undergo rehabilitation. She regained flexion range of movements from 0° to 90° but a further flexion was painful. An arthroscopic arthrolysis was performed to regain flexion deficit. (**c**) While viewing from the anterolateral portal, multiple fibrotic bands were identified in the patellofemoral and anterior compartment. These bands were rubbing against the articular surface of the medial femoral condyle and (**d**) had caused the multiple fissures of the chondral surface with a few loose flaps

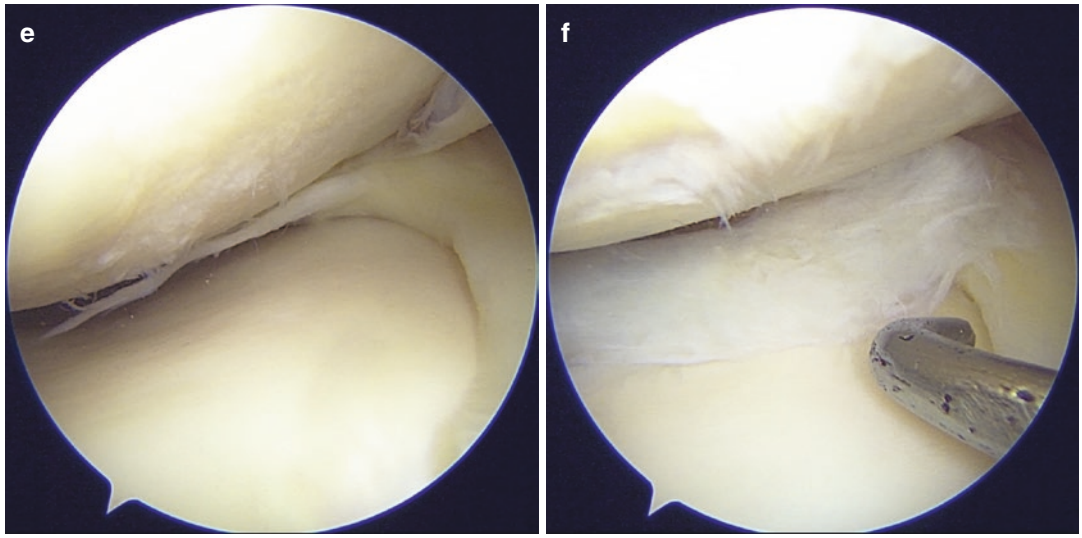

Figure 5.2.5: A 26-year-old male patient had a right knee twisting injury while playing football, resulting in a complex medial meniscus tear. His consulting sports surgeon advised arthroscopy, but he ignored the advice and continued to play. Six months later, he reported back to his sports consultant with an increase in pain and persistent swelling. (**e**) Right knee arthroscopy revealed a flap tear of the medial meniscus while viewing from the anterolateral portal, with an evidence of a cartilage damage on the medial femoral condyle. (**f**) On a closer look, the flap had been displacing into the joint causing an impingement on the medial femoral condylar cartilage leading to fissuring on its surface

5.3 Take-Home Message

The biomechanics play a crucial role in the load distribution on the chondral and the osteochondral surfaces. The type of injury will depend on the type, the direction and the angle of the force put on the chondral/osteochondral surface. Any acute biomechanical load, exceeding the elastic threshold of the chondral or the osteochondral surface, will lead to its damage. While an acute sudden load can lead to a one-time injury, a chronic repetitive load will cause a gradually increasing wear and tear.

A cartilage surgeon should develop a habit of recreating the biomechanics behind each chondral damage, for a better understanding of the characteristic of the lesion. Once the biomechanics behind a lesion are understood, it will become quite clear to the surgeon about the needed management towards the correction of the biomechanics before a cartilage repair procedure is attempted.

References

1. Beran MC, Samora WP, Klingele KE. Weight-bearing osteochondral lesions of the lateral femoral condyle following patellar dislocation in adolescent athletes. Orthopedics. 2012;35:e1033–7.
2. Farr J, Covell DJ, Lattermann C. Cartilage lesions in patellofemoral dislocations: incidents/locations/when to treat. Sports Med Arthrosc Rev. 2012;20:181–6.
3. Chen G, Tang X, Li Q, Zheng G, Yang T, Li J. The evaluation of patient specific factors associated with meniscal and chondral injuries accompanying ACL rupture in young adult patients. Knee Surg Sports Traumatol Arthrosc. 2015;23(3):792–8.
4. Sommerfeldt M, Goodine T, Raheem A, Whittaker J, Otto D. Relationship between time to ACL reconstruction and presence of adverse changes in the knee at the time of reconstruction. Orthop J Sports Med. 2018;6(12):2325967118813917.
5. Ralles S, Agel J, Obermeier M, Tompkins M. Incidence of secondary intra-articular injuries with time to anterior cruciate ligament reconstruction. Am J Sports Med. 2015;43(6):1373–9.
6. Brambilla L, Pulici L, Carimati G, Quaglia A, Prospero E, Bait C, et al. Prevalence of associated lesions in anterior cruciate ligament reconstruction:

correlation with surgical timing and with patient age, sex, and body mass index. Am J Sports Med. 2015;43(12):2966–73.
7. Goyal D, Goyal A, Adachi N. Joint preservation surgery for medial compartment osteoarthritis. Arthrosc Tech. 2017;6(3):e717–28.
8. Hayashi D, Xu L, Guermazi A, Kwoh CK, Hannon MJ, Jarraya M, Green SM, et al. Prevalence of MRI-detected mediopatellar plica in subjects with knee pain and the association with MRI-detected patellofemoral cartilage damage and bone marrow lesions: data from the Joints On Glucosamine study. BMC Musculoskelet Disord. 2013;14:292.

6 The Classifications of the Chondral Lesions

Deepak Rajkumar Goyal

6.1 Introduction

The diagnosis and classification of the chondral lesions are very crucial due to the ever-rising reported incidence of the cartilage lesions detected on arthroscopy, the complexity involved in their clinical presentations and treatment, and in the varied prognosis that various treatments offer [1]. An ideal classification system should properly document a lesion, guide for the best treatment options, help in interpreting and comparing the results of various treatments and help in determining the prognosis.

The available cartilage classification systems are of two types, the magnetic resonance imaging (MRI) based and the arthroscopy based. MRI has a moderate sensitivity to detect chondral lesions, which may be due to less cartilage thickness (<4 mm) and the curved chondral knee surfaces [2, 3]. Type of injury, location, size of the lesion, MRI sequence, strength, etc. can also influence MRI sensitivity [2]. Arthroscopy is considered as the gold standard, however there is a risk of missing a deeper hidden injury [3]. Thus, MRI and arthroscopy are complementary with MRI being an important non-invasive tool to evaluate the symptomatic knee and arthroscopy being an optimal confirmatory method [3].

The Outerbridge classification [4] proposed in 1961 was aimed at classifying the macroscopic changes in chondromalacia patellae, which was later used to describe cartilage lesions at other locations. The original Outerbridge grade 2 and 3 lesions were based on the size of the lesion (<½ in. or >½ in.) and not on the depth of the lesion as later modified in the International Cartilage Regeneration and Joint Preservation Society (ICRS) classification [5]. The size-based grading may be relevant in the context of the patella which has a comparatively smaller articular surface but may not be uniformly relevant at other articular surfaces.

ICRS proposed an arthroscopy-based classification system in 2003, to provide a uniformity to the cartilage lesions and its repair. This ICRS classification is a depth-based classification that can be used for the focal cartilage lesion. The lesions can be traumatic, osteochondritis dissecans (OCD), or a localised degeneration. However, it should not be used for generalised osteoarthritis that doesn't qualify for localised cartilage repair[1]. Any loose flaps or partially detached chondral fragments must be removed, and the firm stable margins are created. Any fissure that is present must be probed to see if the lesion is going down deep to the bone or is just superficial as it looks on arthroscopy [5]. ICRS grade 4 lesions exclude OCD lesions as it has its own classification system [5].

D. R. Goyal (✉)
Saumya Arthroscopy and Sports Knee Clinic, Ahmedabad, India

Visiting Professor of Orthopaedics, Graduate School of Biomedical and Health Sciences, Hiroshima University, Hiroshima, Japan
e-mail: deepak@knee.in

[1]Personal Communication - Brittberg Mats.

D. R. Goyal (ed.), *The Illustrative Book of Cartilage Repair*,
https://doi.org/10.1007/978-3-030-47154-5_6

6.1.1 Outerbridge Macroscopic Classification (1961) for Chondromalacia Patellae

- Grade 1: Softening and swelling of the cartilage
- Grade 2: Fragmentation and fissuring, less than ½ in. in diameter
- Grade 3: Fragmentation and fissuring, greater than ½ in. in diameter
- Grade 4: Erosion of cartilage down to the exposed subchondral bone

6.1.2 International Cartilage Regeneration and Joint Preservation Society (ICRS) Classification (2003) for Focal Chondral Lesions

- Grade 0: Normal cartilage
- Grade 1: Nearly normal (soft indentation and/or superficial fissures, lesions and cracks)
  - Grade1A: Superficial lesions or softening
  - Grade 1B: Superficial fissures and lacerations
- Grade 2: Lesions extending down to <50% of cartilage depth
- Grade 3: Severely abnormal (cartilage defects >50% of cartilage depth as well as down to the calcified layer of the cartilage)
  - Grade 3A: A defect of more than 50% but not down to the calcified layer
  - Grade 3B: A defect down to the calcified layer
  - Grade 3C: A defect thru calcified layer but not thru the subchondral bone
  - Grade 3D: A defect with blisters
- Grade 4: Severely abnormal (full-thickness cartilage loss with exposed subchondral bone)
  - Grade 4A: Defect includes a superficial subchondral bone plate
  - Grade 4B: Defect includes deep subchondral bone

6.1.3 International Cartilage Regeneration and Joint Preservation Society (ICRS) Classification (2003) for Osteochondritis Dissecans (OCD)

- ICRS OCD I: Stable lesion with a continuous but softened area covered by intact cartilage
- ICRS OCD II: Lesion with partial discontinuity, stable on probing
- ICRS OCD III: Lesion with complete discontinuity, "dead in situ," not dislocated
- ICRS OCD IV: Dislocated fragment or loose within the bed or empty defect. A lesion depth of >10 mm is a B-subgroup

6.2 The Illustrations

6.2.A Arthroscopic Classification of the Focal Cartilage Lesions: The ICRS Classification

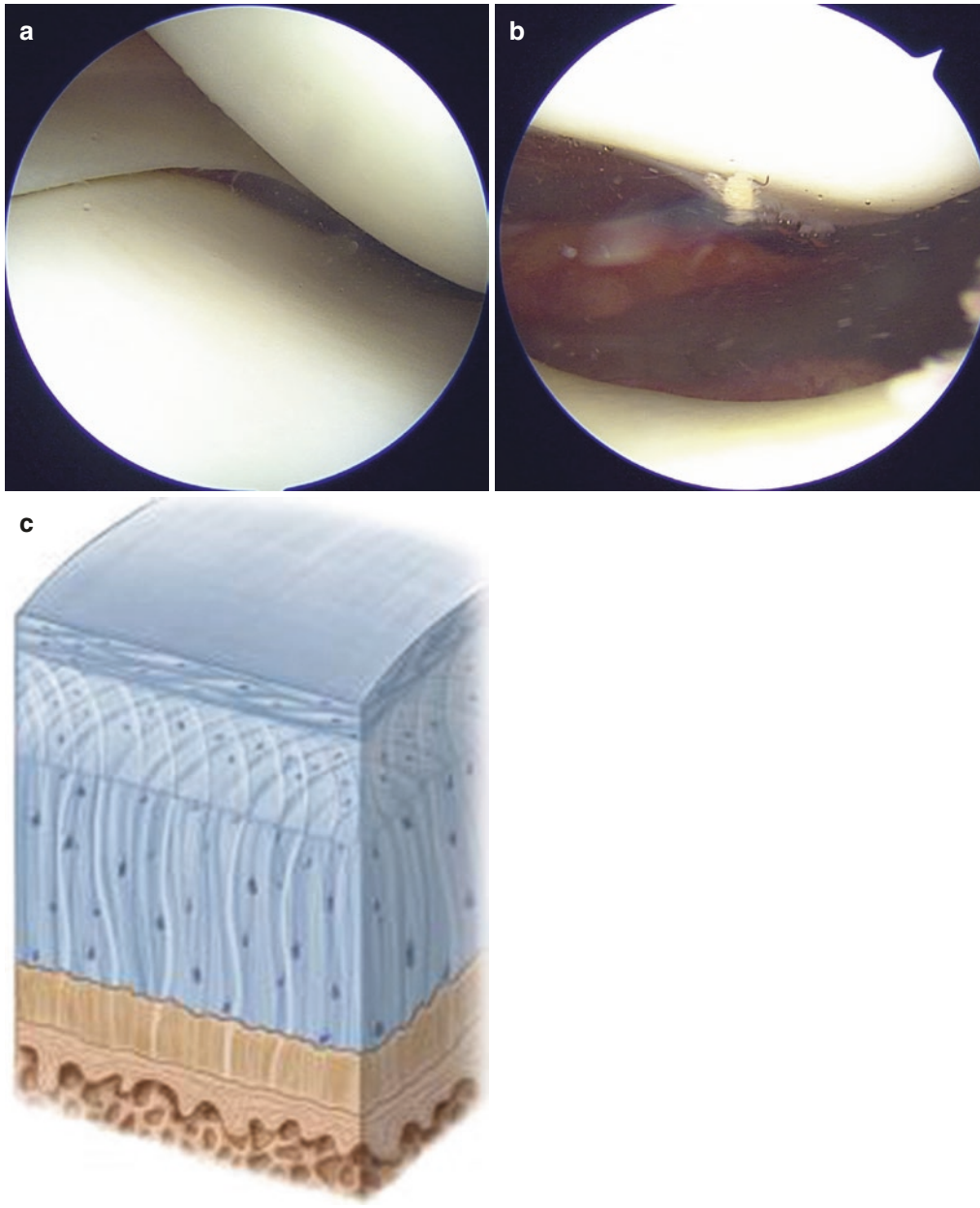

Figure 6.2.A.1: The ICRS Classification for the Focal Chondral Lesions: Grade 0. Grade 0 in the ICRS classification system represents normal cartilage. (**a**) The normal cartilage of left medial compartment of a 21-year-old male patient having anterior cruciate ligament tear while playing football 2 months back, as viewed from the anterolateral portal. The tibial and femoral cartilage are showing a smooth, glistening, white surface that was of normal consistency on probing, indicating grade 0 of ICRS classification. (**b**) The patellofemoral joint is seen from the anterolateral portal of the same patient showing the similar smooth, glistening, white surface of patella and trochlea, suggestive of grade 0 chondral surface of ICRS classification system. (**c**) A pictorial representation of grade 0 cartilage as per ICRS classification. *(reprinted with permission from International Cartilage Regeneration and Joint Preservation Society (ICRS).* www.cartilage.org*)*

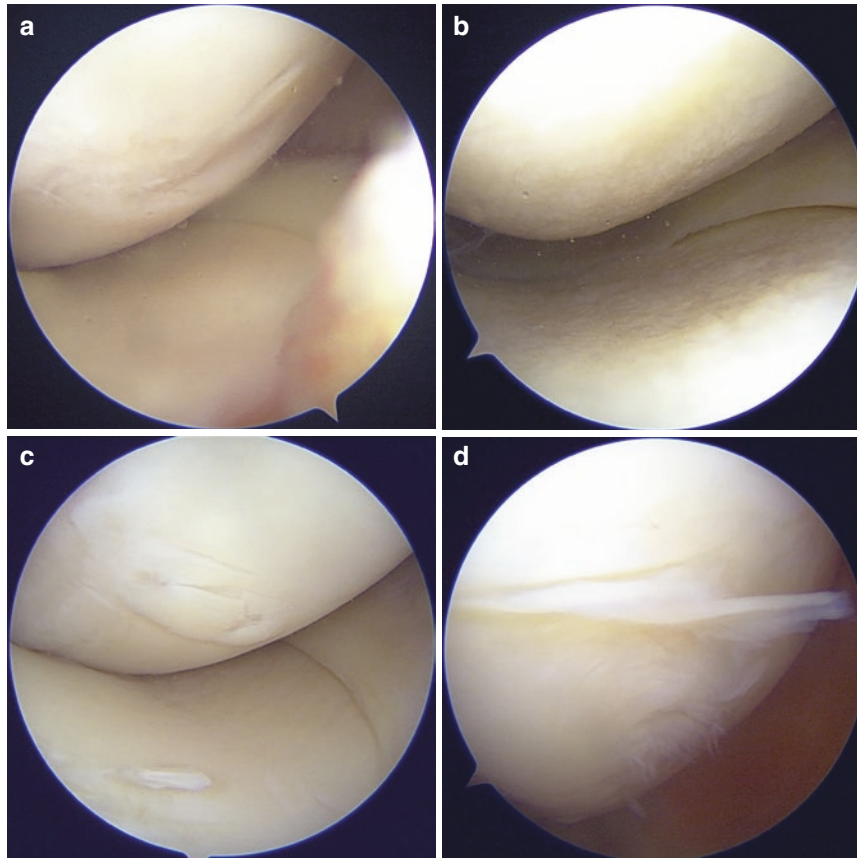

Figure 6.2.A.2: The ICRS Classification for the Focal Chondral Lesions: Grade 1. Grade 1 in the ICRS Classification system represents nearly normal cartilage but with soft indentations/superficial fissures/superficial lesions and cracks. Grade 1 is further subclassified into grade 1A representing superficial lesions or softening and grade 1B representing superficial fissures or lacerations. (**a**) The medial compartment of 19-year-old female having right knee pain following a blunt injury over anteromedial knee 2 years back, as viewed from the anterolateral portal. There is a superficial lesion of around 12 mm × 8 mm on lateral half of medial femoral condyle (ICRS grade 1A) that was caused by hypertrophied synovium impinging on the cartilage near the lesion. (**b**) A 38-year-old male underwent right knee arthroscopy for lateral meniscus tear following a 6-week-old trauma, shows ICRS grade 1A changes in form of softening of the medial femoral condyle and medial tibial plateau cartilage. (**c**) The right-side medial compartment of 48-year-old female with anterior cruciate ligament tear for last 1 year, as viewed from the anterolateral portal. There are superficial fissures on the lateral half of medial femoral condyle that can be due to persistent instability causing abnormal loading on the medial joint leading to fissures. The fissures are superficial on probing and are therefore ICRS grade 1B. (**d**) A 26-year-old female suffered left knee posterior cruciate ligament tear, posterolateral corner injury and lateral meniscus tear 3 months back but continued to walk with a brace without any active treatment leading to ICRS grade 1B lesion on the lateral femoral condyle surface in form of superficial lacerations (view from the anterolateral portal). A pictorial representation of grade 1A (**e**) and grade 1B (**f**) chondral lesions as per ICRS classification. *(reprinted with permission from International Cartilage Regeneration and Joint Preservation Society (ICRS).* www.cartilage.org*)*

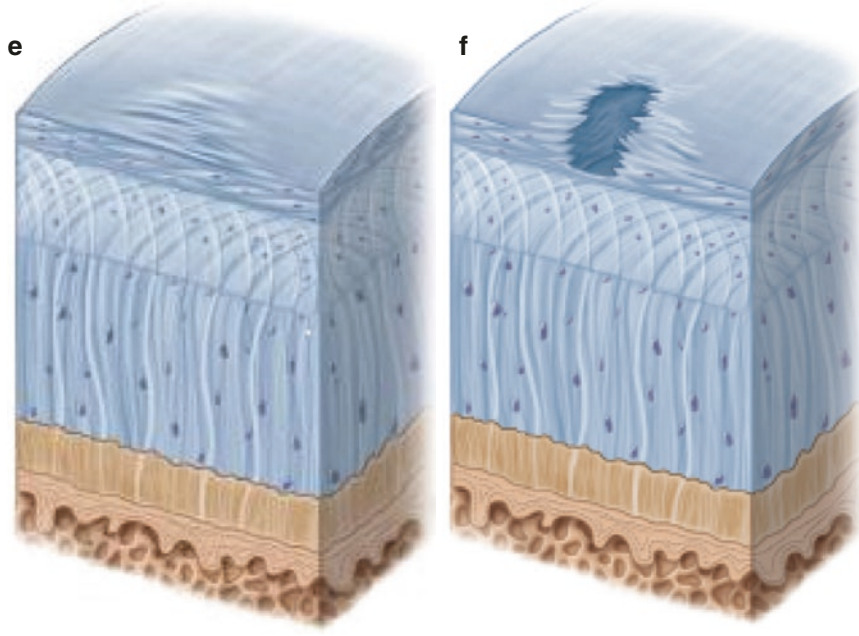

Figure 6.2.A.2: (continued)

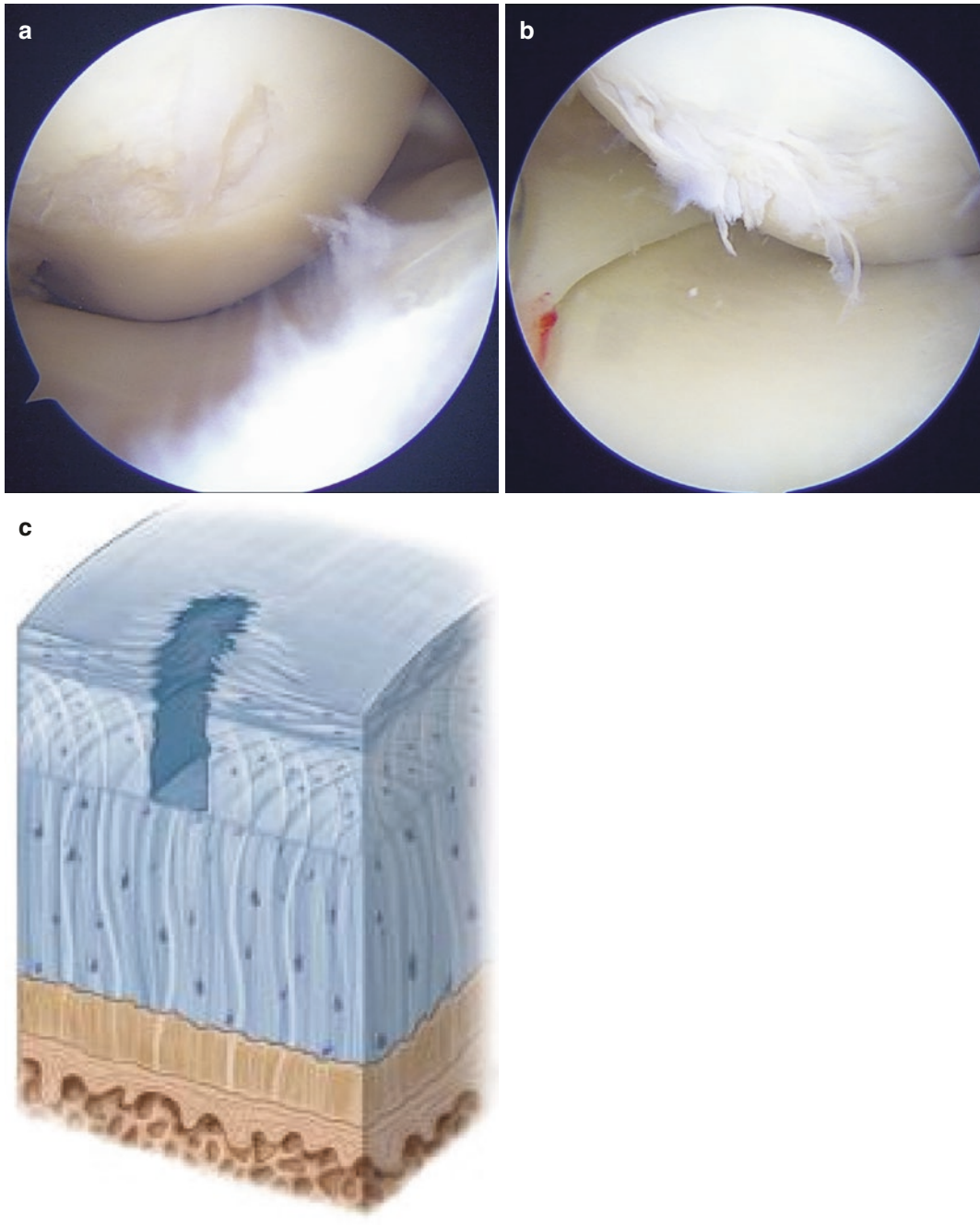

Figure 6.2.A.3: The ICRS Classification for the Focal Chondral Lesions: Grade 2. Grade 2 in the ICRS classification system represents abnormal cartilage, having lesions or fissures extending down to the thickness of the cartilage but covering <50% thickness of the cartilage. (**a**) A 21-year-old female with 10-month-old untreated right-side anterior cruciate ligament tear, presented with 14 mm × 8 mm grade 2 chondral lesion on the medial femoral condyle involving <50% of cartilage thickness, as seen from the anterolateral viewing portal. (**b**) A 20-year-old male patient with 2-year-old untreated left-side anterior cruciate ligament tear, showing multiple lacerations and fissures on the lateral half of the medial femoral condyle, as viewed from the anterolateral portal. On probing the fissures were not extending deeper than the 50% thickness of the cartilage and hence are ICRS grade 2 lesions. (**c**) A pictorial representation of grade 2 chondral lesions as per ICRS classification. *(reprinted with permission from International Cartilage Regeneration and Joint Preservation Society (ICRS).* www.cartilage.org*)*

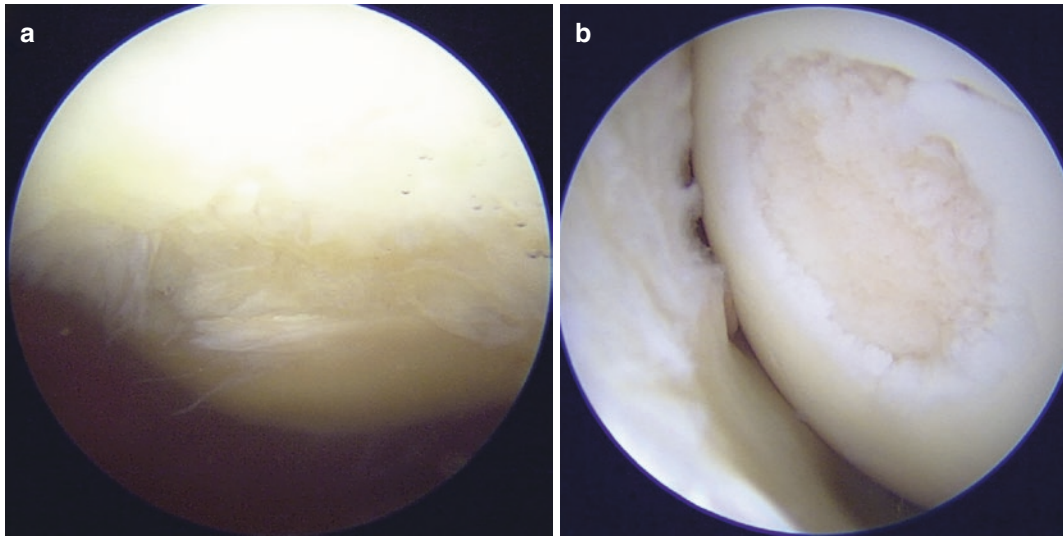

Figure 6.2.A.4: The ICRS Classification for the Focal Chondral Lesions: Grade 3. Grade 3 in the ICRS classification system represents severely abnormal cartilage, having lesions or fissures extending down to the calcified layer of the cartilage and covering >50% thickness of the cartilage. Grade 3 is further divided into grade 3A representing a defect more than 50% but not down to the calcified layer, grade 3B representing a defect down to the calcified layer, grade 3C representing a defect thru the calcified layer reaching up to the subchondral bone and grade 3D representing the defect with >50% thickness and blisters. (**a**) A 35-year-old male had persistent left anterior knee pain for 3 years due to gross patellar mal tracking. Viewing from the superolateral portal, there was a large grade 3A chondral lesion on lateral patellar facet extending >50% thickness of the cartilage. (**b**) A 46-year-old female had neglected left side anterior cruciate ligament tear for 4 years, developed grade 3B chondral lesion on medial femoral condyle that is extending up to the cementing layer (seen as whitish irregular base). (**c**) A 47-year-old male soldier presented with medial side right knee pain since 2 years showed a focal degenerative grade 3C chondral damage on medial femoral condyle. The lesion extends beyond cementing layer and seen reaching the subchondral bone plate which is seen as the smooth reddish bony base. (**d**) A 38-year-old female with left side anterior knee pain for 3 years showed grade 3D lesion in the centre of the trochlea, seen in the form of a bleb formation from the anterolateral portal. On probing, the superficial cartilage got peeled off leading to the bone-deep chondral lesion. A pictorial representation of grade 3A (**e**), grade 3B (**f**), grade 3C (**g**) and grade 3D (**h**) chondral lesions as per ICRS classification. *(reprinted with permission from International Cartilage Regeneration and Joint Preservation Society (ICRS).* www.cartilage.org*)*

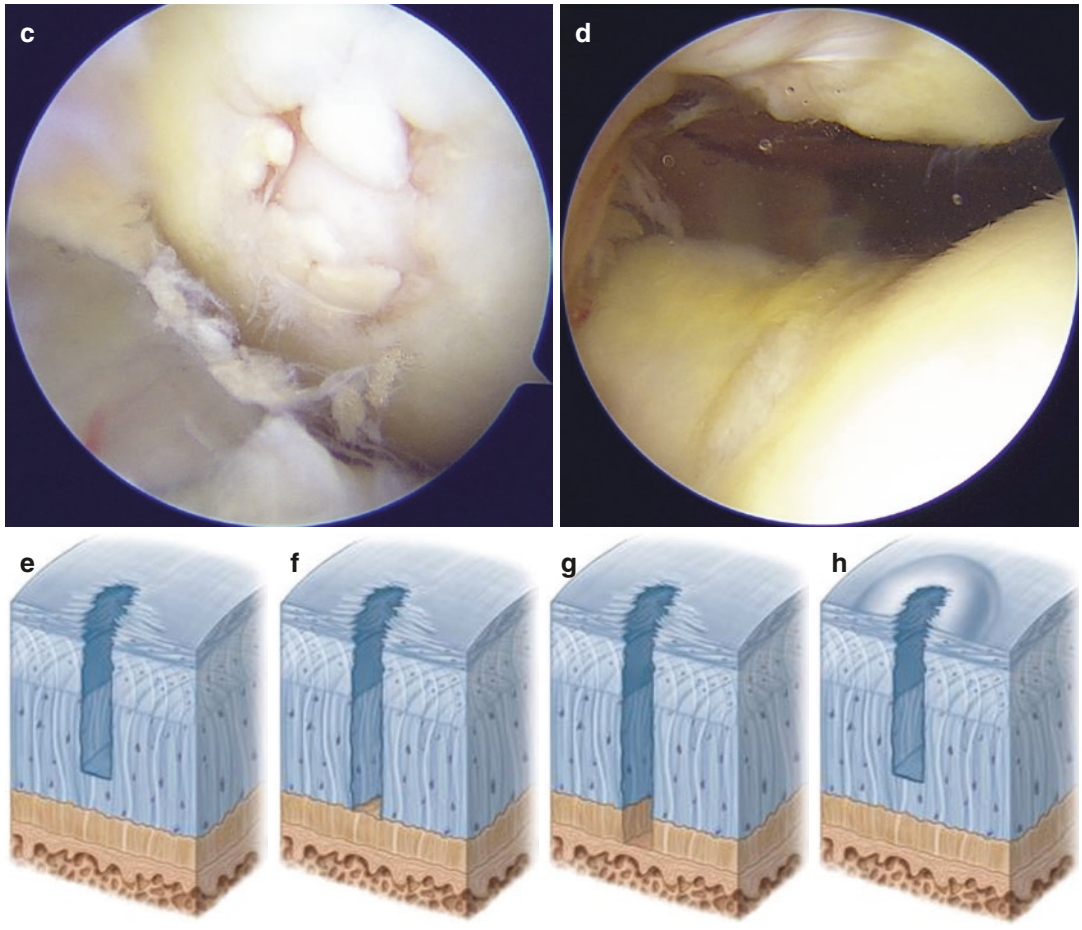

Figure 6.2.A.4: (continued)

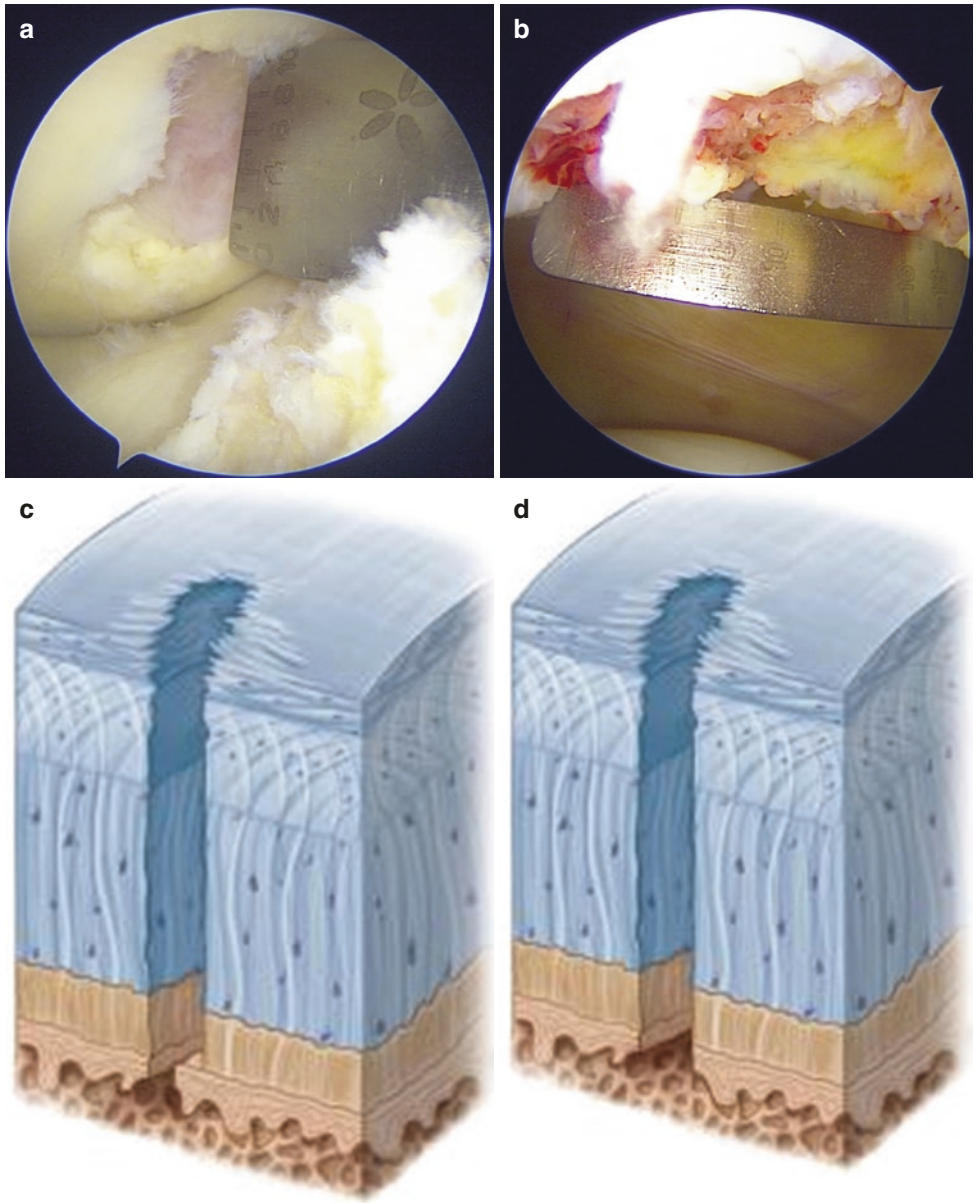

Figure 6.2.A.5: The ICRS Classification for the Focal Chondral Lesions: Grade 4. Grade 4 in the ICRS classification system represents severely abnormal cartilage, having full-thickness cartilage loss with an exposed subchondral bone. Grade 4 is further subdivided into grade 4A representing cartilage defect including the subchondral bone plate and grade 4B representing cartilage defects including the deep subchondral bone. (**a**) A 32-year-old male patient suffered left-side acute patella dislocation 3 years back that was treated conservatively but had persistent lateral joint pain. On arthroscopy, while viewing through the anteromedial portal, a grade 4A lesion is seen that is deeper than the surrounding cartilage thickness with evidence of loss of partial subchondral bone plate with an attempt of fibrocartilage formation from the base. (**b**) A 17-year-old female suffered from left-side acute lateral patellar dislocation with separation of an osteochondral fragment from the medial patellar facet leading to grade 4B defect, as seen from the superolateral portal. A pictorial representation of grade 4A (**c**) and grade 4B (**d**) chondral lesions as per ICRS classification. *(reprinted with permission from International Cartilage Regeneration and Joint Preservation Society (ICRS).* www.cartilage.org*)*

6.2.B Arthroscopic Classification of Osteochondritis Dissecans (OCD): The ICRS Classification

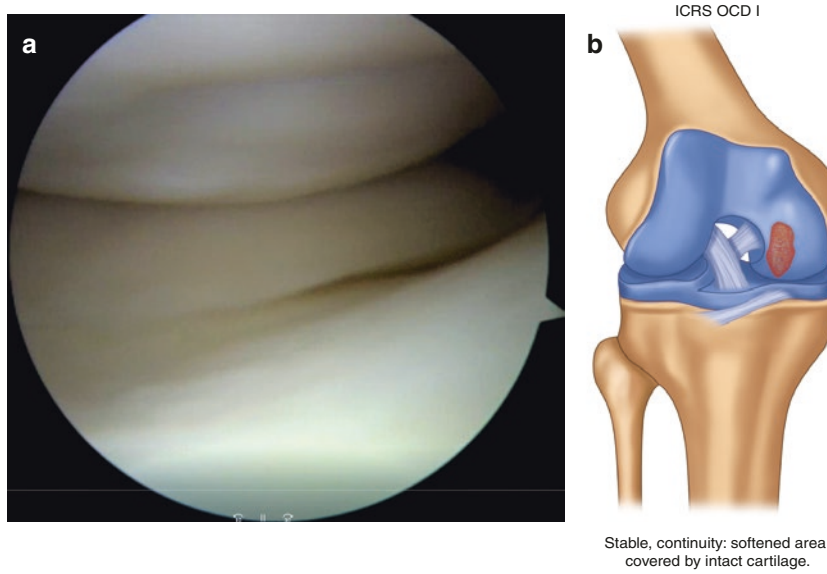

Figure 6.2.B.1: The ICRS Classification for OCD: ICRS OCD Grade I. ICRS OCD grade I represent an osteochondritis dissecans lesion which is stable, is in continuity with surrounding chondral surface and has softened but intact cartilage over it. (**a**) A 25-year-old paramilitary soldier complained of pain in his left knee with 2 years of duration; the pain used to get aggravated on parade. The left medial femoral condyle showed ICRS OCD grade I in form of an 18 mm × 20 mm area of softened cartilage with underlying osteochondritis dissecans lesions that were previously confirmed on MRI. (**b**) A pictorial representation of grade ICRS OCD grade I lesion as per ICRS OCD classification. *(reprinted with permission from International Cartilage Regeneration and Joint Preservation Society.* www.cartilage.org*)*

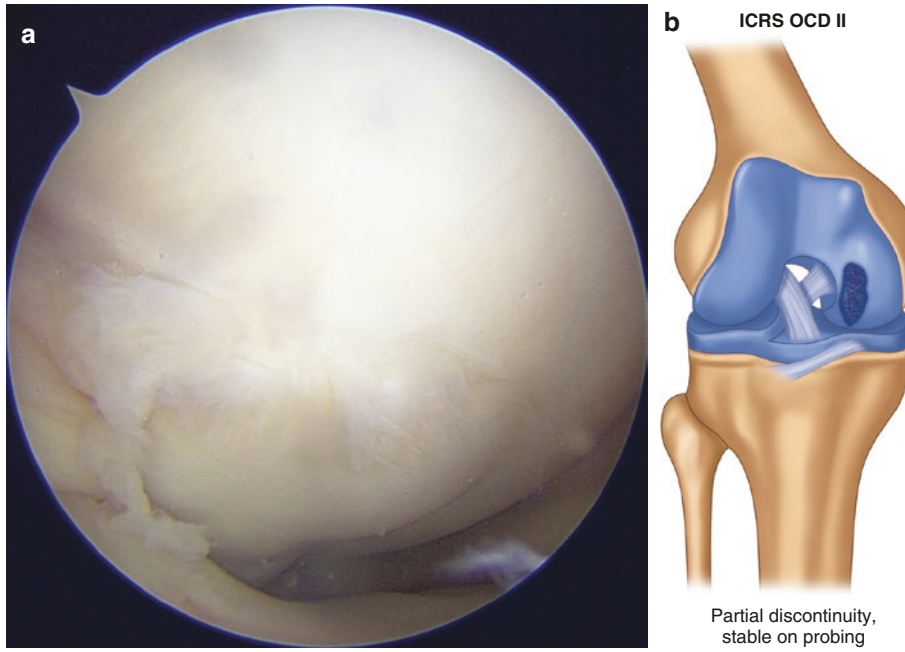

Figure 6.2.B.2: The ICRS Classification for OCD: ICRS OCD Grade II. ICRS OCD grade II represents an osteochondritis dissecans lesion which is in partial discontinuity with the surrounding cartilage, however, is stable on probing. (**a**) A 20-year-old medical student had right knee pain of 3 years duration that got aggravated on playing football. Arthroscopy confirmed ICRS OCD grade II lesion of the right medial femoral condyle that was around 16 mm × 22 mm in size, stable on probing but showed a discontinuity near its anterior margin. (**b**) A pictorial representation of grade ICRS OCD grade II lesion as per ICRS OCD classification. *(reprinted with permission from International Cartilage Regeneration and Joint Preservation Society.* www.cartilage.org*)*

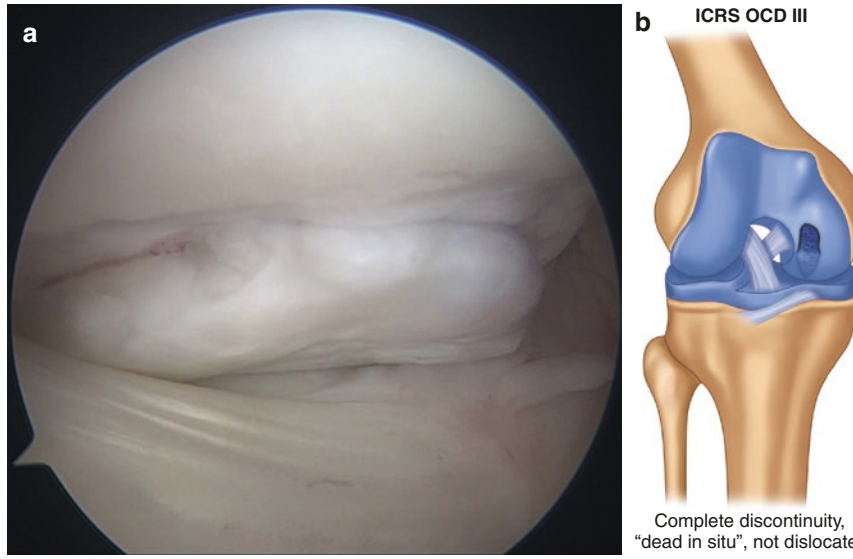

Figure 6.2.B.3: The ICRS Classification for OCD: ICRS OCD Grade III. ICRS OCD grade III represents an osteochondritis dissecans (OCD) lesion which is in complete discontinuity with all its margins but is till seated 'in situ' and is not separated from its base. (**a**) A 20-year-old female had right knee dull aching pain with 2 years duration that had increased in severity for the last 3 weeks along with locking and catching sensations in the knee. Arthroscopy showed ICRS OCD grade III lesion of the right lateral femoral condyle that was nearly separated from its surrounding but was still located at its base. (image courtesy: Dr. Dinshaw Pardiwala, Mumbai, India) (**b**) A pictorial representation of grade ICRS OCD grade III lesion as per ICRS OCD classification. *(reprinted with permission from International Cartilage Regeneration and Joint Preservation Society.* www.cartilage.org*)*

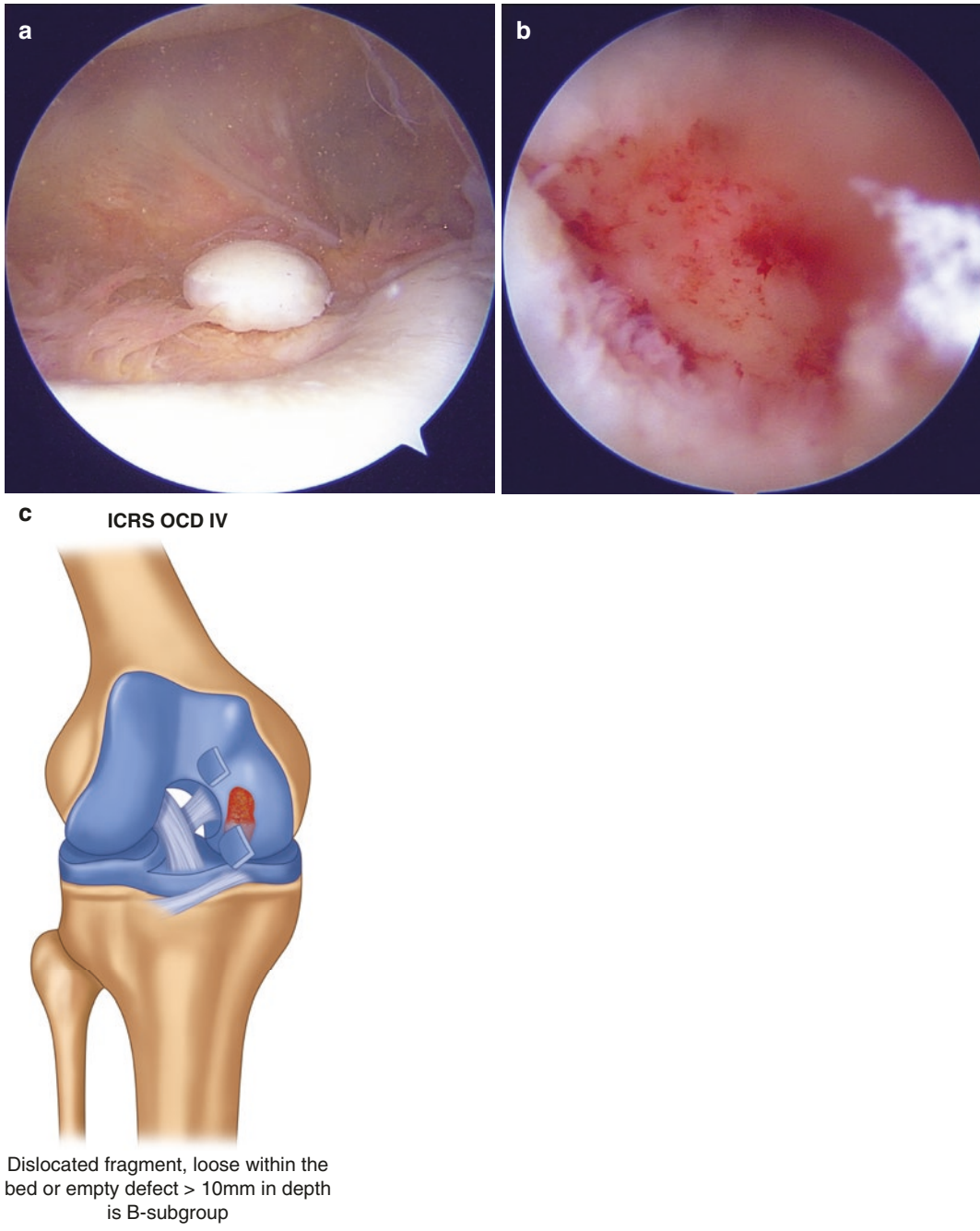

Figure 6.2.B.4: The ICRS Classification for OCD: ICRS OCD Grade IV. ICRS OCD grade IV represents an osteochondritis dissecans (OCD) lesion which is completely separated from its base and is loose in the joint with an empty bed. (**a**) A 16-year-old boy presented with sudden locking of the left knee since 10 days and gave a history of diffuse pain in the knee for 6 months without any concomitant history. Left knee arthroscopy revealed an approximately 12 mm diameter osteochondral loose body arising from (**b**) lateral trochlear surface suggesting a case of juvenile trochlear osteochondritis dissecans (OCD) having ICRS OCD grade IV lesion. (**c**) A pictorial representation of grade ICRS OCD grade IV lesion as per ICRS OCD classification. *(reprinted with permission from International Cartilage Regeneration and Joint Preservation Society.* www.cartilage.org*)*

6.3 Take-Home Message

The ICRS classification has served its purpose of bringing uniformity in describing various cartilage lesions since 2003 [5]. It is important to understand that all the treatments suggested for cartilage repair are generally for ICRS grade 3 and 4 lesions and not for grade 0, 1 or 2 lesions. Hence, it is very crucial to differentiate between nearly normal (ICRS grade 1) and abnormal cartilage (ICRS grade 2) from the severely abnormal cartilage (ICRS grade 3 and 4) on arthroscopy. A careful probe examination should help the surgeon. While superficial crack, fissure or laceration (ICRS grade 1) can easily be confirmed through gently moving the probe along the lesion; it requires little more patience to differentiate between ICRS grade 2 and 3 lesions. The ICRS grade 2 and 3 lesions require probing the depth of lesion at its various locations and then assessing the grade. ICRS grade 4 lesions are relatively easy to diagnose as either the subchondral bone plate or the subchondral spongiosa is exposed.

ICRS classification has been a benchmark in comparing the outcome of various treatments as it has been validated for the macroscopic evaluation of cartilage repair as a research tool [6]. A high correlation with histological assessment of the depth has also provided evidence of validity for this classification system [7]. In addition, the arthroscopic ICRS classification system has shown a good interobserver and intra-observer reliability [7].

References

1. Zhang M, Min Z, Rana N, Liu H. Accuracy of magnetic resonance imaging in grading knee chondral defects. Arthroscopy. 2013;29(2):349–56.
2. Ho YY, Stanley AJ, Hui JH-P, Wang S-C. Postoperative evaluation of the knee after autologous chondrocyte implantation: what radiologists need to know. Radiographics. 2007;27(1):207–20.
3. Danieli MV, Guerreiro JPF, Queiroz Ad, Pereira Hd, Tagima S, Marini MG et al. Diagnosis and classification of chondral knee injuries: comparison between magnetic resonance imaging and arthroscopy. Knee Surg Sports Traumatol Arthrosc. 2016;24(5):1627–33.
4. Outerbridge RE. The etiology of chondromalacia patellae. J Bone Joint Surg Br. 1961;43(4):752–7.
5. Brittberg M, Winalski CS. Evaluation of cartilage injuries and repair. J Bone Joint Surg Am. 2003;85-A(Suppl 2):58–69.
6. van den Borne MPJ, Raijmakers NJH, Vanlauwe J, Victor J, de Jong SN, Bellemans J et al. International cartilage repair society (ICRS) and oswestry macroscopic cartilage evaluation scores validated for use in autologous chondrocyte implantation (ACI) and microfracture. Osteoarthr Cartil. 2007;15(12):1397–402.
7. Dwyer T, Martin CR, Kendra R, Sermer C, Chahal J, Ogilvie-Harris D et al. Reliability and validity of the arthroscopic international cartilage repair society classification system: correlation with histological assessment of depth. Arthroscopy. 2017;33(6):1219–24.

7 The Illustrative Magnetic Resonance Imaging of the Chondral and the Osteochondral Lesions

Drushi Patel, Ankur Shah,
and Deepak Rajkumar Goyal

7.1 Introduction

Approximately two-thirds of the routine knee magnetic resonance imaging (MRI) demonstrates an articular cartilage damage [1]. Chondral injuries can occur de novo or in association with degenerative or traumatic etiologies. Therefore, a careful evaluation of the articular cartilage is an integral part of the knee MRI examination. With an increase in the availability of the treatment options for the articular cartilage lesions, MRI has taken a front seat in the identification and determination of the extent and severity of the chondral lesions. MRI is the investigation of choice and the best non-invasive modality for the evaluation of chondral lesions with an arthroscopy being accepted as the gold standard.

Fast spin-echo (with or without fat suppression) and/or fat-suppressed spoiled gradient-echo image acquisitions are strongly recommended imaging techniques for the cartilage evaluation [2]. Water-sensitive MR sequences such as fat-suppressed T2-weighted or proton density (PD)-weighted or short tau inversion recovery (STIR) sequences best demonstrate the bone marrow lesions in conjunction with the cartilage damage or osteoarthritis (OA). Changes in the signal intensity of the subchondral bone marrow can be an indirect sign of an overlying cartilage lesion [3]. In the absence of obvious visualization of a direct communication between the cartilage defect and the cyst on MRI, a direct communication should be suspected and sought for. Similarly, if there is a focal edema-like signal in the marrow beneath a cartilage lesion, it may indicate that the lesion extends to, or into, the subchondral bone plate, except in the setting of an acute trauma when a bone bruise may be present.

The purpose of this chapter is to differentiate between chondral, osteochondral, subchondral, and osteoarthritis lesions on MRI and to discuss the various radiological terminologies pertaining to these lesions. The chapter also utilizes the commonly recommended grading systems for the chondral and the osteochondral lesions.

D. Patel (✉)
Gujarat Imaging Centre, Samved Hospital,
Ahmedabad, India
e-mail: drushi43@yahoo.com

A. Shah
Sadbhav Imaging Centre, Ahmedabad, India
e-mail: drankur203@gmail.com

D. R. Goyal
Saumya Arthroscopy and Sports Knee Clinic,
Ahmedabad, India

Visiting Professor of Orthopaedics,
Graduate School of Biomedical and Health Sciences,
Hiroshima University, Hiroshima, Japan
e-mail: deepak@knee.in

D. R. Goyal (ed.), *The Illustrative Book of Cartilage Repair*,
https://doi.org/10.1007/978-3-030-47154-5_7

7.2 The Illustrations

7.2.A Focal Chondral Lesions

To date, no standardized MRI classification system for the articular cartilage lesions has been accepted. The modified Outerbridge grading of chondromalacia was modified for MRI, typically using fat-saturated proton density (PD) sequences and considering the depth of the lesion [4]. Later, a working group of International Cartilage Repair Society (ICRS) developed a common, easy system for the clinical and arthroscopic classification of the chondral lesions [5, 6] that was also adopted for the MRI classification and evaluation. Even though an arthroscopic assessment is the gold standard, MRI provides the first insight of the chondral lesions with some limitations. MRI tends to underestimate the true size of the dimensions of a cartilage defect [7]. Since most cartilage defects have irregular or ovoid shape, it is unlikely that any one magnetic resonance image will be perfectly aligned to demonstrate the maximal length or width of the lesion. Therefore, a measurement of the distance between the margins of a defect may extend over several image slice locations and will increase the difficulty of obtaining an accurate assessment of the lesion size. MRI may also underestimate the dimensions of a lesion when unstable fragments remain in place along the margins of a defect [7].

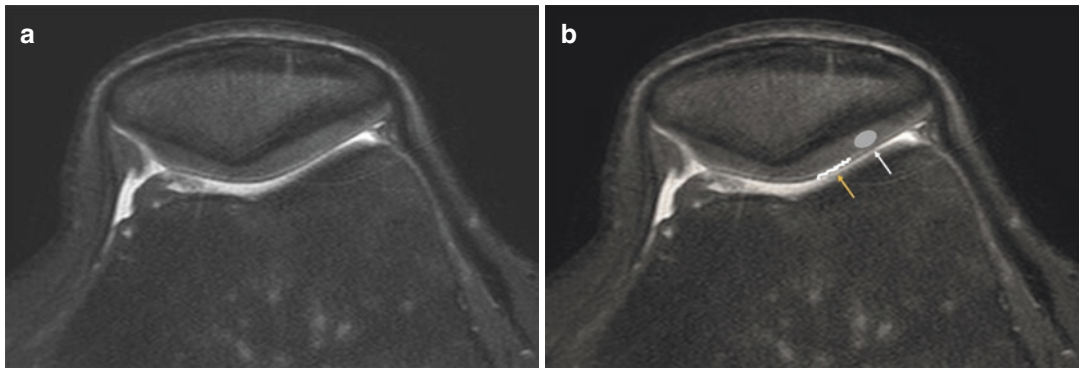

Figure 7.2.A.1: Magnetic Resonance Imaging Adaptation of International Cartilage Repair Society (ICRS) Classification for the Focal Chondral Lesions. A working group of International Cartilage Repair Society (ICRS) developed a common, easy system for the clinical and arthroscopic evaluation of the focal chondral lesions [5, 6] that was further adopted for MRI evaluation [4]. (**a**) ICRS grade 0 is a normal cartilage showing homogenous signals on the fat-suppressed PD images with a normal layered appearance of the articular cartilage throughout its thickness. The surface appears congruous with no evident fissuring or surface irregularity. (**b**) ICRS grade 1 describes superficial lesions which is further divided into grade 1a featuring intrinsic cartilage signal abnormality (as marked by white arrow) without detectable morphologic changes and grade 1b showing superficial fissures or lacerations (as marked by yellow arrow). Occasionally ICRS grade 1b might be difficult to differentiate from ICRS grade 1a or ICRS grade 2 on MRI [8]. (**c**) Focal chondral lesions involving less than 50% thickness of the cartilage are described as ICRS grade 2. (**d**) Cartilage defects extending to >50% of cartilage depth but not through the subchondral bone are classified as ICRS grade 3 lesions. Chondral blisters are also included in this grade which are detected as a bulge on the cartilage surface. (**e**) Chondral lesions extending through the subchondral bone plate or deeper are classified as ICRS grade 4 lesions

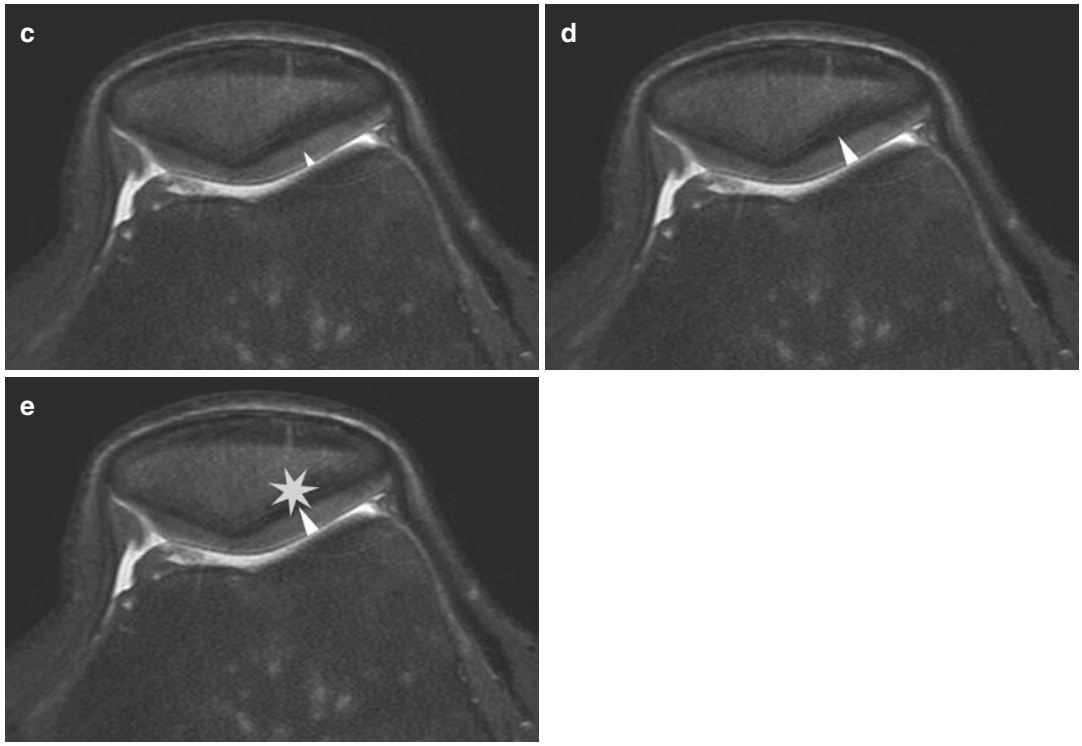

Figure 7.2.A.1: (continued)

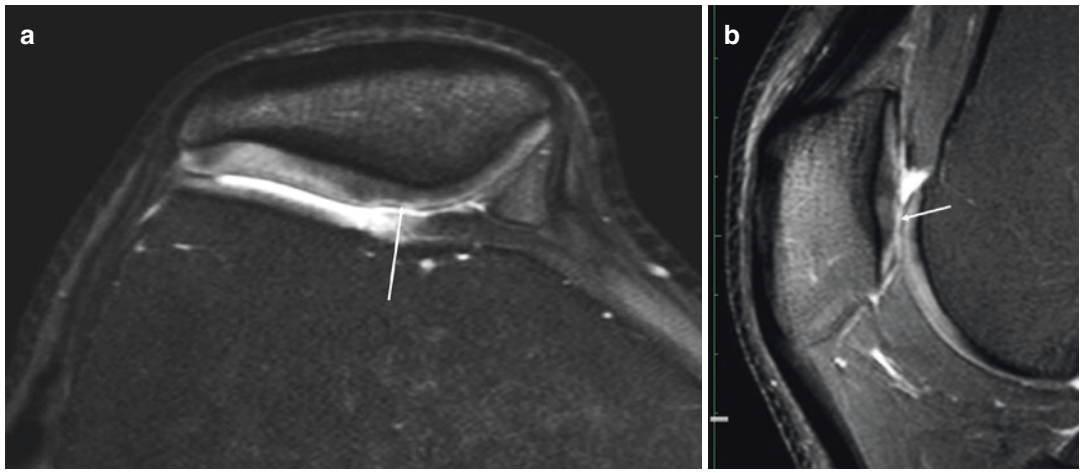

Figure 7.2.A.2: International Cartilage Repair Society (ICRS) Grade 1 Focal Chondral Lesion on Magnetic Resonance Imaging. A 32-year-old male patient who complained of an anterior knee pain in the right knee for 6 months while climbing stairs underwent magnetic resonance imaging (MRI) study. (**a**) The fat-suppressed PD-weighted axial, (**b**) sagittal images revealed subtle chondral surface irregularity at the patellar apex suggestive of grade 1 focal chondral lesion. No evident fragmentation or fissuring or subchondral marrow edema was noted

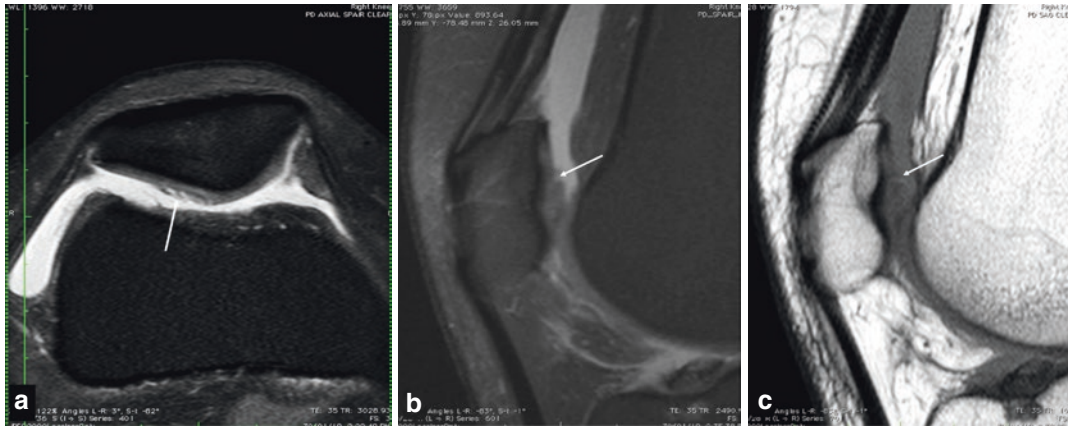

Figure 7.2.A.3: International Cartilage Repair Society (ICRS) Grade 2 Focal Chondral Lesion on Magnetic Resonance Imaging. A 48-year-old female presented with a right-sided anterior knee pain and underwent a magnetic resonance imaging (MRI) examination. (**a**) The fat-suppressed PD-weighted axial, (**b**) PD-weighted sagittal images, and (**c**) non-fat-suppressed PD-weighted sagittal images revealed superficial linear chondral fissuring at the lateral patellar facet extending less than 50% of chondral thickness suggestive of grade 2 chondral lesion. No evident subchondral marrow edema was observed. The sagittal images demonstrated the cranio-caudal extent of the chondral involvement. Note that if the fissure would have been extending more than 50% or up to the subchondral bone, it would have been classified as ICRS grade 3 lesion

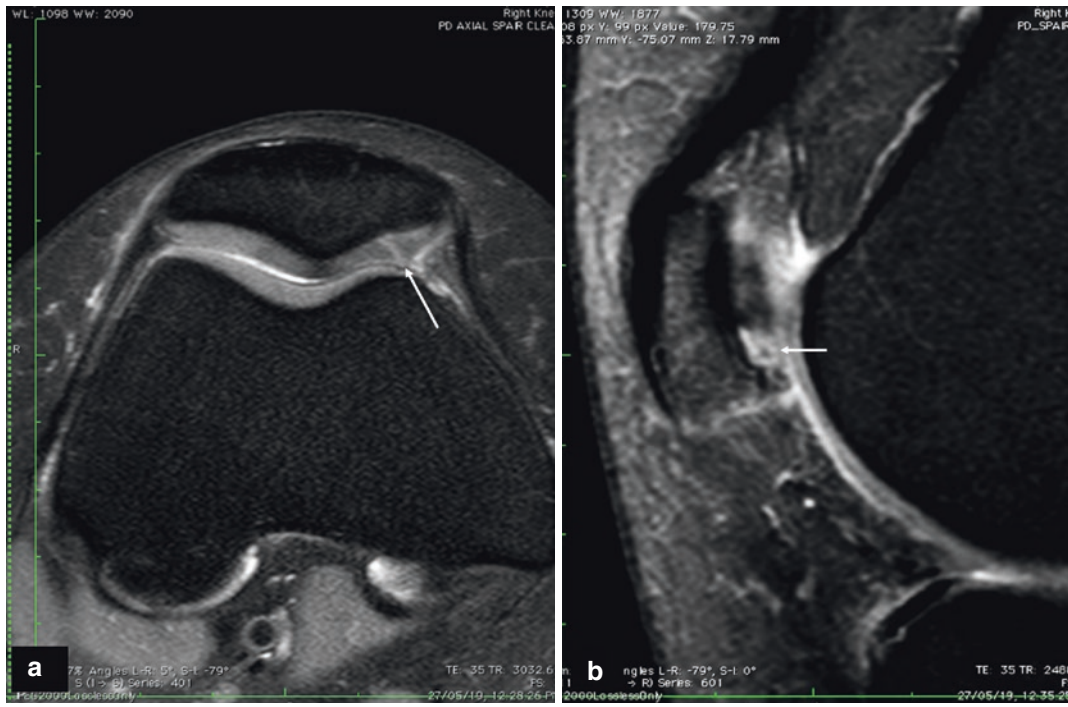

Figure 7.2.A.4.a: International Cartilage Repair Society (ICRS) Grade 3 Focal Chondral Lesion on Magnetic Resonance Imaging. A male aged 45 years complaining of left-sided anterior knee pain for a duration of 6 months showed a focal near full thickness chondral fissure (>50% articular thickness) without subchondral marrow edematous changes at the inferior aspect of the medial patellar facet on (**a**) fat-suppressed PD-weighted axial and (**b**) sagittal images of magnetic resonance imaging study. The axial image demonstrated the linear fissure like configuration of the chondral lesion, while the sagittal image slice along the fissure demonstrated the cranio-caudal extent of the fissure. The adjacent cartilage appeared normal and homogenous in signal intensity. More than 50% thickness involvement and the absence of the subchondral marrow edema are the features to classify the lesion as ICRS grade 3 lesion

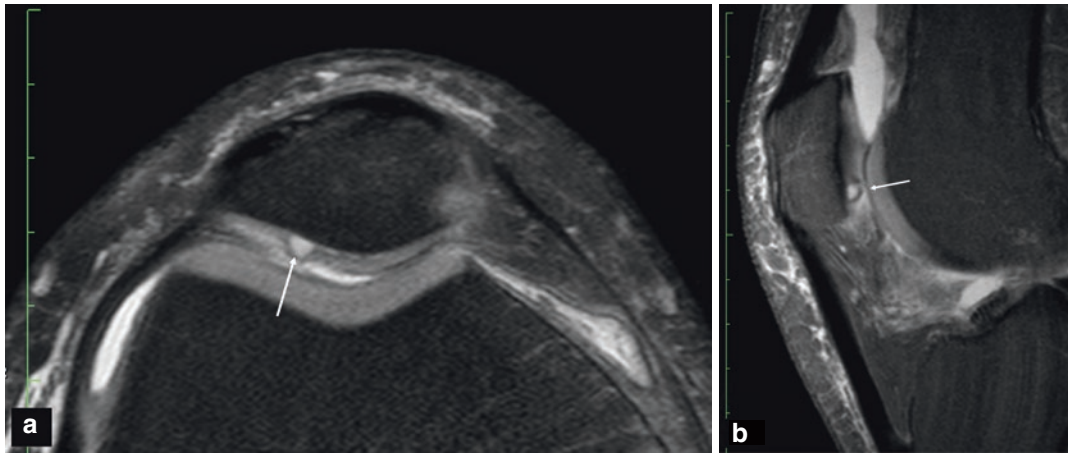

Figure 7.2.A.4.b: International Cartilage Repair Society (ICRS) Grade 3 Focal Chondral Lesion on Magnetic Resonance Imaging. A 35-year-old female presented with a right-sided anterior knee pain following a knee jerk 1 year ago. (**a**) Fat-suppressed PD-weighted axial and (**b**) sagittal images on magnetic resonance imaging (MRI) showed a small focal chondral fluid signal intensity at the tide mark with a smooth overlying chondral surface along the lateral patellar facet, suggestive of a chondral delamination or a blister formation. No evident subchondral marrow edema was noted. Delamination is the separation of the articular cartilage from the subchondral bone with a cleavage plane situated at the level of the base of the cartilage. It is associated with smooth overlying chondral surface and hence may be occult on arthroscopy. Blister formations are categorized as ICRS grade 3 lesions. Delamination may also result in complete separation of the articular cartilage from the subchondral bone and its displacement from the parent bone

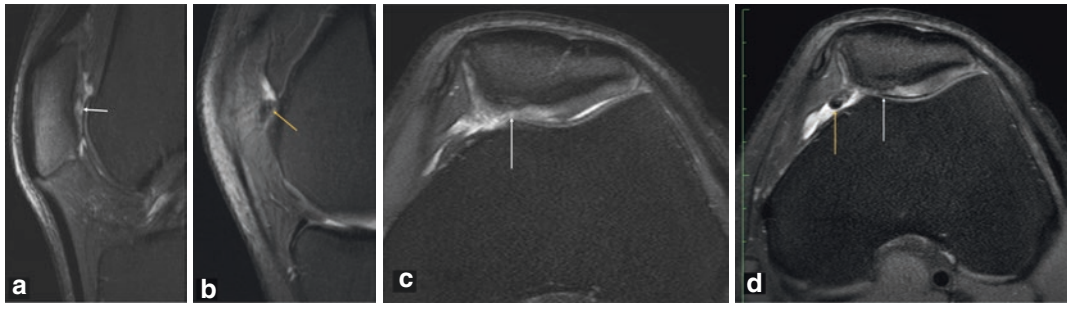

Figure 7.2.A.4.c: International Cartilage Repair Society (ICRS) Grade 3 Focal Chondral Lesion on Magnetic Resonance Imaging. A young football player had a sudden onset of pain in left knee following a forceful jerk of the knee while playing. The fat-suppressed PD-weighted (**a**, **b**) sagittal and (**c**, **d**) axial images on magnetic resonance imaging revealed focal near full thickness chondral defect (white arrow) at the patellar apex and medial patellar facet with an associated chondral flap (yellow arrow) hanging in the medial suprapatellar pouch, attached to the medial edge of the defect. There was a chondral surface irregularity at the patellar apex with hyperintense chondral edematous changes. However, no evident subchondral marrow edema-like signal changes were noted. This type of chondral injury comprising of chondral fissuring with horizontal extension along the base of the cartilage and a flap formation without subchondral marrow edema is included in ICRS grade 3 lesion as it involves >50% thickness of the cartilage

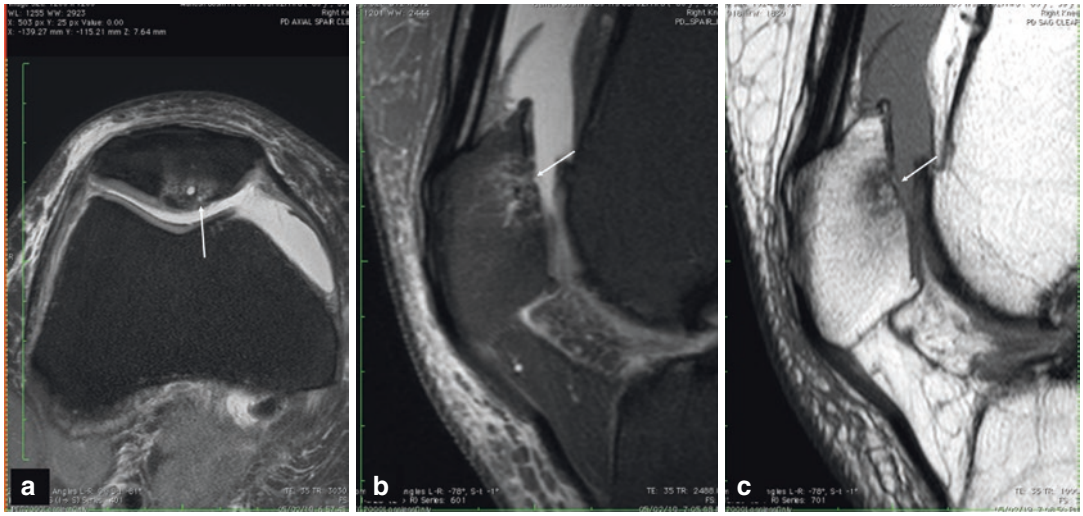

Figure 7.2.A.5.a: International Cartilage Repair Society (ICRS) Grade 4 Focal Chondral Lesion on Magnetic Resonance Imaging. A 45-year-old male suffered with right knee pain for 3 years and underwent a magnetic resonance imaging (MRI). (**a**, **b**) The fat-suppressed PD-weighted axial and sagittal images revealed a large full thickness chondral loss at the patellar apex with subchondral cyst-like changes and edema-like marrow signal intensity suggestive of ICRS grade 4 chondral lesion. (**c**) A non-fat-suppressed PD-weighted sagittal image confirmed chondral changes with a better delineation of the subchondral marrow lesion

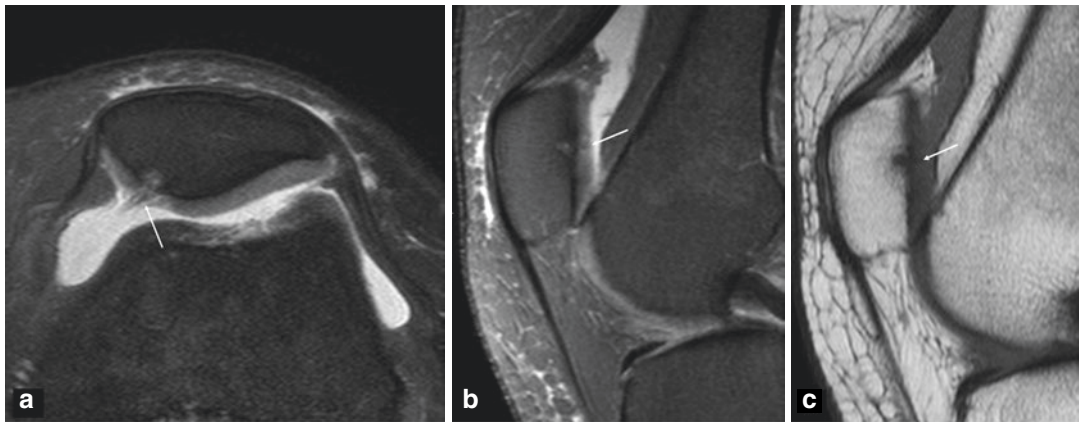

Figure 7.2.A.5.b: International Cartilage Repair Society (ICRS) Grade 4 Focal Chondral Lesion on Magnetic Resonance Imaging. A 42-year-old male with history of left-sided anterior knee pain while climbing stairs for 6 months was advised a magnetic resonance imaging (MRI) examination. The PD-weighted fat-suppressed (**a**) axial and (**b**) sagittal and (**c**) PD-weighted non-fat-suppressed sagittal image showed a focal full thickness chondral fissure involving the entire thickness of the articular cartilage at the medial patellar facet with a focal edema-like marrow signal intensity. The sagittal image did not truly demonstrate the full thickness involvement of the cartilage due to the oblique morphology of the chondral fissure, a partial volume averaging effect of the true sagittal plane and an oblique orientation of the patellar facet. However, the presence of edema-like marrow signal intensity should prompt the clinician to search the true extent of the chondral fissure in another imaging plane, as is evident on (**a**) axial plane, with the fissure extending to the subchondral bone cortex. Such lesions are graded as ICRS grade 4 lesions

7.2.B Osteochondral Lesions

Osteochondral lesion is a broad and nonspecific term that is used to refer to any lesion that involves the articular surface and the subchondral region of a joint, affecting both the cartilage and the bone. Recently a white paper was published by the Society of Skeletal Radiology (SSR) Subchondral Bone Nomenclature Committee [9] after a comprehensive review of the medical literature, and the paper recommended a pattern for the use of terms like osteochondral defects, osteochondritis dissecans, and osteochondral fractures. The term "osteochondral defect" was recommended to describe a focal defect in the articular cartilage and the subchondral bone. A specific diagnosis or cause and chronicity of the osteochondral defect should be stated wherever possible. The term "osteochondritis dissecans" should be reserved for a chronic osteochondral

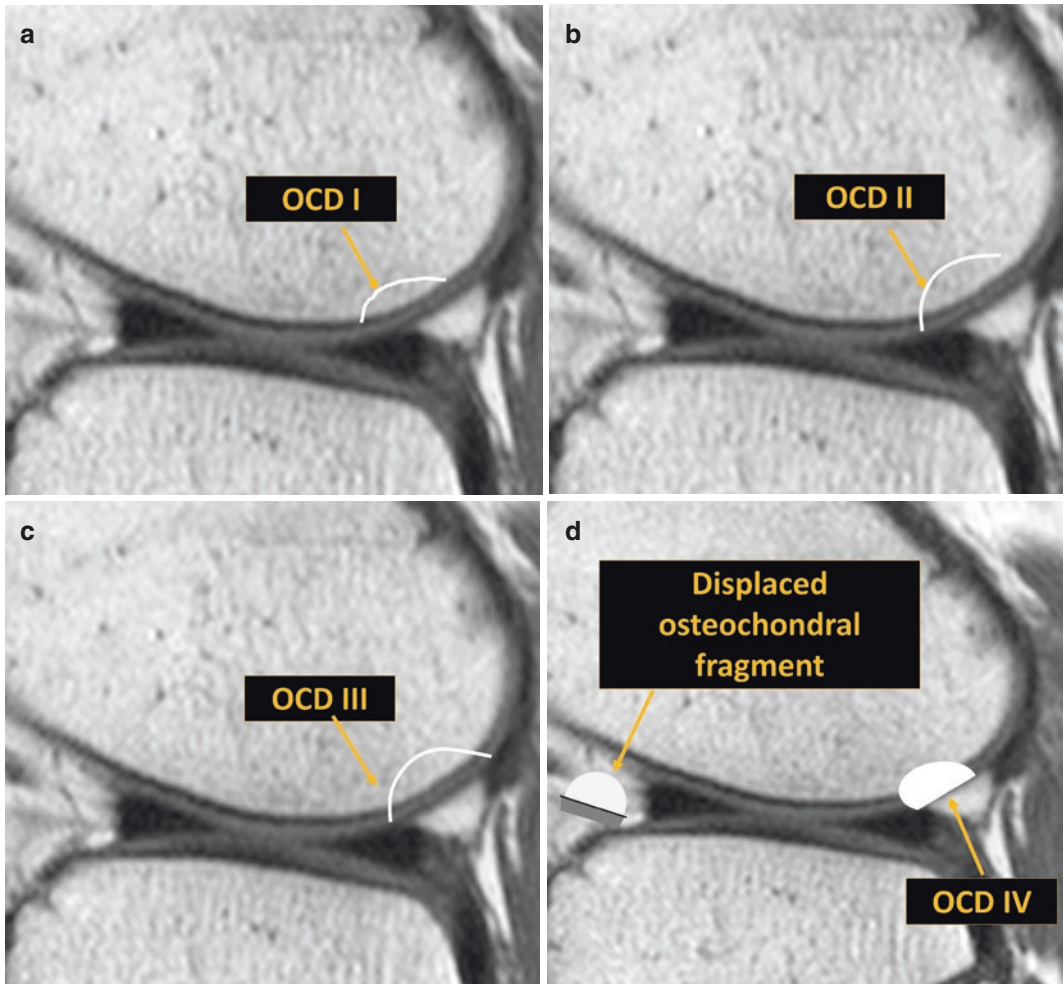

Figure 7.2.B.1: Osteochondritis Dissecans: Magnetic Resonance Imaging-Based Adaptation of International Cartilage Repair Society Staging. Schematic presentation of magnetic resonance imaging-based adaptation of the ICRS (International Cartilage Repair Society) staging system of osteochondritis dissecans (OCD) [15]. (**a**) Stable lesion in continuity with the host bone and covered by an intact articular cartilage is categorized as stage 1 OCD. (**b**) Stable lesion showing partial discontinuity of the cartilage from the host bone is categorized as stage 2 OCD. (**c**) Stage 3 OCD is characterized when there is an unstable lesion showing a complete discontinuity of the "dead in situ" lesion. However, the fragment is not dislocated. (**d**) Presence of an osteochondral defect with a dislocated fragment is categorized as stage 4 OCD

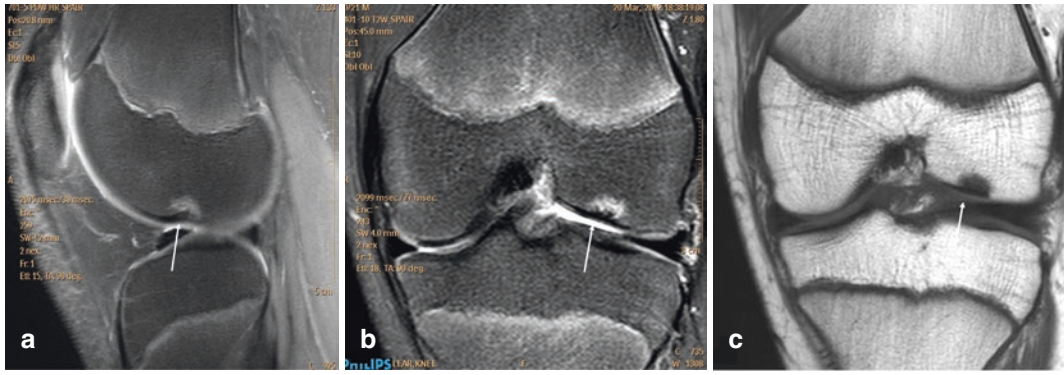

Figure 7.2.B.2: Osteochondritis Dissecans (OCD): International Cartilage Repair Society-Adapted Magnetic Resonance Imaging Stage 1 OCD. Magnetic resonance imaging (MRI)-based classification of OCD is adapted from the International Cartilage Repair Society (ICRS) classification [15] and classifies stage 1 as a stable lesion that is in continuity with the host bone and is covered by an intact articular cartilage. A 14-year-old male patient presenting with an insidious onset left-sided knee pain came for an MRI examination. (**a**, **b**) A fat-suppressed PD-weighted sagittal and coronal image and (**c**) a non-fat-suppressed PD-weighted coronal image revealed a smooth cartilage surface and the associated subchondral hypointense area with a subchondral collapse/cortical depression and the adjacent edema-like marrow signal intensity involving the anterior weight-bearing aspect of the lateral femoral condyle. No evident focal chondral fissuring or cleavage plane was visible. This is a stable lesion graded as ICRS stage 1 osteochondritis dissecans

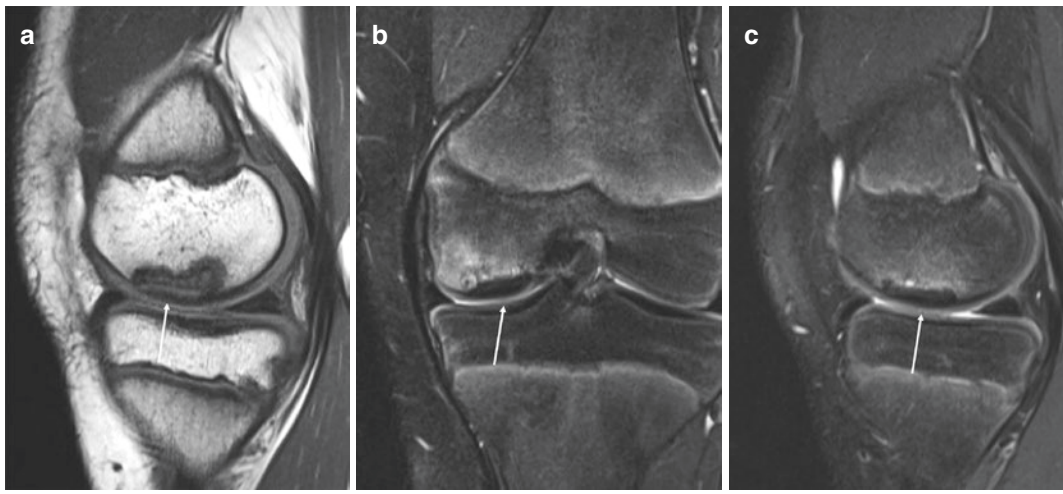

Figure 7.2.B.3: Osteochondritis Dissecans (OCD): International Cartilage Repair Society-Adapted Magnetic Resonance Imaging Stage 2 OCD. Stable osteochondritis dissecans showing partial discontinuity of the lesion from the host bone is classified as stage 2 lesions on magnetic resonance imaging (MRI), the classification being adapted from the International Cartilage Repair Society (ICRS) classification [15]. The hyperintense cleavage or partial discontinuity may be visible as a fissure on the arthroscopy. These lesions are further divided into stage 2-A lesions having a marrow edema and stage 2-B lesions without a marrow edema. A 16-year-old male patient presenting with the left-sided knee pain underwent MRI. (**a**) A non-fat-suppressed PD-weighted sagittal image and (**b**, **c**) fat-suppressed PD-weighted coronal and sagittal images revealed a large osteochondral lesion involving medial femoral condyle with the adjacent subchondral cyst-like changes and edema-like marrow signal intensity. Focal fluid signal was noted between the parent bone and the osteochondral lesion without an evidence of a complete separation suggesting a stage 2 OCD. No evidence of displacement of the fragment was noted

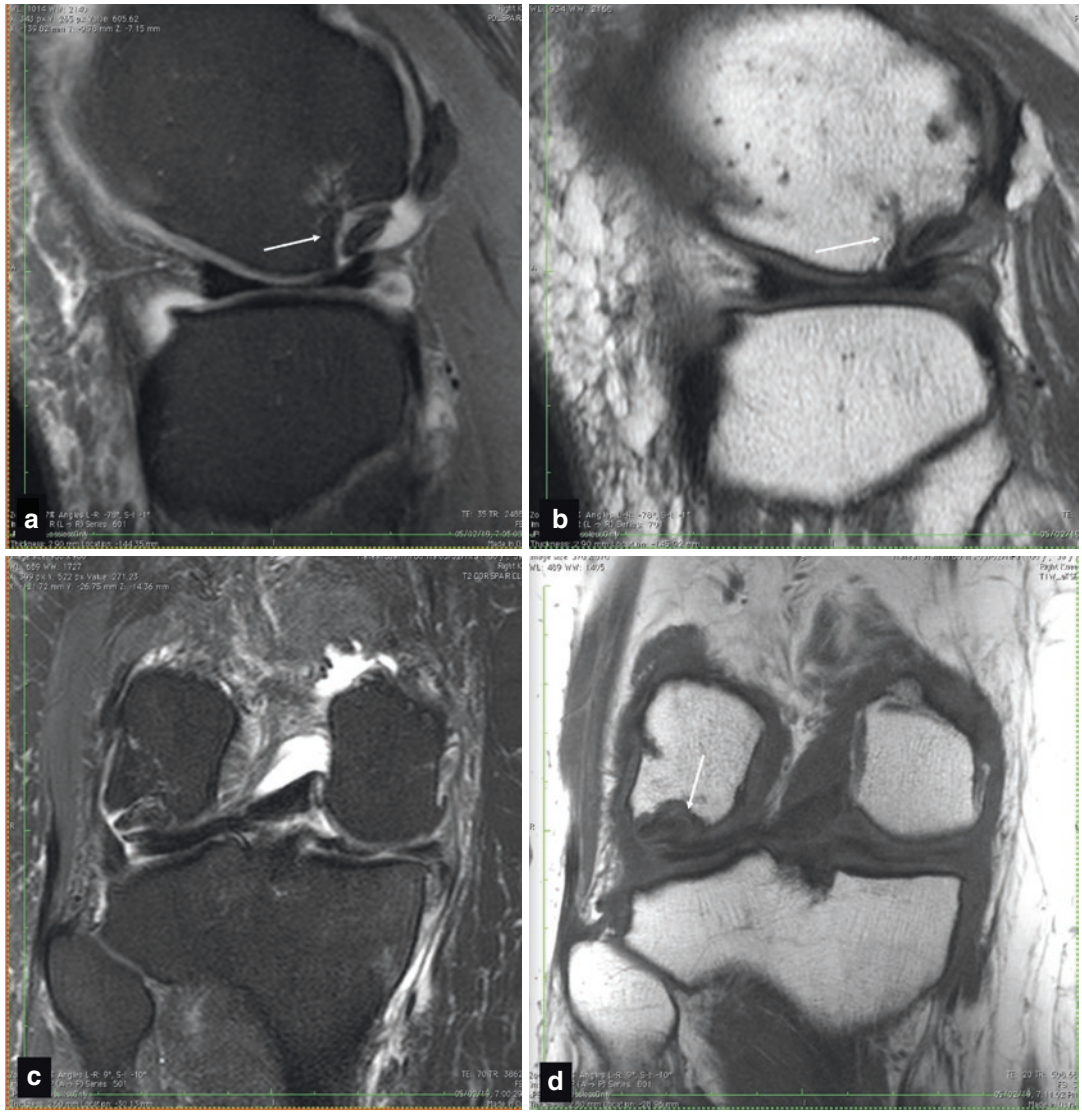

Figure 7.2.B.4: Osteochondritis Dissecans (OCD): International Cartilage Repair Society-Adapted Magnetic Resonance Imaging Stage 3 OCD. An unstable un-displaced osteochondral fragment with a complete discontinuity from the parent bone is classified as a stage 3 osteochondritis dissecans (OCD) on magnetic resonance imaging (MRI) (adapted from the International Cartilage Repair Society (ICRS) classification) [15]. A 30-year-old male patient presented with a lateral right-sided knee pain and underwent an MRI examination. (**a**, **b**) The fat-suppressed and non-fat-suppressed PD-weighted sagittal images and (**c**, **d**) the fat-suppressed and non-fat-suppressed PD-weighted T1-weighted coronal images revealed a focal unstable completely detached osteochondral lesion involving the postero-lateral weight-bearing aspect of the lateral femoral condyle without dislocation of the osteochondral fragment from the parent bone suggestive of a stage 3 OCD. The complete discontinuity of the fragment was noted. Edema-like marrow signal intensity was also noted in the parent bone adjacent to the osteochondral lesion. These findings confirmed the diagnosis of a stage 3 OCD

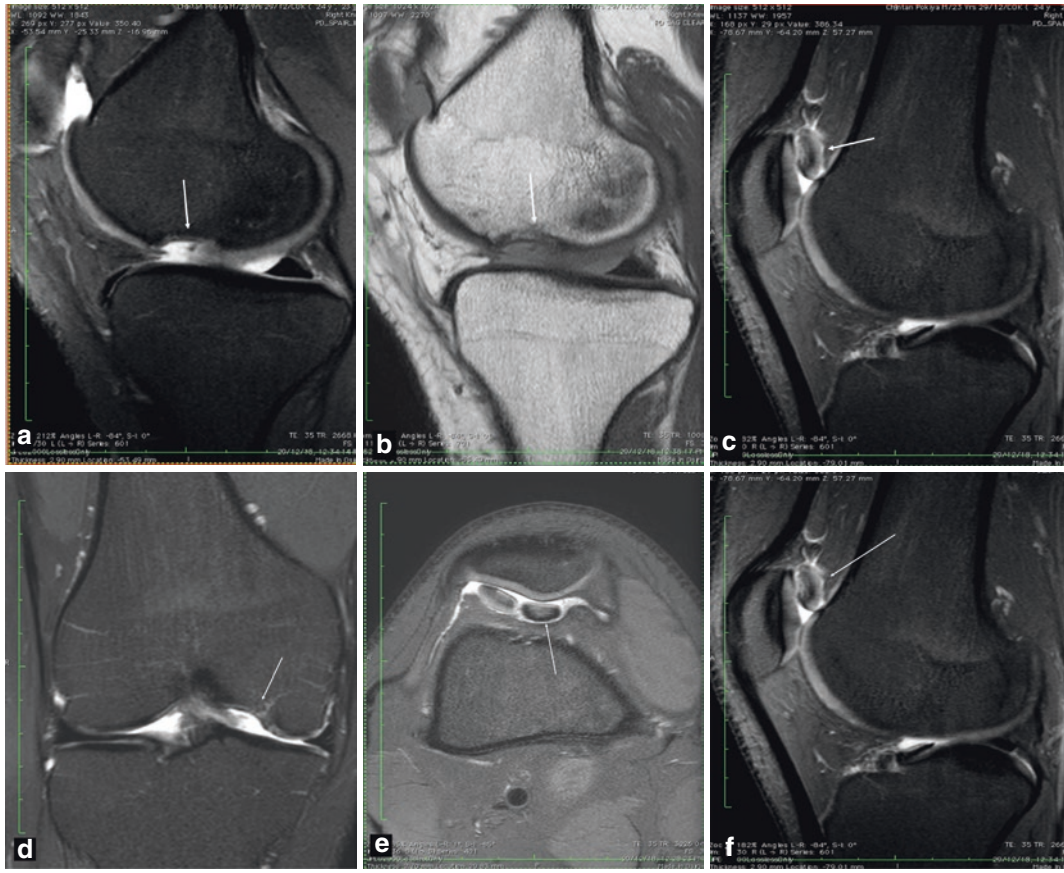

Figure 7.2.B.5: Osteochondritis Dissecans (OCD): International Cartilage Repair Society-Adapted Magnetic Resonance Imaging Stage 4 OCD. A completely separated and dislocated osteochondral fragment is classified as a stage 4 osteochondritis dissecans on magnetic resonance imaging (adapted from the International Cartilage Repair Society (ICRS) classification) [15]. A 22-year-old male patient presented with a long-standing right-sided medial knee pain and intermittent episodes of knee locking. (**a**, **b**) The fat-suppressed and non-fat-suppressed PD-weighted sagittal images and (**c**, **d**) the 3D gradient echo sagittal and T2-weighted fat-suppressed coronal images showed osteochondral defect involving the medial femoral condyle with a dislocated fragment. (**e**, **f**) The fat-suppressed PD-weighted axial and sagittal images showed two dislocated osteochondral fragments in the patellofemoral region. Note the intermediate signal chondral surface with a T2 dark subchondral plate in the dislocated fragments and the size of the displaced fragments corresponding to the osteochondral defect. These findings confirmed the diagnosis of a stage 4 OCD

lesion occurring in the young adults and children at a classic location. The recognized sites of osteochondral dissecans are the femoral condyle (most common), the humeral head, the talus, and the capitulum of the humerus. It describes a progressive separation of the articular cartilage and the underlying subchondral bone with the cleavage plane situated in the subchondral bone and eventually involving the full thickness of the overlying articular cartilage. The term "osteochondral fracture" should be used in the setting of an acute trauma, and it may manifest as a subchondral bone depression or fragmentation creating an osteochondral fragment.

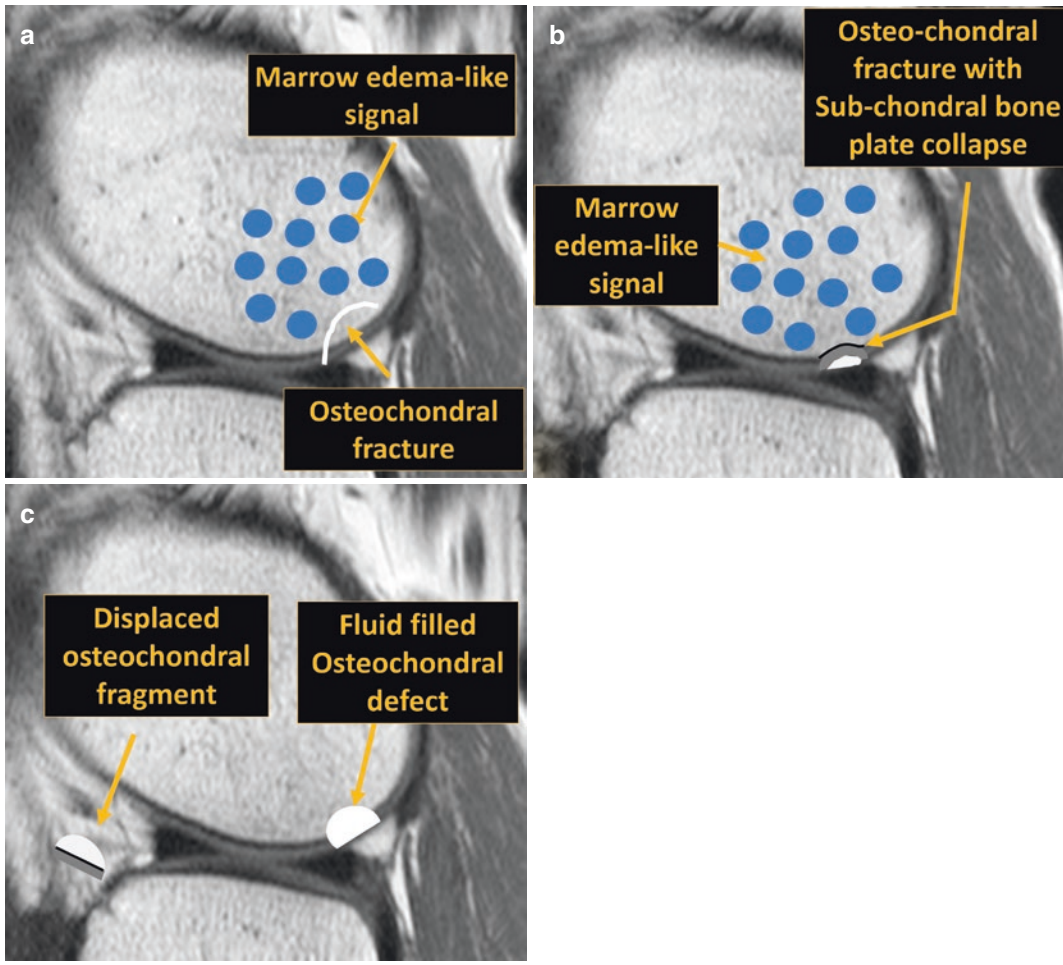

Figure 7.2.B.6: Schematic Presentation of Types of Osteochondral Fractures. The schematic presentation of types of osteochondral fractures [9]. (**a**) In the setting of an acute trauma, osteochondral fracture may present as an osteochondral lesion with a complete or incomplete fracture line through the articular cartilage and the subchondral bone. (**b**) Occasionally the osteochondral fracture line may also be associated with a subchondral bone plate depression. (**c**) The osteochondral fracture can also be associated with a localized defect involving the cartilage and the subchondral bone leading to a displaced osteochondral fracture fragment

Magnetic resonance imaging is the modality of choice for determining the extent and stability of the osteochondral lesions [10, 11] and acts as a guide for the further management. A three-dimensional gradient echo (GRE) T1-weighted MR imaging combined with the routine sequences demonstrates excellent diagnostic capabilities in detecting the unstable osteochondral lesions. De Smet et al. [12, 13] suggested the presence of any one of the four MRI findings indicative of an unstable osteochondral lesion. These findings include (1) a high signal line deep to the fragment as seen on the T2-weighted images, (2) an articular fracture indicated by a high signal passing through the subchondral bone plate, (3) a focal osteochondral defect, and (4) a 5-mm-diameter fluid-filled

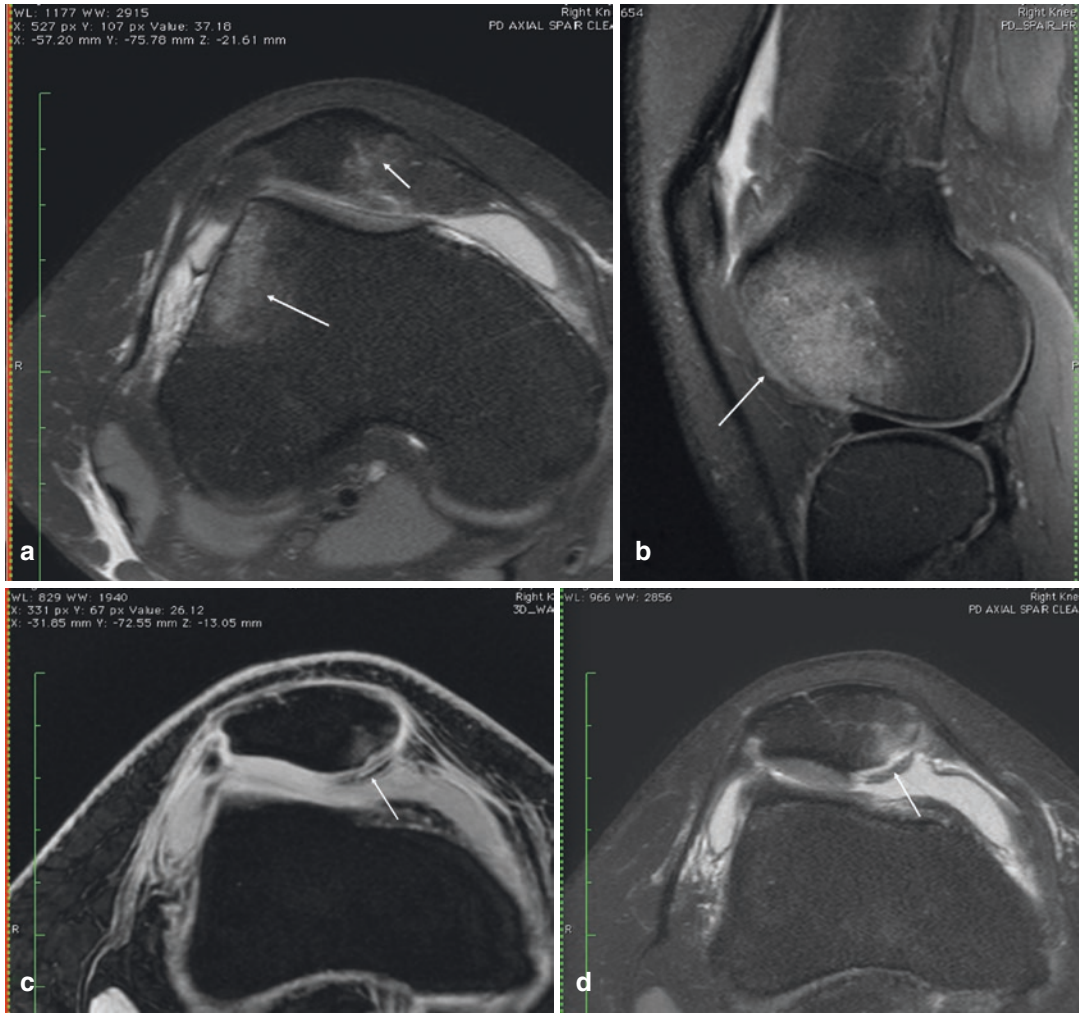

Figure 7.2.B.7: The Osteochondral Fracture: Complete Un-displaced Fragment. The unstable osteochondral fracture involving the right-sided infero-medial patellar facet in a 17-year-old boy with a history of transient lateral patellar dislocation was detected on magnetic resonance imaging. (**a**, **b**) The fat-suppressed PD-weighted axial and sagittal images revealed a bone marrow contusion at the antero-lateral aspect of the lateral femoral condyle. (**b**) Note the high-lying patella on the sagittal images. (**c**) The gradient echo axial image and (**d**) the fat-suppressed PD-weighted axial image revealed a focal unstable completely detached osteochondral fragment at the infero-medial aspect of the patella as evident by the fluid signal undermining the osteochondral fragment and the adjacent edema-like marrow signal intensity at the site of impact. Though the fragment is completely detached, it has not dislodged from the host location

cyst deep to the lesion. Other authors [14] have suggested that the presence of a bright line deep to the osteochondral fragment may result from a granulation tissue and that a break in the articular surface must be demonstrated with MRI to be sure that the fragment is unstable. Therefore, ICRS grade 1 osteochondral lesions may not demonstrate any of the four criteria described by De Smet et al. [12] on MRI. Magnetic resonance imaging can detect a displacement of the fragment from the bed, which would allow a proper staging of the ICRS grade 4 osteochondral lesions.

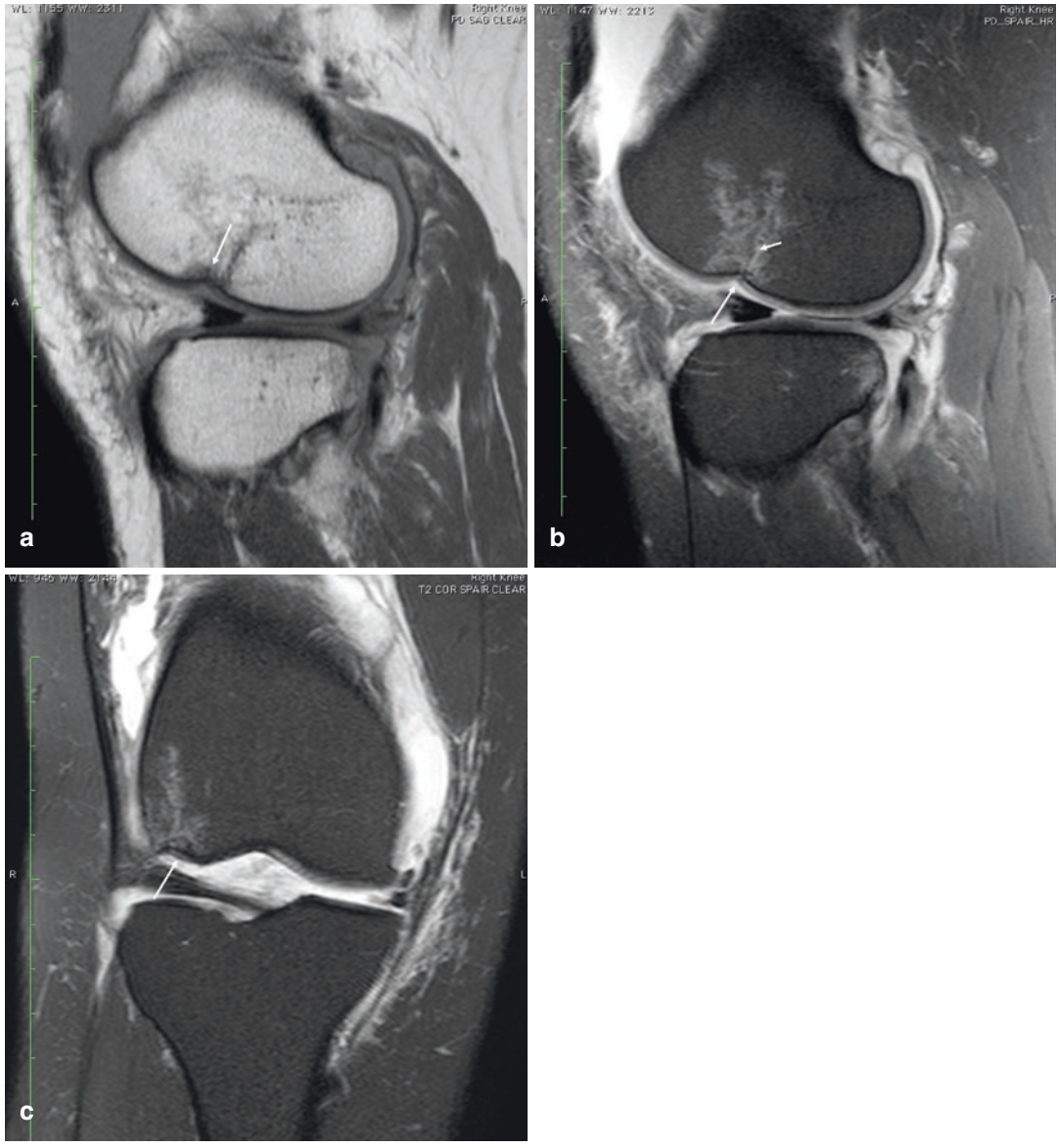

Figure 7.2.B.8: The Osteochondral Fracture: Subchondral Bone Depression. An impaction/osteochondral fracture with collapse of the subchondral bone involving the anterior weight-bearing aspect of the right-sided lateral femoral condyle was detected on magnetic resonance imaging in a 23-year-old female with a history of twisting injury while playing tennis. (**a**, **b**) The non-fat-suppressed and fat-suppressed PD-weighted sagittal images revealed subchondral marrow edema-like signal at the anterior weight-bearing aspect of the lateral femoral condyle with an associated focal cortical depression suggestive of a subchondral collapse (characteristic site of the trabecular injury associated with an anterior cruciate ligament injury representing "footprint" of the injury). (**c**) The fat-suppressed PD-weighted coronal image revealed focal cortical depression with a subchondral marrow edema-like signal at the characteristic location. No evident unstable osteochondral fragment was noted. This pattern of contusion is classically related to a complete anterior cruciate ligament tear

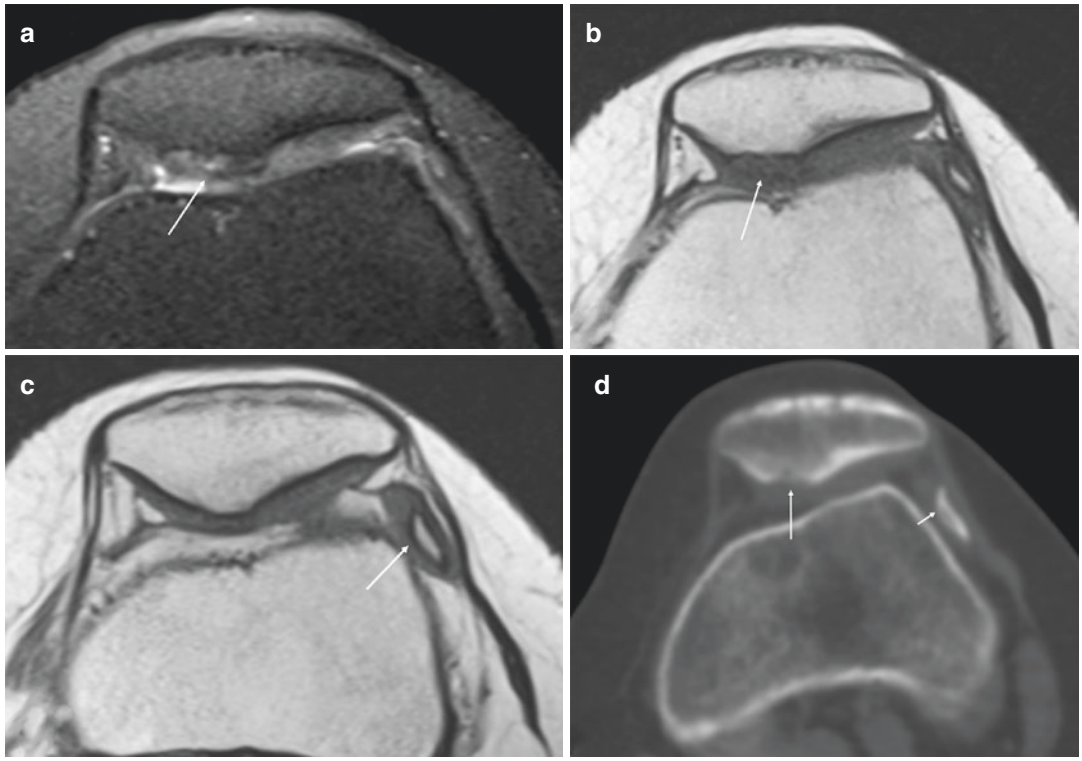

Figure 7.2.B.9: The Osteochondral Fracture: Dislocated Fragment. An unstable dislocated osteochondral fracture involving the patellar apex in a 26-year-old female with a past history of lateral patellar dislocation a year ago presented with an occasional locking of the left knee joint. (**a**, **b**) The non-fat-suppressed and fat-suppressed PD-weighted axial images showed an osteochondral defect involving the patellar apex and the medial patellar facet. (**b**) The subchondral bone plate irregularity is better appreciated in the non-fat-suppressed axial image. (**c**) A non-fat-suppressed PD-weighted axial image showed a dislocated osteochondral fragment in the lateral suprapatellar recess. The intermediate signal chondral surface with hypointense rim of subchondral plate and bone marrow signal intensity of the rest of the dislocated fragment was noted. (**d**) The CT scan image of the same patient better delineated the osteochondral defect at the medial patellar facet and patellar apex (as marked by long white arrow) and the corresponding sized dislocated osteochondral fragment in the lateral suprapatellar recess. The above findings represented an unstable dislocated osteochondral fracture

7.2.C Subchondral Lesions

The white paper published by the Society of Skeletal Radiology (SSR) Subchondral Bone Nomenclature Committee [9] after a comprehensive review of the medical literature also provided recommendations for the use of the terms like subchondral fractures, subchondral insufficiency fractures, epiphyseal collapse, spontaneous osteonecrosis of the knee and osteonecrosis, etc. Subchondral insufficiency fractures (SIF) are the fractures that occur below the chondral surface, particularly in the older patient, and characterized clinically by the sudden onset of severe knee pain in the absence of trauma or following minor trauma [9]. Patients with subchondral insufficiency fracture characteristically have unremarkable plain radiographs, while MRI examination may reveal extensive edema-like marrow signal intensity with or without subchondral bone collapse, which when present represents irreversibility and a poor prognosis. The metaphyseal burst sign [16] described as a soft tissue edema in the meta-epiphyseal region of the affected condyle has been recently described as a secondary sign on MRI of a subchondral insufficiency fracture of the knee. Correlation with clinical history is essential to differentiate an acute trau-

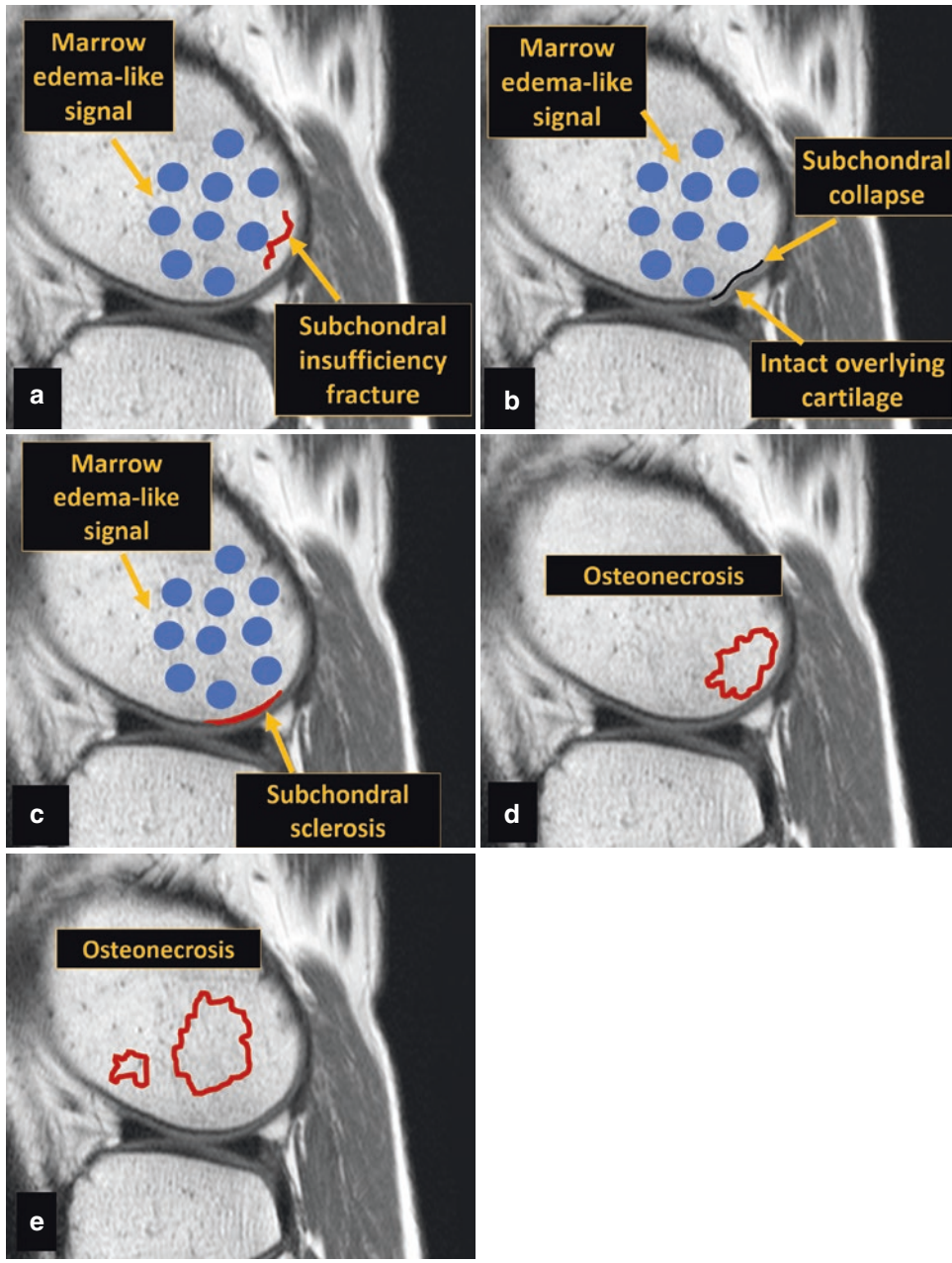

Figure 7.2.C.1: Schematic Presentation of Subchondral Lesion. A schematic presentation of the subchondral lesions [9]. (**a**) A subchondral fracture is defined as an irregular, serpentine, discontinuous subchondral linear signal intensity located subjacent to the subchondral bone plate but at a distance away from the bone plate. If there is an associated chondral involvement, then the term osteochondral fracture is used. (**b**) The subchondral bone collapse refers to the fracture of the subchondral bone plate with a resultant focal cortical depression or step-off, asphericity, and a subchondral plate flattening. It is important to identify the presence of subchondral bone collapse as it represents irreversibility and possibility of the disease progression. (**c**) The subchondral sclerosis presents as a subchondral crescentic hypointense area subjacent to the subchondral bone producing an apparent thickening of the subchondral plate. It may or may not be associated with subchondral plate collapse. It is a manifestation of the mechanical stresses endured by the subchondral bone and can be observed in a subchondral insufficiency fracture, acute traumatic subchondral fracture, and osteoarthritis. (**d**, **e**) A geographic serpiginous marginated subchondral lesion with a central area of preserved marrow signal intensity is termed as osteonecrosis. It may involve the marrow immediately subjacent to the bone plate (**d**) or can be away from it. (**e**) The peripheral rim of osteonecrotic lesion completely encircles the infarcted area without interruption and is typically concave to the articular surface

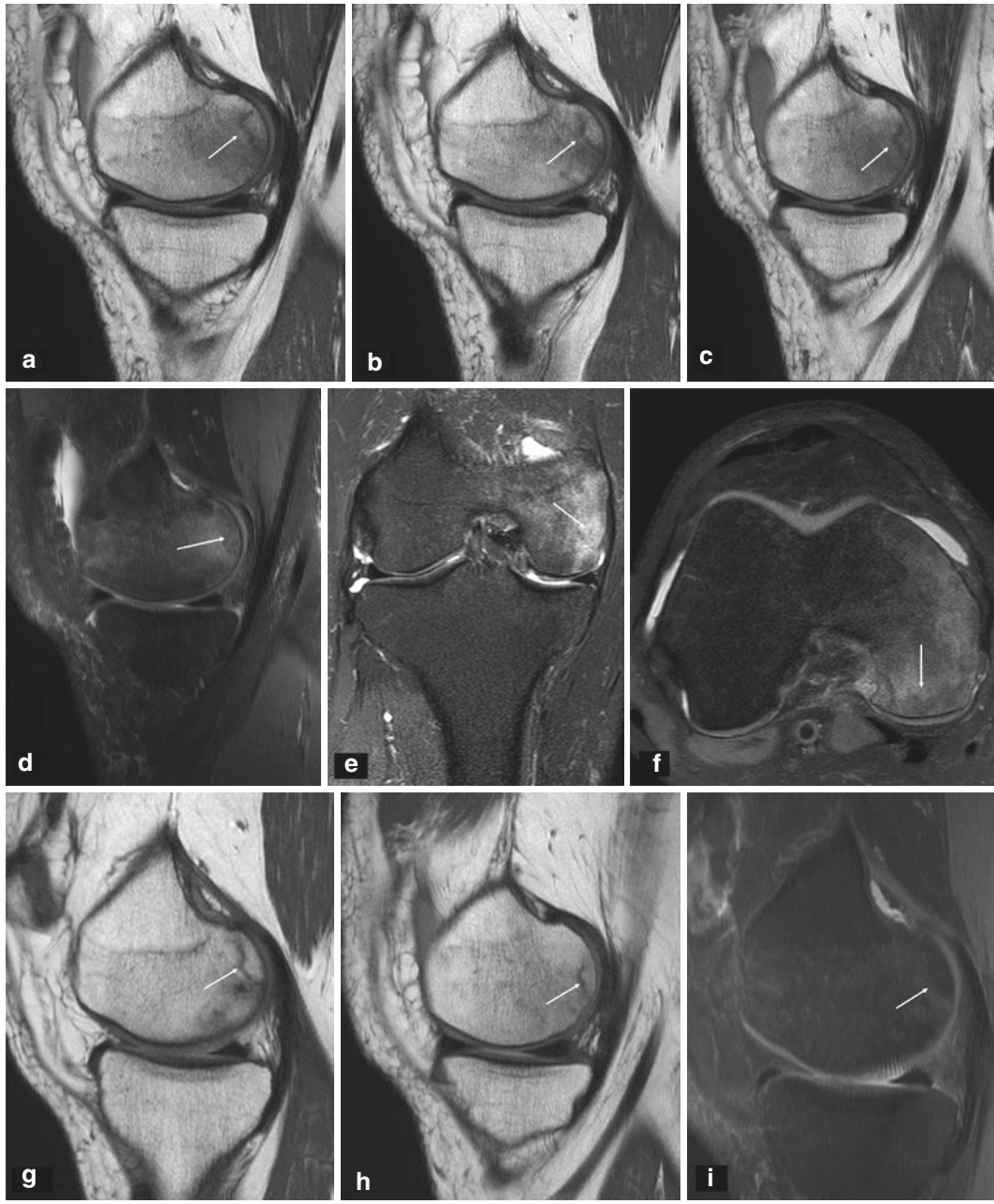

Figure 7.2.C.2.a: Lesions of the Subchondral Bone: Subchondral Insufficiency Fracture. A subchondral insufficiency fracture involving the medial femoral condyle in a 55-year-old male with an insidious onset of right knee pain while walking. (**a**–**c**) The non-fat-suppressed PD-weighted sagittal images showed an incomplete curvilinear hypointense rimmed lesion involving the subchondral bone at the posterior non-weight-bearing aspect of the medial femoral condyle. (**d**–**f**) The fat-suppressed PD-weighted sagittal, coronal, and axial images revealed a diffuse adjacent subchondral edema-like marrow signal intensity. The intact smooth overlying chondral surface suggests an absence of any chondral injury. It was difficult to differentiate from an osteonecrosis on primary imaging. (**g**–**i**) However, a 3-month follow-up with non-fat-suppressed and fat-suppressed PD-weighted sagittal images of above patient showed a near static curvilinear subchondral hypointense rimmed lesion at the posterior non-weight-bearing aspect of the medial femoral condyle with a significant regression in the extent of the adjacent subchondral edema-like marrow signal intensity suggesting a reversibility on imaging and confirmation of the radiological diagnosis of a subchondral insufficiency fracture

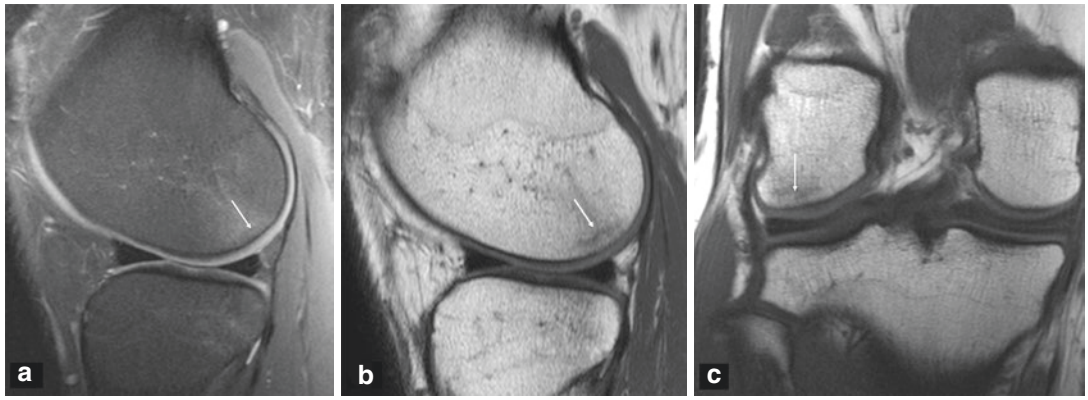

Figure 7.2.C.2.b: Lesions of the Subchondral Bone: Acute Traumatic Subchondral Insufficiency Fracture. An acute traumatic subchondral fracture involving the lateral femoral condyle in a 23-year-old male with a sudden onset right knee pain following a jump from 5′ height. (**a**, **b**) The fat-suppressed and non-fat-suppressed PD-weighted sagittal and (**c**) non-fat-suppressed PD-weighted coronal images showing an incomplete curvilinear hypointense line parallel to, but away from the T2 hypointense subchondral bone plate at the posterior weight-bearing aspect of the lateral femoral condyle with an adjacent subchondral edema-like marrow signal intensity. Note the intact smooth overlying chondral surface and an absence of an associated chondral injury. The clinical history of trauma in a young patient with the above findings clinches the diagnosis of an acute traumatic subchondral fracture

matic subchondral fracture from the subchondral insufficiency fractures [9]. SIF are associated with a more extensive edema-like marrow signal intensity and mostly show hypointense fracture line on all pulse sequences, as compared from the acute traumatic subchondral fractures, which typically show T1 hypointense and T2 hyperintense fracture lines [9].

The term "SONK (spontaneous osteonecrosis of knee)" is now replaced by "subchondral insufficiency fracture" as it is now believed that it is almost always preceded by and indeed caused by an underlying subchondral insufficiency fracture [17–19]. An MRI helps determine the associated irreversible findings such as a subchondral bone plate collapse and the findings associated with a poor prognosis like a subchondral hypointense area which denotes a secondary osteonecrosis. It typically appears in the elderly women presenting as a sudden onset knee pain in an atraumatic setting. The differential diagnosis may be challenging and includes bone infarcts in the other locations and the underlying systemic conditions causing necrosis.

Osteonecrosis or avascular necrosis represents complete loss of blood supply to the bone and includes bone infarcts (metaphyseal) and avascular necrosis (epiphyseal). It manifests as uninterrupted geographic area with a central mummified fat or yellow marrow as compared from SIF which typically appears as low signal intensity discontinuous irregular fracture line parallel to the articular surface [20, 21]. The depth of low signal intensity band from the articular surface has also been reported as a helpful discriminating finding of SIF from osteonecrosis; the mean depth is 1.56 mm for SIF and 15.36 mm for osteonecrosis [22]. "Double line sign" on T2-weighted images comprising of an outer low signal intensity rim of sclerosis and an inner high signal intensity zone of reparative granulation tissue at the reactive interfaces is seen in 65–85% of patients and is pathognomic of osteonecrosis [19, 23].

Contrast-enhanced studies can help the differentiation of osteonecrosis from subchondral insufficiency fractures on MR imaging. A SIF is enhancing compared with non-enhancing devitalized bone in osteonecrosis [24]. The SIF is rarely bilateral, whereas osteonecrosis is quite often bilateral (50–70%) [25].

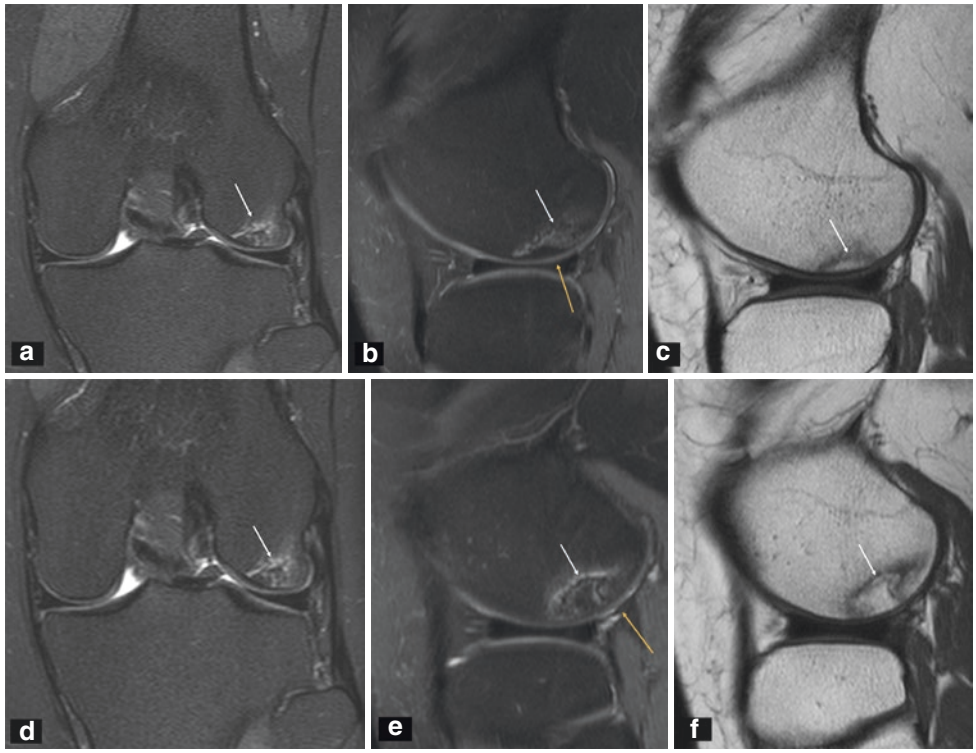

Figure 7.2.C.3.a: Lesions of the Subchondral Bone: Osteonecrosis. A 29-year-old female patient with known interstitial lung disease on long-standing steroid treatment and a known avascular necrosis of the hip joint presented with a left-sided knee pain. The magnetic resonance imaging examination revealed a subchondral bone marrow lesion of the lateral femoral condyle representing an osteonecrosis. The fat-suppressed coronal (**a**, **d**) and sagittal (**b**, **e**) and the non-fat-suppressed PD-weighted sagittal images (**c**, **f**) revealed a well-defined subchondral lesion with a serpiginous peripheral rim and a central preserved fatty marrow and a mild adjacent edema-like marrow signal intensity involving the posterior weight-bearing aspect of the lateral femoral condyle suggestive of an osteonecrosis. The intact overlying articular cartilage (yellow arrow) suggests an absence of a chondral injury. No osseous fragmentation/collapse of the subchondral bone was observed in this case, a feature that represents advanced stages of irreversibility

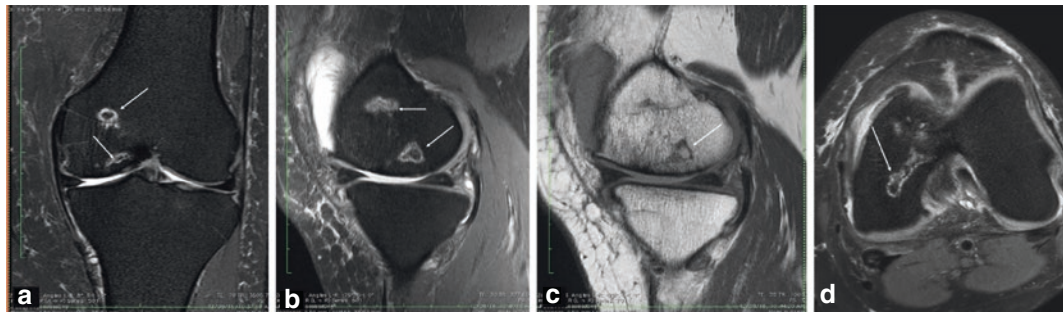

Figure 7.2.C.3.b: Lesions of the Subchondral Bone: Osteonecrosis. A known case of sickle cell disease in a 48-year-old female patient with primary osteonecrosis/bone infarcts had complaints of left-sided knee pain for 2 months. (**a**, **b**, **d**) The fat-suppressed PD-weighted coronal, sagittal, and axial and (**c**) non-fat-suppressed PD-weighted sagittal images of the left knee revealed a well-defined subchondral lesion with a serpiginous peripheral rim and a central preserved fatty marrow and a mild adjacent edema-like marrow signal intensity involving the posterior weight-bearing aspect of the lateral femoral condyle suggestive of osteonecrosis. The overlying articular cartilage appeared intact. No evident fragmentation/collapse of the subchondral bone was seen, the features usually seen in advanced cases

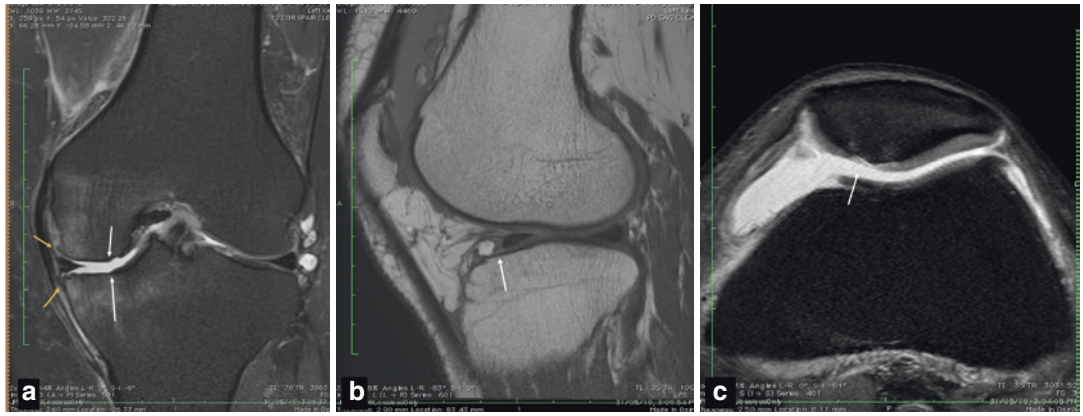

Figure 7.2.D.1 Degenerative Osteoarthritis. A 60-year-old man with the left-sided knee pain revealed medial tibio-femoral and patella-femoral compartment osteoarthritic changes on magnetic resonance imaging. (**a**) The fat-suppressed T2-weighted coronal image revealed diffuse full thickness chondral loss with diffuse subchondral edema-like marrow signal intensity involving the weight-bearing aspect of the medial tibio-femoral joint. The marginal lipping (yellow arrows) at the distal medial condyle of the femur and the proximal medial tibial plateau favored osteoarthritis. (**b**) The non-fat-suppressed PD-weighted sagittal image showed a small osseous loose body at the anterior aspect. (**c**) The fat-suppressed PD-weighted axial image revealed a focal full thickness chondral loss at the medial patellar facet with subtle subchondral edema-like marrow signal intensity. All the changes confirmed the diagnosis of osteoarthritis

7.2.D Degenerative Osteoarthritis

Diffuse ill-defined subchondral bone sclerosis and marrow edema in conjunction with varying degrees of adjacent cartilage alterations is hallmark of knee osteoarthritis on an MRI [26]. The higher grade of cartilage loss is associated with a higher prevalence and a greater volume of concomitant bone marrow lesions [3]. As the disease progresses, there is an increase in the volume of the bone marrow lesions at the sites of progressive cartilage damage and the resultant increasing joint space narrowing. An associated subchondral edema-like marrow signal intensity is best depicted on fat-suppressed PD- or T2-weighted or STIR images [2]. A non-fat-suppressed T1-weighted image best depicts the subchondral sclerosis as low signal intensity compared from the physiologic fatty marrow [2].

7.3 Take-Home Message

MRI is the investigation of choice and is the best non-invasive imaging modality for the evaluation of the chondral, the osteochondral, and the subchondral lesions. The newer nomenclature of the osteochondral and subchondral lesions allows further clarity in the use of various conflicting terms. Being an adaptation of the arthroscopic grading systems, MR grading systems allow the radiologists and orthopedic surgeons to document and to compare these lesions with concurring terminologies. It also allows better pre-operative understanding of the lesions and assists in the management and the surgical planning, wherever necessary.

Acknowledgments Disclaimer: The magnetic resonance images produced in this article are duly consented by the patients.

References

1. Disler DG, McCauley TR, Kelman CG, Fuchs MD, Ratner LM, Wirth CR, Hospodar PP. Fat-suppressed three-dimensional spoiled gradient-echo MR imaging of hyaline cartilage defects in the knee: comparison with standard MR imaging and arthroscopy. AJR Am J Roentgenol. 1996;167:127–132.
2. Recht M, Bobic V, Burstein D, Disler D, Gold G, Gray M, Kramer J, Lang P, McCauley T, Winalski C. Magnetic resonance imaging of articular cartilage. Clin Orthop Relat Res. 2001;S379–396.
3. Rubin DA, Harner CD, Costello JM. Treatable Chondral Injuries in the Knee: Frequency of

Associated Focal Subchondral Edema. American Journal of Roentgenology. 2000;174:1099–1106.
4. Cole BJ, Malek MM. Articular Cartilage Lesions: A Practical Guide to Assessment and Treatment. Springer New York, New York, NY. 2004. ISBN: 0387955402.
5. Goyal D. The Classifications of the Chondral Lesions. In: Goyal D, editor. The illustrative book of cartilage repair, Springer 2021; In Press.
6. Brittberg M, et al. Evaluation of cartilage injuries and cartilage repair. Osteologie. 2000;9:17–25.
7. Brittberg M, Winalski CS. Evaluation of cartilage injuries and repair. J Bone Joint Surg Am. 2003;85(2):58–69.
8. Casula V, Hirvasniemi J, Lehenkari P, Ojala R, Haapea M, Saarakkala S, Lammentausta E, Nieminen MT. Association between quantitative MRI and ICRS arthroscopic grading of articular cartilage. Knee Surg Sports Traumatol Arthrosc. 2016;24:2046–2054.
9. Gorbachova T, Amber I, Beckmann NM, Bennett DL, Chang EY, Davis L, Gonzalez FM, Hansford BG, Howe BM, Lenchik L, Winalski CS, Bredella MA. Nomenclature of Subchondral Nonneoplastic Bone Lesions. AJR Am J Roentgenol. 2019;213:963–982.
10. O'Connor MA, Palaniappan M, Khan N, Bruce CE. Osteochondritis dissecans of the knee in children. A comparison of MRI and arthroscopic findings. J Bone Joint Surg Br. 2002;84:258–262.
11. Bohndorf K. Osteochondritis (osteochondrosis) dissecans: a review and new MRI classification. Eur Radiol. 1998;8:103–112.
12. De Smet AA, Ilahi OA, Graf BK. Untreated osteochondritis dissecans of the femoral condyles: prediction of patient outcome using radiographic and MR findings. Skeletal Radiol. 1997;26:463–467.
13. De Smet AA, Ilahi OA, Graf BK. Reassessment of the MR criteria for stability of osteochondritis dissecans in the knee and ankle. Skeletal Radiol 1996;25:159–163.
14. Zbojniewicz AM, Stringer KF, Laor T, Wall EJ. Juvenile Osteochondritis Dissecans: Correlation Between Histopathology and MRI. AJR Am J Roentgenol. 2015;205:W114–123.
15. Kohyama S, Ogawa T, Mamizuka N, Hara Y, Yamazaki M. A Magnetic Resonance Imaging-Based Staging System for Osteochondritis Dissecans of the Elbow: A Validation Study Against the International Cartilage Repair Society Classification. Orthop J Sports Med. 2018;6:2325967118794620.
16. Vidoni A, Shah R, Mak D, Beale D, Beale S, James S, Botchu R. Metaphyseal burst sign: A secondary sign on MRI of subchondral insufficiency fracture of the knee. J Med Imaging Radiat Oncol. 2018;62:764–768.
17. Kattapuram TM, Kattapuram SV. Spontaneous osteonecrosis of the knee. European Journal of Radiology. 2008;67:42–48.
18. Yamamoto T, Bullough PG. Subchondral insufficiency fracture of the femoral head and medial femoral condyle. Skeletal Radiol. 2000;29:40–44.
19. Yamamoto T, Bullough PG. Spontaneous osteonecrosis of the knee: the result of subchondral insufficiency fracture. J Bone Joint Surg Am. 2000a;82:858–866.
20. Zhao G, Yamamoto T, Ikemura S, Nakashima Y, Mawatari T, Motomura G, Iwamoto Y. A histopathological evaluation of a concave-shaped low-intensity band on T1-weighted MR images in a subchondral insufficiency fracture of the femoral head. Skeletal Radiol. 2010;39:185–188.
21. Ikemura S, Yamamoto T, Motomura G, Nakashima Y, Mawatari T, Iwamoto Y. MRI evaluation of collapsed femoral heads in patients 60 years old or older: Differentiation of subchondral insufficiency fracture from osteonecrosis of the femoral head. AJR Am J Roentgenol. 2010;195:W63–68.
22. Iwasaki K, Yamamoto T, Motomura G, Ikemura S, Yamaguchi R, Iwamoto Y. Radiologic measurements associated with the prognosis and need for surgery in patients with subchondral insufficiency fractures of the femoral head. AJR Am J Roentgenol. 2013;201:W97–103.
23. Zurlo JV. The double-line sign. Radiology. 1999;212:541–542.
24. Miyanishi K, Hara T, Kaminomachi S, Maeda H, Watanabe H, Torisu T. Contrast-enhanced MR imaging of subchondral insufficiency fracture of the femoral head: a preliminary comparison with that of osteonecrosis of the femoral head. Arch Orthop Trauma Surg. 2009;129:583–589.
25. Murphey MD, Foreman KL, Klassen-Fischer MK, Fox MG, Chung EM, Kransdorf MJ. From the radiologic pathology archives imaging of osteonecrosis: radiologic-pathologic correlation. Radiographics. 2014;34:1003–1028.
26. Li G, Yin J, Gao J, Cheng TS, Pavlos NJ, Zhang C, Zheng MH. Subchondral bone in osteoarthritis: insight into risk factors and microstructural changes. Arthritis Res Ther. 2013;15:223.

The Illustrative Role of Cells in Cartilage Repair

8

Byoung-Hyun Min

8.1 Introduction

Autologous chondrocyte implantation (ACI) introduced over 25 years ago has been a milestone treatment for the articular cartilage defects and has produced hyaline cartilage like repair and excellent clinical results [1, 2]. However, the need for two surgical procedures and cell engraftment issues has long been major shortcomings, leading to the development of alternative cell sources such as the mesenchymal stem cells.

Compared to chondrocytes, stem cells hold advantages in terms of securing a large number of cells as well as a differentiation potential for various tissue types. In order for stem cells to be reliably used in clinic, key issues must be addressed regarding the actual survival and continuing chondrogenic differentiation of the transplanted cells.

Implanting the cells from an outside or an inside source to the defect area will lead to the following sequences of events. The cells should attach to the subchondral bone and then shall proliferate as they are stimulated by surrounding stimuli such as the growth factors mechanical stimuli, etc. In addition, the cells should differentiate into chondrocytes, secrete extracellular matrix, and eventually repair cartilage tissue.

Ongoing research regarding stem cells aim to improve the survivorship and differentiation of the transplanted cells by providing a favorable environment as well as stimulation of endogenous stem cells, thereby improving the currently existing surgical methods. A variety of biomaterials are being used to enhance the engraftment of the endogenous or the implanted cells. Researchers and clinicians must understand the mode of action, pros and cons, and posttransplantation behavior of each biomaterial of interest in order to appropriately utilize them.

B.-H. Min (✉)
Department of Orthopedic Surgery, Ajou University School of Medicine, Suwon, South Korea

Department of Molecular Science and Technology, Ajou University, Suwon, South Korea

Cell Therapy Center, Ajou University Hospital, Suwon, South Korea
e-mail: dr.bhmin@gmail.com

D. R. Goyal (ed.), *The Illustrative Book of Cartilage Repair*,
https://doi.org/10.1007/978-3-030-47154-5_8

8.2 The Illustrations

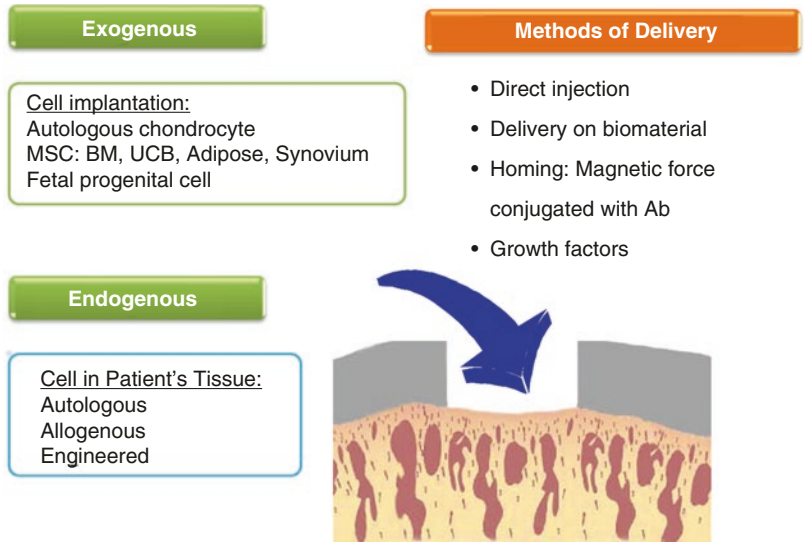

Figure 8.2.1: Cartilage Repair: Different Source of the Cells. The biologic sources for cartilage repair largely includes the use of endogenous cells or the exogenous cell by multiplication. To induce repair by endogenous stem cells, a bone marrow stimulation method is often used. For exogenous cells induced repair, cells that are proliferated by culture are used, such as chondrocytes, mesenchymal stem cells, fetal progenitor cells, etc. The exogenous cells may be implanted to the defect area by direct injection [1, 3] or by seeding into the biomaterials [4–10] or can be navigated by attaching with a magnetic bead [11, 12] or an antibody [13, 14]

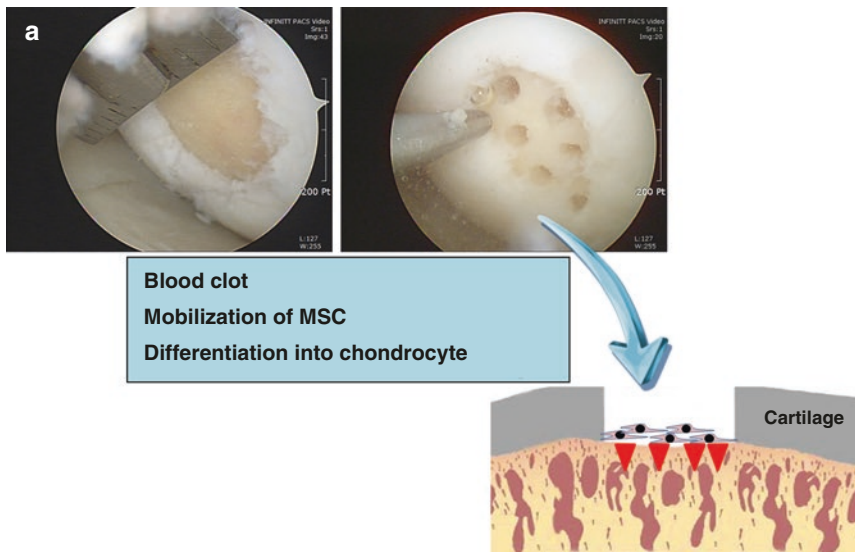

Figure 8.2.2: Cartilage Repair: The Endogenous Stem Cells from the Bone Marrow. The most commonly used method of accessing the endogenous stem cells is the bone marrow stimulation technique. (**a**) One such technique is the microfracture technique, that has been practiced relatively more commonly. This method requires making of multiple holes through the subchondral bone into the bone marrow using an awl, through which the stem cells in the marrow flow to the defect area. These stem cells undergo differentiation and proliferation within the blood clots (mesenchymal blood clot or super clot) to create a cartilage tissue [15, 16]. (**b**) The stem cells in the blood clot formed after a microfracture technique can be identified by colony-forming unit method. Stem cells attached to the culture plates are proliferated to form a colony, and the number of these colonies corresponds to the number of stem cells. The number of colonies varies depending on the diameter and the number of holes

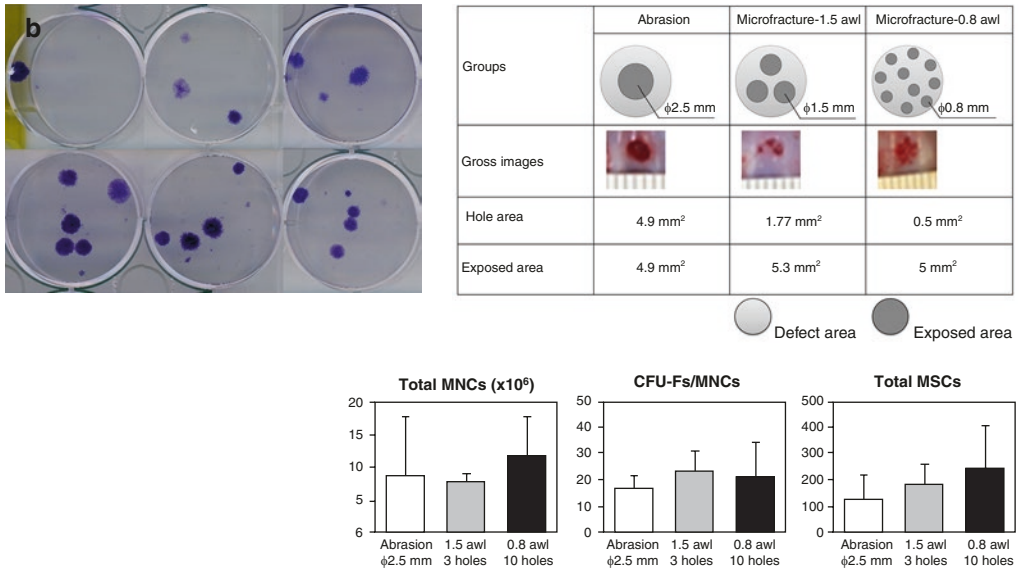

Figure 8.2.2: (continued)

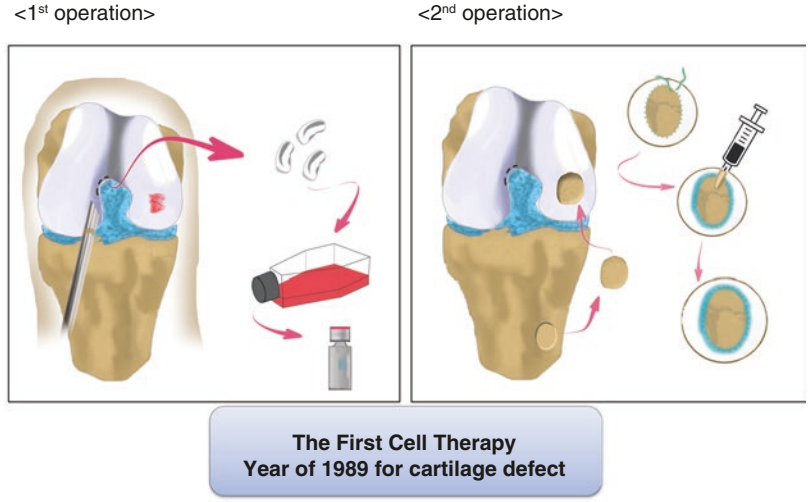

Figure 8.2.3: Cartilage Repair: The Cultured Chondrocytes. The autologous chondrocytes implantation (ACI) is a typical biological method of cell therapy, first reported in 1994. It is two-stage surgery, with the cartilage biopsy collected primarily and then chondrocytes multiplied to minimum of more than five million cells [1]. As a second-stage surgery, the patient's periosteum is harvested to cover the chondral defect, and then the multiplied chondrocytes are injected into the cavity created by it

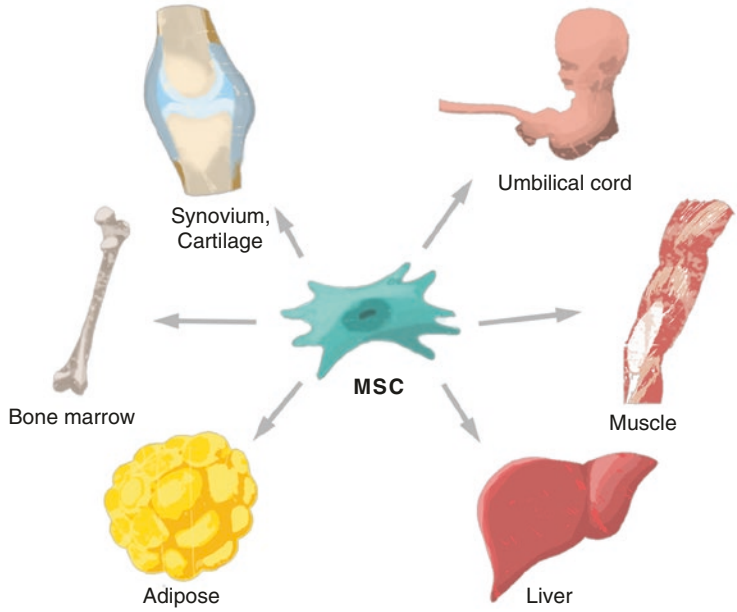

Figure 8.2.4: Cartilage Repair: The Sources of the Stem Cells. There are many different sources of the stem cells, from the embryonic stem cells to the induced pluripotent stem cells. Mesenchymal stem cells (MSC) are known to exist in all the tissues of the body. As far as stem cells for cartilage repair are concerned, the research on stem cells taken from the following tissues have been reported: umbilical cord, umbilical cord blood, fat tissue, bone marrow, synovium, fetal cartilage, iPS, and the embryonic stem cell [17, 18]. For cartilage regeneration, MSCs derived from the bone marrow are studied the most, and MSCs originated from the fat tissues or the umbilical cord blood have been started in clinical application. MSCs cells derived from patient's synovial tissue are reported to have the most potent cartilage differentiation, and their clinically effective application is being studied [17–21]

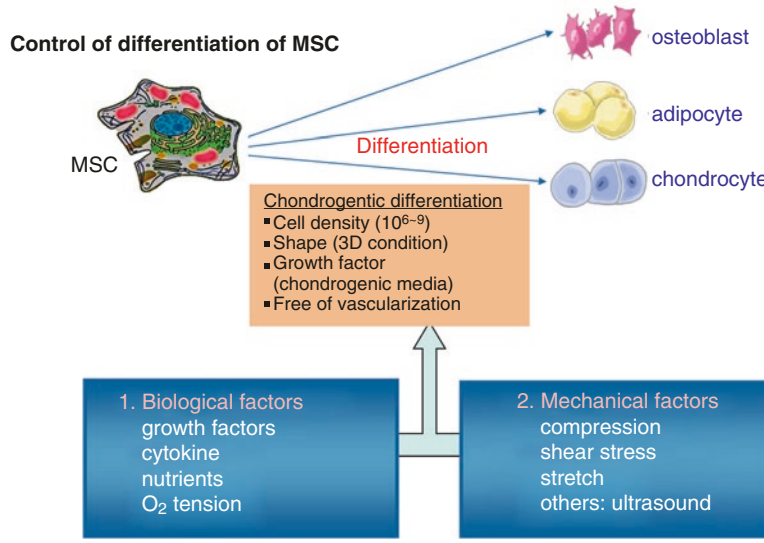

Figure 8.2.5: Factors Controlling Differentiation of Stem Cells into the Chondrocytes In Vitro/In Vivo. Stem cells can differentiate into numerous cells of lineage by biologic or mechanical factors in vitro and in vivo. To differentiate into chondrocytes, the cell density should be high, incubation must be done under the conditions of three-dimensional culture, and chondrogenic media that promotes chondrogenesis should be used [22]. Vascularization during chondrogenesis in vivo should be inhibited if possible, as it can lead to dedifferentiation and calcification [23]. Certain dynamic culture conditions involving compression, shear stress, stretch, and ultrasound improve chondrogenesis [24, 25]

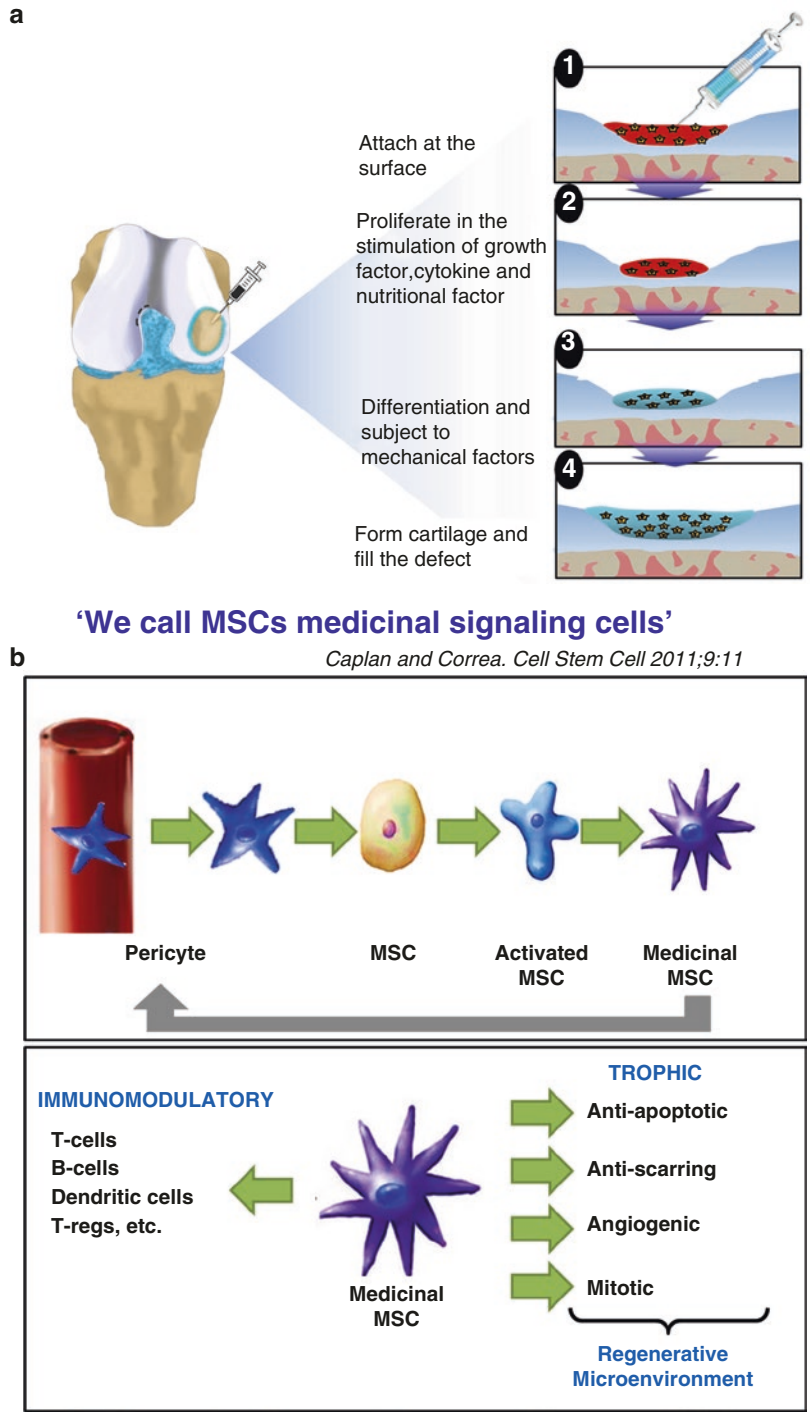

Figure 8.2.6: The Mode of Action of the Transplanted Cells. (**a**) In the classical concept, implanting the cells from an outside source or from an inside source to the defect area will inevitably lead to the following mechanisms. The cells attach on to the surface of the defect to the subchondral bone. The implanted cells proliferate as they are stimulated by surrounding stimuli such as growth factors, cytokine, mechanical stimuli, and other nutritional factors released by neighboring tissues. Cells differentiate, synthesize, and secrete extracellular matrix, eventually filling the cartilage defect with the repaired cartilage tissue. (**b**) The mechanism of cartilage repair by stem cell implantation is being interpreted differently than in the past. According to many current studies, stem cells work like drugs. Since the survival of transplanted cell is very limited, the cells release biologically active factors (paracrine factors) to promote tissue regeneration and inhibit fibrosis, apoptosis, and inflammation by modulating the survival, proliferation, migration, and gene expression of the cells around them

Title/Journal	Cell type	Animal	Duration
Behavior of transplanted bone marrow-derived GFP mesenchymal cells in osteochondral defect as a simulation of autologous transplantation/ Journal of Histochemistry & Cytochemistry 53(2):2-7-216,2005	Autologous MSC	Rat 12-week-old female GFP transgenic rats, genetically identical with wild-type rats.	▪GFP positive cells were observed in the regenerated tissues for 24 weeks although GFP positive cells decreased in number with time
Mesenchymal stem cells are short-lived and do not migrate beyond the lungs after intravenous infusion/ Frontiers in Immunology 3: 1-8, 2012	Allogeneic MSC	▪MSC donors: DsRed C57BL/6 mice ▪MSC recipients: would-type C57BL/6 mice	▪DsRed-MSC were present in lung after 1h, but strongly reduced after 24h. ▪No living DsRed-MSC were detected in cultures of any of the other tissues established at 1, 24, or 72h after MSC infusion
Survival of transplanted rat bone marrow-derived osteogenic stem cells in vivo/ Tissue Eng. Part A 7(7-8): 1147-1156, 2011	Autologous MSC	▪Isogenic adult male rats (Lewis)	▪On day 3, cell numbers had decreased by more than two-thirds of day 1. ▪On day 14, cells could no longer be identified
Transplanted embryonic stem cells survive, differentiate and promote recovery in injured rat spinal cord/ Nature Medicine 5(12): 1410-1412, 1999	Xenogenic ESC	▪Adult long evans female rats	▪At 2-5 weeks after transplantation, ES cell-derived cells were found in aggregates or dispersed singly through-out the injury site
Bone marrow-derived mesenchymal stem cell transplant survival in the injured rodent spinal cord/ Journal of Bone Marrow Research 2(2): 1000146, 2014	MSC		▪0-52%: 1 week after transplantation ▪0-8%: 1 month after transplantation ▪In some cases, presence of MSCs up to 2 months and even 3 months ▪Usually no or very few cells survive at 2 or 3 months
Human adipose-derived stromal/stem cells demonstrate short-lived persistence after implantation in both an immunocompetent and an immunocompromised murine model/ Stem Cell Research & Therapy 5(6):142, 2014	Xenogenic ADSC	▪Immunocompetent wildtype mice: C57BL/6NCr ▪Immunocompromised mice: Athymic NCr-nu/ nu)	▪The persistence of human ASCs is correlated to the percent ERV-3 amplicational. ▪Human ASCs survive for less than 3 weeks after injection

Figure 8.2.7: The Survival of Transplanted Cells. Numerous researches have shown that regardless of the method in which the cells are transplanted, including injection, surgery, or transplantation with the use of biomaterials, the number of cells significantly decreases in a matter of weeks [26–30]. This time-dependent decrease in cell number is also observed in both autologous and allogeneic cells. The mode of action of the transplanted cells, limited by the time within the transplantation site, may not be due to the continued differentiation and functioning of the transplanted cells

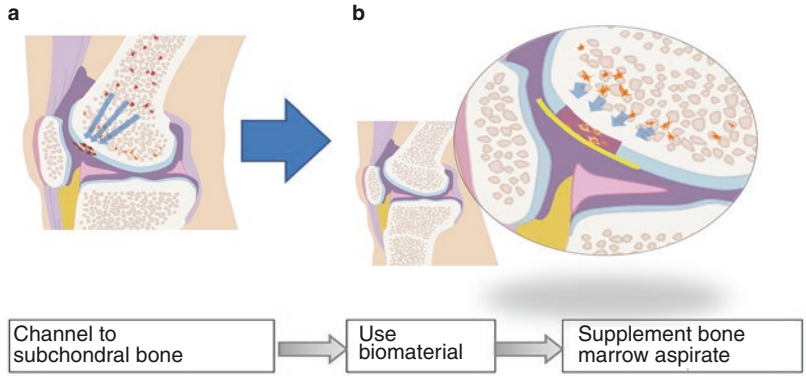

Figure 8.2.8: Supporting the MSC in the Defect Area with Biomaterials. (**a**) Blood clots that contain stem cells and fill the defect areas can be easily lost by gravity, by a shear force or washed by the synovial fluid. Also, cells present in the synovial fluid and cytokine can kill or disrupt the differentiation process. (**b**) Thus, to avoid this, a method of either covering the defect area or scaffolding the defect area; is being sought. Alternatively, increase in the stem cell numbers that participate in regeneration can be done via transplantation of MSCs extracted from the bone marrow or adipose tissue to the area of the defect [31, 32]

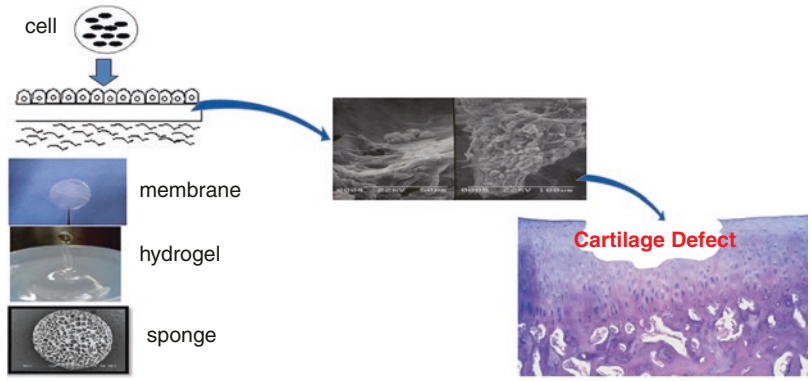

Figure 8.2.9: Concepts of Biomaterials in the Cartilage Repair. The downside of the cell therapy is that the efficiency of engraftment is reduced by the leakage of implanted cells from the damaged area. The survivorship and differentiation success rate are seriously threatened in the unfamiliar environment of the implant. Biomaterials, when used as a carrier of implanting cells, can increase the efficiency of engraftment and survivorship by providing a beneficial environment for growth and differentiation of the grafted cells. Biomaterials used with cells can be membrane-type, gel-type, and three-dimensional scaffold-type. Scaffold with growth factor is also used to promote a differentiation into the cartilage cells

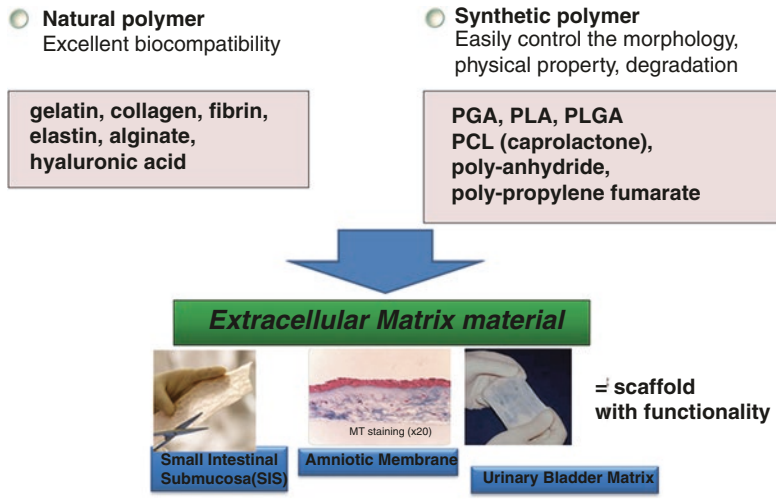

Figure 8.2.10: The Optimal Biodegradable Biomaterial. Biomaterials include natural polymers and synthetic polymers. Each has its advantages and disadvantages. While natural polymers exhibit superior biocompatibility, the physical and chemical processing and degradation control are difficult. While the synthetic polymers have advantages in controlling morphology, physical property, and degradation, biocompatibility may not be good, such as the occurrence of posttransplant inflammation. Biomaterials that are made of extracellular matrix of tissues are useful as a complement to their strengths and weaknesses. The biggest strength of these materials is their biocompatibility with the strong biologic functions. The small intestinal mucosa, amniotic membrane, the urinary bladder matrix, and cartilage are various examples of currently used clinical applications

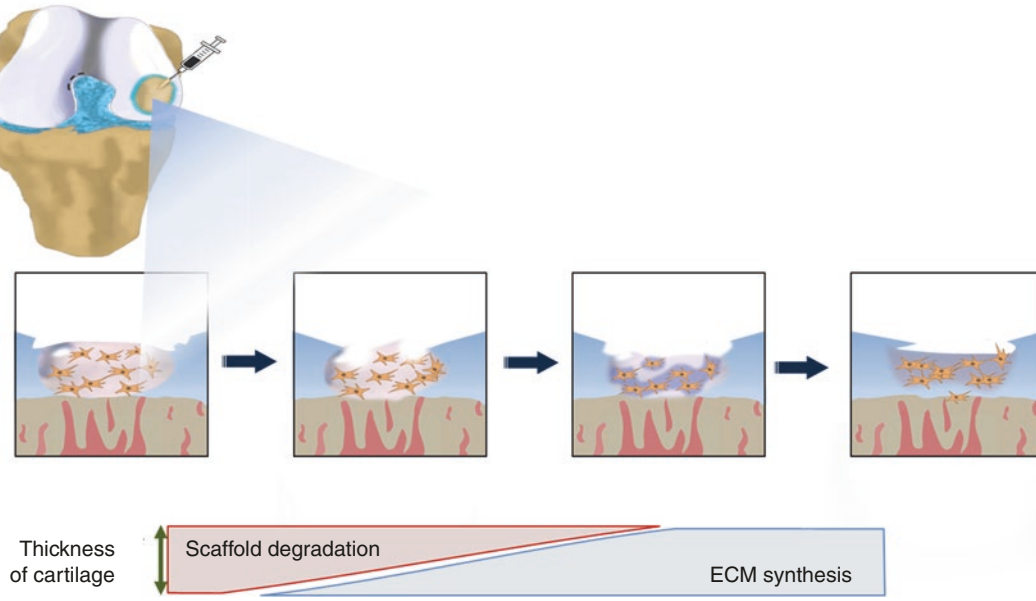

Figure 8.2.11: The Balanced Degradation of the Biomaterial. The stem cells that are transferred into the biomaterials proliferate and differentiate, and they secrete an extracellular matrix. The biomaterials must degrade to accommodate the extracellular matrix that is produced by the cells. When biodegradation of the biomaterial occurs rapidly, the mechanical support becomes mechanically weak, while a slow degradation can inhibit the production of the extracellular matrix. This harmonized degradation of biomaterials is called "balanced degradations"

8.3 Take-Home Message

Stem cells can either originate from cultured autologous, allogeneic cells, or endogenous cells from the patients' bone marrow or other niche tissue. Stem cells have many beneficial qualities compared to adult cells making them an attractive treatment modality. Continued survival and differentiation toward cartilage requires the stem cells to be exposed to certain biological cues and chondrogenic environment, which still requires a further research.

We need a clear understanding of the differentiation process after stem cell transplantation. Understanding of an in vivo stem cell behavior and differentiation mechanism will lead to more advanced cell therapies that will maximize the differentiation process toward cartilage. As for the biomaterials, each material (whether synthetic or natural origin) holds unique advantages and disadvantages. Change in the biomaterial itself after transplantation, such as degradation, should continually support the differentiation and survival of the transplanted cells.

References

1. Brittberg M, Lindahl A, Nilsson A, Ohlsson C, Isaksson O, Peterson L. Treatment of deep cartilage defects in the knee with autologous chondrocyte transplantation. N Engl J Med. 1994;331:889–95.
2. Peterson L, Vasiliadis HS, Brittberg M, Lindahl A. Autologous chondrocyte implantation: a long-term follow-up. Am J Sports Med. 2010;38:1117–24.
3. Nejadnik H, Hui JH, Feng Choong EP, Tai BC, Lee EH. Autologous bone marrow-derived mesenchymal stem cells versus autologous chondrocyte implantation: an observational cohort study. Am J Sports Med. 2010;38:1110–6.
4. Andriano KP, Tabata Y, Ikada Y, Heller J. In vitro and in vivo comparison of bulk and surface hydrolysis in absorbable polymer scaffolds for tissue engineering. J Biomed Mater Res. 1999;48:602–12.
5. Brun P, Cortivo R, Zavan B, Vecchiato N, Abatangelo G. In vitro reconstructed tissues on hyaluronan-based temporary scaffolding. J Mater Sci Mater Med. 1999;10:683–8.
6. Guo JF, Jourdian GW, MacCallum DK. Culture and growth characteristics of chondrocytes encapsulated in alginate beads. Connect Tissue Res. 1989;19:277–97.
7. Homminga GN, Buma P, Koot HW, van der Kraan PM, van den Berg WB. Chondrocyte behavior in fibrin glue in vitro. Acta Orthop Scand. 1993;64:441–5.
8. Lahiji A, Sohrabi A, Hungerford DS, Frondoza CG. Chitosan supports the expression of extracellular matrix proteins in human osteoblasts and chondrocytes. J Biomed Mater Res. 2000;51:586–95.
9. Lee CH, Singla A, Lee Y. Biomedical applications of collagen. Int J Pharm. 2001;221:1–22.
10. Vunjak-Novakovic G, Martin I, Obradovic B, Treppo S, Grodzinsky AJ, Langer R, Freed LE. Bioreactor cultivation conditions modulate the composition and mechanical properties of tissue-engineered cartilage. J Orthop Res. 1999;17:130–8.
11. Kobayashi T, Ochi M, Yanada S, Ishikawa M, Adachi N, Deie M, Arihiro K. A novel cell delivery system using magnetically labeled mesenchymal stem cells and an external magnetic device for clinical cartilage repair. Arthroscopy. 2008;24:69–76.
12. Ochi M. Challenging for cartilage repair. Sports Med Arthrosc Rehabil Ther Technol. 2009;1:13.
13. Choi SM, Lee KM, Ryu SB, Park YJ, Hwang YG, Baek D, Choi Y, Park KH, Park KD, Lee JW. Enhanced articular cartilage regeneration with SIRT1-activated MSCs using gelatin-based hydrogel. Cell Death Dis. 2018;9:866.
14. Lin H, Zhou J, Cao L, Wang HR, Dong J, Chen ZR. Tissue-engineered cartilage constructed by a biotin-conjugated anti-CD44 avidin binding technique for the repairing of cartilage defects in the weight-bearing area of knee joints in pigs. Bone Joint Res. 2017;6:284–95.
15. Min BH, Choi WH, Lee YS, Park SR, Choi BH, Kim YJ, Jin LH, Yoon JH. Effect of different bone marrow stimulation techniques (BSTs) on MSCs mobilization. J Orthop Res. 2013;31:1814–9.
16. Min BH, Truong MD, Song HK, Cho JH, Park DY, Kweon HJ, Chung JY. Development and efficacy testing of a "hollow awl" that leads to patent bone marrow channels and greater mesenchymal stem cell mobilization during bone marrow stimulation cartilage repair surgery. Arthroscopy. 2017;33:2045–51.
17. De Bari C, Roelofs AJ. Stem cell-based therapeutic strategies for cartilage defects and osteoarthritis. Curr Opin Pharmacol. 2018;40:74–80.
18. Lee WY, Wang B. Cartilage repair by mesenchymal stem cells: clinical trial update and perspectives. J Orthop Translatol. 2017;9:76–88.
19. de Sousa EB, Casado PL, Moura Neto V, Duarte ME, Aguiar DP. Synovial fluid and synovial membrane mesenchymal stem cells: latest discoveries and therapeutic perspectives. Stem Cell Res Ther. 2014;5:112.
20. Koizumi K, Ebina K, Hart DA, Hirao M, Noguchi T, Sugita N, Yasui Y, Chijimatsu R, Yoshikawa H, Nakamura N. Synovial mesenchymal stem cells from osteo- or rheumatoid arthritis joints exhibit good potential for cartilage repair using a scaffold-free tissue engineering approach. Osteoarthr Cartil. 2016;24:1413–22.

21. Mak J, Jablonski CL, Leonard CA, Dunn JF, Raharjo E, Matyas JR, Biernaskie J, Krawetz RJ. Intra-articular injection of synovial mesenchymal stem cells improves cartilage repair in a mouse injury model. Sci Rep. 2016;6:23076.
22. Yasui Y, Ando W, Shimomura K, Koizumi K, Ryota C, Hamamoto S, Kobayashi M, Yoshikawa H, Nakamura N. Scaffold-free, stem cell-based cartilage repair. J Clin Orthop Trauma. 2016;7:157–63.
23. Marsano A, Medeiros da Cunha CM, Ghanaati S, Gueven S, Centola M, Tsaryk R, Barbeck M, Stuedle C, Barbero A, Helmrich U, Schaeren S, Kirkpatrick JC, Banfi A, Martin I. Spontaneous in vivo chondrogenesis of bone marrow-derived mesenchymal progenitor cells by blocking vascular endothelial growth factor signaling. Stem Cells Transl Med. 2016;5:1730–8.
24. Choi WH, Choi BH, Min BH, Park SR. Low-intensity ultrasound increased colony forming unit-fibroblasts of mesenchymal stem cells during primary culture. Tissue Eng Part C Methods. 2011;17:517–26.
25. Park IS, Choi WH, Park DY, Park SR, Park SH, Min BH. Effect of joint mimicking loading system on zonal organization into tissue-engineered cartilage. PLoS One. 2018;13:e0202834.
26. Agrawal H, Shang H, Sattah AP, Yang N, Peirce SM, Katz AJ. Human adipose-derived stromal/stem cells demonstrate short-lived persistence after implantation in both an immunocompetent and an immunocompromised murine model. Stem Cell Res Ther. 2014;5:142.17.
27. Eggenhofer E, Benseler V, Kroemer A, Popp FC, Geissler EK, Schlitt HJ, Baan CC, Dahlke MH, Hoogduijn MJ. Mesenchymal stem cells are short-lived and do not migrate beyond the lungs after intravenous infusion. Front Immunol. 2012;3:297.
28. McDonald JW, Liu XZ, Qu Y, Liu S, Mickey SK, Turetsky D, Gottlieb DI, Choi DW. Transplanted embryonic stem cells survive, differentiate and promote recovery in injured rat spinal cord. Nat Med. 1999;5:1410–2.
29. Oshima Y, Watanabe N, Matsuda K, Takai S, Kawata M, Kubo T. Behavior of transplanted bone marrow-derived GFP mesenchymal cells in osteochondral defect as a simulation of autologous transplantation. J Histochem Cytochem. 2005;53:207–16.
30. Zimmermann CE, Gierloff M, Hedderich J, Acil Y, Wiltfang J, Terheyden H. Survival of transplanted rat bone marrow-derived osteogenic stem cells in vivo. Tissue Eng Part A. 2011;17:1147–56.
31. Jin LH, Choi BH, Kim YJ, Park SR, Jin CZ, Min BH. Implantation of bone marrow-derived buffy coat can supplement bone marrow stimulation for articular cartilage repair. Osteoarthr Cartil. 2011;19:1440–8.
32. Yang SS, Jin LH, Park SH, Kim MS, Kim YJ, Choi BH, Lee CT, Park SR, Min BH. Extracellular matrix (ECM) multilayer membrane as a sustained releasing growth factor delivery system for rhTGF-beta3 in articular cartilage repair. PLoS One. 2016;11:e0156292.

9 The Illustrative Chondral and Osteochondral Scaffolds in Cartilage Repair

Alberto Poggi, Luca Andriolo, Angelo Boffa, Sante Alessandro Altamura, Iacopo Romandini, Alessandro Di Martino, Stefano Zaffagnini, and Giuseppe Filardo

9.1 Introduction

Articular chondral lesions are one of the most challenging conditions for the orthopaedic surgeon, representing a painful pathology which can evolve into osteoarthritis (OA). Several surgical techniques have been developed to restore the articular surface and to prevent joint degeneration. Among these, scaffold-based procedures are emerging as potential therapeutic options. Scaffolds are matrices acting as a support for cell adhesion and proliferation. Constructs of different materials are available. Monolayer collagen or hyaluronan-based scaffolds are the most used for chondral defects, while biphasic scaffolds, made of different layers for chondral and subchondral bone tissues, have more recently been proposed to treat the entire osteochondral unit. Scaffolds can be used with cultured cells, concentrated cells, or directly without cell addition.

The earliest chondral scaffold was used in the second-generation autologous chondrocytes implantation (ACI) technique, instead of the periosteum patch, to cover the cartilage defect filled with cultured chondrocytes. Matrix-assisted autologous chondrocytes implantation (MACI®, based on a porcine collagen membrane) and matrix-assisted autologous chondrocytes transplantation (MACT, including different scaffolds) techniques were later developed, seeding autologous chondrocytes onto the scaffold to facilitate their growth. The advantages of these techniques were the ability to maintain the chondrocyte phenotype and matrix production and to avoid the dedifferentiation into fibroblasts that was typical of 2-D cultures. Moreover these techniques considerably reduced some of the typical complications of first-generation ACI, like periosteum hypertrophy, and brightened the prospects of arthroscopic implantation. Nevertheless, MACI/MACT was still affected by some drawbacks like a 2-step technique, requiring a least of 2–3 weeks to cultivate chondral cells, and high costs of cell cultures. Thus, two different strategies were proposed, scaffold augmentation with mesenchymal stem cells not requiring cultures (e.g. bone marrow concentration) or the use of chondral or osteochondral cell-free scaffolds. The most extensively described cell-free chondral technique is autologous matrix-induced chondrogenesis (AMIC), where microfractures are augmented with a scaffold acting as a substrate to increase the potentiality of bone marrow mesenchymal cells coming from the perforation of the subchondral bone plate. Another cell-free chondral scaffold is Cargel, obtained by mixing a soluble chitosan polymer with autologous peripheral blood and applying the solu-

A. Poggi · L. Andriolo · A. Boffa · S. A. Altamura
I. Romandini · A. Di Martino · S. Zaffagnini
II Clinica Ortopedica e Traumatologica, IRCCS Istituto Ortopedico Rizzoli, Bologna, Italy
e-mail: poggialberto8@gmail.com; lucas.andriolo@gmail.com; angeloboffal@libero.it; s.aless.altamura@gmail.com; iacoporoma@gmail.com; alessandro.dimartino@ior.it; Stefano.zaffagnini@ior.it

G. Filardo (✉)
Applied and Translational Research center (ATRc), IRCCS Istituto Ortopedico Rizzoli, Bologna, Italy
e-mail: g.filardo@biomec.ior.it

D. R. Goyal (ed.), *The Illustrative Book of Cartilage Repair*,
https://doi.org/10.1007/978-3-030-47154-5_9

tion to a microfractured cartilage lesion to stabilize the clot, thus guiding and enhancing the cartilage repair. Regarding osteochondral cell-free scaffolds, different biphasic scaffolds has been proposed, like Cartiheal (an aragonite-hyaluronate (Ar-HA) bilayer scaffold) or Maioregen (a three-layer scaffold available in different thickness) aiming to replace, in the same surgical step, not only the cartilage layer but also the subchondral bone. While we are aware of the impossibility to correctly represent all the options/variations currently available worldwide, in the following illustrations, we aim at describing the surgical techniques of the aforementioned procedures underlining their main characteristics.

9.2 The Illustrations

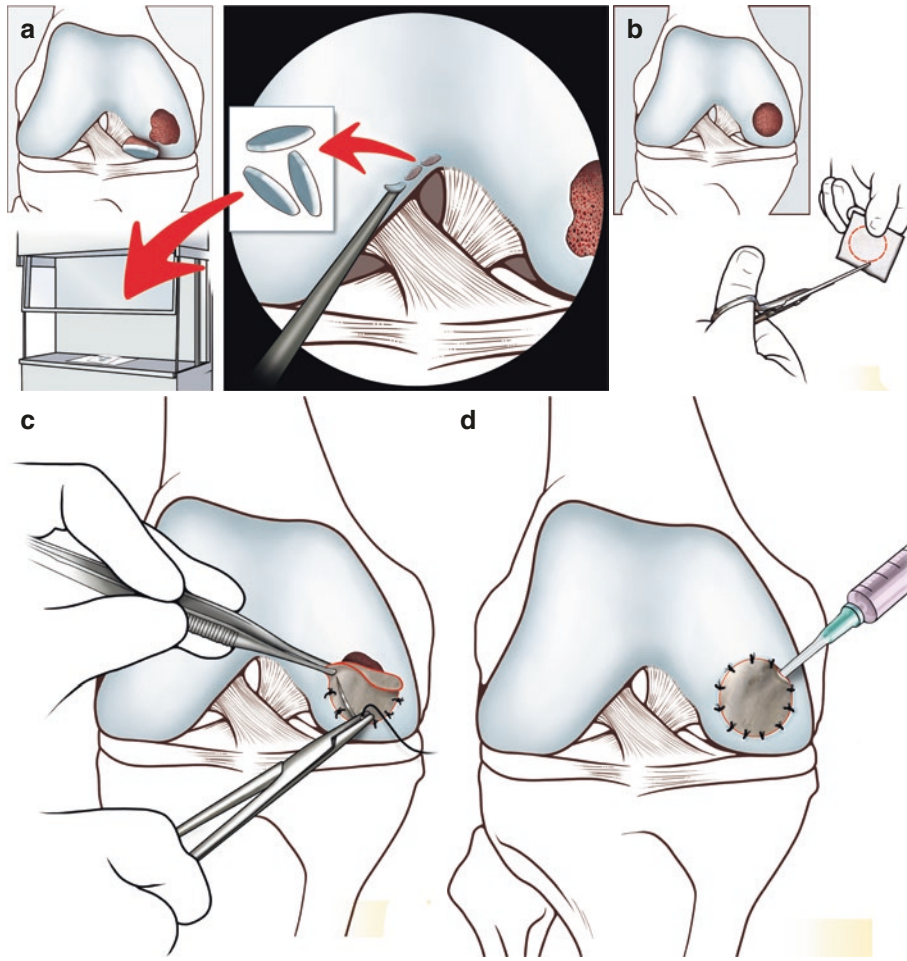

Figure 9.2.1: The Chondral Scaffolds: Second-Generation Autologous Chondrocyte Implantation (ACI) Technique. Autologous chondrocyte implantation (ACI) is a two-step procedure. In the first surgery, (**a**) cartilage biopsies from a less weight-bearing surface (e.g. trochlear notch) are harvested and subsequently sent to the GMP certified cartilage laboratory for enzymatic digestion and cell culture. After a least of 2–3 weeks, the cultured cells are ready for the implantation or can be cryopreserved for future use. (**b**) The second surgery is an open surgery where the size, location, depth of the defect, and the status of the surrounding cartilage are evaluated, and a debridement is performed to prepare the lesion site, with perpendicular margins and avoiding bleeding from the subchondral bone. (**c**) Then type I-III collagen membrane (for first-generation ACI, periosteum patch was used) is accurately sized and sutured to the margins of the chondral lesion and (**d**) is filled underneath with a liquid suspension of cultivated chondrocytes (the integrity of the graft can be tested before by using 1 mL of saline solution injected with 18G plastic angiocatheter underneath the collagen membrane) [1, 2]. (see Chap. 13 for a detailed description of the procedure)

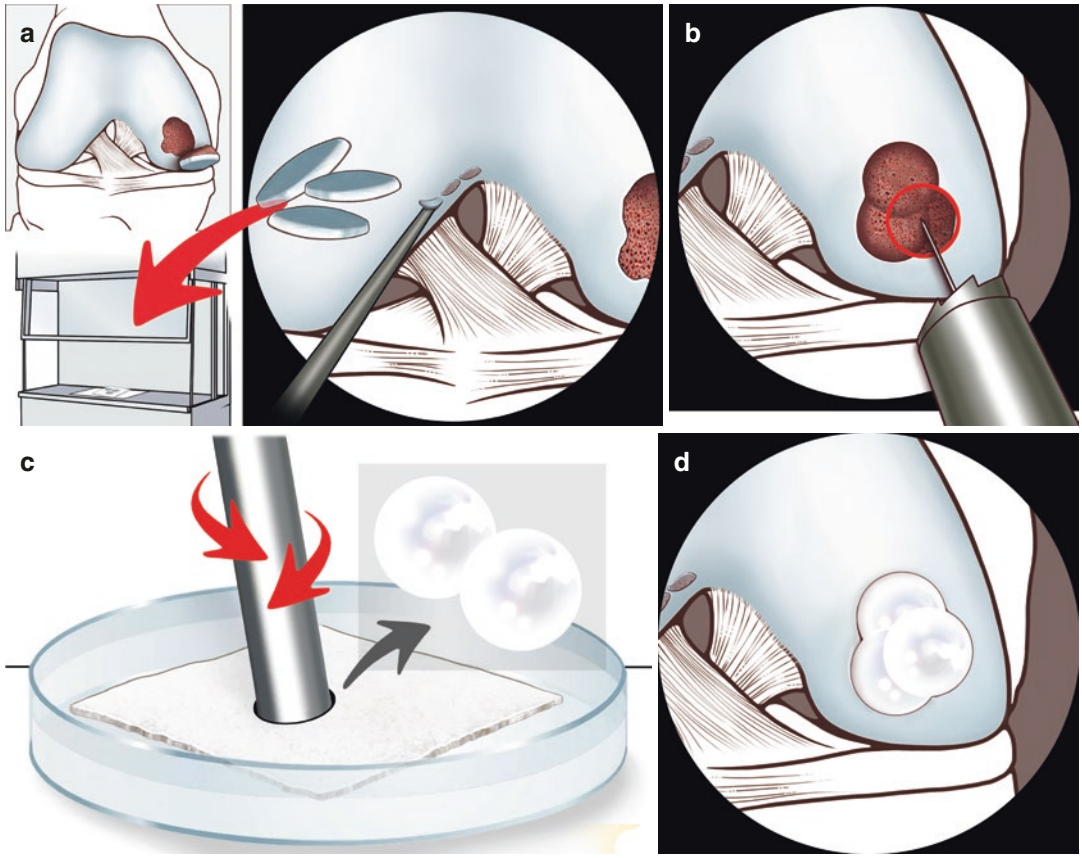

Figure 9.2.2: The Chondral Scaffolds: Matrix-Assisted Autologous Chondrocytes Transplantation (MACT) Technique. Matrix-assisted autologous chondrocyte transplantation (MACT) technique is also a two-step procedure that can be performed with an arthrotomic approach or arthroscopically (suitable for femoral condylar and trochlear cartilage defects). (**a**) The first surgery requires harvest of a 150–200 mg biopsy of healthy cartilage from a lesser weight-bearing area of the knee (e.g. trochlear notch) with a sharp curette. After an enzymatic digestion, chondral cells are isolated and cultivated for 2–4 weeks. Afterwards, the cultured cells (approximately one million cells per cm^2) are seeded onto a hyaluronan-based three-dimensional scaffold 4 days before implantation. In the second step surgery, (**b**) after an accurate debridement, (**c**) the bioengineered tissue is sized and shaped and (**d**) finally implanted in the chondral defect. Scaffold fixation is obtained through the scaffold adherence properties and checked intra-operatively with knee motion cycles [3]

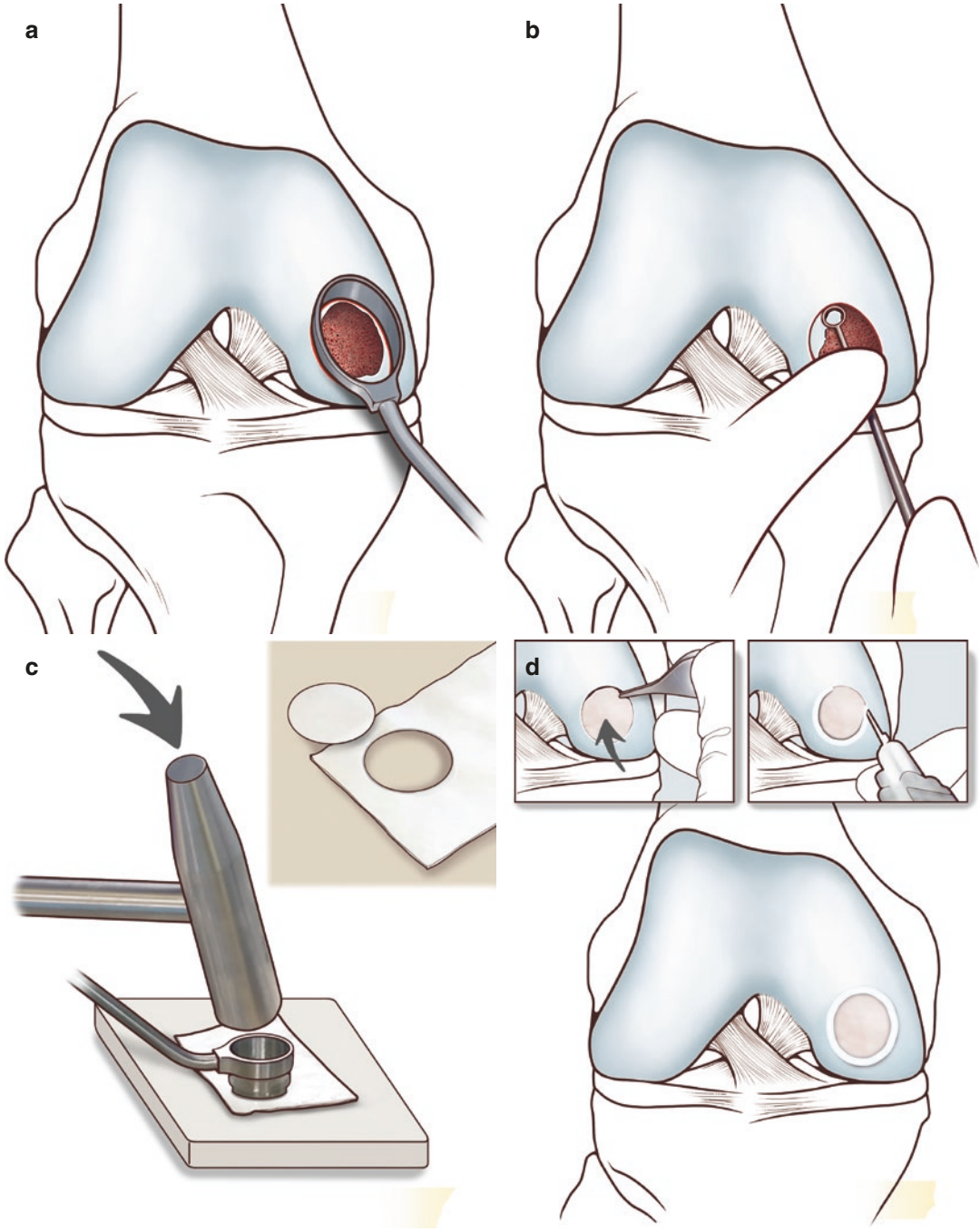

Figure 9.2.3: The Chondral Scaffolds: Matrix-Assisted Autologous Chondrocytes Implantation (MACI) Technique. In matrix-assisted autologous chondrocytes implantation (MACI) technique, as compared to matrix-assisted autologous chondrocytes transplantation (MACT) technique, chondrocyte cells are seeded and cultured directly onto the scaffold to have a temporary 3-D structure of a biodegradable polymer allowing the growth of the living cells [4]. The cartilage biopsy is harvested in a similar fashion as in any other ACI procedure. Next, the harvested chondrocytes are seeded and cultured on a porcine collagen membrane to obtain approximately one million cells per cm^2 [5]. (**a**, **b**) During second-stage surgery, the chondral defect is visualized and prepared with an accurate debridement to remove all nonviable cartilage, and the subchondral bone is exposed. (**c**) The cell-based scaffold is shaped to fit the defect using a foil template or a dedicated instrumentation and then (**d**) implanted and stabilized with a thin layer of fibrin glue [5]. (see Chap. 14 for a detailed description of the procedure)

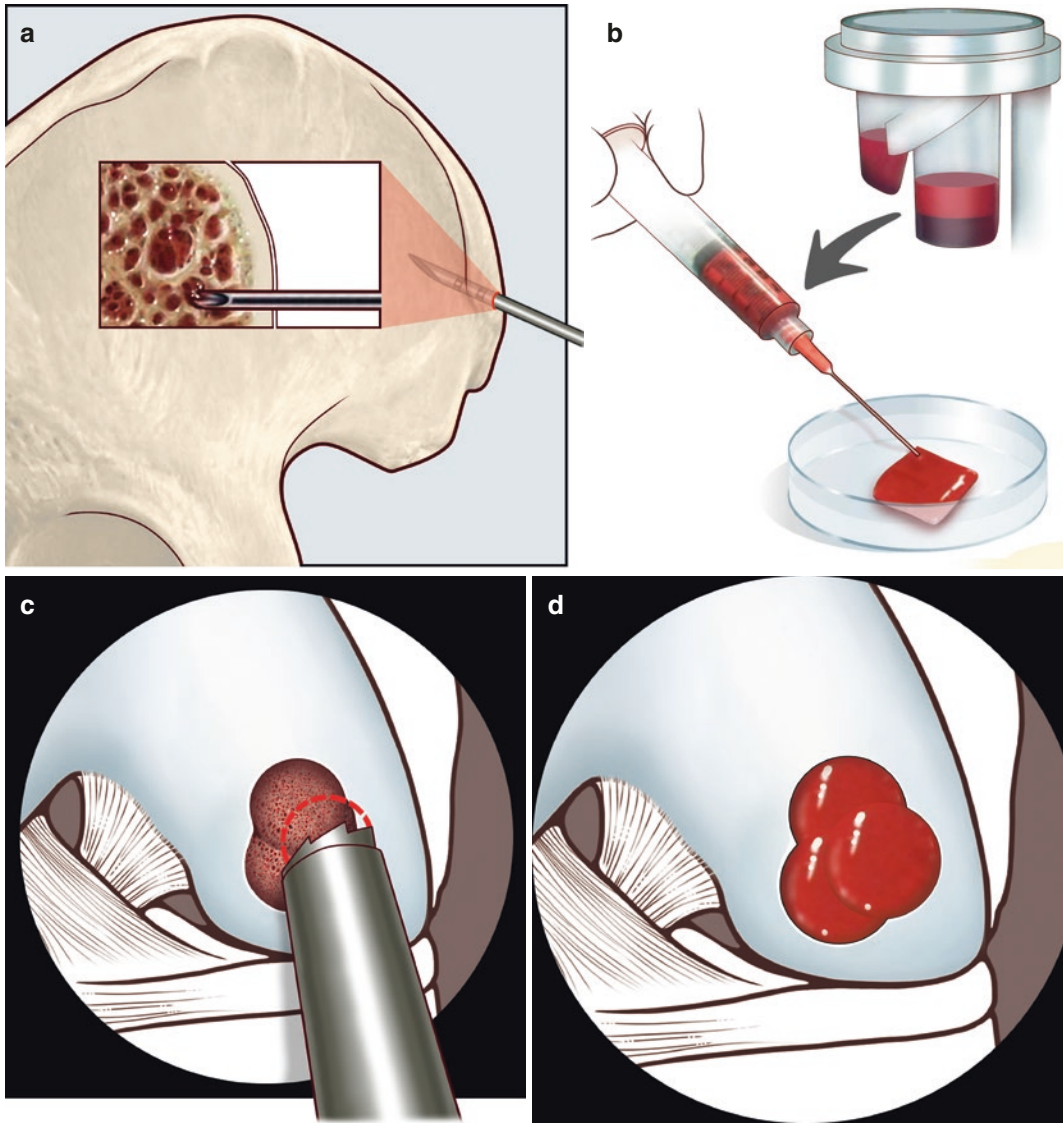

Figure 9.2.4: The Chondral Scaffolds: The Bone Marrow Concentrate (BMC) Augmented Technique. Bone marrow concentrate (BMC) augmented technique is a single-step procedure. (**a**) About 60 cc of bone marrow is harvested from the ipsilateral iliac crest through an aspiration kit. (**b**) The harvested bone marrow is concentrated 4–6 times above the baseline value with a specific centrifuge, which can be subjected to enzymatic activation to obtain an adhesive and stable material. The three-dimensional collagen/hyaluronate scaffold, opportunely shaped according to the size defect, is filled with the BMC to obtain the final implant. (**c**) An arthroscopic evaluation and debridement of chondral lesion is done and then (**d**) the BMC construct is applied onto the defect. Fibrin glue or PRF (platelet-rich fibrin) can be applied to further stabilize the scaffold [6, 7]. (see Chap. 19 for a detailed description of the procedure)

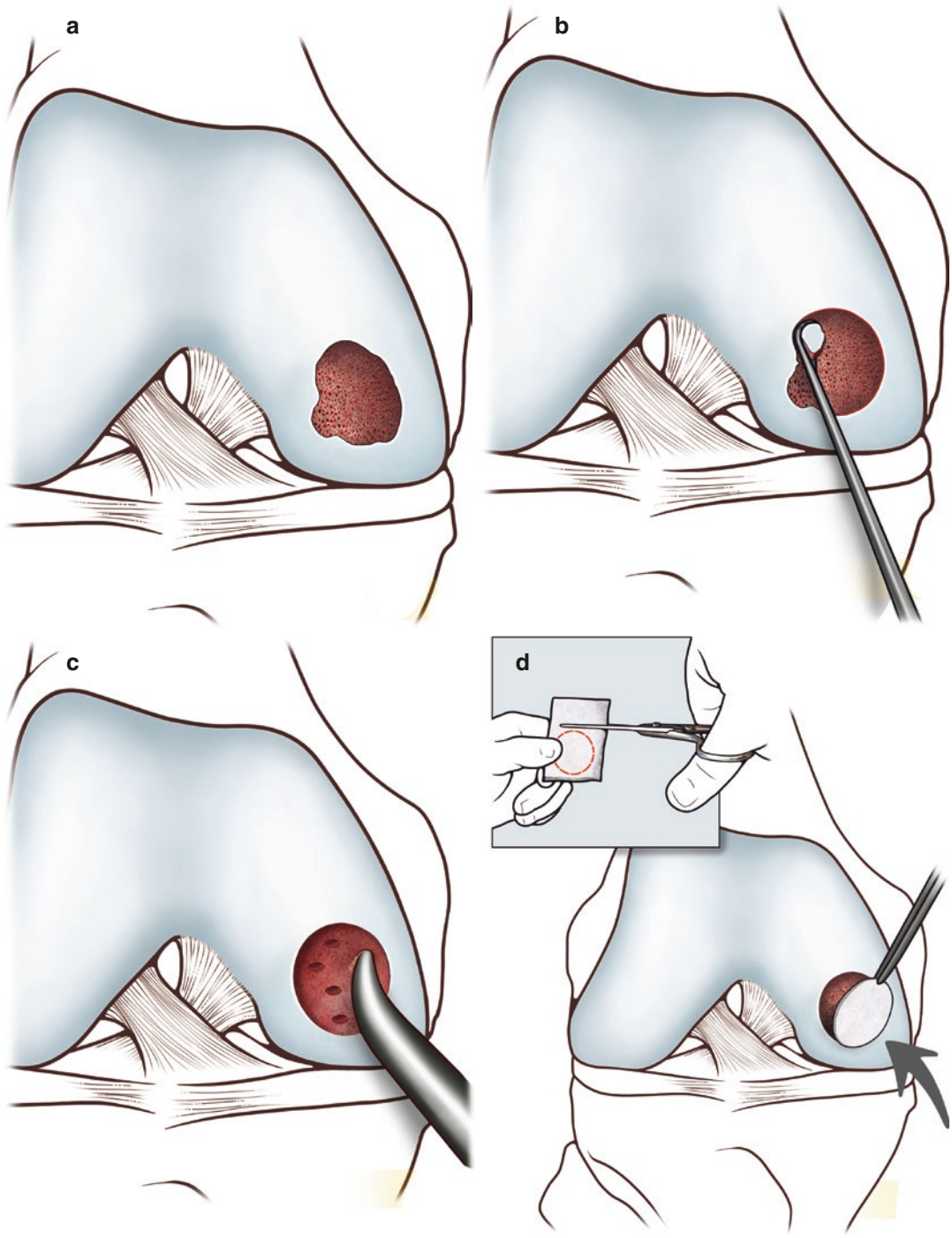

Figure 9.2.5: The Chondral Scaffolds: The Autologous Matrix-Induced Chondrogenesis (AMIC) Technique. In autologous matrix-induced chondrogenesis (AMIC) technique, the cell-free chondral scaffolds are implanted in a single-step procedure. (**a**, **b**) After an accurate arthroscopic or arthrotomic cartilage lesion debridement, (**c**) microfractures are performed according to the technique described by Steadman et al. [8]. (see Chap. 10 for the detailed procedure). (**d**) Then, a collagen matrix (membrane) opportunely sized and shaped is applied to the site of the cartilage defect. Finally, construct fixation is obtained pressing the collagen matrix into the chondral defect paying attention to perform a smooth transition between the matrix and the healthy cartilage (with fibrin glue in case further stability is necessary) [9]

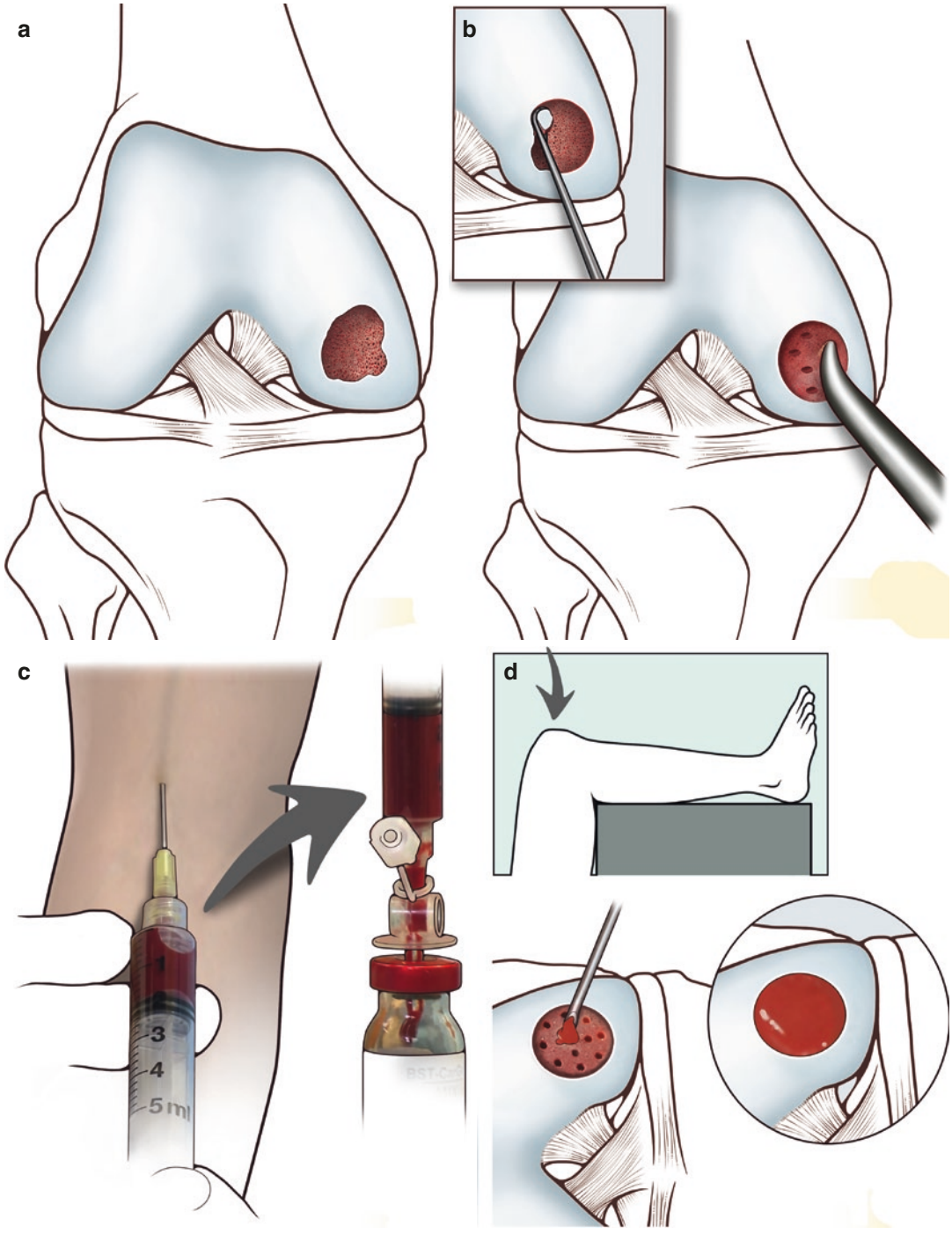

Figure 9.2.6: The Chondral Scaffolds: The Cargel Bio-scaffold Technique. The Cargel technique is a single-step procedure. As in other methods, the cartilage defect is accessed through either an arthrotomic or arthroscopic approach, and (**a**) then the defect is debrided removing the calcified layer. (**b**) A perpendicular stable rim of healthy surrounding cartilage is ensured for the scaffold stability and then the microfractures are performed as a standard procedure. (**c**) The Cargel bio-scaffold is prepared combining 4.5 mL of autologous venous blood with a cytocompatible chitosan solution. (**d**) Finally, the prepared bio-scaffold is implanted in the cartilage defect maintaining the lesion in a horizontal position to allow scaffold solidification, usually obtained in 15 min, thus avoiding any material loss [10]. (see Chap. 16 for a detailed description of the procedure)

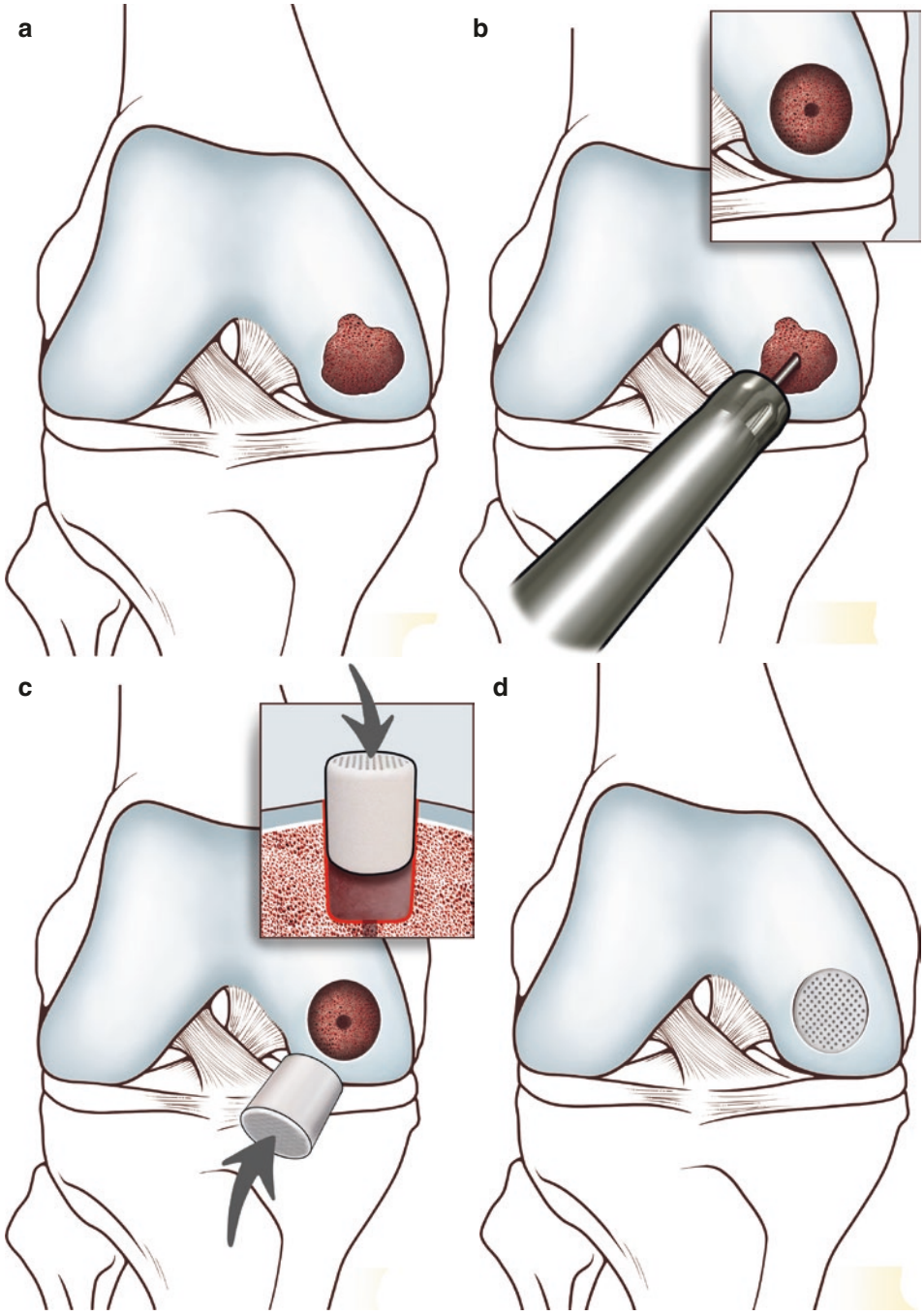

Figure 9.2.7: The Osteochondral Scaffolds: The Cartiheal Technique. The Cartiheal implantation is a single-step surgery for the treatment of the osteochondral defects. (**a**) After an accurate arthrotomic evaluation of the osteochondral defect, (**b**) the lesion site is prepared using a motorized drill and a reamer applied perpendicularly to obtain the desired depth and shape. The cartilage lesion is perfectioned to obtain the correct defect wall inclination for the tapered implants with the help of a shaper. (**c**) Once the preparation is complete, the aragonite-hyaluronate bilayer scaffold is manually inserted and (**d**) subsequently gently impacted to a position 2 mm below the surface of the articular cartilage with a silicone-covered tamper. This favours the chondrocytes migration and subsequent cartilage growth without any impingement-related complications, neither the risk to jeopardize the implant. The stability of the transplant is tested by cyclic bending of the knee while the graft is under direct vision, both before and after the tourniquet removal [11]

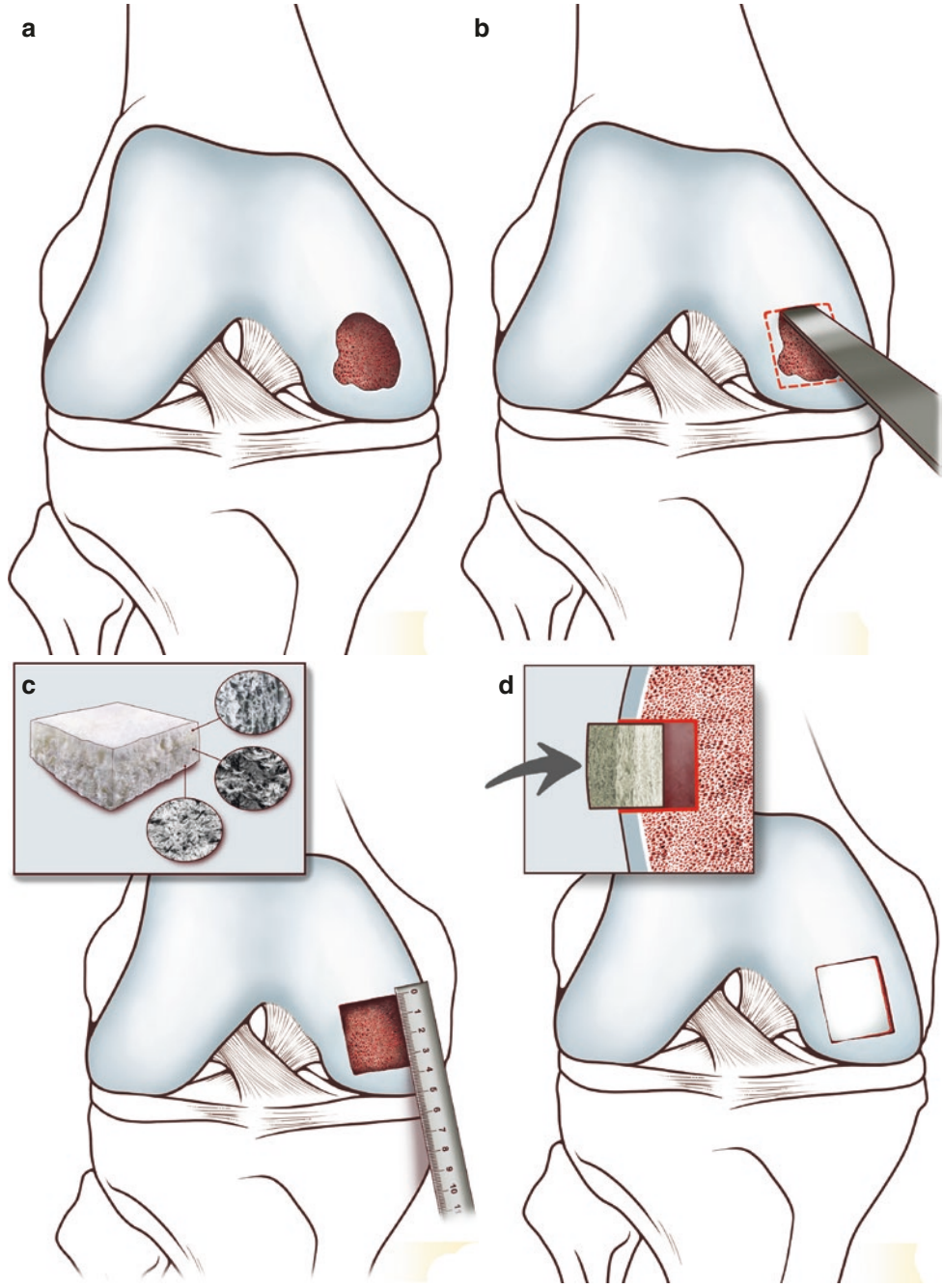

Figure 9.2.8: The Osteochondral Scaffolds: The MaioRegen(T) Technique. The MaioRegen technique is a single-step technique for the treatment of osteochondral defects. (**a**) After an arthrotomic access to analyse the osteochondral lesion, all the diseased subchondral bone is carefully removed with a curette. (**b**) A squared, regular-shaped lodging is created through the use of an osteotome or with a dedicated reamer and shaper. The depth of the lodging should be up to 6–8 mm for MaioRegen trilayer. The collagen-hydroxyapatite graft is a porous, three-dimensional, composite, three-layered structure mimicking the whole osteochondral unit. The scaffold can be sized and shaped with a scalpel to obtain an optimum fitting into the defect, which has been previously prepared. (**c**) The bed of the lesion must have stable shoulders perpendicular to the articular surface to ensure implant stability. (**d**) Finally, the scaffold is applied by press-fit, and a slight scaffold swelling caused by the subchondral bleeding increases the stability. The use of fibrin glue is advisable to ensure the implant stability [12]. Recently, new instruments for the implantation of pre-shaped circular scaffolds have been developed. (see Chap. 17 for a detailed description of the procedure)

9.3 Take-Home Message

Several scaffold-based procedures are available for the treatment of cartilage lesions. Among these, cell-based and cell-free procedures have been proposed, with different biomaterials and implant techniques. It has been quite understood that for any cartilage repair to take place, we need cells and scaffolds. The sources of the cells can be autologous, allogenic and endogenous, or the cells may be sourced from a microfracture technique. We need scaffolds for anchoring, proliferation and differentiation of these cells into mature matrix-producing chondrocytes. While no gold standard is currently available for scaffolds, multiple options of different scaffolds have been tested with variable results. The subsequent chapters discuss many of these options.

There is also an increasing understanding about the importance of evaluating the entire osteochondral unit and, in case of lesions involving the subchondral bone, to consider an osteochondral strategy. Regardless of the specific scaffold chosen, the treatment of concomitant joint issues such as malalignment and instability is paramount to ensure a good outcome of scaffold-based procedures for the restoration of the articular surface.

Acknowledgements Mariapia Cumani for the graphic contribution.

References

1. Brittberg M, Lindahl A, Nilsson A, Ohlsson C, Isaksson O, Peterson L. Treatment of deep cartilage defects in the knee with autologous chondrocyte transplantation. N Engl J Med. 1994;331(14):889–95.
2. Gillogly SD, Wheeler KS. Autologous chondrocyte implantation with collagen membrane. Sports Med Arthrosc Rev. 2015;23(3):118–24.
3. Kon E, Filardo G, Gobbi A, Berruto M, Andriolo L, Ferrua P, Crespiatico I, Marcacci M. Long-term results after hyaluronan-based MACT for the treatment of cartilage lesions of the patellofemoral joint. Am J Sports Med. 2016;44(3):602–8.
4. Saris D, Price A, Widuchowski W, Bertrand-Marchand M, Caron J, Drogset JO, Emans P, Podskubka A, Tsuchida A, Kili S, Levine D, Brittberg M, SUMMIT Study Group. Matrixapplied characterized autologous cultured chondrocytes versus microfracture: two-year follow-up of a prospective randomized trial. Am J Sports Med. 2014;42(6):1384–94. Epub 2014 Apr 8.
5. Meyerkort D, Ebert JR, Ackland TR, Robertson WB, Fallon M, Zheng MH, Wood DJ. Matrix-induced autologous chondrocyte implantation (MACI) for chondral defects in the patellofemoral joint. Knee Surg Sports Traumatol Arthrosc. 2014;22(10):2522–30. Epub 2014 May.
6. Gobbi A, Chaurasia S, Karnatzikos G, Nakamura N. Matrix-induced autologous chondrocyte implantation versus multipotent stem cells for the treatment of large patellofemoral chondral lesions: a nonrandomized prospective trial. Cartilage. 2015;6(2):82.
7. Buda R, Vannini F, Cavallo M, Baldassarri M, Luciani D, Mazzotti A, Pungetti C, Olivieri A, Giannini S. One-step arthroscopic technique for the treatment of osteochondral lesions of the knee with bone-marrow-derived cells: three years results. Musculoskelet Surg. 2013;97(2):145–51. Epub 2013 Feb 19.
8. Steadman JR, Rodkey WG, Briggs KK. Microfracture: its history and experience of the developing surgeon. Cartilage. 2010;1(2):78–86.
9. Kusano T, Jakob RP, Gautier E, Magnussen RA, Hoogewoud H, Jacobi M. Treatment of isolated chondral and osteochondral defects in the knee by autologous matrix-induced chondrogenesis (AMIC). Knee Surg Sports Traumatol Arthrosc. 2012;20(10):2109–15.
10. Steinwachs M, Cavalcanti N, Mauuva Venkatesh Reddy S, Werner C, Tschopp D, Choudur HN. Arthroscopic and open treatment of cartilage lesions with BST-CARGEL scaffold and microfracture: a cohort study of consecutive patients. Knee. 2019;26(1):174–84. Epub 2018 Dec 19.
11. Kon E, Robinson D, Verdonk P, Drobnic M, Patrascu JM, Dulic O, Gavrilovic G, Filardo G. A novel aragonite-based scaffold for osteochondral regeneration: early experience on human implants and technical developments. Injury. 2016;47(Suppl 6):S27–32.
12. Perdisa F, Filardo G, Sessa A, Busacca M, Zaffagnini S, Marcacci M, Kon E. One-step treatment for patellar cartilage defects with a cell-free osteochondral scaffold: a prospective clinical and MRI evaluation. Am J Sports Med. 2017;45(7):1581–8. Epub 2017 Mar 1.

10 The Illustrative Marrow Stimulation Techniques for Cartilage Repair: The Microfracture Technique

Katarzyna Herman, Eleonora Irlandini, Ignacio Dallo, Ezequiel Santa Coloma, and Alberto Gobbi

10.1 Introduction

Cartilage lesions can occur as a result of an acute injury (i.e., chondral fracture from shear and/or compression forces) or following a repetitive microtrauma during sporting activities. Some studies have shown that the chondral lesions are present in approximately 60% of knee arthroscopies, usually coexisting with the other pathologies [1]. One of the most common coexisting pathology is an anterior cruciate ligament (ACL) tear, where the cartilage lesion acts as a source of a continuing pain and a gradual cartilage degeneration takes place [2].

The articular cartilage distributes the loads across the knee joint to protect the subchondral bone. After an injury, the chondral tissue has a limited healing potential because of its relative avascularity, paucity of cells, and their low mitotic activity. Thus, untreated cartilage injuries have little or no potential to heal spontaneously [3].

Marrow stimulation technique like the Pridie drilling, abrasion arthroplasty, and microfracture has remained the first line of treatment for almost 60 years in the management of chondral defects, especially for the lesions in the knees. Microfracture (MF) is one of the most commonly used bone marrow stimulation techniques, first described by Steadman et al. [7]. This technique stimulates the production of a fibrocartilage repair tissue which has a higher proportion of type I collagen; leading to different properties and durability compared to the normal cartilage [9, 10]. Patient selection is extremely important, as not all type of lesion can be treated with this method. Studies have shown that it is a viable option when performed in young athletes with small, single lesions leading to good results at a short-term follow-up [4]. The simplicity and the low cost of the instruments make this technique so appealing, that this technique has been used for over 20 years. However, in some cases the positive outcome may decrease in the longer follow-up [5]. Even though microfracture is a commonly performed method of treatment, it should not be described as a state-of-the-art procedure in the cartilage repair [6].

K. Herman · E. Irlandini · I. Dallo · E. S. Coloma
A. Gobbi (✉)
Orthopaedic Arthroscopic Surgery International (O.A.S.I.) Bioresearch Foundation, Gobbi N.P.O., Milan, Italy
e-mail: kkapturkiewicz@gmail.com; e.irlandini@oasiortopedia.it; ignaciodallo@hotmail.com; ezequielsantacoloma@gmail.com; gobbi@cartilagedoctor.it

D. R. Goyal (ed.), *The Illustrative Book of Cartilage Repair*,
https://doi.org/10.1007/978-3-030-47154-5_10

10.2 The Illustrations

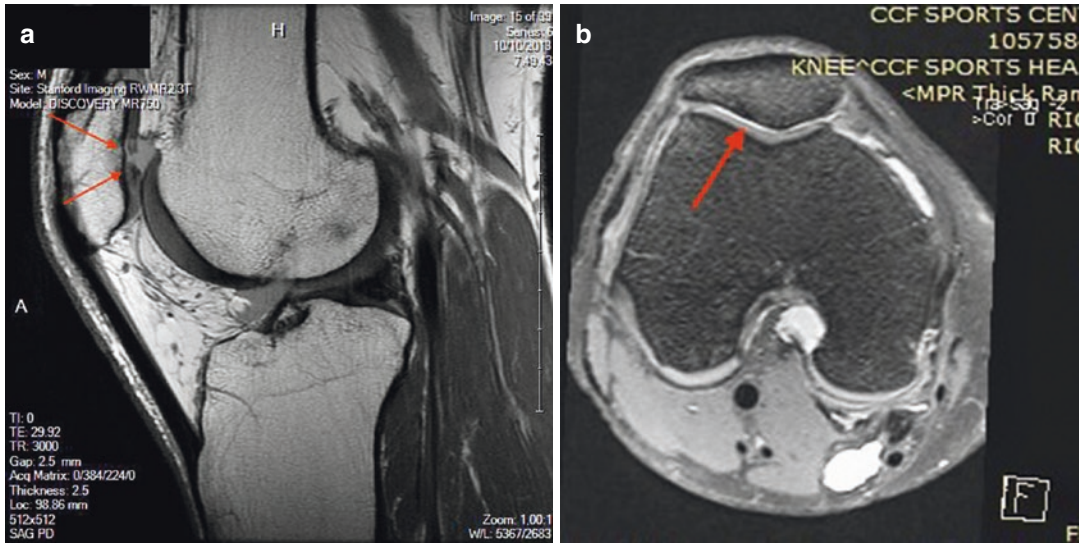

Figure 10.2.1: The Microfracture Technique: The Ideal Case Selection. A 27-year-old male professional ice hockey player complained of pain in the patella-femoral region of the right knee for more than 6 months. He had discomfort while squatting and had difficulty in performing maneuvers while playing, which affected his routine training. He had a history of blunt trauma to the affected knee few months back which was managed conservatively. On examination, the patient had a mild effusion of the right knee, with crepitus and painful range of movement from 40° to 80° without any signs of instability or mal-tracking of the patella. Further, there were no signs of anteroposterior instability or malalignment of the knee. The patient had to return to play for the next season. (**a**) The magnetic resonance imaging (MRI) (T2 sequence sagittal section) showed a full-thickness (ICRS Grade 3c) chondral defect over the mid-level of patella facet. (**b**) T2-weighted axial section on MRI showed signal changes in the articular cartilage at the lateral patellar facet. Microfracture is a viable option as a first line of treatment for the small articular cartilage defects of the knee joint. Lesions <1 cm^2 may be considered to be treated with this technique. However, there is still no consensus and no studies to support it, as a superior cartilage repair technique

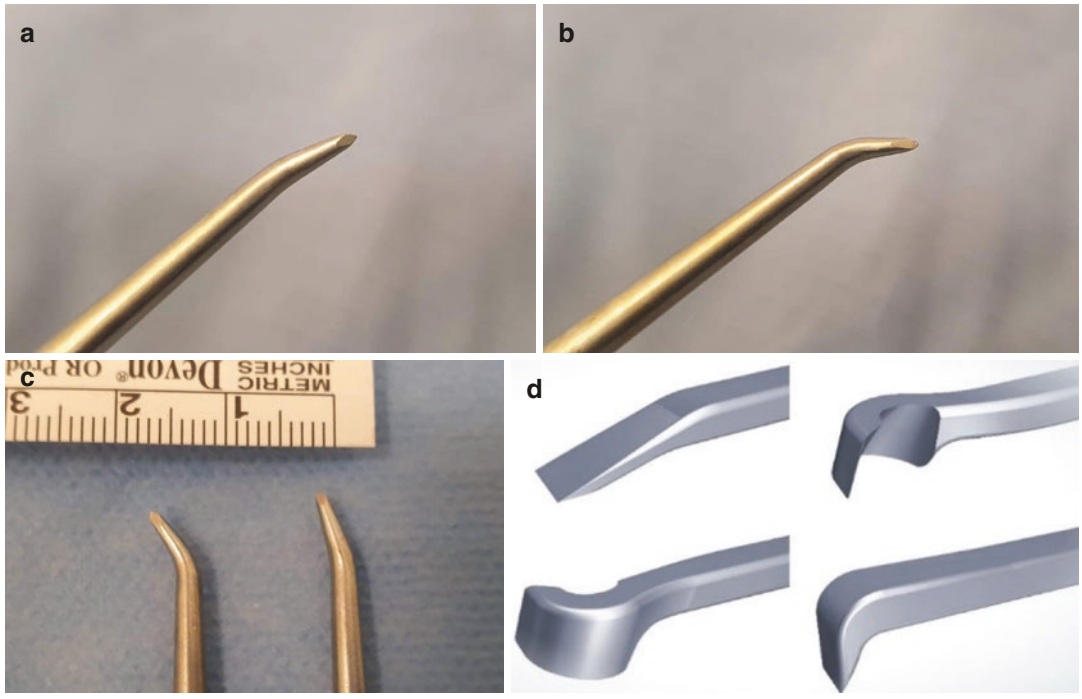

Figure 10.2.2: The Microfracture Technique: The Instruments Required. Most of the commercially available microfracture awls are of different sizes and tip configurations. This allows the surgeon to access chondral lesions in different locations of the hip, the knee, or the ankle joint. Different angles also allow perpendicular position of the awl during the procedure, since it is crucial not to damage the subchondral bone. (**a**, **b**) Microfracture (MF) awls bent at 65° and 40° angles, respectively, with a sharp tip are one such option for the MF technique. (**c**) The tip of the awl is approximately 1 mm as seen in reference to the ruler. Ring curettes or (**d**) special curettes called the chondrectomes (ATMED-Z. Rafalski, Katowice, Poland) can also be used for preparing the defect

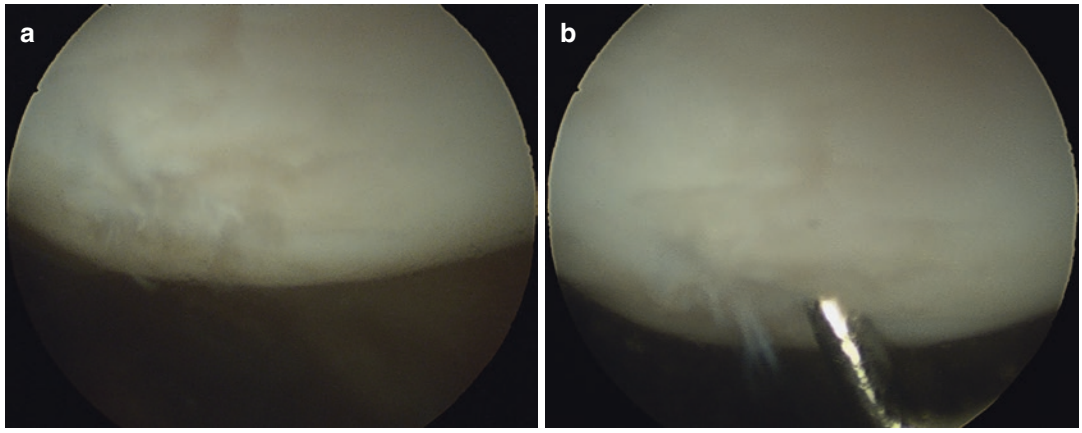

Figure 10.2.3: The Microfracture Technique: The Arthroscopic Assessment of the Lesion. The right knee arthroscopy, viewing from the anterolateral portal, of a 27-year-old male shows (**a**) a full-thickness chondral defect of approximately 1 cm × 1 cm in size at the distal patella facet. (**b**) The probe examination reconfirmed the normal subchondral bone, underneath. Due to the relatively small size (<1 cm^2) of the lesion and the normal subchondral bone underneath, the microfracture technique was chosen as a primary treatment. This technique uses arthroscopic awls (Figure 10.2.2) via standard portals, nullifying the need for an additional incision. The angulated tips of commercially available sets allow the surgeon to reach the lesion at various locations

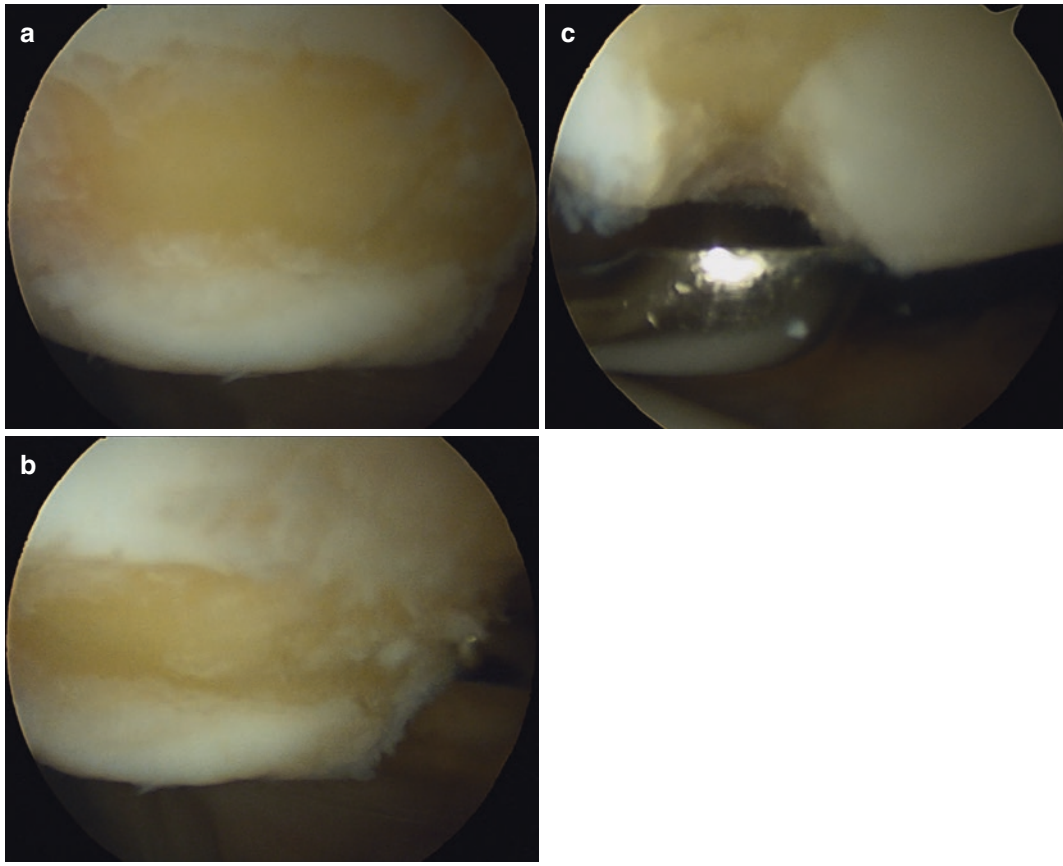

Figure 10.2.4: The Microfracture Technique: The Preparation/Debridement of the Base of the Lesion. The right knee arthroscopy of a 27-year-old male patient undergoing the microfracture technique, while viewing from the anterolateral portal, and working through an anteromedial portal. (**a**, **b**) All the loose and delaminated cartilage should be thoroughly removed. A rotary shaver is helpful in debriding the defect. The periphery of the lesion should create a stable rim. It is crucial to create the walls of the lesion perpendicular to the underlying bone. (**c**) Removal of the calcified layer is the final step in the lesion preparation that can be done using a curette and expose the subchondral layer. However, care should be taken not to damage the subchondral layer

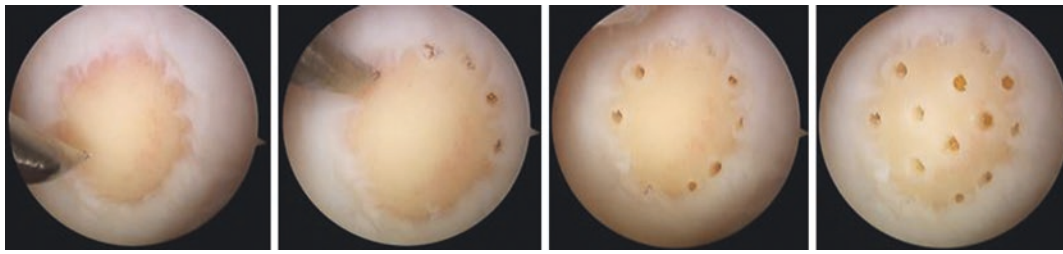

Figure 10.2.5: The Microfracture Technique: The Technical Details. Arthroscopic image of a 22-year-old male right knee with a 2 cm^2 ICRS grade 3A chondral lesion over the weight-bearing region of the medial femoral condyle. Following a thorough debridement of the lesion, multiple holes are made using a custom-angled arthroscopic awl. The holes are placed starting from the periphery to the center, perpendicular to the joint surface, about 3–4 mm apart and about 2–4 mm deep. Care must be taken not to damage the subchondral plate in between the holes. (the case is different from the pictures shown in Figures 10.2.1, 10.2.3, and 10.2.4)

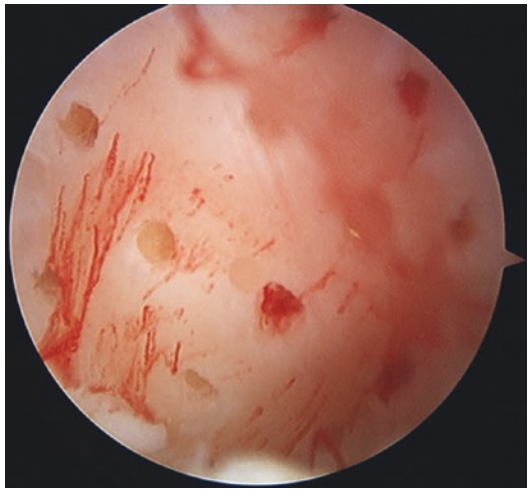

Figure 10.2.6: The Microfracture Technique: The Final Assessment of the Procedure. Right knee arthroscopic image of a 22-year-old male showing an access to the bone marrow in the form of fat cells and blood coming out. Reducing the fluid pressure allows the blood flow from the marrow space to bring mesenchymal stem cells (MSC) into the defect, forming a "superclot" that covers the lesion. (the case is different from the pictures shown in Figures 10.2.1, 10.2.3, and 10.2.4)

Figure 10.2.7: The Microfracture Technique: Postoperative Care and Rehabilitation. Post microfracture technique, the patient is put in a postoperative knee brace restricting the range of motion (ROM) based on the location of the repaired lesion. The detailed postoperative rehabilitation program as suggested by Steadman [7] is recommended. Immediately after the surgery, the patient is placed on a continuous passive motion (CPM) machine with an added cold therapy. The range of motion of the CPM exercises depends on the treated region. The lesions on the weight-bearing surfaces are started initially at a range of 10–70°, which is then gradually increased by 10–20° to achieve a full range. The CPM machine is used for 6–8 h daily. Immediately after the surgery, the patient starts with the isometric exercises and a limited dynamic quadriceps training. The patient is allowed a crutch-assisted touchdown weight-bearing ambulation from 4 to 6 weeks according to the size and the location of the lesion. After this period of time, the weight-bearing loading can be gradually increased, as well as the strength training. The goal is to achieve a full weight-bearing walk at 8 weeks. The lesions in the patellofemoral joint are treated differently. The immediate ROM is 0–30° for 8 weeks, where the operated limb is placed in a brace locked at 0–30°. Partial weight bearing is allowed after 7 days together with the isometric quadriceps exercises. The patients can remove the brace during the passive range of motion exercise in a CPM and can also start the hydrotherapy and bicycling at 2 weeks. After 8 weeks, the full weight-bearing walk without the brace is introduced and the strength training program is gradually advanced

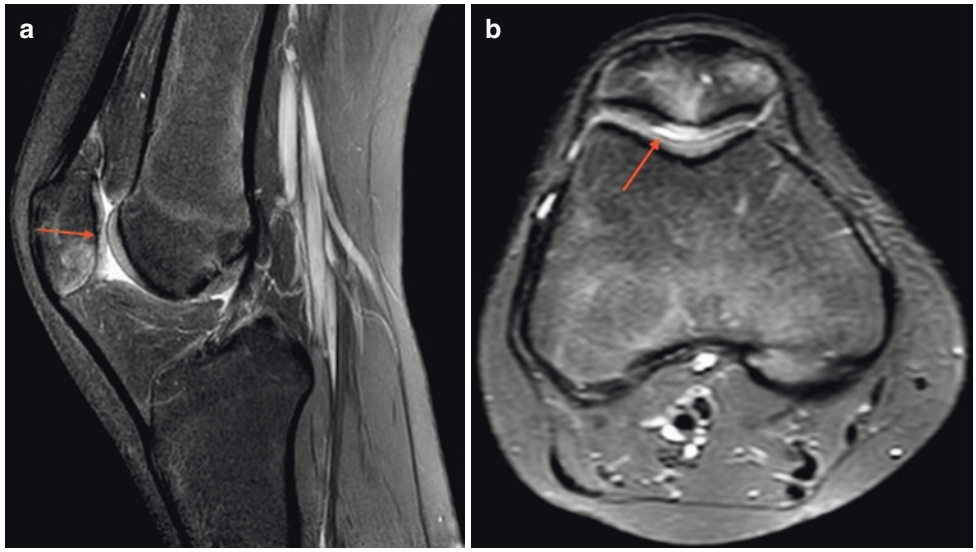

Figure 10.2.8: The Microfracture Technique: The Results on MRI. 6-month postoperative magnetic resonance imaging (MRI) results in a 27-year-old patient, who underwent the microfracture technique for a lateral patellar facet lesion. The T2-weighted sagittal (**a**) and the axial (**b**) sections of MRI show a completely filled defect with a minor hyperintense signal indicating a fairly good quality of a regenerative tissue which has integrated well with the adjacent tissue. The axial view shows the presence of the subchondral changes with edema-like signals on the patella at 6 months following the microfracture, indicating an ongoing marrow activity. (the case is same as shown in Figures 10.2.1, 10.2.3, and 10.2.4)

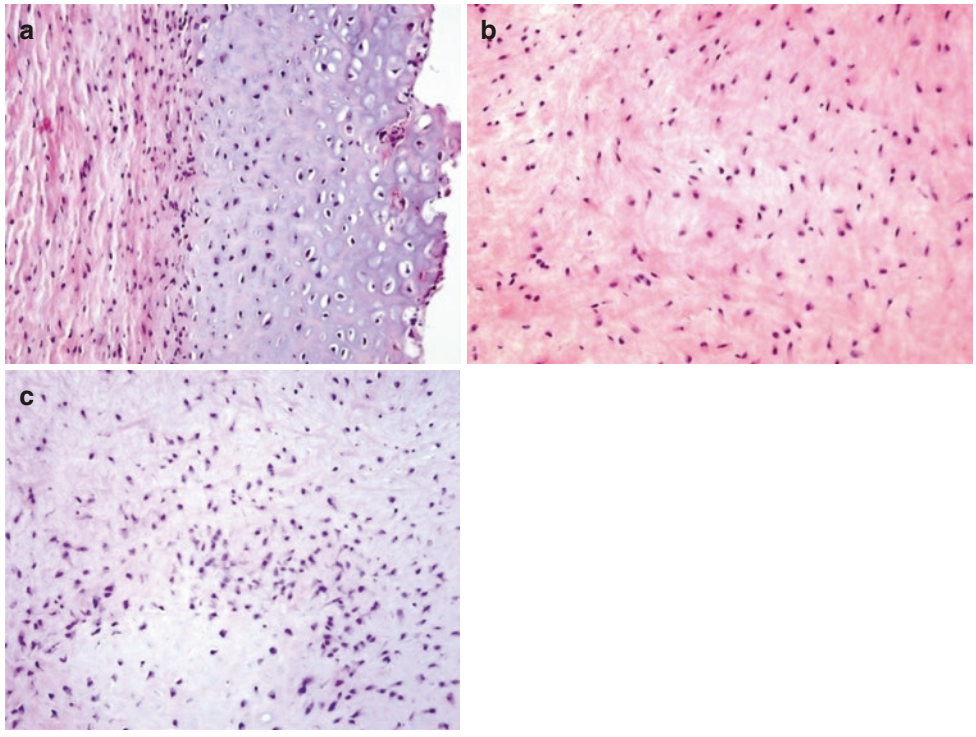

Figure 10.2.9: The Microfracture Technique: The Results on Histopathology. The histologic sections with hematoxylin and eosin staining at 6 months after microfracture demonstrating different areas of fibromyxoid tissue with differentiation. (**a**) The transitional zone with some cartilage tissue; (**b**) the fibromyxoid "hybrid tissue" without differentiation"; and (**c**) initiation of hyaline transformation. Though the repair tissue is inferior to the quality of a normal hyaline cartilage, the regenerative tissue might be beneficial for the joint function and pain relief

10.3 Take-Home Message

Microfracture is the most popular remedy for managing small chondral defects due to its simplicity, low cost, and a quick return to play. However, the quality of cartilage repair is inconsistent leading to poor long-term outcomes [11]. Based on the studies, this method can give optimal results in smaller lesions and in the defects in the weight-bearing region of the femoral condyle [8]. Many new developments are being studied like the microdrilling and the scaffold augmented microfracture, which has shown better clinical and histological results. However, long-term outcomes of these procedures are also yet to be evaluated.

References

1. Arøen A, Løken S, Heir S, Alvik E, Ekeland A, Granlund OG, Engebretsen L. Articular cartilage lesions in 993 consecutive knee arthroscopies. Am J Sports Med. 2004;32:211–5.
2. Johnson DL, Urban WP Jr, Caborn DN, Vanarthos WJ, Carlson CS. Articular cartilage changes seen with magnetic resonance imaging-detected bone bruises associated with acute anterior cruciate ligament rupture. Am J Sports Med. 1998;26:409–14.
3. Newman AP. Articular cartilage repair. Am J Sports Med. 1998;26:309–24.
4. Gobbi A, Karnatzikos G, Kumar A. Long-term results after microfracture treatment for full-thickness knee chondral lesions in athletes. Knee Surg Sports Traumatol Arthrosc. 2014;22(9):1986–96.
5. Gobbi A, Whyte GP. One-stage cartilage repair using a hyaluronic acid-based scaffold with activated bone marrow-derived mesenchymal stem cells compared with microfracture: five-year follow-up. Am J Sports Med. 2016;44(11):2846–54.
6. Frehner F, Benthien JP. Microfracture: state of the art in cartilage surgery? Cartilage. 2018;9(4):339–45.
7. Steadman JR, Rodkey W, Rodrigo J. Microfracture: surgical technique and rehabilitation to treat chondral defects. Clin Orthop. 2001;391S:362–9.
8. Erggelet C, Vavken P. Microfracture for the treatment of cartilage defects in the knee joint—a golden standard? J Clin Orthop Trauma. 2016;7:145–52.
9. Hunziker EB. Articular cartilage repair: basic science and clinical progress: a review of the current status and prospects. Osteoarthr Cartil. 2002;10:432–63.
10. Shapiro F, Koide S, Glimcher MJ. Cell origin and differentiation in the repair of full-thickness defects of articular cartilage. J Bone Joint Surg Am. 1993;75:532–53.
11. Goyal D, Keyhani S, Lee EH, Hui JH. Evidence-based status of microfracture technique: a systematic review of level I and II studies. Arthroscopy. 2013;29:1579–88.

11 The Illustrative Osteochondral Cylinder Transfer Techniques for Cartilage Repair: The Mosaicplasty Technique

Laszlo Hangody

11.1 Introduction

The successful surgical treatment of chondral and osteochondral defects is based on two main pillars: the restoration of the biomechanics and the effective cartilage repair. Several new surgical techniques have been developed in the recent three decades for the cartilage repair like transplantation of autologous and allogenic osteochondral grafts, cell therapies, cell-free biodegradable scaffolds, and other regenerative surgical adjuvants. Autologous osteochondral mosaicplasty is a surgical technique to treat focal chondral and osteochondral defects of the weight-bearing articular surfaces of the joints. During arthroscopic or mini-arthrotomy mosaicplasty, cylindrical osteochondral grafts are harvested from the less or non-weight-bearing periphery of the patellofemoral joint and implanted into the defected area in a mosaic-like fashion, hence the name of the technique. This technique is used most frequently for femoral condylar lesions, but there are specific indications in the ankle, hip, elbow, and shoulder joints as well. Mosaicplasty is recommended for 1.0–4.0 cm^2 full-thickness chondral or osteochondral focal defects of the weight-bearing articular surfaces. [1–4]

Based on actual biomechanical alterations, parallel with the cartilage repair methods; realignment osteotomies, meniscus surgery, and correction of tracking may be necessary to restore the pathoanatomical background.

L. Hangody (✉)
Hungarian Academy of Sciences, Budapest, Hungary

Department of Traumatology, Semmelweis University, Budapest, Hungary

Department of Orthopaedics, Uzsoki Hospital, Budapest, Hungary
e-mail: laszlohangody@gmail.com

D. R. Goyal (ed.), *The Illustrative Book of Cartilage Repair*,
https://doi.org/10.1007/978-3-030-47154-5_11

11.2 The Illustrations

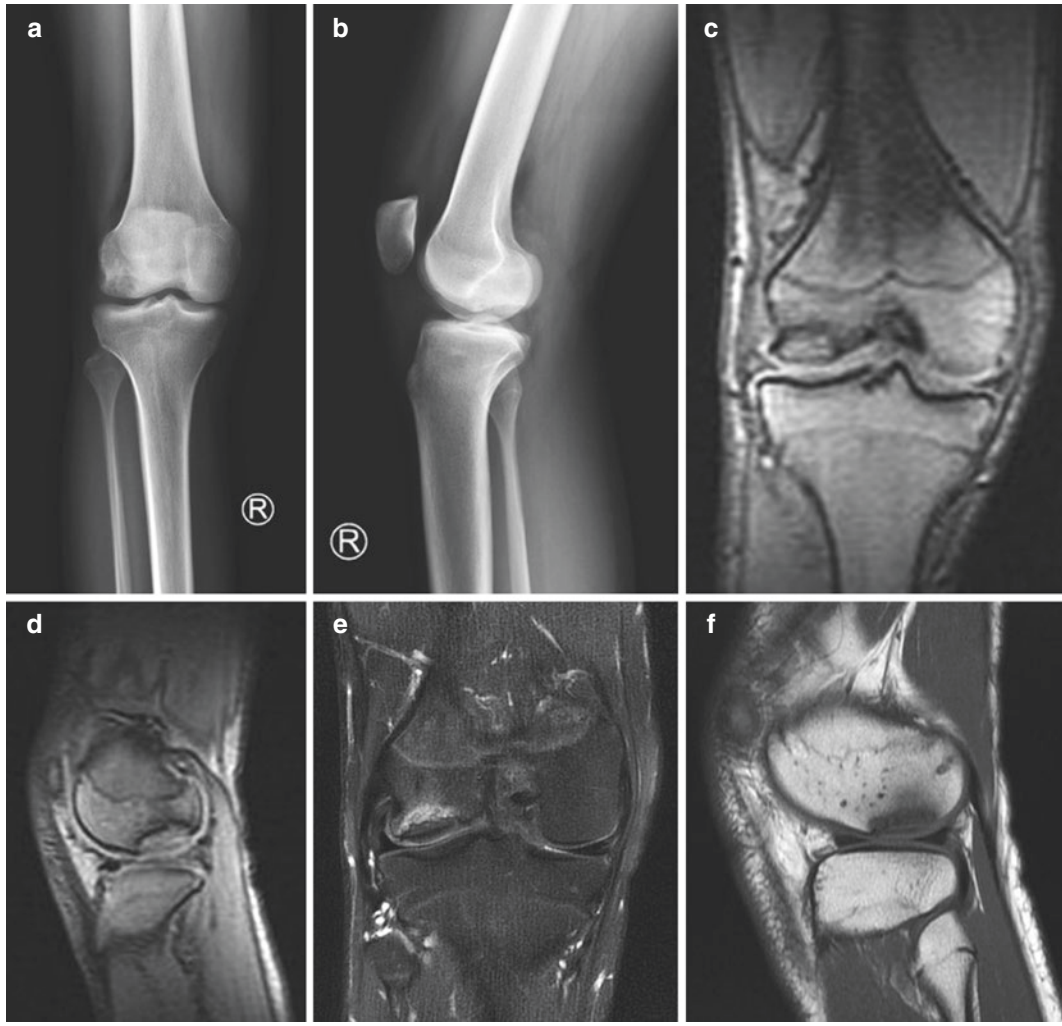

Figure 11.2.1: The Mosaicplasty technique: The Ideal Case Selection. A 22-year-old male patient suffered from right knee pain and moderate effusion after physical training for 1 year. (**a**, **b**) Right knee standing X-ray (the anteroposterior view and the lateral view) showed an osteochondral defect caused by a grade III osteochondritis dissecans of the lateral femoral condyle. (**c**) T1-weighted MR images in the frontal section and (**d**) sagittal section confirmed the diagnosis. (**e**, **f**) The lesion size was 23 mm at its maximal length in the sagittal section and 25 mm at its maximal diameter in the frontal section

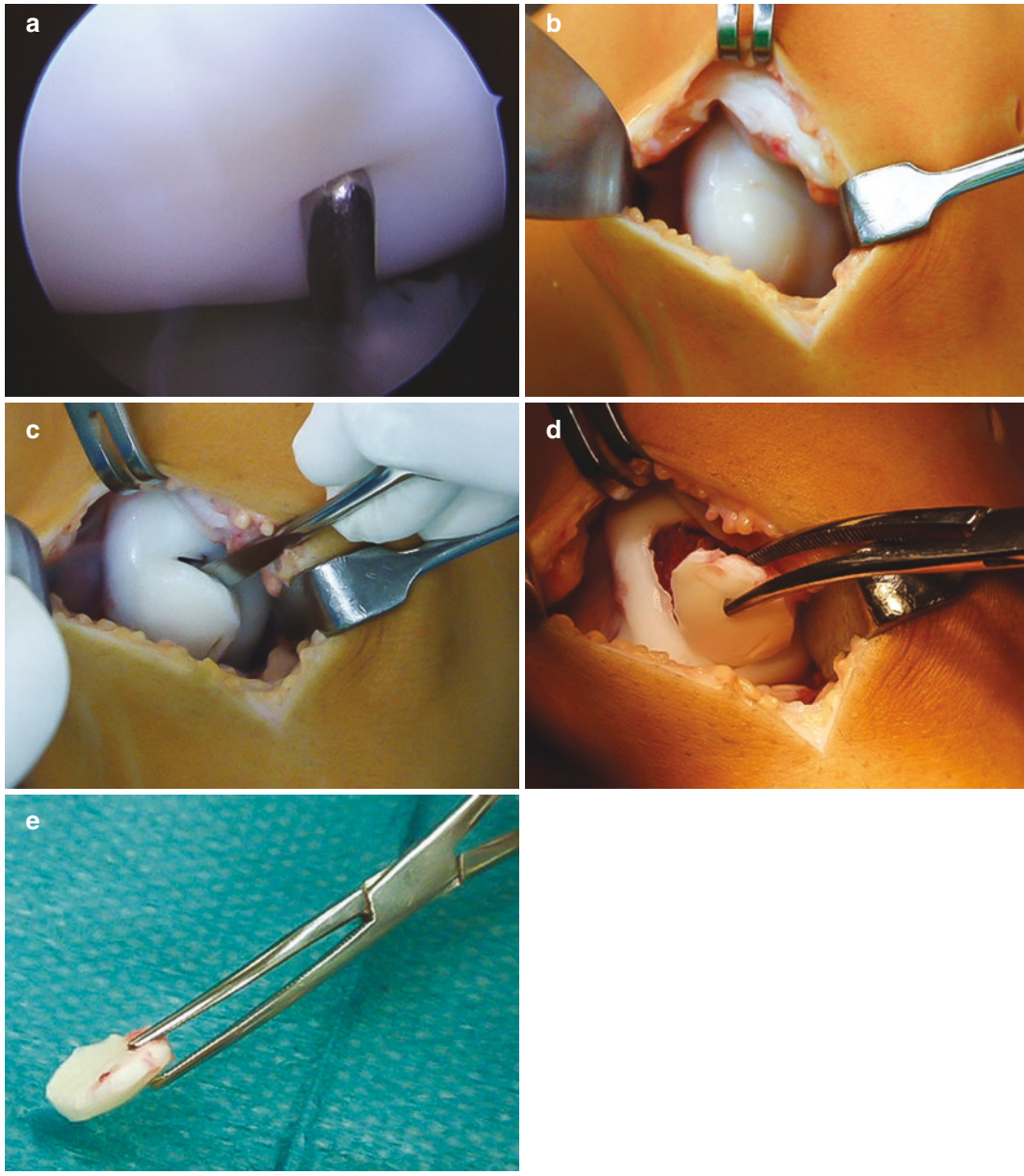

Figure 11.2.2: The Mosaicplasty technique: The Illustrations Assessment of the Ideal Lesion. (**a**) Arthroscopic examination of the right side lateral femoral condyle defect area was done in a 22-year-old male patient, viewing from standard anterolateral portal and instrument from the anteromedial portal, and it showed a well visible groove between the defect and the surrounding areas. (**b**) The defect area was explored through a lateral parapatellar mini-arthrotomy, (**c**, **d**) and an osteochondral fragment of approximately 3.0 cm^2 was excised. (**e**) The maximal thickness of the dissected osteochondral fragment was about 6–7 mm. This well contained 3.0–3.5 cm^2 superficial osteochondral lesion is ideal for mosaicplasty, as the surrounding articular cartilage is intact and the thickness of the bone loss is only 3–4 mm [3]. 15–20 mm long osteochondral cylinders are perfect to substitute not only the cartilage defect but also the bone loss. Proper press-fit fixation of the grafts allows quick rehabilitation [3, 4]

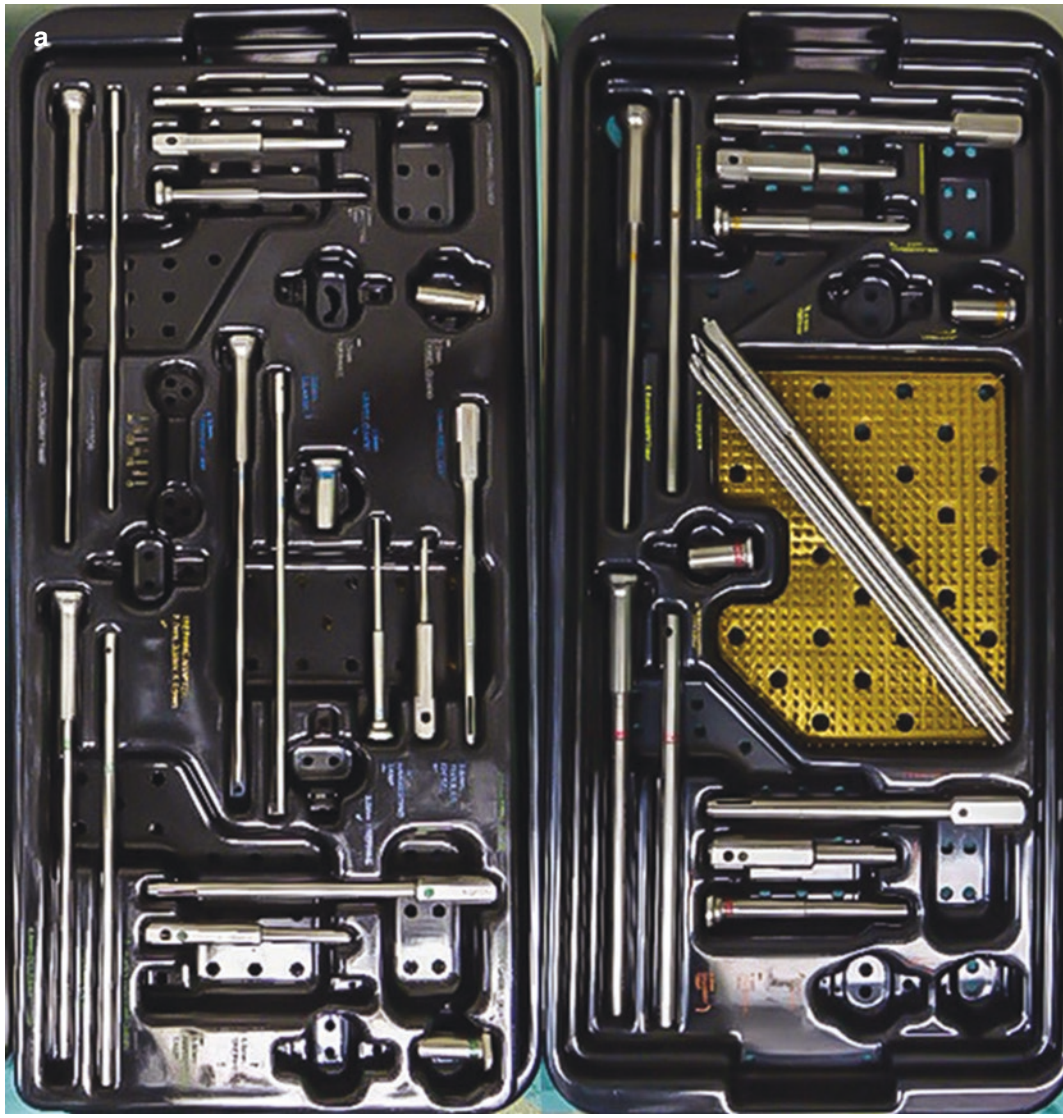

Figure 11.2.3: The Mosaicplasty technique: The Illustrations Instruments required. (**a**) The reusable mosaicplasty instruments sets (Smith and Nephew Inc., Andover, MA) are available in five sizes (2.7, 3.5, 4.5, 6.5, and 8.5 mm diameters). Bigger size osteochondral cylinders are used first, and then smaller sizes osteochondral cylinders can be used to fill the dead spaces in between, to improve the filling rate. (**b**) Tubular harvesters are designed for graft harvest from the less weight-bearing periphery of the patellofemoral joint. Tubular guides are used to provide proper support for all the steps of the implantation. Implantation is supported by drill bits to create recipient tunnels, and conical shape rods (dilators) are provided for proper dilation of these tunnels for easy graft insertion. Finally, insertion tamps with adjustable knob are used to implant the grafts to the appropriate level, keeping flush to the surrounding articular surface [3]

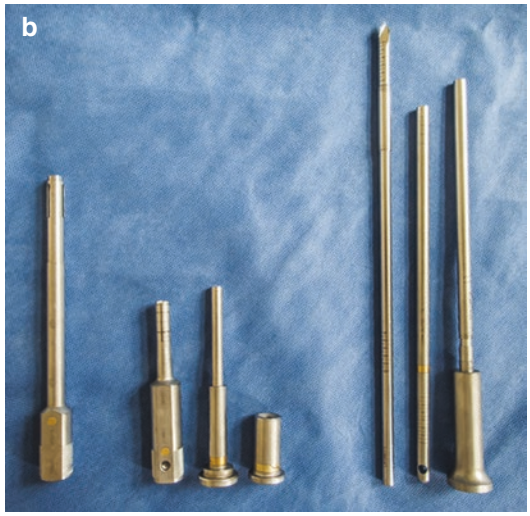

Figure 11.2.3: (continued)

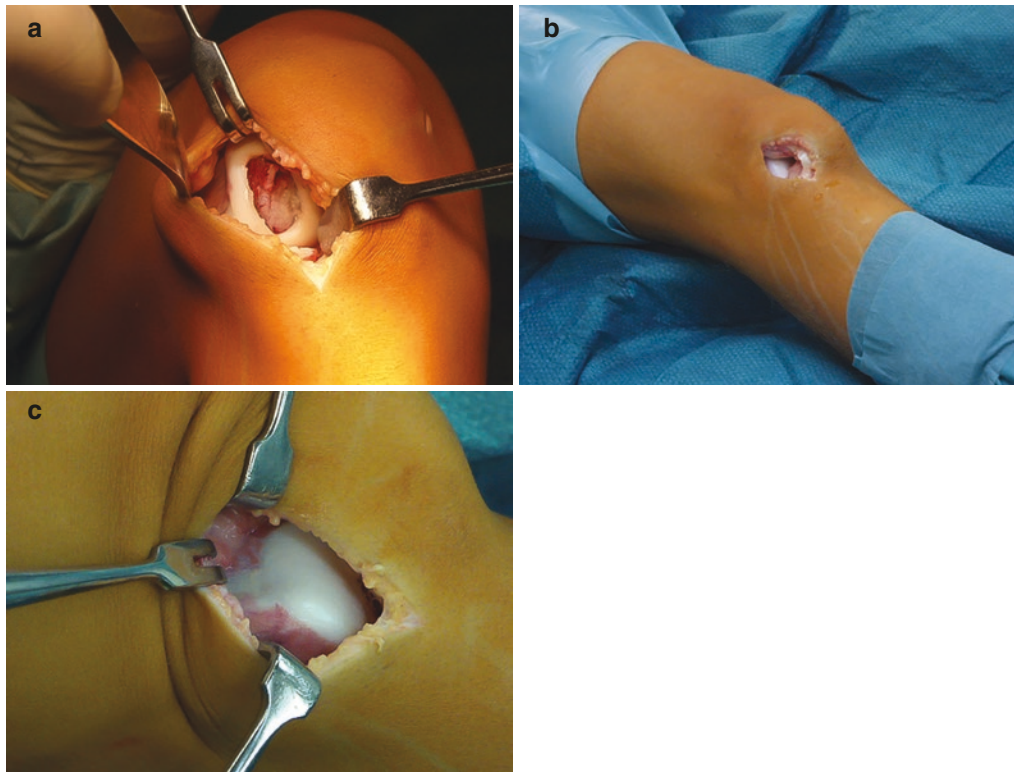

Figure 11.2.4: The Mosaicplasty Technique: Understanding the Surgical Approach. A perpendicular access for the graft harvest and the implantation is obligatory. Implantation of 1–3 grafts on the femoral condyles can be managed easily arthroscopically, but perpendicular access for proper positioning of further implants usually requires a mini-arthrotomy approach [1, 5]. Mosaicplasty for patellofemoral and tibial lesions or indications outside the knee can also be performed by arthrotomy. (**a**) A perpendicular access to the defect area in the right knee is achieved in a flexed knee position, in a 22-year-old male patient with the lateral parapatellar mini-arthrotomy approach. The same approach in the (**b**) fully extended knee position allows access to the most cranial part of the periphery of the lateral femoral condyle for the graft harvest. (**c**) A slight flexion may provide perpendicular access to the lower part of the donor area on the non- or less weight-bearing portion of the lateral femoral condyle for the graft harvest [4, 6]

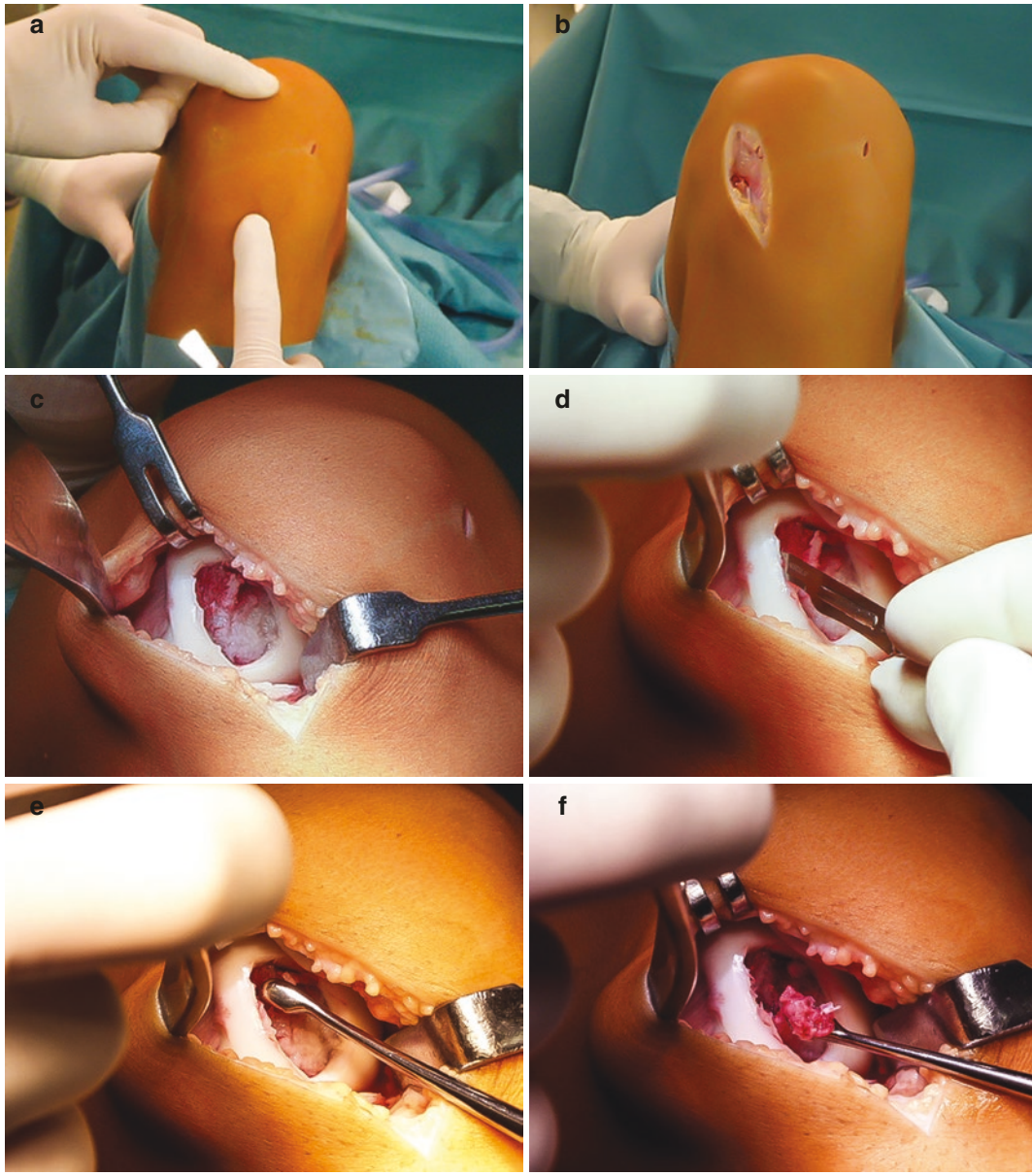

Figure 11.2.5: The Mosaicplasty Technique: The Defect Preparation. A 22-year-old male patient undergoes the mosaicplasty procedure for the osteochondral defect of the lateral femoral condyle of the right knee. (**a**) The landmarks for lateral mini-arthrotomy are the points lateral to the lower pole of the patella and the upper lateral corner of the tibial tubercle. (**b**) The skin incision is put for the lateral parapatellar approach, and (**c**) the defect area is explored. (**d**) The margins of the defect are excised by putting a vertical sharp cut perpendicular to the surface. (**e**) The bony base of the defect area is curetted with a sharp curette, and the (**f**) debris are removed

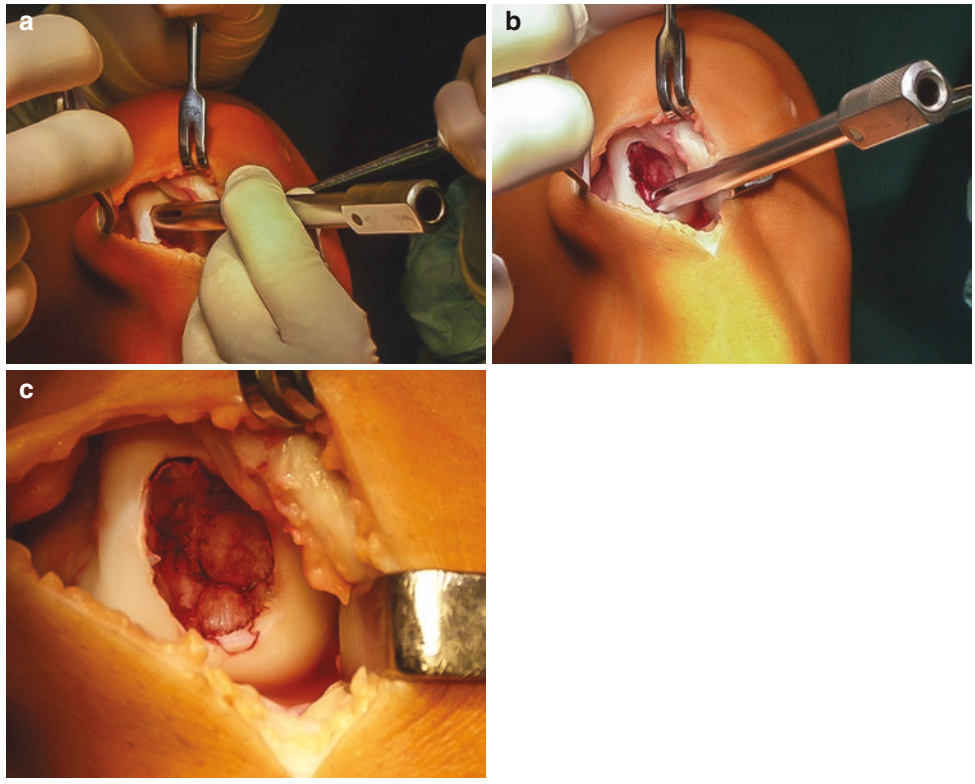

Figure 11.2.6: The Mosaicplasty Technique: The Planning to Fill the Cartilage Defect with the Osteochondral Cylinder Grafts. The osteochondral cylinder harvesting of the grafts is planned in a male aged 22 years with an osteochondral defect in the lateral femoral condyle of the right knee. The tubular chisels of the different sizes have a sharp cutting edge. Light tapping of these cutting edges can mark the bony base of the defected area by circumferences of different sizes. This marking may help to plan an optimal filling rate. (**a**) The sharp cutting edge of a chisel guard (size 8.5 mm) is used to mark the bony base of the defect, and then (**b**) step-by-step planning is performed to find the optimal filling by different graft sizes. (**c**) The optimal filling rate is achieved by contacting rings and deciding the best sizes and number of the grafts

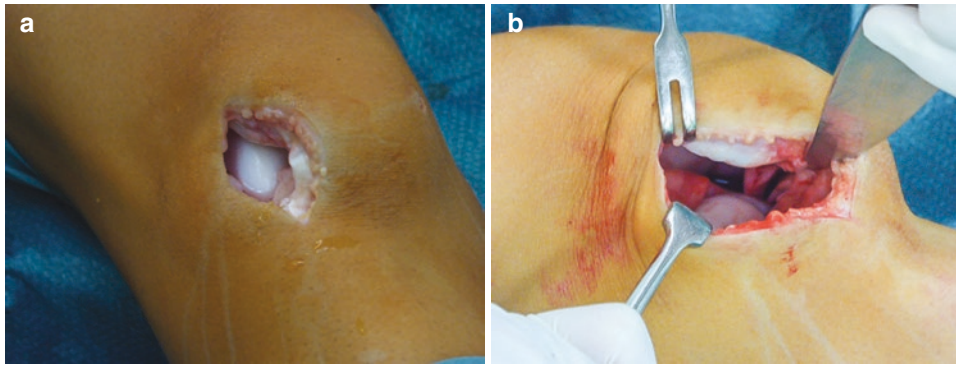

Figure 11.2.7: The Mosaicplasty Technique: The Donor Site Selection. The medial and lateral borders of the medial and the lateral femoral condyles above the level of sulcus terminalis are the less weight-bearing surfaces and may serve as the primary donor sites. In the case of arthroscopic graft harvest, perpendicular access to the medial side is usually easier. In the case of extended graft harvest, the periphery of the notch area may also serve as the secondary harvest site. However, the concave chondral surface of the notch area and the stiffer underlying bone are less optimal compared to the primary harvest areas. (**a**) The right knee of a male patient aged 22 years is explored thru the lateral parapatellar arthrotomy for the possible donor area assessment, and the area of the lateral femoral condyle is noted as easily accessible primary donor site in the extended knee position. (**b**) Opposite side donor area (periphery of the medial femoral condyle) from the same approach may be reached by special retractors but can be challenging to harvest

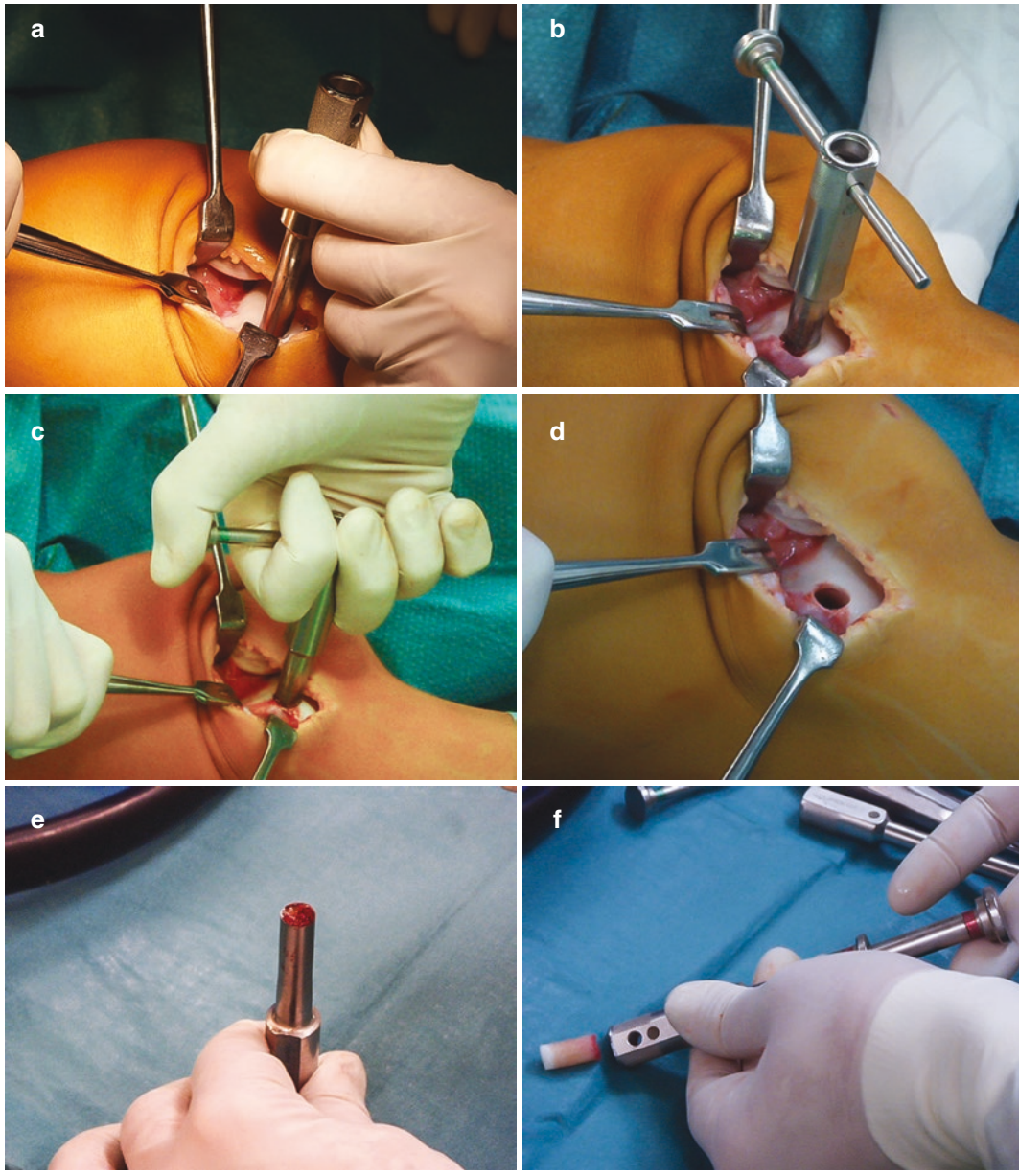

Figure 11.2.8: The Mosaicplasty Technique: Harvesting of the Osteochondral Cylinder Grafts. The osteochondral cylinder graft harvest should be performed strictly perpendicular to the surface of the donor site. In a male aged 22 years with a lesion on weight-bearing area of the right side lateral femoral condyle, graft harvesting is done from the non-weight-bearing area of the lateral femoral condyle. (**a**) Perpendicular placement of the harvester (8.5 mm diameter in this case) on the articular surface is mandatory for the graft harvest. (**b**) Once the harvester is inserted to the desired length (15 mm in this case), removal of the graft is promoted by a tommy bar inserted to the harvester and then by (**c**) performing a slight toggling of the harvesting chisel. (**d**) The empty donor tunnel after graft harvest at the upper part of the lateral donor area is inspected. (**e**) The harvester has a bevel edge to break the graft directly at the level of the cutting edge providing proper graft length. (**f**, **g**) Graft delivery tube is put over the harvesting chisel, and osteochondral cylinder graft is pushed out by pressing of the bony end of the graft. A gentle graft removal from the harvester tube is also recommended. (**h**) The properly delivered osteochondral graft is inspected that is of 8.5 mm diameter and 15 mm length. (**i**) As per requirement, the second or (**j**) third graft can be harvested similarly while remaining proximal to sulcus terminalis all the time and keeping a distance of around 3–4 mm in between. (**j**) The harvested grafts are stored in saline while the recipient area is prepared. The dissected OCD piece is also seen next to the harvested grafts

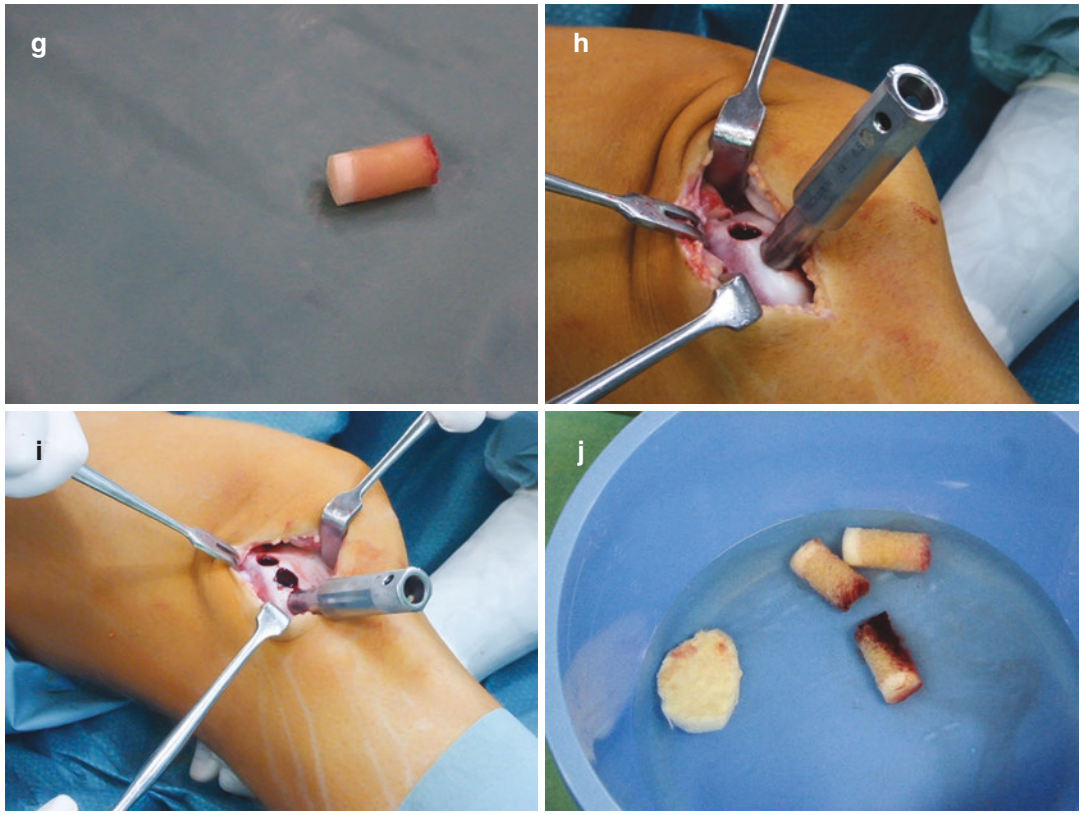

Figure 11.2.8: (continued)

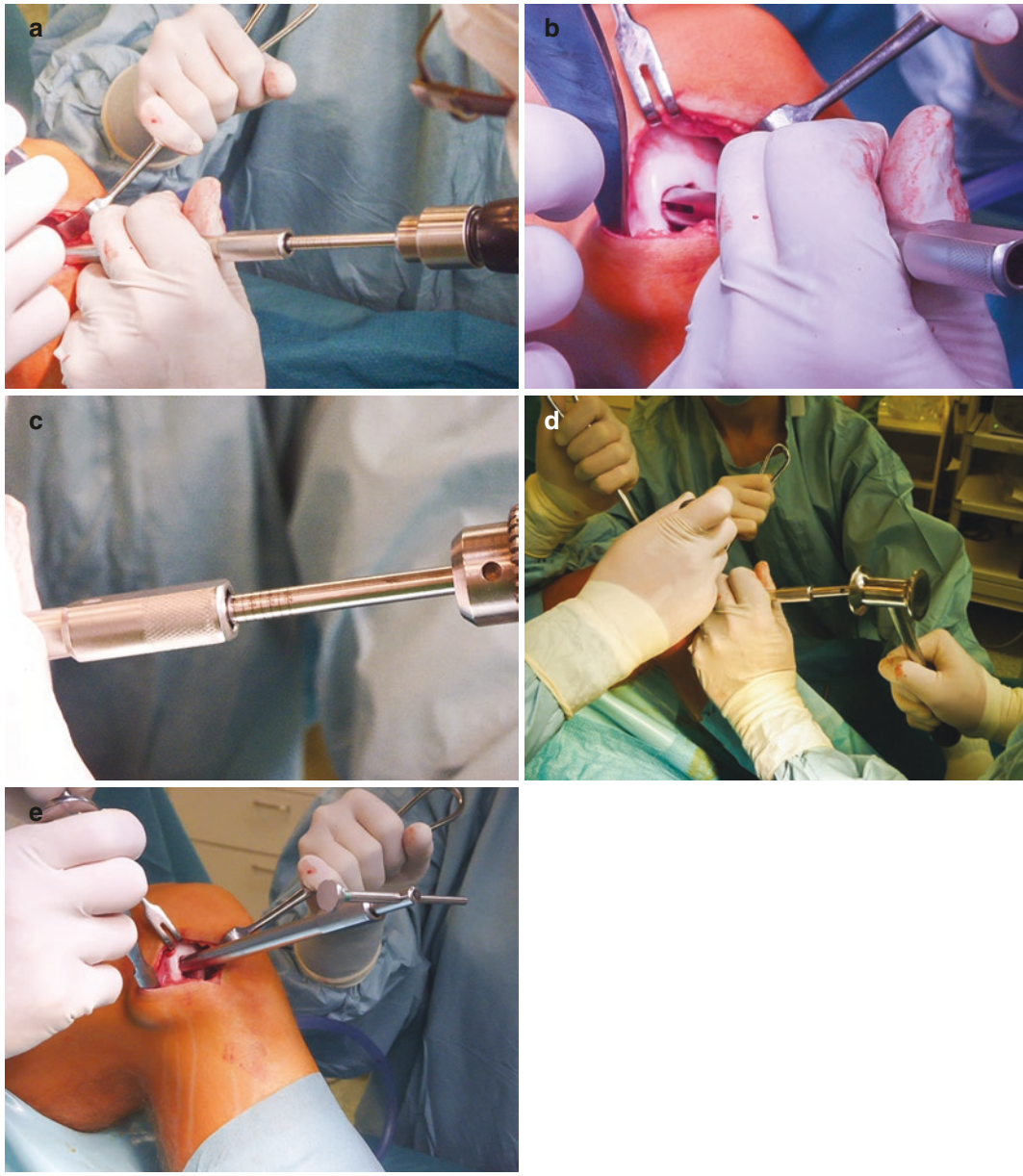

Figure 11.2.9: The Mosaicplasty Technique: The Preparation of the Recipient Area. The recipient tunnels are prepared as per planning done in Figure 11.2.6. The respective graft harvester chisel diameter, delivery tube diameter, and drill bit diameter should match. (**a**, **b**) A drilling guide of respective diameter (8.5 mm in this case) is used to provide safe perpendicular access for drilling in a 22-year-old male with osteochondral lesion in the right side lateral femoral condyle. (**c**) The depth of the drilling can be checked by laser marks. (**d**) The appropriate size of dilator (8.5 mm) is used to properly shape the recipient tunnel so that the graft insertion can be done with minimum pressure on the cartilage and thus providing better cartilage tissue protection. The 8.5 mm diameter dilator is tapped into the recipient tunnel till 20 mm depth, which is supported by the tubular guide. Recipient tunnels usually should be drilled deeper than the length of the grafts. Fixation of the graft doesn't depend on the sitting on the bottom but rather on the press-fit created by slightly bigger graft diameter and conical shape preparation of recipient tunnels. In this case the young patient had a very strong, elastic bone so the recipient tunnels were drilled for 20 mm long and dilation was also performed in the same length. In case of less good bone quality, a less deep dilation could be performed [3, 4]. (**e**) Removal of the dilator is done using the tommy bar

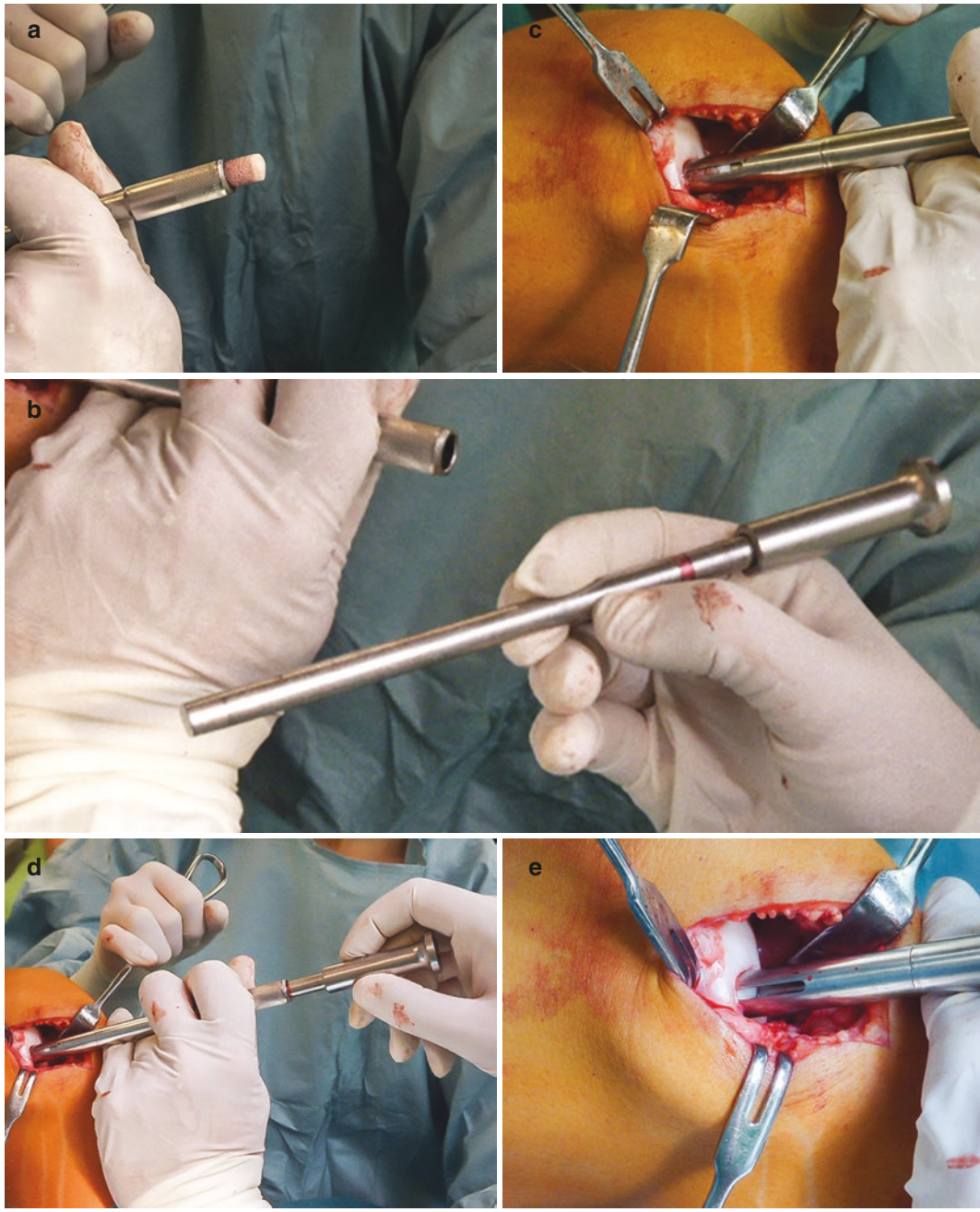

Figure 11.2.10: The Mosaicplasty Technique: The Insertion of the Harvested Osteochondral Grafts. The osteochondral graft insertion is done in a 22-year-old male patient with an osteochondral lesion in the lateral femoral condyle of the right knee. The insertion is supported by the tubular guide and the tamp with the adjustable knob. All graft surfaces should be seated flush to the surrounding chondral surface to achieve maximum congruency. (**a**) The 8.5 mm diameter osteochondral graft is inserted into the tubular guide keeping chondral surface up and should be pressed in, in a gentle manner. (**b**) The laser marks and the adjustable knob of the graft delivery tamp support the gentle insertion of the grafts. (**c**, **d**) The adjustable knob of the delivery tamp should be turned counterclockwise to provide step-by-step delivery. (**e**) The proper position of the osteochondral graft can be checked through the windows in the delivery tube. (**f**) The graft should be seated flush to the surrounding articular surface. (**g**) The implantation of the second graft should be done similarly, and the proper congruency is checked (**h**, **i**) from different views to evaluate possible prominence. (**j**) The best filling rate can be achieved by insertion of different sizes of the graft in between the primary grafts

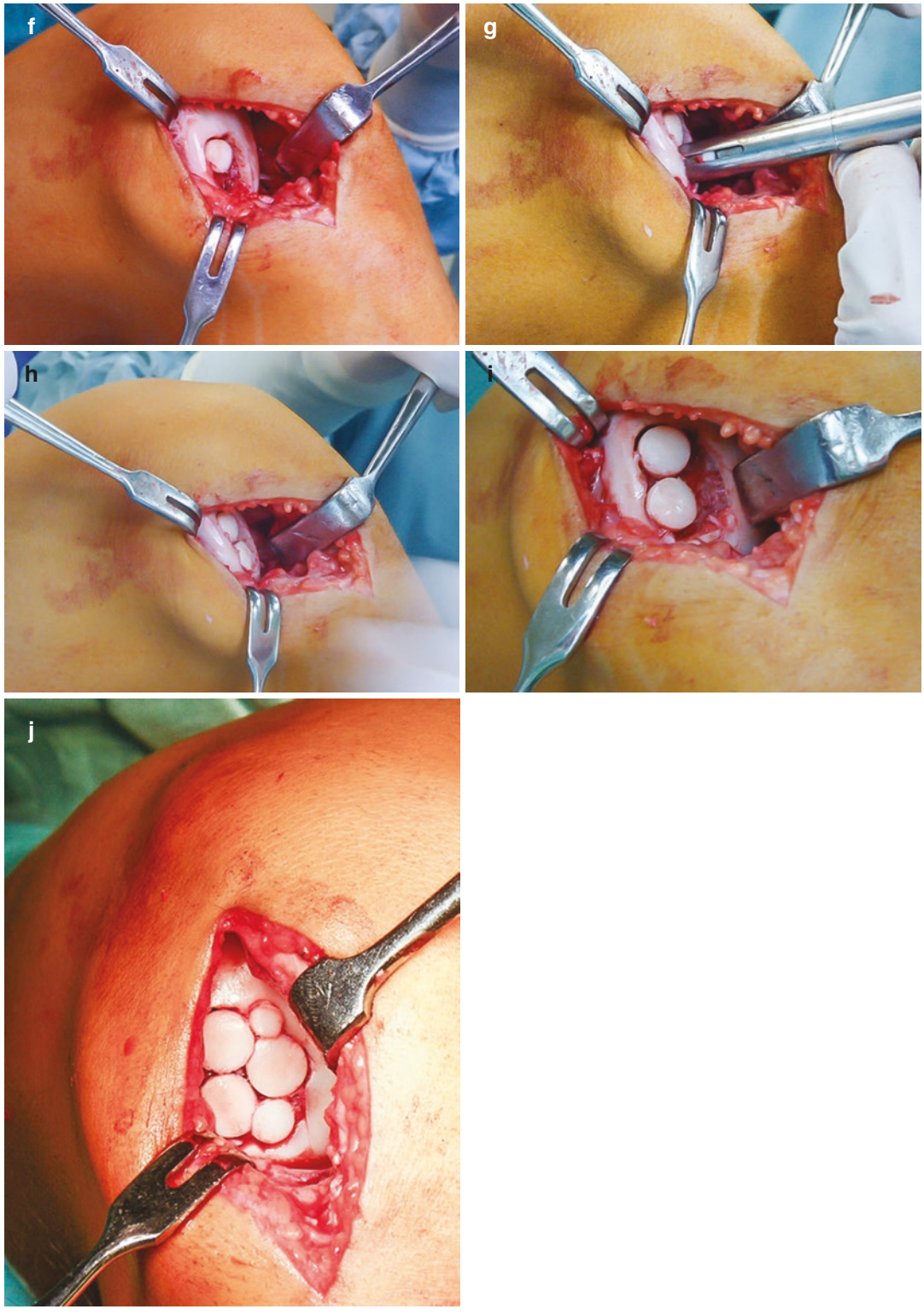

Figure 11.2.10: (continued)

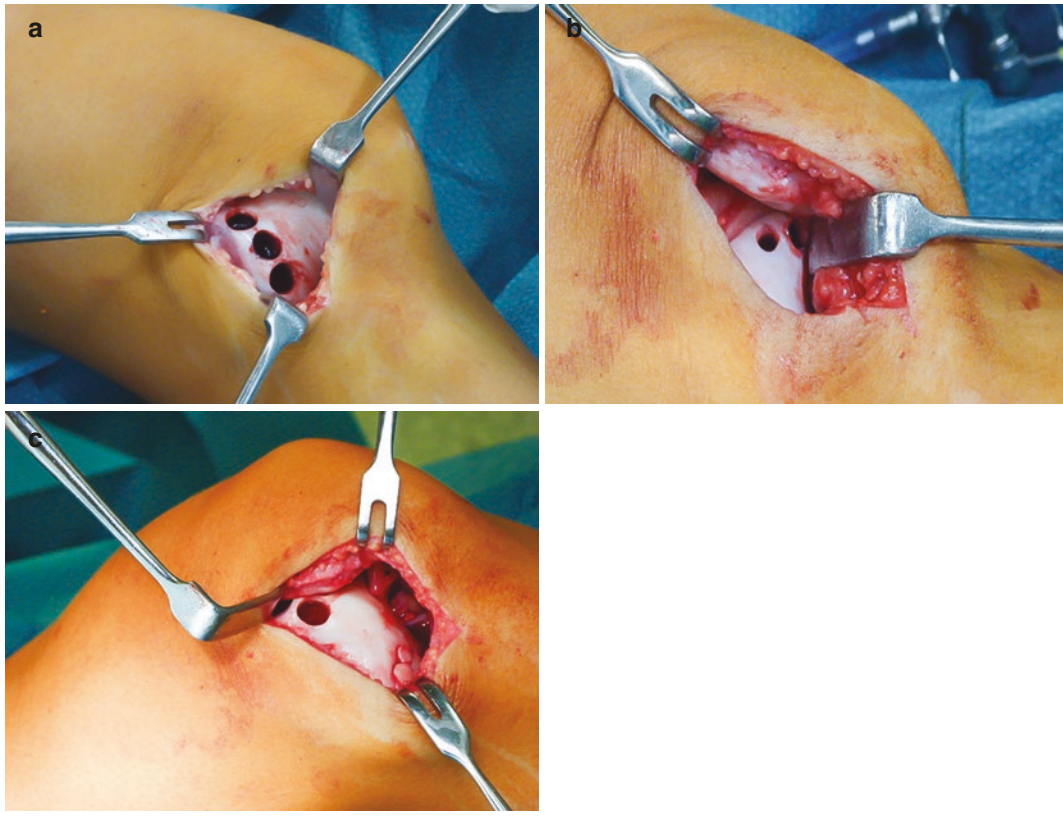

Figure 11.2.11: The Mosaicplasty Technique: Inspection of the Donor Sites. Final inspection of the donor sites is needed to check whether bony bridges between donor tunnels are intact or not. Any possible damage may require slower rehabilitation progress or filling them by biodegradable scaffolds to promote the healing process. A 22-year-old male patient has undergone harvesting of osteochondral donor plugs from the non-weight-bearing zones of the lateral and medial femoral condyles of the right knee. The empty donor tunnels on (**a**, **b**) the periphery of the lateral femoral condyle and (**c**) on the medial periphery of the medial femoral condyle down to the sulcus terminalis are inspected, and the distance between the donor and the recipient areas is checked

Figure 11.2.12: The Mosaicplasty Technique: The Rehabilitation. The surgeon should instruct and guide physiotherapist for a dedicated rehab program in each patient. Customization may be needed depending on the site and extent of the cartilage lesions being treated with mosaicplasty. Proprioceptive training and open-chain strengthening exercises are the keys to faster and swifter return to sports. (**a**) A proprioceptive training for 12-week-old mosaicplasty patient has been administered. (**b**) Muscle strengthening exercises by open-chain training for 8-week-old mosaicplasty patient is given

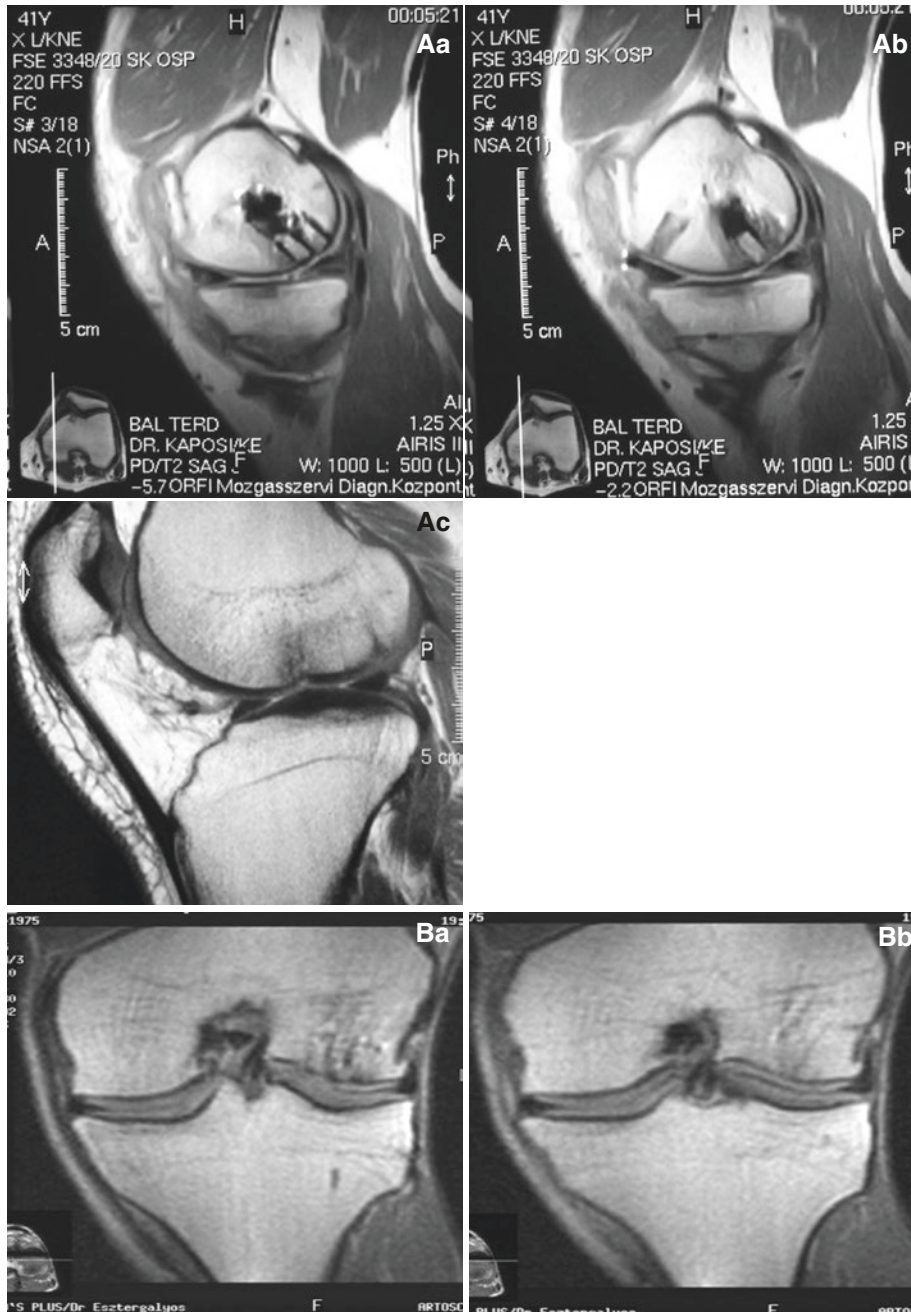

Figure 11.2.13: The Mosaicplasty Technique: The Follow-Up MRI. (**A**): A short-term and mid-term MRI follow-up of a mosaicplasty case done for a shallow OCD defect on the medial femoral condyle. The operation was performed arthroscopically to treat painful, swollen left knee of a 30-year-old dentist. The patient was complaint free at 6 weeks follow-up, and no further deterioration was detected at 2 years follow-up. (**a**) Sagittal view of a 6-week-old mosaicplasty on the medial femoral condyle. (**b**) Donor and recipient sites are seen on the same sagittal section. (**c**) 2 years follow-up sagittal MRI view showing well-healed mosaicplasty plugs on the medial femoral condyle. (This case is different from the case shown from Figures 11.2.1, 11.2.2, 11.2.4, 11.2.5, 11.2.6, 11.2.7, 11.2.8, 11.2.9, 11.2.10, 11.2.11, 11.2.13B, and 11.2.14.) (**B**) A 21-year-old athlete suffered from a painful 4 cm^2-sized OCD lesion of the lateral femoral condyle and was treated by an open mosaicplasty using six grafts of 6.5 mm diameter and two grafts of 4.5 mm diameters. (**a**, **b**) He recovered perfectly, and a follow-up MRI was done at 2 years that showed well-healed osteochondral plugs with homogenous healing with the surrounding bone and the cartilage. (This case is different from the case shown from Figures 11.2.1, 11.2.2, 11.2.4, 11.2.5, 11.2.6, 11.2.7, 11.2.8, 11.2.9, 11.2.10, 11.2.11, 11.2.13A, and 11.2.14)

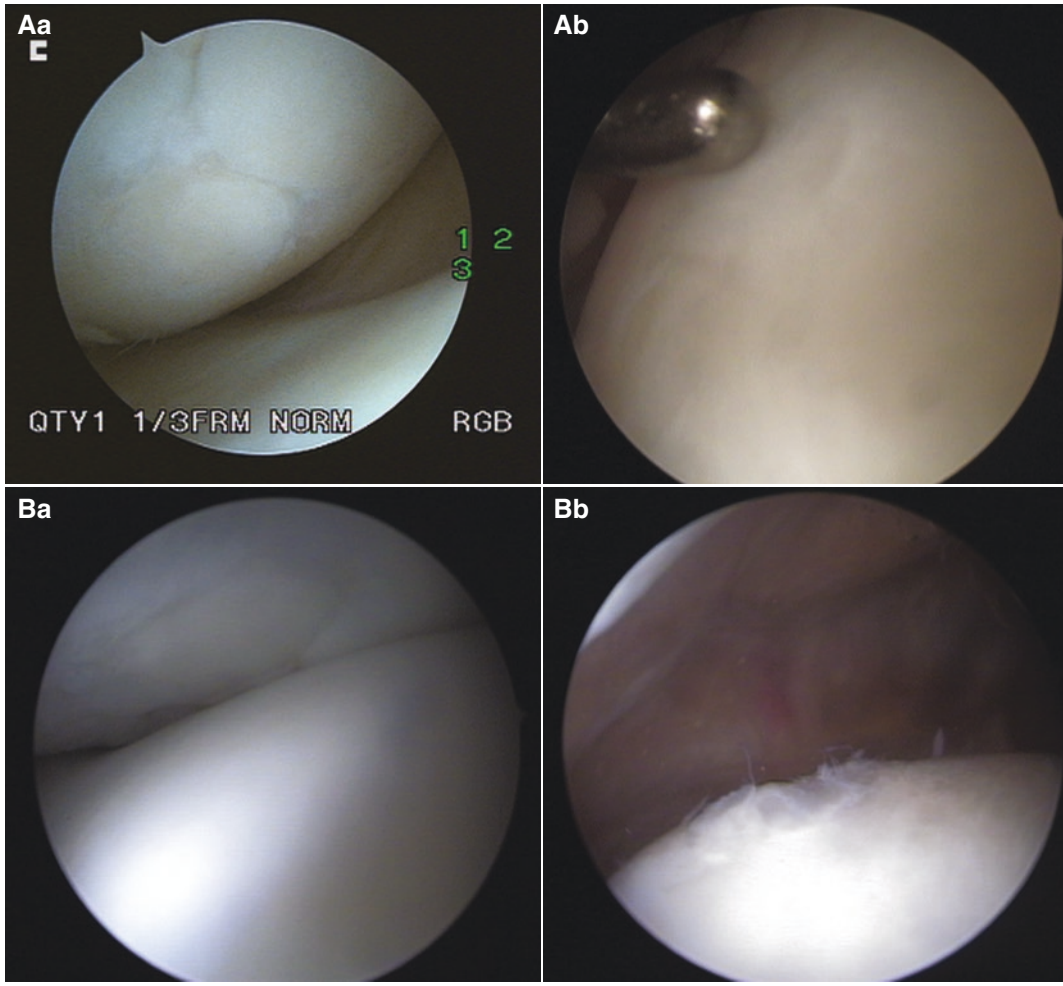

Figure 11.2.14: The Mosaicplasty Technique: The Follow-Up Arthroscopy. (**A**) A 32-year-old female dancer suffered from right knee anterior cruciate ligament tear along with 2 cm^2 chondral defect on the medial femoral condyle and was treated with anterior cruciate ligament reconstruction and arthroscopic mosaicplasty. Four osteochondral grafts of 6.5 mm diameter were harvested, three from the medial femoral condyle and one from the lateral femoral condyle. (**a**) Control arthroscopy of 1-year-old mosaicplasty on the medial femoral condyle shows well-healed 8.5 mm plugs in the center of the medial femoral condyle. All the plugs and intermediary tissue between the plugs are flush to the surrounding articular surface. (**b**) Fibrocartilage coverage of the donor tunnel located on the lateral margin of the lateral femoral condyle in the same case is seen. (This case is different from the case shown from Figures 11.2.1, 11.2.2, 11.2.4, 11.2.5, 11.2.6, 11.2.7, 11.2.8, 11.2.9, 11.2.10, 11.2.11, 11.2.13, and 11.2.14B.) (**B**) An open mosaicplasty was performed for a 35-year-old male patient suffering from retro-patellar pain and effusion of his right knee. Anteromedialization was also performed at the time of the same surgery. Control arthroscopy was done at the time of removal of the screws. (**a**) 3-year-old control arthroscopy of a mosaicplasty on the patella for a 1.5 cm^2 chondral defect shows well-healed mosaicplasty plugs with surrounding tissues. (**b**) Properly healed donor site on the lateral margin of the trochlea of the same case. (This case is different from the case shown from Figures 11.2.1, 11.2.2, 11.2.4, 11.2.5, 11.2.6, 11.2.7, 11.2.8, 11.2.9, 11.2.10, 11.2.11, 11.2.13, and 11.2.14A.)

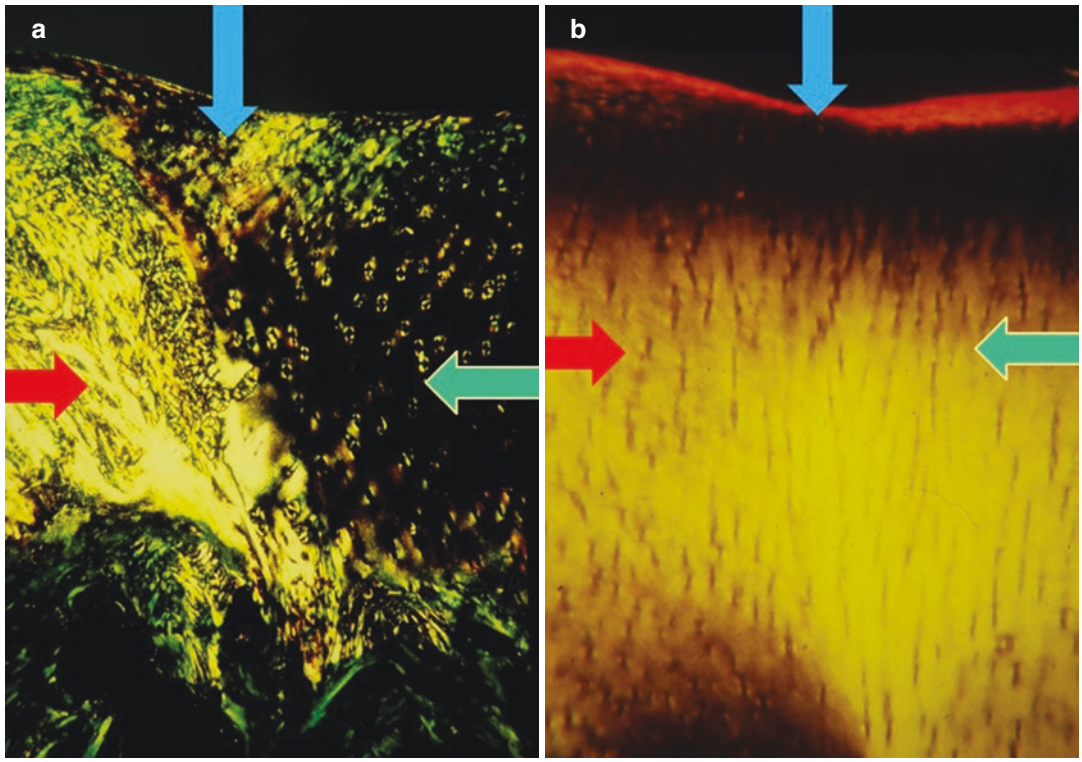

Figure 11.2.15: The Mosaicplasty Technique: The Follow-Up Histological Assessment. A 2 mm diameter osteochondral specimen was harvested by a tubular harvester during a control arthroscopy of a 29-year-old male patient. Implantation was performed to treat a 2 cm^2 chondral defect on the medial femoral condyle, 1 year ago. Second look arthroscopy was indicated for a second sports injury. (This case is different from the case shown from Figures 11.2.1, 11.2.2, 11.2.4, 11.2.5, 11.2.6, 11.2.7, 11.2.8, 11.2.9, 11.2.10, 11.2.11, 11.2.13, and 11.2.14.) (**a**) Transitional area of 1-year-old transplanted graft (picrosirius red at polarized light, 50×) shows healthy hyaline cartilage of the transplanted graft located to the right (green arrow) and intermediate fibrocartilage tissue to the left (red arrow) along with the deep matrix integration between the tissue layers (blue arrow). (**b**) Transitional area of 1-year-old transplanted graft (picrosirius red at polarized light, 50×) shows excellent quality of transplanted hyaline cartilage located to the right (green arrow) and host hyaline cartilage to the left (red arrow) with deep matrix integration of transplanted tissue to the host area (blue arrow)

11.3 Take-Home Message

In the last three decades, many techniques were developed to treat full-thickness chondral and osteochondral defects. Decision-making at the indication is determined by the type and the size of the defect, location of the defect area, activity level of the patient, concomitant biomechanical problems, and many other factors. In spite of promising results with other surgical alternatives, mosaicplasty is still a valuable treatment option for small- and medium-sized focal defects of the weight-bearing articular surfaces. Significant advantages of this procedure are reliable medium- and long-term results (over 90% good to excellent 5-year results in femoral condyle and over 78% good to excellent outcome at 10 years follow-up) [4, 5, 7–9], low rate of donor site morbidity (3% patellofemoral pain due to graft harvest in our material) [4, 5, 8, 9], and quick rehabilitation. Best outcome can be achieved in the cases of well-indicated femoral condylar and ankle implantations, while less favorable results can be expected in the patellofemoral joint.

References

1. Hangody L, Kish G, Kárpáti Z, Szerb I, Udvarhelyi I. Arthroscopic autogenous osteochondral mosaicplasty for the treatment of femoral condylar articular defects. Knee Surg Sports Traumatol Arthrosc. 1997;5:262–7.
2. Hangody L, Füles P. Autologous osteochondral mosaicplasty for the treatment of full thickness defects of weight bearing joints—10 years experimental and clinical experiences. J Bone Joint Surg. 2003;85-A(Suppl 2):25–32.
3. Hangody L, Ráthonyi G, Duska ZS, Vásárhelyi G, Füles P, Módis L. Autologous osteochondral mosaicplasty—surgical technique. J Bone Joint Surg. 2004;86-A(Suppl I):65–72.
4. Hangody L, Vásárhelyi G, Hangody LR, Sükösd Z, Tibay G, Bartha L, Bodó G. Autogenous osteochondral grafting—technique and long term results. Injury. 2008;39(Suppl 1):32–9.
5. Hangody L, Dobos J, Baló E, Pánics G, Hangody LR, Berkes I. Clinical experiences with autologous osteochondral mosaicplasty in athletic population—a 17-years prospective multicenter study. Am J Sports Med. 2010;38:1125–33.
6. Simonian PT, Sussmann PS, Wickiewicz TL, Paletta GA, Warren RF. Contact pressures at osteochondral donor sites in the knee. Am J Sports Med. 1998;26:491–4.
7. Barber FA, Chow JCY. Arthroscopic osteochondral transplantation: histologic results. Arthroscopy. 2001;17(8):832–5.
8. Gudas R, Kalesinskas RJ, Kimtys V, Stankevicius E, Toliusis V, Bernotavicius G, Smailys A. A prospective randomized clinical study of mosaic osteochondral autologous transplantation versus microfracture for the treatment of osteochondral defects in the knee joint in young athletes. Arthroscopy. 2005;21:1066–75.
9. Pareek A, Reardon PJ, Maak TG, Levy BA, Stuart MJ, Krych AJ. Long-term outcomes after osteochondral autograft transfer: a systematic review at mean follow-up of 10.2 years. Arthroscopy. 2016;32:1174–84.

12 The Illustrative Osteochondral Cylinder Transfer Techniques for Cartilage Repair: The OATS Technique

Sachin Ramchandra Tapasvi, Anshu Shekhar, and Shantanu Sudhakar Patil

12.1 Introduction

Cartilage injuries of the knee can have myriad presentations and need to be managed appropriately based on the site, size, and merits of the case. The surgeries can be either reparative procedures or restorative techniques. Transfer of osteochondral plug(s) allows restoration of hyaline cartilage at the defect and is suitable even in the high-demand patients as it is associated with greater longevity, durability, and improved outcomes [1, 2]. It is done in a single stage without aggravated costs or extensive rehabilitation later [3]. This technique also provides better long-term survival compared to the microfracture technique when matched for age or size of lesion [4]. Although suitable for the defects up to 2.5 cm^2, it can be used to cover the defects as large as 4 cm^2. The disadvantage of this technique is related to the donor-site morbidity (for autografts) and contour mismatch. The baseline factors predicting good outcome are single lesion, normal cartilage around the lesion, higher baseline Lysholm score, shorter duration of symptoms, normal patellofemoral joint, young age, and small defect size [5].

This surgery can be done using osteochondral cylinder grafts harvested from a non-weight-bearing area of the same knee as an autograft. A single plug can be used for smaller defect of 6–10 mm diameter, but multiple small- or variable-diameter plugs may be needed for the larger defects. All issues related to stability, alignment, and menisci must be managed simultaneously or prior to the cartilage surgery. There are multiple commercially available systems to perform an osteochondral cylinder transfer. One such system is Osteochondral Autograft Transplant System (OATS™, Arthrex, Naples, FL). These devices allow harvest and transfer of the osteochondral cylinders of various sizes like 4.75, 6, 8, and 10 mm, with 8 or 10 mm single plugs being the most commonly used.

S. R. Tapasvi (✉) · A. Shekhar
The Orthopaedic Speciality Clinic, Pune, India
e-mail: stapasvi@gmail.com;
dr.anshushekhar@gmail.com

S. S. Patil
SRM Medical College and Hospitals, SRM University, Kattankulathur, Tamil Nadu, India
e-mail: shantanusp@gmail.com

D. R. Goyal (ed.), *The Illustrative Book of Cartilage Repair*,
https://doi.org/10.1007/978-3-030-47154-5_12

12.2 The Illustrations

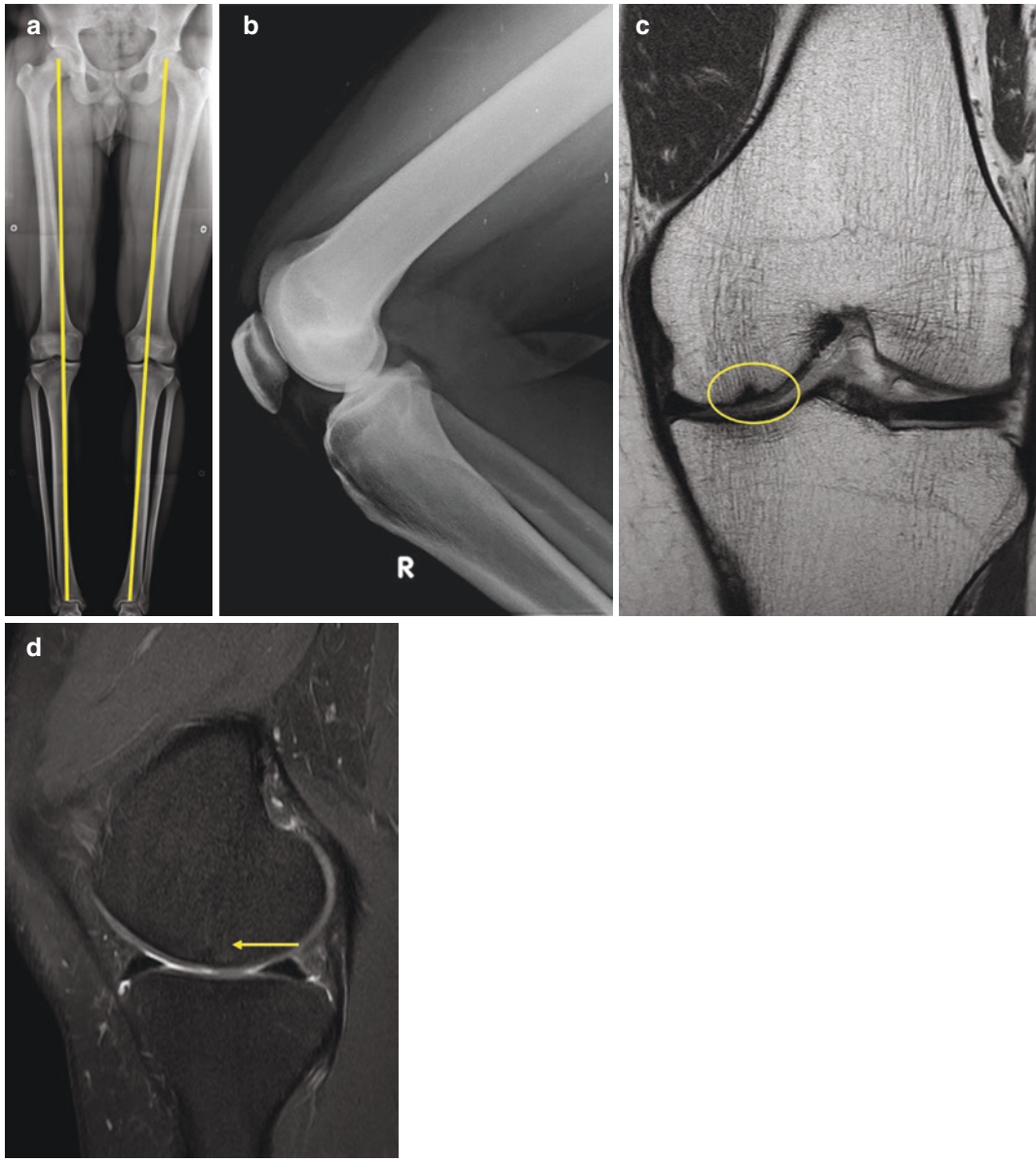

Figure 12.2.1.A: The OATS Technique: The Ideal Case Selection. Preoperative imaging of a 26-year-old female physical therapist and hiking enthusiast, who presented with complaint of right-knee pain of 3-month duration, sustained after a fall. (**a**) An anteroposterior long limb standing scanogram is essential when planning an osteochondral cylinder transfer surgery. The alignment must be neutral or within the physiological range. (**b**) A lateral radiograph is essential to rule out any bony defect or subchondral cysts which are absent in this case. (**c**) MRI of a focal grade 4 (ICRS) post-traumatic chondral lesion in the weight-bearing portion of the medial femoral condyle in proton density (PD) nonfat-saturated coronal MRI image seen as area of hyperintensity (yellow circle). (**d**) The same lesion seen in sagittal proton density (PD) fat-saturated sequence with surrounding bone marrow edema (yellow arrow). (The images shown in Figure 12.2.14a–d belong to the same case as shown in Figure 12.2.1.Aa–d)

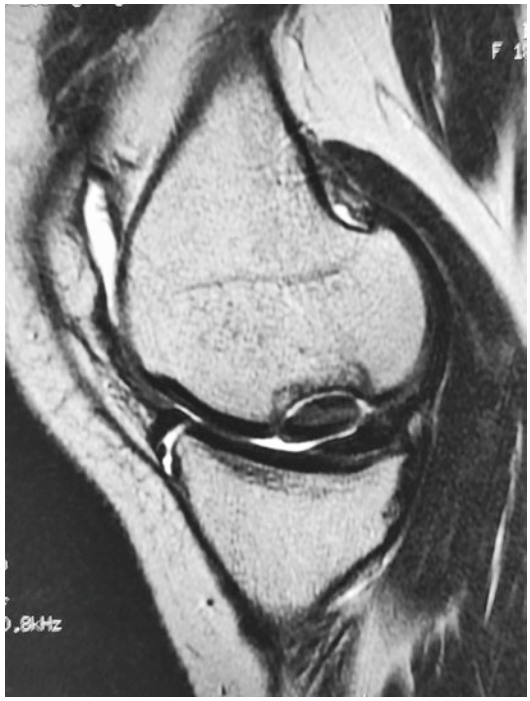

Figure 12.2.1.B: The OATS Technique: The Ideal Case Selection. A T2-weighted sagittal MRI section showing a case of osteochondritis dissecans involving the weight-bearing portion of the medial femoral condyle in a 16-year-old female professional dancer who complained of persistent knee pain, which aggravated on dancing. This is another excellent indication for single-plug OATS. (This image is from a different patient then shown in Figure 12.2.1.Aa–d)

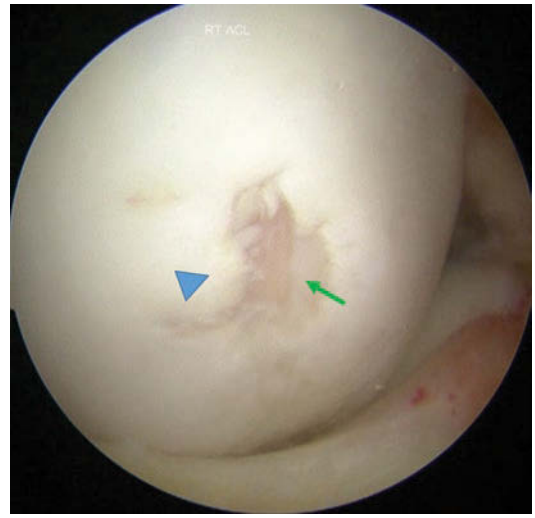

Figure 12.2.2: The OATS Technique: Arthroscopic Assessment of the Lesion. Arthroscopy right knee of a 26-year-old female, viewing from the anterolateral portal, knee in about 60° flexion. An isolated, contained defect in the lateral femoral condyle (LFC) is seen. Such a defect can have an excellent outcome when treated with autologous osteochondral cylinder plug transfer. It is worthwhile noting that although the lesion does not appear very large on inspection (green arrow), there lies an area of unstable cartilage (blue arrowhead) adjacent to it. (The images in Figures 12.2.2, 12.2.4, 12.2.5, 12.2.6, 12.2.8, 12.2.9, 12.2.10, 12.2.11, 12.2.12, and 12.2.13 belong to the same patient)

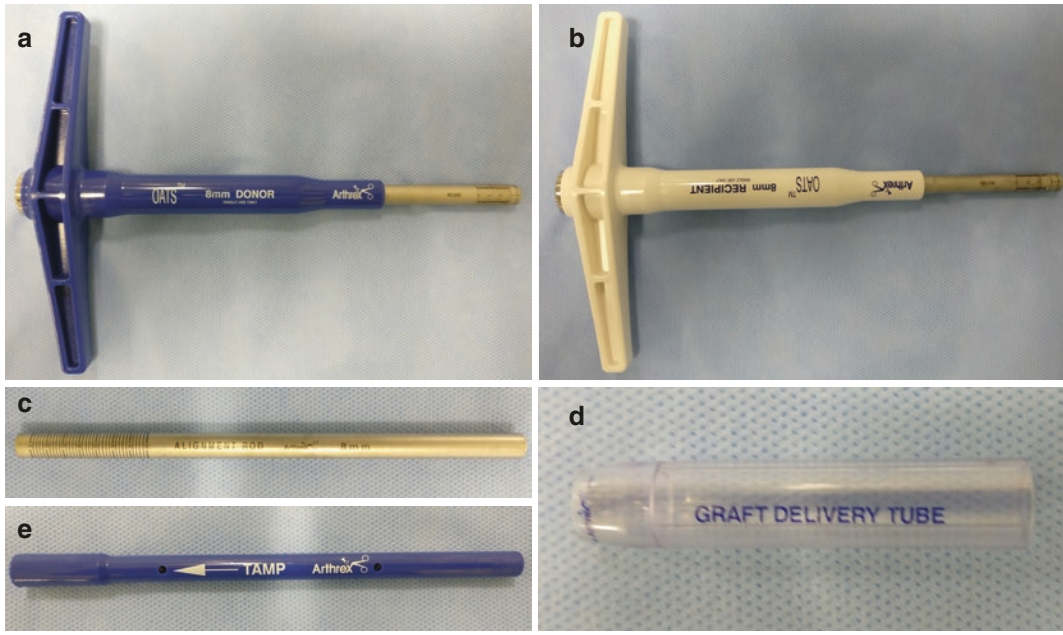

Figure 12.2.3: The OATS Technique: The Instruments Required. (**a**) A donor harvester for harvesting and delivering the osteochondral plug from the donor site, with markings to know the depth of insertion. (**b**) A recipient harvester to remove a bony cylinder from the defect up to a predetermined depth and create tunnel for insertion of the harvested plug. This is undersized by 1 mm in diameter than the donor harvester to allow a press-fit graft fixation. (**c**) An alignment rod is needed to ascertain the angle of the graft insertion, to assess accurate depth of the tunnel prepared, and to smoothen the walls of the prepared defect site. (**d**) A graft delivery tube to deliver the osteochondral plug into the defect without slippage or loss of orientation. (**e**) A tamp which is used for tapping the graft into the defect for the final sit. The tamp prevents damage to cartilage cells

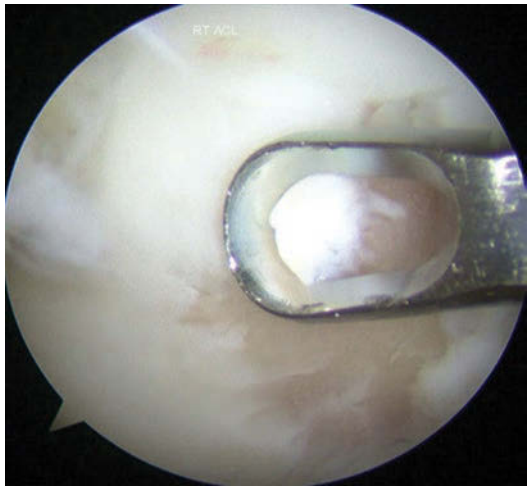

Figure 12.2.4: The OATS Technique: The Assessment of the lesion. Arthroscopy right knee in a 26-year-old female (same patient as in Figure 12.2.2), viewing from the anterolateral portal, instrumentation from the anteromedial portal, knee in about 60° flexion. The edges of the chondral lesion are curetted to create a stable margin. Any sclerotic bone in the bed is also removed with a curette. (The images in Figures 12.2.2, 12.2.4, 12.2.5, 12.2.6, 12.2.8, 12.2.9, 12.2.10, 12.2.11, 12.2.12, and 12.2.13 belong to the same patient)

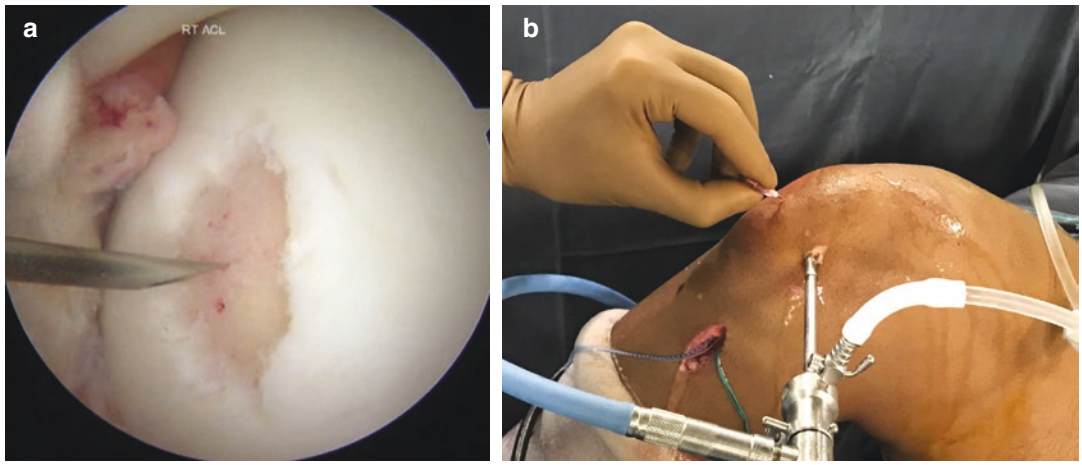

Figure 12.2.5: The OATS Technique: The Lesion Preparation. Arthroscopy right knee in a 26-year-old female, viewing lateral femoral condyle from the anteromedial portal, knee in about 90° flexion. (**a**) An 18G hypodermic or spinal needle is inserted perpendicular to the lesion to assess if it can be approached arthroscopically. The knee must be flexed to the appropriate degrees of flexion for the perpendicular approach; and if this is not possible then an arthrotomy may be required for optimal approach. Most medial or lateral femoral condyle defects can be approached arthroscopically but not very posterior defects of femoral condyles or lesions in the tibia. (**b**) External view of the step described in (**a**). (The images in Figures 12.2.2, 12.2.4, 12.2.5, 12.2.6, 12.2.8, 12.2.9, 12.2.10, 12.2.11, 12.2.12, and 12.2.13 belong to the same patient)

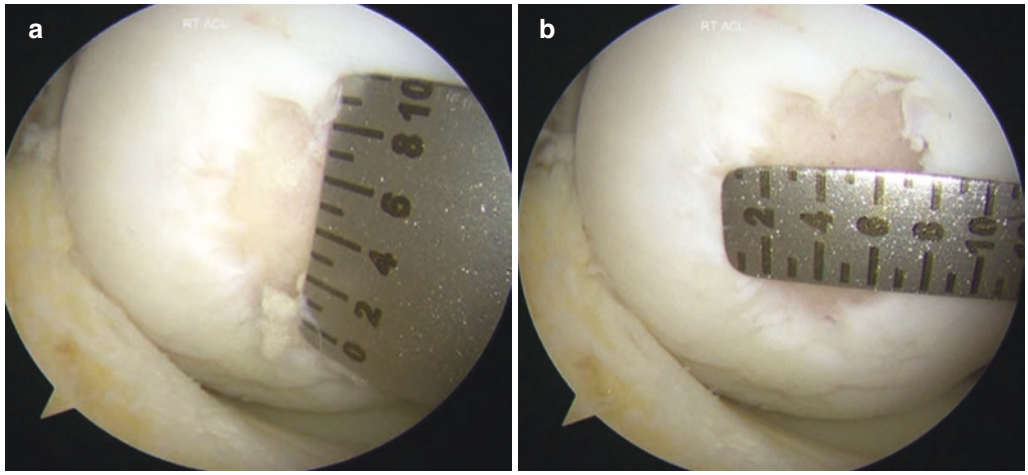

Figure 12.2.6: The OATS Technique: The Final Lesion Size Assessment and Planning for the Osteochondral Graft. Arthroscopy right knee in a 26-year-old female, viewing lateral femoral condyle from the anterolateral portal, instrumentation from the anteromedial portal, knee in about 90° flexion. An arthroscopic ruler is inserted to evaluate the final size of the lesion in (**a**) superoinferior and (**b**) mediolateral planes. This gives the idea about the number and the size of OATS plugs to be harvested. A single 8 mm osteochondral plug in this particular case would cover >95% of the defect. (The images in Figures 12.2.2, 12.2.4, 12.2.5, 12.2.6, 12.2.8, 12.2.9, 12.2.10, 12.2.11, 12.2.12, and 12.2.13 belong to the same patient)

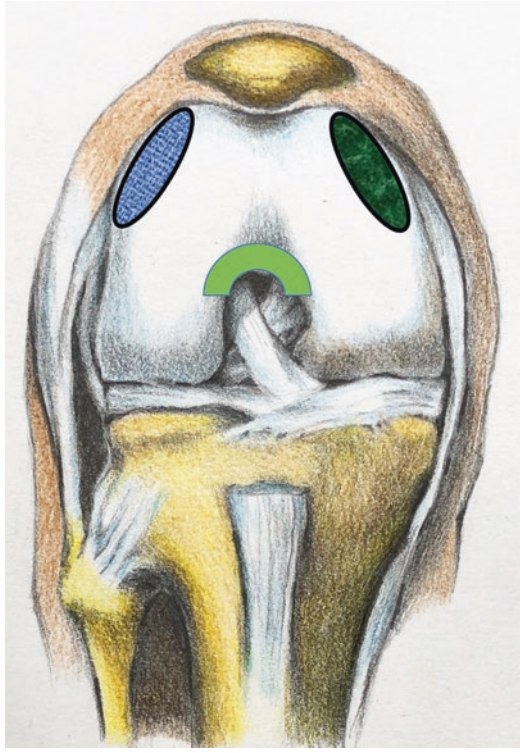

Figure 12.2.7: The OATS Technique: The Selection of the Donor Site. A non-weight-bearing and non-articulating area like the lateral margin of lateral femoral condyle above the sulcus terminalis (blue-shaded area) or medial margin of medial femoral condyle about the sulcus terminalis (green-shaded area) or around the notch for small plugs (marked in green) can be used for harvesting the graft from the same knee

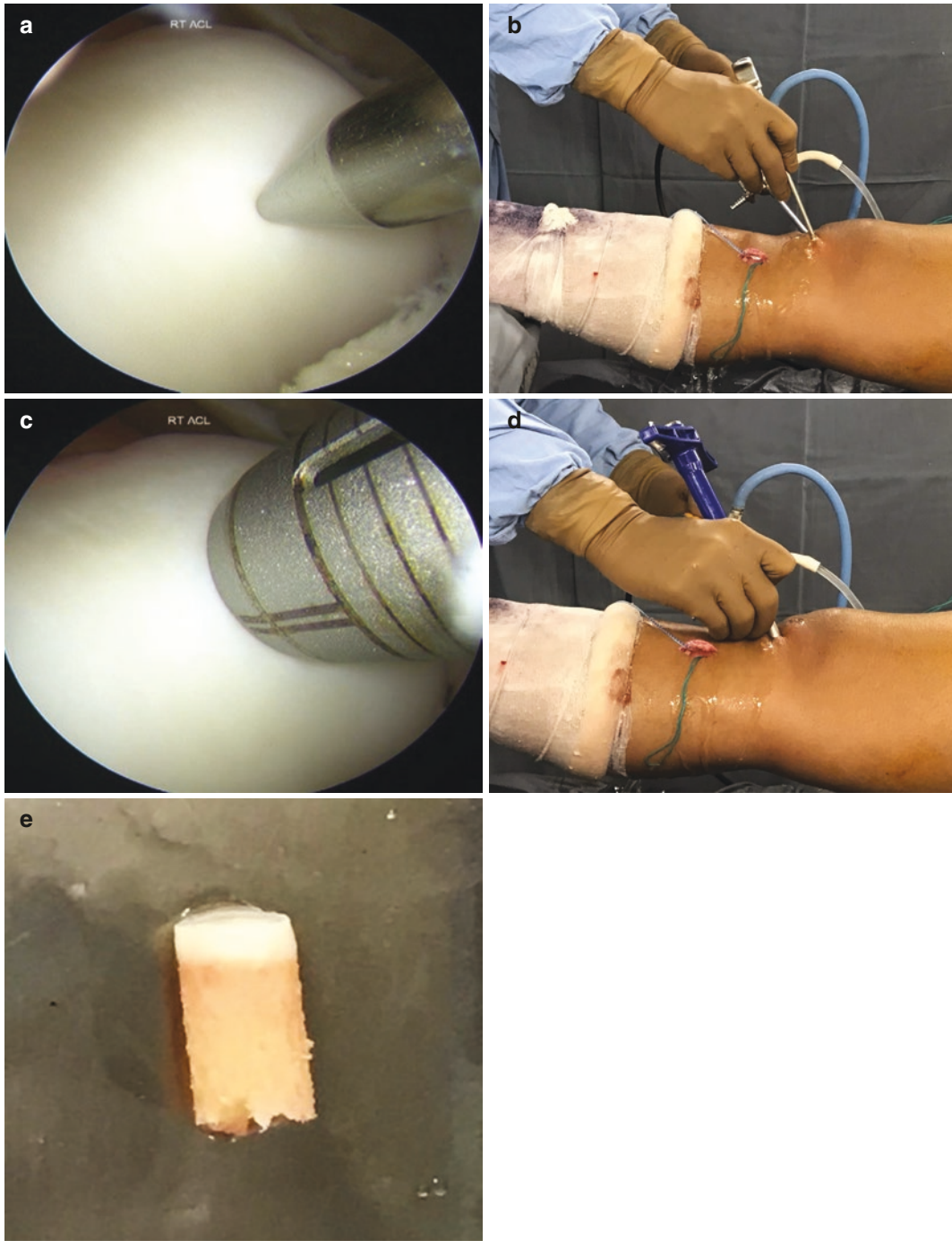

Figure 12.2.8: The OATS Technique: The Osteochondral Graft Harvest from the Donor Area. Arthroscopy right knee in a 26-year-old female, viewing medial femoral condyle from the anterolateral portal, instrumentation from the anteromedial portal, knee in extension. (**a**) The selected donor site is the medial margin of medial femoral condyle in this case. A perpendicular trajectory to the tentative donor area is confirmed using a blunt trocar. (**b**) The external view of the step described in (**a**). (**c**) The obturator is inserted into the donor harvester and is placed perpendicular to the cartilage surface at the point of planned graft harvest site through the anteromedial portal. (**d**) The external view of step described in (**c**). (**e**) The donor harvester is advanced by gentle blows of a mallet up to a depth of 15 mm. The harvested osteochondral plug in this case was 18 mm long although a 15 mm long plug was aimed for. (The images in Figures 12.2.2, 12.2.4, 12.2.5, 12.2.6, 12.2.8, 12.2.9, 12.2.10, 12.2.11, 12.2.12, and 12.2.13 belong to the same patient)

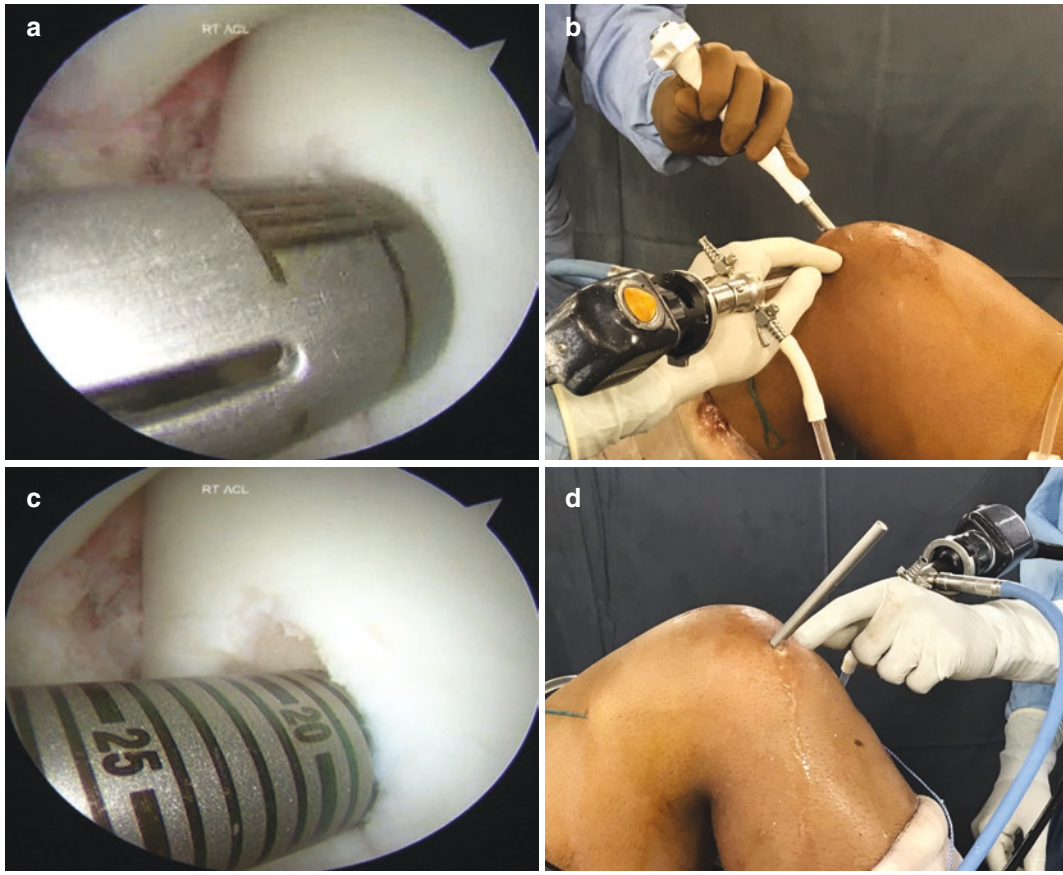

Figure 12.2.9: The OATS Technique: The Preparation of the Recipient Area. Arthroscopy right knee in 26-year-old female, viewing lateral femoral condyle from the anteromedial portal, instrumentation from the anterolateral portal, knee in about 90° flexion. (**a**) The recipient harvester is inserted though the anterolateral portal (which must be enlarged if needed) and placed over the chondral defect. This is hammered up to the exact depth as the length of the harvested plug (18 mm in this case). Gradual removal of this harvester yields an even cylindrical socket of required depth. (**b**) External view of the step shown in (**a**). (**c**) The direction and orientation of the recipient site are determined by using the alignment rod. This instrument also helps to confirm the exact depth of the cylindrical tunnel to avoid the plug from being proud after insertion. This must never be lesser than the length of the plug obtained. If this is the case, then either the plug length must be shortened or the alignment rod should be impacted by a millimeter or two. (**d**) External view of the step described in (**c**). (The images in Figures 12.2.2, 12.2.4, 12.2.5, 12.2.6, 12.2.8, 12.2.9, 12.2.10, 12.2.11, 12.2.12, and 12.2.13 belong to the same patient)

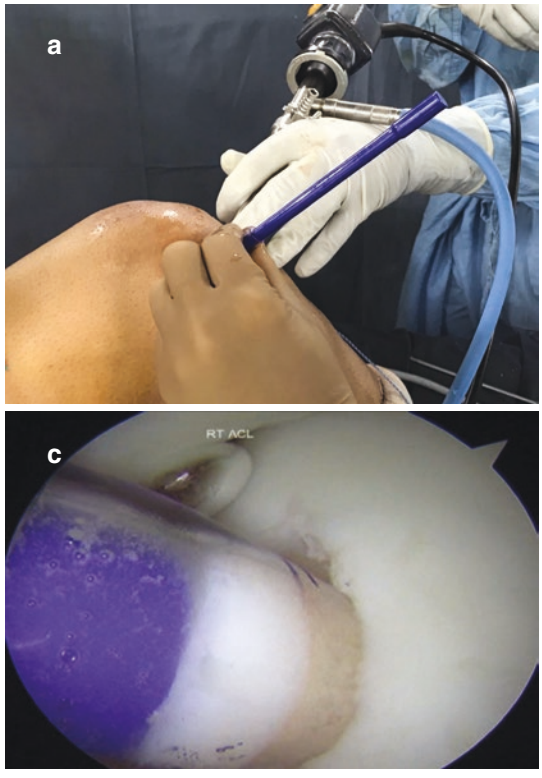

Figure 12.2.10: The OATS Technique: The Insertion of the Osteochondral Graft into the Recipient Area. Arthroscopy right knee in 26-year-old female, viewing lateral femoral condyle from the anteromedial portal, instrumentation from the anterolateral portal, knee in about 90° flexion. The cylindrical osteochondral graft plug is delivered into the joint through the graft delivery tube and placed at the recipient site through the anterolateral portal. The portal may be enlarged as needed to avoid struggle and soft-tissue entrapment. Arthroscopic visualization is maintained continuously. The osteochondral plug is inserted into the delivery tube maintaining proper orientation for sphericity and tamp placed over it to push the graft. The saline infusion may be stopped for a while when this is being done. (**a**) External view of this step. (**b**) Insertion of the graft must be done very gently by tapping with a small mallet and (**c**) under vision to avoid sinking of the graft in the socket. This is a modification of the technique described by the manufacturers of the OATS™ system. The original technique advises direct implantation of the osteochondral plug from the donor harvester into the defect site by gently screwing the core extruder. Only final insertion is to be done by tapping using the tamp in the original technique [6]. (The images in Figures 12.2.2, 12.2.4, 12.2.5, 12.2.6, 12.2.8, 12.2.9, 12.2.10, 12.2.11, 12.2.12, and 12.2.13 belong to the same patient)

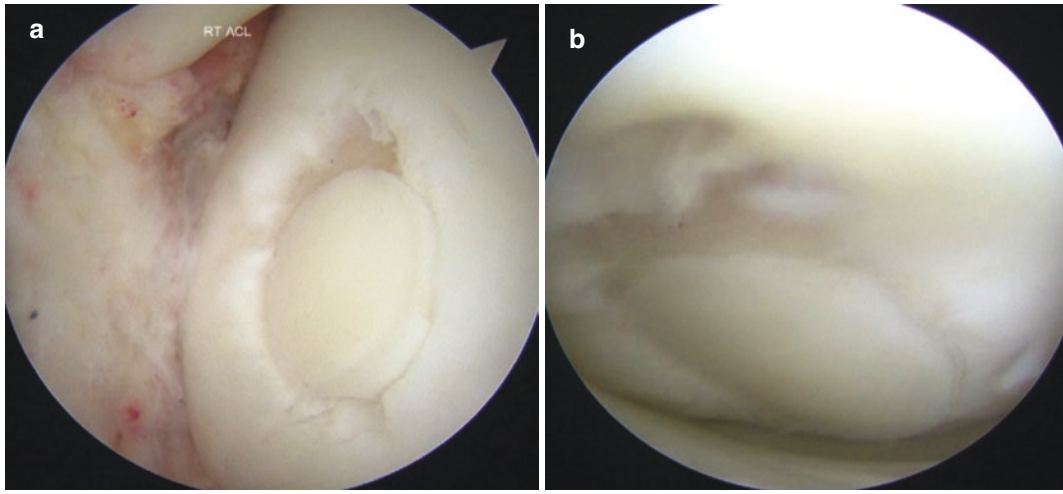

Figure 12.2.11: The OATS Technique: The Final Assessment after the Osteochondral Plug Insertion. Arthroscopy right knee in 26-year-old female, viewing lateral femoral condyle from the anteromedial portal, knee in different degrees of flexion. (**a**) Final appearance of the implanted osteochondral plug. (**b**) The knee is taken through a full range of motion to assess stability and congruity. (The images in Figures 12.2.2, 12.2.4, 12.2.5, 12.2.6, 12.2.8, 12.2.9, 12.2.10, 12.2.11, 12.2.12, and 12.2.13 belong to the same patient)

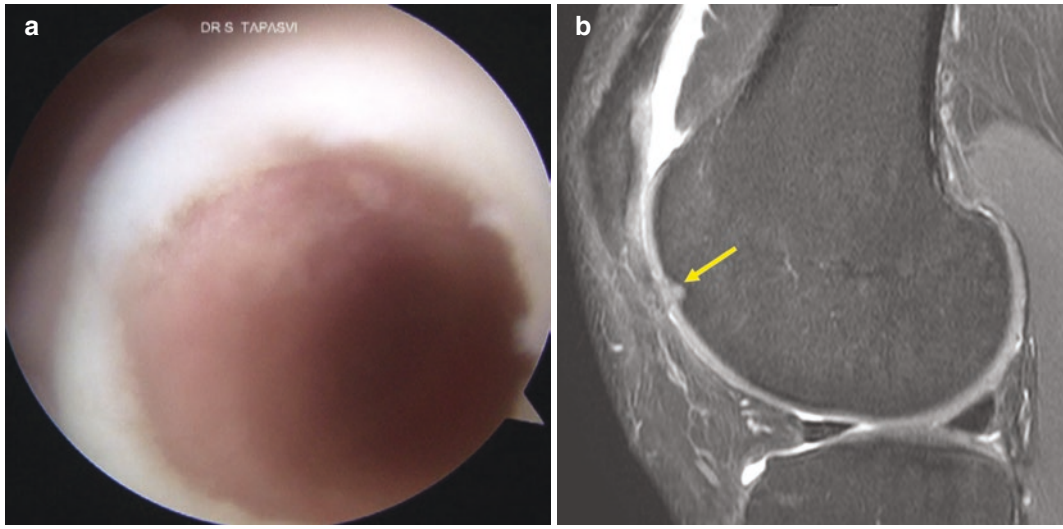

Figure 12.2.12: The OATS Technique: The Final Assessment of the Donor Area. Arthroscopy right knee, viewing medial femoral condyle from the anterolateral portal, knee in extension. (**a**) The donor site is left as a void. (**b**) A proton density, fat-saturated sagittal MRI image showing the fate of donor site with some bone growth and cartilage formation 15 months after the harvest (yellow arrow). (The images in Figures 12.2.2, 12.2.4, 12.2.5, 12.2.6, 12.2.8, 12.2.9, 12.2.10, 12.2.11, 12.2.12, and 12.2.13 belong to the same patient)

Figure 12.2.13: The OATS Technique: The Rehabilitation and Bracing. (**a**, **b**) Lateral unloader brace (OA Adjuster, DJO Global, St. Vista, CA) for the right knee. This is typically used after an OATS procedure of the lateral femoral condyle. Here a key is provided to adjust the amount of unloading of the lateral side

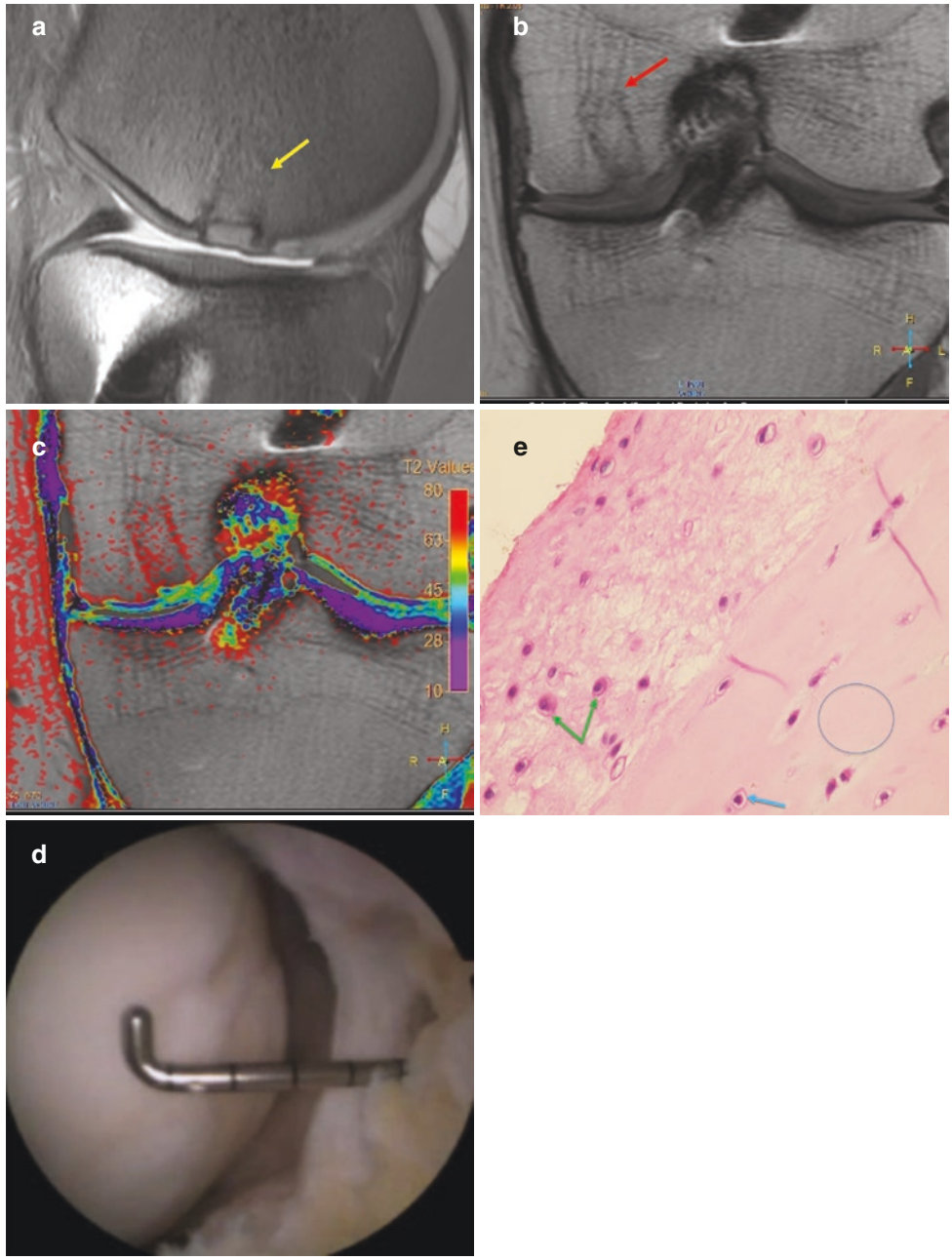

Figure 12.2.14: The OATS Technique: The Long-Term Results. Two-year follow-up of OATS procedure for a patient who had undergone the procedure for a 10 × 10 mm contained, grade 4 ICRS defect in the right-side medial femoral condyle along with a concomitant anterior cruciate ligament reconstruction. (**a**) PD sagittal fat-saturated image and (**b**) PD coronal nonfat-saturated coronal image of the osteochondral graft in situ. The articular surface is congruous and smooth. There is a continuity between the graft and the native cartilage, and between the graft and the underlying bone. Intact subchondral lamina is present with the absence of marrow edema, indicative of a good graft integration. (**c**) The cartilage mapping of the osteochondral graft shows normal T2 values in the graft and in the adjacent cartilage. (**d**) A relook arthroscopy of the right knee, viewing from the anterolateral portal, instrumentation from anteromedial portal, knee in about 90° flexion. A hook probe placed at the site of plug implantation with normal appearance of the cartilage. (**e**) The hematoxylin-eosin stain (100×) of the biopsy from the implanted plug clearly shows chondrocytes within lacunae in the superficial (green arrows) and deep (blue arrow) zones, the characteristic of hyaline cartilage. The chondroid matrix (blue circle) is also seen. (This case is the same patient whose preoperative images are shown in Figure 12.2.1.Aa–d)

12.3 Take-Home Message

- Cartilage injuries of the knee joint are amenable to treatment, with multiple treatment options being available.
- Autologous osteochondral plug transfer is an excellent procedure for a single-stage hyaline cartilage restoration for focal chondral defects of the femur.
- Thorough preparation of the defect to remove free cartilage or loose flaps followed by sizing is important for accurate surgery.
- Defects in weight-bearing areas of both condyles are usually approachable arthroscopically and single-plug OATS is possible by this technique.
- Larger defects requiring multiple plugs (mosaicplasty) or defects of the posterior femoral condyles are better treated with open surgery.
- Strict adherence to surgical technique for a particular device helps improve accuracy and avoid errors which can lead to a catastrophic failure.

References

1. Richter DL, Tanksley JA, Miller MD. Osteochondral autograft transplantation: a review of the surgical technique and outcomes. Sports Med Arthrosc Rev. 2016;24(2):74–8.
2. Richter DL, Schenck RC Jr, Wascher DC, Treme G. Knee articular cartilage repair and restoration techniques: a review of the literature. Sports Health. 2016;8(2):153–60.
3. Patil S, Tapasvi SR. Osteochondral autografts. Curr Rev Musculoskelet Med. 2015;8(4):423–8.
4. Solheim E, Hegna J, Inderhaug E. Long-term survival after microfracture and mosaicplasty for knee articular cartilage repair: a comparative study between two treatments cohorts. Cartilage. 2020;11(1):71–76.
5. Solheim E, Hegna J, Inderhaug E. Early determinants of long-term clinical outcome after cartilage repair surgery in the knee. J Orthop. 2018;15(1):222–5.
6. https://www.arthrex.com/knee/oats-technique.

13 The Illustrative First and Second Generation Autologous Chondrocyte Implantation (ACI) for Cartilage Repair

Mats Brittberg

13.1 Introduction

Autologous chondrocyte implantation (ACI) was first introduced clinically in 1987 [1]. In this procedure, cartilage biopsies are harvested from a minor load-bearing area of the knee. These cartilage slices are then sent to a cartilage laboratory for cell isolation and expansion for several weeks. The expanded increased numbers of cells are returned to the surgeon as a chondrocyte suspension. The cell suspension is to be injected into the defect covered with a membrane of periosteum (first generation, P-ACI). The periosteum being a living tissue could develop into a hypertrophy with mechanical symptoms as a consequence, requiring a revision surgery to shave off the hypertrophied periosteum. Hence some years later, use of the collagen membrane (second generation, C-ACI) started instead of a periosteum patch to reduce the chances of hypertrophy, graft delamination, etc. The second-generation ACI with a collagen membrane had less chances of a revision surgery.

The indications of ACI are cartilage defects larger than 2 cm^2. A patient with a cartilage lesion that has not been repaired to satisfaction with other techniques is also an indication for ACI. Newer generations of ACI, the third generation and the fourth generation with cells grown in different types of scaffolds, are now also available. Biomechanical corrections are important for all the cartilage repair surgeries and should be done before/along with the ACI procedure.

M. Brittberg (✉)
Cartilage Research Unit, University of Gothenburg, Region Halland Orthopaedics, Kungsbacka Hospital, Kungsbacka, Sweden
e-mail: mats.brittberg@telia.com

D. R. Goyal (ed.), *The Illustrative Book of Cartilage Repair*,
https://doi.org/10.1007/978-3-030-47154-5_13

13.2 The Illustrations

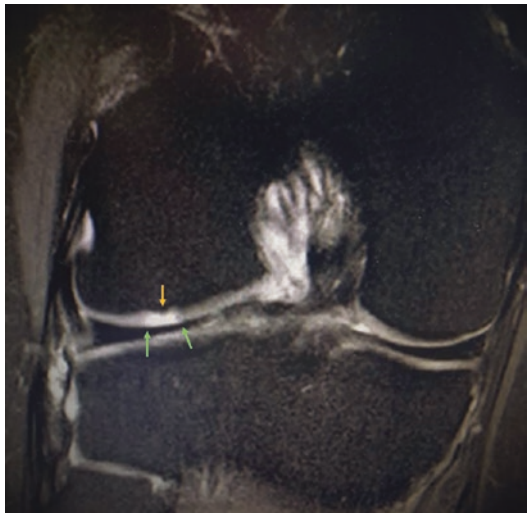

Figure 13.2.1: The PACI/C-ACI Technique: The Ideal Case Selection. An MRI (coronal image, PD FS cor) of a male patient aged 37 years, showing cartilage lesion on the lateral femoral condyle (between two green arrows). The lesion is a full-thickness cartilage lesion, ICRS Grade III–C with an approximate size of 1.5 × 2 cm. A small central osteophyte is also visible in the center of the lesion (yellow arrow). The patient had sustained a rotational trauma when playing football (soccer) and complained of pain on weight bearing, hydrops, and limping

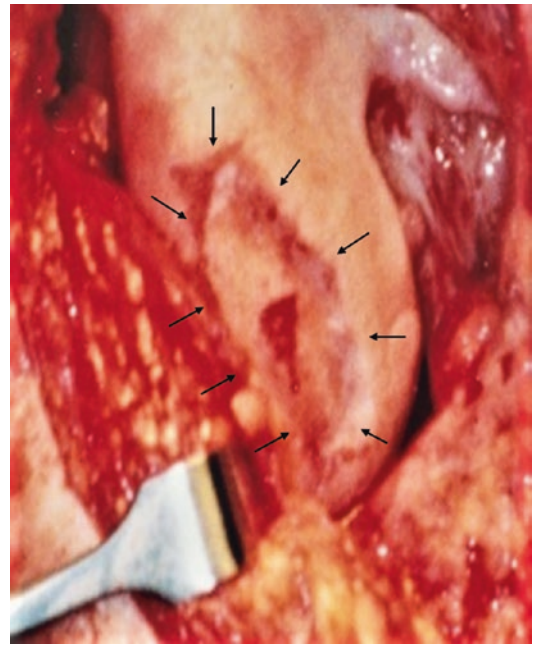

Figure 13.2.2: The P-ACI/C-ACI Technique: The Assessment of the Lesion. A male patient aged 37 years with full-thickness large chondral defect of 3 × 1 cm size (final size after debridement and preparation of the lesion, marked with black arrows) on the lateral femoral condyle. The lesion is a good indication for ACI, as it is a large symptomatic lesion on the weight-bearing zone of the lateral femoral condyle. Patient had no biomechanical malalignment

Figure 13.2.3: The P-ACI/C-ACI Technique: The Instruments Required. Instruments required for P-ACI/C-ACI technique are different raspatories and ring curettes to use for the debridement of the cartilage defect

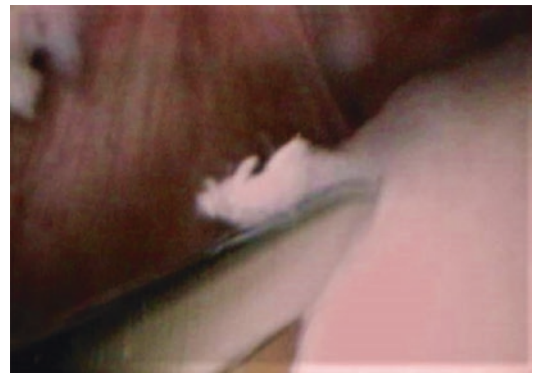

Figure 13.2.4: The P-ACI/C-ACI Technique: The Cartilage Biopsy. Cartilage biopsy is taken via a diagnostic arthroscopy and cartilage slices (2–300 mg) are harvested from a minor load-bearing area. The commonly used harvest area is the lateral part of the intercondylar notch, but the upper medial or lateral part of the trochlear area could also be used as harvest areas. A sharp rasparator is convenient to harvest the cartilage slices

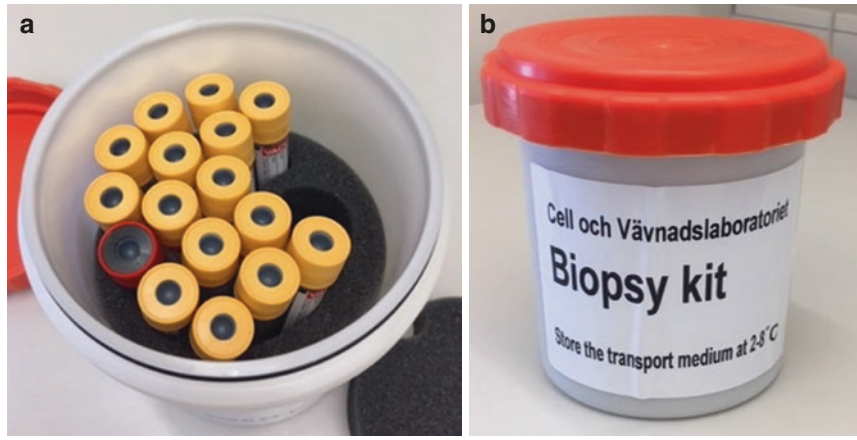

Figure 13.2.5: The P-ACI/C-ACI Technique: The Transport of the Cartilage Biopsy to the Cartilage Lab. (**a**) The cartilage biopsy is transferred to a sterile transport tube (black cap with red ribbon) with biopsy medium consisting of 40 mL sodium chloride (9 mg/mL) with gentamycin and fungizone. Medium has been kept at 2–8 °C before the harvest. Biopsy tube is then packed and sent to a high-quality good manufacturing practice (GMP) cartilage laboratory for further processing, together with 15 × 9 mL autologous blood collected from the patient (tubes with yellow caps). The serum is used in the culture process as an additive to the culture medium. (**b**) There are different transport kits from different companies

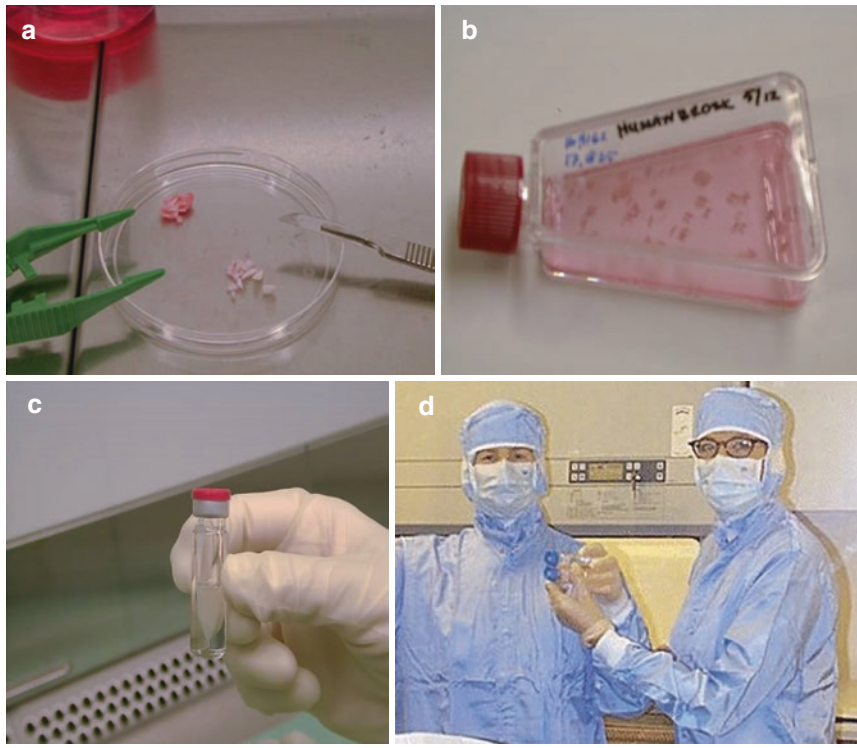

Figure 13.2.6: The P-ACI/C-ACI Technique: The Chondrocyte Culture in the Cartilage Lab. Chondrocytes are isolated from the cartilage biopsy by mechanical mincing (**a**) followed by treatment with collagenase. After the digestion process, in which the chondrocytes are released from the matrix, (**b**) the cells are seeded in culture flasks. Around 2102 cells/mg of cartilage are isolated. The mean number of cells isolated per patient at *cell matrix laboratory* is 5.3×10^5 cells. After a total culture time of 3–5 weeks, enough cell numbers have been reached and the implantation of the cells can be performed. (**c**) This cell product is aseptically filled in syringes or vials. (**d**) The syringes or vials are then packed for shipment to the operating theatre

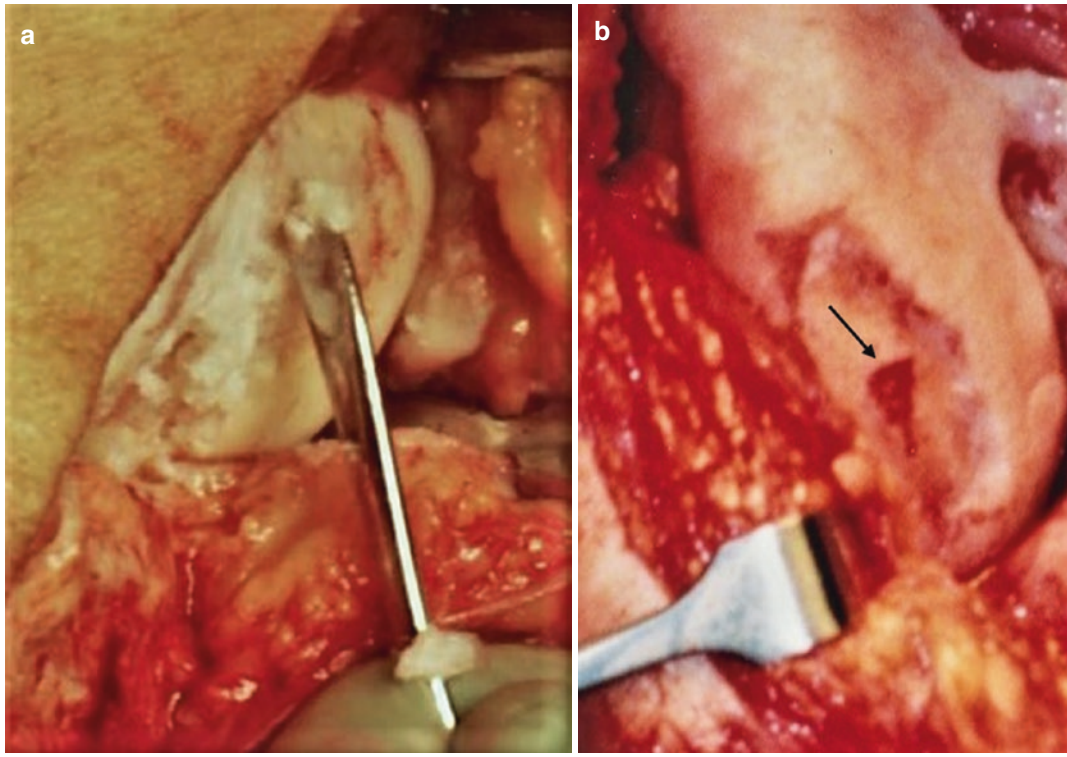

Figure 13.2.7: The P-ACI/C-ACI Technique: The Preparation of the Lesion. In a male patient, 37 years old, a medial parapatellar arthrotomy has been performed and the lateral femoral condyle accessed with the help of retractors. (**a**) A rasparator is used to debride the defect. (**b**) The defect area has been debrided to clean bony bottom and vertical surrounding walls are created. A central osteophyte (black arrow) has been taken away which was seen on MRI in Figure 13.2.1

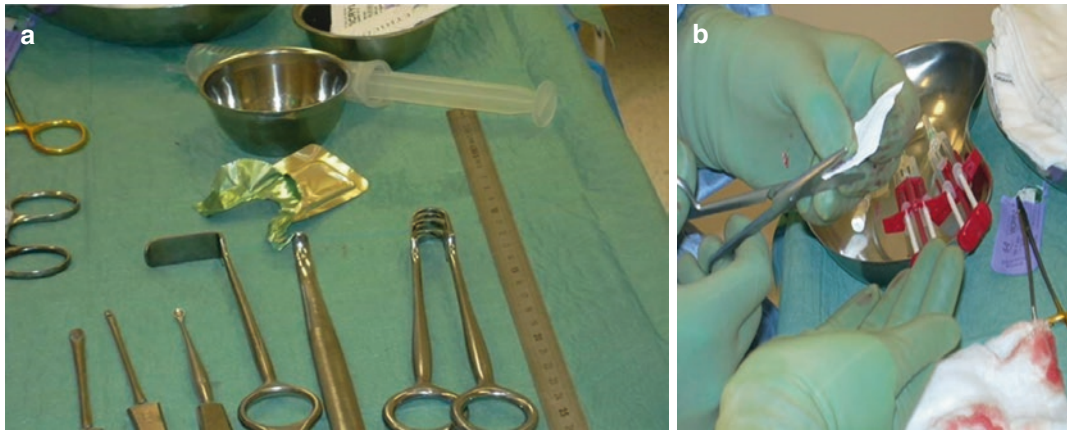

Figure 13.2.8: The P-ACI/C-ACI Technique: The Sizing of the Defect. (**a**) To help assist with obtaining the right-size periosteal or a collagen patch, a template made from either a sterile paper or an aluminum (for example, aluminum suture foil) can be placed over the defect and outlined with a sterile marking pen, oversizing by 1–2 mm. (**b**) The template is then cut out and used during the periosteal patch harvest to ensure an accurate size and the shape. The purpose of adding 1–2 mm in size when cutting the periosteal graft is to account for the fact that the periosteum has a tendency to shrink after harvest even though one may stretch the periosteum considerably

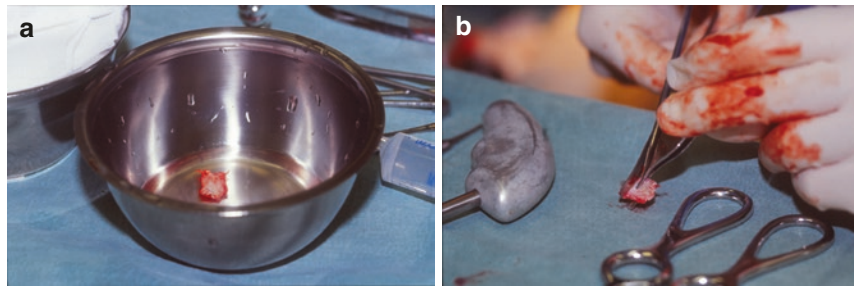

Figure 13.2.9: The P-ACI/C-ACI Technique: The Harvesting of the Periosteum or Preparing the Collagen Membrane. For the first-generation ACI (P-ACI), periosteum is harvested from the upper medial tibia. After marking the size of the periosteum to be harvested, a sharp knife is used to cut out the periosteum, of the required size. One may then use a sharp rasparator to release the outlined periosteal flap. If second generation of ACI is to be used, a collagen membrane can be used in the same way as the periosteum is used. (**a**) Shows periosteal flap just harvested and preserved in saline. (**b**) Shows how the periosteal flap is cut with a scissor to fit exact the size of the lesion

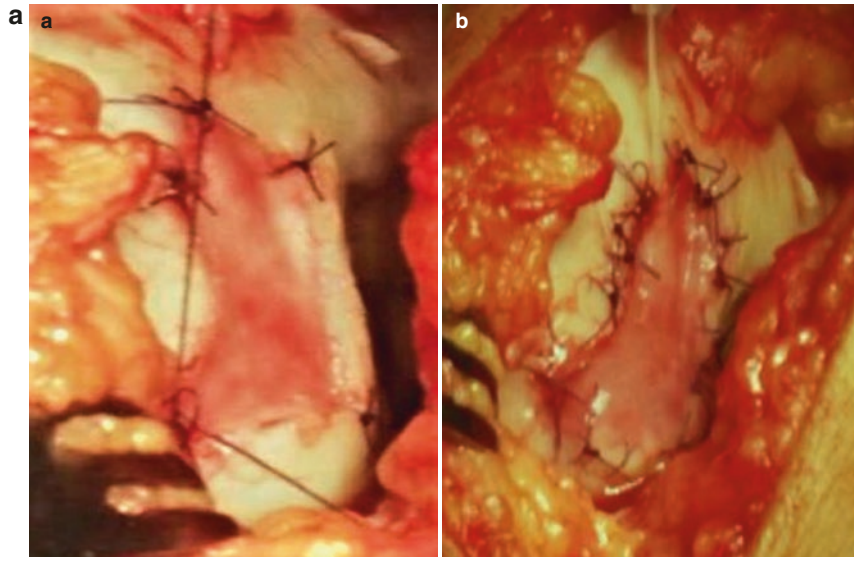

Figure 13.2.10.A: The P-ACI/C-ACI Technique: The Suturing of the Periosteum. The periosteum (cambium layer-chondrogenic area facing the defect) should be attached to the defect area by taking interrupted sutures using 5-0 or 6-0 vicryl sutures (Ethicon vicryl polyglactin 910 P-1 cutting needle, Johnson-Johnson International). (**a**) One starts by putting sutures at the four corners. The suture needle should be passed through the periosteum/collagen membrane from outside to inside about 2 mm from the edge of the periosteum. The needle should be passed through the cartilage from inside to outside with the needle entering the cartilage approximately 2 mm in the defect and perpendicular to the defect wall. An approximately 2–3 mm bite from the defect edge is recommended. The periosteum should reach up to, but not extending over, the cartilage rim to avoid the risk of early delamination due to frictional forces. (**b**) The sutures are then placed one by one around the defect and spaced approximately 3 to 4 mm from each other

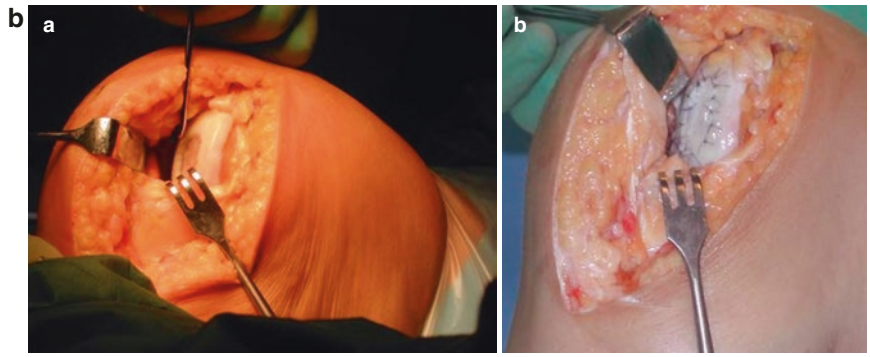

Figure 13.2.10.B: The P-ACI/C-ACI Technique: The Suturing of the Collagen Membrane. The grade IV chondral defect on the medial femoral condyle is treated with C-ACI. (**a**) The lesion is exposed thru medial parapatellar arthrotomy and prepared using rasparator as described in Figure 13.2.7. (**b**) The collagen membrane (rough side facing the defect) is attached to the defect area by taking interrupted sutures using 5-0 or 6-0 vicryl sutures (Ethicon vicryl polyglactin 910 P-1 cutting needle, Johnson-Johnson International). The collagen membrane should reach up to, but not extending over, the cartilage rim to avoid the risk of early delamination due to frictional forces. (This case is different from the cases described in Figures 13.2.1, 13.2.2, 13.2.7, 13.2.10.A, 13.2.11, 13.2.12, 13.2.14, and 13.2.15)

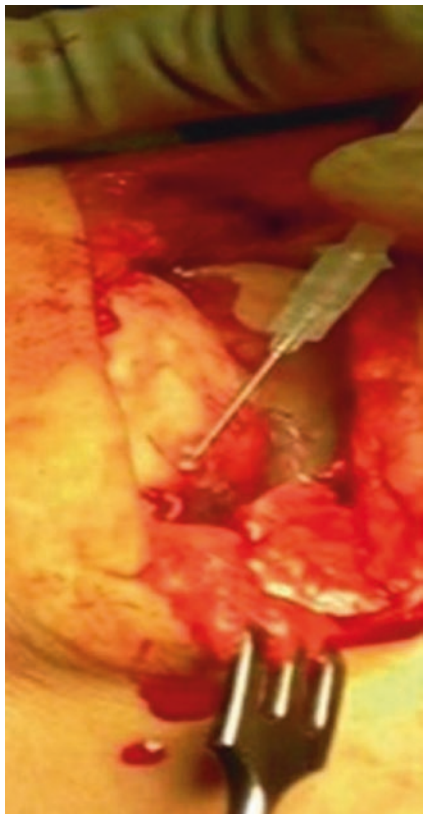

Figure 13.2.11: The P-ACI/C-ACI Technique: The Sealing of the Chondrogenic Chamber. An 18-gauge catheter attached to a saline-filled 1 mL syringe is placed under the periosteum or collagen membrane and the defect area is slowly filled with saline to test water tightness. Any leakage is blocked with additional sutures. The suture line is finally sealed with fibrin glue acting as insurance to assure a watertight compartment

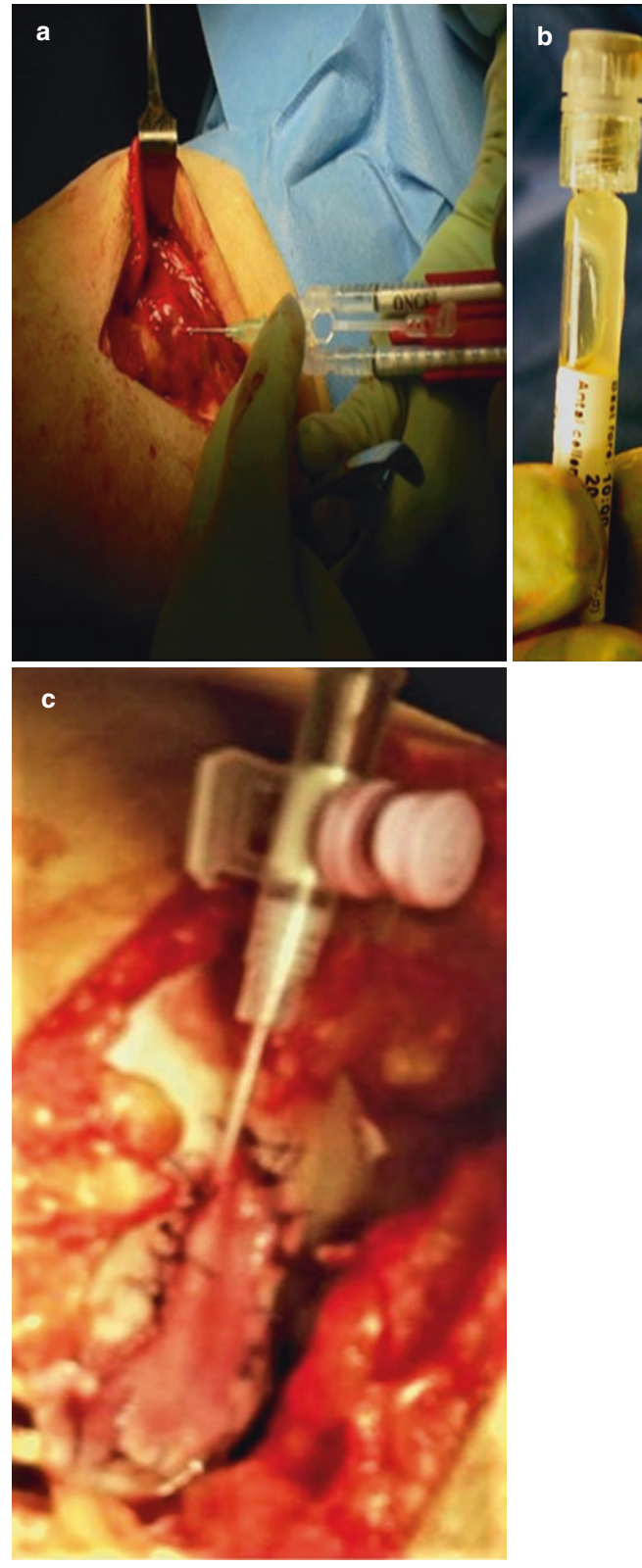

Figure 13.2.12: The P-ACI/C-ACI Technique: The Implantation of the Cultured Chondrocytes. (**a**) The empty space under the periosteum or collagen membrane is filled with fibrin glue to let the injected cell suspension spread evenly. (**b**) The surgeon attaches a catheter on to the syringe with the cell suspension and (**c**) introduces it through the small opening of the cartilage defect and advances to the distal end of the defect. The cells are slowly injected under the periosteal or collagen patch as the catheter is slowly withdrawn to the opening of the defect. Finally, the small opening is then closed with one or two additional sutures, and then sealed with fibrin glue. The arthrotomy is closed in a layered fashion, and a soft sterile dressing is applied to the knee. No drains are used

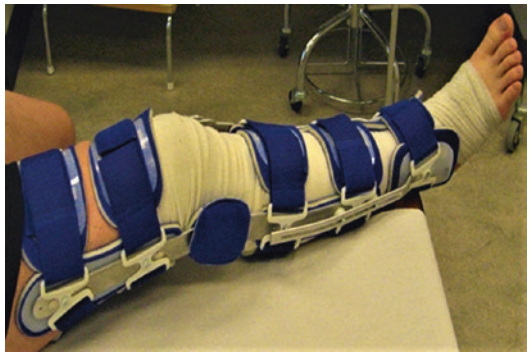

Figure 13.2.13: The P-ACI/C-ACI Technique: The Postoperative Management and Rehabilitation. It is important to protect the repair tissue from excessive intra-articular forces during the early postoperative period and especially avoiding twisting and rotational shearing forces. A brace locked in extension is used for the first 2 weeks with full-weight bearing and crutches. After initial 2 weeks, the locked brace is opened and used just outdoors for the next 4 weeks. Isometric quadriceps training, straight leg raises, and hamstring strengthening should be introduced early and progressively advance to the resisted exercises and return to greater degrees of functional activities. From 3 weeks post-operative period, progressive closed-chain exercises with light resistance are also started. Open-chain exercises can be initiated around the eighth week. Running is not advised until the 7 months post-ACI, with high-level activities being initiated at the 12th month. The gradual progression of active extension exercises depends on the size and location of the defect as observed in the operating room; therefore, it is essential that the surgeon provide guidance to the physio-therapist and reassurance to the patient. If the defects are large, one may consider using an unloader brace

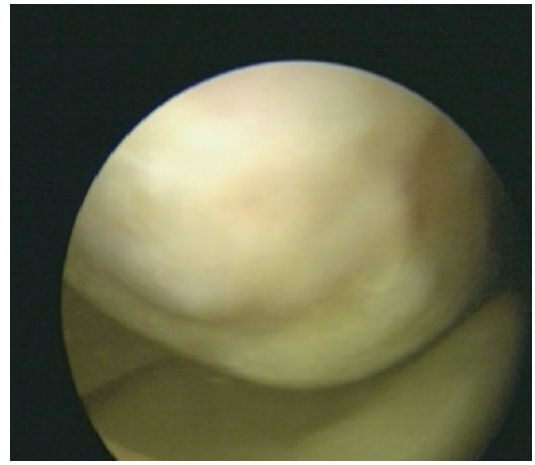

Figure 13.2.15: The P-ACI/C-ACI Technique: The Long-Term Results of a Successful Surgery on Arthroscopy. The male patient aged 37 years with follow-up arthroscopy showing lateral femoral condyle at 1 year post-surgery. The repair tissue is still a bit soft in indentation and is bulging slightly but is stable at border zones

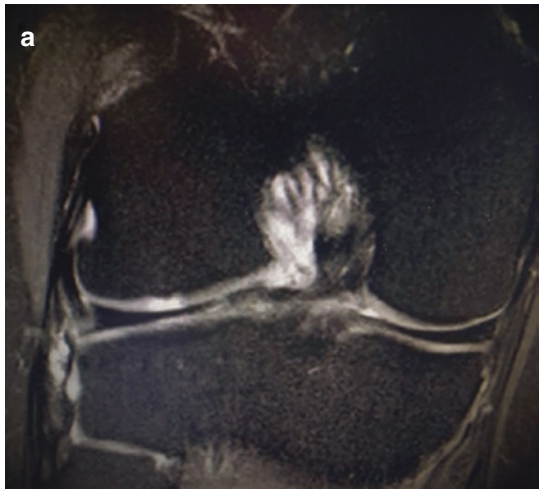

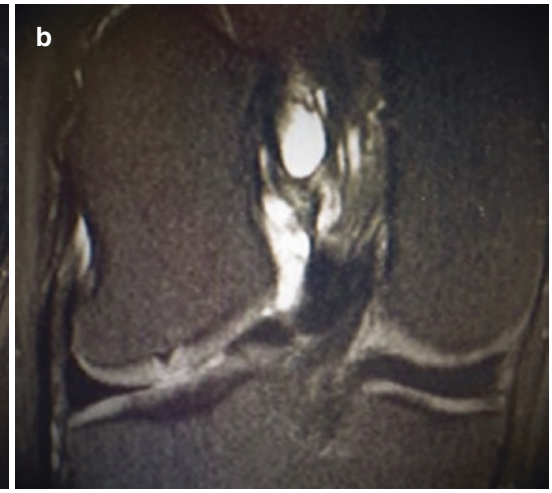

Figure 13.2.14: The P-ACI/C-ACI Technique: The Long-Term Results of a Successful Surgery on MRI. A male aged 37 years with (**a**) the initial defect as already described in Figure 13.2.1. (**b**) The repaired defect at 1.5 years post-surgery on MRI. The MRI shows a bony prominence in the defect area that could be the osteophyte area that was debrided as explained in Figure 13.2.7. The osteochondral defect has healed with some new bone ingrowth. Patient improved after surgery

13.3 Take-Home Message

First- and second-generation ACI have been used for more than 30 years and there are many long-term results with those techniques showing high degree of success in pain relief and functional recovery [2–21]. Today, most surgeons are using third- and fourth-generation ACI. However, first- and second-generation ACI are still useful for large defects and bipolar lesions, especially the first-gen ACI where the stretching capacity of the periosteum is useful. It is important to harvest a thin periosteum without superficial fibrous tissue that might contribute to hypertrophy of the grafted area. The suturing technique is time consuming but when paying extra attention to the careful suturing of the periosteum/collagen membrane, the chances of long-term success will increase.

References

1. Brittberg M, Lindahl A, Nilsson A, Ohlsson C, Isaksson O, Peterson L. Treatment of deep cartilage defects in the knee with autologous chondrocyte transplantation. N Engl J Med. 1994;331(14):889–95.
2. Peterson L, Vasiliadis HS, Brittberg M, Lindahl A. Autologous chondrocyte implantation: a long-term follow-up. Am J Sports Med. 2010;38(6):1117–24.
3. Nawaz SZ, Bentley G, Briggs TW, Carrington RW, Skinner JA, Gallagher KR, Dhinsa BS. Autologous chondrocyte implantation in the knee: mid-term to long-term results. J Bone Joint Surg Am. 2014;96(10):824–30.
4. Rosa D, Balato G, Ciaramella G, Soscia E, Improta G, Triassi M. Long-term clinical results and MRI changes after autologous chondrocyte implantation in the knee of young and active middle aged patients. J Orthop Traumatol. 2016;17(1):55–62.
5. Ogura T, Mosier BA, Bryant T, Minas T. A 20-year follow-up after first-generation autologous chondrocyte implantation. Am J Sports Med. 2017;45(12):2751–76.
6. Horas U, Pelinkovic D, Herr G, Aigner T, Schnettler R. Autologous chondrocyte implantation and osteochondral cylinder transplantation in cartilage repair of the knee joint. A prospective, comparative trial. J Bone Joint Surg Am. 2003;85-A(2):185–92.
7. Schneider U, Andereya S. [First results of a prospective randomized clinical trial on traditional chondrocyte transplantation vs CaReS-technology]. Z Orthop Ihre Grenzgeb. 2003;141(5):496–97.
8. Bentley G, Biant LC, Carrington RW, Akmal M, Goldberg A, Williams AM, et al. A prospective, randomised comparison of autologous chondrocyte implantation versus mosaicplasty for osteochondral defects in the knee. J Bone Joint Surg Br. 2003;85(2):223–30.
9. Visna P, Pasa L, Cizmár I, Hoch J. Treatment of deep cartilage defects of the knee using autologous chondrograft transplantation and by abrasive techniques—a randomized controlled study. Acta Chir Belg. 2004;104(6):709–14.
10. Knutsen G, Engebretsen L, Ludvigsen TC, Drogset JO, Grøntvedt T, Solheim E, et al. Autologous chondrocyte implantation compared with microfracture in the knee. A randomized trial. J Bone Joint Surg Am. 2004;86-A(3):455–64.
11. Bartlett W, Skinner JA, Gooding CR, Carrington RW, Carrington RW, Flanagan AM, Briggs TW, et al. Autologous chondrocyte implantation versus matrix-induced autologous chondrocyte implantation for osteochondral defects of the knee: a prospective, randomised study. J Bone Joint Surg Br. 2005;87(5):640–5.
12. Dozin B, Malpeli M, Cancedda R, Bruzzi P, Calcagno S, Molfetta L, et al. Comparative evaluation of autologous chondrocyte implantation and mosaicplasty: a multicentered randomized clinical trial. Clin J Sport Med. 2005;15(4):220–6.
13. Gooding CR, Bartlett W, Bentley G. A prospective, randomised study comparing two techniques of autologous chondrocyte implantation for osteochondral defects in the knee: periosteum covered versus type I/III collagen covered. Knee. 2006;13(3):203–10.
14. Zeifang F, Oberle D, Nierhoff C, Richter W, Moradi B, Schmitt H. Autologous chondrocyte implantation using the original periosteum-cover technique versus matrix-associated autologous chondrocyte implantation: a randomized clinical trial. Am J Sports Med. 2010;38(5):924–33.
15. Basad E, Ishaque B, Bachmann G, Stürz H, Steinmeyer J. Matrix-induced autologous chondrocyte implantation versus microfracture in the treatment of cartilage defects of the knee: a 2-year randomised study. Knee Surg Sports Traumatol Arthrosc. 2010;18(4):519–27.
16. Vanlauwe J, Saris DB, Victor J, Almqvist KF, Bellemans J, Luyten FP, et al. Five-year outcome of characterized chondrocyte implantation versus microfracture for symptomatic cartilage defects of the knee: early treatment matters. Am J Sports Med. 2011;39(12):2566–74.
17. Cole BJ, Farr J, Winalski CS, Richmond J, Mandelbaum B, De Deyne PG. Outcomes after a single-stage procedure for cell-based cartilage repair: a prospective clinical safety trial with 2-year follow-up. Am J Sports Med. 2011;39(6):1170–9.

18. Crawford DC, DeBerardino TM, Williams RJ 3rd. NeoCart, an autologous cartilage tissue implant, compared with microfracture for treatment of distal femoral cartilage lesions: an FDA phase-II prospective, randomized clinical trial after two years. J Bone Joint Surg Am. 2012;94(11):979–89.
19. Saris D, Price A, Widuchowski W, Bertrand-Marchand M, Caron J, et al. Matrix-applied characterized autologous cultured chondrocytes versus microfracture: two-year follow-up of a prospective randomized trial. Am J Sports Med. 2014;42(6):1384–94.
20. Clavé A, Potel JF, Servien E, Neyret P, Dubrana F, Stindel E. Third-generation autologous chondrocyte implantation versus mosaicplasty for knee cartilage injury: 2-year randomized trial. J Orthop Res. 2016;34(4):658–65.
21. Brittberg M, Recker D, Ilgenfritz J, Saris DBF; SUMMIT Extension Study Group. Matrix-applied characterized autologous cultured chondrocytes versus microfracture: five-year follow-up of a prospective randomized trial. Am J Sports Med. 2018;46(6):1343–51.

14 The Illustrative Membrane Based Autologous Chondrocyte Implantation for Cartilage Repair

Nicholas Ramos, Bert Mandelbaum, and Michael Banffy

14.1 Introduction

First described in 1994 by Brittberg and colleagues [1], autologous chondrocyte implantation (ACI) is a cartilage restoration technique in which a patient's chondrocytes are harvested via cartilage biopsy, cultured and expanded ex vivo, and then reimplanted into the cartilage defect. While this does entail a two-stage surgical procedure, the repair tissue produced by ACI has been shown to produce a hyaline-like cartilage repair tissue that closely resembles the native articular cartilage [1]. The surgical technique for ACI has evolved over the past two decades. First-generation ACI (pACI) involved the use of a periosteal patch to seal the cultured chondrocytes into the cartilage defect; however, the periosteal harvest added additional surgical morbidity. Additionally, periosteal overgrowth and hypertrophy were established postoperative complications [2, 3]. Second-generation ACI (cACI) incorporated a collagen membrane to overlay the chondral defect and implanted chondrocytes which eliminated the complications associated with the periosteal harvest and overgrowth. The third generation of the ACI technique, matrix autologous chondrocyte implantation (MACI), which is described in this chapter, utilizes a collagen membrane pre-seeded with the patient's harvested chondrocytes in the laboratory itself. This pre-seeded implant affords the benefit of facile implantation, and its fixation with the fibrin glue can eliminate the need for tedious circumferential suturing. The current surgical indications for the MACI implantation include patients with medium to large (>2 cm^2) full-thickness articular cartilage defects within the knee who have failed conservative treatment measures. Treatment outcomes for MACI have been promising, producing durable mid- to long-term results in multiple studies [4–6].

N. Ramos · B. Mandelbaum (✉) · M. Banffy
Kerlan Jobe Institute, Los Angeles, CA, USA
e-mail: nikko.ramos@gmail.com;
bmandelbau@aol.com;
BMandelbaum@smog-ortho.net;
mbanffy@gmail.com

D. R. Goyal (ed.), *The Illustrative Book of Cartilage Repair*,
https://doi.org/10.1007/978-3-030-47154-5_14

14.2 The Illustrations

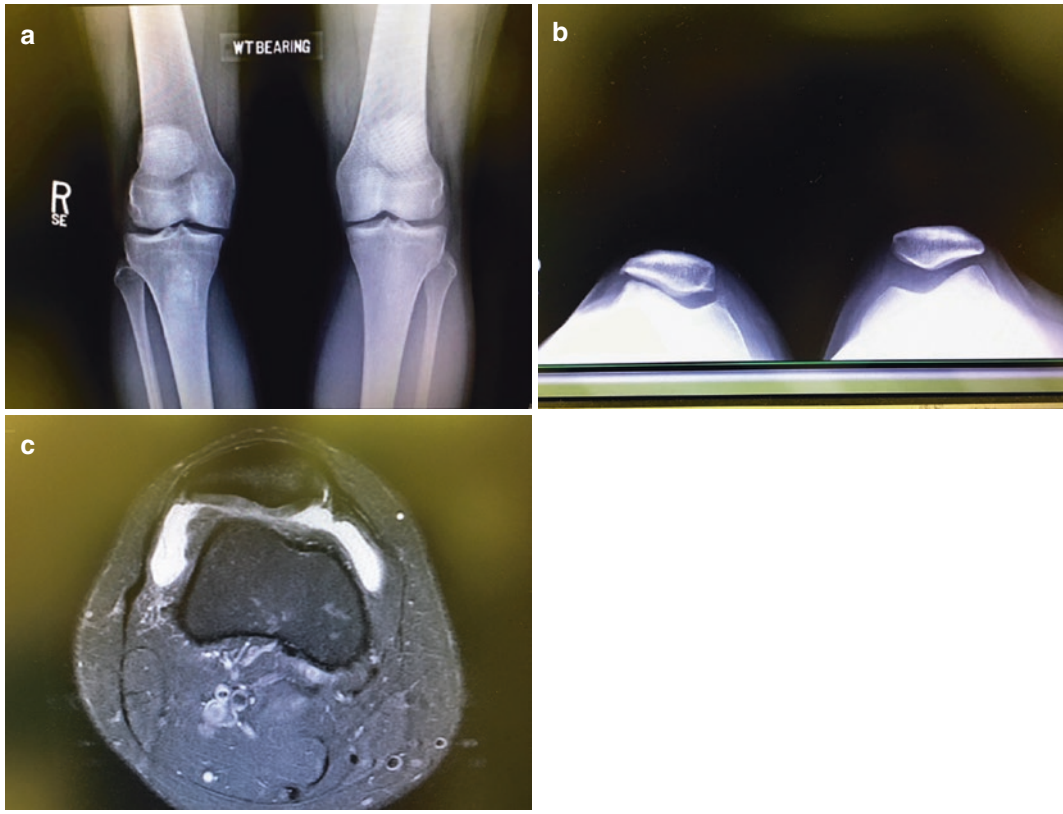

Figure 14.2.1: The MACI Technique: The Ideal Case Selection. A 22-year-old female collegiate volleyball player presented with persistent right anterior knee pain after previous tibial tubercle osteotomy (TTO) and lateral release done 6 years ago for patellar instability. Her symptoms precluded participation in her desired level of elite sport. (**a**) X-rays demonstrated previous TTO with (**b**) loss of joint space in the lateral patellofemoral joint as well as slight lateral tilt and translation of the patella within the trochlear groove. There was no gross varus/valgus malalignment at the knee. (**c**) MRI examination revealed grade IV cartilage lesions in both the lateral patellar facet and the lateral trochlear groove

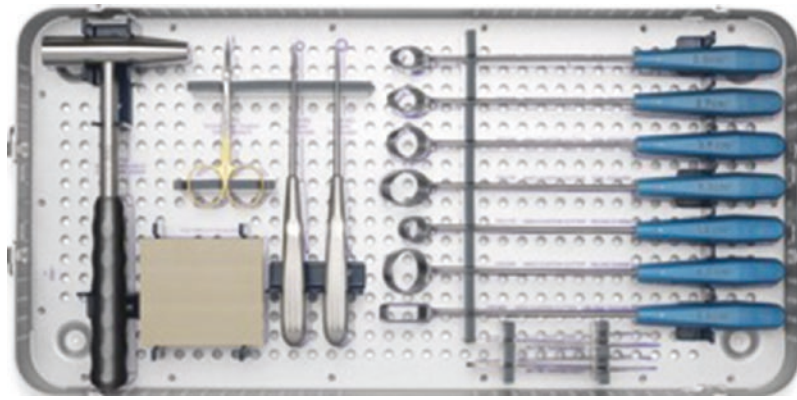

Figure 14.2.2: The MACI Technique: The Instruments. The MACI technique requires variable sized ring curettes to assist in the defect preparation. The PEEK cutting block can be used as a surface on which the MACI membrane can be cut to appropriate size. The mallet can be used in conjunction with ring curettes to prepare the walls of the defect for MACI implantation

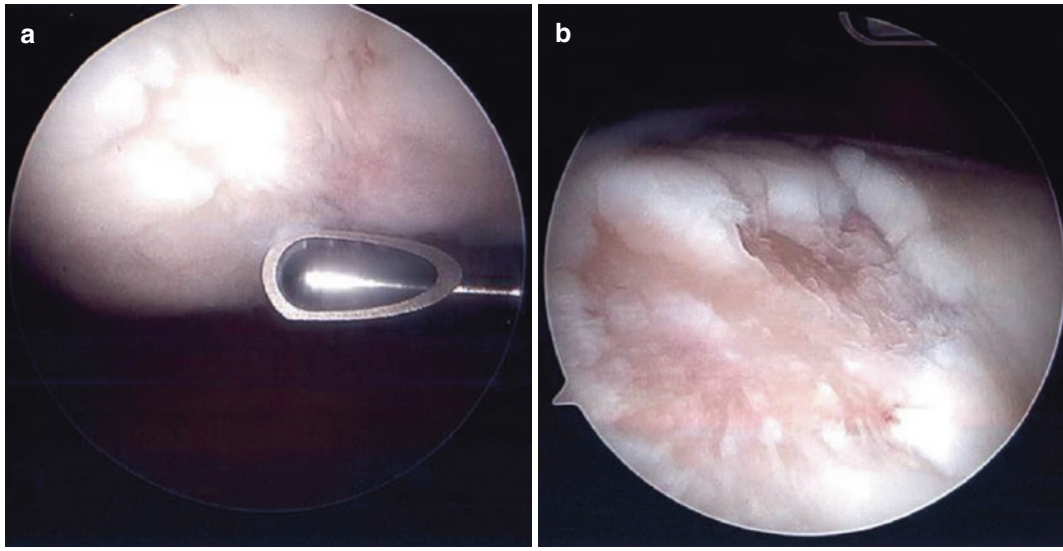

Figure 14.2.3: The MACI Technique: The Arthroscopic Assessment of the Lesion. Arthroscopic visualization of (**a**) the patellar (ICRS grade III, 2 × 2 cm) and (**b**) the trochlear (ICRS grade IV, 3 × 3 cm) lesions of the right knee in a 22-year-old female from the anterolateral viewing portal. The MACI technique is ideal for these lesions given their large size, irregular contour, and defect location which may impede contouring and implantation of osteochondral allograft/autografts. Durable outcomes have been reported with ACI for kissing lesions such as these within the patellofemoral joint [7]

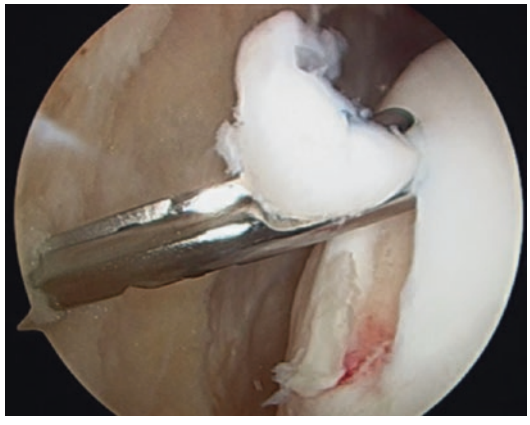

Figure 14.2.4: The MACI Technique: The Cartilage Biopsy. Cartilage biopsy may be taken from either the non-weight-bearing portions of the peripheral trochlea (as depicted here) or the roof of the intercondylar notch using provided curettes. Harvesting 2–3 samples of articular cartilage (approximately 5 mm × 3 mm in size) is recommended to obtain an appropriate cell count for the chondrocyte culturing

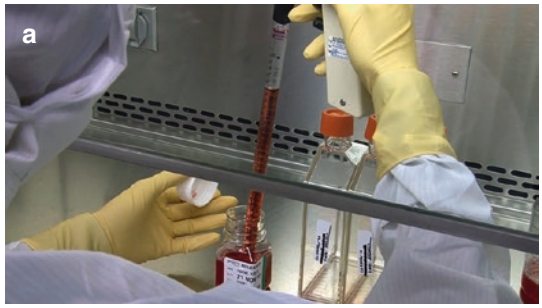

Figure 14.2.5: The MACI Technique: The Chondrocyte Culture and Membrane Seeding in the Laboratory. (**a**) The laboratory cultures human autologous chondrocytes in Dulbecco's modified Eagle medium supplemented with fetal bovine serum and gentamicin over a period of approximately 3–4 weeks to obtain sufficient cells to manufacture MACI at a density of at least 500,000 cells per cm^2 and (**b**) performs assessments for morphology, viability, and sterility. MACI is a uniformly seeded suspension of the chondrocyte cells attached to a collagen type I/III membrane that exhibit differential expression of a chondrocyte-specific marker gene for hyaluronan and proteoglycan link protein 1 (HAPLN1) compared to microfibrillar associated protein 5 (MFAP5) [8]. Each patient's chondrocytes are cryopreserved and remain available for 5 years as per company protocol

Figure 14.2.6: The MACI Technique: The Delivery of the MACI Implant. The MACI implant is a 3 × 5 cm porcine collagen matrix onto which patient's previously harvested chondrocytes are pre-seeded. Chondrocytes are cultured for approximately 3–4 weeks prior to delivery. The MACI implant is delivered in a sterile dish with the culture media hydrating the implant, typically the day prior to the surgery, and can be stored for 6 days. The MACI implant has two sides: rough and smooth. The rough side is implanted with the patient's chondrocytes and is presented facing up in the ceiling package. Care must be taken to ensure continued hydration of the implant with the culture media during the preparation prior to the implantation (image reproduced with permission from Vericel)

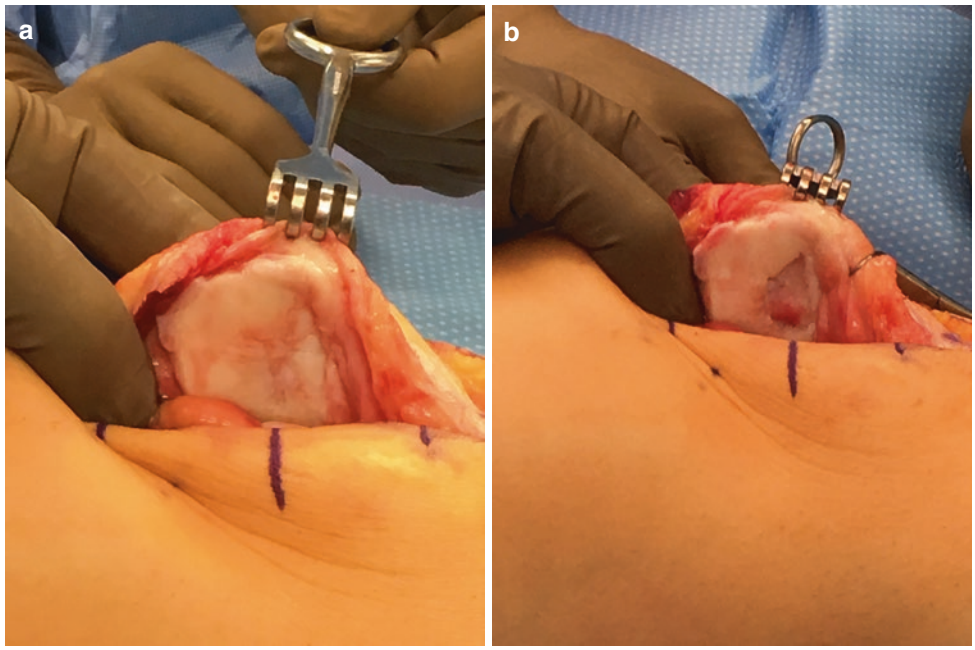

Figure 14.2.7: The MACI Technique: Preparations of the Walls of the Lesion. The patellar lesion in 22-year-old female (**a**) before and (**b**) after the preparation. An open approach to the lesion is performed according to lesion location. In this case, a limited lateral parapatellar approach is utilized to visualize the defect. The lesion is debrided back to stable cartilage borders with vertical walls surrounding the defect. All damaged cartilage and fibrous tissues are removed from the base of the defect, taking care not to violate the subchondral bone plate. A similar lesion preparation was carried out for the trochlear lesion as well

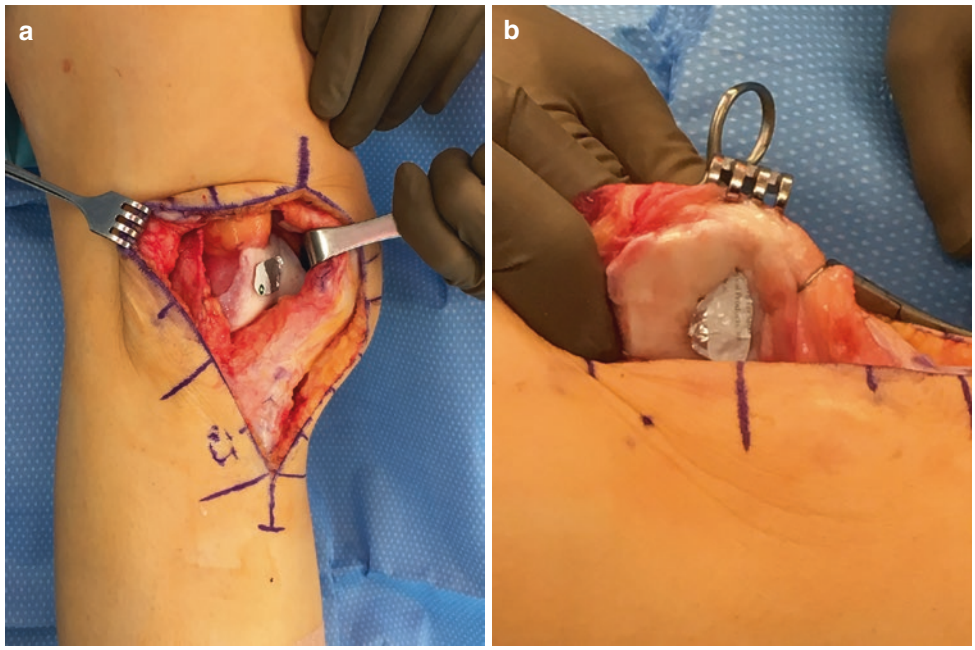

Figure 14.2.8.A: The MACI Technique: Templating the Lesion. Templating of the lesion is performed typically with the suture foil packaging. The foil is prepared to approximate the size and the contour of the prepared defect. The foil is cut to sit within the vertical walls of the prepared defect. In this figure foil templates have been cut and inset into the (**a**) the trochlea and (**b**) the patellar defects

Figure 14.2.8.B: The MACI Technique: Templating the Lesion. The MACI graft is cut according to the foil template. Using a firm surface as a cutting board, the MACI graft is overlaid on top of the template with the rough side (cell side up) and cut to match the template size. Care should be taken to minimize handling of the seeded side of the graft

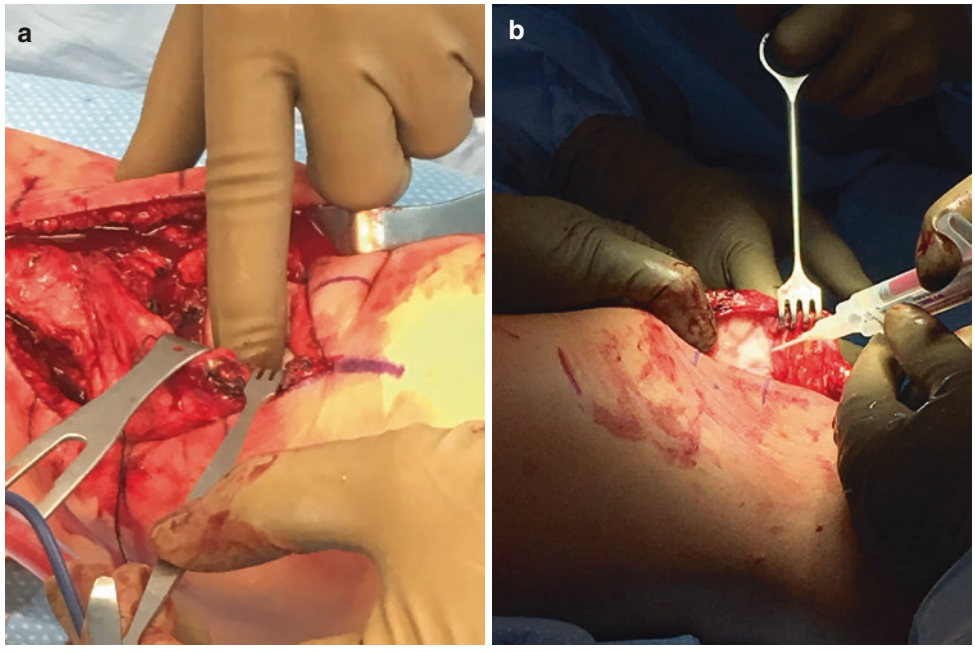

Figure 14.2.9: The MACI Technique: Implantation of the MACI Graft. The tourniquet is deflated and hemostasis is achieved within the defect using epinephrine-soaked pledgets. A thin layer of the fibrin glue is then applied to the base of the defect. (**a**) The cut implant is then placed into the defect and light digital pressure is applied for 3 min. (**b**) Fibrin glue is then used around the periphery of the defect to seal the edges. Supplemental fixation of the graft with interrupted resorbable suture to the surrounding cartilage can be added if conditions warrant

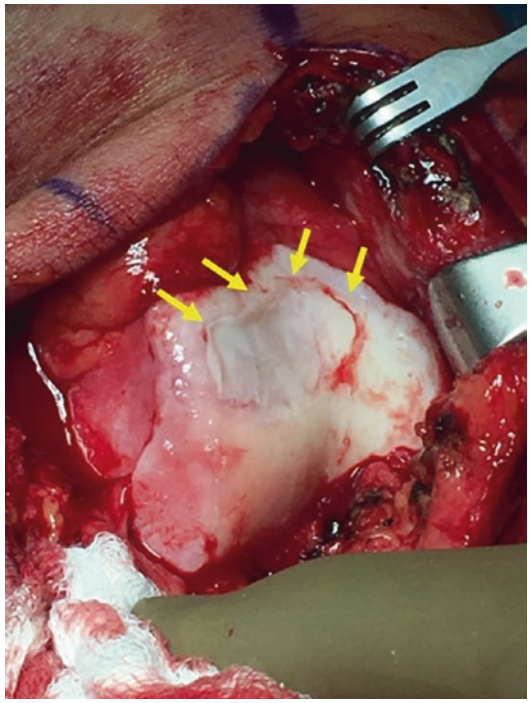

Figure 14.2.10: The MACI Technique: The Final Picture of the Implanted Graft. The MACI graft is implanted on the lateral trochlear defect of a 22-year-old female. Once the fibrin glue is dried, the knee is cycled throughout its "range of movement" (ROM) and the grafts are reassessed for displacement. Supplemental fixation can be added at this stage if graft edges are found to be unstable

a

Post Operative Protocol

- WBAT in full length hinged knee brace locked in extension x 6 weeks
- NWB ROM 0-20 degrees with CPM during first week
- Progress ROM 0-90 degrees over next 6 weeks. Light stationary bike, patellar mobilization, isometric exercises, and blood flow restriction treatment with physical therapist
- WBAT with patellar stabilization brace Weeks 6-12, progressive strengthening with physical therapy, progress to full ROM
- Cycling and pool exercises after Week 12
- Running allowed at 9 months

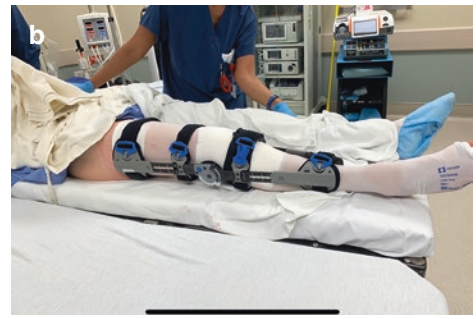

Figure 14.2.11: The MACI Technique: The Postoperative Rehabilitation and Bracing. (**a**) Postoperative protocol following the MACI procedure. (**b**) Immediate post-op weight bearing is permitted with the full-length hinged knee brace locked in extension as seen in picture. Regaining ROM is the focus of the first 6 weeks of therapy with progressive strengthening and return to the sport thereafter

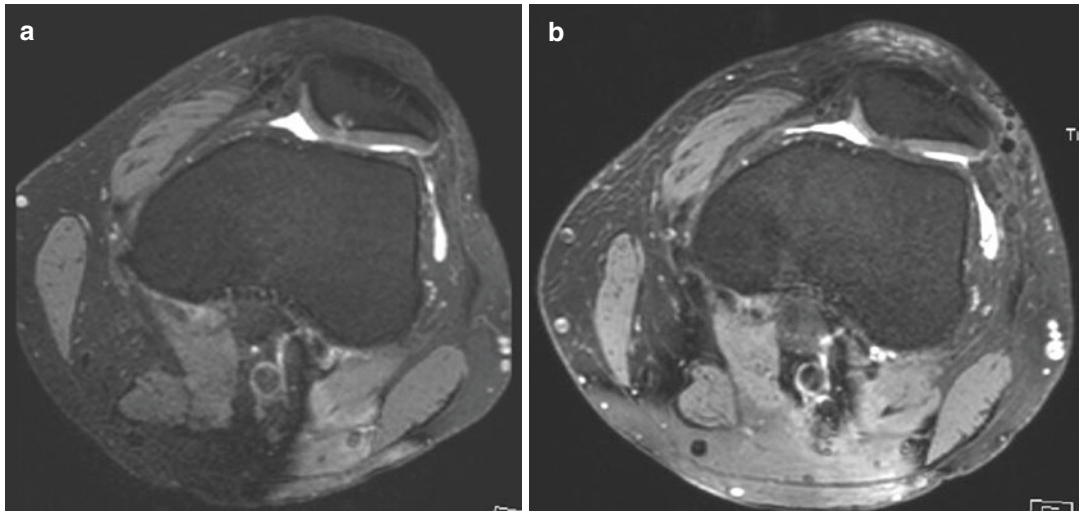

Figure 14.2.12: The MACI Technique: The Long-Term Results of a Successful MACI Technique on MRI. (**a**) Preop MRI images of 38-year-old male with symptomatic osteochondral defect of the central patella of left knee. The patient underwent MACI implantation for the patellar lesion with concomitant off-loading tibial tubercle osteotomy. (**b**) One-year post-op MRI reveals good lesion fill with resolution of underlying bone marrow edema. (The patient in Figures 14.2.12 and 14.2.13 is different from those shown in Figures 14.2.1–14.2.10.) MACI was only recently FDA approved in the USA in 2016. As such there is a relative paucity of second-look arthroscopy cases with robust follow-up and outcome data

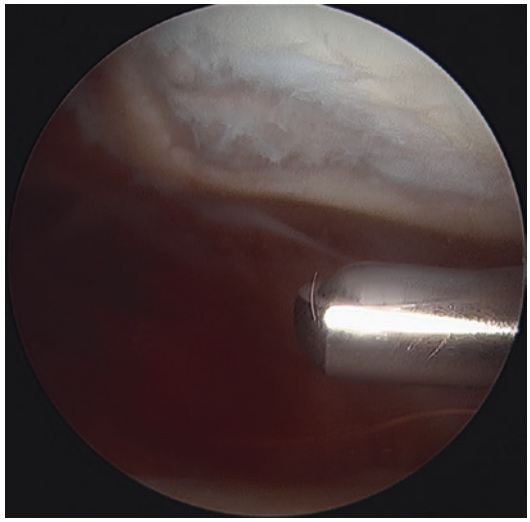

Figure 14.2.13: The MACI Technique: Long-Term Results of Successful MACI Technique on Arthroscopy. Left-knee arthroscopic evaluation of 38-year-old male patient who previously underwent MACI implantation for a patellar chondral defect. Picture of the patellofemoral compartment obtained from anteromedial viewing portal. Arthroscopy was performed at 1-year post-implantation for scarring and impingement of Hoffa's fat pad with anterior interval release. Note the good fill of the defect with stable cartilage repair tissue. (The patient in Figure 14.2.13 is same as in Figure 14.2.12, while both the figures are different from those shown in Figures 14.2.1–14.2.10)

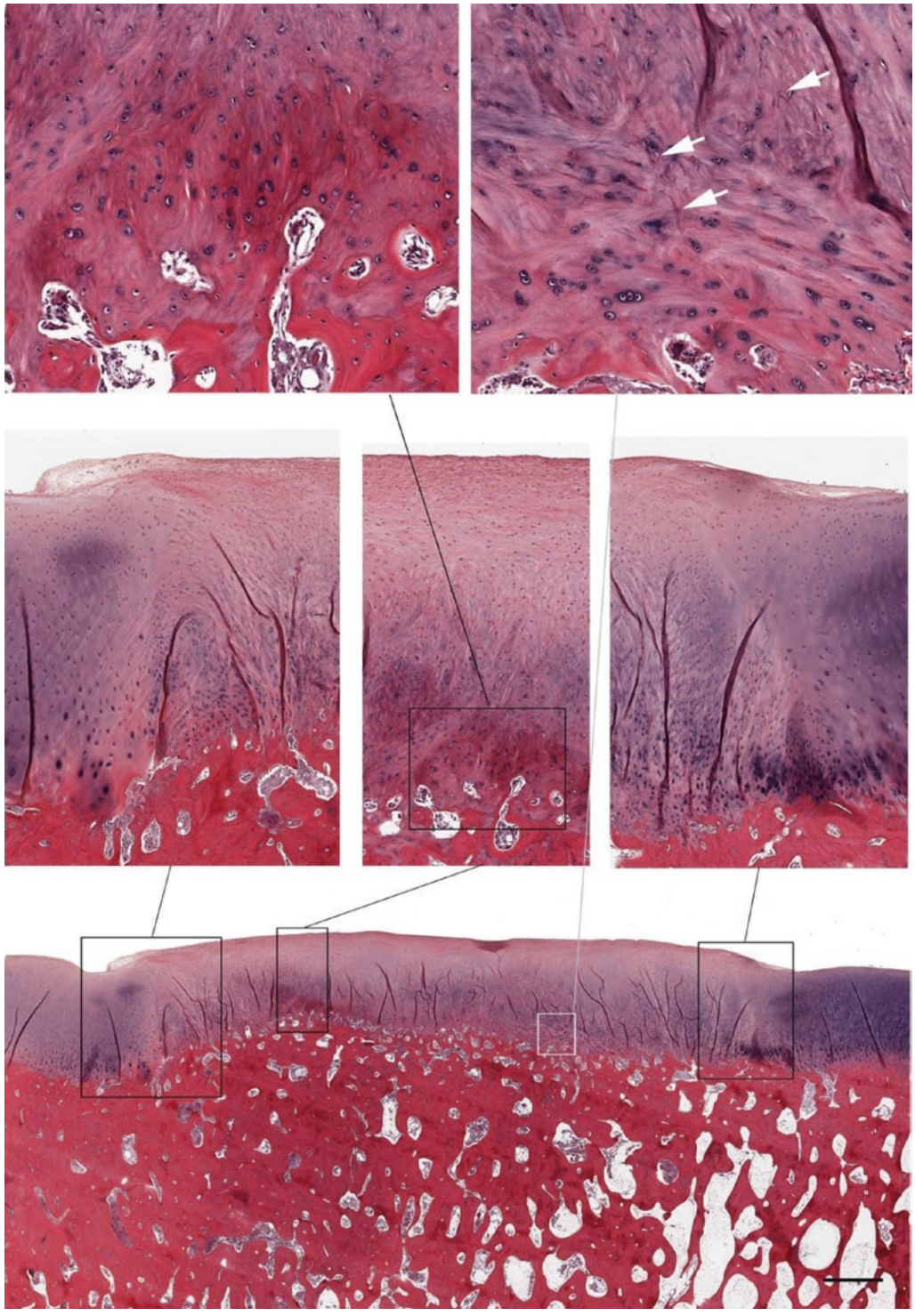

Figure 14.2.14: The MACI Technique: Long-Term Results of Successful MACI Technique on HPE. Photomicrograph of MACI-implanted defect in equine model 52 weeks after repair. Insets show left attachment to cartilage perimeter, center chondrocyte-rich region, and right attachment to perimeter cartilage. Top panels are higher magnification showing chondrocyte predominance (left), and minor residual MACI membrane (arrows; right) (reproduced with permission from Vericel)

14.3 Take-Home Message

- MACI technique is indicated for the large (>2 cm^2) articular cartilage defects within the knee.
- A careful clinical and radiographic assessment is required preoperatively to identify the pathologic factors (tibiofemoral malalignment, patellar mal-tracking, meniscal and/or ligamentous insufficiency) which may need to be addressed concomitantly with the MACI procedure.
- The initial cartilage biopsy is a low-morbidity procedure which also allows for arthroscopic evaluation of the lesion and surgical planning for the future chondrocyte implantation.
- Defect preparation is paramount. Debridement of damaged cartilage should be performed to create circumferential, vertical, and stable cartilage walls. The base of the defect should be cleared of nonviable cartilage tissue, taking care not to violate the subchondral bone plate.
- Ensure stability of the MACI implant after implantation by cycling the knee throughout its ROM. Add absorbable suture to the defect edges if found to be unstable.
- Patients should be counselled on the importance of rehabilitation preoperatively. Return to sport is typically delayed until 6–12 months after the surgery to allow full graft maturation.

References

1. Brittberg M, Lindahl A, Nilsson A, Ohlsson C, Isaksson O, Peterson L. Treatment of deep cartilage defects in the knee with autologous chondrocyte transplantation. N Engl J Med. 1994;331(14):889–95.
2. Gooding CR, Bartlett W, Bentley G, Skinner JA, Carrington R, Flanagan A. A prospective, randomised study comparing two techniques of autologous chondrocyte implantation for osteochondral defects in the knee: periosteum covered versus type I/III collagen covered. Knee. 2006;13(3):203–10.
3. Zaslav K, Cole B, Brewster R, DeBerardino T, Farr J, Fowler P, Nissen C; STAR Study Principal Investigators. A prospective study of autologous chondrocyte implantation in patients with failed prior treatment for articular cartilage defect of the knee: results of the Study of the Treatment of Articular Repair (STAR) clinical trial. Am J Sports Med. 2009;37(1):42–55.
4. Schuette HB, Kraeutler MJ, McCarty EC. Matrix-assisted autologous chondrocyte transplantation in the knee: a systematic review of mid- to long-term clinical outcomes. Orthop J Sports Med. 2017;5(6):2325967117709250.
5. Basad E, Ishaque B, Bachmann G, Stürz H, Steinmeyer J. Matrix-induced autologous chondrocyte implantation versus microfracture in the treatment of cartilage defects of the knee: a 2-year randomised study. Knee Surg Sports Traumatol Arthrosc. 2010;18(4):519–27.
6. Saris D, Price A, Widuchowski W, Bertrand-Marchand M, Caron J et al. Matrix-applied characterized autologous cultured chondrocytes versus microfracture: two-year follow-up of a prospective randomized trial. Am J Sports Med. 2014;42(6):1384–94.
7. Ogura T, Bryant T, Merkely G, Minas T. Autologous chondrocyte implantation for bipolar chondral lesions in the patellofemoral compartment: clinical outcomes at a mean 9 years' follow-up. Am J Sports Med. 2019;47(4):837–46.
8. Rapko S, Zhang M, Richards B, Hutto E, Dethlefsen S, Duguay S. Identification of the chondrocyte lineage using microfibril-associated glycoprotein-2, a novel marker that distinguishes chondrocytes from synovial cells. Tissue Eng Part C Methods. 2010;16(6):1367–75.

15 The Illustrative Third Generation Autologous Chondrocyte Implantation for Cartilage Repair: The Gel Based ACI Technique

Deepak Rajkumar Goyal

15.1 Introduction

Autologous chondrocyte implantation (ACI) has evolved over many generations. The third-generation ACI evolved with cultured chondrocytes directly seeded on a membrane in the laboratory itself and then transported to the operating room for an implantation. This eliminated the need for suturing of a periosteum/membrane during the surgery [1–4]. The third-generation ACI technique further evolved from a monolayer distribution of the cells to the 3-dimensional distributions of the cells by using 3-dimensional scaffolds. Hyalograft-C and BioSeed C are some of the third-generation 3-dimensional scaffold-based ACI [5, 6]. These techniques helped to overcome many disadvantages associated with the first- and second-generation ACI, like graft hypertrophy, poor access to the lesion, membrane suturing and monolayer distribution [5–8]. Chondrocytes grown on a monolayer have a tendency for a slow growth, dedifferentiation and a switch of collagen synthesis from type II to type I [7, 8]. As any chondral defect is a 3-dimensional defect, it is quite logical to fill the defect with a 3-dimensional repair method. Gel-based ACI is a third-generation 3-dimensional scaffold-based technique that allows a 3-dimensional distribution of the autologous cultured chondrocytes in a scaffold that is made of fibrin glue [9–12]. As it is gel based, the scaffold can take any shape and does not require lesion preparation in the form of an oval/round shape.

A symptomatic young patient (14–50 years old depending on their physiological fitness) with a mid- to large-size (size >1.5–2 cm^2) full-thickness focal chondral defect of ICRS grade 3/4 in a biomechanically normal/corrected joint is an ideal indication for a gel-based ACI. Inflammatory or immunological conditions, diffuse or degenerative lesions, obesity, abnormal biomechanics and smokers are the conditions where ACI should not be attempted [10].

The purpose of this chapter is to illustrate the step-by-step technique and the postoperative rehabilitation of a gel-based third-generation ACI in an ideally indicated case.

D. R. Goyal (✉)
Saumya Arthroscopy and Sports Knee Clinic, Ahmedabad, India

Visiting Professor of Orthopaedics, Graduate School of Biomedical and Health Sciences, Hiroshima University, Hiroshima, Japan
e-mail: deepak@knee.in

D. R. Goyal (ed.), *The Illustrative Book of Cartilage Repair*,
https://doi.org/10.1007/978-3-030-47154-5_15

15.2 The Illustrations

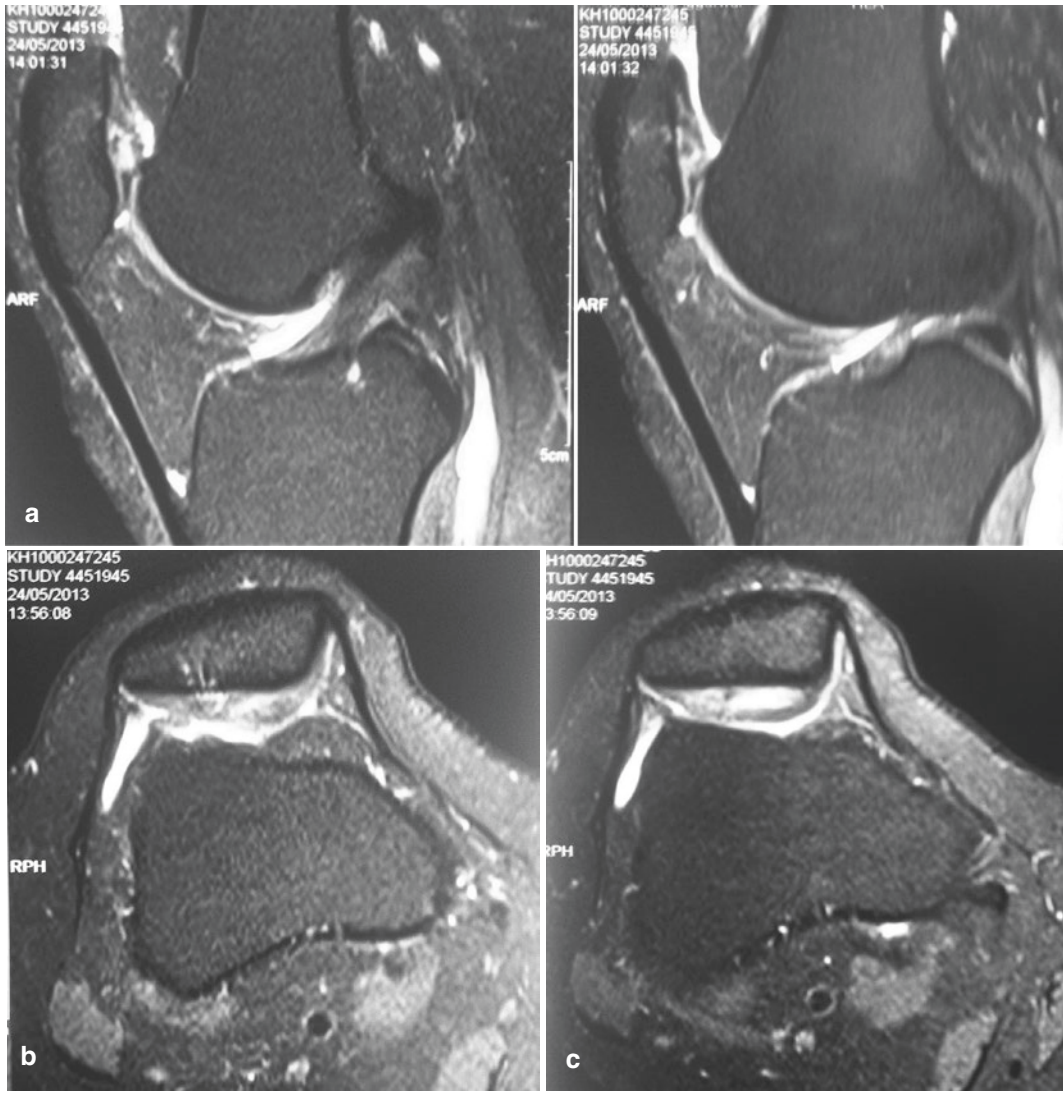

Figure 15.2.1: The Gel-Based ACI Technique: The Ideal Case Selection. A 39-year-old housewife complained of anterior knee pain during the household activities for 2 years; the pain was more on knee-bending activities and on using stairs. She did not give any history of trauma, fall or twisting injury. She already had completed sessions of physiotherapy and medications at her previous ortho surgeon's clinic and had been referred for further management. Her clinical examination revealed mild parapatellar synovitis with tenderness on the lateral patellar facet. Her knee was otherwise stable and had free range of movements. Her X-ray did not reveal any abnormality except trochlea dysplasia grade B. She underwent magnetic resonance imaging and was diagnosed to have a large patellar chondral lesion on the lateral patellar facet. (**a**) Fat-suppressed proton density sagittal images showed areas of chondral hyperintensities in the centre of the patella with a fluid interface. The chondral surface showed some discontinuity. The images also showed mild subchondral (SC) bone oedema. (**b**, **c**) The fat-suppressed proton density axial images confirmed the same findings that were present on the lateral patellar facet with multiple areas of chondral hyperintensity and fluid interface. The SC bone was showing mild bone marrow oedema with intact SC bone plate and SC lamina. As the lesion was a full-thickness large lesion with no SC bone involvement in a young symptomatic female, it was a right indication for choosing autologous chondrocyte implantation technique (ACI). The third-generation ACI was chosen as the treatment of choice

Figure 15.2.2: The Gel-Based ACI Technique: The Instruments. The instruments needed to prepare the chondral lesion for the receipt of the gel-based autologous chondrocyte implantation are not very specific and are generally present in any arthroscopy set. A combination of sharp curettes (1–3) are required to scrap the defective cartilage from the subchondral (SC) bone. Different types of thin and sharp periosteum elevators (4–7) are needed to sharply create the lesion border by separating the healthy cartilage from the unhealthy cartilage. A measuring scale like Trukor depth gauze (8) (Smith & Nephew, USA) is also helpful for measuring the prepared lesion size for the final size assessment and documentation. A special trocar and cannula (9) (Regrow Biosciences Pvt. Ltd., India) are utilised for the cartilage biopsy. However, a routine scoop that can take a deeper bite of the biopsy is also acceptable (more details can be found in Chap. 19, Figure 19.2.2b) [11]

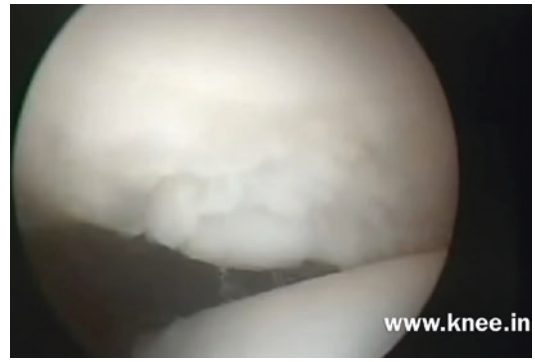

Figure 15.2.3: The Gel-Based ACI Technique: The Arthroscopic Assessment of the Lesion. A 39-year-old female suffering from right-side chronic anterior knee pain underwent a right-knee arthroscopy. Her magnetic resonance imaging had shown a full-thickness chondral lesion on the lateral patellar facet (Figure 15.2.1). While viewing from the anterolateral portal, a full-thickness chondral lesion was reconfirmed on the lateral patellar facet. On probing, the defect was bone deep and was extending till the patellar apex. As arthroscopy had confirmed the clinico-radiological assessment, it was decided to proceed with the first stage of the gel-based autologous chondrocyte implantation

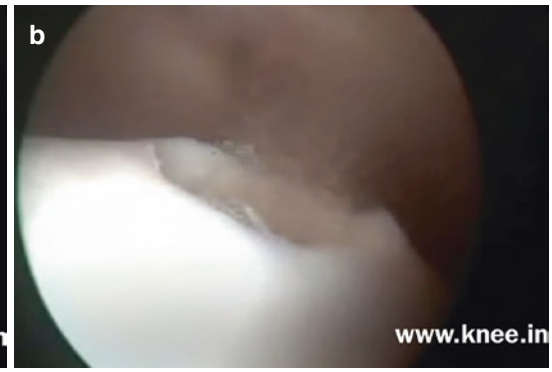

Figure 15.2.4: The Gel-Based ACI Technique: The Cartilage Biopsy. A 39-year-old female suffering from right-side chronic anterior knee pain underwent a right-knee arthroscopy. (**a**) A hexagonal harvester and trocar (Figure 15.2.2(9)) from the biopsy kit were used to harvest the chondral biopsy. The gel-based autologous chondrocyte implantation technique requires harvesting of a hexagonal cylinder from the non-weight-bearing lateral or medial margin of the trochlea above the sulcus terminalis. The best way to ensure this is to take biopsy while the knee is in hyperextension. (**b**) The biopsy is taken bone deep to ensure the full-thickness cartilage harvest [10]. The harvested biopsy material is sent to the cartilage lab for the chondrocyte culture

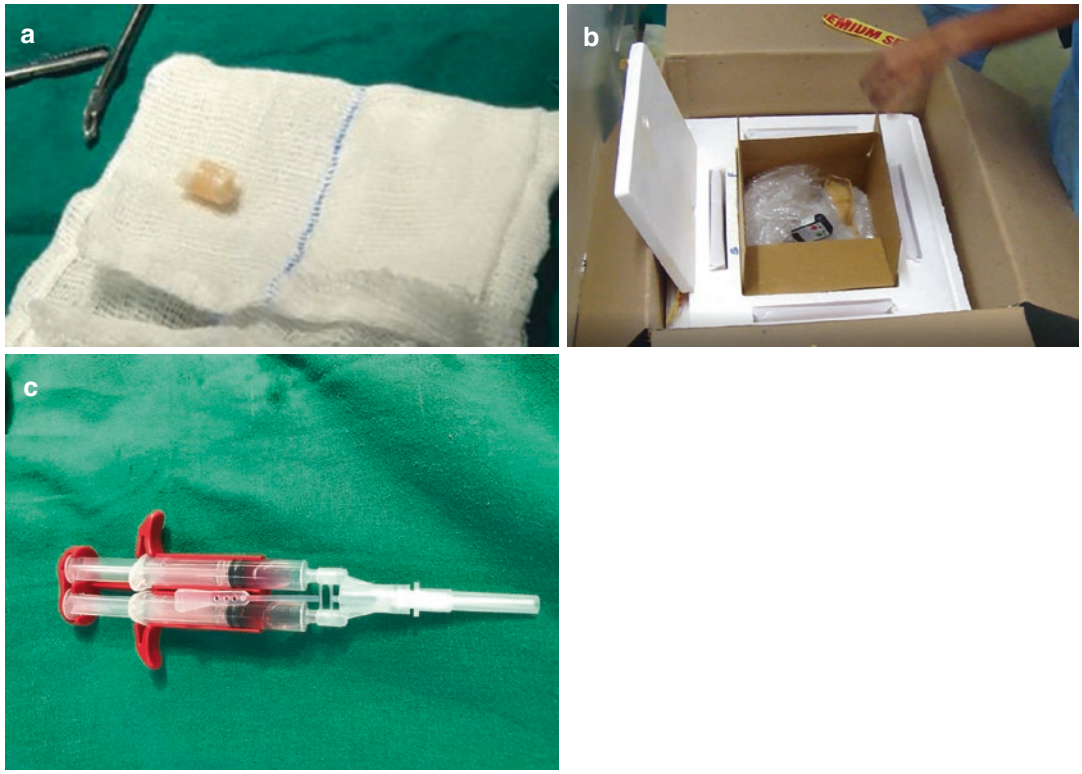

Figure 15.2.5: The Gel-Based ACI Technique: The Chondrocyte Culture in the Cartilage Laboratory and Delivery to the Operation Theatre. (**a**) The donor chondral tissue undergoes enzymatic digestion, cleaning and then cell expansion at a GMP-certified cartilage lab for 4–6 weeks (see Chap. 19, Figure 19.2.5, for more details) [11]. When the culture process is nearly complete, the cartilage lab informs the operating surgeon about the final date of delivery of the cultured chondrocytes. The final cartilage lab report of the chondrocyte culture must state the cell count, cell viability, cell characterisation and cell morphology of the cultured cells. In addition, the presence of any pathogens and endotoxins must be ruled out and supported by the cartilage lab report [10]. (**b**) The cultured chondrocytes are delivered in a temperature-controlled box by a dedicated courier service on the day of the implantation. (**c**) The laboratory assistant prepares the autologous cultured chondrocytes in two syringes with a common 'Y' connector for implantation into the prepared chondral defect (see Chap. 19, Figure 19.2.8, for more details) [11]

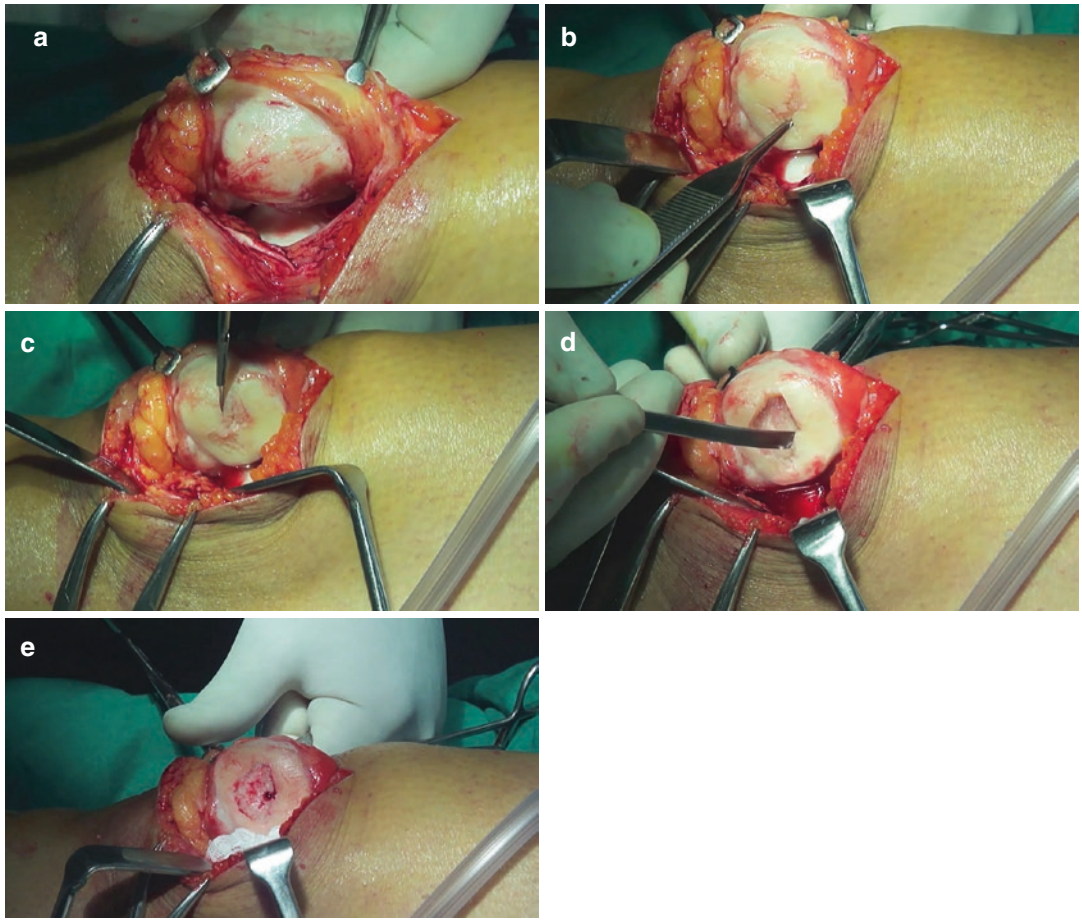

Figure 15.2.6: The Gel-Based ACI Technique: Preparations of the Walls and the Base of the Lesion. A 39-year-old female suffering from a large right-sided lateral patellar chondral lesion is taken for surgery for the second stage of autologous chondrocyte implantation. (**a**) The patellar autologous chondrocyte implantation required a mini medial parapatellar arthrotomy. The cartilage lesion was exposed completely by everting the patella and exposing the patellar articular surface. (**b**) A probe was used to palpate the chondral surface and feel for the fibrillations, depth of the lesion, loose chondral flap and floating chondral area over a fluid interface. (**c**) The margins of the cartilage lesion were prepared using a 15 # blade, sharp ring curettes and a sharp periosteum. An oblique cut on the periphery of the cartilage lesion was put in such a way that the margins are bevelled shaped with more tissue removed from the depth than from the surface. This was important so that the gel-based ACI implant gets an inherent stability from the overhanging margins of the surrounding healthy cartilage. (**d**) Then a sharp ring curette or periosteum was used to remove the remaining irregular and damaged cartilage from the subchondral bone. This was ensured by curetting the tissues from the previously created bevelled margins towards the centre of the lesion. This also ensured that only the healthy cartilage remains all around the prepared cartilage defect, which was important for a good integration of the regenerating cartilage. The size of the prepared defect was then measured for the documentation purpose and for the follow-up assessment. (**e**) A few tiny holes (1.9 mm k wire) were added on the base of the lesion, not penetrating thru the subchondral bone plate, to assist the anchoring of the ACI implant with the base of the lesion [10]

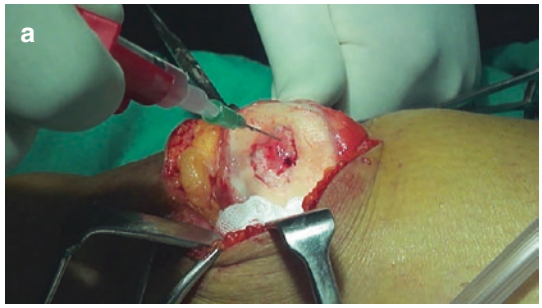

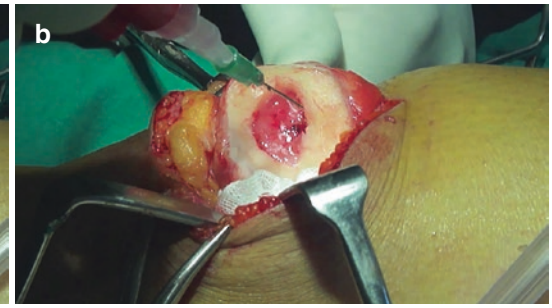

Figure 15.2.7: The Gel-Based ACI Technique: Implantation of the ACI Graft. A 39-year-old female underwent gel-based autologous chondrocyte implantation for a large lateral patellar chondral lesion. The gel-based autologous chondrocyte implantation technique uses fibrinogen in one syringe and a mixture of chondrocytes with thrombin in second syringe, both connected with a 'Y' mixing connector. (**a**, **b**) As each drop was implanted into the defect, a 3-dimensional layer-by-layer scaffold was created on the cartilage defect by the adherent cultured chondrocytes, ultimately forming a multilayered ACI implant [10]. It was carefully observed to keep the base of the defect as gravity neutral, in order to keep the drops of the gel contained inside the defect; otherwise the gel with the chondrocytes may flow out. Any gel flowing out of the defect was wiped out repeatedly with the help of dry patties. The gel got solidified in 8–10 min (see Chap. 19, Figures 19.2.9 and 19.2.10, for more details) [11]

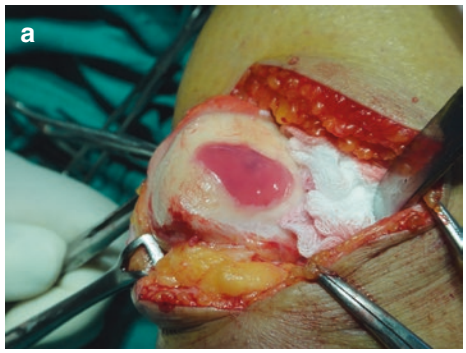

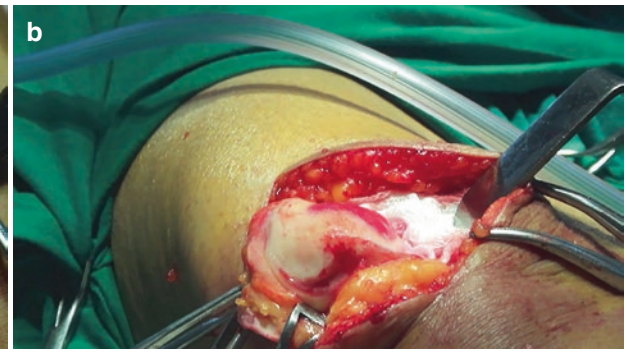

Figure 15.2.8: The Gel-Based ACI Technique: The Final Inspection of the Implanted Graft. A 39-year-old female underwent a gel-based autologous chondrocyte implantation for a large lateral patellar chondral lesion. (**a**) A final inspection was done to ensure that all the implanted autologous chondrocyte implantation graft is contained inside the defect with no empty spaces or bubbles. (**b**) The graft is slightly proud, beyond the surrounding surface of the cartilage defect, but this was intentional to account for some retraction of the fibrin that is commonly seen with this transplantation. However, care must be taken to keep this to a minimum level (<0.5–1 mm) [10]. A gentle flexion-extension range of movement was carried out for 3–5 repetitions and then a reinspection was done to cross-check the stability of the implant. Gentle lavage was done of the graft and the surrounding tissue, and a closure was done in layers

Figure 15.2.9: The Gel-Based ACI Technique: The Post-operative Rehabilitation and Bracing. Ice application, compression bandage and elevation to the limb are important in the immediate post-operative period to manage the pain and inflammation [10]. While it is necessary to avoid premature overloading of the graft in the early phase, it is equally necessary to start an early controlled range of motion and weight bearing to stimulate the cellular orientation and the chondrocyte development. The critical motion to be avoided is shear force moments such as flexion while traversing the stairs; in this instance a full extension should be maintained on the stairs. The physiotherapist must start active and active assisted flexion and range of movements early to achieve a full range by 3–6 weeks, unless instructed by the surgeon due to case-specific reasons. Once the pain subsides, patient is encouraged to walk. Hence, the static strengthening exercises are added to allow an early functional gait. CPM is also advocated to encourage cartilage healing. It must be emphasised that both CPM and active movements are essential and have different roles to play [10]. The transplanted tissues are firm and durable within 6–9 months and hence any sudden shear or extreme loading forces are avoided until that time. Low-impact activities like swimming and biking can be started after 12 weeks. Moderate activities like jogging and dancing should be deferred for 9 months [13, 14]. A 39-year-old female underwent patellar gel-based ACI for a large lateral patellar chondral lesion. (**a**) Continuous passive motion machine (CPM) was started 6–12 h after surgery and was continued for 6–8 h per day and for up to 6–8 weeks. (**b**) As the patient had undergone ACI on the patellar regions, partial weight bearing was allowed during the early phases of rehabilitation with a long-limb brace locked in full extension (it must be noted that the cases with tibio-femoral ACI are usually kept non-weight bearing for 3–4 weeks post-operatively, in contrast to patella ACI cases). (**c**) An increase in the range of motion in ROM brace by 40° per week was allowed until the patient obtains full range by 6 weeks

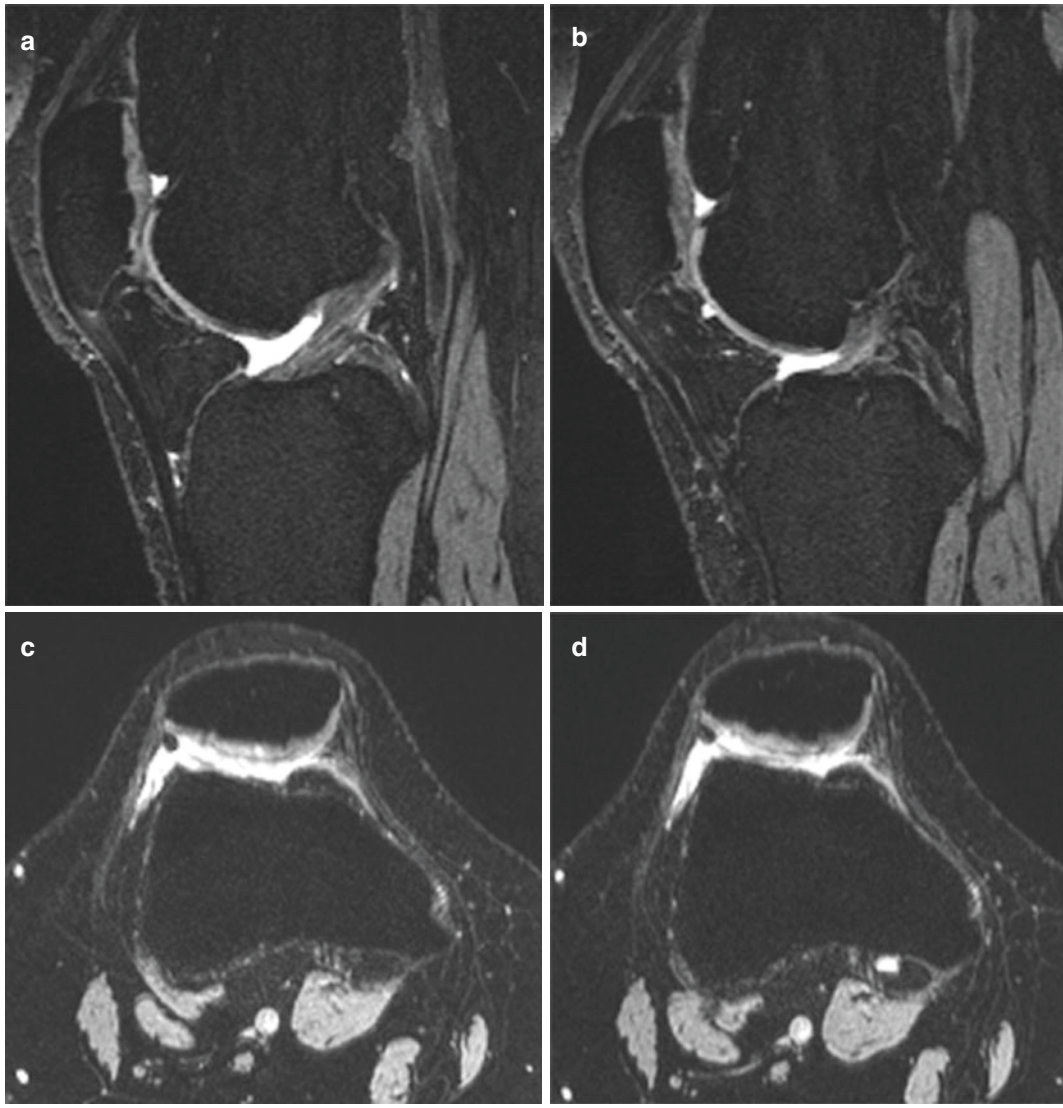

Figure 15.2.10: The Gel-Based ACI Technique: The Long-Term Results. A 39-year-old female that underwent right-side patella ACI came back for follow-up after 6.5 years at the age of 46 years. She had no complaints in her right knee, and she is socially active and pursuing her hobby of dancing. Her right-knee examination was clinically normal with no evidence of synovitis, effusion or tenderness. Her movements were full and pain free. Follow-up magnetic resonance imaging demonstrated the following outcome of the patella ACI. (**a**, **b**) T2 fat-suppressed sagittal images showed well-healed chondral defect with intact chondral surface. The homogeneity of the chondral regenerate was isotense with the surrounding cartilage tissue. The subchondral bone was also intact throughout with no evidence of subchondral (SC) cysts or oedema. There were two small internal osteophytes seen on the SC surface that might have come from a possible over-drilling of the SC bone before the implantation of a gel-based ACI transplant (see Figure 15.2.6e). (**c**, **d**) The T2-weighted fat-suppressed axial images confirmed the findings seen in the sagittal images

15.3 Take-Home Message

The literature has consistently shown gradually improving results of ACI, from the first generation to the third generation [10]. There is a strong short- to mid-term evidence in favour of all the generations of the ACI. Literature supports long-term results with many case series using a first-generation ACI; however, there are not many publications supporting the long-term results of the third-generation ACI at present. Kim et al. [12] published clinical and functional improvement at 2-year results following fibrin ACI for deep defects of the femoral condyle in 30 patients. Arthroscopic assessments performed 12 months post-operatively produced nearly normal (grade II) International Cartilage Repair Society score in 8 of the 10 patients with no graft-associated complications. Choi et al. [9] published data of 98 patients operated with a gel-based ACI, with a mean age of 43.7 years and the mean lesion size of 5.23 cm^2 at a mean follow-up of 24.35 months (range 13–52 months). They observed an improvement of tKSS-A (telephone Knee Society Score-A) from 43.52 to 89.71 and an improvement on the tKSS-B (telephone Knee Society Score-B) from 50.66 to 89.38 [9, 10]. Goyal et al. [8] performed a systematic review of second- and third-generation ACI over the first-generation ACI using level I and II studies. The third-generation ACI was found to give comparable results as in first-generation ACI with minimum complications up to 2-year follow-up. The third-generation ACI gives added advantages of fewer complications and ease of surgical technique as compared to the previous generations [10]. The gel-based ACI provides a 3-dimensional distribution of the cultured cells in a fibrin scaffold. The procedure has a very specific set of indications and contraindications, guiding the selection process of choosing the third-generation ACI. Consideration of the possible abnormal biomechanics is required, and corrected if needed, as with any cartilage repair procedure.

References

1. Brittberg M. The illustrative 1st and 2nd generation autologous chondrocyte implantation (ACI) for the cartilage repair. In: Goyal D, editor. The illustrative book of cartilage repair. Springer; 2021; In Press.
2. Ramos N, Mandelbaum B, Banffy M. The illustrative membrane based autologous chondrocyte implantation for the cartilage repair. In: Goyal D, editor. The illustrative book of cartilage repair. Springer; 2021, In Press.
3. Bartlett W, Skinner JA, Gooding CR, Carrington RW, Flanagan AM, Briggs TW, et al. Autologous chondrocyte implantation versus matrix-induced autologous chondrocyte implantation for osteochondral defects of the knee: a prospective, randomised study. J Bone Joint Surg Br. 2005;87(5):640–5.
4. Behrens P, Bitter T, Kurz B, Russlies M. Matrix-associated autologous chondrocyte transplantation/implantation (MACT/MACI)—5-year follow-up. Knee. 2006;13(3):194–202.
5. Pavesio A, Abatangelo G, Borrione A, Brocchetta D, Hollander AP, Kon E, et al. Hyaluronan-based scaffolds (Hyalograft C) in the treatment of knee cartilage defects: preliminary clinical findings. Novartis Found Symp. 2003;249:203–17; discussion 229–233, 234–238, 239–241.
6. Ossendorf C, Kaps C, Kreuz PC, Burmester GR, Sittinger M, Erggelet C. Treatment of posttraumatic and focal osteoarthritic cartilage defects of the knee with autologous polymer-based three-dimensional chondrocyte grafts: 2-year clinical results. Arthritis Res Ther. 2007;9(2):R41.
7. Grigolo B, Lisignoli G, Piacentini A, Fiorini M, Gobbi P, Mazzotti G, et al. Evidence for redifferentiation of human chondrocytes grown on a hyaluronan-based biomaterial (HYAff 11): molecular, immunohistochemical and ultrastructural analysis. Biomaterials. 2002;23:1187–95.
8. Goyal D, Goyal A, Keyhani S, Lee EH, Hui JHP. Evidence-based status of second- and third-generation autologous chondrocyte implantation over first generation: a systematic review of level I and II studies. Arthroscopy. 2013;29(11):1872–8.
9. Choi NY, Kim BW, Yeo WJ, Kim HB, Suh DS, Kim JS, et al. Gel-type autologous chondrocyte (Chondron) implantation for treatment of articular cartilage defects of the knee. BMC Musculoskelet Disord. 2010;11:103.

10. Goyal D, Vishvas M. Gel based autologous chondrocyte implantation: the surgical technique. Asian J Arthroscopy. 2019;4(1):27–33.
11. Goyal D. The illustrative overlay autologous chondrocytes implantation (overlay ACI) technique for repair of the extra-large osteochondral defects. In: Goyal D, editor. The illustrative book of cartilage repair. Berlin: Springer; 2021, In Press.
12. Kim MK, Choi SW, Kim SR, Oh IS, Won MH. Autologous chondrocyte implantation in the knee using fibrin. Knee Surg Sports Traumatol Arthrosc. 2010;18(4):528–34.
13. Peterson L, Minas T, Brittberg M, Nilsson A, Sjögren-Jansson E, Lindahl A. Two- to 9-year outcome after autologous chondrocyte transplantation of the knee. Clin Orthop Relat Res. 2000;374:212–34.
14. Peterson L, Brittberg M, Kiviranta I, Akerlund EL, Lindahl A. Autologous chondrocyte transplantation. Biomechanics and long-term durability. Am J Sports Med. 2002;30(1):2–12.

16 The Illustrative Single-Stage Cartilage Repair Technique with Chitosan-Based Bioscaffold (BST-CarGel)

Ivan Wong
and Anjaneyulu Purnachandra Tejaswi Ravipati

16.1 Introduction

Articular cartilage damage and osteochondral defects remain major orthopaedic challenges. In a study reviewing over 30,000 arthroscopic procedures, approximately 60% of the patients were found to have some cartilaginous defects, a majority (41.0% of all chondral lesions had grade III changes, and 19.2% of all had grade IV changes) of them being high-grade defects [1]. If left untreated, these can progress to degenerative arthritis requiring arthroplasty at an earlier age [2]. The goal of any cartilage repair treatment is to achieve a repair tissue with structural characteristics comparable with the native hyaline cartilage, which may result in long-term durability, joint function and pain relief [3]. Although several strategies have been described to treat the chondral lesions, microfracture is currently the first line of surgical treatment recommended for the small chondral defects [4, 5]. However, microfracture technique is not without its drawbacks. Microfracture results in a fibrocartilaginous repair tissue lacking hyaline articular structure [6–8] and clinical benefit that is variable beyond 5 years [9]. It is postulated that the inconsistency and suboptimal repair tissue both in quantity and in quality may result from the instability of the fibrin clot formed from marrow blood in the lesion [6, 7, 10, 11], which may shrink as a result of platelet-driven clot retraction [11, 12]. It has been demonstrated by studies that improved repair can be achieved with a more adherent and a voluminous clot [13]. This clot in turn modulates the repair events that result in optimum cartilage regeneration and repair. Hence the critical component for the bone marrow-derived cartilage repair is the quantity of the initial blood clot present in the cartilage lesion after the microfracture [13, 14].

Recently, gel-forming chitosan-based biopolymer has gained interests as a scaffolding material that can be injected into the site of the microfracture to stabilise the clot and facilitate the cartilage repair [15]. Chitosan is a natural polysaccharide which is biocompatible and biodegradable and it has been studied extensively as an effective scaffolding biomaterial with low toxicity and great adhesiveness to the tissues [16].

BST-CarGel (Smith and Nephew Inc., USA) is an injectable chitosan-based medical device, which is designed to be used in conjunction with the bone marrow stimulation technique [3]. While the microfracture initiates the reparative process by inducing bleeding in the subchondral space, followed by proliferation and migration of inflammatory and stromal cells from the cancellous

I. Wong (✉) · A. P. T. Ravipati
Division of Orthopaedic Surgery,
Dalhousie University, Halifax, NS, Canada
e-mail: iw@drivanwong.com;
drpurnateju@gmail.com

D. R. Goyal (ed.), *The Illustrative Book of Cartilage Repair*,
https://doi.org/10.1007/978-3-030-47154-5_16

marrow into a fibrin clot, the cationic nature of the chitosan in the BST-CarGel increases the adhesivity of the mixture to cartilage lesions, ensuring longer clot residency [17]. This maintenance of critical blood components above the marrow holes ensures activation of adequate repair process [18]. The safety and efficacy of BST-CarGel in treating chondral lesions in femoral condyles have been shown in a well-designed randomised controlled trial [3]. The 5-year superiority of the BST-CarGel over microfracture alone was also demonstrated in a multicentre, randomised controlled trial [17].

16.2 The Illustrations

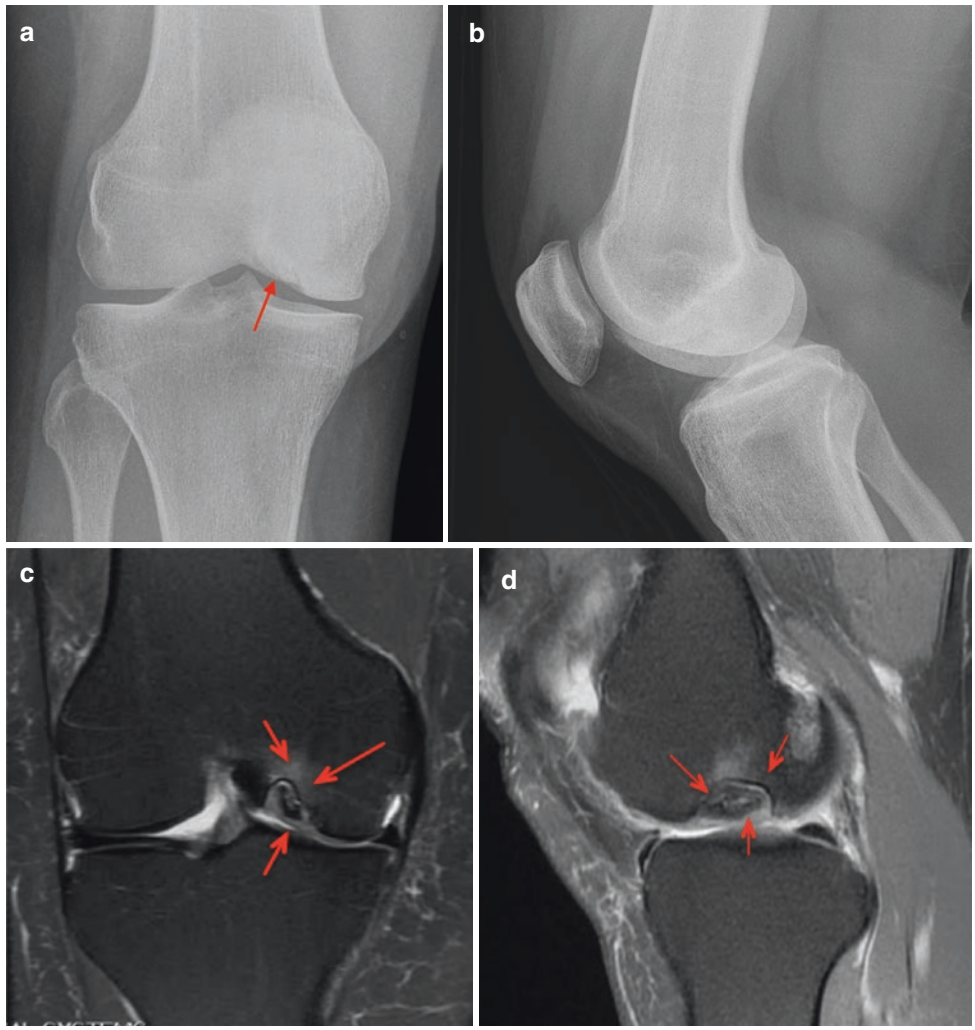

Figure 16.2.1: The Single-Stage Cartilage Repair Technique Using Chitosan-Based Bioscaffold: The Ideal Case Selection. A 33-year-old female presented with clicking and pain in the right knee for 1 year. She gave no history of trauma to her knee. Clinically, her knee was silent except for the medial joint line tenderness. A clinical examination and the radiographs confirmed good alignment of the lower limbs. An antero-posterior weight-bearing X-ray of the right knee (**a**, **b**) revealed an osteochondral defect in the lateral part of the medial femoral condyle. An magnetic resonance imaging (MRI) revealed a stable osteochondral defect on the medial femoral condyle. MRI COR T2 FSE (**c**, **d**) and SAG FSE (**d**) (red arrows) images showed the osteochondral defect measuring 2 cm × 2 cm × 1 cm on the medial femoral condyle

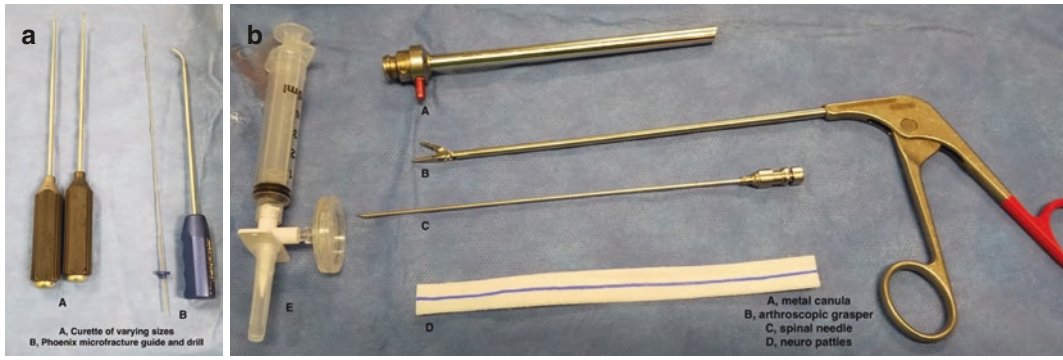

Figure 16.2.2: The Single-Stage Cartilage Repair Technique Using Chitosan-Based Bioscaffold: The Instruments. Instruments that are typically used for the BST-CarGel technique include (**a**) arthroscopic curettes of varying sizes along with the microfracture instruments (phoenix microfracture guide and drill used in this case). This instrument is particularly useful to avoid skiving of the awl and achieve optimum depth of microfracture. (**b**) Other instruments include an arthroscopic grasper, neuropatties for drying the lesion and a spinal needle for delivery of the BST-CarGel implant

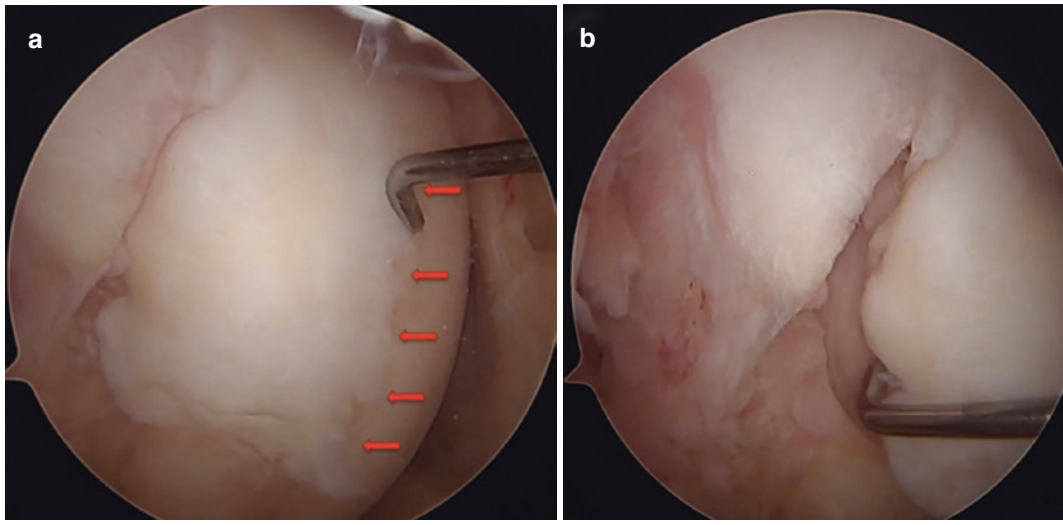

Figure 16.2.3: The Single-Stage Cartilage Repair Technique Using Chitosan-Based Bioscaffold: The Arthroscopic Case Selection. The 33-year-old female patient is positioned supine on the operating table. A tourniquet is applied to the right upper thigh. A post is placed against the upper thigh so as to get the valgus stress to the knee when supported against the surgeon's hip. View from the anterolateral portal with a probe in the anteromedial portal (**a**). Arrows outline the edge of the OCD lesion on the medial femoral condyle. The osteochondral defect was found to be unstable with a probe (**b** & **c**) and was removed with a grasper (**d**) through the anteromedial portal. On measuring with a graduated probe, the osteochondral piece measured 20 mm in height and 20 mm in width. BST-CarGel is indicated for osteochondral involvement as it can enhance the filling of the entire lesion [14, 18]. The decision was made to do a single-stage cartilage repair with the microfracture technique for the bone marrow stimulation and add a chitosan-based bioscaffold

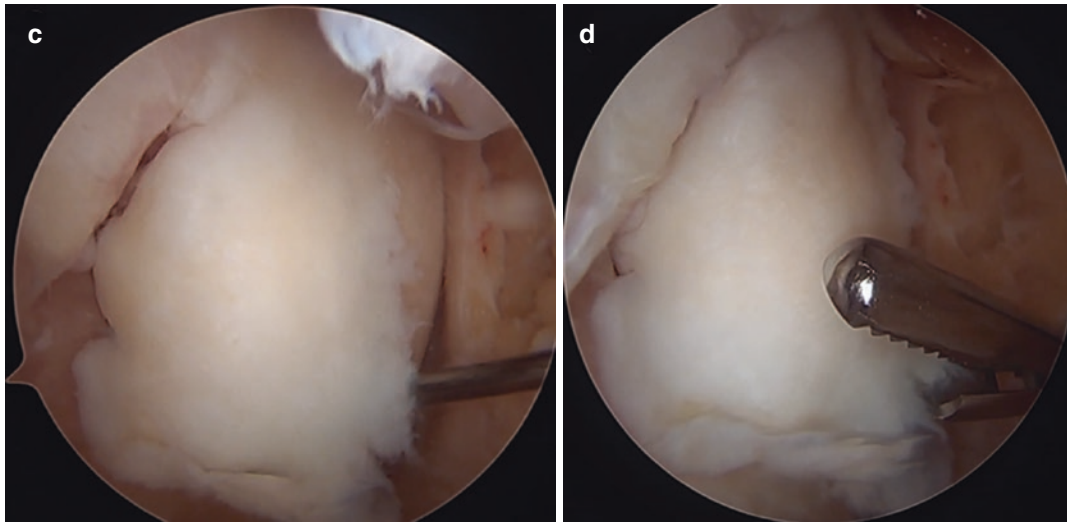

Figure 16.2.3: (continued)

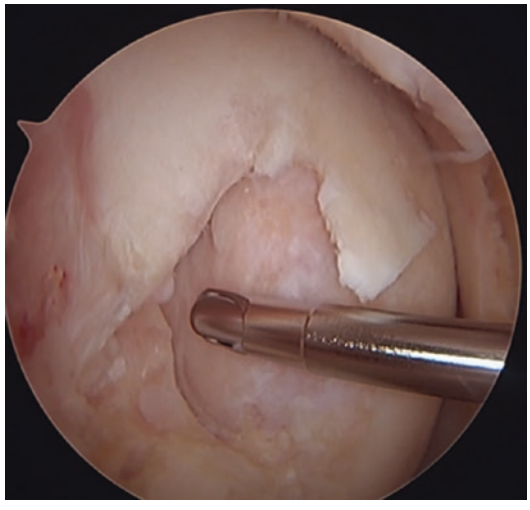

Figure 16.2.4: The Single-Stage Cartilage Repair Technique Using Chitosan-Based Bioscaffold: The Debridement of the Cartilage Defect. A 33-year-old female, right knee, view from the anterolateral portal. The lesion was debrided to remove the chondral flakes with an arthroscopic shaver from the anteromedial portal

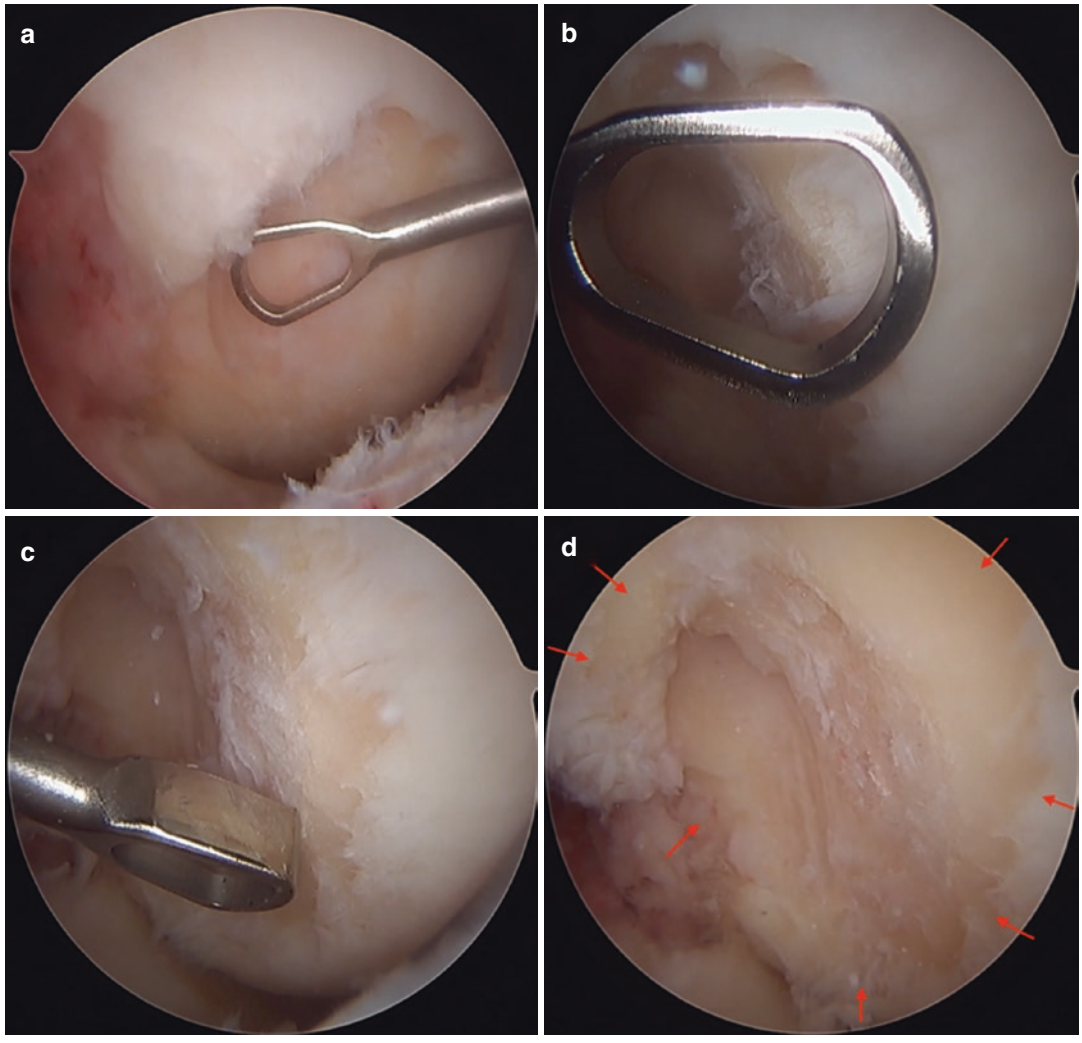

Figure 16.2.5: The Single-Stage Cartilage Repair Technique Using Chitosan-Based Bioscaffold: The Preparation of the Cartilage Defect. A 33-year-old female, right knee, viewing from the anterolateral portal and with a curette in the anteromedial portal; the lateral wall of the lesion was debrided to achieve the vertical walls (**a**). The scope was switched to the anteromedial portal and the medial wall of the lesion was debrided with a curette from the anterolateral portal (**b**, **c**). Any calcific tissue was removed from the base and the final lesion preparation can be seen in (**d**)

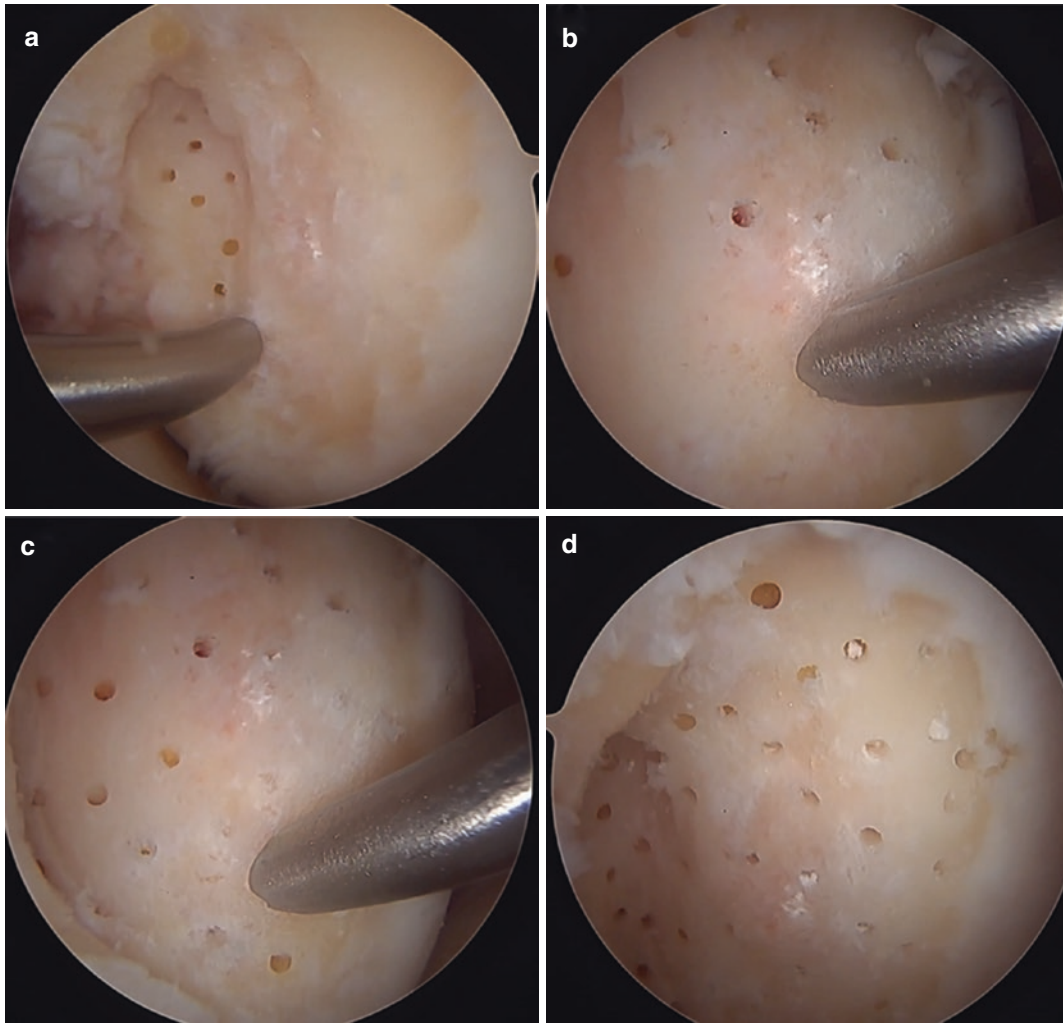

Figure 16.2.6: The Single-Stage Cartilage Repair Technique Using Chitosan-Based Bioscaffold: The Bone Marrow Stimulation Using the Microfracture Technique. The Phoenix microfracture system (Stryker) was used for the lesion in the right-side medial femoral condyle of a 33-year-old female. The awl/drill guide was positioned in a perpendicular fashion to the exposed subchondral bone to achieve optimal results. The lesion was viewed from anteromedial portal, while an awl was passed from the anterolateral portal (**a**) to achieve the desired angle for the microfracture procedure. The scope was switched to the anterolateral portal and a Phoenix guide and drill were used (**b**, **c**) to complete the microfracture to obtain the final result (**d**). This step ensures access to the autosomal bone marrow stem cells to the lesion

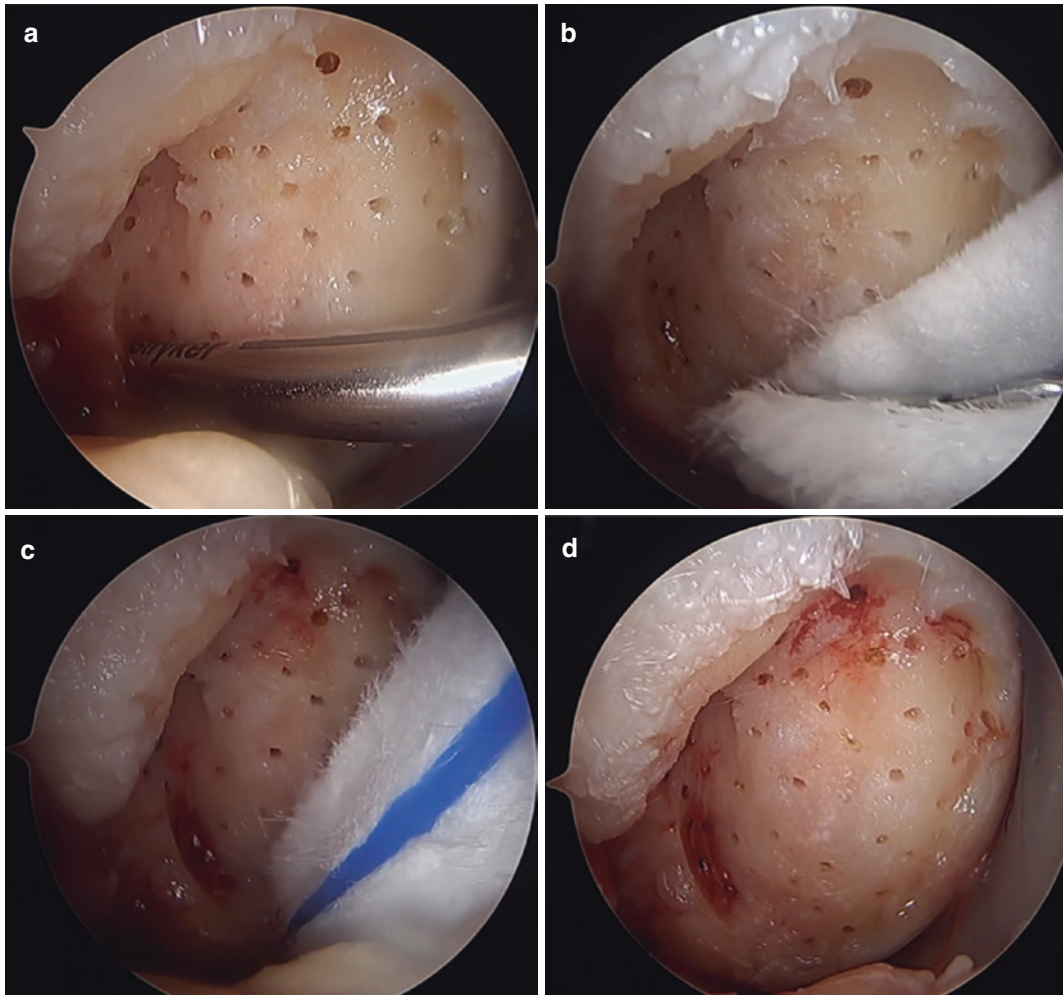

Figure 16.2.7: The Single-Stage Cartilage Repair Technique Using Chitosan-Based Bioscaffold: The Preparation of the Lesion for the BST-CarGel Implantation. A 33-year-old female, right knee. Preparation of the defect for the BST-CarGel implantation requires clearing the joint of the irrigation fluid. With the arthroscope in the anterolateral portal, fluid inside the joint was drained with suction attached to the shaver from the anteromedial portal (**a**). Residual fluid was cleared with a swab (**b**, **c**) and the defect was dried in preparation for the BST-CarGel implant (**d**)

Figure 16.2.8: The Single-Stage Cartilage Repair Technique Using Chitosan-Based Bioscaffold: The Preparation of the BST-CarGel on Table. (**a**) BST-CarGel preparation, the 'Mix vial' (red cap) and 'Add vial' (blue cap) are warmed to 37 °C (physiological temperature) using a thermostat. (**b**) The 'Mix vial' contains 1.2 mL of chitosan polymer solution and 'Add vial' contains 1.9 mL disodium beta-glycerophosphate solution. The floor nurse withdraws exactly 0.3 mL from the 'Add vial' and adds it (**c**) to the 'Mix vial' in a dropwise manner. This makes contents of 'Mix vial' as 1.5 mL. (**d**) This mixture is left untouched for 10 min in the warmer at physiological temperature. (**e**) Once the microfracture is completed, 5 mL of autologous blood is drawn from the patients' arm. (**f**) Using a dispensing pin 4.5 mL of autologous blood is injected into the 'Mix vial' (BST-CarGel:blood ratio of 1:3) and vigorously mixed for 10 s. (**g**) At this point the scrub nurse or the operating surgeon withdraws 4–5 mL of BST-CarGel/blood mixture from the 'Mix vial' taking sterile precautions which is delivered to the prepared defect in a dropwise manner

Figure 16.2.8: (continued)

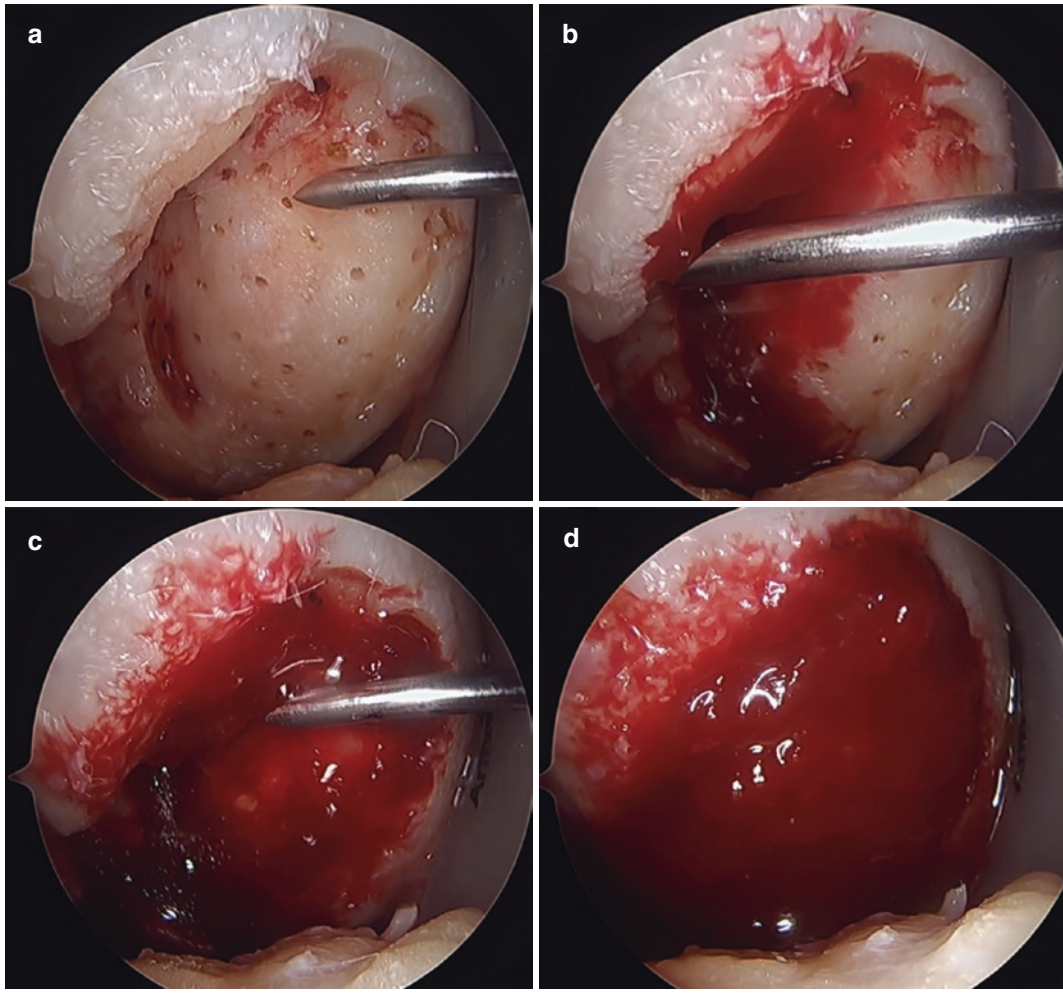

Figure 16.2.9: The Single-Stage Cartilage Repair Technique Using Chitosan-Based Bioscaffold: The Implantation of the BST-CarGel. A 33-year-old female, right knee, viewing from the anterolateral portal; a 23-gauge spinal needle was inserted into the joint from the anteromedial portal (**a**) and the prepared BST-CarGel was implanted to cover the entire defect (**b**, **c**). The knee was immobilised for 10–12 min to allow for the BST-CarGel mixture to clot (**d**). The portals were sutured and the knee was immobilised in extension with a brace for 24 h

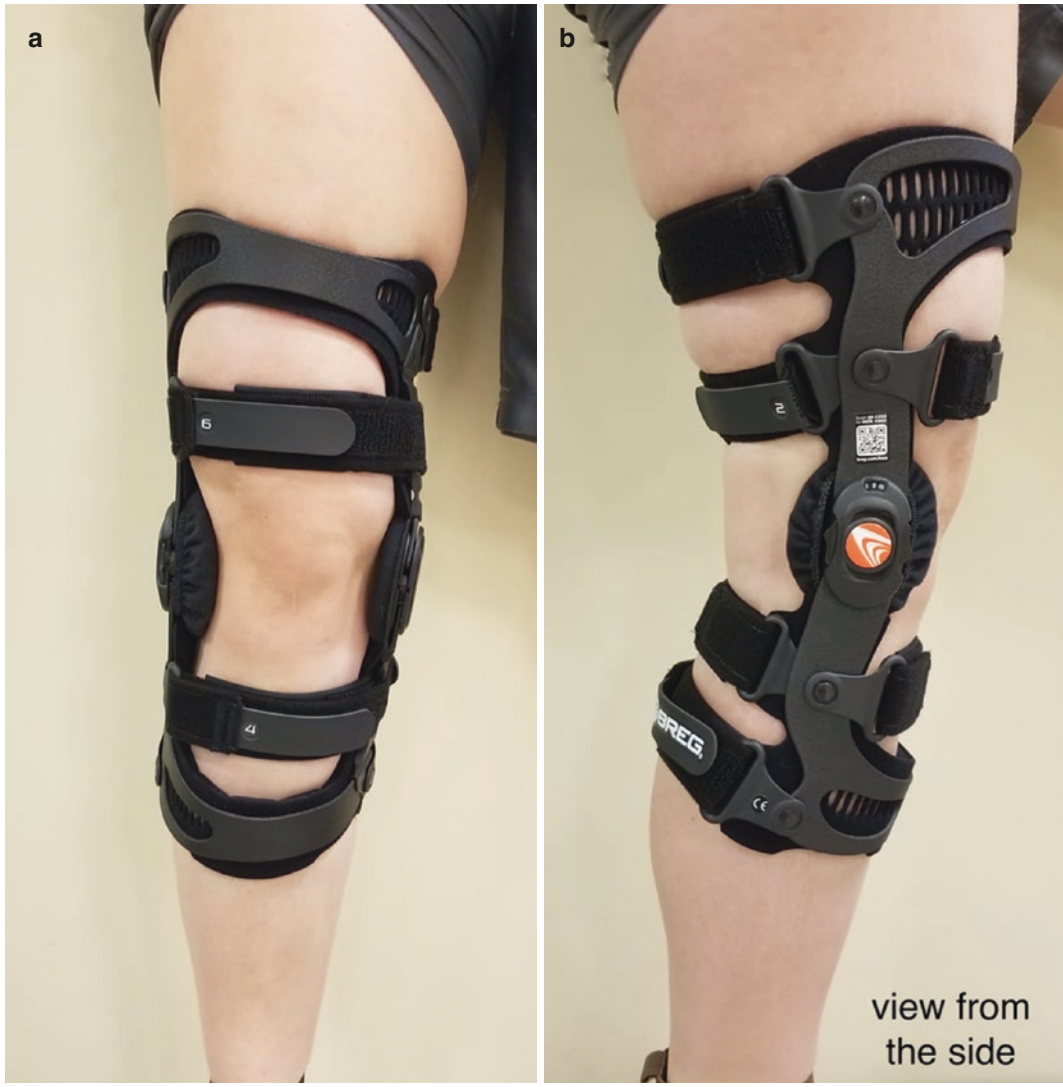

Figure 16.2.10: The Single-Stage Cartilage Repair Technique Using Chitosan-Based Bioscaffold: The Post-operative Rehabilitation Protocol and the Bracing. A hinged 'off-loader' knee brace is applied after the procedure, viewing from the front (**a**) and viewing from the side (**b**). The knee is immobilised in full extension for 24 h. Patient is allowed complete range of motion from the second post-operative day. This brace is replaced by a custom-made off-loader brace as soon as the swelling subsides. Patient is allowed 25% weight bearing for the initial 6 weeks, 50% from the seventh week and 75% from the eighth week and then allowed to go back to full weight bearing by the end of ninth week

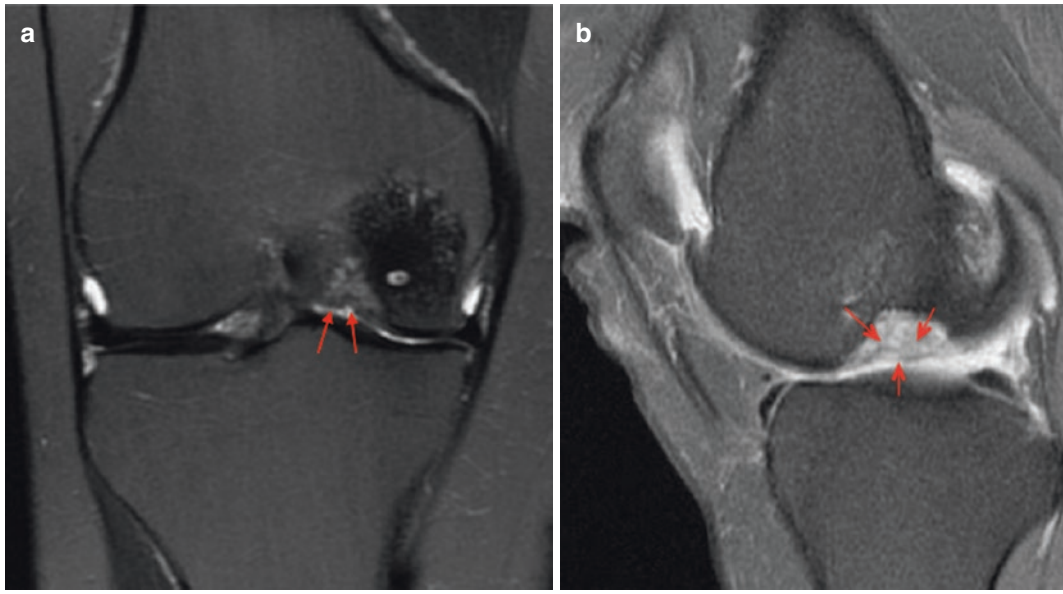

Figure 16.2.11: The Single-Stage Cartilage Repair Technique Using Chitosan-Based Bioscaffold: The Short-Term Results on MRI. A 15-month post-operative right-knee MRI of a 33-year-old female shows regeneration of the cartilage covering the initial defect. T2 COR FSE (**a**) and T2 SAT FSE (**b**) MRI images showing smooth congruous chondral surface. The osteochondral defect has filled in completely with no gap seen in the defect. Subchondroplasty seen adjacent to the filled defect (darker area)

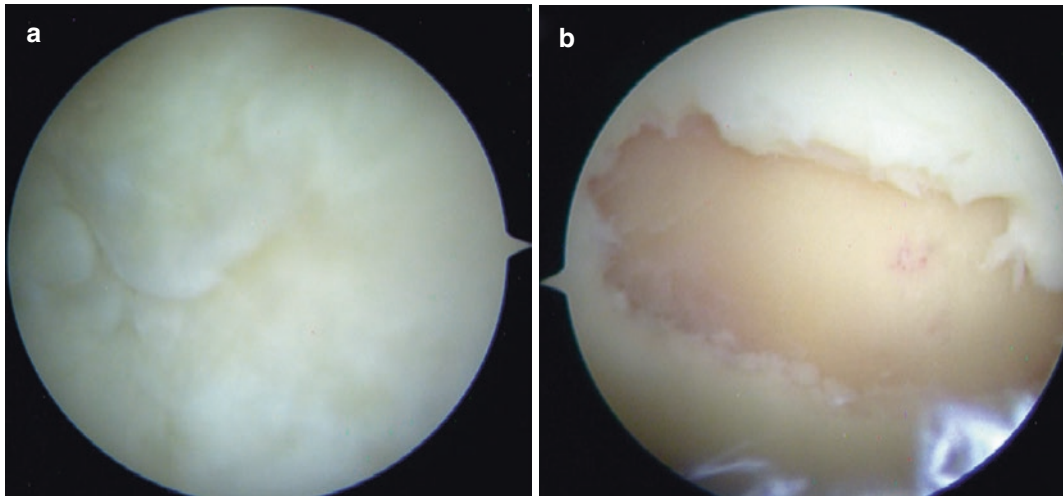

Figure 16.2.12: The Single-Stage Cartilage Repair Technique Using Chitosan-Based Bioscaffold: The Short-Term Results on Arthroscopy. A 36-year-old male with a history of chondral defect just below the trochlea of the left femoral condyle (**a**) was treated with BST-CarGel-based cartilage repair technique (case different from the case shown in Figures 16.2.1, 16.2.2, 16.2.3, 16.2.4, 16.2.5, 16.2.6, 16.2.7, 16.2.8, 16.2.9, 16.2.10, and 16.2.11). The defect after the initial preparation can be seen in (**b**). A second-look arthroscopy done 22 months after the index operation (**c**) shows excellent healing of almost the entire defect with the regenerated cartilage looking similar to the surrounding native cartilage

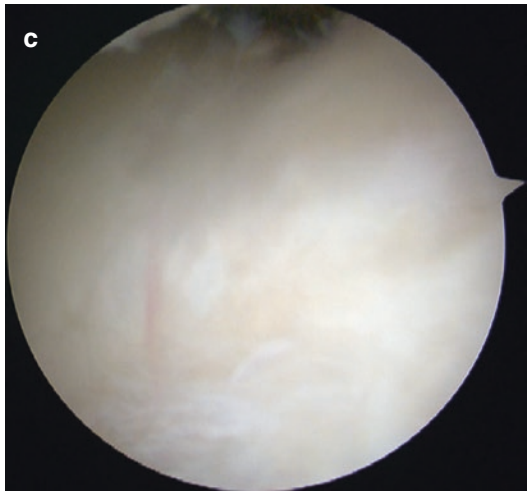

Figure 16.2.12: (continued)

16.3 Take-Home Message

Microfracture is currently considered as the standard first line of care for the treatment of the cartilage defects. Microfracture initiates a repair response that is similar to the natural wound-healing sequence. BST-CarGel when used in combination with bone marrow stimulation (e.g. microfracture) overcomes the major pitfall of the standard microfracture technique, namely the quantity of the initial blood clot present in the cartilage lesion to trigger the wound-healing cascade. The soluble and physiological characteristics of this chitosan polymer solution permit its combination with a freshly drawn autologous whole blood to form a hybrid polymer-blood mixture. This mixture when applied to the cartilage and bone surfaces of prepared lesions, regardless of their geometry and size, adheres and solidifies as a polymer-stabilised hybrid clot [11] maximising the clot available and tissue healing response. A randomised controlled trial involving 80 patients by Shive et al. showed that at 5 years, BST-CarGel treatment resulted in a sustained and a significantly superior repair tissue quantity and quality over the microfracture technique alone [17].

Although traditionally cartilage restorative options for osteochondritis have been limited, the mechanistic evidence from animal data has shown that BST-CarGel has a reproducible and positive effect on subchondral bone remodelling, suggesting that cartilage loss emanating from subchondral bone pathologies, such as osteochondritis dissecans or cysts, may be addressed through BST-CarGel treatment [12, 14, 19].

Proper visualisation and assessment of the lesion is a prerequisite for arthroscopic cartilage repair approach. Adequate care should be taken to prepare the lesion and the calcified layer should be removed to allow adequate adhesion of bone marrow cells. A stable rim of healthy surrounding cartilage should be respected with regard to the containment of the defect. The advantages of this less invasive approach include reduced morbidity and a faster recovery. Further Steinwachs et al. reported fewer postoperative complications and promising reductions in pain and swelling, when cartilage restoration was done with bone marrow stimulation and CarGel combined [20]. Nevertheless, the long-term outcome is still unknown, and these results need to be further confirmed by long-term clinical studies.

References

1. Curl WW, Krome J, Gordon ES, Rushing J, Smith BP, Poehling GG. Cartilage injuries: a review of 31,516 knee arthroscopies. Arthroscopy. 1997;13(4):456–60.
2. Bhosale AM, Richardson JB. Articular cartilage: structure, injuries and review of management. Br Med Bull. 2008;87(1):77–95.
3. Stanish WD, McCormack R, Forriol F, Mohtadi N, Pelet S, Desnoyers J, et al. Novel scaffold-based BST-CarGel treatment results in superior cartilage repair compared with microfracture in a randomized controlled trial. J Bone Joint Surg Am. 2013;95(18):1640–50.
4. Bedi A, Feeley BT, Williams RJ. Management of articular cartilage defects of the knee. J Bone Joint Surg Am. 2010;92(4):994–1009.
5. Cole BJ, Pascual-Garrido C, Grumet RC. Surgical management of articular cartilage defects in the knee. J Bone Joint Surg Am. 2009;91(7):1778–90.

6. Mithoefer K, McAdams T, Williams RJ, Kreuz PC, Mandelbaum BR. Clinical efficacy of the microfracture technique for articular cartilage repair in the knee. Am J Sports Med. 2009;37(10):2053–63.
7. Frisbie DD, Oxford JT, Southwood L, Trotter GW, Rodkey WG, Steadman JR, et al. Early events in cartilage repair after subchondral bone microfracture. Clin Orthop Relat Res. 2003;407:215–27.
8. Nehrer S, Spector M, Minas T. Histologic analysis of tissue after failed cartilage repair procedures. Clin Orthop Relat Res. 1999;365:149–62.
9. Goyal D, Keyhani S, Lee EH, Hui JHP. Evidence-based status of microfracture technique: a systematic review of level I and II studies. Arthroscopy. 2013;29(9):1579–88.
10. Fortier LA, Potter HG, Rickey EJ, Schnabel LV, Foo LF, Chong LR, et al. Concentrated bone marrow aspirate improves full-thickness cartilage repair compared with microfracture in the equine model. J Bone Joint Surg Am. 2010;92(10):1927–37.
11. Hoemann CD, Hurtig M, Rossomacha E, Sun J, Chevrier A, Shive MS, et al. Chitosan-glycerol phosphate/blood implants improve hyaline cartilage repair in ovine microfracture defects. J Bone Joint Surg Am. 2005;87(12):2671–86.
12. Shapiro F, Koide S, Glimcher MJ. Cell origin and differentiation in the repair of full-thickness defects of articular cartilage. J Bone Joint Surg Am. 1993;75(4):532–53.
13. Chevrier A, Hoemann CD, Sun J, Buschmann MD. Temporal and spatial modulation of chondrogenic foci in subchondral microdrill holes by chitosan-glycerol phosphate/blood implants. Osteoarthr Cartil. 2011;19(1):136–44.
14. Chevrier A, Hoemann CD, Sun J, Buschmann MD. Chitosan–glycerol phosphate/blood implants increase cell recruitment, transient vascularization and subchondral bone remodeling in drilled cartilage defects. Osteoarthr Cartil. 2007;15(3):316–27.
15. Chenite A, Chaput C, Wang D, Combes C, Buschmann MD, Hoemann CD, et al. Novel injectable neutral solutions of chitosan form biodegradable gels in situ. Biomaterials. 2000;21(21):2155–61.
16. Kumar MNVR, Muzzarelli RAA, Muzzarelli C, Sashiwa H, Domb AJ. Chitosan chemistry and pharmaceutical perspectives. Chem Rev. 2004;104(12):6017–84.
17. Shive MS, Stanish WD, McCormack R, Forriol F, Mohtadi N, Pelet S, et al. BST-CarGel® treatment maintains cartilage repair superiority over microfracture at 5 years in a multicenter randomized controlled trial. Cartilage. 2015;6(2):62–72.
18. Mestriner LA. Osteochondritis dissecans of the knee: diagnosis and treatment. Rev Bras Ortop. 2012;47(5):553–62.
19. Hoemann CD, Duval N, Restrepo A, Stanish W, Buschmann MD, Shive MS, et al. BST-CarGel: in situ chondroinduction for cartilage repair. Oper Tech Orthop. 2006;16(4):271–8.
20. Steinwachs M, Cavalcanti N, Mauuva Venkatesh Reddy S, Werner C, Tschopp D, Choudur HN. Arthroscopic and open treatment of cartilage lesions with BST-CARGEL scaffold and microfracture: a cohort study of consecutive patients. Knee. 2019;26(1):174–84.

17 The Illustrative Multilayer Scaffolds for the Single-Stage Cartilage Repair in the Osteochondral Lesions

Elizaveta Kon and Alessandra Nannini

17.1 Introduction

There is increasing awareness about the involvement of the subchondral bone in the majority of chondral lesions and this has resulted in the need to develop cell-free treatment strategies focused on the entire osteochondral unit. Heterogeneous scaffolds have been currently proposed that combine distinct but integrated layers, corresponding to the cartilage and the bone regions, to regenerate both the components of the osteochondral unit [1]. These "cell-free osteochondral scaffolds" have been developed with the aim to give specific regenerative signals to the mesenchymal cells coming from the bone marrow [2, 3]. An ideal graft would be an 'off-the-shelf' product from both the surgical and the commercial standpoint.

One of currently approved scaffolds with these characteristics is *MaioRegen*®, a nanostructured biomimetic scaffold (Fin-Ceramica SpA, Faenza, Italy). *MaioRegen* is available in three different configurations: (1) *MaioRegen Prime* for the treatment of osteochondral lesions with severely compromised subchondral bone (the one used in the clinical case described in this chapter), (2) *MaioRegen Slim* for the treatment of osteochondral lesions with slightly compromised subchondral bone and (3) *MaioRegen Chondro+* for the treatment of cartilage lesions. *MaioRegen Prime* mimics the whole osteochondral anatomy with its porous 3-dimensional tri-layer composite structure: the smooth superficial cartilaginous layer consisting of type I collagen, the intermediate tidemark-like layer consisting of a combined type I collagen (60%) and the hydroxyapatite (40%) and the lower layer consisting of a mineralised blend of type I collagen (30%) and hydroxyapatite (70%) reproducing the subchondral bone (Figures 17.2.4 and 17.2.5). This scaffold was introduced into the clinical practice because a cell-free approach after animal studies showed good results in terms of both the cartilage and the bone tissue formation [4]. It provided similar macroscopic, histological and radiographic results when implanting a scaffold loaded with autologous chondrocytes or scaffold alone, probably inducing an in situ regeneration through stem cells coming from the surrounding bone marrow. Clinical studies further showed that the implantation of this biomimetic scaffold to treat chondral and osteochondral knee defects proved to be effective in terms of clinical outcome at a short and long follow-up time in a large patient population, even though altered findings have been detected at MRI [5]. MaioRegen is mainly used in the knee. A study by Kaipel et al. showed conflicting results of this scaffold in osteochondral

E. Kon (✉) · A. Nannini
Department of Biomedical Sciences, Humanitas University, Milan, Italy

Humanitas Clinical and Research Center- IRCCS, Milan, Italy
e-mail: elizaveta.kon@humanitas.it; alessandra.nann@gmail.com

D. R. Goyal (ed.), *The Illustrative Book of Cartilage Repair*,
https://doi.org/10.1007/978-3-030-47154-5_17

lesions of the talus. In their study, MaioRegen provided substantial clinical improvement; however, there was a strong evidence that the quality of the superficial repair tissue was limited and osteoconduction as well as subchondral ossification was unfavourable [6].

MaioRegen is indicated in cases where it is necessary to restore osteochondral lesions of traumatic, post-traumatic, degenerative origin or due to osteochondritis dissecans, with grade III–IV lesions (*Outerbridge* classification), and with focal, single or multiple lesions. *MaioRegen* should not be used in patients with advanced osteoarthritic conditions, immune system disorders, neoplastic diseases, infectious diseases or obesity (BMI >30) or who are above 60 years of the age.

17.2 The Illustrations

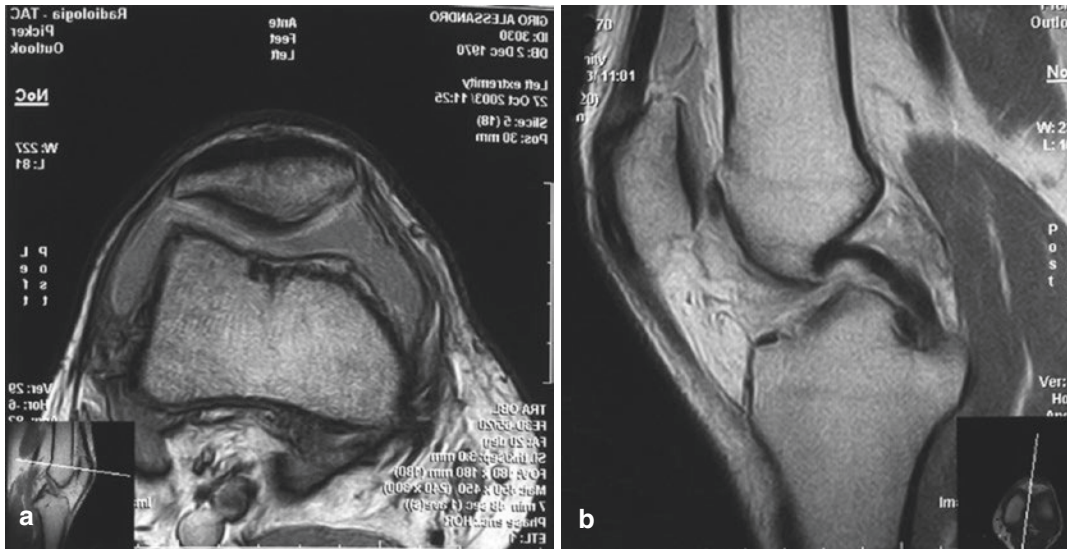

Figure 17.2.1: The Biomimetic Scaffold Technique for the Single-Stage Cartilage Repair: The Ideal Case Selection. A 36-year-old male patient presented with a degenerative lesion of the trochlea with the duration of 8 months. His BMI was 23 and he had an active lifestyle. His basal IKDC subjective score was 54.0 and KUJALA score was 53. The MRI image (sagittal (**b**) and patellar axial (**a**) T1 sequence) showed an ICRS grade IV (severely abnormal, through the subchondral bone) single osteochondral lesion with the compromised bone. Patellofemoral biomechanics were normal, but the patient was feeling severe pain, mainly going down the stairs, and was experiencing limitations in the sport practice

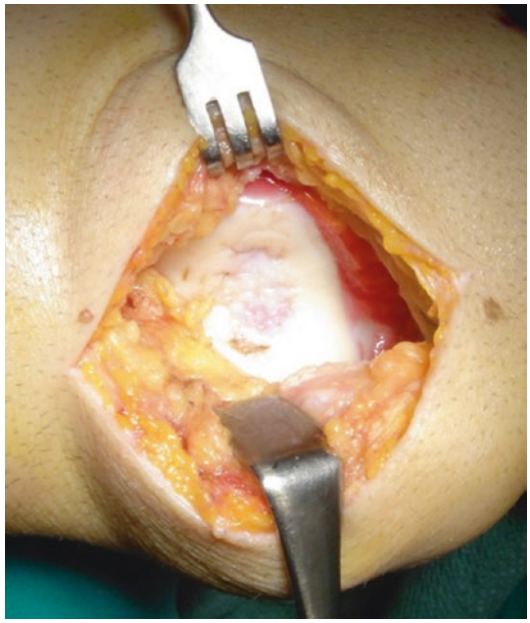

Figure 17.2.2: The Biomimetic Scaffold Technique for the Single-Stage Cartilage Repair: The Peroperative Assessment of the Lesion. A 36-year-old man with an active lifestyle had ICRS grade IV lesion of the trochlea with the moderate involvement of the subchondral bone which was sclerosed. *MaioRegen* is indicated for osteochondral lesions with the moderate-to-severe bone involvement because of its 3-D tri-layer composite structure, mimicking the whole osteochondral anatomy, and because of its thickness of 7 mm

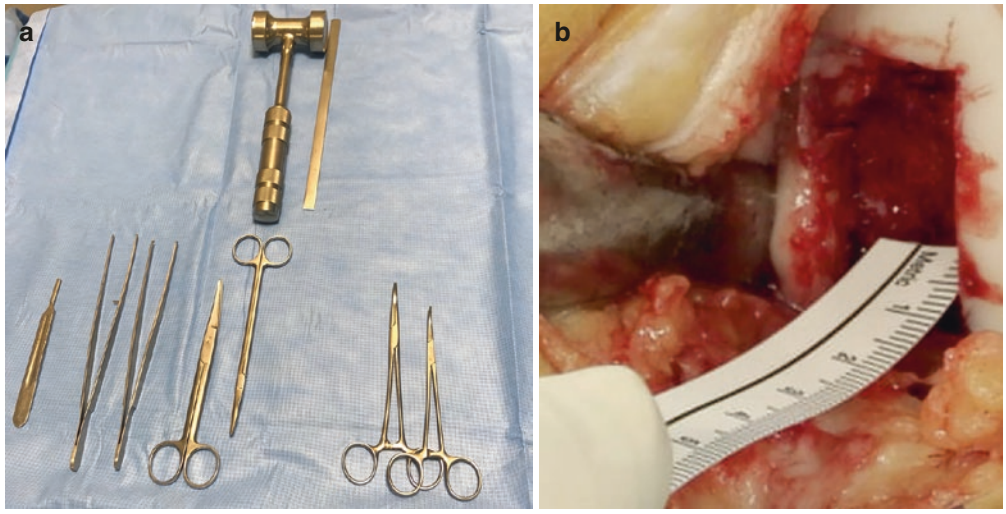

Figure 17.2.3: The Biomimetic Scaffold Technique for the Single-Stage Cartilage Repair: The Instruments Required. There is not a specific toolset for the implantation of *MaioRegen*. (**a**) Standard instruments necessary to perform a medial parapatellar minimal invasive arthrotomy to expose the lesions are required. The sclerotic subchondral bone is removed using an osteotome and (**b**) the defect depth is checked using a ruler. A scalpel is used to cut the smooth cartilage-like layer of the scaffold and surgical scissors are used to cut the deeper layer(s). As implantation is press fit, no specific tool is necessary. A syringe of fibrin glue is used to enhance the stability

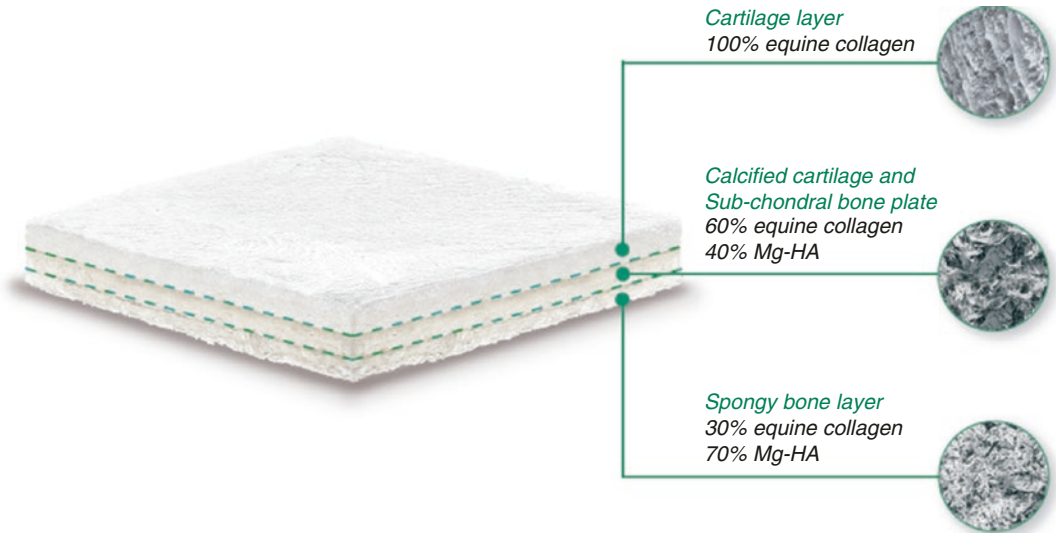

Figure 17.2.4: The Biomimetic Scaffold Technique for the Single-Stage Cartilage Repair: The Morphological Properties. The osteochondral nanostructured biomimetic scaffold (Fin-Ceramica SpA, Faenza, Italy) has a porous 3-D tri-layer composite structure, mimicking the whole osteochondral anatomy. The cartilaginous layer, consisting of type I collagen, has a smooth surface to favour the joint flow (1). The intermediate layer (tidemark-like) (2) consists of a combination of type I collagen (60%) and hydroxyapatite (40%), whereas the lower layer consists of a mineralised blend of type I collagen (30%) and hydroxyapatite (70%) reproducing the subchondral bone layer (3). Each layer is separately synthesised by a standardised process starting from an atelocollagen aqueous solution (1% w/w) in acetic acid, isolated from the equine tendon (picture courtesy—Fin-Ceramica SpA, Faenza, Italy)

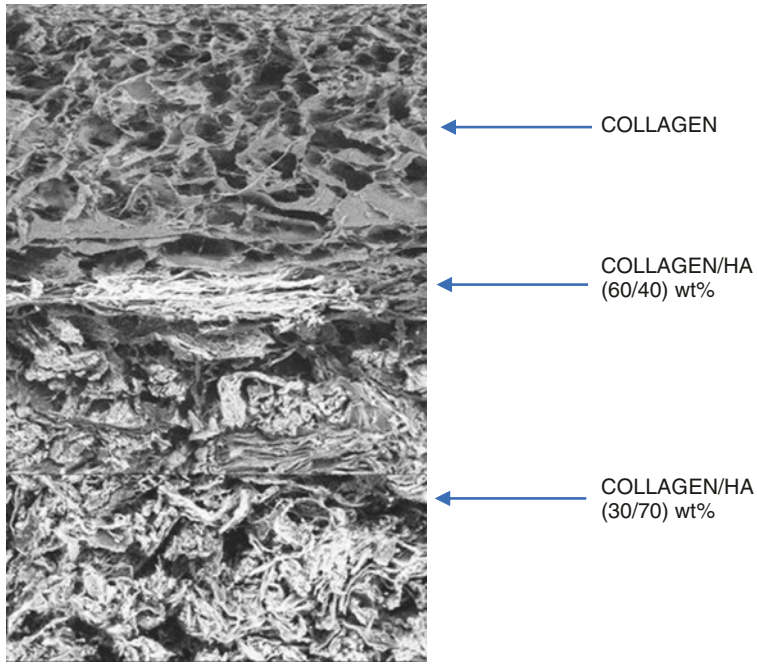

Figure 17.2.5: The Biomimetic Scaffold Technique for the Single-Stage Cartilage Repair: The Histological Properties. The deeper mineral phase is made of magnesium–hydroxyapatite (Mg–HA), nucleated onto collagen fibres in proportion of 70 and 30%. The intermediate tidemark-like layer consists of a combination of type I collagen (60% of weight) and Mg–HA (40% of weight), whereas the superficial cartilage-like layer is entirely made of type I collagen, with a smooth surface. The upper non-mineralised chondral layer is of type I collagen (Opocrin S.p.A., Modena, Italy); the intermediate and the lower layers are obtained by nucleating bone-like nanostructured non-stoichiometric hydroxyapatite into self-assembling collagen fibres, as occurs in the biological neo-ossification process. The final construct is obtained by physically combining the layers on top of a mylar sheet and finally freeze-dried and gamma-sterilised at 25 KGray (picture courtesy—Fin-Ceramica SpA, Faenza, Italy)

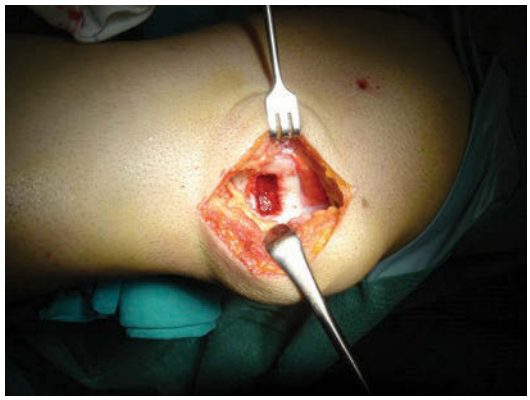

Figure 17.2.6: The Biomimetic Scaffold Technique for the Single-Stage Cartilage Repair: Preparation of the Walls and the Base of the Lesion. A 36-year-old male with localised trochlear lesion, exposed through minimally invasive medial parapatellar arthrotomy. The damaged osteochondral tissues are removed, and a squared, regular-shaped lodging is created using an osteotome that is 8 mm deep. A surgical ruler is used to be sure about the depth and about making the base as flat and regular. The lodging size (3.4 cm^2) is finally measured

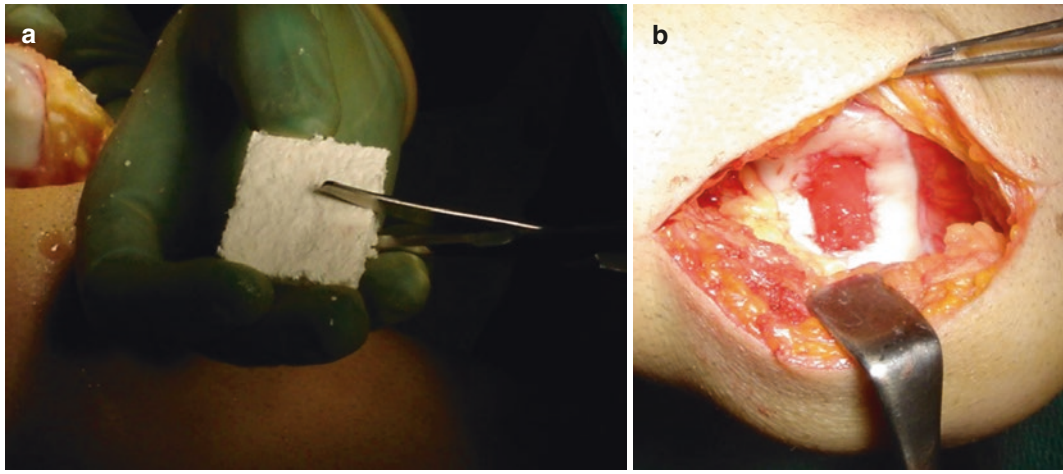

Figure 17.2.7: The Biomimetic Scaffold Technique for the Single-Stage Cartilage Repair: Implantation of the Scaffold into the Defect. (**a**) The scaffold is prepared according to the site dimension. The smooth cartilage-like layer of the scaffold is cut using a scalpel and deeper layer(s) are cut using the surgical scissors (Figure 17.2.3). (**b**) The scaffold is inserted into the trochlear defect of a 36-year-old male patient by a gentle press fit, making sure that the bottom layer gets in contact with the bone floor. Fibrin glue is applied on the upper perimeter to ensure adequate mechanical stability. The scaffold perfectly adapts to the anatomical conformation of the lesion and is able to auto-stabilise in situ. The scaffold should not be bigger than the lesion site; otherwise the stability would be poor, and the risk of scaffold dislodgement would be high

Figure 17.2.8: The Biomimetic Scaffold Technique for the Single-Stage Cartilage Repair: The Final Check. Three flexion/extension cycles are performed in order to verify the stability of the scaffold after 5 min of implantation of the scaffold. The implanted scaffold is again inspected for the adherence and the stability before the closure

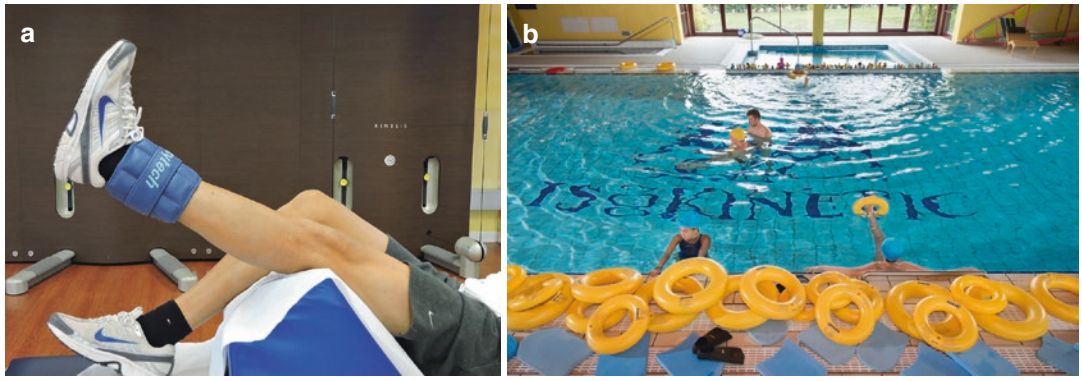

Figure 17.2.9: The Biomimetic Scaffold Technique for the Single-Stage Cartilage Repair: The Rehabilitation and Bracing. Early rehabilitation protocol is advocated. Knee joint is mobilised early in order to help the resolution of swelling, and to favour joint nutrition and healing. At the same time, patient is encouraged to perform early isometric and isotonic exercises, and controlled mechanical compressions. Voluntary muscular contraction and electrical neuromuscular stimulation (NMES) are started at the time of discharge. No weight bearing is allowed, and crutches are maintained for 3–4 weeks. After that, patient is allowed to progressively reach the full weight bearing. Exercises in the swimming pool are suggested after third week (picture courtesy—Bologna Isokinetic Srl)

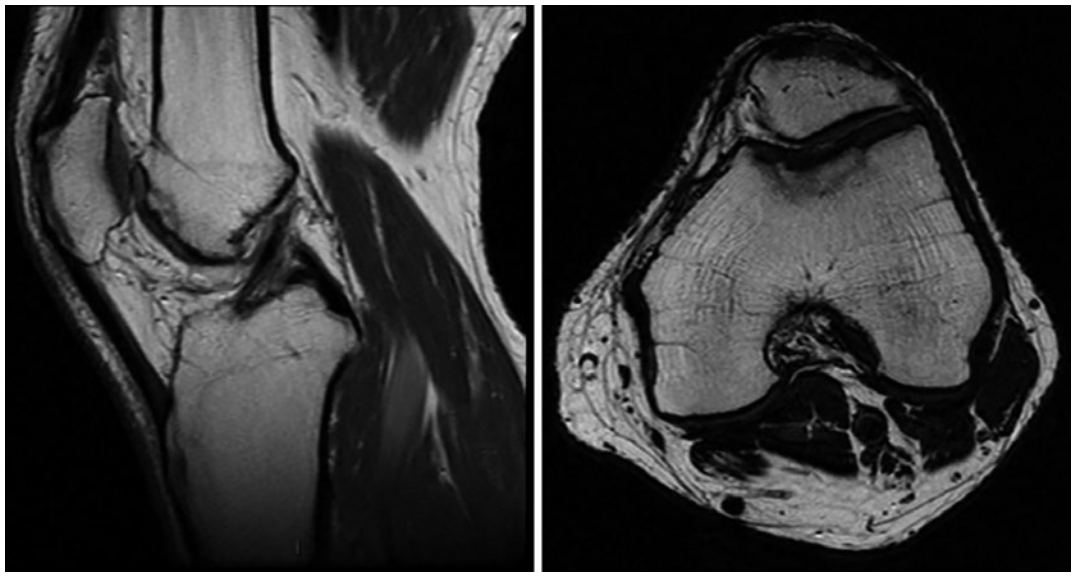

Figure 17.2.10: The Biomimetic Scaffold Technique for the Single-Stage Cartilage Repair: The Mid-Term Results on MRI at 24 Months. Male patient operated with biomimetic scaffold at the age of 36 years for the ICRS grade IV cartilage defect at trochlea, presented with mid-term follow-up at 2 years. His IKDC subjective score had improved from 54.0 to 93.0 and Kujala score had improved from 53 to 100. MRI scan was performed and analysed (sagittal and axial T1 sequence) with MOCART scoring system. MOCART system revealed filling of the defect (complete 70%), cartilage integration (complete 70%) and tissue structure (homogenous 48%). The follow-up MRI study revealed overall judgement of the results at 2 years as marked improvement

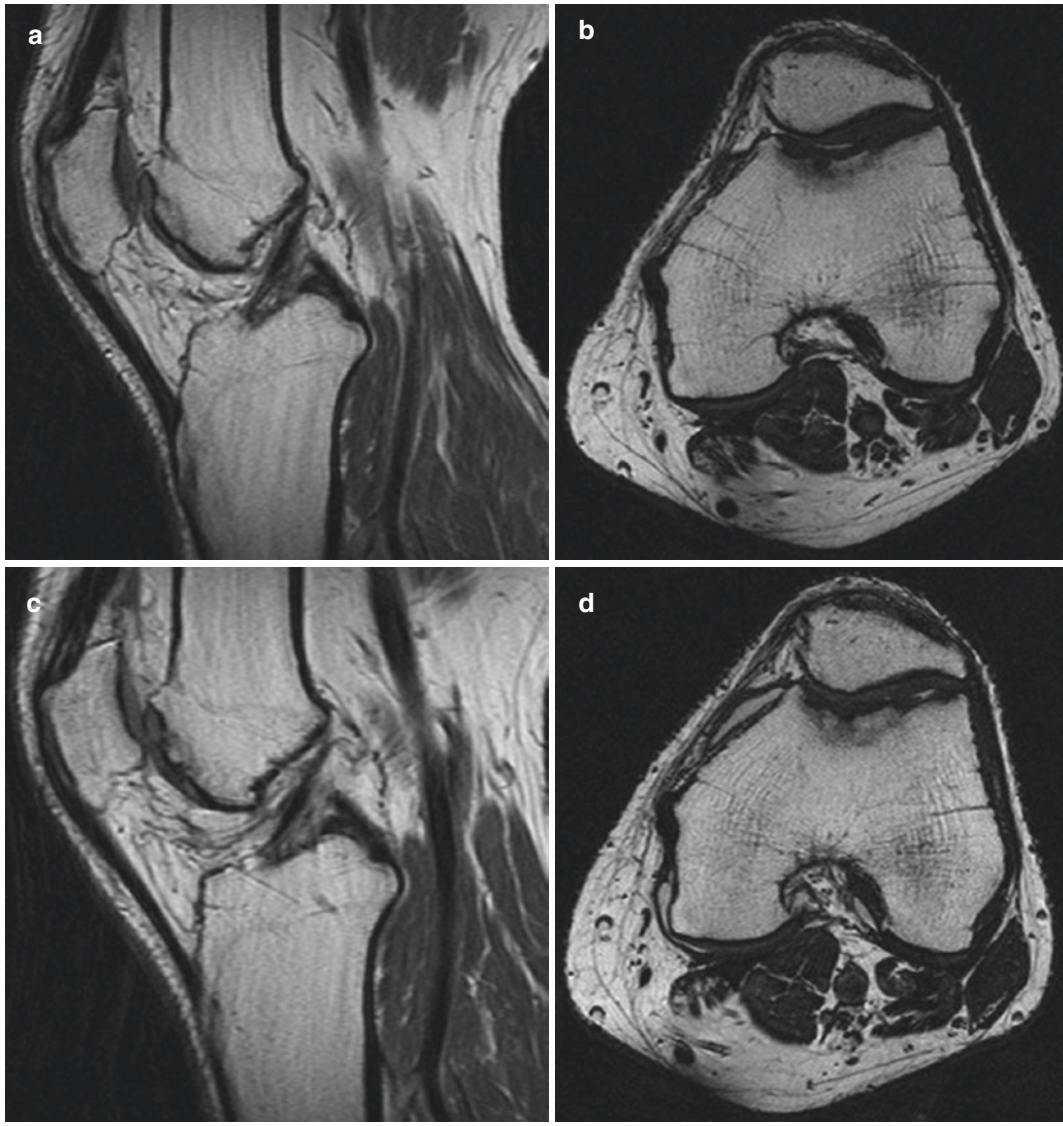

Figure 17.2.11: The Biomimetic Scaffold Technique for the Single-Stage Cartilage Repair: The Long-Term Results on MRI at 48 and 60 Months of Follow-Up. Male patient operated with biomimetic scaffold at the age of 36 years for the ICRS grade IV cartilage defect at trochlea, presented with long-term follow-up at 48 months (**a**, **b**) and 60 months (**c**, **d**). His IKDC subjective score had improved from 54.0 to 92.0 at 48 months and remained 92.0 at 60 months. MRI scan was performed and analysed (sagittal and axial T1 sequence) with MOCART scoring system. MOCART system revealed filling of the defect (complete 87% at 48 and 60 months), cartilage integration (complete 65% at 48 months and 67% at 60 months) and tissue structure (homogenous 52% at 48 and 60 months). The follow-up MRI study revealed overall judgement of the results at 4 years and at 5 years as marked improvement. Subsequent MRI from 24-month follow-up till 60-month follow-up documents a slow but steady progression over time and persistent abnormalities that do not correlate with the good clinical scores

17.3 Take-Home Message

The innovations in the field of biomaterials are providing the clinicians with new fascinating options to treat articular lesions. In our prospective study published in 2014 [5], we enrolled 82 patients complaining of clinical symptoms, such as knee pain and swelling, in association with grade III–IV chondral and osteochondral lesion or osteochondritis dissecans. Seventy-nine of them were evaluated at 12 and 24 months, and recently 24 of them were re-evaluated at 10-year follow-up. At 24 months, IKDC subjective score statistically significantly increased (76.2 ± 19.6) when compared to baseline evaluation (47.4 ± 17.1), and similarly did the IKDC objective score, changing from 72.1% at baseline to 88.6% at 12-month follow-up, and further improving at 24 months ($P = 0.012$). The improvement reached at 24 months and remained stable over time up to 10 years ($P < 0.0005$). This improvement has slowly been seen also with MRI, even though the presence of persistent abnormalities did not correlate with the clinical picture. The implantation of this biomimetic scaffold to treat chondral and osteochondral knee defects proved to be effective in terms of clinical outcome at a short-, medium- and long-term follow-up time in a large patient population, even though altered findings have been detected at MRI.

References

1. Kon E, Robinson D, Verdonk P, Drobnic M, Patrascu J, Dulic O. A novel aragonite-based scaffold for osteochondral regeneration: early experience on human implants and technical developments. Injury. 2016;47(Suppl 6):S27–32.
2. Wang X, Grogan SP, Rieser F, Winkelmann V, Maquet V, La Berge M. Tissue engineering of biphasic cartilage constructs using various biodegradable scaffolds: an in vitro study. Biomaterials. 2004;25:3681–8.
3. Woodfield TB, Malda J, de Wijn J, Péters F, Riesle J, van Blitterswijk CA. Design of porous scaffolds for cartilage tissue engineering using a three-dimensional fiber-deposition technique. Biomaterials. 2004;25:4149–61.
4. Filardo G, Kon E, Roffi A, Di Martino A, Marcacci M. Scaffold-based repair for cartilage healing: a systematic review and technical note. Arthroscopy. 2013;29(1):174–86.
5. Kon E, Filardo G, Perdisa F, Di Martino A, Busacca M, Balboni F, Sessa A, Marcacci M. A one-step treatment for chondral and osteochondral knee defects: clinical results of a biomimetic scaffold implantation at 2 years of follow-up. J Mater Sci Mater Med. 2014;25(10):2437–44.
6. Kaipel M, Schreiner M, Kellner R, Klikovits J, Apprich S, Brix M, Boszotta H, Domayer S, Trattnig S. Beneficial clinical effects but limited tissue quality following osteochondral repair with a cell-free multilayered nano-composite scaffold in the talus. Foot Ankle Surg. 2017;23(4):302–6.

18 The Illustrative Bone Marrow Aspirate Concentrate and Hyaluronan-Based Scaffold Technique for Single-Stage Cartilage Repair

Alberto Gobbi, Ignacio Dallo, Katarzyna Herman, and Eleonora Irlandini

18.1 Introduction

The limited intrinsic healing potential of the articular cartilage is attributed to the presence of specialized cells which have low mitotic activity and lack of blood supply to promote tissue repair. Therefore, once injury occurs, surgical intervention is necessary to maximize the chances of articular cartilage repair. A good cartilage repair will lead to good functional outcome and will avoid subsequent cartilage degeneration that could otherwise lead to the development of osteoarthritis (OA) [1].

Several surgical techniques for the regeneration of the articular cartilage have been proposed. Among them, two-step procedures like autologous chondrocyte implantation (ACI) have been shown to provide good results, promoting formation of new hyaline-like cartilage tissue [2–4], while other techniques, such as microfracture, result in fibrous cartilage and less durable repair [5]. Single-stage cell-based procedures are an attractive treatment option, given the potential for cost savings and avoiding a second-stage procedure.

Multipotent mesenchymal stem cells sourced from bone marrow aspirate concentrate (BMAC) in combination with a biologic scaffold have demonstrated good to excellent clinical outcomes at long-term follow-up as with ACI [6–8]. In this chapter, we describe and illustrate the bone marrow aspirate concentrate and hyaluronan-based scaffold technique for single-stage repair in the patellofemoral compartment. This can be used to treat chondral knee injuries in a wide range of patient age and lesion sizes and in all the knee compartments.

A. Gobbi (✉) · I. Dallo · K. Herman · E. Irlandini
Orthopaedic Arthroscopic Surgery International (O.A.S.I.) Bioresearch Foundation, Gobbi N.P.O., Milan, Italy
e-mail: gobbi@cartilagedoctor.it; ignaciodallo@hotmail.com; kkapturkiewicz@gmail.com; e.irlandini@oasiortopedia.it

D. R. Goyal (ed.), *The Illustrative Book of Cartilage Repair*,
https://doi.org/10.1007/978-3-030-47154-5_18

18.2 The Illustrations

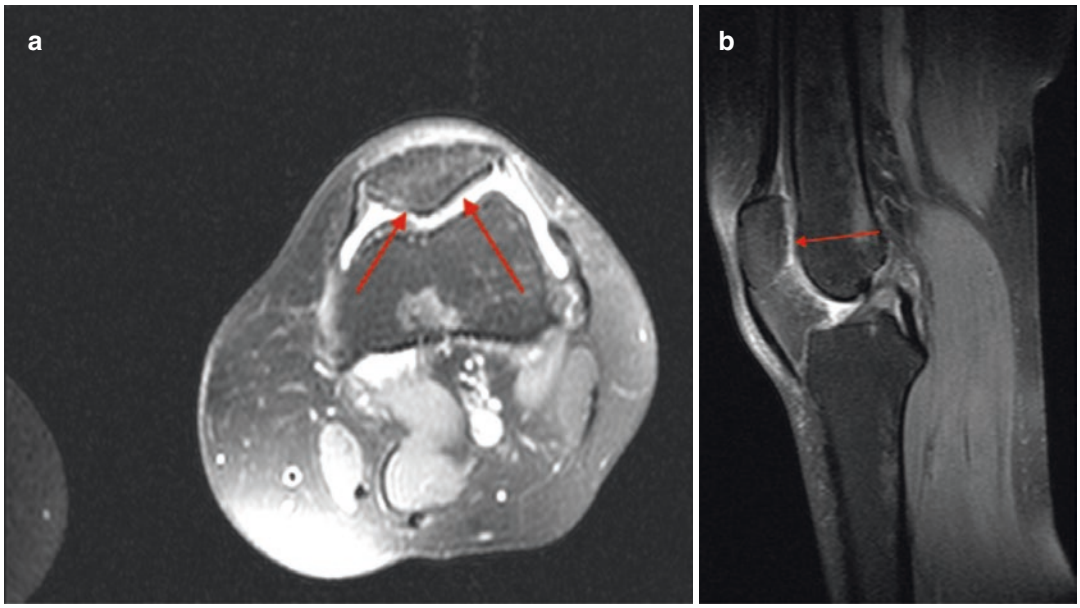

Figure 18.2.1: The Combined BMAC and Hyaluronan Scaffold Procedure: The Ideal Case Selection. A 57-year-old female amateur swimmer complained of chronic pain in the patellofemoral region of the left knee for more than a year. She had discomfort while descending stairs and performing daily activities. Clinical examination revealed mild effusion of the left knee, with painful range of movement from 40° to 80° without any signs of instability or mal-tracking of the patella. Further, there were also no signs of anteroposterior instability or malalignment of the knee. (**a**) Her magnetic resonance imaging (MRI) (T2 sequence axial section) showed a full-thickness (ICRS grade 3c) chondral defect over the lateral patella facet and a partial-thickness chondral defect (ICRS grade 3a) on the medial patellar facet. (**b**) T2-weighted sagittal section showed signal changes in the articular cartilage at the mid-level of the medial patellar facet

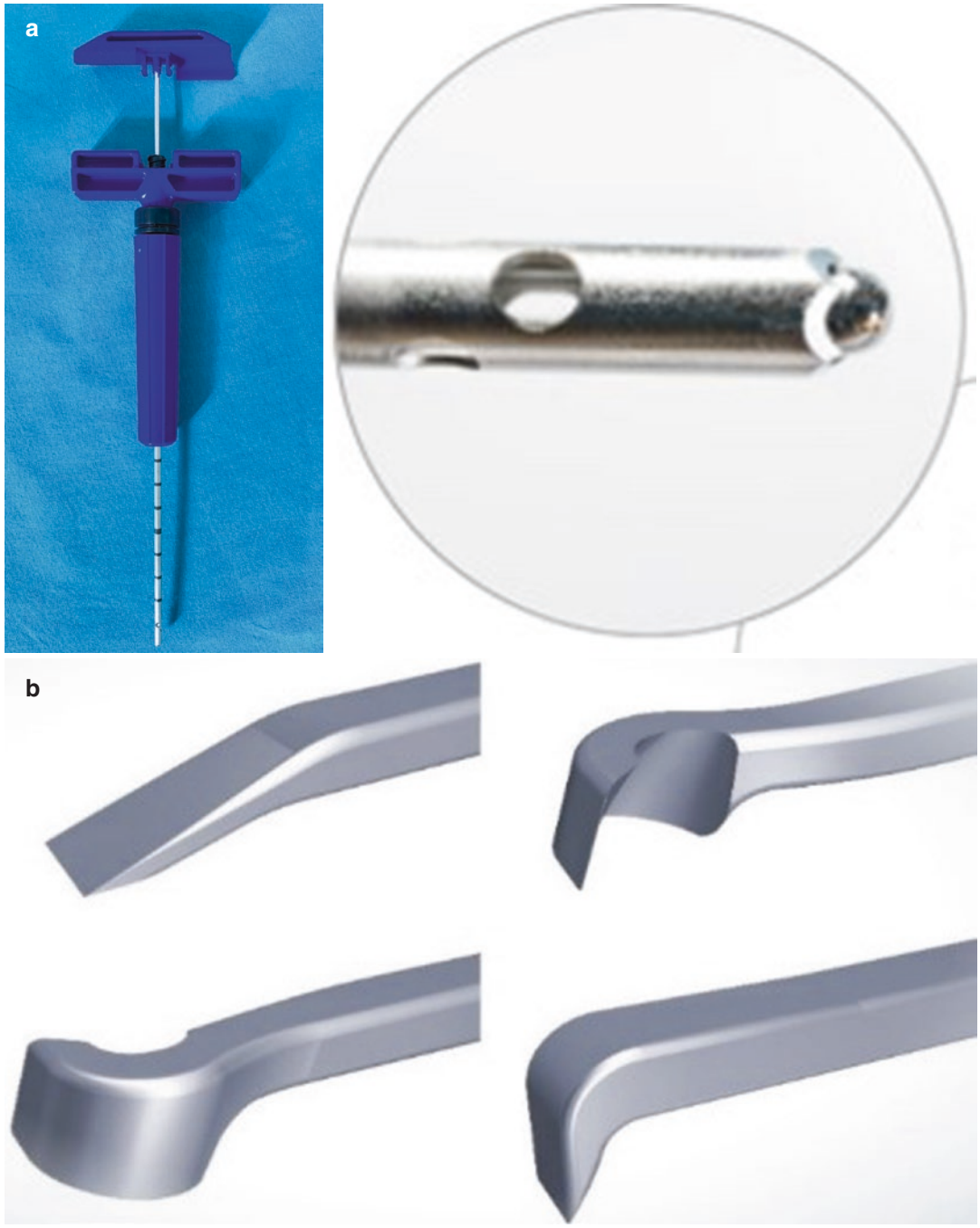

Figure 18.2.2: The Combined BMAC and Hyaluronan Scaffold Procedure: Instruments Required. (**a**) Bone marrow aspirate trocar (Aspire Medical Innovation GmbH, Germany) with depth guide and lateral fenestrations (see subset) for multilevel aspiration. (**b**) Chondrectome set (ATMED-Z. Rafalski, Katowice, Poland). These special curettes are used in the preparation of the chondral defect. (**c**) Hyaluronic based scaffold (Hyalofast, Anika Therapeutics, Italy) is a 3-dimensional biologic scaffold that helps to homogenously hold the mesenchymal stem cells from the bone marrow aspirate concentrate

Figure 18.2.2: (continued)

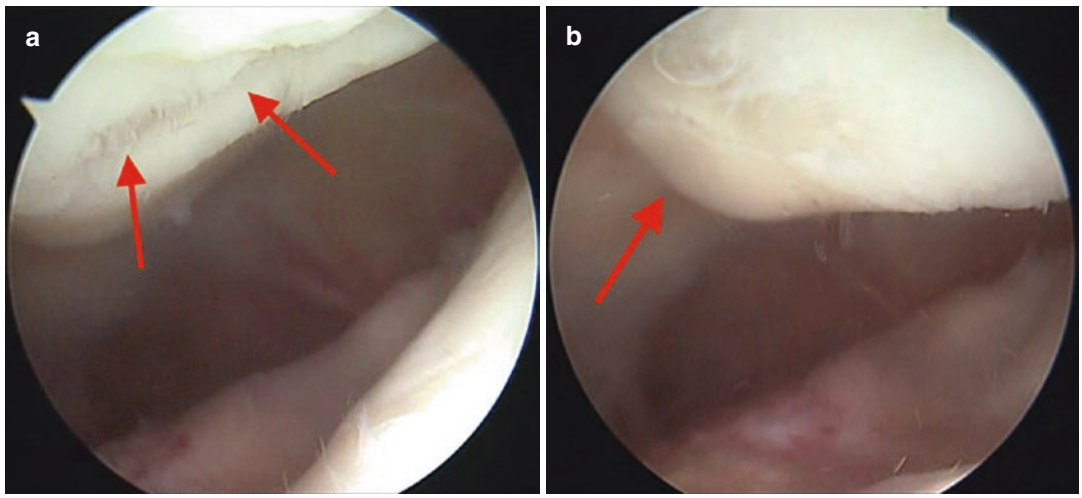

Figure 18.2.3: The Combined BMAC and Hyaluronan Scaffold Procedure: Assessment of the Lesion Selected for the Procedure. Left-knee arthroscopy, viewing from anterolateral portal, of a 57-year-old female revealed (**a**) a full-thickness chondral defect over the lateral patella facet that was approximately 2 × 1 cm in size and (**b**) a chondral flap over the medial patella facet that was approximately 2 cm in size. Cartilage repair using BMAC with HA scaffold was preferred, since the overall lesion size was more than 2 cm^2 without any subchondral involvement. BMAC is reported [2] to give good to excellent outcomes in large patellofemoral defects without "burning bridges" as with the microfracture technique. BMAC is also a single-step procedure causing lesser morbidity. A further surgical decision regarding an open or arthroscopic approach must be decided at this point, based on the size and the location of the defect. The combined BMAC and HA scaffold procedure can be performed arthroscopically, provided that the entire extent of the defect is reachable by the instruments; if not, as in this case, the procedure must be converted to a mini-open technique [9]

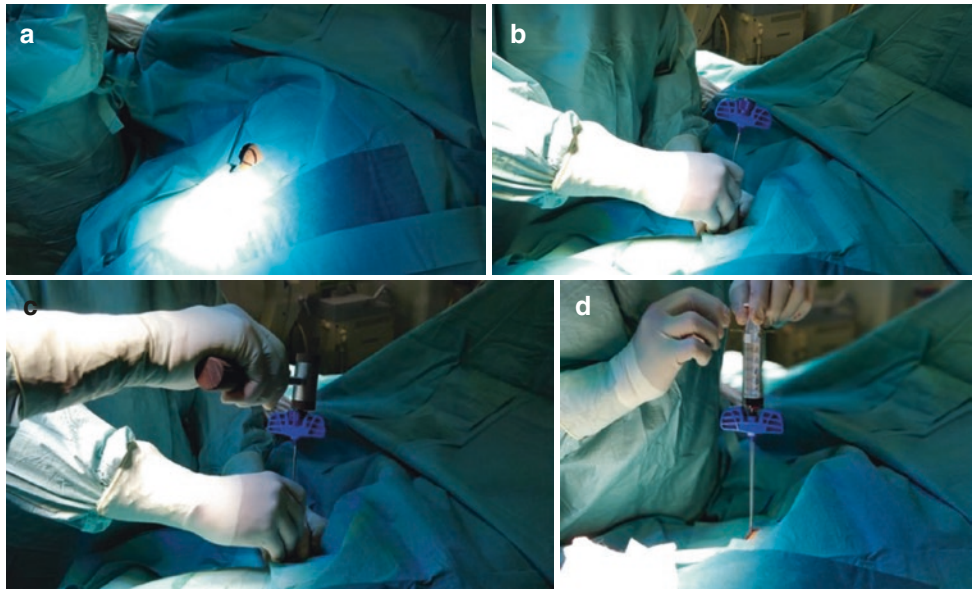

Figure 18.2.4: The Combined BMAC and Hyaluronan Scaffold Procedure: Harvesting of the Bone Marrow Concentrate. The aspiration of the bone marrow is done before the main surgical procedure in order to prepare the concentrate in the meantime. The patient is placed supine and (**a**) the anterior ipsilateral (left) iliac crest is prepared for the aspiration. (**b**) A small incision (about 1 cm) is made and the trocar is placed directly on the iliac crest. (**c**) The trocar is then advanced into the bone about 5–8 cm deep based on the patient morphology with a hammer. (**d**) Around 60 mL of the bone marrow is aspirated with a syringe (quantity of bone marrow required is assessed based on the concentration system and the defect size). It is important to change the direction of the needle for every 5 mL of aspiration in order to collect bone marrow from different zones of the iliac crest

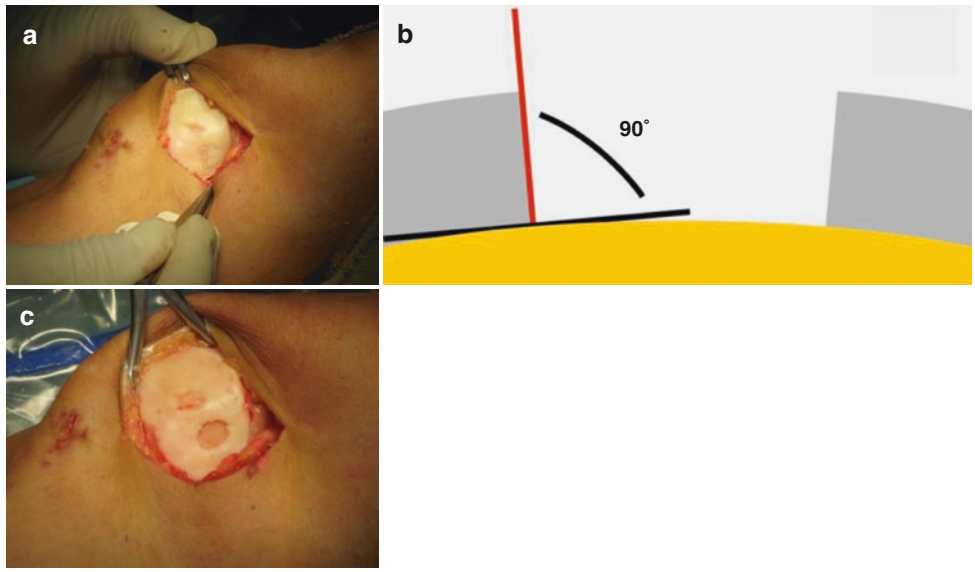

Figure 18.2.5: The Combined BMAC and Hyaluronan Scaffold Procedure: Preparation of the Lesion. The mini-lateral arthrotomy was done in a female aged 57 years to expose the bi-facetal patellar chondral lesions, after the arthroscopy procedure. (**a**) The lesion was exposed for the preparation and the subsequent implantation. (**b**) Chondral defect was prepared to obtain perpendicular edges using the special curettes called chondrectomes (ATMED, Poland). (**c**) Care must be taken to prepare the circumferential border of the lesion which needs to be perpendicular to the subchondral bone

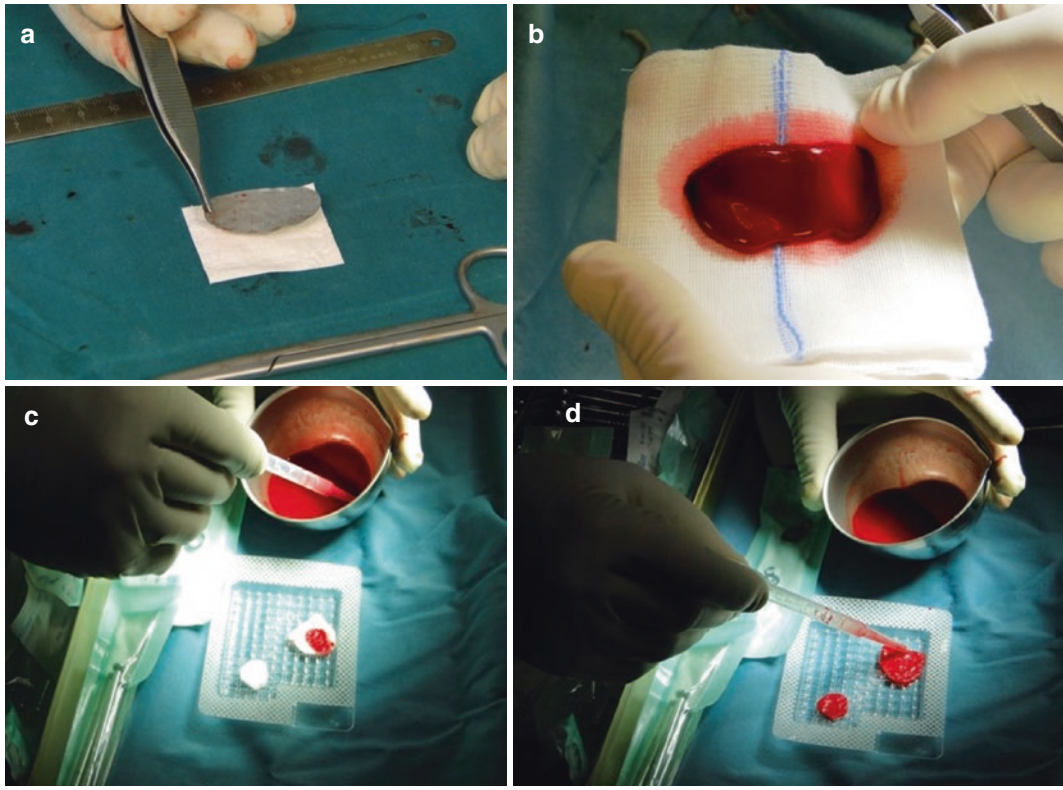

Figure 18.2.6: The Combined BMAC and Hyaluronan Scaffold Procedure: Preparations of the BMAC Graft Before Implantation. After debridement and thorough preparation, the lesion size is measured. (**a**) The lesion is templated on an aluminum foil, which is then used to size match the hyaluronic acid-based scaffold. (**b**) The concentrate of bone marrow was activated with batroxobin enzyme (Plateltex Act, Plateltex SRO, Bratislava, Slovakia) to form a sticky clot. (**c**) The prepared concentrate was then placed on the hyalofast scaffold. (**d**) After a few minutes the activated BMAC was absorbed by the scaffold, creating a sticky implant that is easy to apply onto the lesion

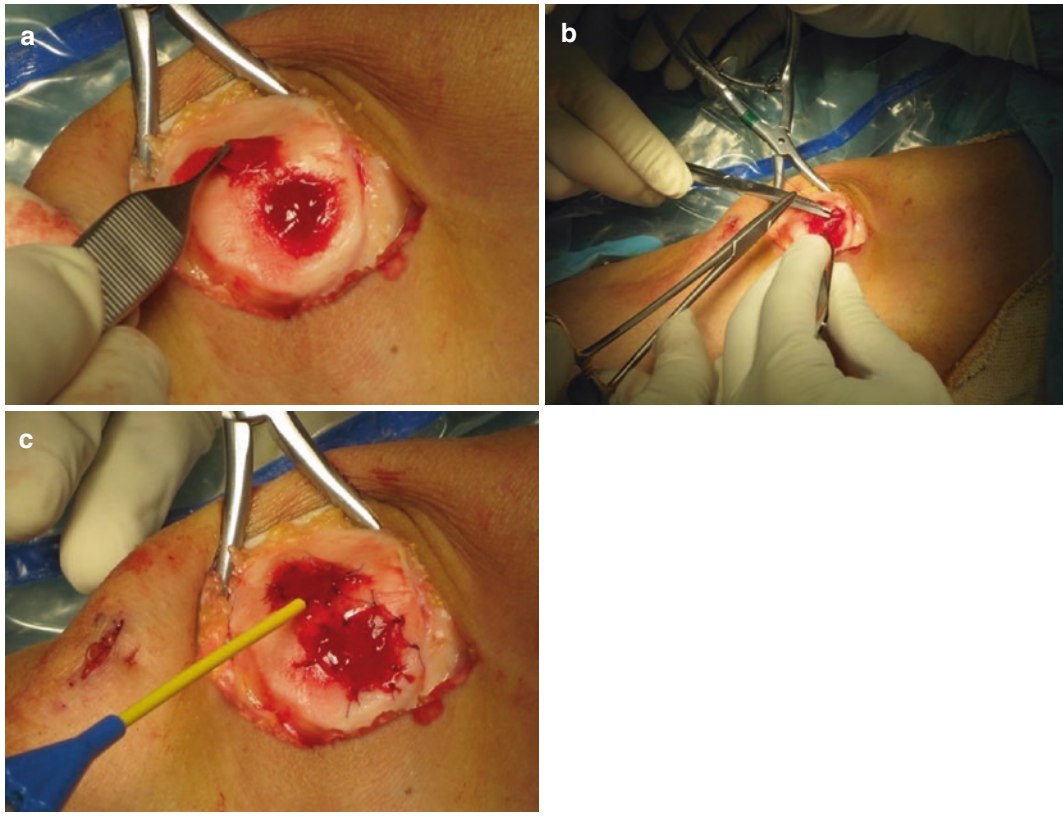

Figure 18.2.7: The Combined BMAC and Hyaluronan Scaffold Procedure: The Graft Implantation. The left-sided patellar bi-facetal chondral lesion was prepared for implantation with bone marrow aspiration concentrate (BMAC)-impregnated hyaluronic acid (HA) scaffold in a female aged 57 years. (**a**) The HA-BMAC (see HA-BMAC preparation in Figure 18.2.6) scaffold was placed into both the lesions. (**b**) Stay stitches were applied using 6-0 absorbable polydioxanone sutures (PDS II, Ethicon Inc.) to anchor the graft. However, in the recent years it has been observed that if the graft is well stabilized, then suturing the implant becomes unnecessary. (**c**) The scaffold was secured with fibrin glue around the implant. The stability of the implant needs to be checked by flexing and extending the knee joint

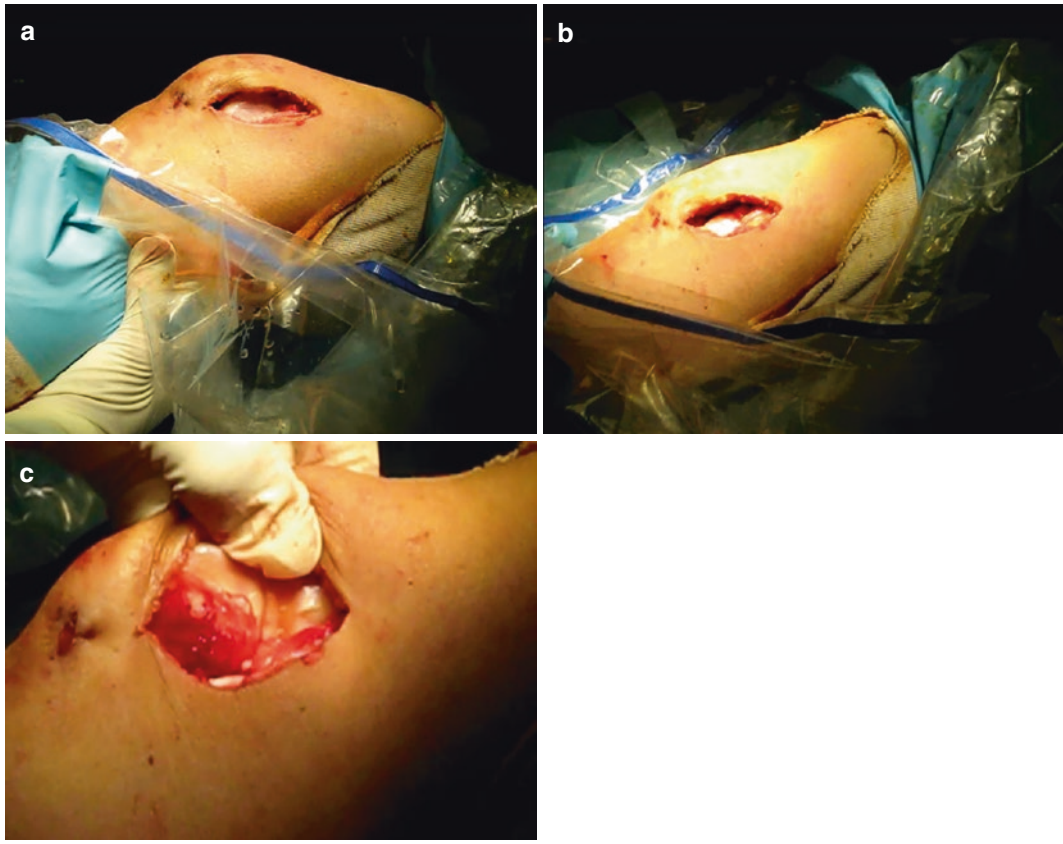

Figure 18.2.8: The Combined BMAC and Hyaluronan Scaffold Procedure: The Final Assessment. A 57-year-old female athlete has undergone bone marrow aspiration concentrate (BMAC)-impregnated hyaluronic acid (HA) scaffold implantation for patellar chondral defects. The knee is then (**a**) flexed and (**b**) extended to check the scaffold stability after 5 min of implantation. (**c**) If stable, instrumentation is removed; stitches are done, and dressing is applied

Figure 18.2.9: The Combined BMAC and Hyaluronan Scaffold Procedure: The Rehabilitation. The rehabilitation program following bone marrow aspiration concentrate-hyaluronic acid scaffold procedure is divided into four phases, each phase lasting from 6 to 12 weeks. The first phase is the proliferative/protective phase that lasts from 0 to 6 weeks. The aim of this phase is to achieve full extension, with gradual increase of flexion and strengthening of the muscles using static exercises. The second phase is the transition phase that lasts from 6 to 12 weeks. During this phase patient is trained to perform some basic functional activities along with strength training. Full-knee range of motion needs to be achieved at the end of this phase. Weight bearing is also initiated during the eighth week. The third phase is the maturation phase that lasts from 12 to 24 weeks. In this phase near-normal quadriceps strength is achieved along with some advanced functional training and pool-based exercises. Fourth phase is the functional recovery phase that lasts from 24 to 52 weeks. In this final phase, patients get trained to return to their sporting activity by proprioception, agility, and coordination training. (**a**, **b**) Resistance strength training exercise of phase three rehabilitation. (**c**) Functional training using antigravity treadmill of phase three rehabilitation

Figure 18.2.9: (continued)

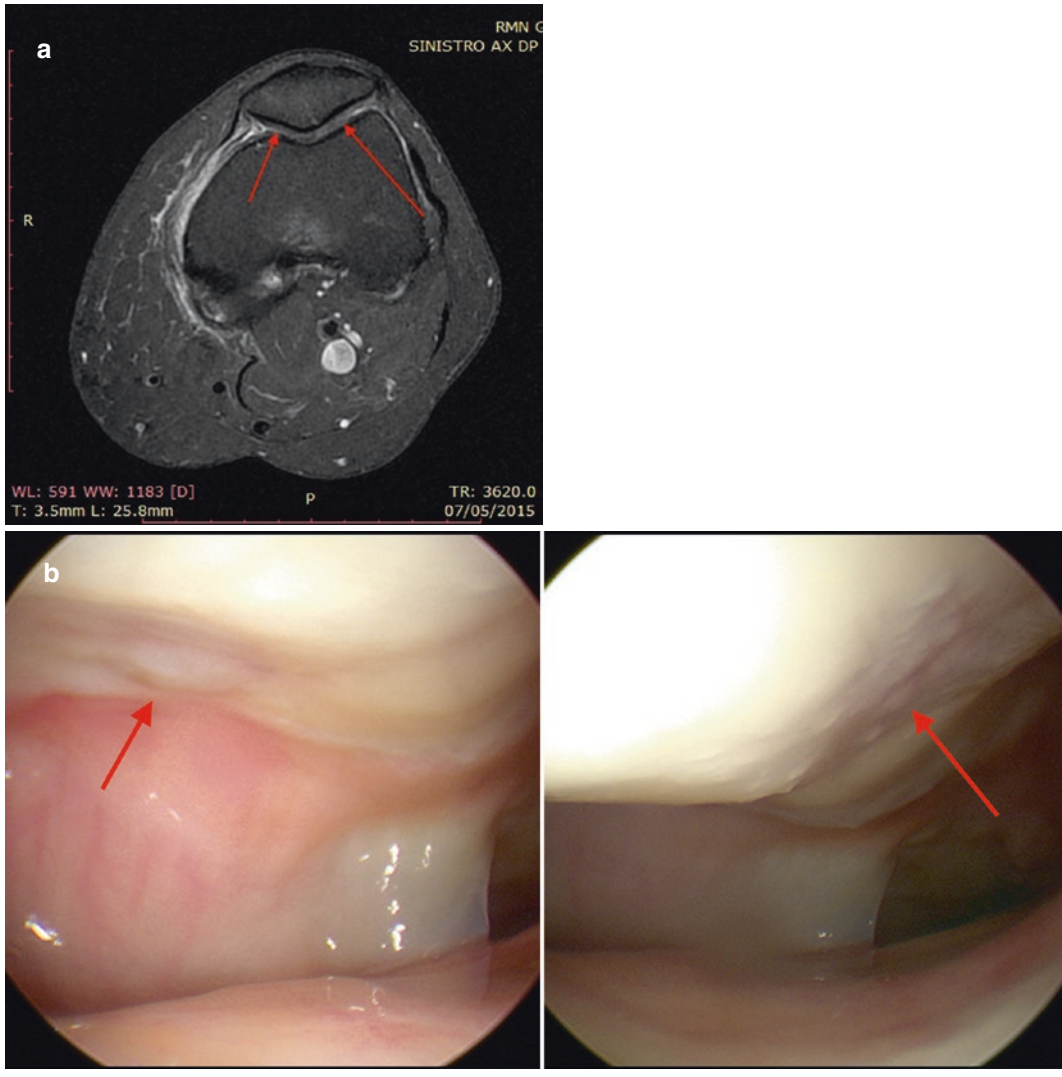

Figure 18.2.10: The Combined BMAC and Hyaluronan Scaffold Procedure: The Long-Term Results. A 57-year-old female underwent bone marrow aspirate concentrate (BMAC) with hyaluronic acid (HA) scaffold procedure for the patellar cartilage lesions. After 6 years, the patient suffered a medial meniscal tear in the same knee. (**a**) On MRI, good quality of a regenerative tissue is seen which has integrated well with the adjacent tissue. (**b**) Arthroscopy was done for the medial meniscal tear that showed a good quality of a regenerative tissue at both the patellar facets. At 9-year follow-up after the HA-BMAC procedure, the patient reports good clinical and functional outcome. The patient-reported outcome scores at 9-year follow-up are as follows: Visual Analogue Scale—1, Knee Injury and Osteoarthritis Outcome Score (KOOS): symptoms—93, pain—89, ADL—69, sports—75, QOL—81

18.3 Take-Home Message

Achieving good long-term outcomes in patellofemoral cartilage defects has always remained a challenge. Repair of such full-thickness cartilage injury using a hyaluronic acid-based scaffold with concentrated bone marrow aspirate concentrate provides good to excellent clinical outcomes at long-term follow-up in small or large lesions, in single or multiple lesions, and in treatment of lesions in multiple compartments [8]. Moreover, single-step cartilage repair eliminates the need for a two-step procedure, thereby reducing the cost and morbidity to the patient. While good to excellent outcomes can be expected in treated patients over 45 years of age, outcomes may be comparatively more successful in younger patients.

References

1. Mankin HJ. The response of articular cartilage to mechanical injury. J Bone Joint Surg Am. 1982;64(3):460–6.
2. Gobbi A, Kon E, Berruto M, Francisco R, Filardo G, Marcacci M. Patellofemoral full-thickness chondral defects treated with Hyalograft-C: a clinical, arthroscopic, and histologic review. Am J Sports Med. 2006;34(11):1763–73.
3. Kon E, Gobbi A, Filardo G, Delcogliano M, Zaffagnini S, Marcacci M. Arthroscopic second-generation autologous chondrocyte implantation compared with microfracture for chondral lesions of the knee: prospective nonrandomized study at 5 years. Am J Sports Med. 2009;37(1):33–41.
4. Battaglia M, Rimondi E, Monti C, Guaraldi F, Sant'Andrea A, Buda R, et al. Validity of T2 mapping in characterization of the regeneration tissue by bone marrow derived cell transplantation in osteochondral lesions of the ankle. Eur J Radiol. 2011;80(2):e132–9.
5. Gobbi A, Karnatzikos G, Kumar A. Long-term results after microfracture treatment for full-thickness knee chondral lesions in athletes. Knee Surg Sports Traumatol Arthrosc. 2014;22(9):1986–96.
6. Gobbi A, Whyte GP. One-stage cartilage repair using a hyaluronic acid-based scaffold with activated bone marrow-derived mesenchymal stem cells compared with microfracture: five-year follow-up. Am J Sports Med. 2016;44(11):2846–54.
7. Gobbi A, Scotti C, Karnatzikos G, Mudhigere A, Castro M, Peretti GM. One-step surgery with multipotent stem cells and Hyaluronan-based scaffold for the treatment of full-thickness chondral defects of the knee in patients older than 45 years. Knee Surg Sports Traumatol Arthrosc. 2017;25(8):2494–501.
8. Gobbi A, Whyte GP. Long-term clinical outcomes of one-stage cartilage repair in the knee with hyaluronic acid-based scaffold embedded with mesenchymal stem cells sourced from bone marrow aspirate concentrate. Am J Sports Med. 2019;47(7):1621–8.
9. Whyte GP, Gobbi A, Sadlik B. Dry arthroscopic single-stage cartilage repair of the knee using a hyaluronic acid-based scaffold with activated bone marrow-derived mesenchymal stem cells. Arthrosc Tech. 2016;5(4):e913–8.

19 The Illustrative Overlay Autologous Chondrocyte Implantation (Overlay ACI) Technique for Repair of the Extra-Large Osteochondral Defects

Deepak Rajkumar Goyal

19.1 Introduction

The importance of the subchondral (SC) bone has been well established [1, 2], which makes the osteochondral (OC) lesions distinctly different from the pure chondral lesions. For the treatment of osteochondral lesions, the subchondral bone must be reconstructed properly before the cartilage repair procedure is carried out [3]. Most of these OC lesions are very big in size and are associated with either subchondral bone damage or large SC cysts or a totally separated large OC fragment [4]. The most common non-degenerative etiologies for such large combined osseous and chondral lesions are osteochondritis dissecans (OCD), regional osteonecrosis, and trauma [5]. Prognosis of such lesions is less favorable and has a strong tendency to leave a painful and/or unstable joint causing early-age osteoarthritis. Treating such large lesions with joint-preservation techniques is a big challenge because there are no proven techniques to treat such lesions; they may require multiple surgeries, and still have a doubtful success rate. Goyal [6] discussed the mid-term results of "The overlay ACI technique" and established the technique for the treatment of the extra-large osteochondral lesions where the autologous chondrocyte implantation (ACI) was overlaid over the reconstructed subchondral bone. The purpose of this chapter is to illustrate the case selection and the surgical technique along with a discussion of the long-term results of the Overlay ACI technique.

D. R. Goyal (✉)
Saumya Arthroscopy and Sports Knee Clinic, Ahmedabad, India

Visiting Professor of Orthopaedics, Graduate School of Biomedical and Health Sciences, Hiroshima University, Hiroshima, Japan
e-mail: deepak@knee.in

D. R. Goyal (ed.), *The Illustrative Book of Cartilage Repair*,
https://doi.org/10.1007/978-3-030-47154-5_19

19.2 The Illustrations

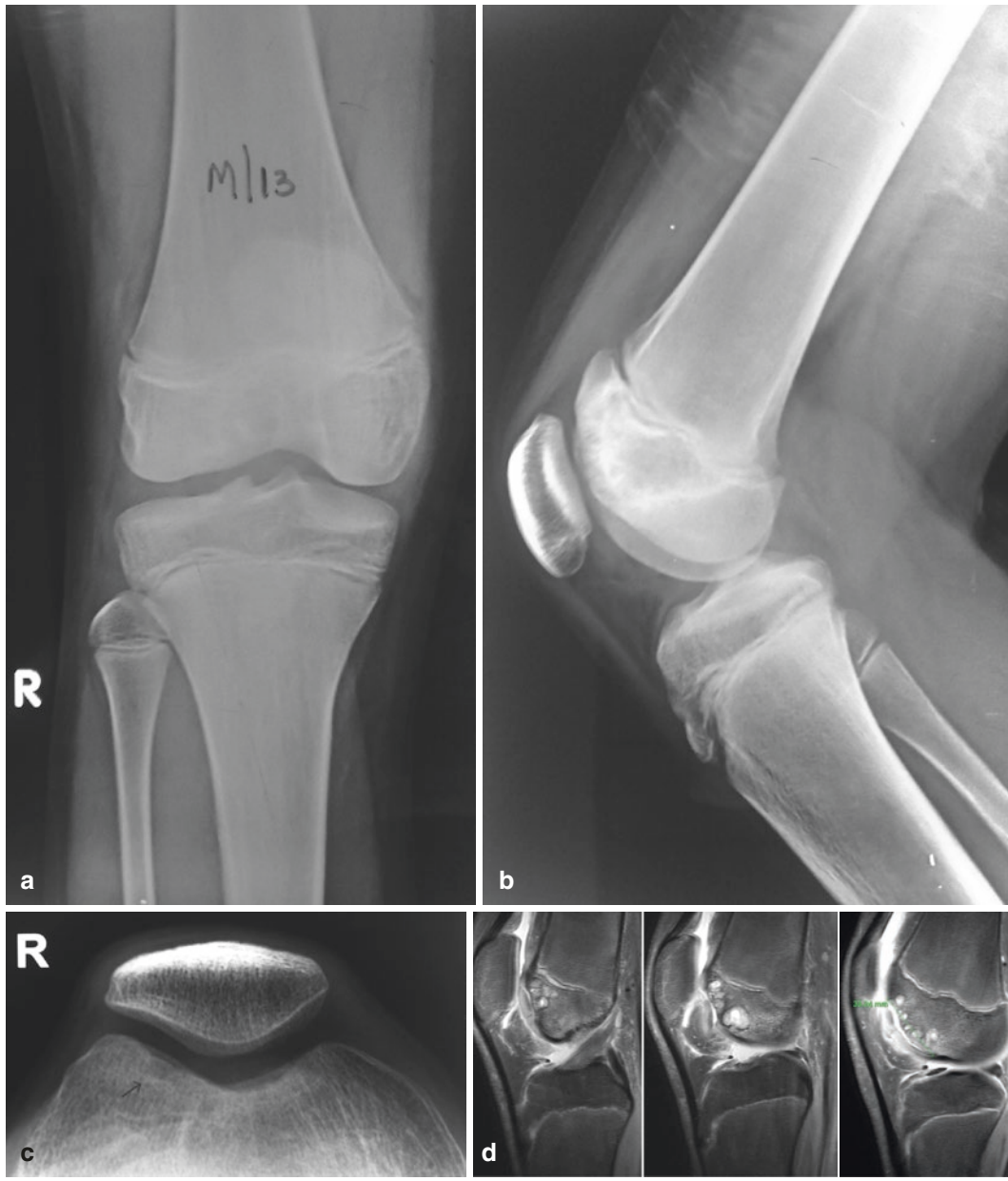

Figure 19.2.1: The Overlay ACI Technique: The Ideal Case Selection. A 13-year-old teen presented with a persistent right-knee pain for 3 months that got aggravated on a leisure mountain climbing incidence with the development of locking of the knee joint. The clinical examination revealed right knee locked in 20° of flexion and painful patellofemoral movements. (**a**–**c**) Routine radiological examination showed the presence of subchondral cysts in the trochlea. (**d**–**f**) The lesion was diagnosed as juvenile osteochondritis dissecans on magnetic resonance imaging (MRI) and it was found to be very extensive involving nearly the complete trochlear surface, with multiple large-size subchondral cysts present at the center and at the lateral trochlear surface. The MRI also revealed the separation of a huge osteochondral piece from the lateral trochlear surface extending till the center of the trochlea. (**g**) A computed tomography imaging was also done to rule out any other pathology and was found to be consistent with the MRI findings

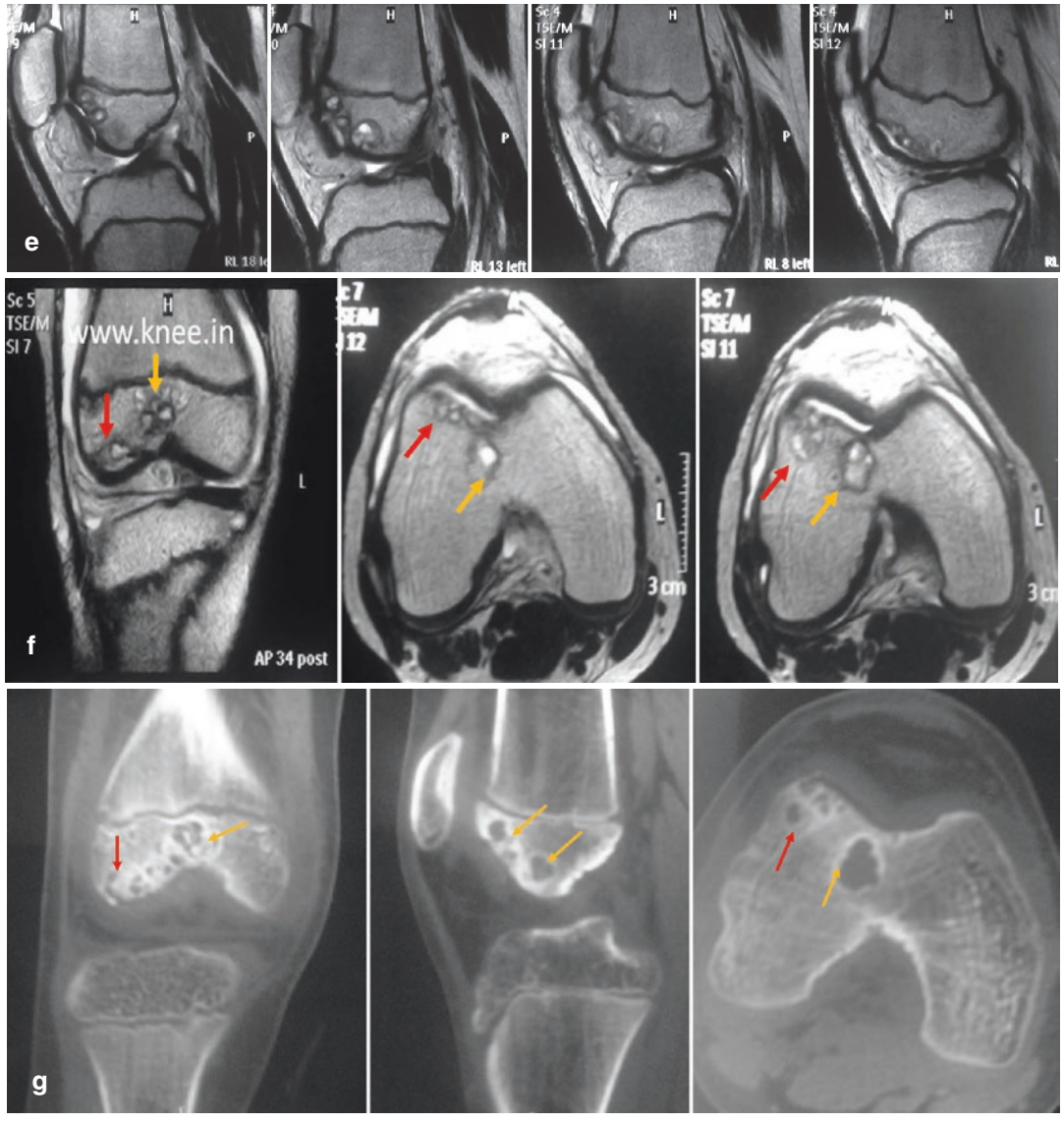

Figure 19.2.1: (continued)

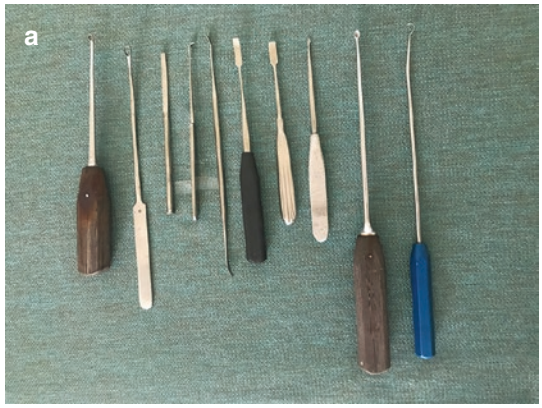

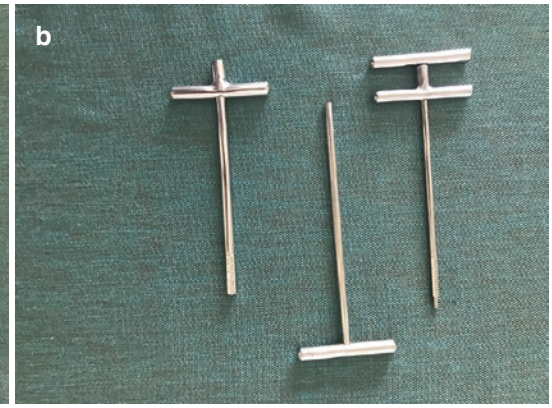

Figure 19.2.2: The Overlay ACI Technique: The Instruments. The overlay ACI technique requires routine instruments needed for any cartilage defect preparation. In addition, it also requires instruments to clean the subchondral (SC) cysts, debride the SC lesion, and scrap the lesion till a healthy SC bone. (**a**) Different type of scoops and ring curettes, of different angles, are needed to prepare the chondral defect. Small osteotomes and angled osteotomes, along with deeper curettes, are needed to prepare the SC bone lesions. (**b**) A special trocar and cannula are advocated for use while taking a cartilage biopsy for ACI by the cartilage lab (Regrow Biosciences Pvt. Ltd., India). The trocar cannula set comes in two sizes, 7 mm and 4 mm, with 4 mm being the preferred size. The surgeon should put the trocar-cannula perpendicular to the chondral biopsy site, then remove the trocar, and hammer the cannula till 5 mm mark. This ensures a complete thickness of the cartilage as well as a minimal base of the SC bone, being harvested as the cartilage biopsy

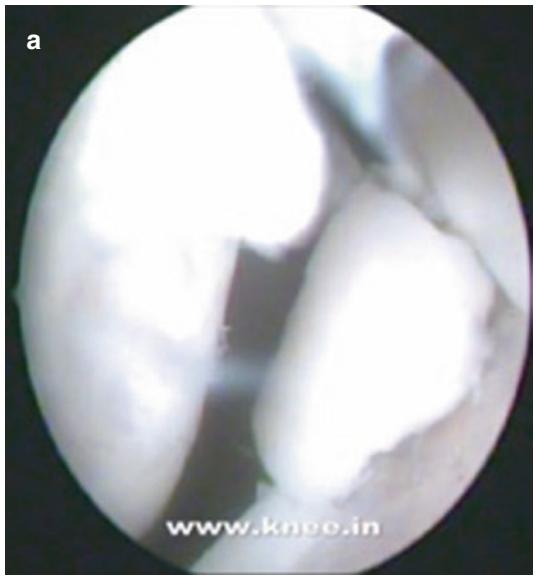

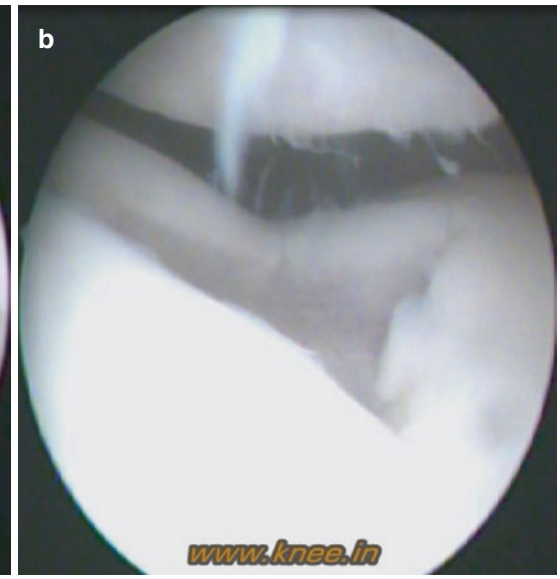

Figure 19.2.3: The Overlay ACI Technique: The Arthroscopic Assessment of the Lesion. A 13-year-old male underwent right-knee arthroscopy for the locked knee. (**a**) The trochlear surface showed a nearly separated chondral piece from the center of the trochlea, as viewed from the anterolateral portal. There was also a loose chondral piece that was found in the anterior compartment (not shown in the picture). (**b**) The removal of both the chondral pieces led to a big chondral defect that was quadrilateral in shape, extending from the center of the trochlea towards the lateral facet of the trochlea. The trochlear bed as well as the subchondral cysts were covered with fibrous tissue throughout the lesion. The corresponding patellar surface was normal, as was the remaining knee joint. (**c**, **d**) The size of the separated chondral pieces measured approximately 32 mm × 20 mm

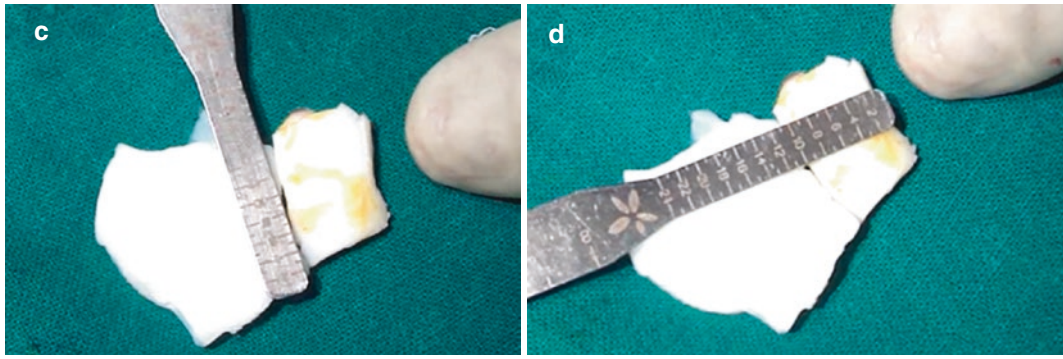

Figure 19.2.3: (continued)

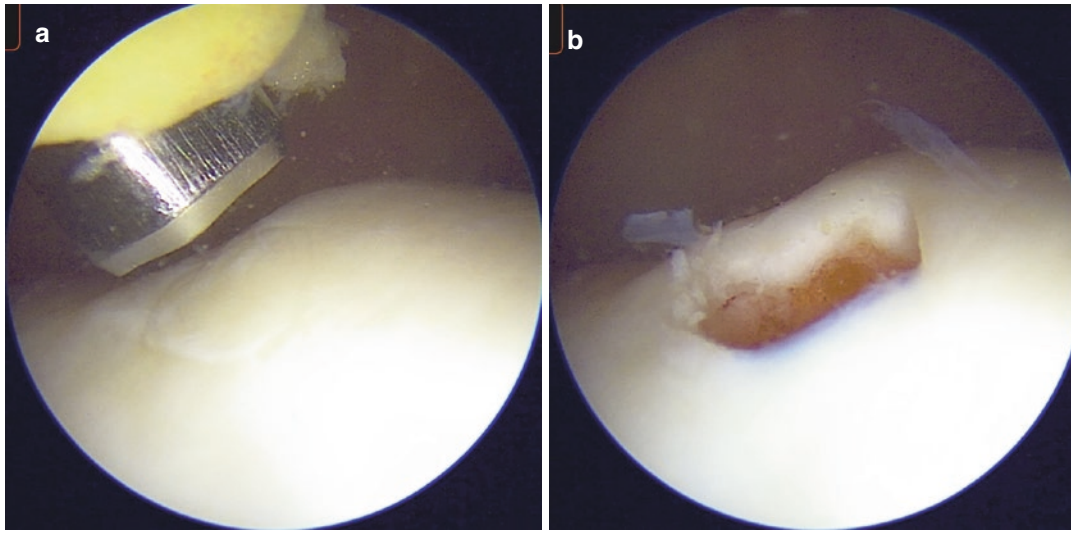

Figure 19.2.4: The Overlay ACI Technique: The Cartilage Biopsy. The cartilage lab (Regrow Biosciences Pvt. Ltd., India) recommends using a hexagonal harvester to harvest the chondral biopsy. The most preferred site is the lateral or the medial trochlear border above the linea terminalis. As this case had trochlear involvement extending mainly on the lateral trochlear surface, the chondral biopsy was taken from the medial trochlear border. (**a**) The harvester with the trocar was placed perpendicular to the articular surface from the anteromedial portal while viewing from the anterolateral portal. The trocar was removed once the perpendicular position of the graft harvester was ascertained. With gradual hammering, the harvester was inserted till the first-level mark which is 5 mm from the surface. (**b**) A 5 mm thick chondral biopsy at the trochlear margins will usually involve the full-thickness cartilage till the subchondral bone plate. The harvester was then gradually rotated clockwise and then counterclockwise and then removed from the biopsy site. (**c**) The trocar was again put in the harvester and gradually pushed while keeping the harvester in the transport vial. (**d**) Thus, the chondral biopsy was directly transferred into the transport media tube (the chondral biopsy is taken out of the transport media for the sake of demonstration)

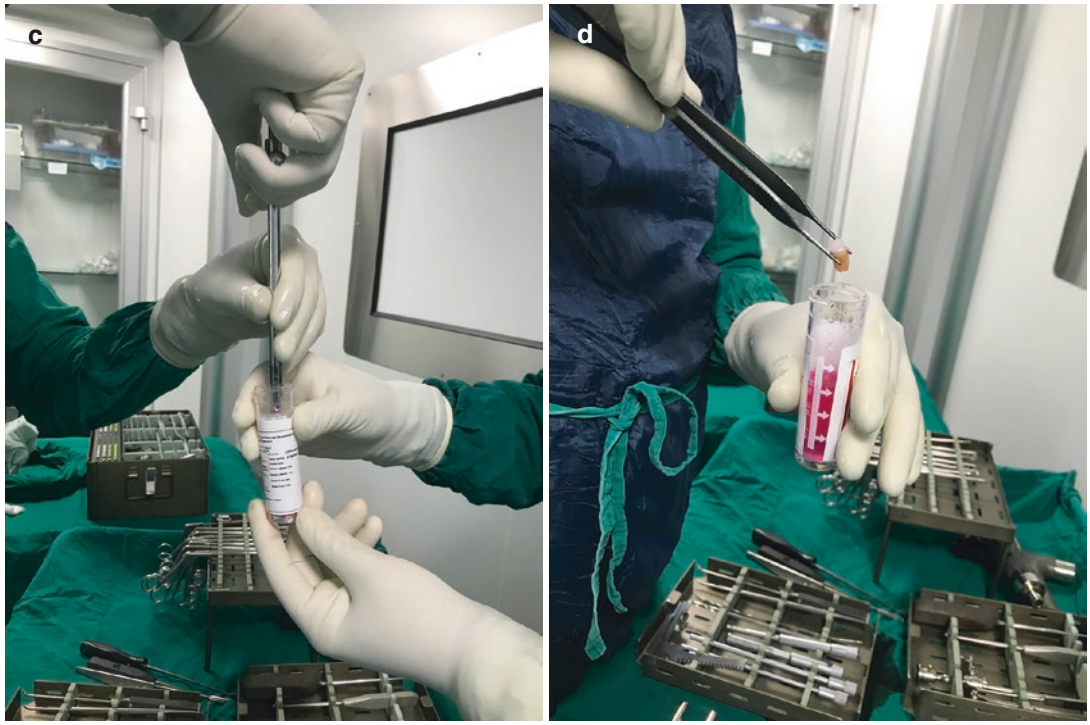

Figure 19.2.4: (continued)

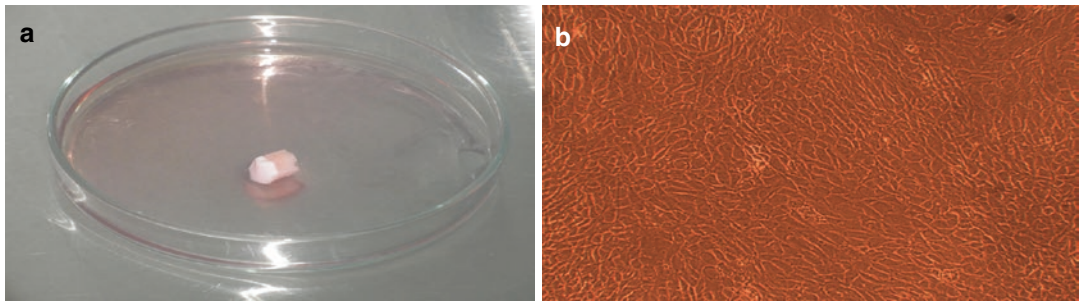

Figure 19.2.5: The Overlay ACI Technique: The Chondrocyte Culture and Cell Delivery from the Cartilage Lab. The cartilage biopsy tissue was collected in a transport vial containing the medium and was transported to the cell-processing center under controlled temperature conditions. (**a**) Cartilage tissue was processed as per the standard operating procedure under cGMP conditions. A 132 mg of cartilage biopsy tissue yielded 1.56×10^5 cells at the time of isolation. (**b**) Further medium changes were given at every 72 h and after reaching the cellular confluency of around 80%, the cells were enzymatically harvested and seeded for the next step. The cell count recorded at this step (P1-passage 1) was 8.87×10^6 and the cell viability was 97.16%. (**c**) The cells were further seeded for P2 stage (passage 2) and harvested after reaching confluency. The cells were now seeded for the final process stage and a fresh culture medium was given at a 2–3-day interval. Cells were enzymatically harvested once reached to a confluency. (**d**) The cell count and cell viability at final process stage were 48.64×10^6 and 98.68%, respectively. A total of 48×10^6 cells were filled in 4 V-vials with 12 million cells per vial and transported at 2–8 °C to hospital for the implantation. Sterility and mycoplasma were tested at every stage of culture and were found to be negative during the entire culture period (with permission from Dr. Vinayak Kedage, Lab Director, Regrow Biosciences Pvt. Ltd.)

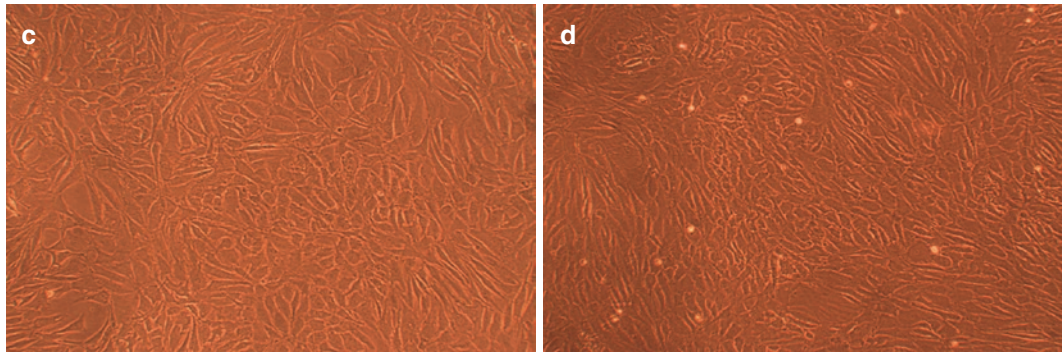

Figure 19.2.5: (continued)

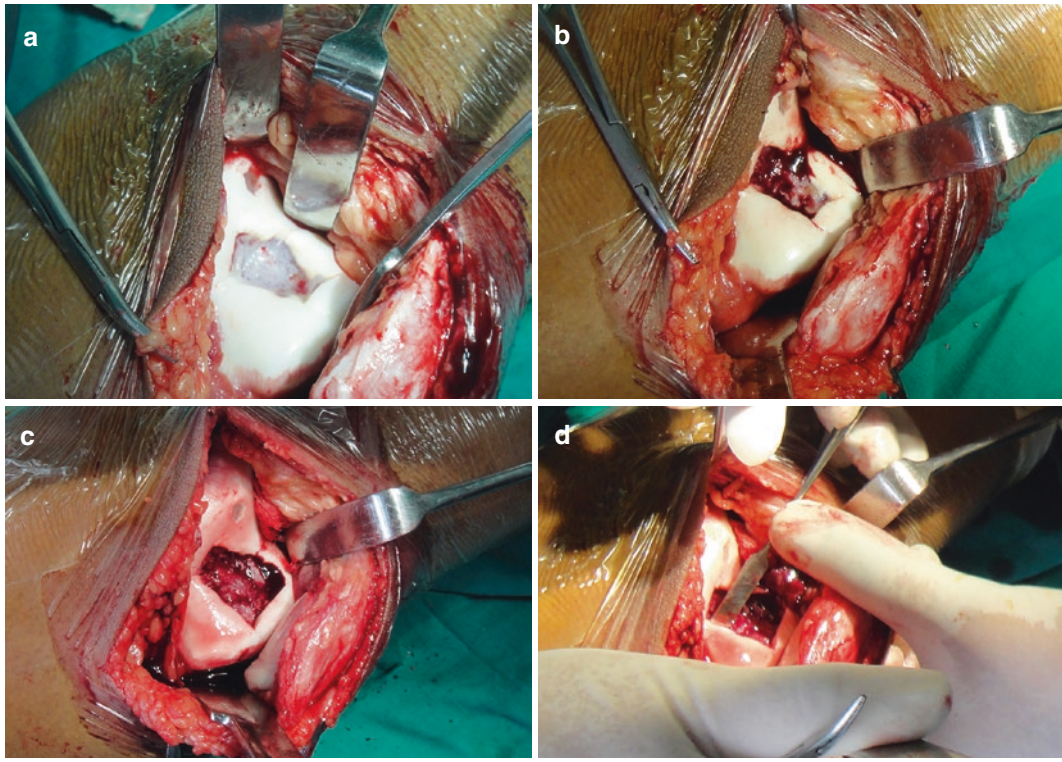

Figure 19.2.6: The Overlay ACI Technique: The Preparation of the Osteochondral Lesion. A 13-year-old male patient with juvenile osteochondritis dissecans of the right trochlea. The lesion was exposed thru a medial parapatellar arthrotomy. A Langenbeck retractor was placed in the intercondylar notch and a Hoffmann's retractor was placed in the lateral gutter while viewing from the superolateral corner of the knee. (**a**) A quadrilateral shaped trochlear osteochondral lesion was visible that was covered by fibrous tissue. A healing cartilage biopsy site was also visible near medial margin of the lower medial trochlear surface. (**b**) The osteochondral lesion extended from the center of the trochlea towards the lateral trochlear surface. On scrapping, multiple subchondral (SC) cysts got exposed (see Figure 19.2.7 for details). (**c**) A thorough debridement of the base of the lesion was carried out with the removal of all the unhealthy cartilage from the margins of the lesion. The final size of the defect was 34 mm × 26 mm in their longest extents. (**d**) The gel-based autologous chondrocyte implantation technique requires walls of the lesions to be beveled to improve the stability of the graft in the lesion. A sharp periosteum was used to create the bevel-shaped margins

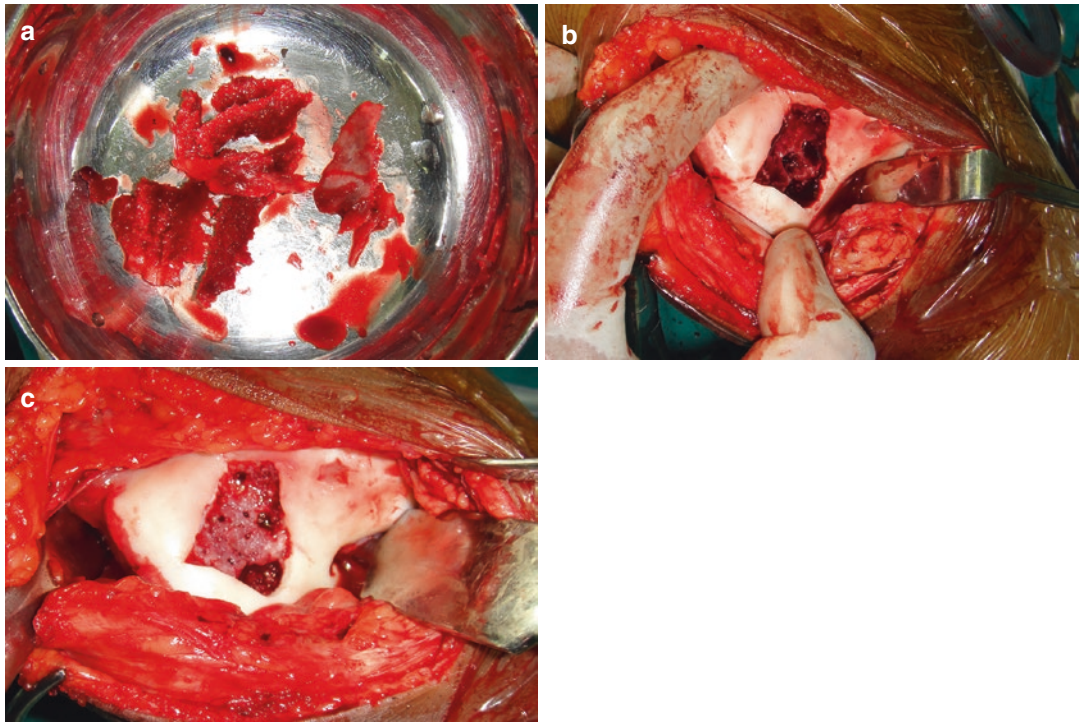

Figure 19.2.7: The Overlay ACI Technique: The Subchondral Bone Reconstruction. The subchondral (SC) bone reconstruction is carried out using the autogenous iliac crest bone graft. Depending on the type of osteochondral damage, either a pure cancellous graft or a tricortical graft is harvested from the iliac crest. If there is a SC cyst then a cancellous graft is needed to fill the cavity after a thorough curettage of the cyst. When there is a loss of large osteochondral surface of the articular surface, a tricortical congruous graft is used to recreate the SC bone. (**a**) Autogenous cancellous iliac crest graft was harvested from the ipsilateral side of a 13-year-old male patient who suffered from juvenile osteochondritis dissecans of the right trochlea. (**b**) A medial parapatellar arthrotomy was done and the lesion was exposed. On scrapping of the base of the lesion, multiple SC cysts were explored as seen in Figure 19.2.1 on MRI. The walls of the cysts were curetted till the healthy surrounding walls. (**c**) The cancellous iliac crest bone graft was impacted into the SC cysts till the level of the SC bone plate, thus reconstructing the SC spongiosa and the SC bone plate

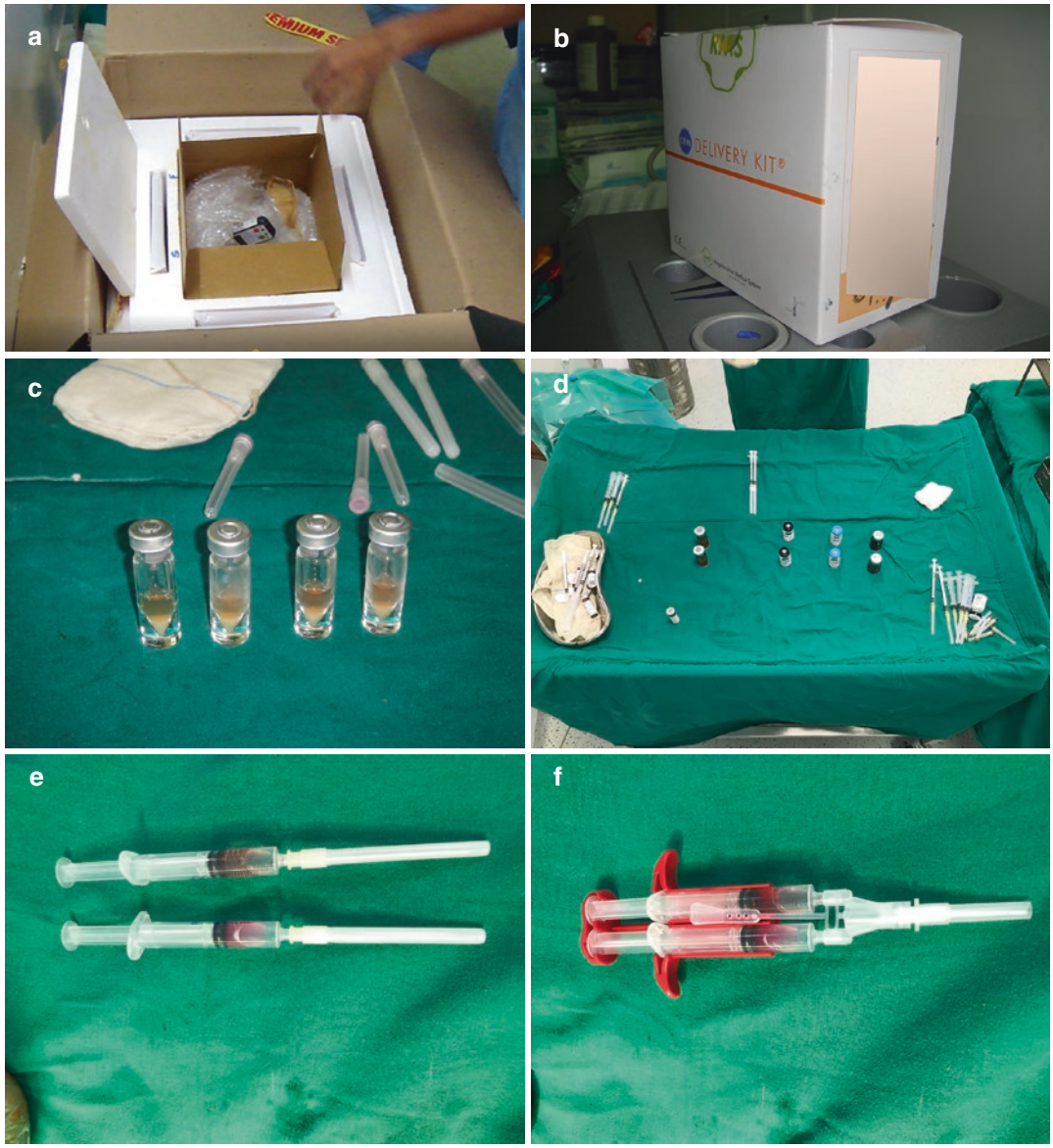

Figure 19.2.8: The Overlay ACI Technique: The Preparation of the ACI Implant. (**a**, **b**) The autologous chondrocyte implant (ACI) is received from the laboratory maintaining the cold chain, 6 weeks after the harvest of the chondral biopsy. (**c**) The cultured chondrocytes are received in conical vials so that a maximum number of the cells can be tapped. (**d**) A proprietary preparation method [7] is used to prepare the final implant using multiple vials and two different syringes. (**e**) The first syringe contains 1 mL fibrinogen while the second syringe contains 0.9 mL of cultured chondrocytes and 0.1 mL of thrombin. (**f**) Two 1 mL syringes are connected with a "Y" mixing connector. Each drop of the syringe contains a mix of chondrocytes and thrombin-fibrinogen mixture that forms the fibrin scaffold

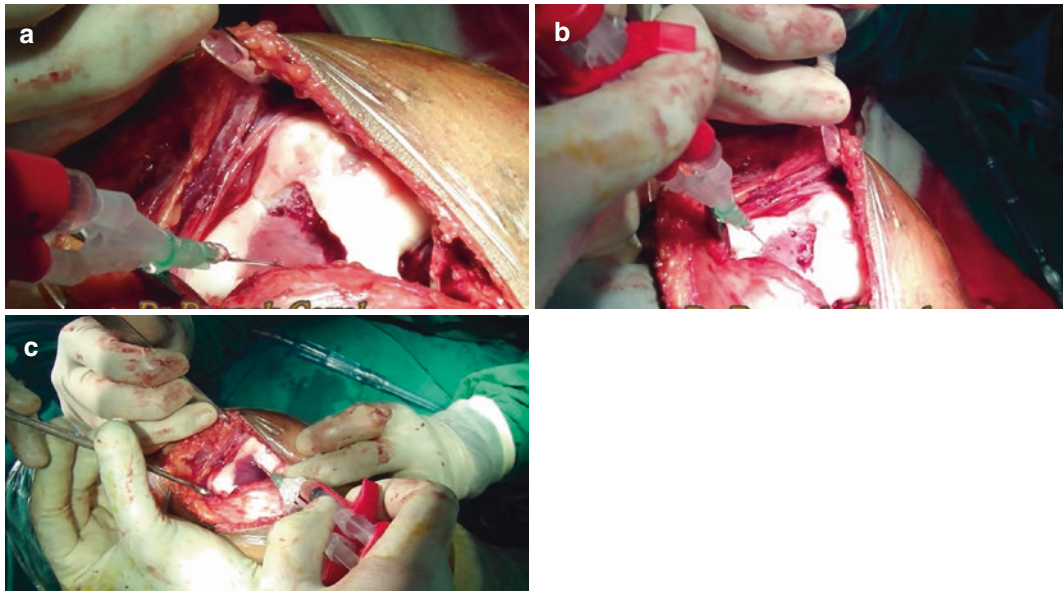

Figure 19.2.9: The Overlay ACI Technique: The Implantation of the ACI. The gel-based ACI is implanted drop by drop on the chondral lesion. When the plunger of the "Y" syringe is gently pressed, the contents of both the syringes mix with each other forming a drop-by-drop gel-based implant containing chondrocytes and thrombin + fibrinogen mixture that on solidification forms a 3-dimensional scaffold of fibrin with 3-dimensional equal distribution of chondrocytes throughout the lesion. The drops are implanted gradually so that it does not flow away into the joint and a gravity-neutral position of the defect is recommended for the same. (**a**) A 13-year-old boy has been treated with osseous reconstruction of the subchondral bone with the iliac cancellous bone graft and then implanted with gel-based ACI on its trochlear region. The knee was tilted laterally to make the lateral trochlear lesion as gravity neutral. (**b**) As the gel-based ACI started solidifying, the knee was tilted medially to continue with the implantation of the ACI gel on the center and adjoining medial trochlear surface, thereby providing a continuous gravity-neutral base. (**c**) The gel-based ACI solidified in 8–10 min forming a final fibrin glue-based scaffold impregnated with the cultured chondrocytes

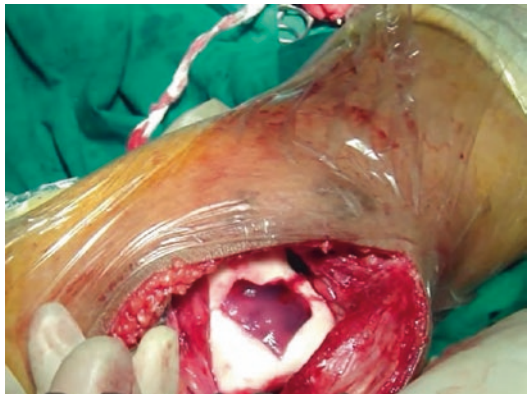

Figure 19.2.10: The Overlay ACI Technique: The Final Assessment of Osteochondral Reconstruction. A 13-year-old boy underwent the overlay autologous chondrocyte implantation (ACI) technique for the juvenile osteochondritis dissecans of the right knee. The gel-based ACI that was put on the underlying reconstructed subchondral bone got solidified in 8–10 min. Then the joint was subjected to a gradual range of movement 2–3 times and then the chondral defect was examined again. The edges of the defect were checked for any overflow of the gel on the surrounding chondral surface and the joint was inspected for any gel remnants. The contour of the implant was also checked from the horizon to see if the surface of the gel ACI is congruous with the surrounding surface or not. Usually less than a mm proud gel is acceptable, but more proud gel should not be accepted as it might get peeled away due to shear stresses during the range of movement. A wash was given, and closure was done in layers

Figure 19.2.11: The Overlay ACI Technique: The Postoperative Care and Rehabilitation. During the early phase, the postoperative rehabilitation should aim for the protection of the osteochondral construct while simultaneously maintaining the range of the movements. The early phase should also aim for maintaining the muscular strength with the help of the static exercises of the quadriceps, the hamstring, the abductor, and the adductor muscles. Dynamic muscle-strengthening exercises are added to the rehabilitation program, 4–6 weeks onwards, depending on the size and the location of the lesion. (**a**) The continuous passive motion (CPM) machine exercises are advised form the postoperative day 1, for 6–8 h every day till 6–8 weeks, to stimulate the chondrocytes to remain differentiated. During the time the patient is not doing CPM exercises, (**b**) the patient is advised to keep the leg in dial-locked range of motion brace (ROM knee brace) with (**c**) a lock kept at zero during the first week. (**d**) Depending on the location and the size of the lesion, range of motion is increasingly allowed using dial lock on the brace. Weight bearing is allowed depending on the location of the treated lesion. For patellofemoral lesions, weight bearing with dial-locked brace at zero (in both the flexion and extension) is allowed as soon as the quadriceps control is gained by the patient. For the tibiofemoral lesions, weight bearing is delayed for 3–6 weeks, depending on the size of the lesion

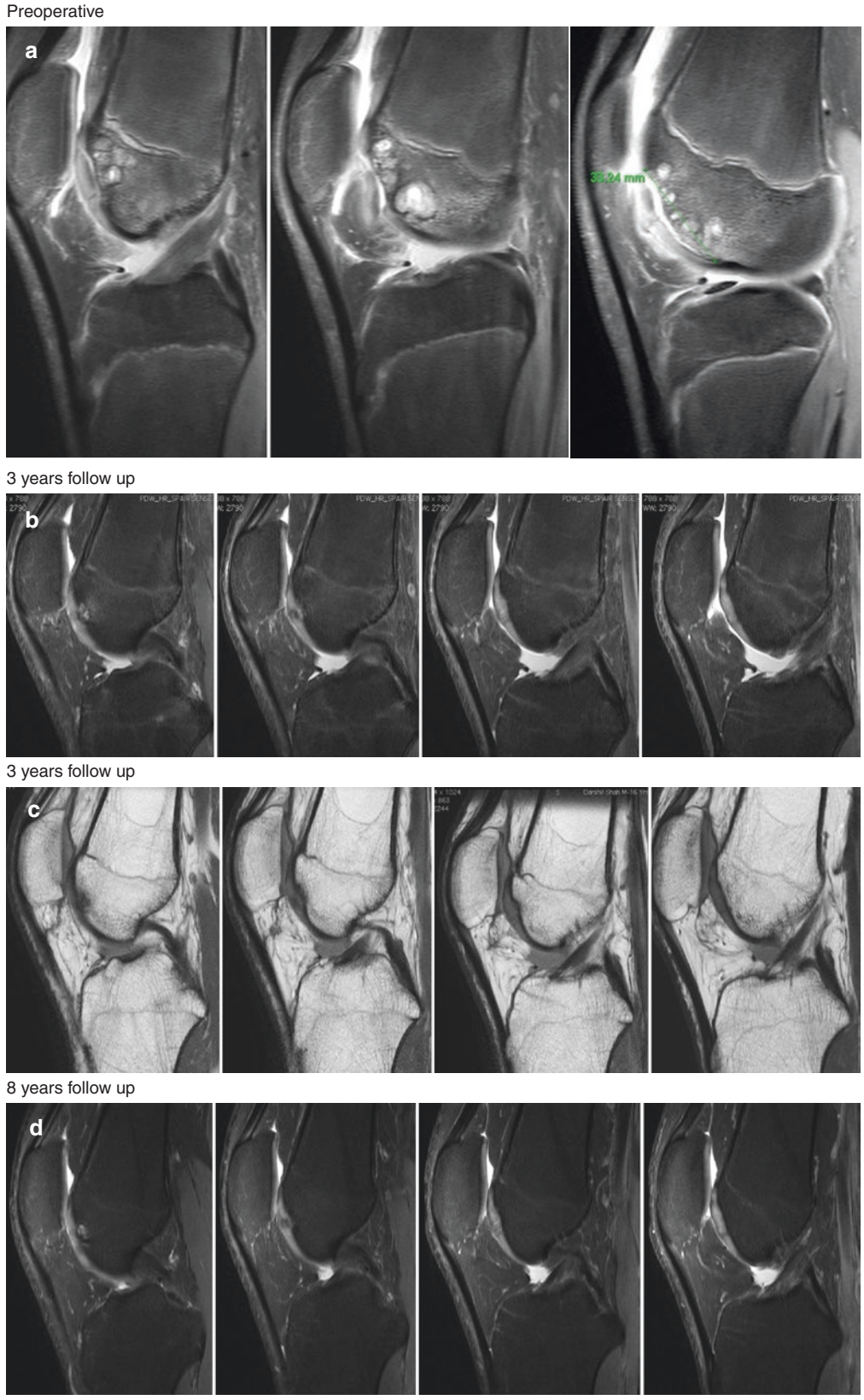

Figure 19.2.12:

Figure 19.2.12: The Overlay ACI Technique: The Long-Term Results. A 13-year-old male patient was treated using the overlay autologous chondrocyte implantation (ACI) technique for the juvenile osteochondritis dissecans of the right trochlea. (**a**) The T2 sagittal images show multiple subchondral (SC) cysts along with near-total separation of the osteochondral piece from the center as well as the lateral trochlear surface. (**b**, **c**) The 3-year postoperative follow-up T2 and T1 sagittal images of the same knee show completely healed SC bony cysts along with well-healed SC bone plate in full extent of the trochlear lesion. The healed cartilage over the trochlea also shows well-congruous, well-filled cartilage repair with full integration of the repaired cartilage with the surrounding cartilage surface. The post-ACI picture also shows homogenous repair throughout its extent. A tiny bony spicule of the SC bone graft is seen on the most medial image leading to a small area of inhomogeneous cartilage along with a minor SC bone edema underneath. (**d**) The 8-year postoperative MRI following the overlay ACI technique shows persistently healed SC bone cysts and SC bone plate. The healthy repaired cartilage seen at 3-year follow-up has remained persistently well healed with a homogenous structure, a complete defect fill, and an integration with the surrounding walls. A tiny spicule of SC graft is persistent, but the underlying SC bone marrow edema has decreased

19.3 Take-Home Message

The overlay ACI technique is an autogenous alternative for the osseous and chondral reconstruction of the large osteochondral defects. Many scaffold-based techniques and allograft options have been discussed in the literature; however, all have some limitations. Sandwich technique [3, 8] has been described; but there are no case studies or clinical data that have been published. Biphasic and triphasic scaffolds have been used to treat midsize OC lesions [9, 10] (Chap. 17), but there are no reports of them being used in extra-large lesions. Osteochondral (OC) allografts (Chap. 20) can be used to treat extra-large OC lesions provided that the surgeon has access to the allografts and there are regulatory approvals. The best results of OC allografts were reported in younger patients (<30 years) having unipolar, traumatic lesions with short duration of symptoms (<12 months) [11]. The overall re-surgery rate after OC allografts has been published to be as high as 35% [12]. Konst et al. [13] also used a combination of gel-based ACI and bone grafting in nine patients with median lesion size of 7.1 cm^2 (2.5–12) with median depth of the lesion as 0.9 cm (range 0.8–1.2 cm). The median follow-up of 9 months showed improvements in KOOS and IKDC scores. Goyal [14] showed encouraging long-term results after the use of the overlay ACI technique in extra-large osteochondral lesions. The overlay ACI technique is a good alternative to allografts or multiphasic scaffolds when the surgeon is looking for an autogenous alternative or when the surgeon does not have access to allografts or artificial scaffolds. Though there are no long-term published comparative reports, each of these techniques should provide good osseous and chondral healing with long-term results.

References

1. Goyal D, Goyal A, Adachi N. Subchondral bone: healthy soil for the healthy cartilage. In: Gobbi A, Espregueira-Mendes J, Lane JG, Karahan M, editors. Bio-orthopaedics. Berlin: Springer Berlin Heidelberg; 2017. p. 479–86.
2. Madry H, Dijk CN, Mueller-Gerbl M. The basic science of the subchondral bone. Knee Surg Sports Traumatol Arthrosc. 2010;18(4):419–33.
3. Gomoll AH, Madry H, Knutsen G, van Dijk N, Seil R, Brittberg M, Kon E. The subchondral bone in articular cartilage repair: current problems in the surgical management. Knee Surg Sports Traumatol Arthrosc. 2010;18(4):434–47.
4. Karataglis D, Learmonth DJA. Management of big osteochondral defects of the knee using osteochondral allografts with the MEGA-OATS technique. Knee. 2005;12(5):389–93.
5. Brucker PU, Braun S, Imhoff AB. [Mega-OATS technique—autologous osteochondral transplantation as a salvage procedure for large osteochondral defects of the femoral condyle]. Operative Orthopädie und Traumatologie. 2008;20(3):188–98.

6. Goyal D. Autologous chondrocyte implantation; international cartilage and osteoarthritis symposium of Korean Orthopaedic Research Society, at Suwon, South Korea. 2014.
7. Goyal D, Modi V. Gel based autologous chondrocyte implantation. The surgical technique. Asian J Arthroscopy. 2019;4(1):27–33.
8. Brittberg M. Autologous chondrocyte implantation—technique and long-term follow-up. Injury. 2008;39(Suppl 1):S40–9.
9. Kon E, Filardo G, Perdisa F, Venieri G, Marcacci M. Clinical results of multilayered biomaterials for osteochondral regeneration. J Exp Orthop. 2014;1(1):10.
10. Perdisa F, Kon E, Sessa A, Andriolo L, Busacca M, Marcacci M, Filardo G. Treatment of knee osteochondritis Dissecans with a cell-free biomimetic osteochondral scaffold: clinical and imaging findings at midterm follow-up. Am J Sports Med. 2018;46(2):314–21.
11. Pisanu G, Cottino U, Rosso F, Blonna D, Marmotti AG, Bertolo C, Rossi R, Bonasia DE. Large osteochondral allografts of the knee: surgical technique and indications. Joints. 2018;6(1):42–53.
12. Sherman SL, Garrity J, Bauer K, Cook J, Stannard J, Bugbee W. Fresh osteochondral allograft transplantation for the knee: current concepts. J Am Acad Orthop Surg. 2014;22(2):121–33.
13. Könst YE, Benink RJ, Veldstra R, van der Krieke TJ, Helder MN, van Royen BJ. Treatment of severe osteochondral defects of the knee by combined autologous bone grafting and autologous chondrocyte implantation using fibrin gel. Knee Surg Sports Traumatol Arthrosc. 2012;20(11):2263–9.
14. Comparative analysis of treatment of large osteochondral lesions treated with SC bone reconstruction alone vs SC bone reconstruction & ACI. APOA sports meeting incorporating Orthopaedic Research 2019, Kuala Lumpur, Malaysia, 2019.

The Illustrative Osteochondral Allograft-Based Cartilage Repair

20

Martyn Snow

20.1 Introduction

The use of osteochondral allograft (OCA) represents a reconstructive solution for treating young, high-demand patients with symptomatic chondral lesions in an attempt to delay or avoid the need for joint replacement. Allografts have the advantage of providing flexibility in terms of the size of the defect treated and the location. Both femoral and tibial defects can be addressed, and reasonable results have also been reported in the patella. It is a single-stage treatment and, in association with autologous osteochondral transplantation, the only method of cartilage repair that results in the regeneration of mature hyaline cartilage with viable chondrocytes [1]. The main indications for the use of fresh osteochondral allografts are avascular necrosis of the femoral condyle, large osteochondritis dissecans and traumatic defects of the knee. As with all forms of cartilage repair, associated malalignment, instability and/or meniscal deficiency must be addressed concomitantly.

An organised transplant service is required as procedures cannot be carried out on an elective basis. Each individual allograft is size matched based on standard anteroposterior and lateral X-rays of the knee with a magnification marker. Donor grafts once harvested are stored at 4 °C in antibiotic-loaded media. Cell viability decreases over time and consequently grafts have an expiration date of 28 days after harvest, the point at which chondrocyte viability is thought to decrease below 70% [1]. As with the use of any allograft tissue, there is a risk of disease transmission which is estimated to be similar to that of homologous blood transfusion (HIV 1:493,000, hepatitis C 1:103,000 and hepatitis B 1:63,000) [2].

M. Snow (✉)
The Royal Orthopaedic Hospital, Birmingham, UK

Department of Chemical Engineering, University of Birmingham, Birmingham, UK
e-mail: snowmartyn@gmail.com

D. R. Goyal (ed.), *The Illustrative Book of Cartilage Repair*,
https://doi.org/10.1007/978-3-030-47154-5_20

20.2 The Illustrations

20.2.A Osteochondral Allograft for Cartilage Repair—The Dowel Technique

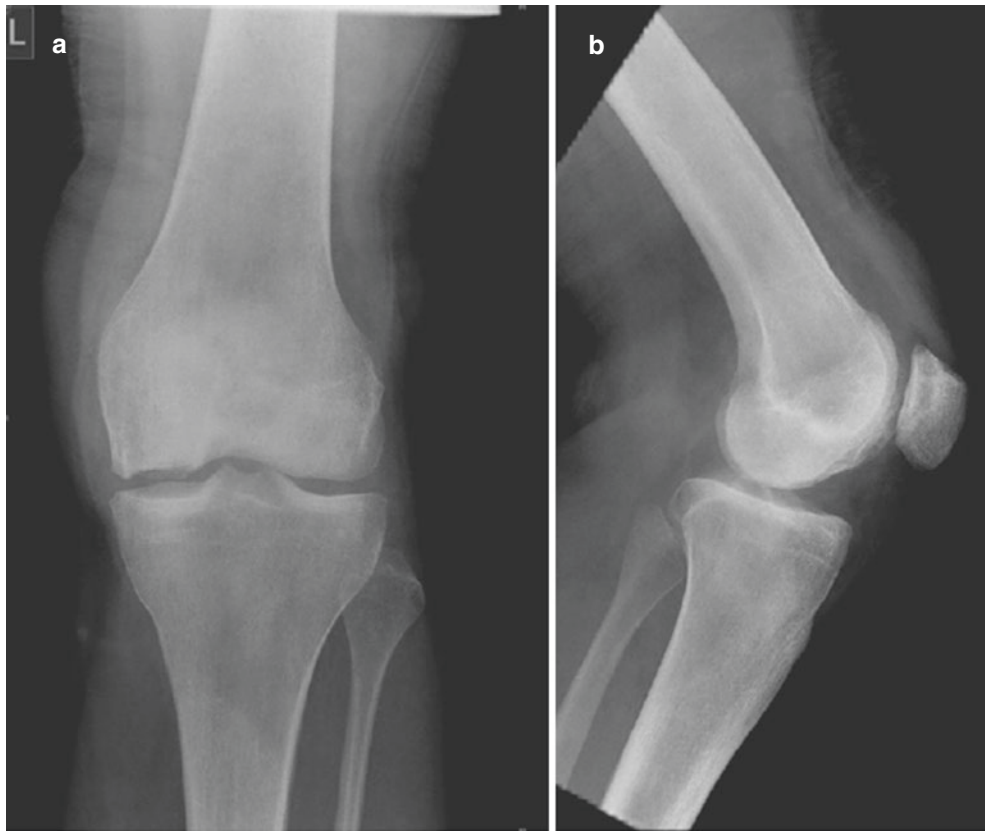

Figure 20.2.A.1: Osteochondral Allograft for Cartilage Repair Using the Dowel Technique: The Ideal Case Selection. A 22-year-old female presented 2 years following treatment for acute lymphoblastic leukaemia. She complained of pain over medial side of the left knee, which limited her walking distance and disturbed her sleep at night despite analgesia. (**a**, **b**) X-ray demonstrated an osteochondral defect of the medial femoral condyle. (**c**, **d**) MRI revealed multiple areas of avascular necrosis secondary to chemotherapy and steroids. The medial femoral condyle had collapsed as a consequence of the extensive subchondral bone involvement and this area correlated with the site of pain and maximal area of tenderness on examination. Whilst there are also areas of avascular necrosis on the lateral femoral condyle and the tibial plateau, there is an area of normal bone between them and the subchondral bone; hence such lesions are invariably asymptomatic

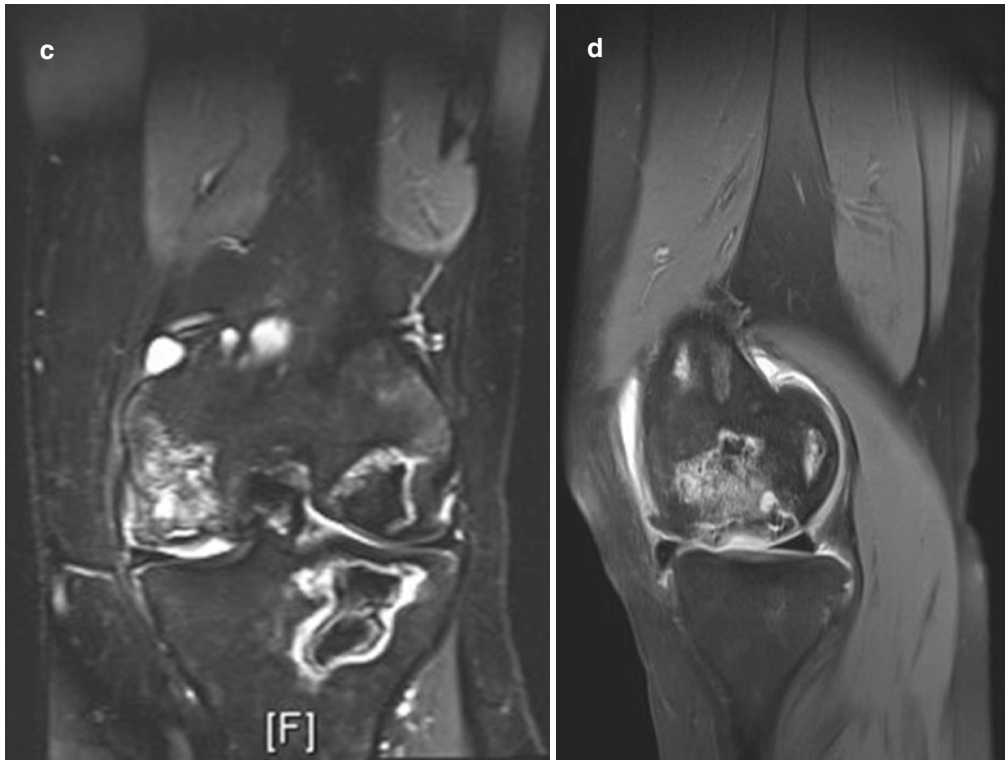

Figure 20.2.A.1: (continued)

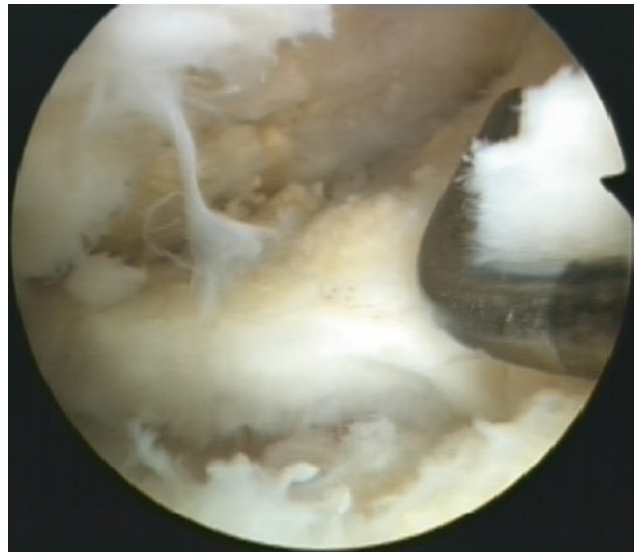

Figure 20.2.A.2: Osteochondral Allograft for Cartilage Repair Using the Dowel Technique: The Assessment of the Lesion. An arthroscopy is commonly carried out to ensure the suitability of the patient for osteochondral allograft (OCA) and to assess associated pathology. Left-knee arthroscopy of the 22-year-old female, viewing from the anterolateral portal, demonstrated delamination of the medial femoral condyle chondral surface with avascular subchondral bone beneath. The meniscus was shown to be intact with minimal damage to the opposing tibial surface. Given the MRI and the arthroscopic appearance of the subchondral bone, a reconstructive technique that reconstructs the bone and cartilage must be considered. As the lesion is greater than 2 cm^2, an autograft is not a viable option. Currently, there is no osteochondral scaffold that has shown comparable results to osteochondral allograft within the literature.

Due to the significant amount of avascular subchondral bone, a decision was made to treat the medial femoral condyle lesion with fresh OCA using a dowel technique. The dowel technique was chosen because the lesion was contained, and a larger amount of bone can be reconstructed compared with the shell technique. When planning an osteochondral allograft, an anteroposterior and lateral X-ray of the knee (with a magnification marker) or the MRI scan is used to measure the femoral condyle size so that the radius of curvature of the allograft closely matches the patient. Once an appropriately sized hemicondyle is found, the allograft should be implanted as early as possible. The success of OCA has been shown to correlate with the percentage of chondrocyte viability at the time of implantation. The cell viability is thought to deteriorate below 70% after 28 days, and so allografts should be implanted before this point [3]

Figure 20.2.A.3: Osteochondral Allograft for Cartilage Repair Using the Dowel Technique: The Instruments Required. To undertake a large-core OCA, a specialist instrument set is required. These are supplied by various manufacturers, e.g. the Mega OATS set from Arthrex (used during the included case) or (**a**) the JRF osteochondral allograft core instrumentation set (as shown in the picture). (**b**) The main elements of the set (from left to right) are a sizing core template, a drill, a guide for the coring device and a corer for the allograft. The sizing core template allows the surgeon to size the defect and determine the size of the allograft core required. The sizing tube will help to ensure perpendicular drilling of the defect and a corresponding perpendicular core from the allograft. The drill allows the creation of the appropriately sized defect; it has 1 mm increments etched on its surface to ensure that the depth of the drilled defect is appropriate. A corresponding corer is required to create a core from the allograft; this is aided with the use of a guide which can be pinned in place

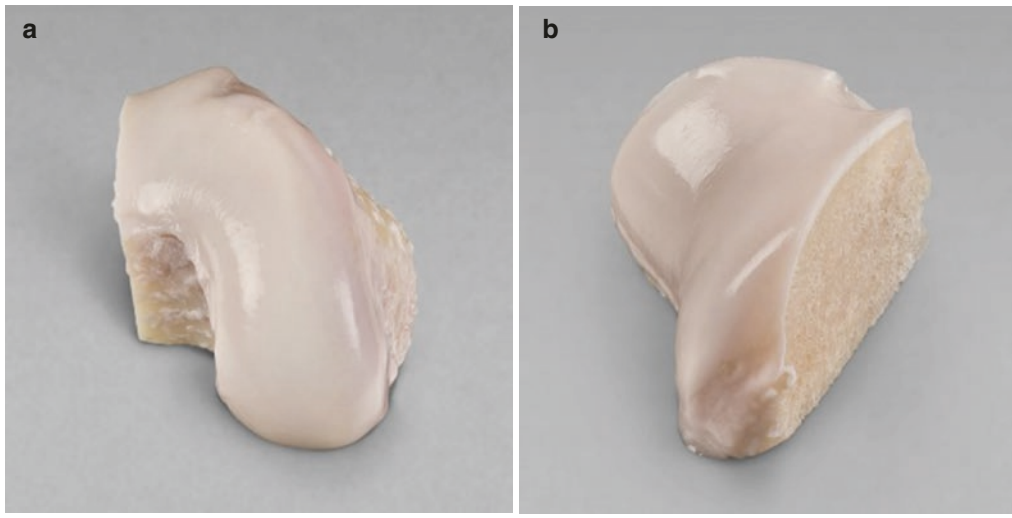

Figure 20.2.A.4: Osteochondral Allograft for Cartilage Repair Using the Dowel Technique: The Allograft Tissue Selection. (**a**) A femoral hemi-condyle is the graft used for the majority of cases. This is requested to treat unilateral lesions anywhere on the medial or lateral femoral condyle, respectively. (**b**) Lesions involving the central trochlea will require a whole trochlear allograft to be ordered. (**c**) The allograft needs to be size matched to the patient to ensure that the allograft matches the radius of curvature of the patient's femoral condyle following insertion. The allograft is sized from the X-rays or MRI scan and is based on the width of the femoral condyle 1 cm below the roof of the notch. When a suitable graft is found, an offer sheet is provided stating the dimensions of the allograft and the patient's condyle, so that a decision can be made as to its suitability. Usually, a tolerance of 2–3 mm is acceptable. There is no need for gender match. Currently, the convention is to use the ipsilateral condyle. However, data does suggest that if the proposed dowel is 20 mm or less then a medial or lateral condyle can be used irrespective of the defect location [4]. The graft expiration date is an important factor; before acceptance, it must be confirmed that the allograft can be implanted prior to this date in order to maintain cell viability and maximise clinical outcome. As the lesion in this case involved the weight-bearing area of the medial femoral condyle, a medial femoral condyle allograft was requested for this particular patient

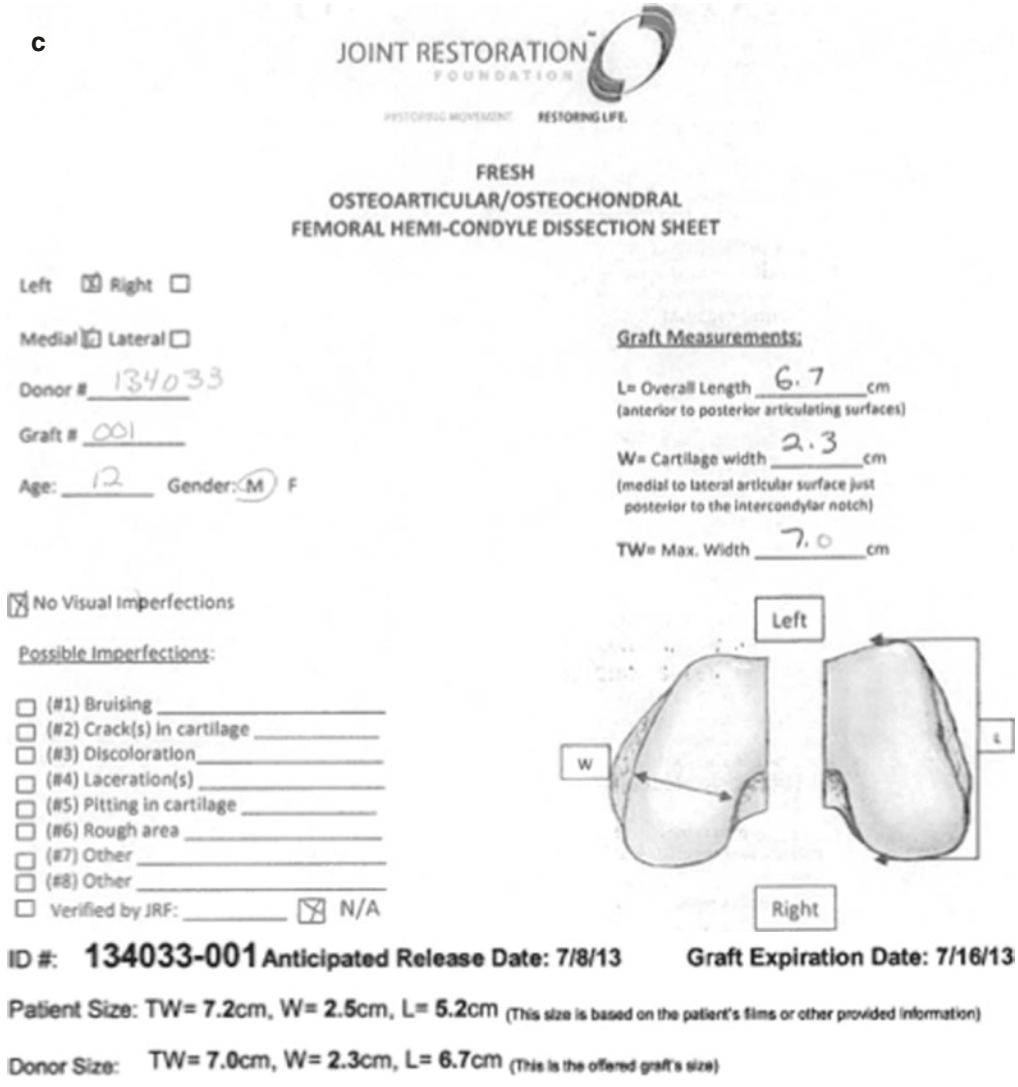

Figure 20.2.A.4: (continued)

Figure 20.2.A.5: Osteochondral Allograft for Cartilage Repair Using the Dowel Technique: The Transport of the Allograft from the Vendors. The allograft is transported in a polystyrene box containing ice blocks. The box does not come with a temperature log but has been validated to keep the allograft at 4 °C for 6 days. The allograft is triple packed with the allograft contained in the third layer stored within antibiotic-loaded media. The allograft must not be frozen, as this will result in cell death and will, therefore, affect the clinical outcome

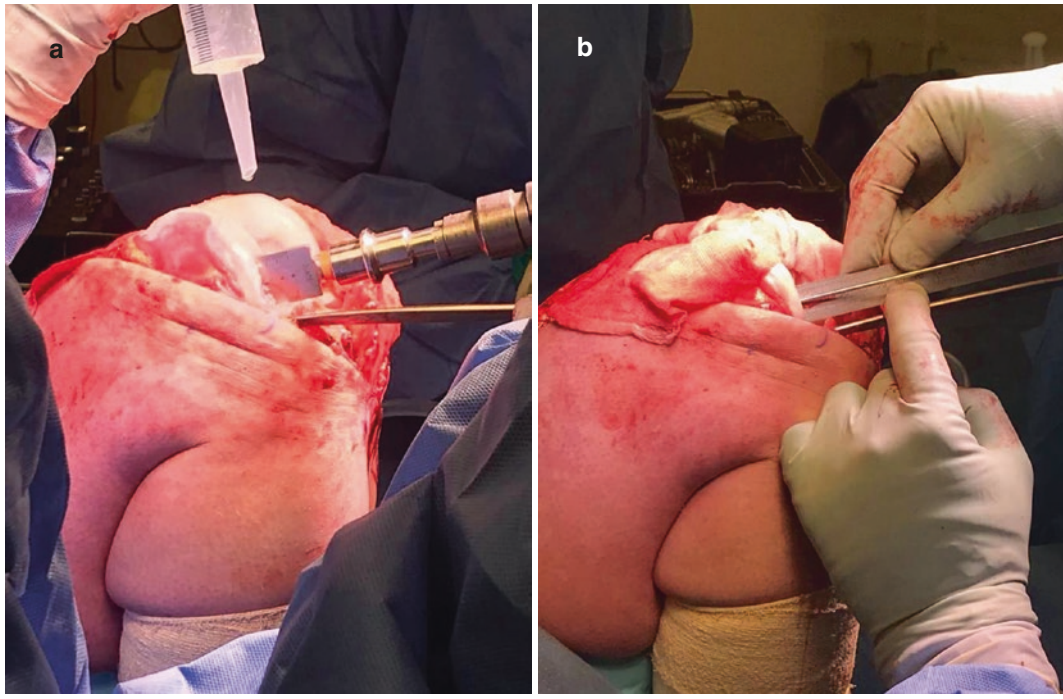

Figure 20.2.A.6: Osteochondral Allograft for Cartilage Repair Using the Dowel Technique: The Preparation of the Lesion. The sizing template is used to determine the size of the allograft core needed to reconstruct the defect. In this case, two 25 mm cores were required. The template is centred over the defect, and it is important to ensure that the template is perpendicular to the articular surface. A guide wire is then drilled through the centre of the template and the position of the template is checked again. The amount of bone on the allograft should be kept to a minimum, and ideally should be between 3 and 5 mm. (**a**) Thus the 25 mm drill is drilled over the guide wire down to the depth of approximately 7–8 mm from the cartilage surface. During drilling, the lesion should be constantly lavaged with normal saline in order to minimise chondrocyte injury of the adjacent cartilage. (**b**) The depth of the defect drilled should then be measured at the 12, 3, 6 and 9 o'clock positions. These measurements should be written down and then used to create an allograft of the corresponding depth. It is vitally important that these measurements are correct; if the depth is overestimated, the allograft created will be too proud relative to the surrounding cartilage and consequently will likely fail. In this case, two wires can be seen, one for each of the 25 mm cores. The position of the defect should be measured relative to the notch, terminal sulcus, and medial and lateral edges of the condyle. This is to ensure that the allograft core can be taken from the same location on the donor hemicondyle

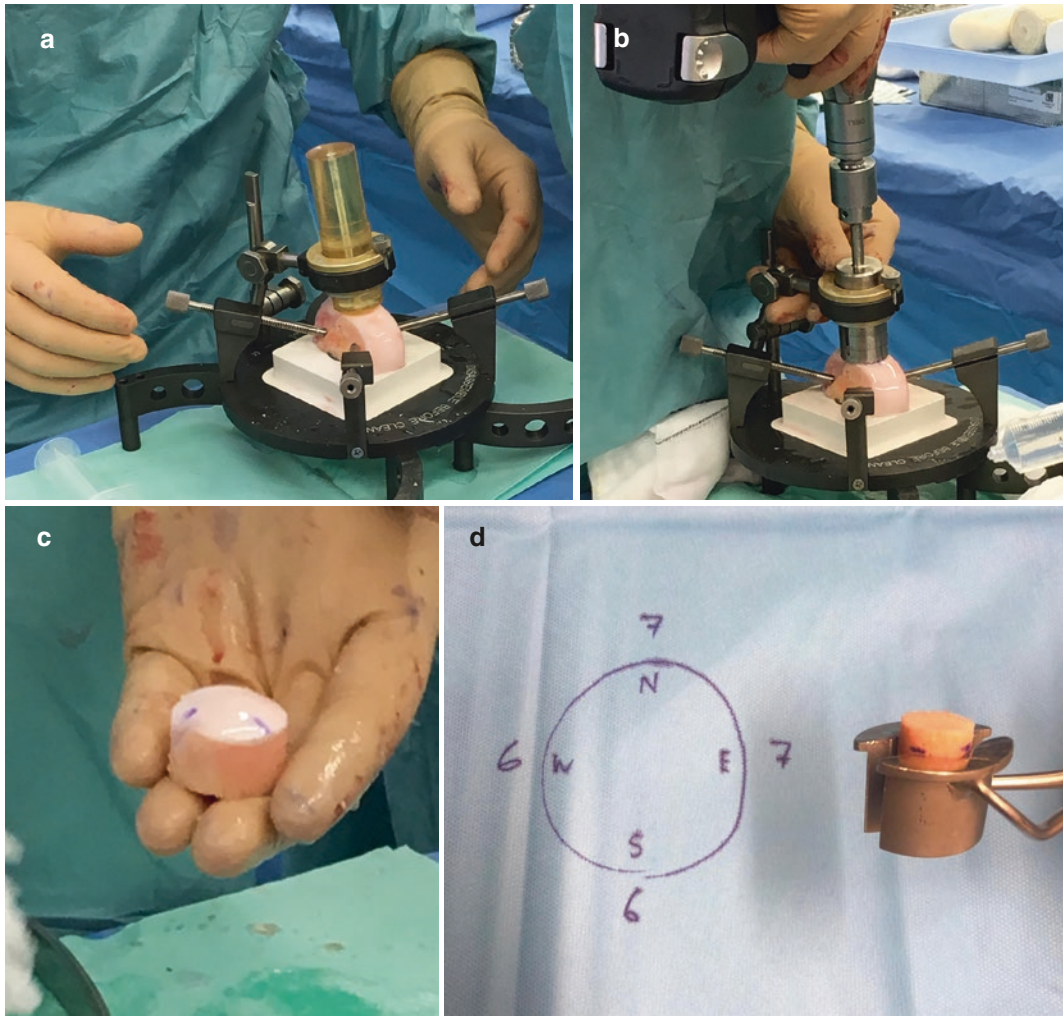

Figure 20.2.A.7: Osteochondral Allograft for Cartilage Repair Using the Dowel Technique: The Preparation of the Osteochondral Allograft. The corresponding location on the fresh hemicondyle is identified based on the previous measurements, and these are used to obtain the two 25 mm diameter dowels required. (**a**) A mega-OATS set (Arthrex, Naples, FL) was used to obtain the dowels from the corresponding location on the hemicondyle without damaging the allograft cartilage surface. The jig allows the 25 mm ring to be held in the required place whilst the core is taken. The 25 mm core template is used to ensure that the ring is in the correct location and perpendicular to the condyle. (**b**) Whilst reaming the allograft dowel the reamer is constantly irrigated to reduce heat and potential chondrocyte injury/death. (**c**) Before removing the dowel from the hemicondyle, the 12 o'clock position is identified using a marker pen to ensure the correct orientation of the allograft when implanted. A saw is often required to undercut the end of the dowel to remove it from the allograft. (**d**, **e**) The allograft dowel is then shaped to match the defect precisely. The amount of allograft bone implanted should be kept to a minimum to reduce the risk of any potential host immune response. 3–5 mm is usually the minimum bone required, but this can be increased up to 10 mm. Beyond this, it is recommended that the base of the defect is bone grafted with autologous bone to ensure that the maximum allograft bone implanted is limited to 10 mm. The previously taken measurements of the defect at 12, 3, 6 and 9 o'clock are then marked on the allograft. The dowel is then shaped to the corresponding measurements to ensure that it is not proud on implantation. This is done using the specialist clamp fixed at the required depth; the clamp then acts as a cutting guide for the sagittal saw. Prior to implantation, a power lavage is used to remove as much of the donor marrow elements from the bone as possible in order to minimise host immune response

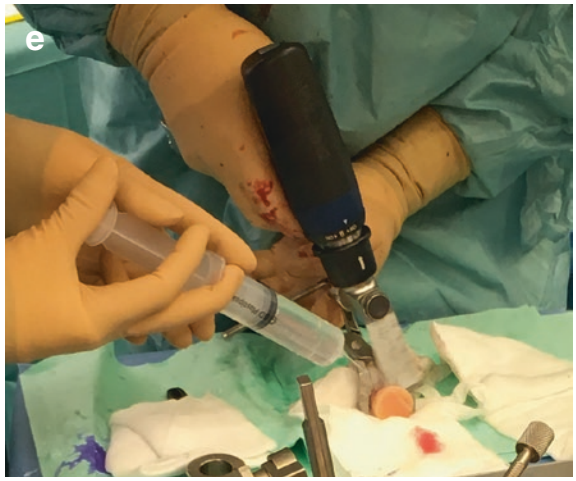

Figure 20.2.A.7: (continued)

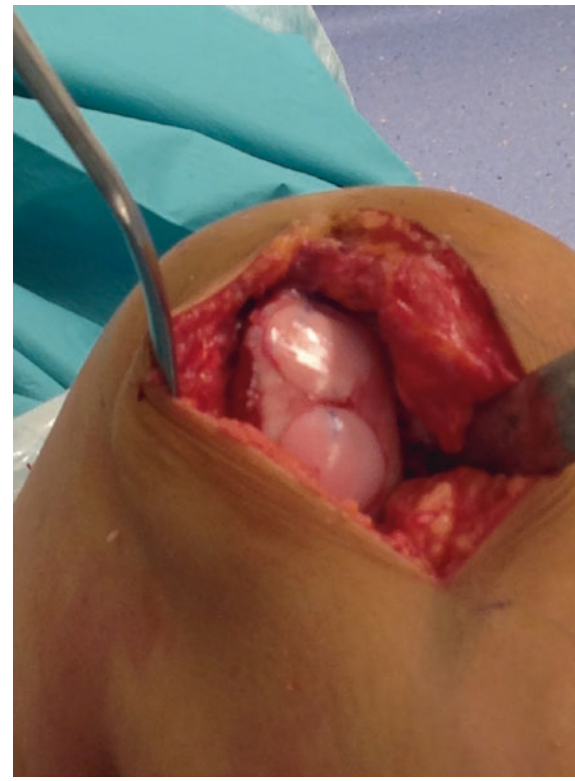

Figure 20.2.A.8: Osteochondral Allograft for Cartilage Repair Using the Dowel Technique: The Fixation of the Allograft. The final dowel is then implanted using only thumb pressure. The dowel is inserted with the previously made mark at the 12 o'clock position. Occasionally the corners of the bone dowel need to be smoothed with a nibbler to enable engagement. The allograft should not be heavily impacted as this will result in significant chondrocyte death. If performed correctly, the allograft should be press fit and so no further fixation is usually required. If the press fit is insufficient, then the dowel requires additional stabilisation with a headless compression screw which can be absorbable or non-absorbable depending on the surgeon's preference

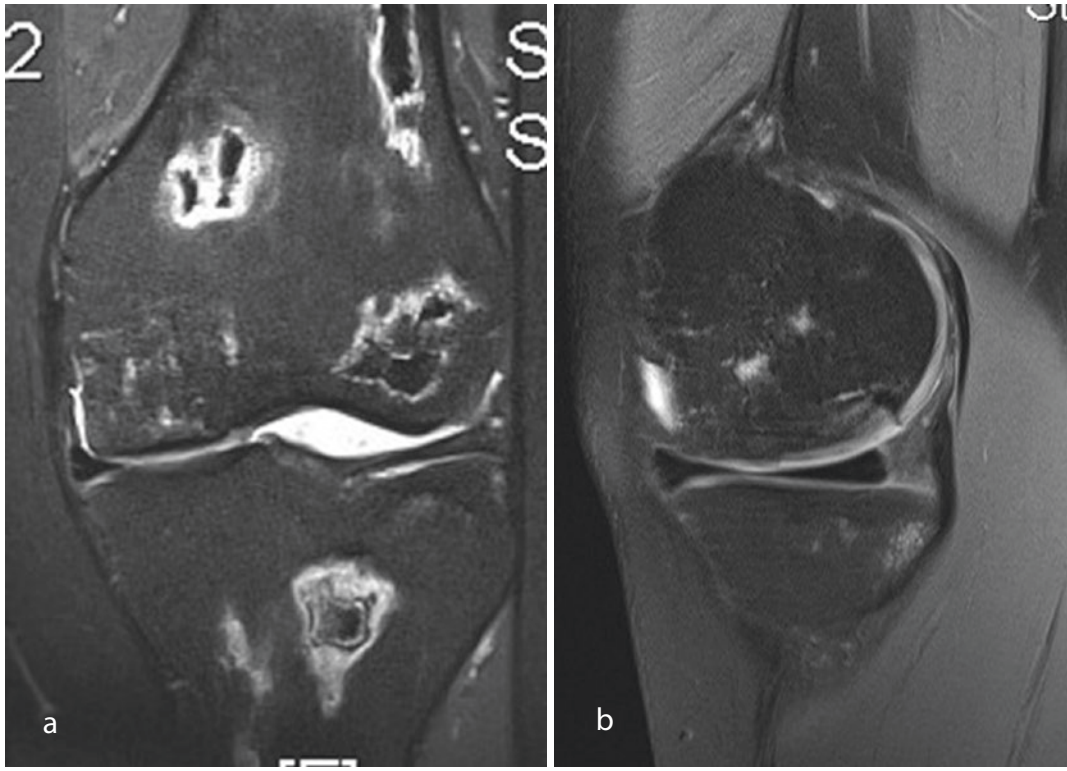

Figure 20.2.A.9: Osteochondral Allograft for Cartilage Repair Using the Dowel Technique: The Results of a Successful Osteochondral Allograft. A 22-year-old female operated with two osteochondral allograft plugs on medial femoral condyle following drug/steroid-induced osteonecrosis. The patient underwent MRI at 2-year follow-up which confirmed good integration of the allograft plugs with maintenance of the chondral layer. The patient's preoperative symptoms had completely resolved, and there was no deterioration in the other previously noted areas of avascular necrosis present within the lateral femoral condyle and tibia

20.2.B Osteochondral Allograft for Cartilage Repair—The Shell Technique

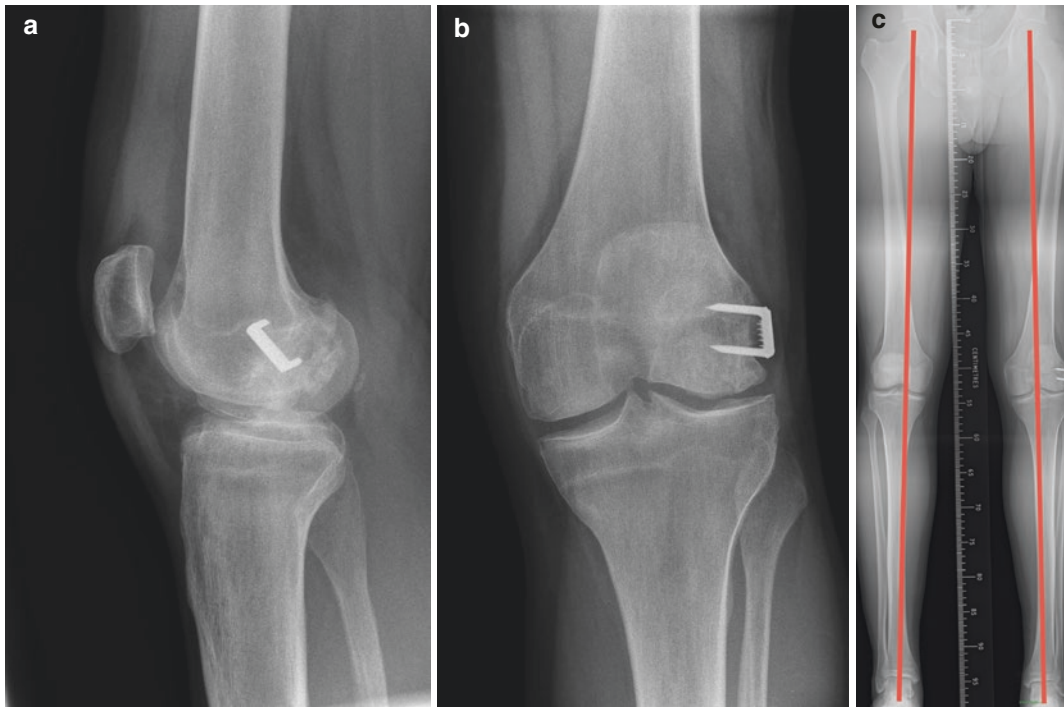

Figure 20.2.B.1: Osteochondral Allograft for the Cartilage Repair Using the Shell Technique: The Ideal Case Selection. A 29-year-old male underwent a frozen osteochondral allograft for a large osteochondritis dissecans of the right lateral femoral condyle 8 years ago. This was undertaken through a lateral parapatellar incision, and the lateral collateral ligament appeared to have been taken down to improve exposure before being reattached using a staple. He had a good clinical result for 3 years following the procedure but then developed lateral based knee pain on activity. (**a**, **b**) This deteriorated, and further investigation demonstrated that the allograft had fragmented with partial absorption. Despite an arthroscopy to remove loose bodies at the previous institution, the patient continued to suffer from locking, pain and swelling. On examination, there was lateral joint-line pain and a grade 2 effusion. (**c**) The knee was in neutral alignment. A decision was made to undertake a fresh osteochondral shell allograft to reconstruct his lateral compartment. A shell allograft was required due to the extensive area of damage and the inability to obtain perpendicular access to the posterior condyle from an anterior incision (even in deep flexion)

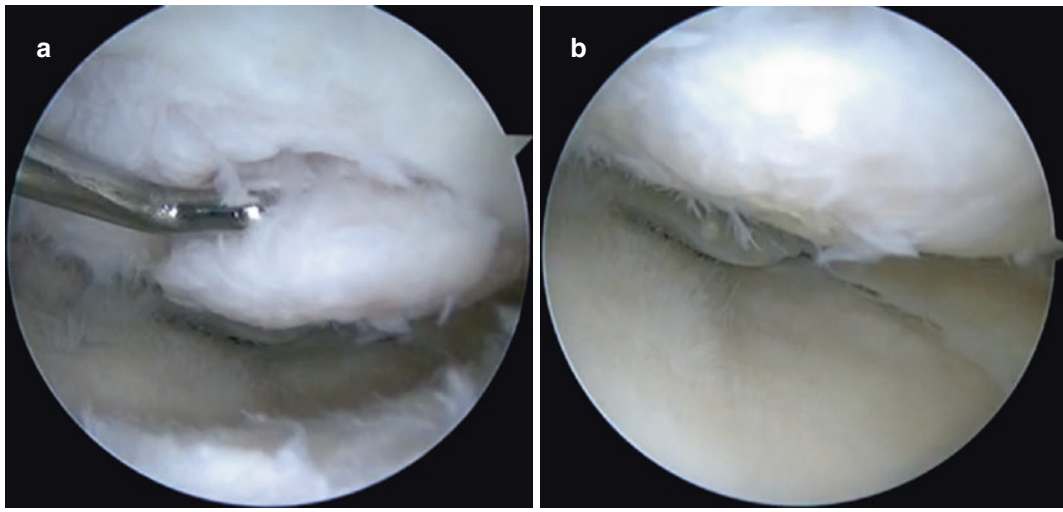

Figure 20.2.B.2: Osteochondral Allograft for Cartilage Repair Using the Shell Technique: The Arthroscopic Assessment of the Lesion. (**a**) Right-knee arthroscopic picture of a 29-year-old male, as viewed from the anterolateral portal, showed fragmentation of the entire lateral femoral condyle. (**b**) There is corresponding wear on the tibial plateau and meniscus. However, the meniscus and tibial surfaces were felt to be sufficiently intact to proceed with a femoral condyle allograft in isolation

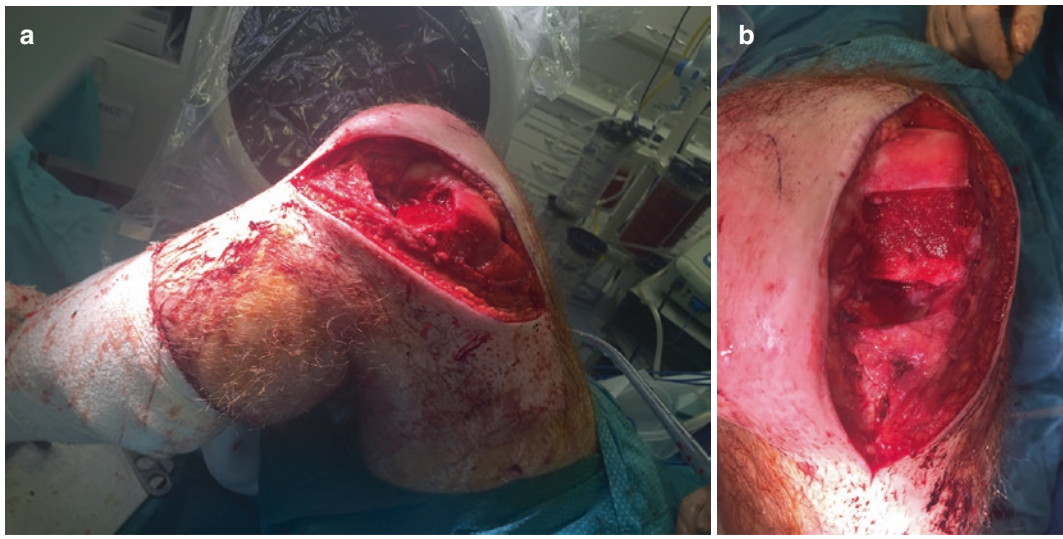

Figure 20.2.B.3: Osteochondral Allograft for Cartilage Repair Using the Shell Technique: The Preparation of the Lesion. (**a**) The previous lateral based incision was used, and a lateral parapatellar arthrotomy was performed to expose the failed previous osteochondral allograft of the lateral femoral condyle. The staple was removed, and the damaged areas of bone and cartilage were removed using a combination of osteotomes, a high-speed burr and an oscillating saw. Intraoperative fluoroscopy was used to guide the resection of the posterior condyle. (**b**) The resection of bone is minimised to 5 mm. However, the resection must be taken back to healthy bone. The extent of the resection carried out is measured relative to the notch and sulcus. These measurements are then translated to the allograft hemicondyle so that the identical area of the condyle is implanted to that resected

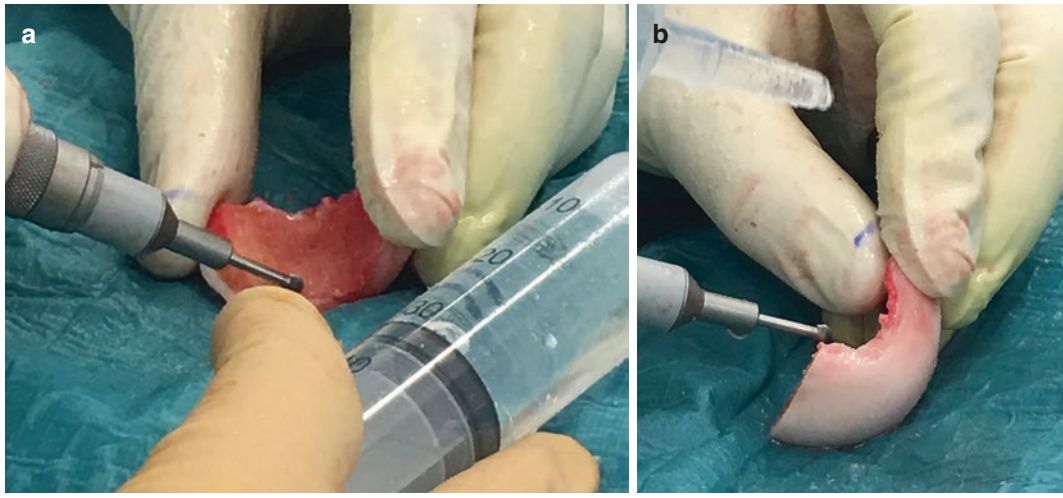

Figure 20.2.B.4: Osteochondral Allograft for Cartilage Repair Using the Shell Technique: The Instruments Required. There is no specialist instrumentation required for a shell osteochondral allograft. The allograft hemicondyle is shaped to match the defect using a sagittal saw and a high-speed burr. Constant lavage is used to prevent thermal injury and chondrocyte death. Care must be taken to ensure that the allograft does not become contaminated during the preparation. There is no specialist holding device, and so the allograft can easily be dislodged out of the surgeon's hand if the burr digs into the graft or gets caught in soft tissue

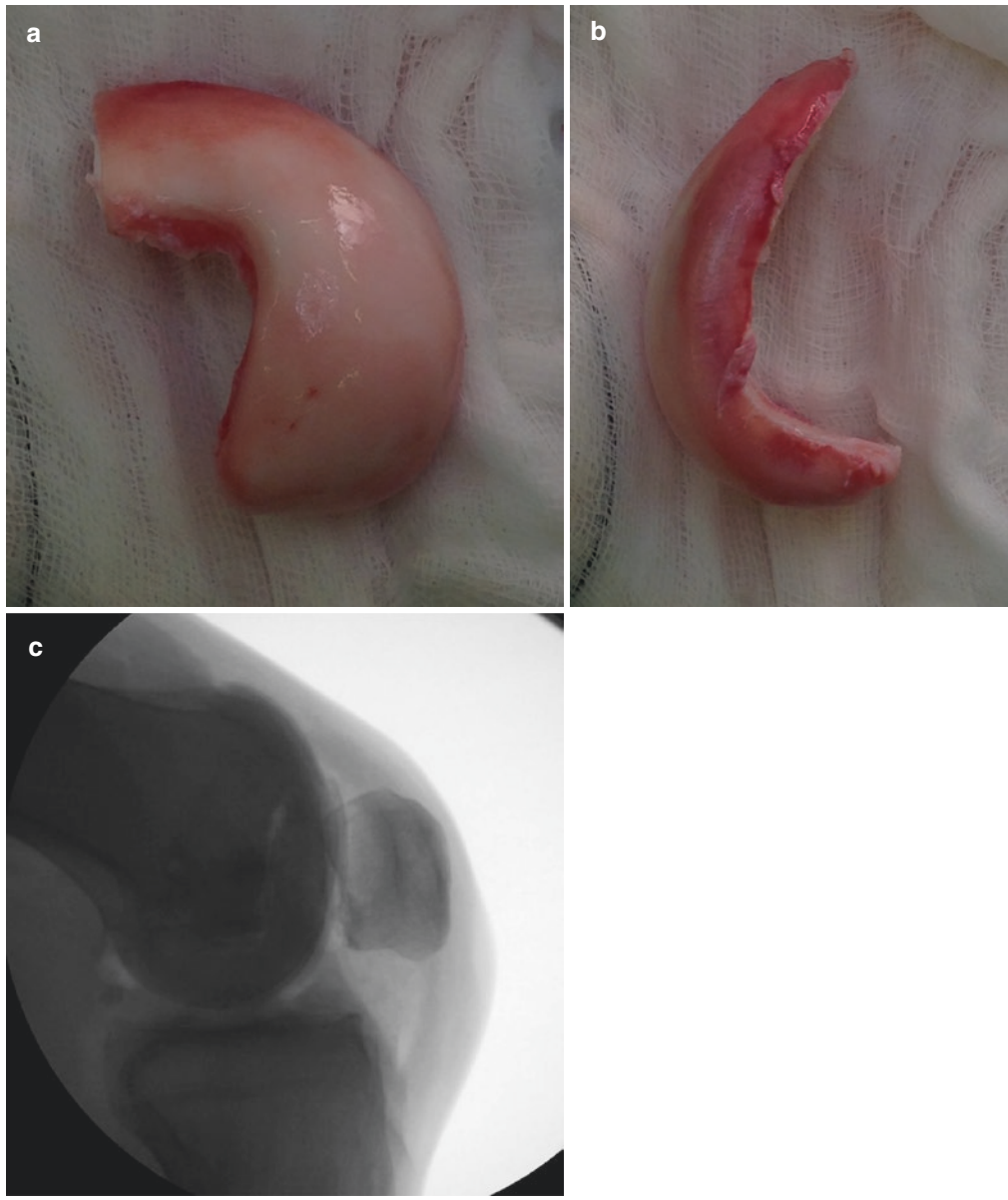

Figure 20.2.B.5: Osteochondral Allograft for Cartilage Repair Using the Shell Technique: The Preparation of the Osteochondral Allograft Tissues. (**a**, **b**) A matching allograft is created free hand to perfectly match the resected area. The previous measurement of the resection site relative to the notch is transferred to the allograft, and it is cut to the appropriate length. The hemicondyle is then shaped using a combination of a small oscillating saw and high-speed burr. Ideally, a maximum of 5 mm of bone is implanted to reduce the risk of a potential immune response. Care is taken to shape the allograft and the resection site so that the shape is slightly curved, as a sharp angle on the cut surface could act as a stress riser and consequently increase the risk of a potential allograft fracture. The shaping process involves a significant amount of trial and error and continues until an acceptable match is achieved both visually and on fluoroscopy. (**c**) The fluoroscopy is particularly useful to help determine where allograft/host mismatch exists and therefore direct further shaping. With large shell allografts, the radius of curvature of the condyle must be recreated, and the interface between the allograft and the native cartilage must not be prominent. The fluoroscopy is also used to ensure that the native coronal angle of the joint line has been recreated. When the shaping process has finished, the bone on the allograft is thoroughly irrigated with power lavage in an attempt to remove as much donor marrow elements as possible; as residual donor marrow has been implicated in a low-grade immune response and potential non-union

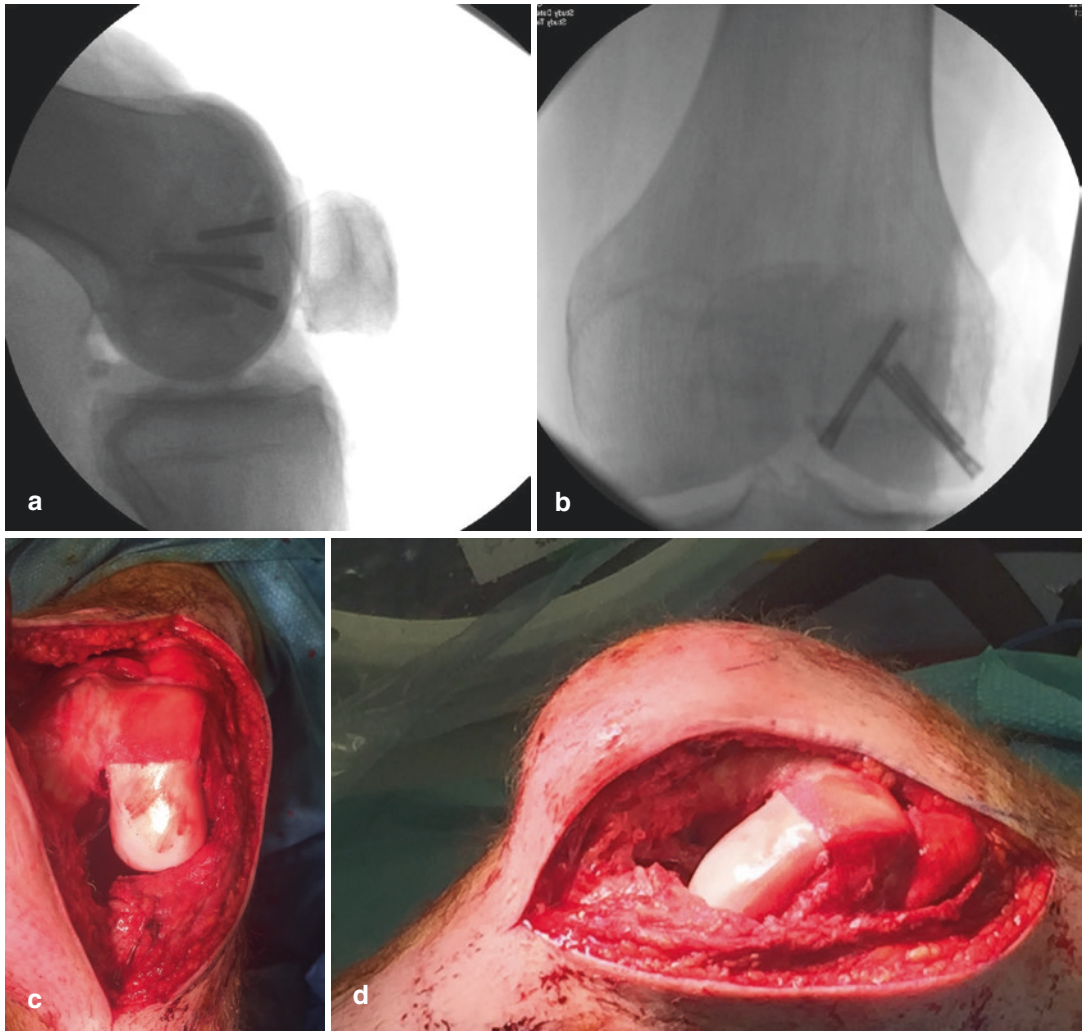

Figure 20.2.B.6: Osteochondral Allograft for Cartilage Repair Using the Shell Technique: The Fixation of Allograft at the Defect Site. A 29-year-old male is treated with an osteochondral shell allograft on the lateral femoral condyle. (**a**, **b**) After a satisfactory position of the allograft is achieved, it is stabilised by placing headless compression screws around the periphery of the allograft. Ideally, the allograft should be compressed against the resection site so that there is no visible gap macroscopically or on fluoroscopy. (**c**, **d**) The stability of the final construct is confirmed by placing the knee through a range of motion and checking for allograft movement. The retinacula, subcutaneous tissue and skin are then closed in the usual manner

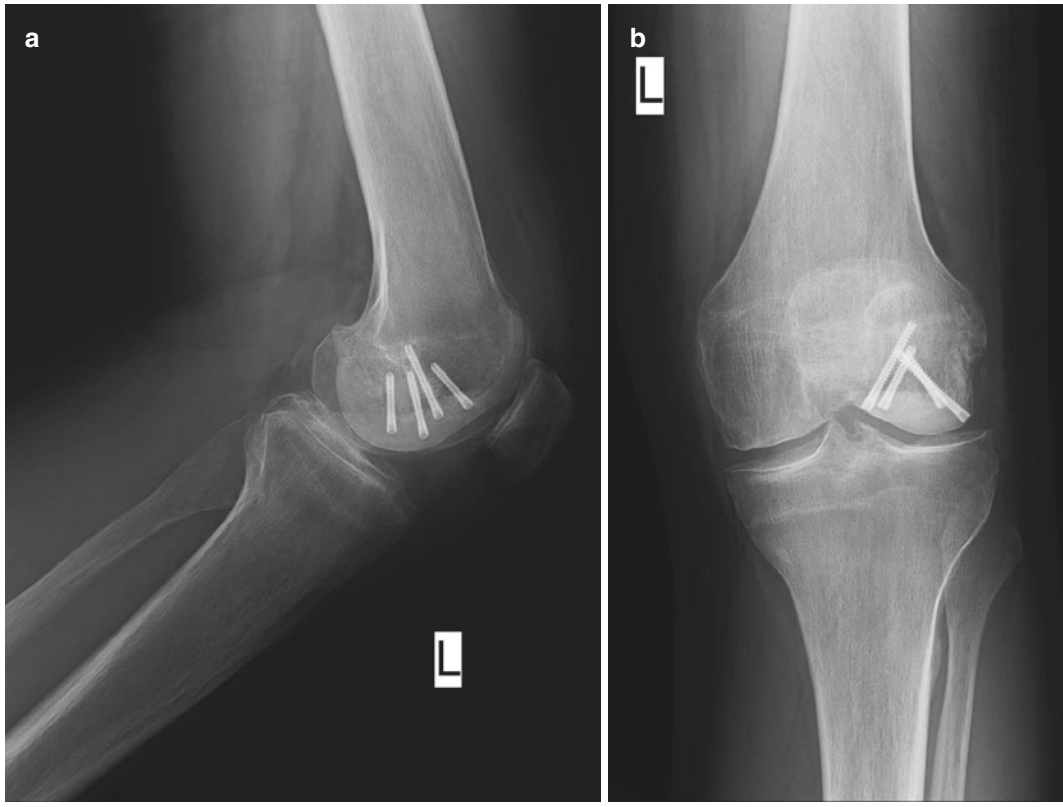

Figure 20.2.B.7: Osteochondral Allograft for Cartilage Repair Using the Shell Technique: The Radiological Results of a Successful Osteochondral Allograft. A 12-month follow-up X-ray of a 29-year-old male treated with an osteochondral shell allograft on the lateral femoral condyle showing good integration. Serial X-rays are usually undertaken to ensure that union between the allograft and the resection site is achieved, which typically occurs by 6 months post-surgery. Follow-up continues until 2 years to ensure graft revascularisation. MRI is of limited benefit given the use of metal screws. Assessment of allograft integration can be made based on the bony integration and maintenance of the joint space

Figure 20.2.B.8: Osteochondral Allograft for Cartilage Repair: The Rehabilitation and Bracing. Patients are generally permitted unrestricted, full range of motion unless a concomitant reconstructive procedure dictates knee motion restriction. Braces are typically used for patellofemoral joint allografts, where flexion is limited to 40° for 4–6 weeks. When a shell technique is used to replace the entire posterior condyle, flexion is limited to 30° for the first 2 weeks, 60° between 2 and 4 weeks and 90° between 4 and 6 weeks. Following a bipolar tibial and femoral allograft, where the femoral and tibial surface has been resurfaced, an unloader brace can be used to prevent excessive stress on the reconstructed sites. CPM can be used for 6–8 h per day for the initial 6 weeks to avoid adhesions, promote the healing process and encourage graft nutrition if available.

Supervised physical therapy commences after the initial post-operative visit, and the patient is kept non-weight bearing or toe-touch weight bearing for the first 6–12 weeks, depending on the size of the graft, type of fixation and radiographic signs of incorporation. By 3 months, patients are expected to have a full range of motion and regain quadriceps strength. At 4–6 months, functional rehabilitation should be complete, and patients can begin light recreational activities avoiding the excessive impact on the allograft. Shell allografts need to be protected for longer given that they are usually larger uncontained lesions and therfore exposed to greater loads compared to dowel grafts

20.3 Take-Home Message

Fresh osteochondral allograft is an established technique for cartilage repair which has been used in clinical practice for more than 20 years. It is an excellent technique for addressing significant osteochondral lesions within the knee from conditions such as osteochondritis dissecans, avascular necrosis and trauma. Unlike autologous chondrocyte implantation, OCA results are not negatively affected when undertaken following previous failed cartilage repair and so provide a good salvage option. Graft availability is the main limitation to use of this form of treatment, and surgeons must work closely with their tissue banks to ensure that correctly sized grafts are implanted prior to graft expiration. There are no comparative trials of osteochondral allograft versus any other forms of cartilage repair. This is principally due to the fact that osteochondral allografts, unlike other forms of cartilage repair, are indicated for large bone and cartilage lesions. The logistics and timing of graft implantation would also make any comparative trial difficult to perform. However, the long-term results (summarised in Table 20.3.1) are excellent and are comparative to those of autologous chondrocyte implantation [30].

Table 20.3.1 A summary of the literature on the survival of fresh osteochondral allograft in the knee

	Graft survival—osteochondral allografts			
Authors	1–5 years	6–10 years	11–15 years	More than 15 years
Aubin [5]		85%—10 years	74%—15 years	
Beaver [6]	75%—5 years	64%—10 years	63%—14 years	
Briggs [7]	89.5%—5 years	74.7%—10 years	74%—15 years	
Cameron [8]	100%—5 years	91.7%—10 years		
Emmerson [9]	91%—5 years	85%—7.7 years 76%—10 years	76%—15 years	
Frank [10]	87%—5 years			
Frank [11]	86%—5 years			
Garrett [12]	94%—2 to 9 years			
Ghazavi [13]	95%—5 years	85%—7.5 years 71%—10 years		66%—20 years
Görtz [14]	89%—5.6 years			
Gracitelli [15]		86–87.6%—10 years		
Gracitelli [16]	87.8%—5 years	82%—10 years	74.9%—15 years	
Gracitelli [17]	78.1%—5 years	78.1%—10 years		
Gross [18]	95%—5 years	85%—10 years	74%—15 years	
Horton [19]		61%—10 years		
Jamali [20]		75%—7.8 years 67%—10 years		
LaPrade [21]	100%—3 years			
Levy [22]		82%—10 years	74%—15 years	66%—20 years
Marco [23]	86.6%—3.2 years			
McCarthy [24]		100%—6 years		
McCulloch [25]*	96%—3 years			
Murphy [3]	93%—5 years	90%—10 years		
Raz [26]		91%—10 years	84%—15 years	69%—20 years 59%—25 years
Shasha [27]	95%—5 years	80%—10 years	65%—15 years	
Shasha [28]	95%—5 years	71%—10 years		66%—20 years
Tirico [29]	97.2%—5 years	93.5%—10 years		

*adolescents and pediatric

References

1. Pearsall AWT, Tucker JA, Hester RB, Heitman RJ. Chondrocyte viability in refrigerated osteochondral allografts used for transplantation within the knee. Am J Sports Med. 2004;32(1):125–31.
2. Zou S, Dodd RY, Stramer SL, Strong DM. Probability of viremia with HBV, HCV, HIV, and HTLV among tissue donors in the United States. N Engl J Med. 2004;351(8):751–9.
3. Murphy RT, Pennock AT, Bugbee WD. Osteochondral allograft transplantation of the knee in the pediatric and adolescent population. Am J Sports Med. 2014;42(3):635–40.
4. Yanke AB, Urita A, Shin JJ, Cvetanovich GL, Moran EK, Bach BR Jr, Cole BJ, Inoue N, Verma NN. Topographic analysis of the distal femoral condyle articular cartilage surface: adequacy of the graft from opposite condyles of the same or different size for the osteochondral allograft transplantation. Cartilage. 2019;10(2):205–13. Epub 2018 Jan 16.
5. Aubin PP, Cheah HK, Davis AM, Gross AE. Long-term follow-up of fresh femoral osteochondral allografts for posttraumatic knee defects. Clin Orthop Relat Res. 2001;(391 Suppl):S318–327.
6. Beaver RJ, Mahomed M, Backstein D, Davis A, Zukor DJ, Gross AE. Fresh osteochondral allografts for post-traumatic defects in the knee. A survivorship analysis. J Bone Joint Surg Br. 1992;74(1):105–10.
7. Briggs DT, Sadr KN, Pulido PA, Bugbee WD. The use of Osteochondral allograft transplantation for primary treatment of cartilage lesions in the knee. Cartilage. 2015;6(4):203–7.
8. Cameron JI, Pulido P, DeYoung A, Gortz S, Bugbee W. Outcome following isolated osteochondral allograft transplantation of the femoral trochlea. Orthop J Sports Med. 2015;3(3 Suppl):2325967115S2325900002.
9. Emmerson BC, Gortz S, Jamali AA, Chung C, Amiel D, Bugbee WD. Fresh osteochondral allografting in the treatment of osteochondritis dissecans of the femoral condyle. Am J Sports Med. 2007;35(6):907–14.
10. Frank RM, Lee S, Cotter EJ, Hannon CP, Leroux T, Cole BJ. Outcomes of osteochondral allograft transplantation with and without concomitant meniscus allograft transplantation: a comparative matched group analysis. Am J Sports Med. 2018;46(3):573–80.
11. Frank RM, Lee S, Levy D, Poland S, Smith M, Scalise N, Cvetanovich GL, Cole BJ. Osteochondral allograft transplantation of the knee: analysis of failures at 5 years. Am J Sports Med. 2017;45(4):864–74.
12. Garrett JC. Fresh osteochondral allografts for treatment of articular defects in osteochondritis dissecans of the lateral femoral condyle in adults. Clin Orthop Relat Res. 1994;(303):33–37.
13. Ghazavi MT, Pritzker KP, Davis AM, Gross AE. Fresh osteochondral allografts for post-traumatic osteochondral defects of the knee. J Bone Joint Surg Br. 1997;79(6):1008–13.
14. Görtz S, De Young AJ, Bugbee WD. Fresh osteochondral allografting for steroid-associated osteonecrosis of the femoral condyles. Clin Orthop Relat Res. 2010;468(5):1269–78.
15. Gracitelli GC, Meric G, Briggs DT, Pulido PA, McCauley JC, Belloti JC, Bugbee WD. Fresh osteochondral allografts in the knee: comparison of primary transplantation versus transplantation after failure of previous subchondral marrow stimulation. Am J Sports Med. 2015;43(4):885–91.
16. Gracitelli GC, Meric G, Pulido PA, McCauley JC, Bugbee WD. Osteochondral allograft transplantation for knee lesions after failure of cartilage repair surgery. Cartilage. 2015;6(2):98–105.
17. Gracitelli GC, Moraes VY, Franciozi CE, Luzo MV, Belloti JC. Surgical interventions (microfracture, drilling, mosaicplasty, and allograft transplantation) for treating isolated cartilage defects of the knee in adults. Cochrane Database Syst Rev. 2016;9:CD010675.
18. Gross AE, Kim W, Las Heras F, Backstein D, Safir O, Pritzker KP. Fresh osteochondral allografts for posttraumatic knee defects: long-term followup. Clin Orthop Relat Res. 2008;466(8):1863–70.
19. Horton MT, Pulido PA, McCauley JC, Bugbee WD. Revision osteochondral allograft transplantations: do they work? Am J Sports Med. 2013;41(11):2507–11.
20. Jamali AA, Emmerson BC, Chung C, Convery FR, Bugbee WD. Fresh osteochondral allografts: results in the patellofemoral joint. Clin Orthop Relat Res. 2005;(437):176–185.
21. LaPrade RF, Botker J, Herzog M, Agel J. Refrigerated osteoarticular allografts to treat articular cartilage defects of the femoral condyles. A prospective outcomes study. J Bone Joint Surg Am. 2009;91(4):805–11.
22. Levy YD, Görtz S, Pulido PA, McCauley JC, Bugbee WD. Do fresh osteochondral allografts successfully treat femoral condyle lesions? Clin Orthop Relat Res. 2013;471(1):231–7.
23. Marco F, Lopez-Oliva F, Fernandez Fernandez-Arroyo JM, de Pedro JA, Perez AJ, Leon C, Lopez-Duran L. Osteochondral allografts for osteochondritis dissecans and osteonecrosis of the femoral condyles. Int Orthop. 1993;17(2):104–8.
24. McCarthy MA, Meyer MA, Weber AE, Levy DM, Tilton AK, Yanke AB, Cole BJ. Can competitive athletes return to high-level play after osteochondral allograft transplantation of the knee? Arthroscopy. 2017;33(9):1712–7.
25. McCulloch PC, Kang RW, Sobhy MH, Hayden JK, Cole BJ. Prospective evaluation of prolonged fresh osteochondral allograft transplantation of the femoral condyle: minimum 2-year follow-up. Am J Sports Med. 2007;35(3):411–20.
26. Raz G, Safir OA, Backstein DJ, Lee PTH, Gross AE. Distal femoral fresh osteochondral allografts: follow-up at a mean of twenty-two years. JBJS. 2014;96(13):1101–7.

27. Shasha N, Aubin PP, Cheah HK, Davis AM, Agnidis Z, Gross AE. Long-term clinical experience with fresh osteochondral allografts for articular knee defects in high demand patients. Cell Tissue Bank. 2002;3(3):175–82.
28. Shasha N, Krywulak S, Backstein D, Pressman A, Gross AE. Long-term follow-up of fresh tibial osteochondral allografts for failed tibial plateau fractures. J Bone Joint Surg Am. 2003;85-A(Suppl 2):33–9.
29. Tirico LEP, McCauley JC, Pulido PA, Bugbee WD. Lesion size does not predict outcomes in fresh osteochondral allograft transplantation. Am J Sports Med. 2018;46(4):900–7.
30. Jones KJ, Kelley BV, Arshi A, McAllister DR, Fabricant PD. Comparative effectiveness of cartilage repair with respect to the minimal clinically important difference. Am J Sports Med. 2019;47(13):3284–93. [Epub ahead of print].

The Illustrative 3D Bioprinting in Cartilage Repair

21

Timothy F. Reed, Pooja N. Swami,
Taylor L. Mustapich, and Daniel A. Grande

21.1 Introduction

Chondral and osteochondral lesions are extremely challenging scenarios in orthopedic health due to their lack of regenerative and repair abilities. 3D bioprinting is an emerging technology with great applications in this field, as it can be used to build constructs that can mimic cartilage anatomy and physiology. 3D bioprinting is the process of dispensing a biocompatible material (bio-ink) in a precise layer-by-layer pattern, creating a three-dimensional cellular construct that preserves cell function and viability and can be expected to mimic the physiological behavior of the native tissue. It is a three-step process: preprinting, where a design is created using computer-aided design (CAD) software to generate a GCode, which is read by the 3D printer; bioprinting, where a cell-laden hydrogel is extruded in a layer-by-layer fashion creating a 3D rendering of the design; and post-printing, where a construct may be incubated and put through various analyses to evaluate properties of the construct and cell viability after undergoing the mechanical stress of printing. This chapter describes and illustrates the workflow of 3D printing and bioprinting, important considerations in the selection of biomaterials, criteria for an ideal bio-ink, and applications of 3D bioprinting in the field of medical research and healthcare and finally its application into cartilage repair.

T. F. Reed
Donald and Barbara Zucker School of Medicine at Hofstra/Northwell, Hempstead, NY, USA

Orthopaedic Research Laboratory at Feinstein Institute for Medical Research, Northwell Health, Manhasset, NY, USA
e-mail: treed3@pride.hofstra.edu

P. N. Swami · T. L. Mustapich
Orthopaedic Research Laboratory at Feinstein Institute for Medical Research, Northwell Health, Manhasset, NY, USA
e-mail: pswami@northwell.edu; mustapic@mail.einstein.yu.edu

D. A. Grande (✉)
Donald and Barbara Zucker School of Medicine at Hofstra/Northwell, Hempstead, NY, USA

Orthopaedic Research Laboratory at Feinstein Institute for Medical Research, Northwell Health, Manhasset, NY, USA

Department of Orthopaedic Surgery, Northwell Health, Great Neck, NY, USA
e-mail: dgrande@northwell.edu

D. R. Goyal (ed.), *The Illustrative Book of Cartilage Repair*,
https://doi.org/10.1007/978-3-030-47154-5_21

21.2 The Illustrations

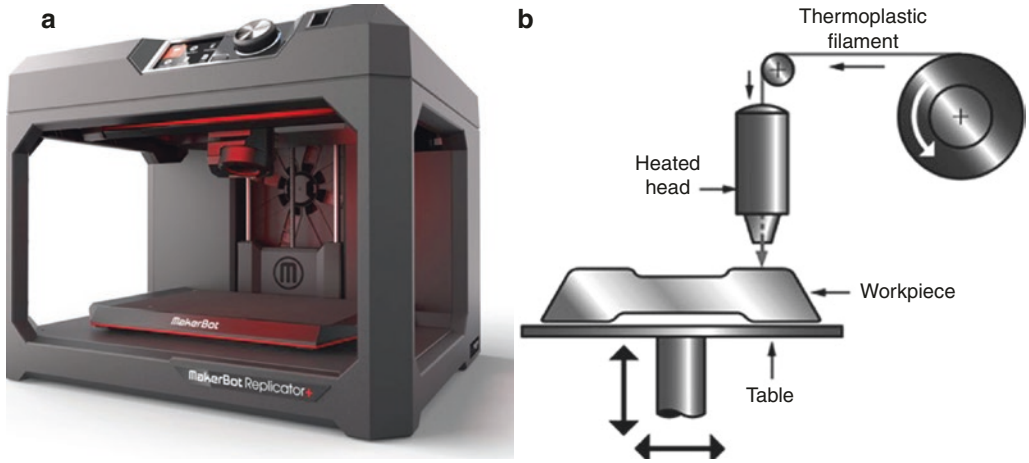

Figure 21.2.1: The Basics of 3D Printing. 3D printing is a process in which a physical object is produced from a three-dimensional digital model, typically by laying down many successive thin layers of a material. A broad array of machines are available, and a wide variety of printing techniques can be implemented to create these objects. (**a**) A sample 3D printer, MakerBot Replicator+. © MakerBot Industries, LLC 2016 [1]. (**b**) Basic schematic for the process of 3D printing involving extrusion of the thermoplastic filament through a heated extruder head, fusing as deposited and solidifying resulting in a 3D construct on the print bed [2]

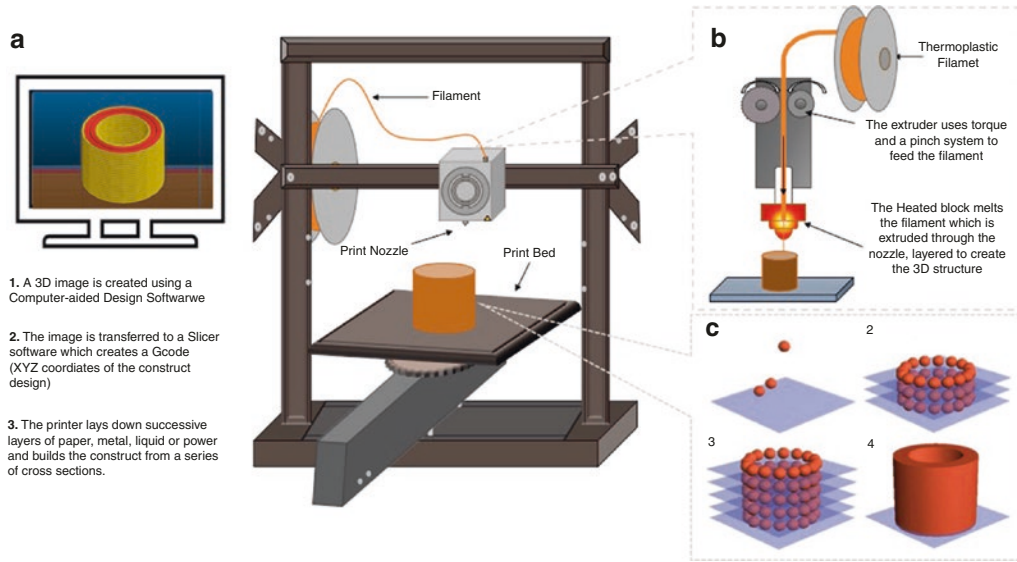

Figure 21.2.2: The Process of 3D Printing. (**a**) In the process of fused deposition modeling (FDM), a 3D image is rendered using computer-aided design (CAD) software, which is subsequently sent to the printer to create the final 3D construct. (**b**) In order to be printed, the filament (orange) is fed through a gear into a heated extruder head to achieve a molten state before being delivered via the nozzle. The extruder head temperature is adjusted as per the filament properties, allowing the filament to melt. As the melted filament is extruded through the nozzle and laid on the print bed, the room temperature cools down the filament, solidifying it to the shape it has been deposited in. (**c**) The printer then deposits successive cross sections of the material to produce the construct. Thermoplastics such as polycaprolactone (PCL), polylactic acid (PLA), and acrylonitrile butadiene styrene (ABS) are commonly used filaments for FDM [3]

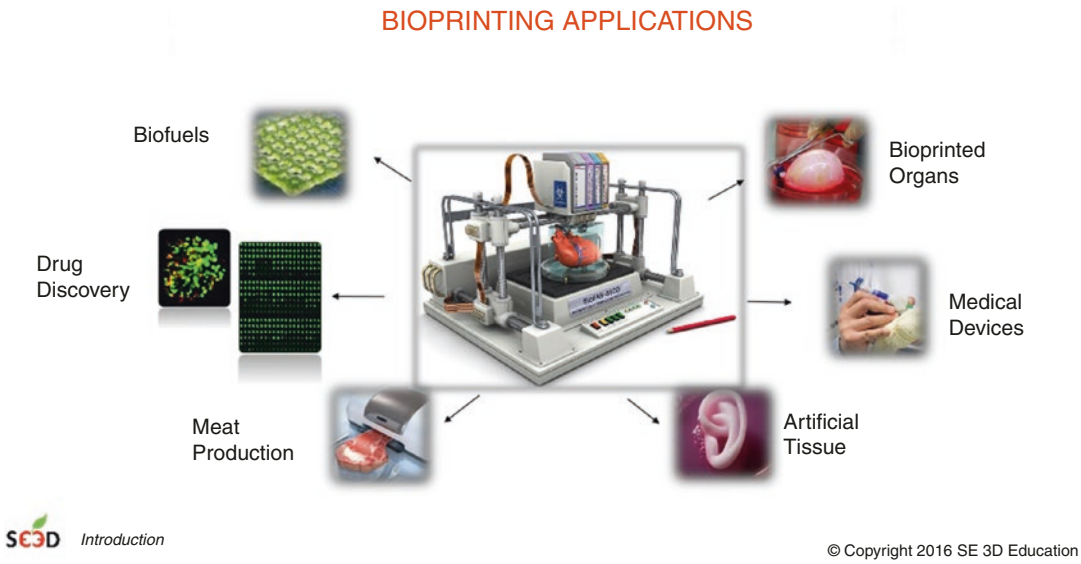

Figure 21.2.3: What Is "Bio"-Printing?. 3D printing and 3D bioprinting follow the same working principle where a material is extruded to build a 3D construct. However, the former technique uses materials such as metal, thermoplastics, and resin, whereas 3D bioprinting involves the use of biocompatible materials (cell-laden bio-ink) to produce bioengineered structures. Briefly, live cells are mixed homogenously with a biocompatible hydrogel and dispensed layer by layer, creating a three-dimensional construct, as seen in standard 3D printing. The value of bioprinted constructs lies in the preservation of cell viability and function. Bioprinting can be applied to a multitude of disciplines, including regenerative medicine, pharmacokinetics, and basic cell biology. As with standard 3D printing, a variety of machinery, methods, and materials can be utilized [4]

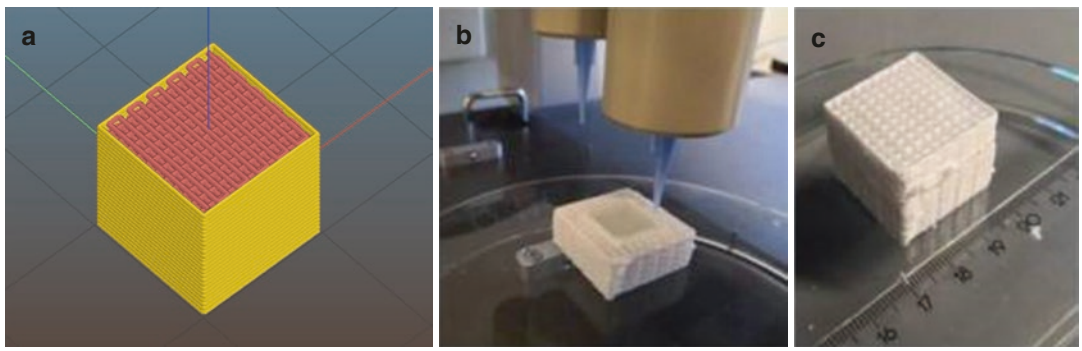

Figure 21.2.4: The 3D Bioprinted Cube. A three-dimensional printed cube with porous faces demonstrates the versatility of bio-inks as a medium for 3D printing. Constructs with microstructures offer a greater surface area for cell attachment and proliferation and provide opportunity for targeted delivery of external stimuli, such as growth factors. In an operative setting, structures with flat surfaces are preferred as they are easy to handle. (**a**) CAD-rendered image of a cube (25 × 25 × 25 mm) with pores (2 × 2 mm) through top and bottom face. (**b**) Layer-by-layer extrusion of the bio-ink to print the rendered model. (**c**) Final 3D-printed construct [5]

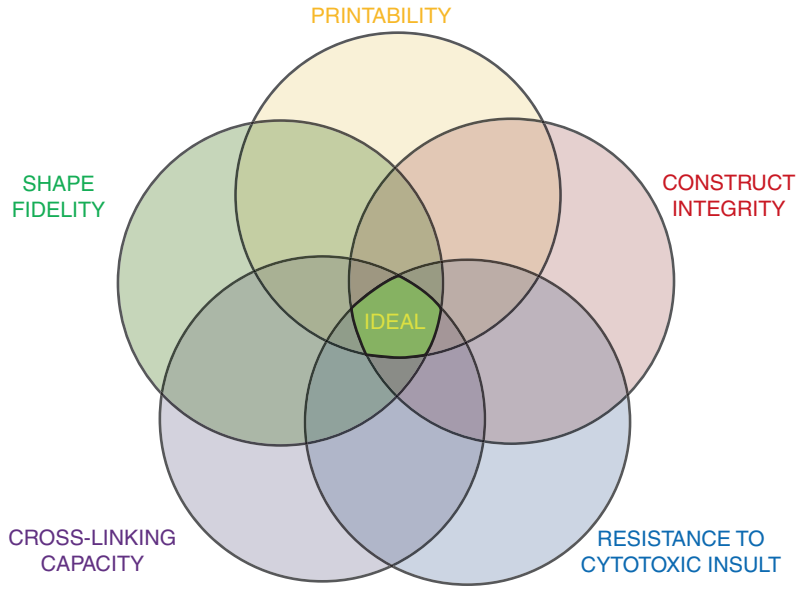

Figure 21.2.5: Ideal Criteria for Hydrogel-Based Bio-Inks in 3D Bioprinting. An ideal biocompatible hydrogel meets five essential criteria: **printability**, to enable consistent and uniform extrusion of the hydrogel; ability to **cross-link**, to avoid deformation post-printing and hence contributing to a high **construct integrity**, that ensures wholeness or strength of a construct through its ability to withstand internal damage due to external environment; **shape fidelity**, to achieve a 3D construct true to the desired shape and structure; **resistance to cytotoxic insult**, to maximize therapeutic effect and avoid immunogenicity

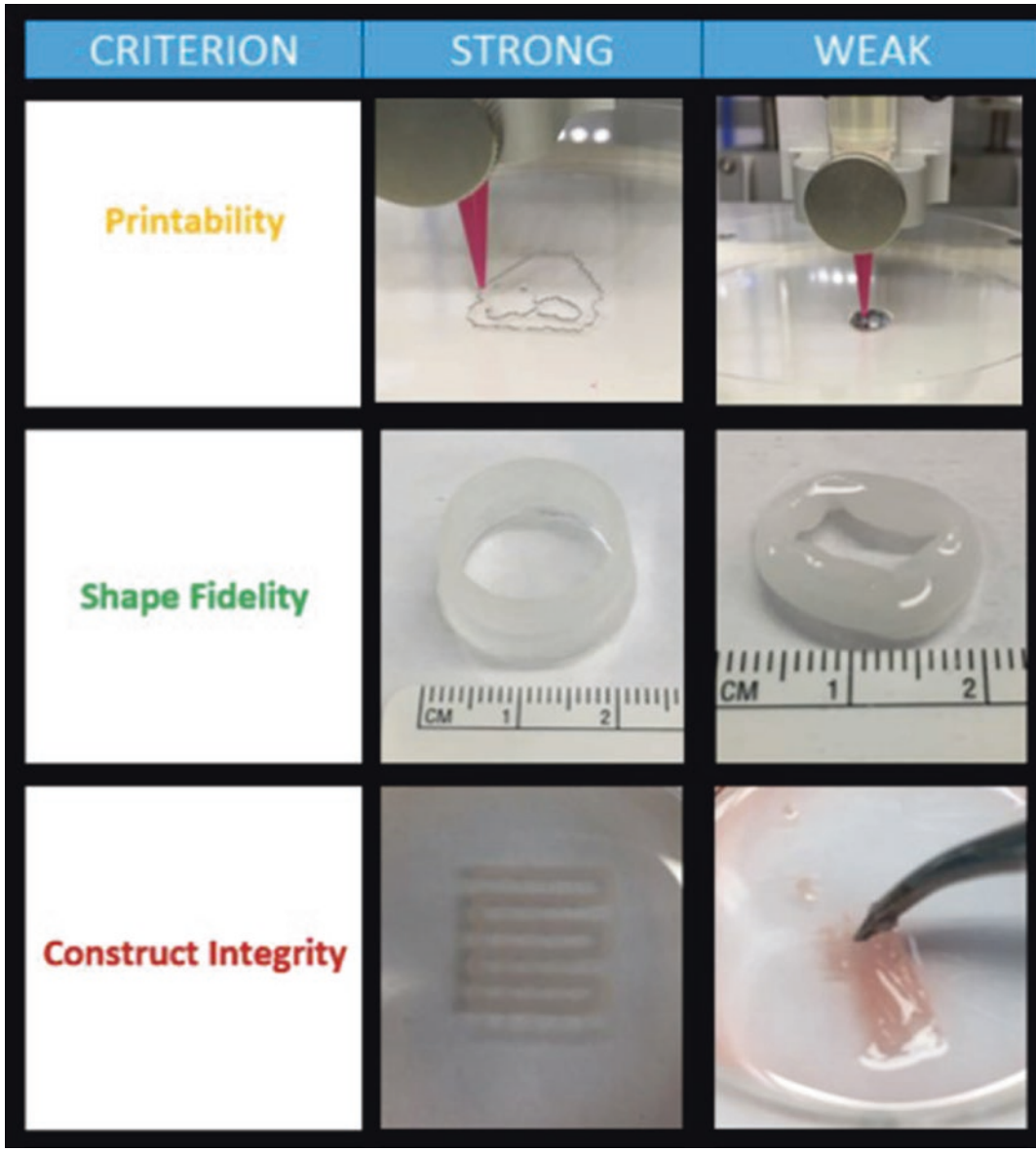

Figure 21.2.6: Variability in Selection Criteria of Hydrogel-Based Bioprinted Constructs. Hydrogels are proposed to be the best candidates for use as a bio-ink due to their ability to mimic the physiological conditions of extracellular matrix as well as their feasible viscoelastic properties. Viscosity is key in achieving a good **printability**. A higher viscosity hydrogel exhibits a stronger resolution whereas a less viscous gel proves challenging to print due to instant deformation. One of the key criteria of an ideal bio-ink is **shape fidelity**, which represents how true a 3D printed construct is to its original design. Certain hydrogels tend to deform post-printing and hence an alternative composition may be required to reinforce the structure. Above is an image of two renditions of the same printing design using two different hydrogels: PF127 (strong shape fidelity) and alginate after cross-linking with calcium chloride (weak shape fidelity). A 3D bioprinted construct must be well cross-linked and maintain its **integrity** to allow cell proliferation and extracellular matrix formation within the desired structure. A construct with weak integrity may deform or collapse upon handling

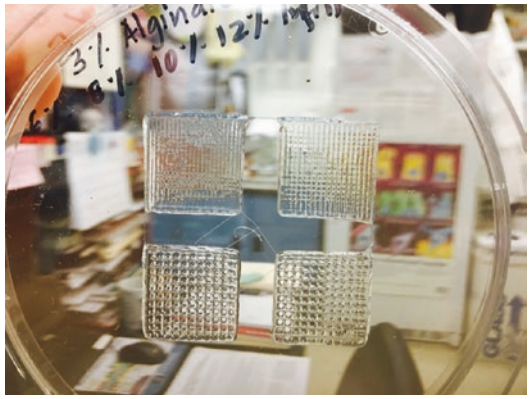

Figure 21.2.7: Variable Resolution in 3D Bioprinting. Though largely dictated by the rendering software and the printer itself, the resolution of the final printed product can also vary with the type of hydrogel-based bio-ink being used. Using hydrogels is advantageous due to their bio-compatibility, biodegradability, and the moist environment they provide facilitating ECM production. Hydrogels are also easily pliable, meaning they could be printed to create a wide range of resolutions by adjusting gel viscosity, nozzle diameter, printing speed, and extrusion pressure. Changing resolutions allow fine control of the ultrastructure of the construct influencing cell migration or accumulation depending on the desired type of tissue. For example, a more porous structure enables exchange of nutrients and provides larger surface area for cell attachment

	Printability	Cross-linking	Shape fidelity	Construct Integrity	Cytotoxicity
Alginate	High	$CaCl_2/CaSO_4$	Moderate	High	-
Alginate +Collagen	Low	$CaCl_2/CaSO_4$	Low	Moderate	-
Pluronic F127	High	Temperature sensitive	High	Low	-
Gelatin Methacrylate	Moderate	Photo-polymerizable	Moderate	Moderate	~70% Cell viability

Figure 21.2.8: Commonly Used Bio-Inks and Their Respective Properties. Key elements to be considered when choosing a bio-ink include the printability, cross-linking capacity, shape fidelity, and construct integrity of the medium, as well as its susceptibility to cytotoxic insult (see Figure 21.2.5). Alginate is an anionic polysaccharide that forms a viscous gum on binding with water, and is purified from brown seaweed. Alginate hydrogels have been particularly attractive in would healing, drug delivery, and tissue engineering applications owing to their biocompatibility, ease of gelation, and structural similarity with natural extracellular matrix (ECM). Collagen is a structural protein and a major component of the ECM. Type II collagen is the most predominant in articular and hyaline cartilage and plays an important role in providing tensile strength to the tissue. Since extrusion bioprinting requires the bio-ink to be self-supporting for layer-by-layer fabrication, collagen, which has a relatively lower viscosity, is mixed with alginate for structural reinforcement. Pluronic F127 gels are widely used as drug carriers due to their low toxicity and reverse thermal gelation, making it highly printable. But since it cross-links only via hydrogen bonding, the printed construct has no integrity and easily deforms if handled. Gelatin methacrylate (GelMA) is a photopolymerizable seminatural hydrogel comprised of modified gelatin with methacrylic anhydride, and it is an attractive biomaterial for cell-based studies and tissue engineering applications. Studies have shown that 3D printed constructs using GelMA hydrogel have the ability to maintain strict control and care of the microenvironment and exhibit long-term cell viability

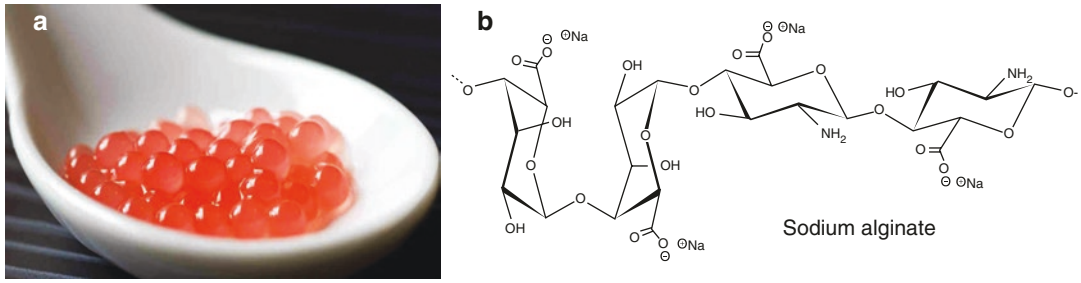

Figure 21.2.9.A: Commonly Used Bio-Ink Materials: Alginate and Cross-Linking. (**a**, **b**) Alginate is an anionic polysaccharide derived from brown seaweed. Due to its ability to allow the transmission of chemical signals to cells in developing tissue, alginate closely replicates native extracellular matrix (ECM), making it an attractive option for scaffolding material in tissue engineering applications [6, 7]

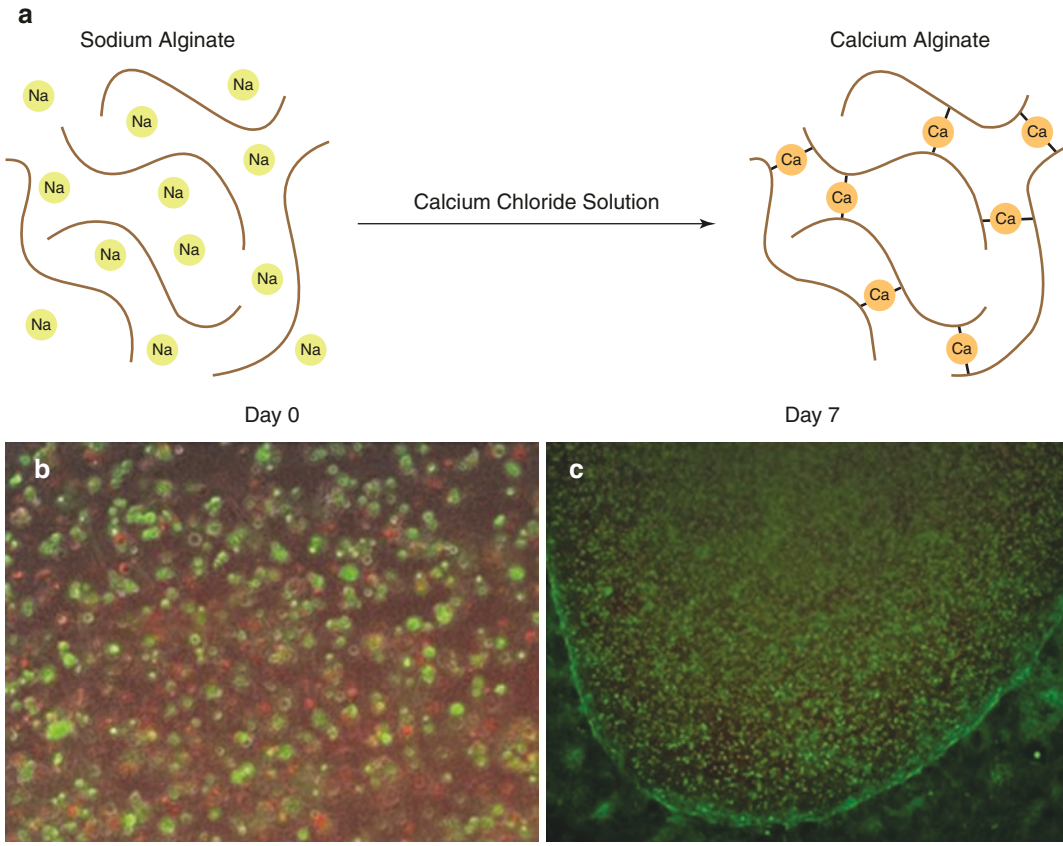

Figure 21.2.9.B: Commonly Used Bio-Ink Materials: Alginate and Cross-Linking. (**a**) In order to induce the formation of reinforcing calcium cross-links, sodium alginate is exposed to a calcium chloride solution ($CaCl_2$/$CaSO_4$). These cations link the monomers to form polymers resulting in gelation [8]. Longer duration of exposure to cross-linking agents may be more toxic to the cells; hence scaffolds are typically cross-linked only for a few minutes depending on the type of hydrogel and the size of the construct. (**b**, **c**) Maintenance of cell viability is demonstrated by the preponderance of live cells (green) over nonviable cells after the biomaterial is allowed to incubate at 37 °C and 5% CO_2 for 1 week

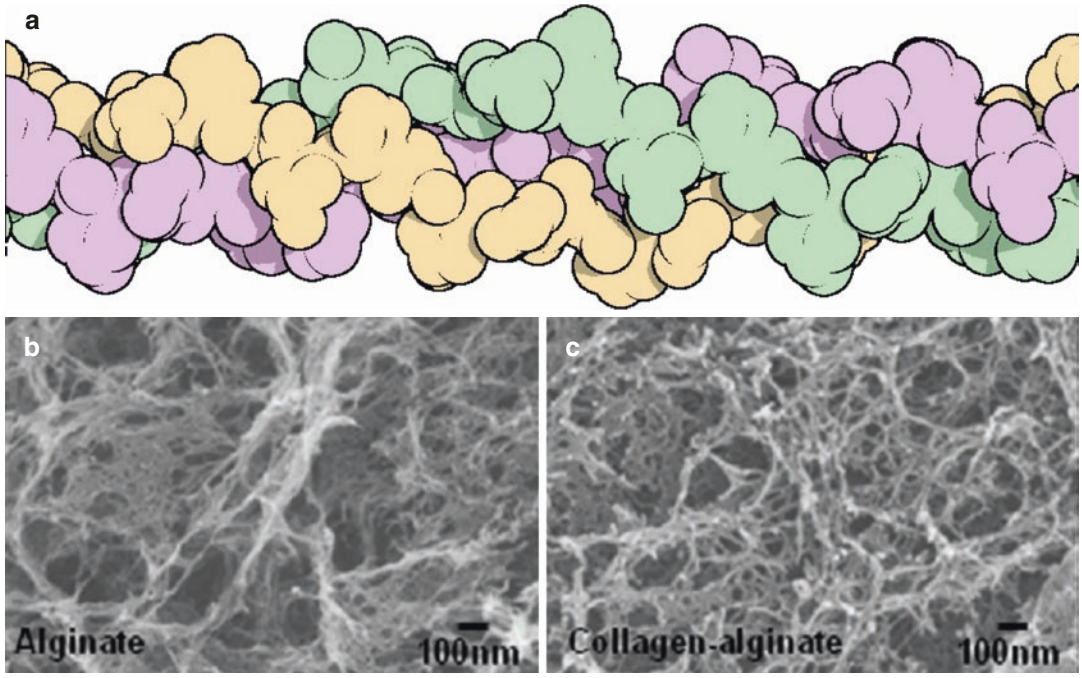

Figure 21.2.10: Commonly Used Bio-Ink Materials: Alginate with Collagen II. (**a**) Molecular structure of collagen II, one of the major components of native extracellular matrix (ECM) [9]. (**b**, **c**) Alginate-based hydrogels can be reinforced with collagen II to resist breakdown of cross-links during 3D printing with bio-inks. However, this comes at the price of moderately reduced fidelity and integrity, as well as drastically reduced printability. Adding other components to the hydrogel such as nanocellulose or constructing an additional synthetic scaffold structure that can reinforce the bioprinted structure could overcome these limitations [10]

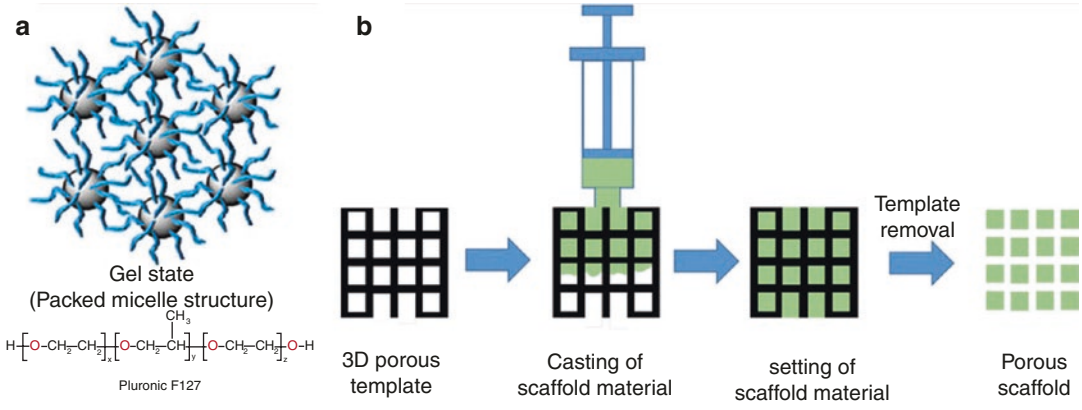

Figure 21.2.11: Commonly Used Bio-Ink Materials: Pluronic F127. (**a**) Pluronic F127 is a widely used thermo-reversible polymer in drug delivery systems that gels at higher temperatures (37 °C) and liquefies at lower temperatures (4 °C). Though Pluronic F127 confers good printability, this benefit is balanced by relatively weak structural integrity of the final printed product [11]. (**b**) However, this weak structural integrity is beneficial in the use of Pluronic F127 as a "sacrificial" bio-ink. Sacrificial materials are highly water soluble at certain temperatures and can act as useful support materials to 3D print in. Printing in a sacrificial bath avoids overhangs or deformations by giving the construct a little extra time to cross-link, and as the construct cross-links or strengthens, the bath can be washed away [12]

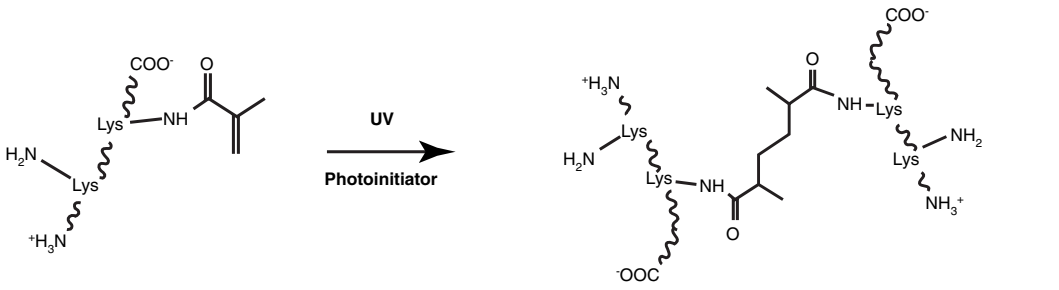

Figure 21.2.12: Commonly Used Bio-Ink Materials: Gelatin Methacrylate. Gelatin methacrylate (GelMA) is a seminatural, photopolymerizable hydrogel comprised of a modified gelatin with methacrylic anhydride. With moderate printability, shape fidelity, and construct integrity, GelMA provides a well-balanced option as a hydrogel for cell-based studies and a feasible bio-ink for 3D bioprinting and tissue engineering applications [13]

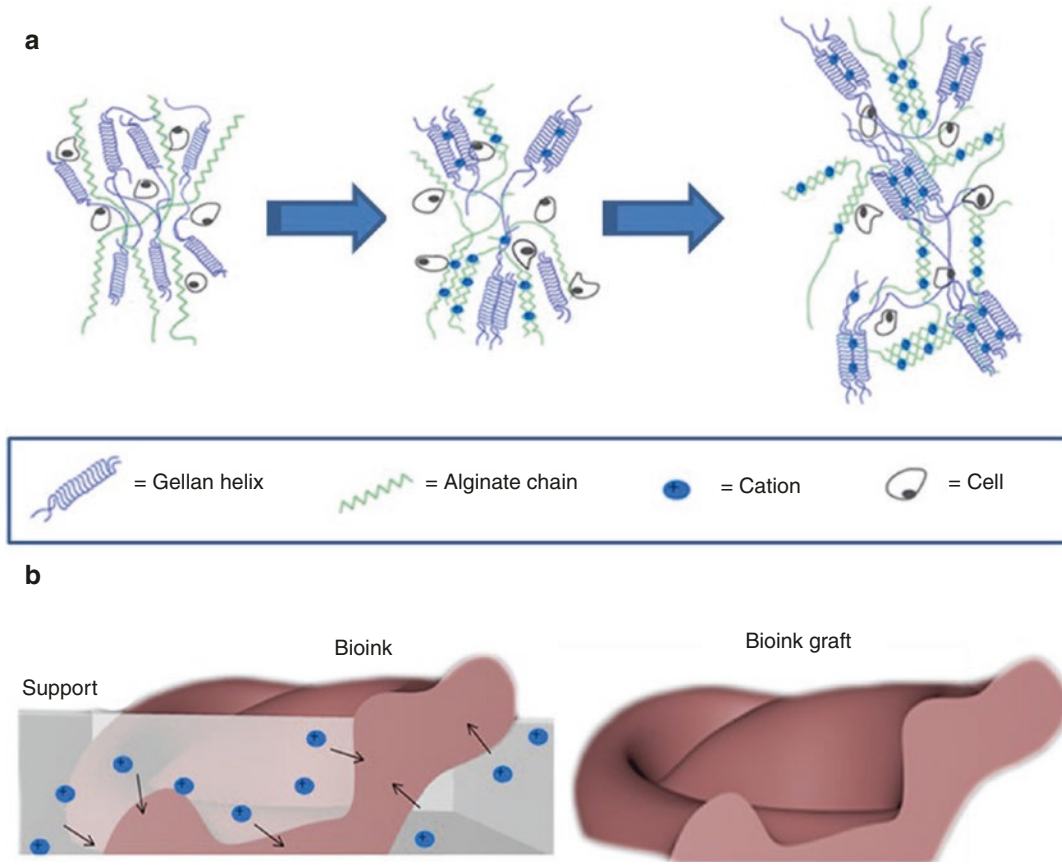

Figure 21.2.13: Cation-Induced Gelation of Hydrogel-Based Bio-Ink. (**a**) Hydrogel-based bio-inks composed of gellan and alginate can be prompted to undergo gelation by the addition of cations. These cations form ionic bonds between the monomers creating a strong, cross-linked polymer. (**b**) Sacrificial bio-inks can be used as cation reservoirs to trigger this gelation process in the permanent 3D bioprinted graft [14]

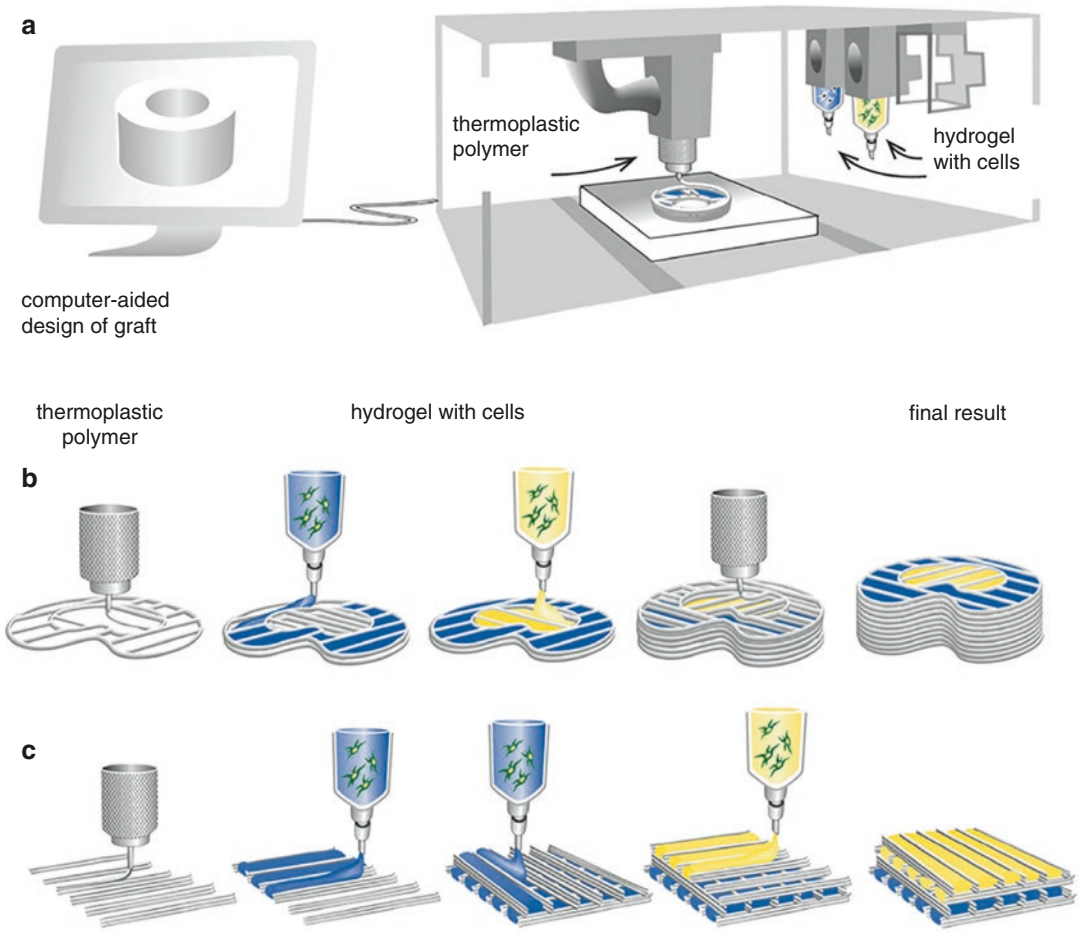

Figure 21.2.14: Fiber Reinforcement: A Shift in the Paradigm of Biofabrication. (**a**) Researchers have begun to utilize separate materials for structural support and cell delivery, to produce viable bioprinting constructs. These constructs exhibit favorable mechanical characteristics closely mimicking those of the native tissue. Furthermore, the hydrogel is supported by the thermoplastic material, which allows a broader range of hydrogel types to be used (relative to bioprinting of hydrogels alone). (**b**, **c**) Thermoplastic polymers serve as skeletal structures into which hydrogels composed of varying cell types and/or bioactive factors can be embedded in an organized, sustainable fashion [15]

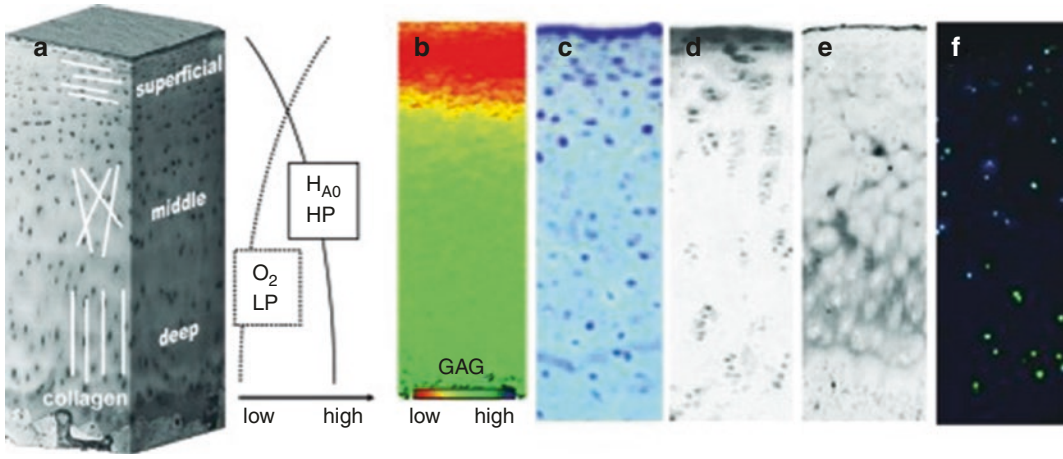

Figure 21.2.15: 3D Bioprinting of Articular Cartilage Tissues: Zonal Variations. Zonal consideration in articular cartilage is an essential consideration when bioprinting articular cartilage tissues. (**a**) Moving from superficial to deep articular cartilage (AC), there is a distinct change in collagen orientation, as well as a gradual increase in hyaluronic acid (H_{A0}) levels and decrease in oxygen (O_2) levels. (**b**) There is a significant increase in the presence of glycosaminoglycan (GAG) in the middle and deep layers of AC relative to the more superficial layers. (**c**) Proteoglycan 4 (PRG4) and (**d**) developmental endothelial locus 1 (Den-1) are present in high levels in the superficial zone and thus may serve as suitable zone-specific markers. (**e**) Cartilage intermediate-layer protein (CILP) and (**f**) Jagged 1 (JAG1) expression are seen predominantly in the middle and deep zones of AC [16]

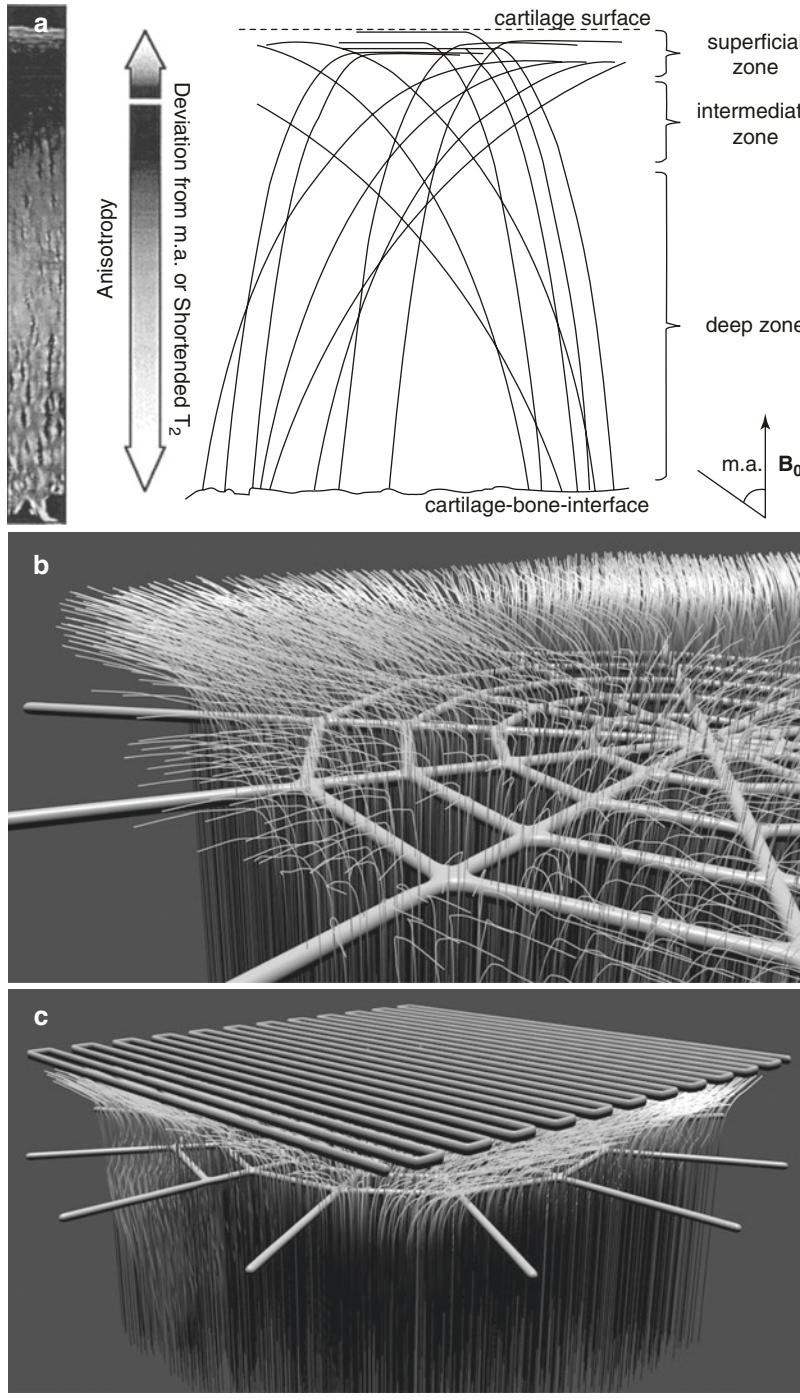

Figure 21.2.16: Potential Strategy for Replicating the Collagenous Structural Architecture of Articular Cartilage. (**a**) Double arrow indicates the directions of increasing anisotropy and deviation of collagen fibrils from the "magic angle" (m.a.) towards both superficial and deep zone. This results in a shortening of T_2 with increasing anisotropy. Bright structures in the polarized light microscopy image (left) reveal arranged structures. The m.a. (54.7°) is indicated with the direction of the B_0 field. This imaging technique, based on the orientation of the collagen fibrils, can detect disease at an early stage before macroscopic changes in tissue appear, and employ tissue-engineered components to prevent an irreversible onset of the disease. (**b**) 3D rendering of the collagen fibril structure and (**c**) 3D rendering of the collagenous structure as a base for overlying bioprinted medium [17]

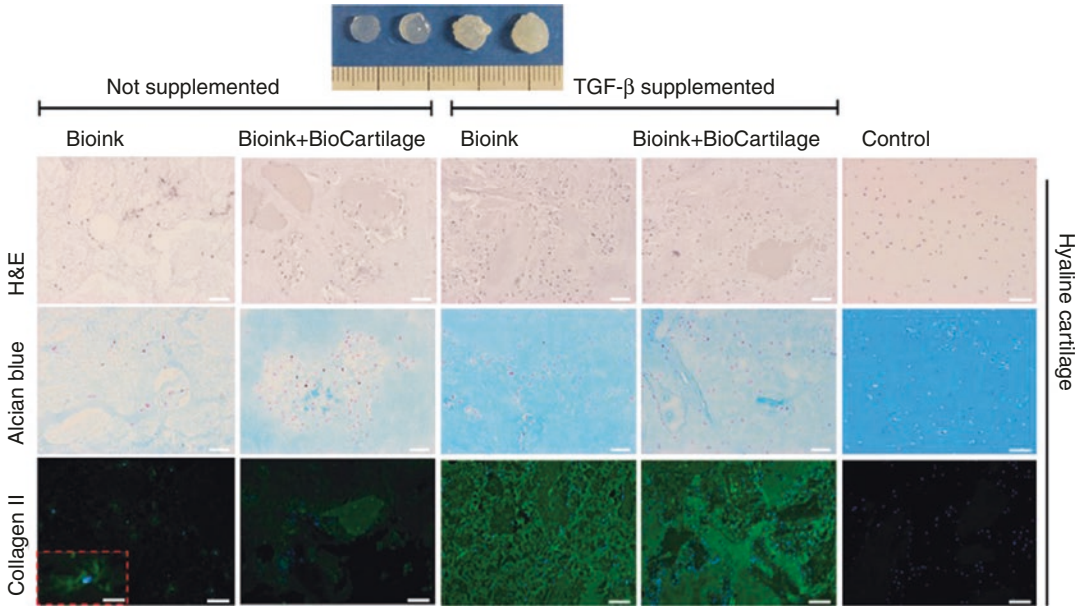

Figure 21.2.17: Post-print Enhancement of 3D Bioprinted Constructs. The addition of extracellular matrix components in the form of micronized biocartilage (Arthrex™) can enhance cell proliferation within the printed construct. The constructs can be further enhanced by post-print exposure of the construct to growth factors, such as transforming growth factor beta-3 (TGF-β3) [14]

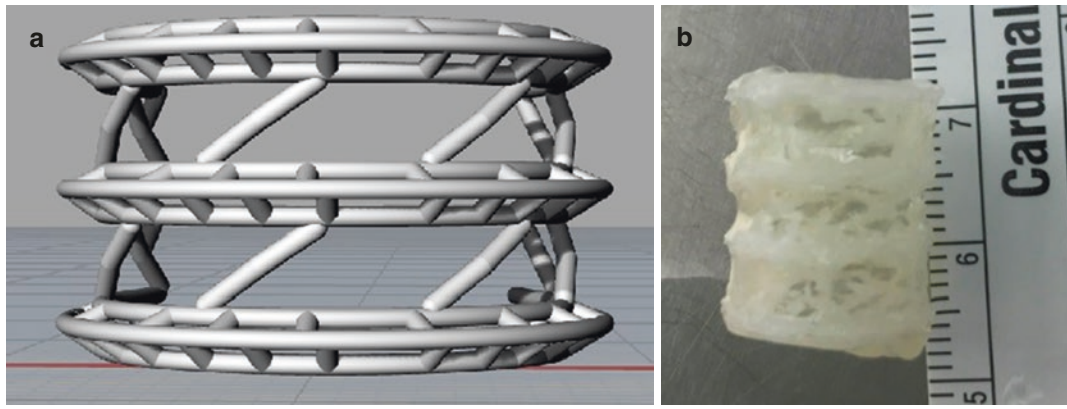

Figure 21.2.18: 3D Bioprinted Tracheal Tissue: An Exemplary Application of Cartilaginous 3D Bio printing. (**a**) CAD-rendered scaffold for cartilaginous tracheal tissue. (**b**) Printed scaffold, preimplantation. (**c**, **d**) Printed scaffold successfully seeded with cartilaginous tissue, 4 weeks in vivo. (**e**) Demonstration of normal cartilage growth in a tracheal replacement graft when chondrocytes are separated from the tracheal lumen by an intervening membrane. When no such membrane exists, there is a propensity for inflammation and stenosis. These findings are important for future construction and implantation of tracheal replacement grafts

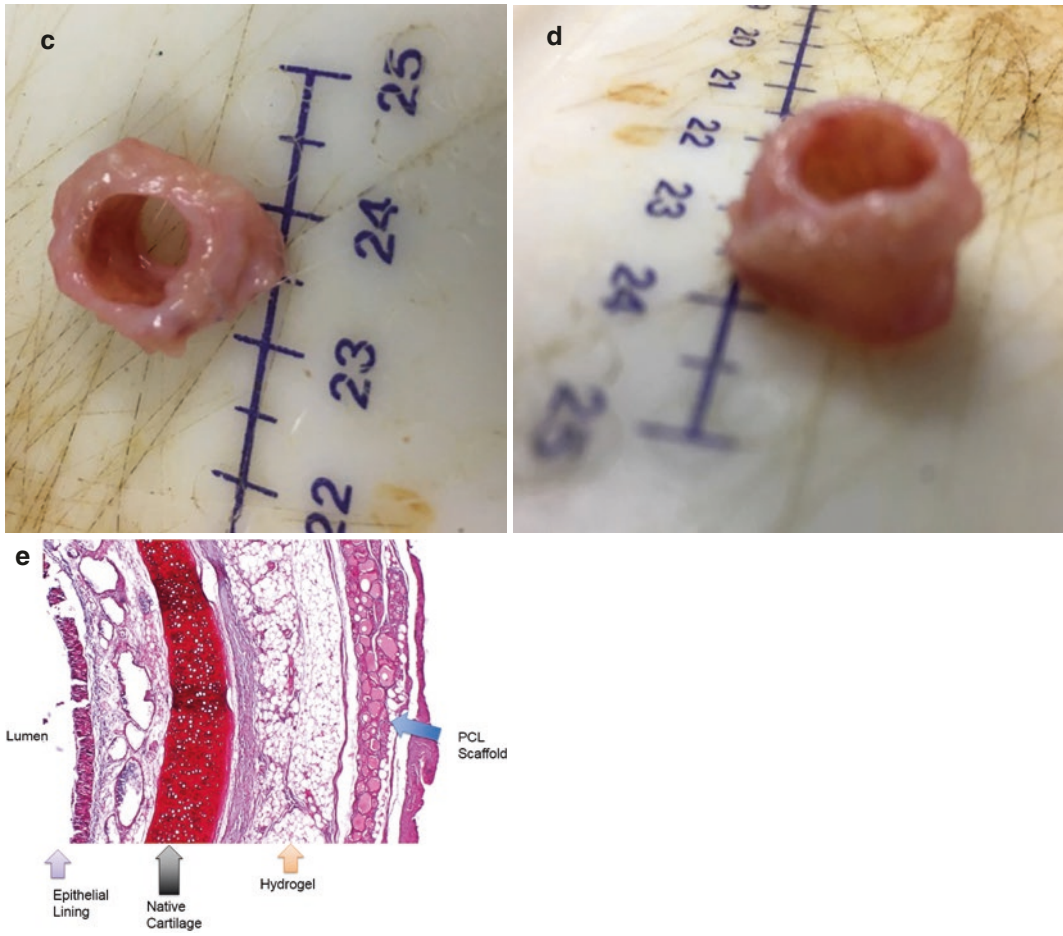

Figure 21.2.18: (continued)

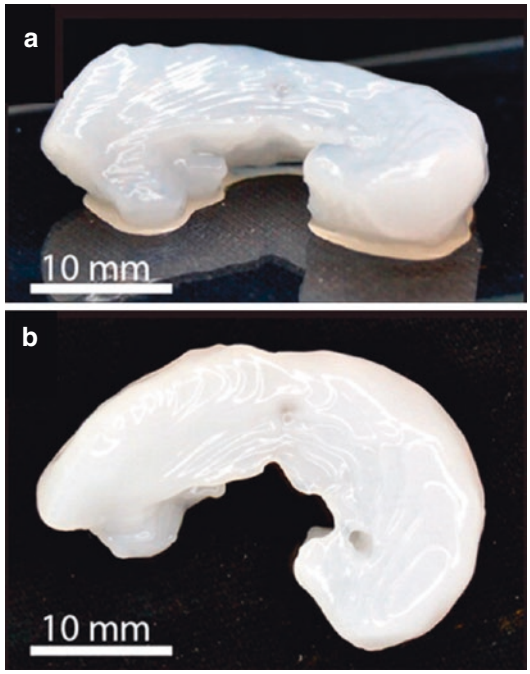

Figure 21.2.19: 3D Bioprinted Meniscus: Future Directions. A top view (**a**) and side view (**b**) of a 3D bioprinted construct of a sheep meniscus. The construct was printed using the 3D Discovery bioprinter from regenHU (Switzerland). Alginate-nanocellulose hydrogel mixture was used as a bio-ink. The construct shape was retained post-printing and the cells remained viable [18]

21.3 Take-Home Message

Cartilage defects prove difficult to manage clinically and surgically due to their avascular structure. Its limited regenerative capacity poses yet another obstacle in the development of long-term solutions for repairing cartilage defects. With the hope of developing more long-standing solutions, many researchers have turned to tissue-engineering cartilage de novo by means of 3D bioprinting. Using 3D bioprinting, various biocompatible materials can be assembled in a highly precise manner, mimicking the ultrastructure and biomechanical properties of target tissue, to produce a personalized, patient-specific construct. Biomaterials can be seeded with extracellular "cues" to promote target tissue type behavior, 3D printed and fabricated to form any complex shape required to fit the patient's defect. Due to the lack of vascularity and lymphatic supply, cartilage may seem like an ideal and relatively simpler candidate for 3D bioprinting. However, its characteristic zonal architecture makes it challenging to reproduce cartilage, artificially. In order to resolve these challenges, in-depth preclinical studies are required to assess the viability of 3D bioprinted cartilage grafts in vivo, prior to clinical translation. Although relatively recent, the field of three-dimensional bioprinting is rapidly advancing and shows enormous potential for developing more personalized and concrete solutions to overcome long-standing medical challenges.

References

1. MakerBot. MakerBot® replicator 2 brochure. Online. http://downloads.makerbot.com/replicator2/MakerBot_Replicator2_brochure.pdf. Accessed 21 July 2019.
2. Burkhardt C, Freigassner P, Weber O, Imgrund P, Hampel S. Fused filament fabrication (FFF) of 316L green parts for the MIM process. Deposition Technologies. World Powder Metallurgy; 2016.
3. Schematics of building a tubular organ module by bioprinting. Organ printing: understanding and employing multicellular self-assembly. University of Missouri; 2007. Online. http://organprint.missouri.edu/www/. Accessed 21 July 2019.
4. Bioprinting applications. SE 3D (permission granted by Dr. Mayasari Lim) Education. 2016. Online. Accessed 21 July 2019.
5. Ahlfeld T, Köhler T, Czichy C, Lode A, Gelinsky M. A methylcellulose hydrogel as support for 3D plotting of complex shaped calcium phosphate scaffolds. Gels. 2018;4(3):68.
6. Alginates in food: sodium alginate uses in food. Culinary Physics. 2014.
7. Matin A, Shafi H, Wang M, Khan Z, Gleason K, Rahman F. Reverse osmosis membranes surface-modified using an initiated chemical vapor deposition technique show resistance to alginate fouling under cross-flow conditions: filtration & subsequent characterization. Desalination. 2016;379:108–17.
8. Calcium promotes the solidification of alginate networks. Deconstructed Apple Pie. Discover Magazine. 2014. Accessed 21 July 2019.
9. The RCSB PDB "molecule of the month": Collagen. D.S. Goodsell. *RCSB PDB.* 2000.
10. Lee BR, Hwang JW, Choi YY, Wong SF, Hwang YH, Lee DY, Lee S-H. In situ formation and collagen-alginate composite encapsulation of pancreatic islet spheroids. Biomaterials. 2012;33(3):837–45.

11. Young-seok J, Park W, Park H, Lee D, Na K. Thermosensitive injectable hydrogel based on the physical mixing of hyaluronic acid and Pluronic F-127 for sustained NSAID delivery. Carbohydr Polym. 2017;156:403–8.
12. Houben A, Van Hoorick J, Van Erps J, Thienpont H, Van Vlierberghe S, Dubruel Pl. Indirect rapid prototyping: opening up unprecedented opportunities in scaffold design and applications. Ann Biomed Eng. 2017;45:58–83.
13. Rose J, Pacelli S, El Haj A, Dua H, Hopkinson A, White L, Rose F. Gelatin-based materials in ocular tissue engineering. Materials. 2014;7(4):3106–35.
14. Kesti M, Eberhardt C, Pagliccia G, Kenkel D, Grande D, Boss A, Zenobi-Wong M. Bioprinting complex cartilaginous structures with clinically compliant biomaterials. Adv Funct Mater. 2015;25(48):7406–17.
15. Schuurman W, Khristov V, Pot M, van Weeren P, Dhert W, Malda J. Bioprinting of hybrid tissue constructs with tailorable mechanical properties. Biofabrication. 2011;3(2):1–7.
16. Klein T, Malda J, Sah R, Hutmacher D. Tissue engineering of articular cartilage with biomimetic zones. Tissue Eng Part B Rev. 2009;15(2):143–57.
17. Nieminen M, Rieppo J, Toyras J, Hakumaki J, Silvennoinen J, Hyttinen H, Jurvelin J. T2 relaxation reveals spatial collagen architecture in articular cartilage: a comparative quantitative MRI and polarized light microscopy study. Magn Resonan Med. 2001;46:487–93.
18. Markstedt K, Mantas A, Tournier I, Martínez Ávila H, Hägg D, Gatenholm P. 3D bioprinting human chondrocytes with nanocellulose–alginate bioink for cartilage tissue engineering applications. Biomacromolecules. 2015;16(5):1489–96.

22 The Illustrative Magnetic Resonance Image (MRI) Assessment of Cartilage Repair

Dinshaw N. Pardiwala, Kushalappa Subbiah, and Pradeep Mandapalli

22.1 Introduction

Magnetic resonance imaging (MRI) is the ideal noninvasive technique to objectively evaluate osteochondral repair due to its superior soft-tissue characterization, lack of ionizing radiation, multiplanar capabilities, and ability to evaluate the structure and surface of not only the articular cartilage but also the subchondral bone. Although several MRI scoring systems for classification and grading of articular cartilage repair tissue have been described, the MOCART (MRI observation of cartilage repair tissue) scoring system is validated and the most practical (Table 22.1.1) [1, 2].

In addition to the structural imaging of articular cartilage, several techniques have been developed to assess the biochemical properties of reparative chondral tissue with an intent to assess the functional efficacy of cartilage repair. These include T2 mapping for collagen content [3], delayed gadolinium-enhanced MRI of cartilage (dGEMRIC) for glycosaminoglycan content [4], and diffusion mapping for collagen ultrastructure and orientation [5].

Table 22.1.1 MOCART[a] score (grading and point scale) [1]

Variable	Classes	Points
Degree of defect repair and defect filling	Complete	20
	Hypertrophy	15
	Incomplete >50%	10
	Incomplete <50%	5
	Subchondral bone exposed	0
Integration to border zone	Complete	15
	Incomplete	
	Demarcating border seen	10
	Defect visible	
	<50% length of repair tissue	5
	>50% length of repair tissue	0
Surface of the repair tissue	Intact	10
	Damaged	
	<50% length of repair tissue	5
	>50% length of repair tissue	0
Structure of the repair tissue	Homogenous	5
	Inhomogeneous	0
Signal intensity of repair tissue	Dual FSE (fast spin echo)	
	Isointense	15
	Moderately hyperintense	5
	Markedly hyperintense	0
	3D gradient	
	Isointense	15
	Moderately hypointense	5
	Markedly hypointense	0
Subchondral lamina	Intact	5
	Not intact	0
Subchondral bone	Intact	5
	Not intact	0
Adhesions	No	5
	Yes	0
Effusion	No	5
	Yes	0
[a]MOCART: Magnetic resonance observation of cartilage repair tissue		**100**

D. N. Pardiwala (✉) · K. Subbiah · P. Mandapalli
Arthroscopy Service, Kokilaben Dhirubhai Ambani Hospital, Mumbai, India
e-mail: pardiwala@outlook.com; kushalappa.s@gmail.com; pradeep.kmc33@gmail.com

D. R. Goyal (ed.), *The Illustrative Book of Cartilage Repair*,
https://doi.org/10.1007/978-3-030-47154-5_22

22.2 The Illustrations

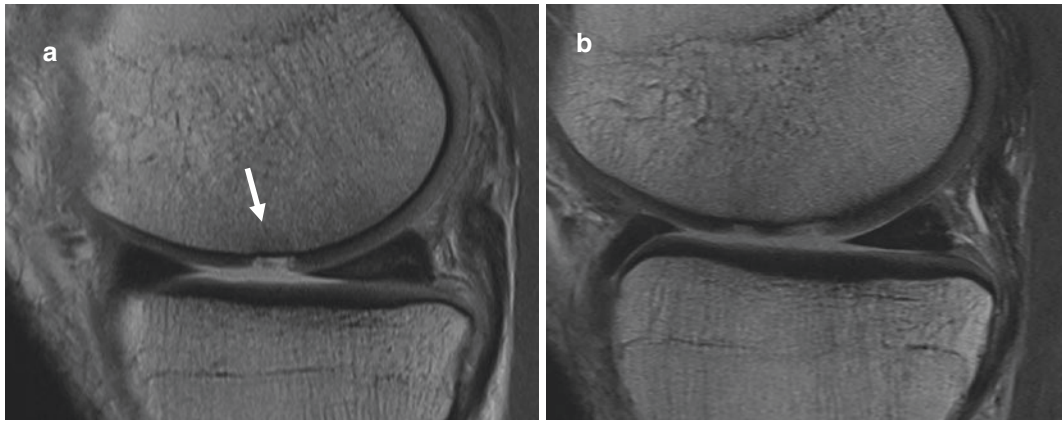

Figure 22.2.1: Natural Progression of Focal Chondral Defects in a Non-operated Case. Natural progression over 7 years of a focal chondral defect of the medial femoral condyle (MFC) of right knee in a 41-year-old distance runner who refused treatment and continued to run despite pain. (**a**) Three weeks following a twisting injury while running, a small focal, isolated full-thickness chondral defect (white arrow) was noted in the MFC. The ligaments and menisci were normal and limb alignment was in mild varus (medial proximal tibia angle—MPTA 82°). (**b**, **c**) Note the progressive MFC chondral loss, followed by subchondral bone edema (8 weeks and 6 months following injury, respectively). (**d**) At 5 years, there is extensive generalized chondral loss of MFC with osteophyte formation (white arrow), and (**e**) ultimately medial tibial chondral loss heralding medial compartment osteoarthritis (7-year follow-up)

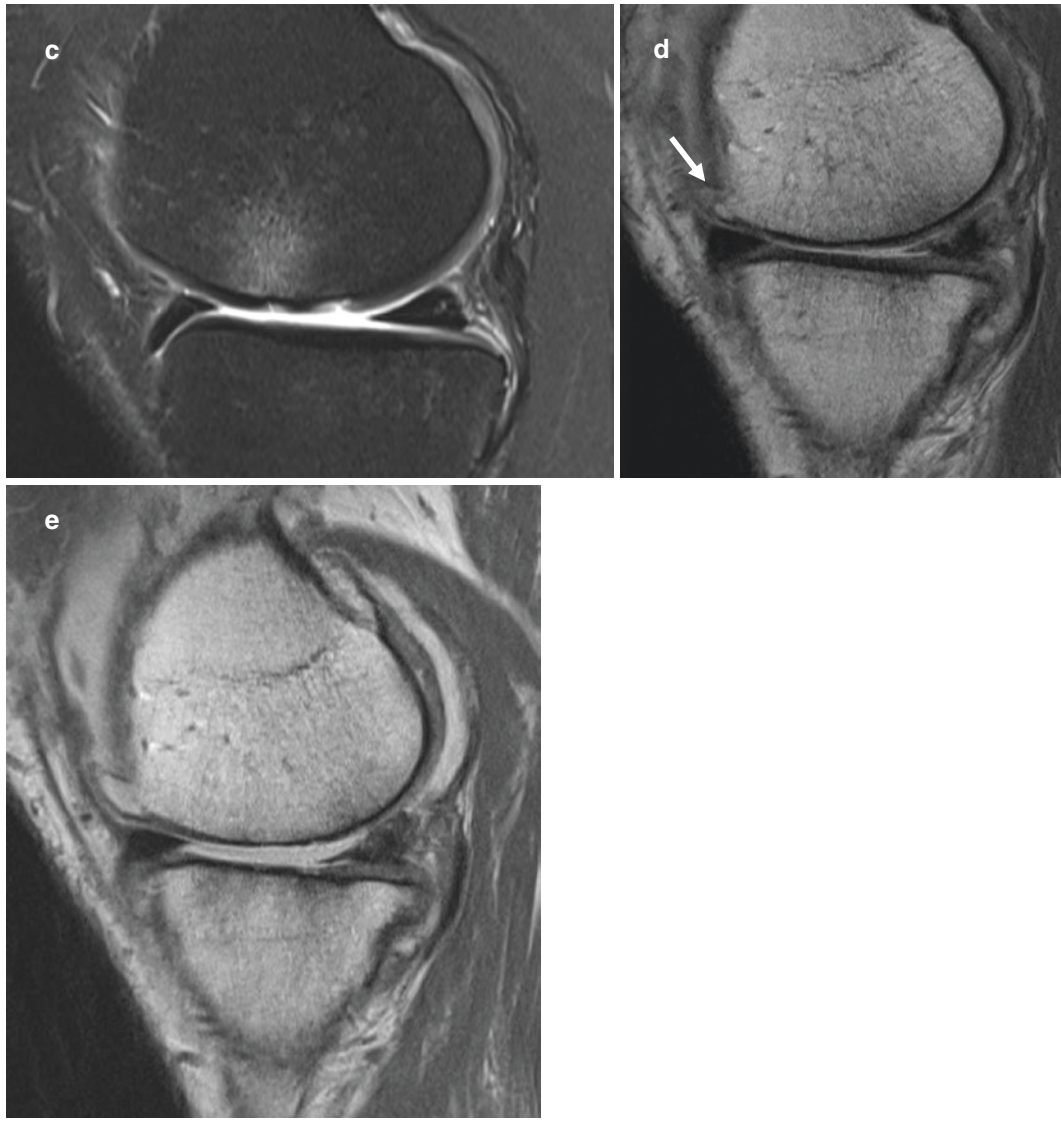

Figure 22.2.1 (continued)

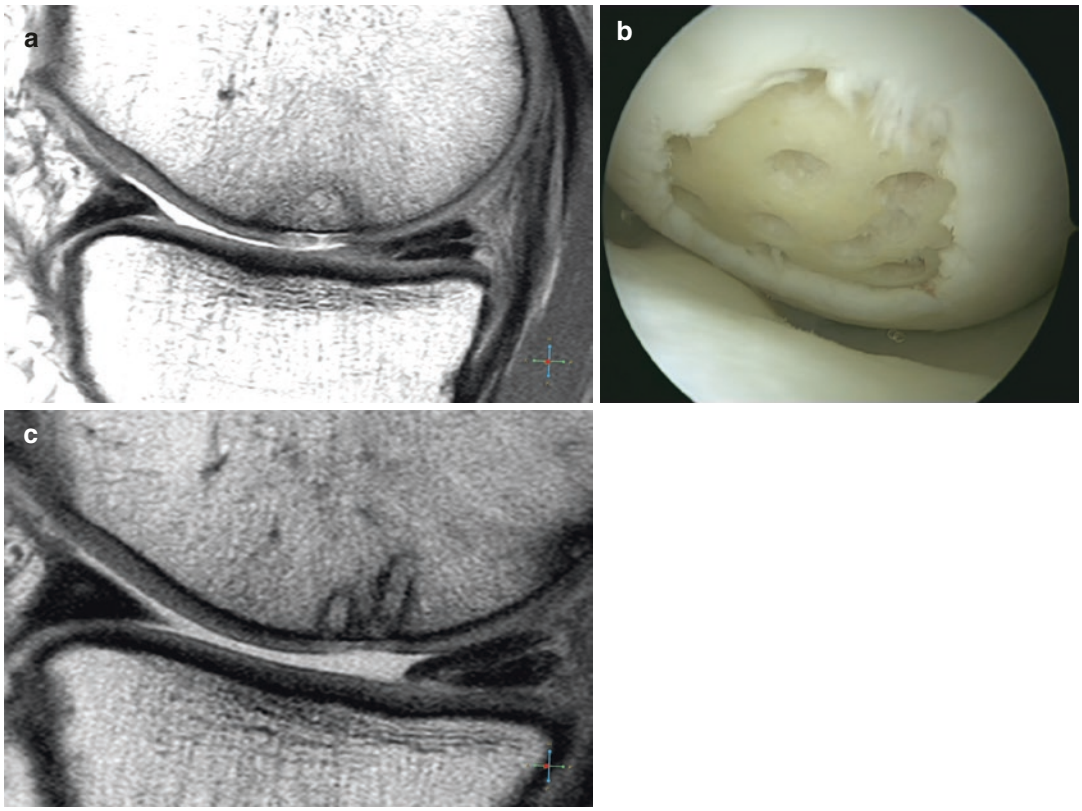

Figure 22.2.2.A: MRI Assessment of Cartilage Repair Following Marrow Stimulation Techniques. Marrow stimulation using microfracture technique for a post-traumatic medial femoral condyle (MFC) full-thickness chondral defect in a 39-year-old male patient. (**a**) The pre-operative MRI T1 sagittal image reveals a 12 mm wide full-thickness chondral defect of MFC along with a stable horizontal tear of the medial meniscus. (**b**) The micro-fracture technique for cartilage repair has been performed using a 2 mm diameter microfracture awl. (**c**) One-year postoperative MRI T1 sagittal image reveals regenerated cartilage at the site of microfracture. Although the defect fill is more than 50%, with border zone integration, the defect repair is incomplete and nonhomogeneous. Since the regenerated cartilage tissue is nonhomogeneous, and the surface of repair tissue is minimally incongruent, the MOCART score is 70 for such a regenerated cartilage

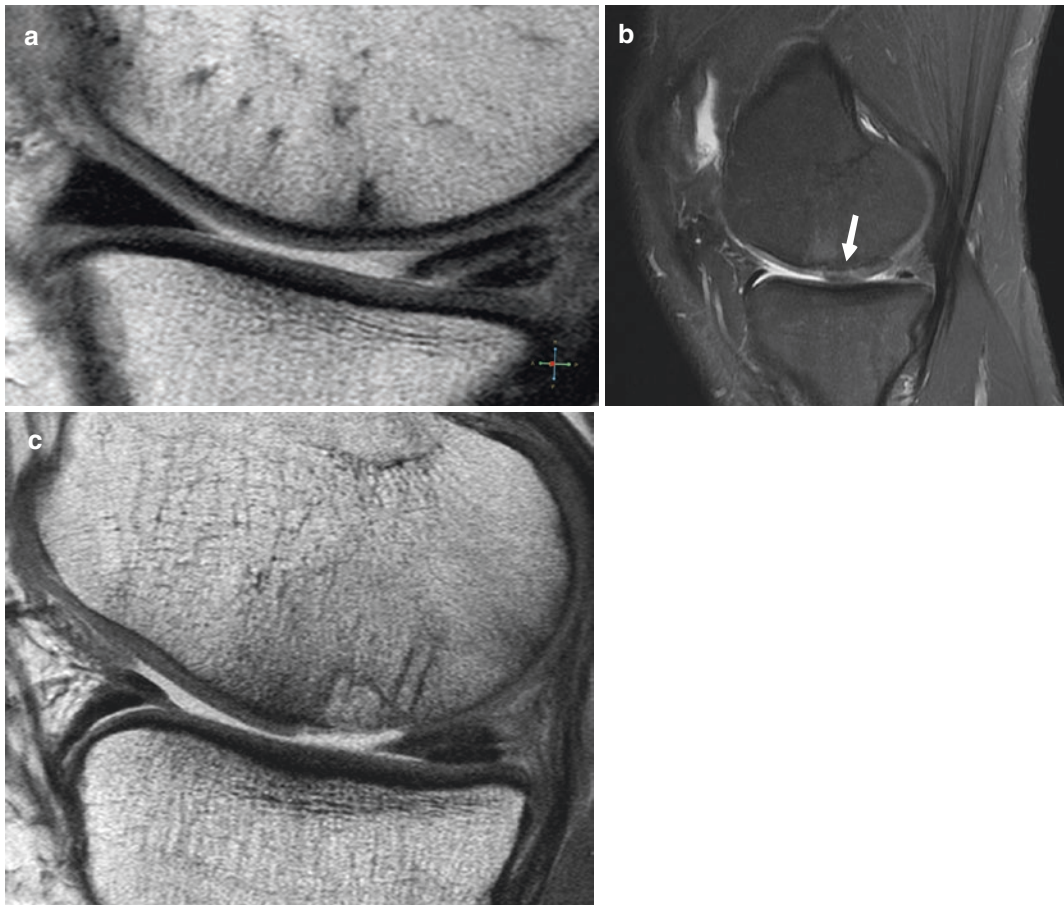

Figure 22.2.2.B: MRI Assessment of Cartilage Repair Following Marrow Stimulation Techniques. Cartilage restoration following marrow stimulation is unpredictable and depends largely on the size and the location of the defect, and compliance with postoperative precautions and rehabilitation. Three cases of medial femoral condyle (MFC) ICRS grade 4 focal chondral defects treated with marrow stimulation using the microfracture technique at 1 year following surgery show different results. (**a**) T1 sagittal image of a 45-year-old female with a 7 mm lesion shows excellent cartilage structure and surface restoration with a MOCART score of 95. (**b**) PD sagittal image of a 23-year-old male patient having undergone microfracture for a 20 mm diameter focal lesion showing complete defect filling (white arrow), incomplete integration to the border zone, and subchondral bone changes, with a MOCART score of 75. (**c**) A 49-year-old male with a 17 × 20 mm lesion shows incomplete filling of the defect with subchondral bone exposed and hence a MOCART score of 30

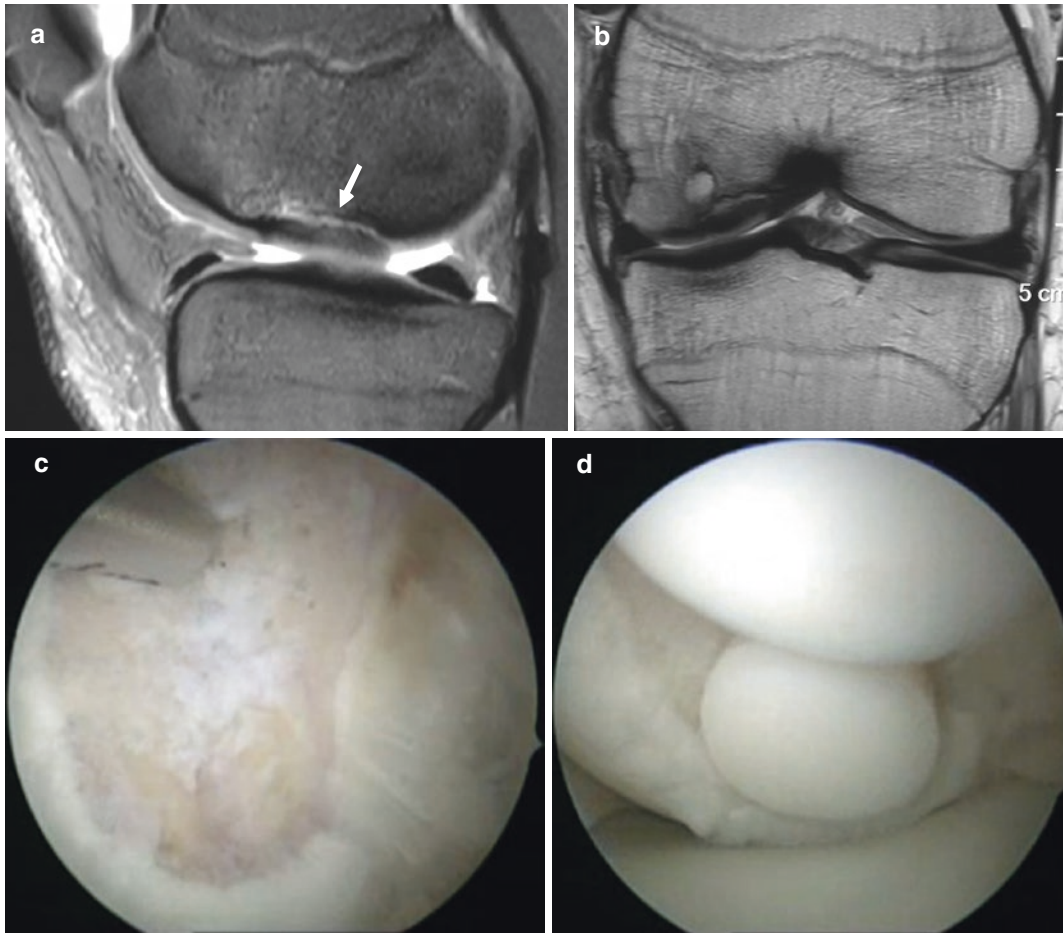

Figure 22.2.3.A: MRI Assessment of the Cartilage Repair Following Osteochondral Cylinder Transfer Technique. Medial femoral condyle (MFC) osteochondritis dissecans (OCD) in a 21-year-old male treated with arthroscopic osteochondral autograft cylinder transfer. (**a**, **b**) Preoperative MRI reveals MFC OCD (white arrow) with a large unstable fragment (ICRS OCD II). (**c**) Viewing from the anterolateral portal, arthroscopy revealed a 22 × 14 mm MFC lesion. (**d**) Post-OCD debridement, the defect received three 8 mm autograft osteochondral cylinders. (**e**–**g**) Postoperative MRI at 1 year reveals MOCART score of 80 with excellent congruity of the cartilage plug tissue with normal surrounding articular cartilage. Although the bone and hyaline cartilage of the autograft cylinders have healed to surrounding normal tissues, the border zones can still be demarcated, and there is a small subchondral cyst (white arrow) 1 year following repair. Note that the intervening articular cartilage gaps between the multiple cylinders have also filled up, and the surface of the repair tissue is remarkably intact both on sagittal and coronal T1 and STIR images

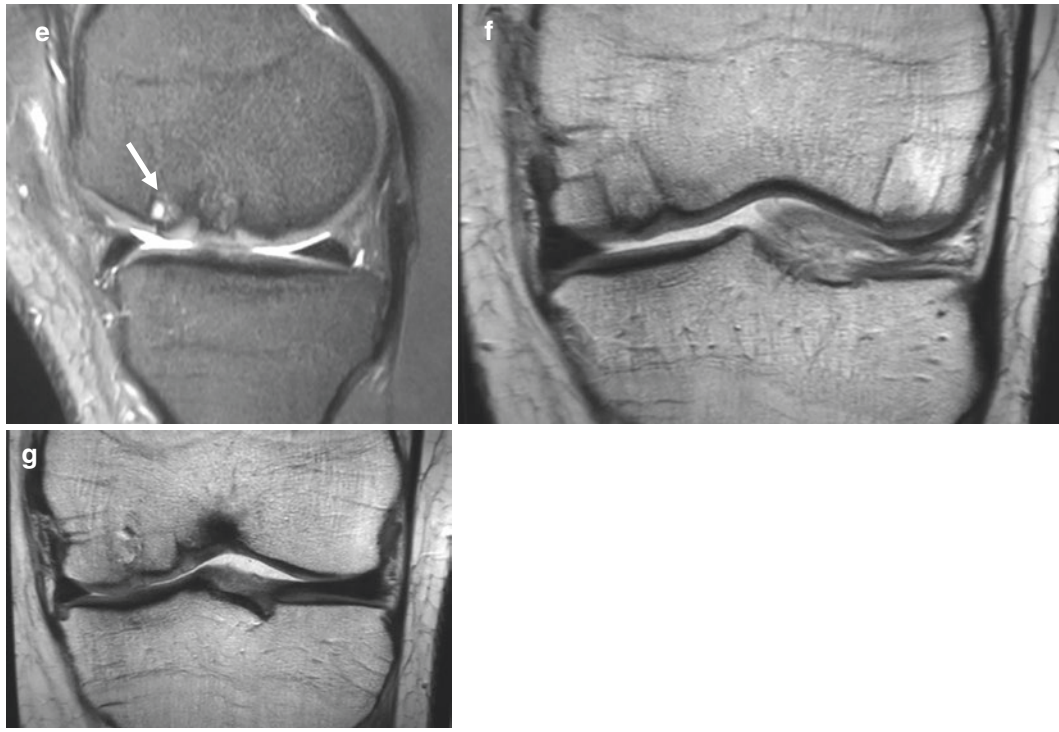

Figure 22.2.3.A (continued)

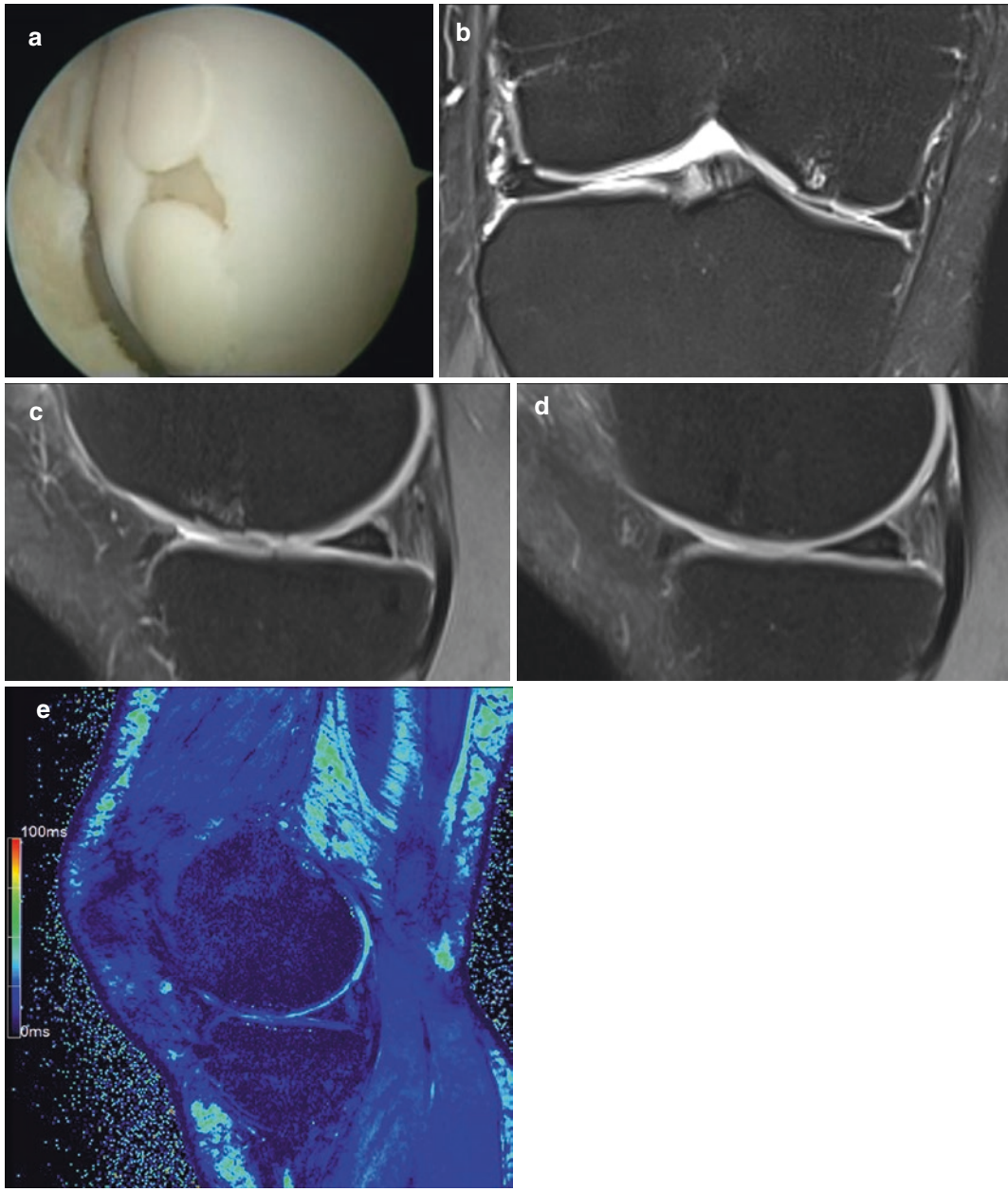

Figure 22.2.3.B: MRI Assessment of the Cartilage Repair Following Osteochondral Cylinder Transfer Technique. (**a**) Medial femoral condyle (MFC) osteochondritis dissecans (OCD) of size 16 × 9 mm treated with the arthroscopic transfer of two osteochondral autograft cylinders in a 24-year-old male athlete. (**b**, **c**) One-year postoperative MRI reveals MOCART score of 75 with healed osteochondral cylinders on the PD coronal and sagittal images. Although there is a complete defect filling with an intact repair surface, the interface between the transferred cartilage and the border zones can still be demarcated, the repair is nonhomogeneous, and subchondral bone is yet not normal. (**d**) Two years following surgery, MRI reveals MOCART score of 100 with repaired area revealing normal thickness and signal of the articular cartilage, an intact smooth surface, and normal subchondral bone. (**e**) Two years following surgery, T2 STAR sagittal cartilage mapping reveals repaired cartilage zonal variation and T2 values similar to those of the adjoining normal cartilage indicating a successful hyaline cartilage repair with normal collagen content

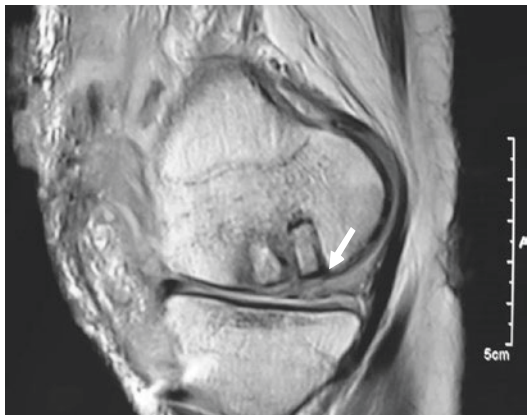

Figure 22.2.3.C: MRI Assessment of the Cartilage Repair Following Osteochondral Cylinder Transfer Technique. Medial femoral condyle (MFC) osteochondritis dissecans (OCD) treated with the transfer of two 8 mm osteochondral autograft cylinders in a 24-year-old female. Graft subsidence resulted in poor surface congruity and hence the MOCART score at 6 months following surgery is just 55

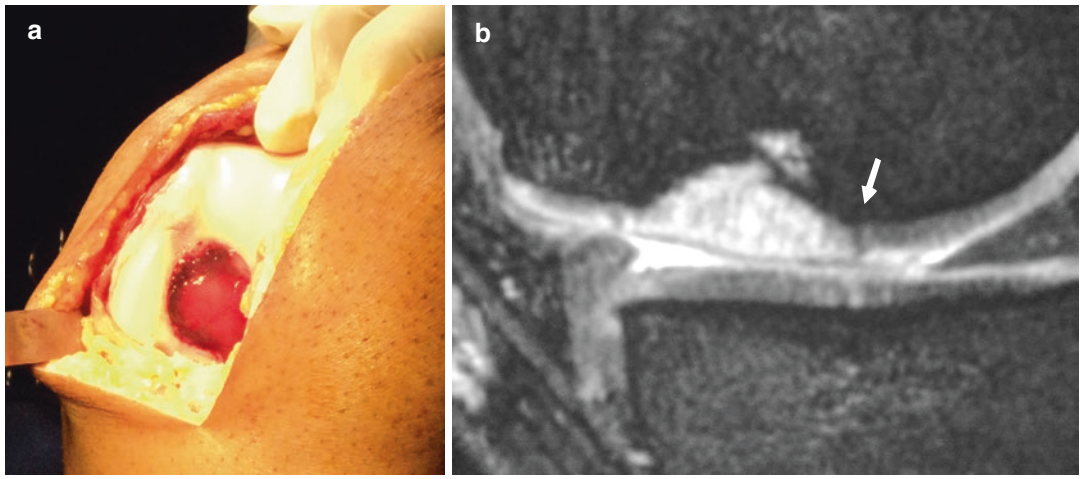

Figure 22.2.4.A: MRI Assessment of the Cartilage Repair Following Autologous Chondrocyte Implantation (ACI). A large medial femoral condyle (MFC) osteochondritis dissecans in a 23-year-old male treated with fibrin ACI. (**a**) Intraoperative postimplantation image reveals three-dimensional restoration of the normal surface topography of the MFC. (**b**) One-year postoperative T1 sagittal MRI reveals complete defect filling and an intact smooth surface. However, interface integration is incomplete with a demarcating border still visible (white arrow), and the subchondral bone is not intact making the overall MOCART score of 80

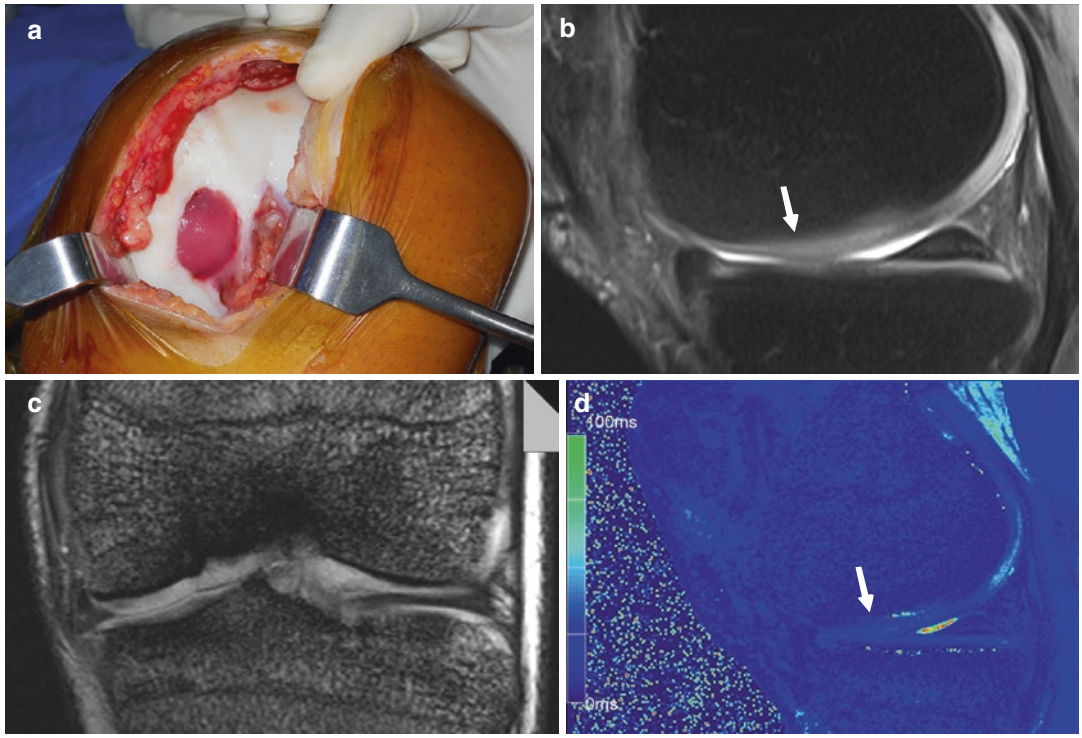

Figure 22.2.4.B: MRI Assessment of the Cartilage Repair Following Autologous Chondrocyte Implantation (ACI). Large medial femoral condyle (MFC) osteochondritis dissecans treated with fibrin ACI in a 19-year-old male. (**a**) Intraoperative postimplantation image with fibrin ACI implanted at the 24 × 20 mm MFC defect site. (**b**, **c**) Two-year postoperative MRI reveals MOCART score of 95 with complete defect filling and an intact smooth surface. The repair is homogenous, interface integration is complete, and subchondral lamina and bone are intact. However, there does appear to be mild hypertrophy in the sagittal image (white arrow). (**d**) T2 STAR cartilage mapping 2 years following surgery reveals repaired cartilage zonal variation and T2 values similar to those of the adjoining normal cartilage indicating a successful hyaline cartilage repair

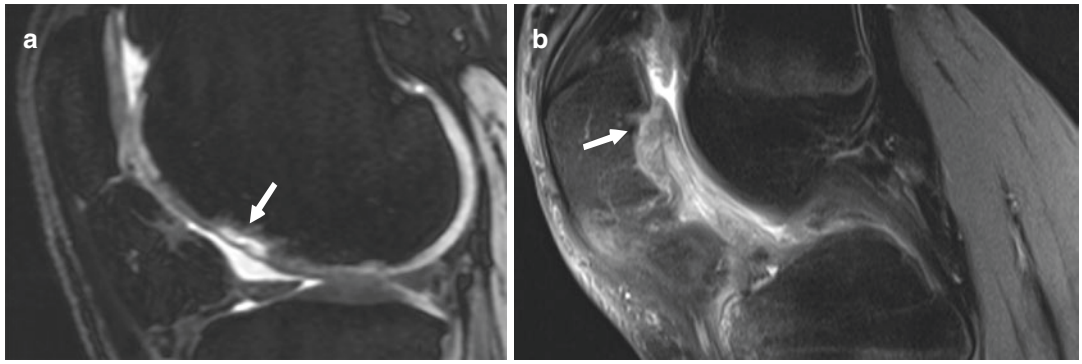

Figure 22.2.4.C: MRI Assessment of the Cartilage Repair Following Autologous Chondrocyte Implantation (ACI). The common postoperative complications in autologous chondrocyte implantation (ACI) that may be demonstrated on MRI include (**a**) cystic changes within the repaired cartilage resulting in a nonhomogeneous repair, as seen on the lateral femoral condyle at 1-year post-ACI in a 38-year-old male and (**b**) graft hypertrophy causing surface incongruity as seen on the patella 1-year post-ACI in a 19-year-old female

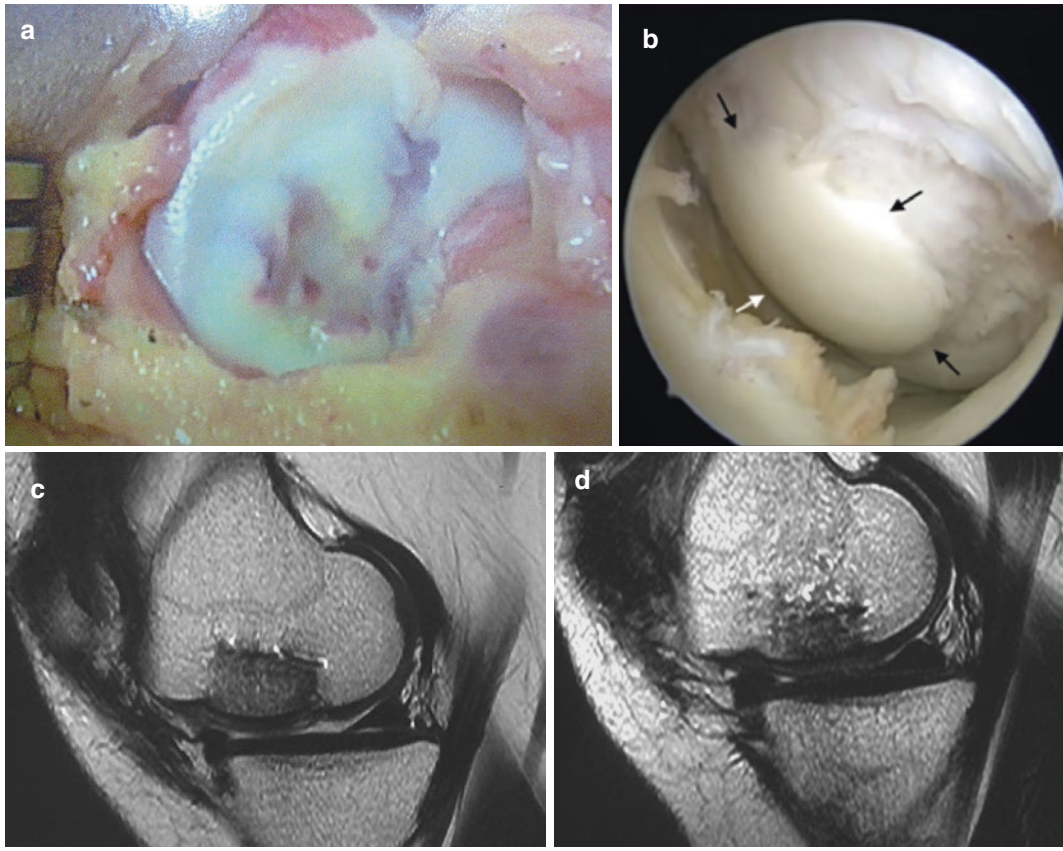

Figure 22.2.5: MRI Assessment of the Cartilage Repair Following Osteochondral Allograft Transplantation. Massive medial femoral condyle (MFC) osteochondral lesion with sectoral collapse treated with osteochondral allograft transplantation in a 21-year-old female. (**a**) Intraoperative image of the MFC prior to transplantation. (**b**) Second-look arthroscopic image 1 year following transplantation reveals complete healing of the allograft, good interface incorporation, normal articular cartilage topography, and firm surface. (**c**) One year following surgery, MRI reveals that the graft has united with no secondary collapse, repaired articular cartilage is homogenous, the repaired surface is intact and smooth, and the subchondral lamina and bone are normal. However, interface integration at the posterior border of allograft is still incomplete, resulting in a MOCART score of 95. (**d**) Two years following surgery, MRI reveals MOCART score of 100 with a complete integration of the interface and no demarcating borders

22.3 Take-Home Message

Focal articular cartilage defects in the knee progress to premature osteoarthritis and should be repaired whenever possible. An objective method of assessing the quality of repair tissue is with the MOCART score determined on a postoperative MRI. This scoring system evaluates nine parameters which include the extent of defect filling, border zone integration, structure, surface and signal intensity of the repair tissue, status of the subchondral lamina and subchondral bone, and presence of adhesions and effusion. Often, MRI is performed for baseline postoperative documentation and prognostication when the postoperative course is uneventful. MRI may also be used to monitor progressive stages of graft healing. More often, MRI is requested in cases with

recurrent or new symptoms after surgery. The four common techniques of articular cartilage repair have unique postoperative features and possible complications that may be apparent on imaging [6]. These include graft loosening, graft protuberance, graft depression, and collapse in osteochondral autograft cylinder transfer. The donor harvest site may develop surface incongruity and associated patellofemoral morbidity. ACI can be complicated by graft hypertrophy or cystic degeneration within 6 months of implantation [7, 8]. Graft collapse and immune rejection with synovitis are complications noted with the cadaveric allografts.

References

1. Marlovits S, Striessnig G, Resinger CT, Aldrian SM, Vecsei V, Imhof H, et al. Definition of pertinent parameters for the evaluation of articular cartilage repair tissue with high-resolution magnetic resonance imaging. Eur J Radiol. 2004;52:310–9.
2. Marlovits S, Singer P, Zeller P, Mandl I, Haller J, Trattnig S. Magnetic resonance observation of cartilage repair tissue (MOCART) for the evaluation of autologous chondrocyte transplantation: determination of interobserver variability and correlation to clinical outcome after 2 years. Eur J Radiol. 2006;57:16–23.
3. Battaglia M, Vannini F, Buda R, Cavallo M, Ruffilli A, Monti C, et al. Arthroscopic autologous chondrocyte implantation in osteochondral lesions of the talus: mid-term T2-mapping MRI evaluation. Knee Surg Sports Traumatol Arthrosc. 2011;19:1376–84.
4. Wiewiorski M, Miska M, Kretzschmar M, Studler U, Bieri O, Valderrabano V. Delayed gadolinium-enhanced MRI of cartilage of the ankle joint: results after autologous matrix-induced chondrogenesis (AMIC)-aided reconstruction of osteochondral lesions of the talus. Clin Radiol. 2013;68:1031–8.
5. Apprich S, Trattnig S, Welsch GH, Noebauer-Huhmann IM, Sokolowski M, Hirschfeld C, et al. Assessment of articular cartilage repair tissue after matrix-associated autologous chondrocyte transplantation or the microfracture technique in the ankle joint using diffusion-weighted imaging at 3 Tesla. Osteoarthr Cartil. 2012;20:703–11.
6. Sanghvi D, Munshi M, Pardiwala D. Imaging of cartilage repair procedures. Indian J Radiol Imaging. 2014;24:249–53.
7. Niemeyer P, Pestka JM, Kreuz PC, Erggelet C, Schmal H, Suedkamp NP, et al. Characteristic complications after autologous chondrocyte implantation for cartilage defects of the knee joint. Am J Sports Med. 2008;36:2091–9.
8. Pietschmann MF, Niethammer TR, Horng A, Gülecyüz MF, Feist-Pagenstert I, Jansson V, et al. The incidence and relevance of graft hypertrophy after matrix based autologous chondrocyte implantation. Am J Sports Med. 2012;40:68–74.